UNIVERSIDADE DE LISBOA
FACULDADE DE CIÊNCIAS

Faculdade de Ciências

Departamento de Biologia

Effects of Rare Earth Elements on aquatic organisms under a changing environment

"Documento Definitivo"

Doutoramento em Biologia e Ecologia das Alterações Globais
Especialidade em Biologia e Ecologia Marinha

Cátia Alexandra Alves Figueiredo

Tese orientada por:
Doutora Joana Raimundo Pimenta
Doutor Pedro Miguel Alfaia Barcia Ré
Doutor Mário Emanuel Campos de Sousa Diniz

Documento especialmente elaborado para a obtenção do grau de doutor

2022

UNIVERSIDADE DE LISBOA
FACULDADE DE CIÊNCIAS

Faculdade de Ciências

Departamento de Biologia

Effects of Rare Earth Elements on aquatic organisms under a changing environment

Doutoramento em Biologia e Ecologia das Alterações Globais

Especialidade em Biologia e Ecologia Marinha

Cátia Alexandra Alves Figueiredo

Tese orientada por:
Doutora Joana Raimundo Pimenta
Doutor Pedro Miguel Alfaia Barcia Ré
Doutor Mário Emanuel Campos de Sousa Diniz

Júri:
Presidente:

- Doutora Sólveig Thorsteinsdottir, Professora Associada com Agregação e Presidente do Departamento de Biologia Animal da Faculdade de Ciências da Universidade de Lisboa

Vogais:

- Doutora Patrícia Alexandra Oliveira Pereira Kowalski, Investigadora equiparada a Investigadora Auxiliar Departamento de Biologia da Universidade de Aveiro
- Doutora Patrícia Isabel Silvestre Pinto, Investigadora Doutorada Auxiliar Faculdade de Ciências e Tecnologia da Universidade do Algarve
- Doutora Joana Raimundo Pimenta, Investigadora Auxiliar Instituto Português do Mar e da Atmosfera, IPMA I.P. (orientadora)
- Doutora Ana Margarida da Silva Faria, Investigadora Escola de Biociências do ISPA-Instituto Universitário de Ciências Psicológicas, Sociais e da Vida
- Doutor Leonel Paulo Sul de Serrano Gordo, Professor Associado com Agregação Faculdade de Ciências da Universidade de Lisboa
- Doutor Carlos Alexandre Sarabando Gravato, Professor Auxiliar Faculdade de Ciências da Universidade de Lisboa

Documento especialmente elaborado para a obtenção do grau de doutor

Fundação para a Ciência e Tecnologia (SFRH/BD/130023/2017)

2022

“Sempre chegamos ao sítio aonde nos esperam.”

- José Saramago

Acknowledgements

Quem diria que esta seria a secção mais difícil de escrever da tese?! Não a deixei para o fim à-toa. É uma pena que durante estes processos não seja comum verbalizarmos regularmente a apreciação que temos pelas pessoas, dentro e fora de instituições e laboratórios, que nos acompanham e ajudam. Dependemos delas a vários níveis, e são fundamentais para os nossos percursos, muitas vezes sem terem noção disso. Chego finalmente aqui, aonde me esperaram, inundada de sentimentos de apreciação e espero que ao longo deste processo de catarse, que é a escrita desta secção, faça um pouco jus ao quão agradecida estou a todos vós por ter conseguido começar e levar a cabo esta tese de doutoramento, que também é vossa. É impossível consegui-lo nestas linhas, mas espero que um dia consigam receber um bocadinho da admiração e agradecimento que vos tenho.

Começo primeiramente, claro, por agradecer aos meus orientadores: à Doutora Joana Raimundo, ao Professor Doutor Mário Diniz e ao Professor Doutor Pedro Ré.

Joana, lembro-me bem quando te escolhi para minha orientadora. Queria uma mulher forte, com um currículo vasto que me pudesse ajudar na temática desta tese que eu pouco conhecia. Fiquei tão contente quando soube que tinha tido bolsa de doutoramento e que iriamos embarcar juntas nesta viagem de quatro anos. Logo de início apercebi-me que eras tão mais do que aquilo e o tempo foi-me mostrando, até, que isso estava longe de ser o mais importante. Não consigo pôr em palavras o quanto te conhecer e trabalhar do teu lado ajudou a complementar a pessoa e profissional que me tornei. É raro encontrar uma pessoa com a qual podemos contar e na qual podemos confiar. Agradeço-te por cada momento de ensinamentos sobre temas que se aprendem nos livros, mas também e principalmente por toda a tua disponibilidade, dentro e fora de horários convencionais. Agradeço-te a companhia e apoio nas amostragens, a ajuda nas experiências, na análise das amostras e dados, nos artigos e em toda a produção massiva que resultou deste nosso trabalho. E fundamentalmente agradeço-te por sempre teres estado lá, principalmente quando fiquei desamparada e foste impecável no processo de *step up* para arranjar soluções e podermos assim

continuar o nosso trabalho. Empoderaste-me e não há nada mais forte do que uma mulher quebrada que se reconstrói. Espero ter-te deixado orgulhosa.

Ao Mário, o meu muito obrigada por teres aceitado este desafio de orientar uma aluna de outra faculdade que mal conhecias. Agradeço-te também a integridade que demonstraste desde início e por sempre teres uma palavra de apoio nos momentos mais difíceis. Estas tuas características fizeram diferença e ajudaram a minha confiança e o meu trabalho. Sempre tiveste disponível para me receber no teu laboratório, reunir comigo e ensinar-me. Ouvir as histórias que sempre tinhas para contar foi um prazer, assim como rir muito delas. Tens o dom de ser um bom comunicador e aprendi muito contigo. Espero que a vida me ceda a oportunidade de voltarmos a trabalhar juntos.

Para o professor Pedro Ré tenho uma palavra de agradecimento por ter aceitado sem hesitações orientar-me e saltar para um barco em movimento, permitindo-me obter este grau. Obrigada pelo apoio e por toda a disponibilidade.

Agradeço também à Fundação para a Ciência e Tecnologia por ter confiado nas minhas capacidades e me ter atribuído bolsa de doutoramento (SFRH/BD/130023/2017), que foi essencial para poder levar a cabo este sonho.

A escolha, mútua, nestes orientadores fez-me pertencer a instituições e conhecer uma série de pessoas que me fizeram sentir em casa, e que foram muito importantes. Ao Mário Mil-Homens e ao Pedro Brito do Instituto Português do Mar e da Atmosfera (IPMA), muito obrigada pelo companheirismo, disponibilidade e ajuda. Foi um enorme prazer conhecer-vos, trabalhar convosco e partilhar gargalhadas. À Clara Lopes deixo um agradecimento particular, obrigada por todo o companheirismo e por me manteres junto a essa casa que é o IPMA. Não é qualquer pessoa que tem a capacidade em partilhar a sua casa dessa forma. Agradeço também por partilhares os teus amigos, meus companheiros das horas de almoço: Rui Oliveira, Lia Godinho, Catarina Churro e Carolina Magro. Obrigada a todos por ouvirem os meus desabafos, me acompanharem neste processo muitas vezes frustrante e exaustivo e por estarem sempre dispostos a ajudar e obrigada ainda por me fazerem rir, partilharem as vossas histórias e tornarem o meu dia-a-dia no IPMA um bocadinho melhor. Guardo-vos com muito carinho por isso.

Por fim, ainda sobre esta casa que se tornou o IPMA, gostaria de mencionar o Doutor Miguel Caetano. Comecei muito tímida a contactar contigo, por te reconhecer

uma série de características que admiro e muito rapidamente se tornou claro para mim que serias uma presença inquestionável em todos os meus trabalhos. Admiro muito a tua ética de trabalho e aprendi com ela, tornou-me melhor aluna e profissional. O percurso do início tímido, porque chegavas sempre com perguntas às quais não sabia responder, até perceber que isso me fazia questionar e olhar de maneira diferente para mim e para o meu trabalho, foi curto. Ter contado com a tua presença e ajuda melhorou a qualidade dos meus trabalhos, mas fundamentalmente melhorou-me e isso levarei para lá desta tese. Obrigada.

Relativamente ao Centro de Ciências do Mar e do Ambiente (MARE) e à minha passagem pelo Laboratório Marítimo da Guia guardo as pessoas que ficaram, amigos e colegas importantíssimos e sem os quais este trabalho não teria sido possível. Aos meus melhores amigos Tiago Grilo e Ana Rita Lopes, pilares fundamentais para a minha existência, estou muito agradecida ao acaso que decidiu juntar-nos e à sorte que tivemos em alinhar-nos. Para além de todo o apoio durante o processo de candidatura a bolsa de doutoramento, a todas as ajudas nas experiências e nos laboratórios e no processo de escrita de artigos estou imensamente agradecida a toda a vossa disponibilidade e presença. Vocês são muito importantes e este sentimento de casa para o qual contribuem o João e o Alex, dá-me parte da força que foi crucial para concluir esta dissertação. Deixo ainda uma palavra extra de agradecimento ao Grilo, que ajudou a financiar parte das minhas experiências e que sempre deu tudo o que tinha e não tinha para que este trabalho fosse concluído com sucesso. Este trabalho não seria o mesmo, e definitivamente não tão rico, se não tivesse contado contigo. E eu também não.

Ainda trazidos até mim graças à minha passagem pelo MARE quero agradecer aos meus amigos Francisco Carvalho, Miguel Baptista e Sara García-Morales. Chico, és das pessoas mais engraçadas que conheço e poder ter partilhado este processo contigo, e com o Tiago, tornou-o mais leve e agradável. O conforto do teu abraço faz parte daquela força que precisei para terminar este doutoramento. Ao Miguel Baptista o meu muito obrigada por toda a disponibilidade e companheirismo, desde antes do início desta tese. Sentir-me querida foi importante e saber que consegues lidar com as minhas ansiedades e atrasos em respostas e afins sem nunca teres cobrado isso é um bom indicador da pessoa que és. Por fim, à Sarita o meu muito obrigada, por saber estar no lado certo da história e por me empoderar a ser melhor ser humano.

| Acknowledgements

Relativamente às pessoas cruciais fora de instituições de investigação e laboratórios tenho um agradecimento muito grande a deixar à amiga da minha vida Ana Gil. Sei-te de cor e partilhar todo este processo contigo tornou-o tão melhor. És conforto, és casa, és orgulho e sou muito agradecida por poder existir contigo. Agradeço o pilar que és, o apoio que és e toda a força que me deste principalmente nos momentos de fraqueza, exaustão e frustração. Guardo com tanto carinho todas as videochamadas à hora de jantar com o Maurício, quando eu ainda estava a trabalhar no computador e como esses momentos de distração me davam força para continuar. Obrigada por me ajudares a concluir este sonho.

Ainda em relação a amizades de uma vida, agradeço também à Sara Fernandes e à Bárbara Gonçalves minhas companheiras ininterruptas desde as aulas do secundário. Comecei a traçar este sonho do vosso lado e a vossa amizade manteve-me sempre do lado certo.

Ao Gustavo Briz e Fahim Cassam, meus companheiros de lutas, um obrigada por me manterem ligada ao mundo que me corre nas veias. Todos os momentos passados com vocês foram importantes para manter a chama, do que é tão estrutural em mim, viva.

A todos estes amigos que fazem parte da minha família lógica um muito obrigada. Escolher-vos com a exigência que tenho para mim fez com que a amostra diversa de pessoas com as mais diferentes posições e valências tornassem esta tese exequível.

Para o fim deixei os agradecimentos à outra família.

Aos meus irmãos, Nuno Figueiredo e Maria Elisabete Figueiredo obrigada pelo vosso companheirismo. Sinto o vosso orgulho e isso é tão importante. São indubitavelmente parte essencial na formação da minha personalidade e agradeço-vos por isso, muito do que aprendi com vocês ajudou-me neste processo. Agradeço também por me terem dado os meus sobrinhos: Andreia e Catarina Paixão e Rodrigo e Bárbara Figueiredo, que foram marcantes no sentimento de casa e na força necessária para concluir esta tarefa.

E um grande obrigada aos meus pais: José Figueiredo e Lúcia Alves. Mesmo sem perceberem muito bem o que seria isto de fazer um doutoramento sempre me apoiaram a fazer o que eu desejasse. Tudo o que nos deram, e o que fizeram de nós é a

base deste trabalho. Os meus traços de personalidade são vossos e aprendi tanto do que sou hoje convosco. A ética de trabalho que permitiu concluir esta dissertação aprendi-a com vocês e estou tão agradecida por tudo. Pai, desde sempre senti que só me querias ver feliz e quando sentimos este tipo de amor, nenhum contratempo ou dificuldade profissional nos abala. Obrigada. Quanto a ti, Mãe, vou-te contar a história de como um dia sonhei em fazer um doutoramento, do quanto trabalhei para conseguir bolsa e de tudo o que passei no curso dos quatro anos de trabalho intenso para o conseguir, das pessoas que fui conhecendo pelo caminho e de como cheguei à fase final de escrever estas palavras, as vezes que forem precisas, para te lembrares e poder sentir aquele orgulho que sei que tens em mim, mesmo que por breves momentos.

Dirijo o meu último agradecimento à Filipa Vassallo e Silva. Não poderia ter escolhido melhor pessoa para ter do meu lado e este processo ajudou-me a ver isso. Não haveria melhor pessoa para me apoiar, ajudar a lidar com as frustrações, aceitar o meu horário e adaptar-se a ele, compreender as partes mais técnicas dos meus devaneios e estar sempre pronta para me receber com um abraço no fim de um dia de trabalho. Agradeço também ao Alfredo por se ter deixado conquistar e à família que construímos. O conforto que encontrei em vocês tornou o processo de escrita desta dissertação mais agradável e definitivamente tornou a vida melhor.

Obrigada.

Table of Contents

ABSTRACT

Anthropogenically increased rare earth elements (REE) availability and climate change constitute a major environmental challenge. Their combined effects are poorly understood; hence, the main objective of this Ph.D. dissertation was to undertake their bioaccumulation, elimination, and interaction through assessing biochemical strategies of several taxonomic groups (sponges, fish, bivalves and algae). The findings show that coastal and deep-sea biomonitoring species can accumulate REE, mimicking environmentally available and seasonal changes in REE concentrations. Although described as chemically coherent, Lanthanum (La) and Gadolinium (Gd) behave differently, and their bioavailability changes with water salinity. Lanthanum accumulation in *Anguilla anguilla* exposed to 120 ng L^{-1} peaked after 3 days and decreased even in a continuously exposed medium. When exposed to 1.5 µg L^{-1} La and warming, the accumulation was exacerbated, and the elimination was less effective. *Ruditapes philippinarum* exposed to 0.3 and 0.9 µg L^{-1} La accumulated after two days, in a dose dependent manner. *Spisula solida* exposed to 15 µg L^{-1} La, or 10 µg L^{-1} of Gd and climate change accumulated after one day and a 7-day elimination phase was insufficient, however warming enhanced it. La and Gd triggered an insufficient biochemical response. La and Gd accumulation in the green macroalgae *Ulva rigida* occurred in 24h and REE exposure in a near future scenario triggered an overproduction of reactive oxygen species that requested a superior antioxidant response. The results emphasize enhanced REE toxicological potential in a changing world. Organisms' responses were species-specific, element-specific, and dose-specific, suggesting that understanding REE accumulation and toxic responses in the near-future is exceptionally intricate. Nonetheless, REE accumulation and toxic effects may be exacerbated by climate change, imposing deleterious consequences to species. Overall, data deriving from this novel Ph.D. dissertation will be pivotal for the decision-making process of policy makers when legislating for these emergent problematics and timely environmental policies.

Keywords: rare earth elements; climate change; bioaccumulation; ecotoxicology; biochemical defense mechanisms.

RESUMO

O aumento da disponibilidade de elementos terras raras (REE) e as alterações climáticas constituem um desafio ambiental com consequências pouco conhecidas; daí, o objetivo desta tese de doutoramento consistiu em investigar a sua bioacumulação, eliminação e interação através da avaliação de estratégias bioquímicas de diversos grupos taxonómicos (esponjas, peixes, bivalves e algas). Os resultados mostram que espécies bioindicadoras costeiras e de alto mar acumulam REE, refletindo mudanças sazonais e concentrações ambientalmente disponíveis. Embora descritos como análogos, o Lantânio (La) e Gadolínio (Gd) comportam-se de forma diferente, e sua biodisponibilidade muda com a salinidade da água. *Anguila anguila* exposta a 120 ng L^{-1} La acumulou durante 3 dias e posteriormente a acumulação diminuiu em meio continuamente exposto. Exposta a 1,5 µg L^{-1} La e aquecimento global, a acumulação aumentou e a eliminação diminui. *Ruditapes philippinarum* exposta a 0,3 e 0,9 µg L^{-1} La acumulou de forma dependente da dose. *Spisula solida* exposta a 15 µg L^{-1} La, ou 10 µg L^{-1} de Gd e a alterações climáticas acumulou em 24h e uma eliminação de 7 dias foi insuficiente, apesar do aquecimento global aumentá-la. A resposta bioquímica desencadeada foi insuficiente. A acumulação de La e Gd em *Ulva rigida* ocorreu em 24h e a exposição em alterações climáticas exigiu uma resposta ao stress oxidativo superior. Os resultados enfatizam um potencial ecotoxicológico de REE aumentado num mundo em mudança. As respostas dos organismos foram específicas por espécie, por elemento e por dose, sugerindo que compreender a acumulação de REE e as respostas ecotoxicológicas num futuro próximo é excecionalmente complexo. Apesar disso, a acumulação de REE e os efeitos tóxicos podem ser exacerbados pelas mudanças climáticas, impondo consequências nocivas às espécies. No geral, os dados desta tese de doutoramento podem ser basilares para o processo de tomada de decisões políticas ao legislar para estas problemáticas emergentes.

Palavras-chave: terras raras; alterações climáticas; bioacumulação; ecotoxicologia; respostas bioquímicas.

RESUMO ALARGADO

Os elementos terras raras, ou REE (*rare earth elements*), são um grupo da tabela periódica que incluem, segundo a definição da IUPAC (*International Union of Pure and Applied Chemistry*) o escândio (Sc), o ítrio (Y) e os 15 elementos da série lantanídeos (Ln), do lantânio ao lutécio. São um grupo coeso, com um comportamento químico bastante similar. Têm várias aplicações industriais, mas também na agricultura como fertilizantes, na criação animal e aquacultura como bactericidas ou em medicina. As técnicas de extração, de mineração e de purificação são as principais fontes antropogénicas de REE. Primeiramente a comunidade científica focou-se no seu estudo do ponto de vista geológico e de impactos ambientais relacionados com a sua extração, o que fez com que fossem considerados como pouco tóxicos. Após se tornar conhecida a capacidade de serem bioacumulados, e assim que um enriquecimento (anomalia positiva) de gadolínio (Gd) em rios na Europa foi diretamente associado a agentes de contraste de ressonância magnética, a preocupação ambiental aumentou. A demanda por REE cresce exponencialmente devido à sua aplicabilidade em tecnologias modernas, como baterias de carros elétricos e híbridos, geradores de turbinas eólicas, entre outros. Prevê-se que esta demanda se mantenha, o que pode originar um risco de escassez. Assim, têm surgidos novos locais de mineração pelo mundo, o que adivinha uma transferência crescente para os ecossistemas aquáticos. A sua utilização desenfreada fez com que fossem considerados como poluentes emergentes pela União europeia, o que ilustra a urgência em desvendar o seu comportamento ecotoxicológico. Na presente tese, o Lantânio (La) e o Gadolínio (Gd) foram escolhidos como representantes de REE leves e pesadas, respetivamente. O La é o primeiro da série de lantanídeos e é um dos mais abundantes e reativos. Sabe-se que é introduzido na hidrosfera através de emissões industriais, e que a sua mineração produz efluentes que entram no ambiente altamente concentrados em La. É acumulado por organismos aquáticos e pode ser tóxico. O Gd é um dos REE mais explorados e é usado desde os anos 80 como agente de contraste em ressonâncias magnéticas. Injetado num complexo estável na corrente sanguínea, é excretado pela urina e chega ao ambiente praticamente inalterado. A sua

acumulação é notória em zonas costeiras altamente populosas e os seus efeitos toxicológicos começam agora a ser desvendados.

As alterações climáticas são outra problemática da atualidade. Os níveis atmosféricos crescentes de dióxido de carbono (CO_2) desde a revolução industrial, impacta as propriedades físico-químicas da hidrosfera e a temperatura da Terra. Devido a estes, prevê-se um aumento de 1-4 °C da temperatura média da superfície dos oceanos até 2100. Tendo em conta que o oceano é um dos maiores reservatórios naturais de CO_2, espera-se ainda que esta absorção aumente a quantidade de iões hidrogénio, que reduzem o pH da água. A ocorrência de contaminantes emergentes, como os REE, irá também interferir nos processos biológicos necessários para a sobrevivência de espécies aquáticas. Adicionalmente, as alterações climáticas interferem na bioacumulação de contaminantes e nas suas respostas ecotoxicológicas. Dada a crescente consciência sobre alterações climáticas, poluentes e os seus impactos, o objetivo principal da presente tese de doutoramento prendeu-se com a criação de conhecimento chave sobre estas problemáticas emergentes. Assim, analisou-se a bioacumulação de REE, a sua interação com o aquecimento global e a acidificação do oceano e ainda as respostas ecotoxicológicas induzidas em espécies aquáticas ecológica e economicamente relevantes. Para atingir este objetivo, a presente dissertação foi dividida em três partes: Parte 1 – para compreender a influência de fatores abióticos na acumulação de REE, os valores basais de REE foram estimados em invertebrados marinhos, biomonitores, capturados ao longo da costa de Portugal, em diferentes épocas, e do mar profundo do Atlântico Norte; Parte 2 – com o objetivo de estudar a bioacumulação e eliminação de REE, e possível interação com alterações climáticas, foram realizados estudos de exposição a La e Gd, e aquecimento global e acidificação dos oceanos, utilizando diferentes modelos biológicos, e avaliadas respostas biológicas e bioquímicas; Parte 3 – onde se pretendeu integrar o conhecimento científico produzido e propor direções de investigação.

Os resultados demonstram que mexilhões *Mytilus galloprovincialis* amostrados junto ao estuário do Tejo apresentam maiores concentrações de REE, em oposição aos localizados em zonas costeiras. As concentrações de REE foram maiores na primavera, do que no outono e o enriquecimento naturalmente existente de REE leves em comparação a pesadas foi demonstrado também nos tecidos dos mexilhões.

Em relação a esponjas do mar profundo (481 a 2656 m) do Atlântico Norte pertencentes a 5 géneros porífera (Jaspis, Geodia, Hamacantha, Leiodermatium, Poliopogon), o espécimen mais profundo apresentou a maior concentração de REE. Uma anomalia negativa de Ce foi observada em *M. galloprovincialis,* ao longo da costa portuguesa, e também nestes espécimenes.

O La e o Gd comportam-se de forma diferente, em diferentes salinidades. A temperatura afeta os níveis de La em água doce, enquanto a acidificação diminui os valores de Gd. Os níveis de La e Gd diminuíram consideravelmente durante as primeiras 24h, o que indica que estudos de exposição em laboratório a REE devem fazer uma monitorização mais rigorosa dos valores de exposição presentes na água. Em água salobra apenas as concentrações de La foram alteradas quando expostos a aquecimento e aquecimento e acidificação. Em água salgada, os níveis de La e Gd permaneceram mais estáveis, mas a disponibilidade de outros complexos aumentou, o que indica que os iões La^{3+} e Gd^{3+} podem estar menos disponíveis.

A fase inicial da ontogenia da enguia Europeia, *Anguilla anguilla,* foi exposta a uma concentração ambientalmente relevante de 120 ng L^{-1} de La durante 7 dias, à qual se sucedeu uma fase de 7 dias de depuração. A acumulação atingiu o máximo após 72 horas, tendo decrescido mesmo num meio continuamente exposto. A acumulação foi maior na víscera seguida do corpo sem pele e da brânquia. Um aumento significativo da atividade da acetilcolinesterase (AChE) foi acompanhado de uma depressão da peroxidação lipídica (LPO) e da atividade da catalase (CAT), ilustrando o impacto fisiológico do La.

Quando exposta a 1.5 µg L^{-1} de La durante 5 dias, aos quais se seguiu uma fase de eliminação de 5 dias, num cenário de aquecimento global, a acumulação e a toxicidade do La foram exponenciadas com o aumento da temperatura. O padrão de acumulação desta concentração foi diferente do estudo anterior sendo maior na víscera seguida pela cabeça e restante corpo. A eliminação do La foi menos eficiente num cenário de aquecimento. Ocorreu LPO e a expressão de proteínas de choque térmico (HSP) foi suprimida em enguias expostas a La, em temperatura controlo e aquecimento global. Enguias expostas a La são incapazes de prevenir de modo eficiente o dano celular, sendo este cenário particularmente dramático em condições de aquecimento.

| Resumo alargado

O bivalve *Ruditapes philippinarum* foi exposto a duas concentrações ambientalmente relevantes de La (0.3 µg L^{-1} e 0.9 µg L^{-1}), durante 6 dias. Ao fim do segundo dia o La tinha sido acumulado de uma forma dependente da dose. A acumulação foi maior nas brânquias seguidas pela glândula digestiva e pelo restante corpo.

Já o bivalve *Spisula solida* foi exposto a 15 µg L^{-1} de La e aquecimento e acidificação, durante 7 dias, seguido de um período de eliminação de 7 dias. O La foi bioacumulado em 24h, em todas as condições abióticas. Sete dias de eliminação foram insuficientes. Uma resposta bioquímica foi desencadeada, no entanto, ocorreu dano lipídico e esta foi insuficiente para desintoxicar La.

A mesma espécie exposta a 10 µg L^{-1} Gd por sete dias, seguidos por uma fase de eliminação de igual período, e alterações climáticas, acumulou após 24h, e o período de eliminação não foi eficiente. O Gd foi o principal impulsionador da resposta ao stresse oxidativo, no entanto, o seu impacto foi exacerbado pelas alterações climáticas. O dano lipídico foi maior em *S. solida* exposta a aquecimento e Gd, o que enfatiza os efeitos tóxicos aumentados num oceano em mudança.

Por fim, a magroalga verde *Ulva rigida* foi exposta a La ou Gd (15 µg L^{-1} ou 10 µg L^{-1}, respetivamente), e aquecimento e acidificação durante 7 dias aos quais se sucedeu uma eliminação de 7 dias. O aquecimento e a acidificação contribuíram para os níveis mais baixos de La e aumentaram a eliminação do mesmo, mas não de Gd. La e Gd ativaram uma defesa antioxidante, evitando dano lipídico. No entanto, a exposição a REE num cenário futuro solicitou uma resposta ao stress oxidativo superior. Adicionalmente, um aumento na clorofila total e nos carotenoides indica um gasto de energia acrescido, em resposta a um ambiente multistressor.

Os dados sugerem que a exposição a REE num mundo em mudança pode implicar efeitos mais graves do que o expectável.

Assim, os resultados descritos nesta dissertação constituem uma valiosa contribuição para o conhecimento do comportamento dos REE em diferentes matrizes, assim como a sua interação com futuras condições ambientais. Os impactos negativos causados por estes em diferentes organismos podem interferir no seu sucesso ecológico, acarretando consequências ecológicas e económicas graves.

Concomitantemente, os dados empíricos desta dissertação de doutoramento podem ser importantes no processo de tomada de decisões políticas.

LIST OF ARTICLES

The present Ph.D. dissertation encompasses nine scientific papers, listed below, corresponding to different chapters (2-10).

Chapter 2

Figueiredo, C., Oliveira, R., Lopes, C., Brito, P., Caetano, M., Raimundo, J., 2022. Rare earth elements biomonitoring using the mussel *Mytilus galloprovincialis* in the Portuguese coast: seasonal variations. Marine Pollution Bulletin 175, 113335 (DOI 10.1016/j.marpolbul.2022.113335)

Chapter 3

Figueiredo, C., Caetano, M., Mil-Homens, M., Tojeira I., Xavier, J. R., Rosa, R., Raimundo, J. 2021. Rare earth and trace elements in deep-sea sponges of the North Atlantic. Marine Pollution Bulletin 166, 112217 (DOI 10.1016/j.marpolbul.2021.112217)

Chapter 4

Figueiredo, C., Grilo, T.F., Lopes, C., Brito, P., Caetano, M., Raimundo, J. 2022. Lanthanum and Gadolinium availability in aquatic mediums: new insights to ecotoxicology and environmental studies. Journal of Trace Elements in Medicine and Biology 71, 136957. (DOI 10.1016/j.jtemb.2022.126957)

Chapter 5

Figueiredo, C.[#], Grilo, T. F.[#], Lopes, C., Brito, P., Diniz, M., Caetano, M., Rosa, R., Raimundo, J. 2018. Accumulation, elimination, and neuro-oxidative damage under lanthanum exposure in glass eels (*Anguilla anguilla*). Chemosphere 206, 414-423 (DOI 10.1016/j.chemosphere.2018.05.029)

Chapter 6

Figueiredo, C.[#], Raimundo, J.[#], Lopes, A.R., Lopes, C., Rosa, N., Brito, P., Diniz, M., Caetano, M., Grilo, T.F. 2020. Warming enhances lanthanum accumulation and toxicity promoting cellular damage in glass eels (*Anguilla anguilla*). Environmental Research 191, 110051

(DOI 10.1016/j.envres.2020.110051)

Chapter 7

Figueiredo, C., Grilo, T.F., Lopes, A.R., Lopes, C., Brito, P., Caetano, m., Raimundo, J., 2022. Differential tissue accumulation in the invasive manila clam, *Ruditapes philippinarum* under two environmentally relevant lanthanum concentrations. Environmental Monitoring and Assessment 194:11.

(DOI 10.1007/s10661-021-09666-y)

Chapter 8

Figueiredo, C., Grilo, T.F., Oliveira, R., Ferreira, I.J., Gil, F., Lopes, C., Brito, P., Ré, P., Caetano, M., Diniz, M., Raimundo, J., 2022. Single and combined ecotoxicological effects of ocean warming, acidification and lanthanum exposure on the surf clam (*Spisula solida*). Chemosphere 302, 134850.

(DOI 10.1016/j.chemosphere.2022.134850)

Chapter 9

Figueiredo, C., Grilo, T.F., Oliveira, R., Ferreira, I.J., Gil, F., Lopes, C., Brito, P., Ré, P., Caetano, M., Diniz, M, Raimundo, J., 2022. Enhanced ecotoxicity of Gadolinium in a warmer and acidified changing ocean using a multibiomarker approach: the case of the surf clam *Spisula solida*. Accepted for publication in Aquatic toxicology.

Chapter 10

Figueiredo, C., Grilo, T.F., Oliveira, R., Ferreira, I.J., Gil, F., Lopes, C., Brito, P., Caetano, M., Ré, P., Caetano, M, Diniz, M., Raimundo, J., 2022. A triple threat: Ocean warming, acidification, and rare earth elements exposure triggers a superior antioxidant response and pigment production in the adaptable *Ulva rigida*. Environmental Advances 8, 100235.

(DOI 10.1016/j.envadv.2022.100235)

LIST OF ABBREVIATIONS AND UNITS

A

Abs – Absorbance

AChE – Acetylcholinesterase

ANOVA – Analysis of variance

ATP – Adenosine triphosphate

atm – atmosphere

B

BCF – Bioconcentration factor

BSA – Bovine serum albumin

C

CAT – Catalase

Ca^{2+} – Calcium ion

$CaCO_3$ – Calcium carbonate ion

CDNB – Chloro-2,4-dinitrobenzene

Ce – Cerium

ChEs – Cholinesterases

Cho – Chondrite

CH_4 – Methane

Cl^- – Chlorine ion

CO_2 – Carbon dioxide

CO_3^{2-} – Carbonate ion

Cont. – Continuation

CRM – Certified reference material

CT – Total dissolved inorganic carbon

D

DL – Detection limit

DNA – Deoxyribonucleic acid

DO – Dissolved oxygen

dw – Dry weight

Dy – Dysprosium

E

e.g. – For example (from the Latin "*exampli gratia*")

ELISA – Enzyme–linked immunosorbent Assay

ETC – Electron transport chain

etc – Etcetera

EU – European Union

EUS – European shale normalized

Er – Erbium

Eu – Europium

F

FAO – Food and Agriculture Organization

FCT – Fundação para a Ciência e Tecnologia

FCUL – Faculdade de Ciências da Universidade de Lisboa

G

g – grams

g – Relative centrifugal force

Gd – Gadolinium

$GdCl_3$ – Gadolinium chloride

GHG – Greenhouse gas

GPx – Glutathione peroxidase

GSH – Reduced glutathione

GST – Glutathione S–transferases

H

h – hour

H^+ – Hydrogen ions

H_2CO_3 – Carbonic acid

H_2O – Water

H_2O_2 – Hydrogen peroxide

H_3BO_3 – Boric acid

HCL – Hydrochloric acid

HCO_3^- – bicarbonate ion

HF – Hydrofluoric acid

HNO_3 – Nitric acid

Ho – Holmium

HREE – Heavy Rare Earth Elements

HSP_{70} – Heat shock protein 70 kDa

HSPs – Heat shock proteins

HSR - Heat shock response

I

ICP-MS – Inductively coupled plasma mass spectrometry

i.e. – That is (from the Latin "*id est*")

IPCC – Intergovernmental Panel on Climate Change

IPMA – Instituto Português do Mar e da Atmosfera

IS – Internal standard

IUCN – International Union for Conservation of Nature and Natural Resources

IUPAC – International Union of Pure and Applied Chemistry

K

KCl – Potassium chloride

kDa – Kilodalton

kg – Kilogram

KH_2PO_4 – Potassium phosphate

KOH – Potassium hydroxide

L

L – litre

L^{-1} – Per litre

La – Lanthanum

$LaCl_3$ – Lanthanum chloride

LC50 – Lethal Concentration 50

L:D – Light:dark

Log – Logarithm

LPO – Lipid peroxidation

LREE – Light Rare Earth Elements

Lu – Lutetium

M

m – Meter

M – Molar concentration

MARE – Marine and Environmental Sciences Centre

MDA – Malondialdehyde bis (dimethylacetal)

mg – milligram

mg Kg^{-1} – miligram per kilogram

Mg^{2+} – Magnesium ion

mg L^{-1} – miligram per litre

min – minute

mL – mililitre

mm – milimetre

mM – milimolar

MS – Mass spectrometry

MΩ – Megaohm

N

n.a. – Not available or not applicable

ng – nanogram

nm – nanometers

nmol – nanomoles

N_2O – Nitrous oxide

Na^+ – Sodium cation

Na_2HPO_4 – Sodium phosphate

NaCl – Sodium chloride

$NADP^+$ – Nicotinamide adenine dinucleotide phosphate

NADPH – Dihydronicotinamide – adenine dinucleotide phosphate

NaOH – Sodium hydroxide

Nd – Neodymium

O

OA – Ocean acidification

OW – Ocean warming

O_2^- – Superoxide ion

O_2 – Oxygen

O_3 – Ozone

P

p – *p*–value

PBS – Phosphate buffered saline

*p*CO2 – Carbon dioxide partial pressure

pH – Power of hydrogen

pH_T – pH total scale

Pm – Promethium

ppm – part per million

Pr – Praseodymium

PSU – Practical salinity unit

Q

QC – Quality control

R

r – Pearson correlation coefficient

REE – Rare Earth Element

ROS – Reactive oxygen species

Rpm – Revolutions per minute

S

s – second

Sc – Scandium

SD – Standard deviation

SE – Standard error

Sm – Samarium

SO_4^{2-} – Sulfate

SOD – Superoxide dismutase

Sp – suprapur

sp. or spp. – Specific epithet of species not identified. Single or several species within a genus

SST – Sea surface temperature

T

TA – Total alkalinity

TAC – Total antioxidant capacity

Tb – Terbium

TBARS – Thiobarbituric acid reactive Substances

TE – Trace elements

Temp – Temperature

Tm – Thulium

U

Ub – Total ubiquitin

UCIBIO – Research Unit on Applied Molecular Biosciences

UK – United Kingdom

USA – United States of America

UV – Ultraviolet

V

v/v – volume/volume

W

ww – Wet weight

WWTP – Wastewater treatment plant

X

XOD – xanthine oxidase

Y

Y – Yttrium

Yb – Ytterbium

Z

Zn – Zinc

SYMBOLS

~ – Approximately

[ ] – Concentration

°C – Degree Celsius

< – Lower than

> – Higher than

% – Percentage

± – Plus minus

Δ – Variation

∑ – Sum

™ – Trademark

µ – Micro

µg – Microgram

µg g^{-1} – Microgram per gram

µatm – Micro atmosphere

µL – Microliter

µm – Micrometer

µM – Micromolar

µm – Micromole

ƐmM – Extinction coefficient

Ω Ara – aragonite saturation state

Ω Cal – calcite saturation state

8 –OHdG – 8 –hydroxy –2'-deoxyguanosine

LIST OF FIGURES

Chapter 9

Chapter 10

LIST OF TABLES

ANNEX 3

ANNEX 4

ANNEX 5

ANNEX 6

PART ONE

1. GENERAL INTRODUCTION

1.1 RARE EARTH ELEMENTS

The rare earth elements (REE) are a group of seventeen strongly related heavy elements, comprising Scandium (Sc), Ytrium (Y) and the Lanthanide Group, as defined by the International Union of Pure and Applied Chemistry (IUPAC), that are unknown to most people. Some may have heard of them, or probably associate them to the poorly known rows of elements beneath the main body of the Periodic Table (Figure 1.1).

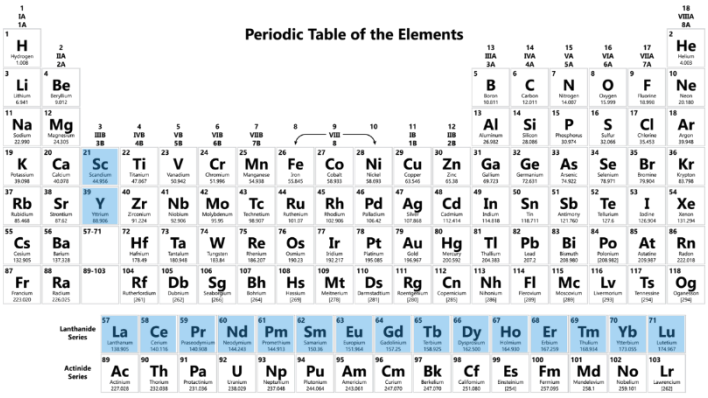

Figure 1.1 – Periodic table of the elements with rare earth elements highlighted in light blue

The REE consist of the following elements: ^{21}scandium (Sc), ^{39}yttrium (Y), ^{57}lanthanum (La), ^{58}cerium (Ce), ^{59}praseodymium (Pr), ^{60}neodymium (Nd), ^{61}promethium (Pm), ^{62}samarium (Sm), ^{63}europium (Eu), ^{64}gadolinium (Gd), ^{65}terbium (Tb), ^{66}dysprosium (Dy), ^{67}holmium (Ho), ^{68}erbium (Er), ^{69}thulium (Tm), ^{70}ytterbium (Yb), and ^{71}lutetium (Lu). Yttrium was the first element to be revealed, at the end of the 18th century, and within the next century, almost all have been discovered. The REE display very similar chemical behavior, forming the largest chemically coherent group (Haxel, 2002). In fact, Sc and Y are considered REE due to their resembling performance to the lanthanides (Ln). The Ln possess similar physicochemical properties since they are majorly trivalent (3+), with the exception of Eu, Yb and Sm that form 2+ ions, and Ce, that can also form 4+ ions (Cotton, 2013). The radii of the Ln^{3+} decreases continuously, with increasing atomic number, in a phenomena known as lanthanide contraction, that is responsible for the remarkable physical and chemical behavior similarity in this series of elements (Hu et al., 2017).

The name REE constitutes an inaccuracy and does not make them justice. This is closely related to their discovery, when only one deposit was known, a single quarry near Ytterby, in Sweden. This misled the scientists to think they were rare, when in fact average REE concentrations in the Earth's crust range from 150 to 200 mg kg $^{-1}$ and are

therefore more abundant than copper, lead, gold and platinum (Humphries, 2010). Vulcanic emissions and parent rock weathering, through rain and watercourses, are the main REE terrestrial sources. While hydrothermal crusts and vents, and Fe-Mn nodules constitute the major natural sources in the deep-sea. Their versatility branded them much more technological, environmental, and economically central than their anonymity might suggest. This realization is key to the understanding of their imperative role in modern life and technologies. Although REE occur naturally on the Earth's crust, with the exception of the radioactive Pm, their individual abundances are very dissimilar, with the most abundant presenting up to two to five orders of magnitude greater concentrations than the least abundant ones (Figure 1.2) (Atwood, 2013; Haxel, 2002).

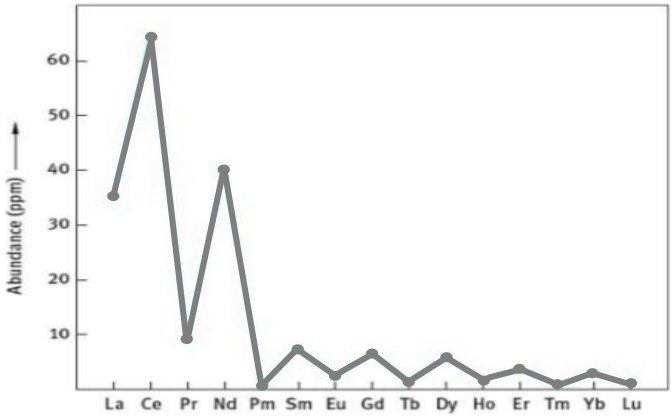

Figure 1.2 – Rare earth element abundance. Adapted from Atwood (2013)

The saw-shaped curve presented in Figure 1.2 can be levelled when each element is normalized with rock patterns (Atwood, 2013). This normalization simplifies data visualization, and allows the identification of possible anomalies, which are positive or negative deviations from their neighboring pairs (Holser, 1997), of a singular element or group of elements. There are several accepted patterns of rocks to normalize REE concentrations, and within this thesis two were used: The European Shale (EUS) proposed by Minami (1935) and improved by Haskin and Haskin (1966); and a mean of chondrites (Schmitt et al., 1963).

Mining, extraction, and purification activities constitute the main REE anthropogenic sources. Rare earth elements mining is known to cause soil erosion, biodiversity loss, land use shift, flooding, and water and air pollution (Carpenter et al., 2015). Furthermore, the worldwide industrial, agricultural, and domestic REE usage has

a direct environmental impact, due to contaminated wastewater. The bioavailability of REE is strongly related to its speciation, which in turn depends on a wide array of factors such as pH, salinity, major anions (Liang et al., 2005) and organic matter. In saltwater, REE are present mainly as carbonate and chloride complexes, while in freshwater are complexed with humic substances and hydroxide anions.

Acid mine drainage is responsible for discharges of low pH and REE high concentrated effluents (Burch et al., 2011), which alters the REE fractionation patterns (Lecomte et al., 2017). Rare earth element fractionation is also altered by urban wastewater treatment systems, and domestic and industrial effluents. These effluents contribute to REE concentration increase and these anthropogenic REE enter the environment in a much more soluble and reactive form, than the naturally occurring REE, increasing their bioavailability. The bioaccessibility and the bioavailability of a given metal determines the amount that can be accumulated by aquatic organisms. Bioaccessibility refers to the compounds that are hypothetically available, nonetheless at present can be out of reach. The portion that are indeed able to cross biological membranes is labeled bioavailable (Semple et al., 2004). Metal speciation, the physicochemical water parameters and the physiological characteristics of the organisms are some of the many abiotic and biotic factors that can alter the bioavailability of metals, such as REE. Toxicity arises when the rates of detoxification and excretion are exceeded by the rate of metal uptake (Luoma and Rainbow, 2005) and REE are known to be bioaccumulated and show toxicity effects on organisms such as aquatic plants, aquatic invertebrates and vertebrates (e.g., Oral et al., 2010; Weltje et al., 2002; Zhang et al., 2012). Although the number of studies on REE bioaccumulation and toxic effect have increased in recent years, due to the growing importance that emerging REE are gathering, few studies exist.

The demand for REE has been growing dramatically as modern technological applications emerged and multiplied in the past decades, which cause their consumption at an unprecedented rate. Their applications range from computer memories, rechargeable batteries, super magnets, mobile phones, LED lighting, fluorescent materials, solar panels and magnetic resonance imaging (MRI) agents (Balaram, 2019). Numerous REE are crucial for the manufacture of “green technologies” such as electric and hybrid-electric vehicles batteries, wind turbine generators, low-

energy lighting, fuel cells, magnetic refrigeration (Atwood, 2013), and their usage is on the rise. REE application is summarized in Table 1.1.

Table 1.1 – Rare earth element applications. Source: (Voncken, 2016)

Z	Rare Earth Element	Major Use
21	Scandium	Alloying metal for aluminum; high intensity streetlamps.
39	Yttrium	Red coloring; fluorescent lamps; ceramics; metal alloy agent.
57	Lanthanum	Hybrid engines; metal alloys; batteries; diesel fuel additive; hydrogen storage; fluid catalyst, special optical glasses; superconductor.
58	Cerium	Auto catalyst; petroleum refining; metal alloys; polishing compound; pigment.
59	Praseodymium	Super-strong magnets; catalyst; lasers.
60	Neodymium	Auto catalyst; petroleum refining; hard drives; hybrid engines; permanent magnets.
61	Promethium	X-rays
62	Samarium	Cancer treatment; nuclear reactor control rods; Magnets.
63	Europium	Red color for television and computer screens.
64	Gadolinium	Magnets; shielding nuclear reactors; neutron radiography.
65	Terbium	Phosphors; permanent magnets; luminescent materials.
66	Dysprosium	Permanent magnets; hybrid engines; cooler of nuclear-reactor rods.
67	Holmium	Glass coloring; lasers.
68	Erbium	Phosphors; safety goggles.
69	Thulium	Medical x-way units; lasers.
70	Ytterbium	Lasers; steel alloys.
71	Lutetium	Catalysts in petroleum refining

The REE industry rose in the sixties, when scientists discovered that the element Eu could emit red luminescence, and was shortly applied in the development of color TV's (Gschneidner Jr, 2011). Before this, REE production was roughly 2 thousand tons per year, however, in 2010 the global demand for REE stood between 110,000 and 113,000 tons (Voncken, 2016) and by 2020 the global demand was estimated at around 170 thousand tons (Dushyantha et al., 2020). Due to the emerging "green technologies", the exponential usage of REE is expected to be upheld in the coming years, which may lead to a supply risk in the near future. Additionally, five countries hold almost 99% of the REE world reserve, which constitutes a major bottleneck for the world's economy. China is the country that grasps the largest REE resource and holds the monopoly of the REE supply chain (Figure 1.3).

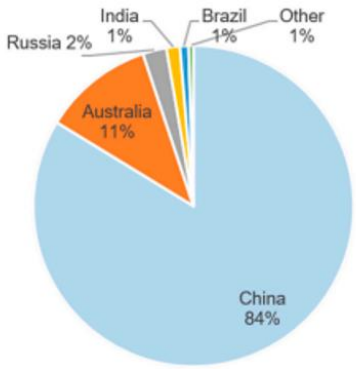

Figure 1.3 – Percentage distribution of world REE reserve by country. Adapted from U.S. Geological Survey Minerals Yearbook – Rare Earths.

This monopoly has already created an economic inequity, when China limited the export of REE in 2007, giving rise to their prices, in what was termed as the REE Crisis (Voncken, 2016). After the REE crisis, many countries understood the vital need to find other REE sources, weakening this dependency. Therefore, new REE mining sites have emerged in recent years, such as Mont Weld in Australia (Lynas Corporation Ltd, 2017), Kvanefjeld in Greenland (Greenland Minerals and Energy Ltd, 2017) and a promising reserve in the deep Pacific Ocean (Takaya et al., 2018).

Higher demand and shorter lifespans of many electronic products have led to alarming production of electronic waste (e-waste). Around 40 million metric tons of e-waste is generated globally, which encompass around 5% of the worldwide waste (Hazra et al., 2019). The recycling of REE is until recently almost never applied (Binnemans and Jones, 2014) and this process uses aggressive solvents and very high temperatures and pressures, which may well impose greater environmental harm than mining new REE. E-waste dismantling, open storage and burning can release its components into the environment (Uchida et al., 2018). Together with popularized utilization of REE in many other areas such as agriculture, forestry, animal husbandry and aquaculture, in which they are used as components of bactericides or fertilizers (Gwenzi et al., 2018), transfer to aquatic ecosystems is expected to continue to increase in coming years. This has led to REE being considered by the European Union as emergent Critical Metals and highlights the urgent need of a better understanding of their biogeochemical behavior and ecotoxicology.

1.1.1 Lanthanum

Lanthanum is the first element of the Ln series and is one of the most abundant REE in the environment (Herrmann et al., 2016). This element was discovered in 1839

by Carl Gustaf Mosander and named *lanthana*. This name is a variation of the Greek word *lanthanein*, which means "concealed", as it is a difficult element to isolate. Lanthanum is a malleable silvery metal, and at room temperature can be cut with a knife. This element is one of the most reactive within the REE (Emsley, 2011).

Previous studies have shown anthropogenic introduced La levels in the hydrosphere, by industrial emissions (Kulaksız and Bau, 2011b). Additionally, La mining and ore processing regularly discharge effluents that contain high concentrations of La. The appraisal of enhanced La levels imposing an environmental risk, is still yet to be entirely accomplished. Nevertheless, La has been described as carcinogenic to humans and genotoxic with particularly damaging consequences to human lymphocytes (Wang et al., 2016). As La strongly binds to carbonate and phosphate, La salts have been used in medicine to impound excess phosphate in the body (Schmidt et al., 2012). This feature has also been useful to remove excess phosphate from natural- and wastewaters (Li et al., 2019; Min et al., 2019). This method has been applied in hundreds of water bodies, in several parts of the world (Copetti et al., 2016) and yet studies on the potential impacts of this practice are still needed (Zhi et al., 2020).

The ability of fresh water and saltwater organisms to bioaccumulate La has been described: Hao et al. (1996) and Qiang et al. (1994) exposed juvenile fresh water carp (*Cyprinus carpio*) to La nitrate and demonstrated that the highest bioconcentration occurred in the internal organs, followed by gills, skeleton and ultimately the muscle. Hao et al. (1996) described that the La elimination of the muscles, gills, and skeleton differed from that of the internal organs. The first, rapidly lost La during the first days, and a slower elimination continued until equilibrium was reached. The internal organs accumulated greater in the first two days as La was distributed from other tissues and then La was detoxified and stored. Donald and Sardella (2010) stated that the La concentration in muscles of female freshwater fish goldeyes (*Hiodon alosoides*) were significantly higher than adult females. In adult specimens the ovaries contained greater amounts than the muscle, which indicates a loss of La via eggs during spawning and that La accumulation in this species is life stage dependent. Landman and Ling (2006) performed a three-year monitoring program of Lake Okareka (New Zealand), during a Phoslock® (La modified clay used for remediation in eutrophic water masses) treatment and quantified La in the freshwater rainbow trout (*Oncorhynchus mykiss*) and in the

freshwater crayfish (*Paranephrops planifrons*) and observed that the uptake in male trout livers was faster and greater than in female livers, indicating a sex-specific accumulation pattern. Additionally, minor La accumulation occurred in the crustacean crayfish, while significant accumulation into the hepatopancreas occurred. Lastly, Zhang et al. (2012) showed that La^{3+} and Yb^{3+} delayed the development of zebrafish embryos and larvae, reducing survival and hatchability rates and observed a concentration-dependent tail malformation. Hence, species-, sex-, and concentration-dependent responses highlight the intricacies of La toxic responses in vertebrates. Regarding invertebrates, Hou and Yan (1998) described a great La adsorption capacity of macroalgae, while studying the La concentration of 35 different algae species from the Chinese coast, highlighted by one of the highest bioaccumulation factor described for metals. This suggests that future studies should further investigate macroalgae REE remediation capabilities. Riget et al. (1996) studied the correlation between La concentration and blue mussel (*Mytilus edulis*) shell length in a Greenland fjord and found a significant positive correlation, which suggests that La is accumulated faster than blue mussels grow, which may impose toxic effects in this species. The scientific information on La toxicity is still very scarce, quite puzzling and showcasing conflicting results. To the best of my knowledge, only a few toxicity trials have been performed on fish species. Different sensitivities have been shown, and early life stages are the most sensitive (Herrmann et al., 2016). Few acute toxicity studies have been performed and the conflicting results of LC50 values, point to a species-specific sensitivity (e.g., Block and Pärt, 1992; Martin and Hickey, 2004). These showcases the important knowledge gap, on La bioaccumulation and possible toxic effects, that this thesis contributed to reduce.

1.1.2 Gadolinium

Gadolinium was discovered in 1880 and named as a tribute after Johan Gadolin, who discover the first REE, yttrium. As its neighboring REE, Gd is a malleable silvery white metal. This metal reacts with water and is soluble in dilute acid (Rogowska et al., 2018). Gadolinium is one of the most commercially exploited REE, has several industrial applications, and since the 1980's has been used as a contrasting agent in magnetic resonance imaging (MRI), due to its paramagnetic properties. After being injected into the blood stream for this medical exam, it is excreted through urine, reaching directly

the aquatic environment virtually unaffected by wastewater-treatment plants (Migaszewski and Gałuszka, 2016; Rogowska et al., 2018). Each MRI uses 1.2 g of Gd, which accounts for 5% of the total Gd production (Künnemeyer et al., 2009). This Gd-based contrast agents are chelates containing Gd^{3+}, as this free ion is highly toxic for inhibiting Ca^{2+}-regulated signaling in animal cells. A Gd anomaly in river water was firstly reported in 1996 (Bau and Dulski, 1996) and has already been described in seawater (e.g., Hatje et al., 2016; Pedreira et al., 2018), groundwater (Johannesson et al., 2017) and tap water (e.g., Kulaksız and Bau, 2011a), due to increased anthropogenic input. The Gd usage is continuingly growing, hence, large Gd quantities will continue to enter the hydrosphere in the recent future. Although Gd is not easily decoupled from their neighboring REE, positive Gd anomalies are now occurring in bivalve shells of densely populated areas, due to pollution (Akagi and Edanami, 2017; Ponnurangam et al., 2016). Gadolinium accumulation has also been detected in the digestive gland and gills of fresh water bivalves (Merschel and Bau, 2015). Perrat et al. (2017) studied the Gd bioaccumulation of two bivalve species (*Dreissena rostriformis bungensis* and *Corbicula fluminea*) close to a wastewater treatment plant output and described that Gd can be accumulated in bivalve tissues even if only present as the stable Gd-contrast agent and Le Goff et al. (2019) investigated the Gd concentration of scallop (*Pecten maximus*) shells from the Bay of Brest (France) and found that although the specifically tested Gd-based contrast agent usage has been reduced in Europe, Gd was still present in shells. These pattern of persistent accumulation may be accoupled with deleterious effects, as Henriques et al. (2019) exposed the Mediterranean mussel (*Mytilus galloprovincialis*) to different Gd concentrations, and found that the Gd exposure strongly affected the mussel biochemical performance, reducing its metabolism, provoking oxidative stress, and proved to be neurotoxic. Gadolinium toxic effect have also been described for other invertebrate species: four sea urchin species (*Paracentrotus lividus*, *Arbacia lixula*, *Heliocidaris tuberculate*, and *Centrostephanus rodgersii*) demonstrated different Gd sensitivities, nonetheless, development of exposed embryos and skeleton growth was impaired, showcasing the need to further study the toxicity of Gd (Martino et al., 2017).

Ferreira et al. (2020) investigated the Gd uptake from contaminated seawater of three macroalgae (*Ulva lactuca*, *Fucus spiralis,* and *Gracilaria* sp.). The three species were able to remove effetely Gd from the water along 72h. Up to 85% of Gd was

removed and the order of accumulation was green algae > red algae > brown algae. In regard to the Gd toxic effects to algae, Tai et al. (2010) investigated REE toxicity on a marine monocellular algae (*Skeletonema costatum*), and showed that all single Ln provoked similar toxic effects. High concentrations caused 50% reduction in this algae growth. A mixed solution with equivalent concentrations of singular Ln had the same inhibition effect as each individual Ln. This behavior is unmatched when compared to other groups of elements.

Concerning vertebrates, Qiang et al. (1994) exposed various tissues of carp (*Cyprinus carpio*) to La, Gd, and Y and found a low uptake ability for this species and the order of bioconcentration factor was internal organs > gills > skeleton > muscle. Nevertheless, Hanana et al. (2017) compared the toxic effects of $GdCl_3$ to Omniscan® (a Gd-based MRI contrast agent) on exposed zebra mussels (*Dresissena polymorpha*) and described the first as modulating mRNA level of metallothionein cytochrome c oxidase and superoxide dismutase (SOD) were increase, while catalase (CAT) and glutathione-S-transferase (GST) were downregulated. On the contrary, mussels exposed to Omniscan® exhibited downregulation of SOD, CAT, GST, and Lipid peroxidation (LPO), and an increase in GST activity, suggesting that the Gd chelated form did not promote reactive oxygen species (ROS) production.

Research data is limited on Gd bioaccumulation and ecotoxicological effects and although this may pose a threat to human and ecological health, they have been overlooked.

1.2 A CHANGING HIGH CO_2 WORLD

The Industrial Revolution constitutes the transitioning of an agrarian and handicraft economy to a machine manufacturing industry. This process began in Britain in the 18th century and soon spread to other areas of the world. Before, humans were fueled by the animals and plants they consumed, had chief aid from domesticated animals, and windmills and waterwheels captured extra energy, with little to no possibility of reserving it. This human labor agrarian times changed forever when people found a more powerful source of energy – coal, oil, and natural gas. By burning these fossil fuels, large quantities of energy, that had been stored for hundreds of millions of years, were released. Great progresses in several fields (e.g., technology, medicine,

education, culture, etc.) were then possible, nonetheless they came with a cost (Allen, 2009). Burning the newly found sources of energy let to increasing greenhouse gases (GHG) emissions, such as carbon dioxide (CO_2), methane (CH_4) and ozone (O_3), into the atmosphere. The GHG act as a layer, around the Earth's atmosphere, creating the known phenomenon "Greenhouse Effect". This layer absorbs and traps solar energy, in the form of heat, which in turn increases global average temperatures (Figure 1.4) (Black and Weisel, 2010).

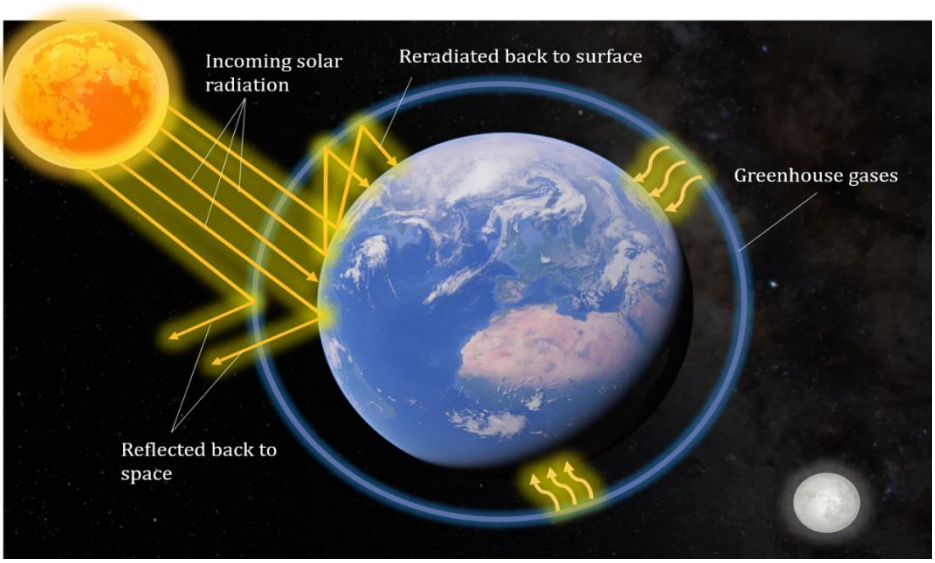

Figure 1.4 – Diagram of the greenhouse effect. Greenhouse gases capture solar radiation, increasing Earth's temperature.

The fifth report of the Intergovernmental Panel on Climate Change (IPCC, 2014), states that the unprecedented levels of GHG emission in the last 50 years, led to the trapped energy, in the form of heat, being stored in the ocean. In fact, the ocean can uptake over 90% of this excessive heat that is now accumulated in our Earth (Black and Weisel, 2010). Consequently, the average seawater surface temperature (SST) has increased around 0.1°C in each decade since the Industrial Revolution. Since the late 18th century, humans have exhaustively exploit natural resources, combusted fossil fuels, and release pollutants into the environment, at continuously faster rates. In fact, a special IPCC report on the Ocean and Cryosphere in a Changing Climate (IPCC, 2019) stated that by 2100 the ocean will warm by 5 to 7 times as much, compared with the observed changes since 1970. These changes are expected to occur with greater expression in the Northern Hemisphere (IPCC, 2014), reaching up to 4°C in temperate coastal areas of the Atlantic Ocean by 2100 (IPCC, 2021). Within the global warming setting, other stressors are arising as: seawater stratification and rising sea water levels

that in turn affect seawater salinity; increased dead oxygen zones; alterations of wind and precipitation; and extreme events, such as heat waves, droughts and floods (IPCC, 2019). The impacts of a changing ocean are experienced when the conditions are stretched outside the array of formerly experienced, at rates that the ecological systems can adapt (Pörtner et al., 2014) and the full consequences of these are, yet, largely unknown.

The continuing emission of GHG has led to increased CO_2 partial pressure (*p*CO2) oceanic uptake, which in turn leads to average seawater pH decrease at a global scale (IPCC, 2019). This CO_2 augmented levels alter profoundly the seawater chemistry. Dissolved CO_2 reacts with the water molecule (H_2O) and produces carbonic acid (H_2CO_3). Later, this acid is dissociated into bicarbonate (HCO_3^-) and hydrogen (H^+), which is the ultimate responsible for the pH decrease, in the known phenomenon named Ocean Acidification (Figure 1.5) (Zeebe and Ridgwell, 2011).

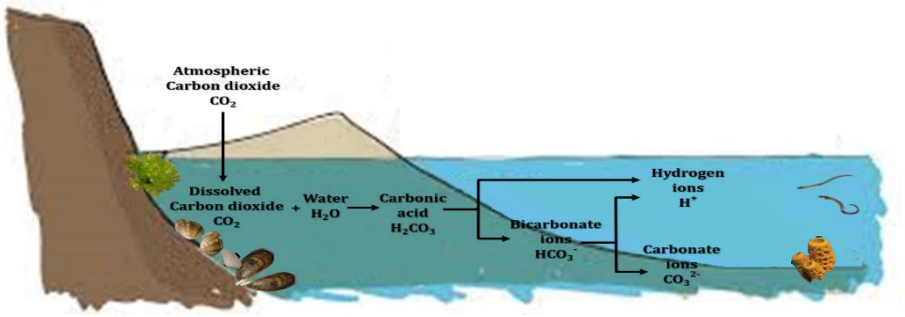

Figure 1.5 – Ocean acidification diagram: atmospheric CO_2 fate, as it dissolves in the water culminating in pH decrease.

After displaying stable values for more than 800 million years, the average seawater surface pH has effectively dropped 0.1 units, since the Industrial Revolution (IPCC, 2021). In fact, in pre-industrial times, CO_2 concentrations have been relatively stable for 10,000 years, displaying about 280 ppm, reaching in present day never registered levels above 400 ppm. In a worst-case scenario, with unreduced anthropogenic CO_2 emissions, at today's rate, by the end of the century, the predicted CO_2 levels will surpass 1000 ppm (Pörtner et al., 2014), which corresponds to a drop of up to 0.4 pH units in temperate coastal areas of the Atlantic Ocean (IPCC, 2021; McNeil and Sasse, 2016).

These two previously described climate change effects can occur isolated or combined with other stressors (e.g., contaminants), which is expected to further challenge marine organisms, in all levels of biological organization, in a cascade of

deleterious effects that can exacerbate their impacts. These impacts can affect their fitness, metabolism, reproduction, and recruitment, affecting populations and ecosystem dynamics, which can in the most extreme cases lead to worldwide decrease of biodiversity (FAO, 2018a).

1.2.1 The effects of warming and acidification in aquatic organisms

Most aquatic species are ectothermic hence temperature shifts may impact their physiological functioning. Although many species are able to thrive with daily and seasonal temperature variations, in the presence of multiple stressors their resilience may be surpassed (Madeira et al., 2012). Species fecundity success is expected to be strongly affected as spawning events are influenced by temperature (Przeslawski et al., 2008). Additionally, higher temperatures increase cell membrane fluidity and it is well known that thermal stress imposes metabolic changes in aquatic biota (e.g., Anacleto et al., 2018). Warming causes enhanced metabolism, attended with increased ventilation and higher feeding rates. These may result in higher bioaccumulation and elimination rates, as dissolved contaminants are incorporated via respiration and contaminants present in preys are also up taken in greater scale (Dijkstra et al., 2013). The warming induced metabolism change may in addition exacerbate contaminants toxicity by means of a lowered organism ability to cope with contaminants, detoxify them or even by means of biotransformation of contaminants to even more toxic compounds (Manciocco et al., 2014).

Calcifying organisms, such as corals, depend directly on the calcium carbonate cycle and therefore could have been expected that these organisms would be the most impacted by acidification. However, in recent years new insights on the impacts of acidification in a wide array of organism are surging. Fish can adjust their internal pH according to the environmental levels (Fabry et al., 2008) and are therefore relatively tolerant to pH discrepancies. Nevertheless, acidification can cause malformation, alterations in buoyancy and spatial orientation (Pimentel et al., 2014). Hypercapnia can also affect species behavior, by disrupting the ionic balance in proton-based neurotransmitter receptors, which renders into species audacity (Lai et al., 2017; Munday et al., 2014).

Aquatic organisms harbor antioxidant and protein repair and removal mechanisms, to offset reactive oxygen species (ROS) and thus avoid oxidative stress

(Lushchak, 2011). However, if exposed to environmental stressors, such as warming, acidification and pollutants, a ROS overrun can occur, which challenges their naturally occurring antioxidant and protective mechanisms. Superoxide dismutase (SOD), acts as the first enzymatic defense response against ROS buildup, converting O^{2-} in H_2O_2. Then, catalase (CAT) detoxifies the H_2O_2 produced, by separating it into two molecules: H_2O and O_2. At the end of this response glutathione-S-transferase (GST) enables the excretion of xenobiotics (Sies, 1997; Wang et al., 2000). These organisms also harbor a protein repair mechanism, which is known to be temperature-dependent as this can alter protein stability (Somero, 1995). When in stressful environments, aquatic organisms display a heat shock response, by synthesizing molecular chaperones – the heat shock protein (HSPs) (Sørensen et al., 2003). When these physiological response fails excess ROS buildup will originate oxidative damage, by means of lipid peroxidation (LPO), protein degradation and DNA damage. The usefulness of this indicators as biomarkers is well recognized and a substantial volume of studies have addressed this physiological defense mechanisms in aquatic organisms under climate change conditions. Nevertheless, it is now known that this response is species-specific and depends on the stressor (Kumar et al., 2017), which highlights the need to study the effects of emergent and not so well known pollutants, such as the REE.

Estuaries and shallow water coastal areas constitute valuable shelter ecosystems to many marine species, being key spawning and nursery areas and harbor early life stages, that are known to be the most vulnerable life stage, and climate change is expected to impact them greatly, which may regrettably result in biodiversity loss.

It can be hypothesized that interactions between climate change variables and REE may impose greater deleterious effects, and this is a hypothesis that deserves to be further investigated.

1.3 THE EFFECTS OF RARE EARTH ELEMENTS IN A CHANGING OCEAN: STATE OF THE ART

Climate change is forecasted to rise the occurrence and harshness of a wide array of pathogens, such as virus, parasites, toxins and to exacerbate the effects of pollutants. Additionally, Ln bioavailability is affected by temperature, pH, and other organic and

inorganic ligands (Byrne and Sholkovitz, 1996), which suggests that interactions with climate change variables are likely to occur.

A great deal of studies have focused on the effects of an acidic pH on REE behavior (e.g., Gammons et al., 2005; Wood et al., 2006) however, these studies do not deal with climate change nor with the possible toxic effects of these combination on aquatic organism and environments. The vast majority are industry oriented or deal with REE mining processes and optimization.

In regard to temperature, Morosetti et al. (2020) exposed the mussel, *Mytilus galloprovincialis,* to cerium oxide nanoparticles (NPs) and mercury (Hg) in a warming scenario and found that the CeO_2 NPs alone did not induce toxic effects. While the Hg accumulation was not impacted by the presence of CeO_2 NPs, the biochemical alterations induced by Hg alone were partially canceled upon co-exposure with CeO_2 NPs. In this study temperature alone caused the greatest impairments to metabolic and biochemical functioning. In another study on mussels (*Mytilus edulis*), Ponnurangam et al. (2016) investigated the possibility of their shells functioning as bioarchives of REE distribution in seawater and studied the impact of pH and temperature on their partitioning. A REE pattern model was hypothesized at pH 8.2 and 7.6 and at temperatures 25 and 5°C and at lower pH, REE concentration in shell increased, although did not affect the shape of the REE fractionation. On another hand, temperature affected the REE pattern, while minorly affecting the concentrations. The authors suggested that REE in mussel shells could be a proxy for paleo-pH and ocean acidification.

To the best of my knowledge, before this Ph.D. thesis no other studies on the bioaccumulation of emergent REE in conditions that are already also changing, such as water temperature and pH, and their possible toxic effects, were published.

The tremendous lack of data and studies highlights the very urgent need to further assess this challenging topic.

1.4 GENERAL AIMS

Humans' dependency on natural resources has by far surpassed their regenerative capacity, and this has led to climate change and outstanding levels of contamination. This new world imposes a great threat to marine and aquatic lifeforms,

as their resilience is pushed to unprecedented extremes. Furthermore, the consequences of these environmental stressors are expected to worsen, as they become more hostile in the future, menacing species' ecological success, in inland waters, estuaries, open ocean and the deep-sea. Nonetheless, before this thesis, the scientific knowhow on the possible interactions between climate change and REE contamination was lacking, as discussed before. Therefore, there is a significant gap of knowledge that research needs to fill with toxicological data on REE and the possible interactions with climate change and their consequences. Within this context, the general aim of this Ph.D. thesis was to deliver key contribution on these emergent yet poorly understood problematics, by addressing the REE bioaccumulation, the effects of the possible interaction of warming and/or acidification on them, and the induced ecotoxicological responses in significant aquatic species. To achieve this objective, this Ph.D. thesis formed the succeeding research questions:

1. Will depth, location and season affect REE bioaccumulation in good biomonitoring species?
2. Will warming and acidification affect REE availability in water?
3. Will warming and/or acidification interact with REE bioaccumulation and affect species' ecotoxicological responses?

To address the first research question, the REE concentrations on marine invertebrates along the Portuguese coast in different seasons and along different depths of the deep-sea of the North Atlantic were assessed.

To address the remaining research questions, two REE have been selected. Although REE are known to behave coherently, as discussed before, their grouping is yet not consistent among authors. Here, La and Gd were chosen as representatives of Light (LREE) and Heavy REE (HREE), respectively, accordingly to the 4f electron configuration (Aide and Aide, 2012; Anastopoulos et al., 2016). Thus, REE can be divided into the LREE group (which includes La, Ce, Pr, Nd, Pm, Sm, Eu), with no unpaired 4f electrons and the HREE (that comprises Y, Gd, Tb, Dy, Ho, Er, Tm, Yb and Lu; Kulaksız and Bau, 2007).

To maintain result consistency, the exposure pathway through water was prioritized in all exposure trials.

As for climate change-related stressors, the water abiotic conditions, such as warming and/or acidification were always replicated in accordance with the worst-case scenario projection (i.e., RCP8.5) of the most recent reports of the Intergovernmental Panel for Climate Change (IPCC, 2014; IPCC, 2019). These projections include a temperate increase of +4 to 5°C and an increase of more than 1000 ppm of pCO_2, which ultimately leads to a decrease of 0.4 pH units.

Independent trials were carried out for La and Gd. For the La exposure experiments, the biological models used were the European eel (*Anguilla anguilla*) and the manila clam (*Ruditapes phillipinarum*), the surf clam (*Spisula solida*) and the sea lettuce (*Ulva rigida*). For the experiments using Gd, the biological models used were the surf clam (*Spisula solida*) and the green macroalgae *Ulva rigida*.

The first experiment described in this Ph.D. thesis focused uniquely on the La and Gd species behavior in three different water types, fresh-, brackish- and saltwater, under warming and acidification, and constituted a pilot study, which permitted the optimization of the following experiments.

1.4.2 Selected biological models

The selection of the biological models (listed below) for this Ph.D. thesis was based on the following principles:

1) The bivalve, mussel (*Mytilus galloprovincialis*);
2) Marine sponges belonging to five porifera genera (*Jaspis, Geodia, Hamachantha, Leiodermatium, Poliopogon*);
3) The catadromous European eel (*Anguilla anguilla*);
4) The bivalve, manila clam (*Ruditapes philippinarum*);
5) The bivalve, surf clam (*Spisula solida*);
6) The green macroalgae (*Ulva rigida*).

Species that are likely to accumulate higher REE levels were selected. Bivalve species are sedentary, and sponges are sessile, while both are benthic filter-feeding organisms. This feeding strategy brands these species particularly vulnerable to element availability in the water. Also, they are more susceptible to present REE from contaminated sediments. Likewise, macroalgae have been appointed as a great

bioremediation tool, due to its aptitude to bioaccumulate a wide array of contaminants, including REE.

Early life stages, particularly of fish species, display greater vulnerability to both climate-change environmental stressors and pollutants, than adult life forms. Furthermore, juvenile ecotoxicological impairments may affect species' recruitment. Therefore, this life stage was prioritized in the two experiments with fish.

Finally, the fish and bivalve species used hold a considerable commercial value, as they are of great importance in human diet. This also allowed for the veil on the REE seafood safety concerns to start being unraveled.

1.5 THESIS OUTLINE

This thesis is divided in four parts:

(i) part one – The first part represents a detailed description of the topics that relate the coming chapters, and the state of the art regarding REE and climate change, possible interactions, and impacts on aquatic organisms (Chapter 1).

(ii) part two – The second part of this thesis is composed of two chapters (Chapter 2 and 3). This part describes baseline REE levels in biomonitoring marine invertebrates, along the coast of Portugal and in the deep-sea areas of the North Atlantic.

(iii) part three – This part is composed of 7 chapters (Chapters 4-10) that focus on the bioaccumulation, elimination, and effects of REE and climate change variables on a wide array of marine organisms. Both single-stressor studies and the interaction between stressors were performed.

(iv) part four – Here the scientific knowledge produced during this thesis is compiled, integrated and future research directions are proposed (Chapter 11).

The present thesis encompasses eleven chapters and the specific objective of each of the following chapters is presented underneath:

PART ONE: GENERAL INTRODUCTION

Chapter 1

This chapter presents an overview of the state of the art regarding REE, their sources and utilizations, and climate change as well as the potential interactive effects between these multiple stressors and their impacts.

PART TWO: BASELINE AND MONITORING REE LEVELS IN THE PORTUGUESE COAST AND NORTH ATLANTIC

Chapter 2

Rare earth elements have been intensively applied in modern technologies and in many other areas and their expanded usage culminates in increasing discharges into the environment. Mussels have been chosen as model species in biomonitoring studies and are known to accumulate REE. Hence, REE concentrations in *Mytilus galloprovincialis* from six locations along the Portuguese coast were accessed to determine environmental concentrations and investigate possible linkage to local ecosystem characteristics and temporal variations, by determining them in two distinct seasons (autumn and spring).

Chapter 3

The available data of REE of deep-sea organisms was nonexistent. Therefore, to seal this gap of knowledge, the aim of this chapter was to characterize REE in five porifere genera (*Jaspis, Geodia, Hamachantha, Leiodermatium, Poliopogon*) collected in deep-sea areas (between 481 and 2656 m) of the North Atlantic. Hence, a baseline for future comparisons was established and the first characterization of REE in a sessile deep-sea marine invertebrate group was assessed.

PART THREE: MULTIPLE STRESSORS IN A NEAR-FUTURE ENVIRONMENT

Chapter 4

In this chapter, La and Gd levels in spiked (1.5 and 1 µg L^{-1}, respectively) fresh-, brackish- and salt-water were quantified, 8 times over 24 hours in present-day and near-future conditions (T°=+4°C, pH=△0.4), with the chief objective of setting the baseline knowledge by which upcoming research towards understanding REE patterns and toxicity in the near-future will build upon.

Chapter 5

With the aim of providing an holistic perspective about physiological processes occurring in European glass eels (*Anguilla anguilla*) under La exposure, and considering the endangered conservation status (International Union for Conservation of Nature Red List) of this species and the vulnerability of early fish life stages to a wide range of contaminants, the accumulation and elimination potential of La (120 ng L^{-1}) and subsequent quantification of acetylcholinesterase, lipid peroxidation and antioxidant enzymatic machinery, in the edible European glass eel was assessed.

Chapter 6

As fish early life stages are more susceptible to both climate change and pollutants, the bioaccumulation and elimination of lanthanum-exposed (1.5 µg L^{-1}) glass eels' (*Anguilla anguilla*) tissues (viscera, head and body) under present-day temperatures and in a warming scenario were evaluated. Additionally, specific biomarkers, indicative of cellular damage, namely acetylcholinesterase, DNA damage, lipid peroxidation, and heat shock protein 70, were estimated with the objective of refining the knowledge on the physiological responses derived from La accumulation in a near-future scenario.

Chapter 7

Due to their known feature as bioindicators of aquatic pollution, the aim of this chapter was to assess the La bioaccumulation ability of the manila clam (*Ruditapes philippinarum*). Differential tissue accumulation was assessed by quantifying La concentrations in gills, digestive gland, and remaining body of *R. philippinarum* exposed to two environmentally relevant concentrations of La (0.3 µg L^{-1} and 0.9 µg L^{-1}) through water. The La bioaccumulation was measured after one, two, and six days of exposure.

Chapter 8

A study dealing with the effects of ocean warming, acidification, and their impacts on La accumulation and elimination had never been conducted. Hence, the surf clam (*Spisula solida*) was exposed to 15 µg L^{-1} of La and climate change for 7 days, plus a 7-day elimination period, with the objective of exploring the effects, combined and as single stressors, of ocean warming, acidification, and La accumulation and elimination. Furthermore, a robust set of membrane-associated, protein, and antioxidant enzymes and non-enzymatic molecules were quantified.

Chapter 9

The objective of this chapter was to assess, for the first time, the combined effects of rising temperature (Δ = +4 °C) and decreasing pH (Δ = − 0.4 pH units) on the bioaccumulation and elimination of Gd in the bioindicator bivalve species, *Spisula solida.* The surf clams were exposed to 10 µg L^{-1} of $GdCl_3$ for seven days, followed by an elimination phase that lasted another seven days and the oxidative stress-related responses were investigated.

Chapter 10

Studies on REE bioaccumulation, elimination, and toxicity in a multi-stressor environment (e.g., warming and acidification) with macroalgae were virtually non-existing. Therefore, the ecotoxicological responses and total chlorophyll and carotenoid content of the green tide forming macroalgae *Ulva rigida* were assessed after 7 days of co-exposure to La or Gd (15 µg L^{-1} or 10 µg L^{-1}, respectively), and ocean warming (+4°C) and acidification (-0.4 pH units) with the objective of diminishing this knowledge gap. Additionally, the La and Gd elimination, after a 7-day phase, was assessed.

PART FOUR: GENERAL CONSIDERATIONS AND FUTURE RESEARCH PERSPECTIVES

Chapter 11

This chapter has the ultimate objective of compiling the results presented in the previous chapters in an integrated method, while being critically analyzed. To conclude, the research topics that rose during this thesis are addressed, in the hopes that near future research can overcome them and contribute to our understanding of the effects of these multiple stressors in a timely manner.

REFERENCES

Aide, M.T., Aide, C., 2012. Rare earth elements: their importance in understanding soil genesis. International Scholarly Research Notices 2012, 783876.

Akagi, T., Edanami, K., 2017. Sources of rare earth elements in shells and soft-tissues of bivalves from Tokyo Bay. Marine Chemistry 194, 55-62.

Allen, R.C., 2009. The British industrial revolution in global perspective. Cambridge University Press.

Anacleto, P., Figueiredo, C., Baptista, M., Maulvault, A.L., Camacho, C., Pousão-Ferreira, P., Valente, L.M., Marques, A., Rosa, R., 2018. Fish energy budget under ocean warming and flame retardant exposure. Environmental research 164, 186-196.

Anastopoulos, I., Bhatnagar, A., Lima, E.C., 2016. Adsorption of rare earth metals: A review of recent literature. Journal of Molecular Liquids 221, 954-962.

Atwood, D.A., 2013. The rare earth elements: fundamentals and applications. John Wiley & Sons.

Balaram, V., 2019. Rare earth elements: A review of applications, occurrence, exploration, analysis, recycling, and environmental impact. Geoscience Frontiers 10, 1285-1303.

Bau, M., Dulski, P., 1996. Distribution of yttrium and rare-earth elements in the Penge and Kuruman iron-formations, Transvaal Supergroup, South Africa. Precambrian Research 79, 37-55.

Binnemans, K., Jones, P.T., 2014. Perspectives for the recovery of rare earths from end-of-life fluorescent lamps. Journal of Rare Earths 32, 195-200.

Black, B.C., Weisel, G.J., 2010. Global Warming. Santa Barbara. CA: Greenwood.

Block, M., Pärt, P., 1992. Uptake of ^{109}Cd by cultured gill epithelial cells from rainbow trout (*Oncorhynchus mykiss*). Aquatic toxicology 23, 137-151.

Burch, K.R., Comer, J.B., Wolf, S.F., Brake, S.S., 2011. REE geochemistry of an acid mine drainage system in western Indiana, Abstr. with Programs—Geological Society of America 43, 5.

Byrne, R., Sholkovitz, E., 1996. Marine chemistry and geochemistry of the lanthanides. Handbook on the physics and chemistry of rare earths 23, 497-593.

Carpenter, D., Boutin, C., Allison, J.E., Parsons, J.L., Ellis, D.M., 2015. Uptake and effects of six rare earth elements (REEs) on selected native and crop species growing in contaminated soils. PLoS One 10, e0129936.

Copetti, D., Finsterle, K., Marziali, L., Stefani, F., Tartari, G., Douglas, G., Reitzel, K., Spears, B.M., Winfield, I.J., Crosa, G., 2016. Eutrophication management in surface waters using lanthanum modified bentonite: a review. Water research 97, 162-174.

Cotton, S., 2013. Lanthanide and actinide chemistry. John Wiley & Sons.

Dijkstra, J.A., Buckman, K.L., Ward, D., Evans, D.W., Dionne, M., Chen, C.Y., 2013. Experimental and natural warming elevates mercury concentrations in estuarine fish. PloS one 8, e58401.

Donald, D.B., Sardella, G.D., 2010. Mercury and other metals in muscle and ovaries of goldeye (*Hiodon alosoides*). Environmental toxicology and chemistry 29, 373-379.

Dushyantha, N., Batapola, N., Ilankoon, I., Rohitha, S., Premasiri, R., Abeysinghe, B., Ratnayake, N., Dissanayake, K., 2020. The story of rare earth elements (REEs): Occurrences, global distribution, genesis, geology, mineralogy and global production. Ore Geology Reviews 122, 103521.

Emsley, J., 2011. Nature's building blocks: an AZ guide to the elements. Oxford University Press.

Fabry, V.J., Seibel, B.A., Feely, R.A., Orr, J.C., 2008. Impacts of ocean acidification on marine fauna and ecosystem processes. ICES Journal of Marine Science 65, 414-432.

FAO, 2018a. Impacts of climate change on fisheries and aquaculture. Synthesis of current knowledge, adaptation and mitigation options. Food and Agriculture Organization of the United Nations. Rome, Italy. 628pp.

Ferreira, N., Ferreira, A., Viana, T., Lopes, C.B., Costa, M., Pinto, J., Soares, J., Pinheiro-Torres, J., Henriques, B., Pereira, E., 2020. Assessment of marine macroalgae potential for gadolinium removal from contaminated aquatic systems. Science of The Total Environment 749, 141488.

Gammons, C.H., Wood, S.A., Pedrozo, F., Varekamp, J.C., Nelson, B.J., Shope, C.L., Baffico, G., 2005. Hydrogeochemistry and rare earth element behavior in a volcanically acidified watershed in Patagonia, Argentina. Chemical Geology 222, 249-267.

Gschneidner Jr, K.A., 2011. The rare earth crisis–the supply/demand situation for 2010–2015. Material Matters 6, 32-37.

Gwenzi, W., Mangori, L., Danha, C., Chaukura, N., Dunjana, N., Sanganyado, E., 2018. Sources, behaviour, and environmental and human health risks of high-technology rare earth elements as emerging contaminants. Science of the Total Environment 636, 299-313.

Hanana, H., Turcotte, P., André, C., Gagnon, C., Gagné, F., 2017. Comparative study of the effects of gadolinium chloride and gadolinium–based magnetic resonance imaging contrast agent on freshwater mussel, *Dreissena polymorpha*. Chemosphere 181, 197-207.

Hao, S., Xiaorong, W., Zhaozhe, H., Chonghua, W., Liansheng, W., Lemei, D., Zhong, L., Yijun, C., 1996. Bioconcentration and elimination of five light rare earth elements in carp (*Cyprinus carpio* L.). Chemosphere 33, 1475-1483.

Haskin, M.A., Haskin, L.A., 1966. Rare earths in European shales: a redetermination. Science 154, 507-509.

Hatje, V., Bruland, K.W., Flegal, A.R., 2016. Increases in anthropogenic gadolinium anomalies and rare earth element concentrations in San Francisco Bay over a 20 year record. Environmental science & technology 50, 4159-4168.

Haxel, G., 2002. Rare earth elements: critical resources for high technology. US Department of the Interior, US Geological Survey.

Hazra, A., Das, S., Ganguly, A., Das, P., Chatterjee, P.K., Murmu, N.C., Banerjee, P., 2019. Plasma Arc Technology: A Potential Solution Toward Waste to Energy Conversion and of GHGs Mitigation. Springer Singapore, Singapore, pp. 203-217.

Henriques, B., Coppola, F., Monteiro, R., Pinto, J., Viana, T., Pretti, C., Soares, A., Freitas, R., Pereira, E., 2019. Toxicological assessment of anthropogenic Gadolinium in seawater: Biochemical effects in mussels *Mytilus galloprovincialis*. Science of The Total Environment 664, 626-634.

Herrmann, H., Nolde, J., Berger, S., Heise, S., 2016. Aquatic ecotoxicity of lanthanum–a review and an attempt to derive water and sediment quality criteria. Ecotoxicology and Environmental Safety 124, 213-238.

Holser, W.T., 1997. Evaluation of the application of rare-earth elements to paleoceanography. Palaeogeography, Palaeoclimatology, Palaeoecology 132, 309-323.

Hou, X., Yan, X., 1998. Study on the concentration and seasonal variation of inorganic elements in 35 species of marine algae. Science of the Total Environment 222, 141-156.

Hu, B., He, M., Jakubowski, N., Meinhardt, J., Meyer, F.M., Niederstraßer, J., Schramm, R., Sindern, S., Stosch, H.-G., Bertau, M., 2017. Handbook of Rare Earth Elements: Analytics. Walter de Gruyter GmbH & Co KG.

Humphries, M., 2010. Rare earth elements: the global supply chain. Diane Publishing.

IPCC, 2014: Impacts, Adaptation, and Vulnerability. Summaries, Frequently Asked Questions, and Cross-Chapter Boxes. A Contribution of Working Group II to the Fifth Assessment Report of the Intergovernmental Panel on Climate Change. World Meteorological Organization, Geneva, Switzerland

IPCC, 2019: IPCC Special Report on the Ocean and Cryosphere in a Changing Climate [H.-O. Pörtner, D.C. Roberts, V. Masson-Delmotte, P. Zhai, M. Tignor, E. Poloczanska, K. Mintenbeck, A. Alegría, M. Nicolai, A. Okem, J. Petzold, B. Rama, N.M. Weyer (eds.)]. In press.

IPCC, 2021: Summary for Policymakers. In: Climate Change 2021: The Physical Science Basis. Contribution of Working Group I to the Sixth Assessment Report of the Intergovernmental Panel on Climate Change [Masson-Delmotte, V., P. Zhai, A. Pirani, S.L. Connors, C. Péan, S. Berger, N. Caud, Y. Chen, L. Goldfarb, M.I. Gomis, M. Huang, K. Leitzell, E. Lonnoy, J.B.R. Matthews, T.K. Maycock, T. Waterfield, O. Yelekçi, R. Yu, and B. Zhou (eds.)]. In Press.

Johannesson, K.H., Palmore, C.D., Fackrell, J., Prouty, N.G., Swarzenski, P.W., Chevis, D.A., Telfeyan, K., White, C.D., Burdige, D.J., 2017. Rare earth element behavior during groundwater–seawater mixing along the Kona Coast of Hawaii. Geochimica et cosmochimica acta 198, 229-258.

Kulaksız, S., Bau, M., 2007. Contrasting behaviour of anthropogenic gadolinium and natural rare earth elements in estuaries and the gadolinium input into the North Sea. Earth and Planetary Science Letters 260, 361-371.

Kulaksız, S., Bau, M., 2011a. Anthropogenic gadolinium as a microcontaminant in tap water used as drinking water in urban areas and megacities. Applied Geochemistry 26, 1877-1885.

Kulaksız, S., Bau, M., 2011b. Rare earth elements in the Rhine River, Germany: first case of anthropogenic lanthanum as a dissolved microcontaminant in the hydrosphere. Environment International 37, 973-979.

Kumar, A., AbdElgawad, H., Castellano, I., Lorenti, M., Delledonne, M., Beemster, G.T., Asard, H., Buia, M.C., Palumbo, A., 2017. Physiological and biochemical analyses shed light on the response of Sargassum vulgare to ocean acidification at different time scales. Frontiers in plant science 8, 570.

Künnemeyer, J., Terborg, L., Meermann, B.r., Brauckmann, C., Möller, I., Scheffer, A., Karst, U., 2009. Speciation analysis of gadolinium chelates in hospital effluents and wastewater treatment plant sewage by a novel HILIC/ICP-MS method. Environmental science & technology 43, 2884-2890.

Lai, F., Fagernes, C.E., Jutfelt, F., Nilsson, G.E., 2017. Expression of genes involved in brain GABAergic neurotransmission in three-spined stickleback exposed to near-future CO_2. Conservation physiology 5.

Landman, M., Ling, N., 2006. Lake Okareka and Tikitapu Fish Health Monitoring. Environment Bay of Plenty.

Le Goff, S., Barrat, J.-A., Chauvaud, L., Paulet, Y.-M., Gueguen, B., Salem, D.B., 2019. Compound-specific recording of gadolinium pollution in coastal waters by great scallops. Scientific reports 9, 1-5.

Lecomte, K.L., Sarmiento, A., Borrego, J., Nieto, J., 2017. Rare earth elements mobility processes in an AMD-affected estuary: Huelva Estuary (SW Spain). Marine pollution bulletin 121, 282-291.

Li, J.-R., Wang, F.-K., Xiao, H., Xu, L., Fu, M.-L., 2019. Layered chalcogenide modified by Lanthanum, calcium and magnesium for the removal of phosphate from water. Colloids and Surfaces A: Physicochemical and Engineering Aspects 560, 306-314.

Liang, T., Zhang, S., Wang, L., Kung, H.-T., Wang, Y., Hu, A., Ding, S., 2005. Environmental biogeochemical behaviors of rare earth elements in soil–plant systems. Environmental Geochemistry and Health 27, 301-311.

Luoma, S.N., Rainbow, P.S., 2005. Why is metal bioaccumulation so variable? Biodynamics as a unifying concept. Environmental Science & Technology 39, 1921-1931.

Lushchak, V.I., 2011. Environmentally induced oxidative stress in aquatic animals. Aquatic toxicology 101, 13-30.

Madeira, D., Narciso, L., Cabral, H.N., Vinagre, C., 2012. Thermal tolerance and potential impacts of climate change on coastal and estuarine organisms. Journal of Sea Research 70, 32-41.

Manciocco, A., Calamandrei, G., Alleva, E., 2014. Global warming and environmental contaminants in aquatic organisms: the need of the etho-toxicology approach. Chemosphere 100, 1-7.

Martin, M., Hickey, C., 2004. Determination of HSNO ecotoxic thresholds for granular Phoslock™(Eureka 1 formulation) phase 1: acute toxicity. Report prepared for Primaxa Ltd, 2004-2137.

Martino, C., Bonaventura, R., Byrne, M., Roccheri, M., Matranga, V., 2017. Effects of exposure to gadolinium on the development of geographically and phylogenetically distant sea urchins species. Marine environmental research 128, 98-106.

McNeil, B.I., Sasse, T.P., 2016. Future ocean hypercapnia driven by anthropogenic amplification of the natural CO_2 cycle. Nature 529, 383-386.

Merschel, G., Bau, M., 2015. Rare earth elements in the aragonitic shell of freshwater mussel *Corbicula fluminea* and the bioavailability of anthropogenic lanthanum, samarium and gadolinium in river water. Science of the Total Environment 533, 91-101.

Migaszewski, Z.M., Gałuszka, A., 2016. The use of gadolinium and europium concentrations as contaminant tracers in the Nida River watershed in south-central Poland. Geological Quarterly 60, 67-76.

Min, X., Wu, X., Shao, P., Ren, Z., Ding, L., Luo, X., 2019. Ultra-high capacity of lanthanum-doped UiO-66 for phosphate capture: Unusual doping of lanthanum by the reduction of coordination number. Chemical Engineering Journal 358, 321-330.

Minami, E., 1935. Gehalte an seltenen Erden in europäischen und japanischen Tonschiefern, von E. Minami. Weidmann.

Morosetti, B., Freitas, R., Pereira, E., Hamza, H., Andrade, M., Coppola, F., Maggioni, D., Della Torre, C., 2020. Will temperature rise change the biochemical alterations induced in *Mytilus galloprovincialis* by cerium oxide nanoparticles and mercury?. Environmental research 188, 109778.

Munday, P.L., Cheal, A.J., Dixson, D.L., Rummer, J.L., Fabricius, K.E., 2014. Behavioural impairment in reef fishes caused by ocean acidification at CO_2 seeps. Nature Climate Change 4, 487-492.

Oral, R., Bustamante, P., Warnau, M., d'Ambra, A., Guida, M., Pagano, G., 2010. Cytogenetic and developmental toxicity of cerium and lanthanum to sea urchin embryos. Chemosphere 81, 194-198.

Pedreira, R.M., Pahnke, K., Böning, P., Hatje, V., 2018. Tracking hospital effluent-derived gadolinium in Atlantic coastal waters off Brazil. Water research 145, 62-72.

Perrat, E., Parant, M., Py, J.-S., Rosin, C., Cossu-Leguille, C., 2017. Bioaccumulation of gadolinium in freshwater bivalves. Environmental Science and Pollution Research 24, 12405-12415.

Pimentel, M.S., Faleiro, F., Dionísio, G., Repolho, T., Pousão-Ferreira, P., Machado, J., Rosa, R., 2014. Defective skeletogenesis and oversized otoliths in fish early stages in a changing ocean. Journal of Experimental Biology 217, 2062-2070.

Ponnurangam, A., Bau, M., Brenner, M., Koschinsky, A., 2016. Mussel shells of *Mytilus edulis* as bioarchives of the distribution of rare earth elements and yttrium in seawater and the potential impact of pH and temperature on their partitioning behavior. Biogeosciences 13, 751-760.

Pörtner, H.-O., Karl, D.M., Boyd, P.W., Cheung, W., Lluch-Cota, S.E., Nojiri, Y., Schmidt, D.N., Zavialov, P.O., Alheit, J., Aristegui, J., 2014. Ocean systems, Climate change 2014: impacts, adaptation, and vulnerability. Part A: global and sectoral aspects. contribution of working group II to the fifth assessment report of the intergovernmental panel on climate change. Cambridge University Press, pp. 411-484.

Przeslawski, R., Ahyong, S., Byrne, M., Woerheide, G., Hutchings, P., 2008. Beyond corals and fish: the effects of climate change on noncoral benthic invertebrates of tropical reefs. Global Change Biology 14, 2773-2795.

Qiang, T., Xiao-Rong, W., Li-Qing, T., Le-Mei, D., 1994. Bioaccumulation of the rare earth elements lanthanum, gadolinium and yttrium in carp (*Cyprinus carpio*). Environmental pollution 85, 345-350.

Riget, F., Johansen, P., Asmund, G., 1996. Influence of length on element concentrations in blue mussels (*Mytilus edulis*). Marine Pollution Bulletin 32, 745-751.

Rogowska, J., Olkowska, E., Ratajczyk, W., Wolska, L., 2018. Gadolinium as a new emerging contaminant of aquatic environments. Environmental toxicology and chemistry 37, 1523-1534.

Schmidt, B.H., Dribusch, U., Delport, P.C., Gropp, J.M., van der Staay, F.J., 2012. Tolerability and efficacy of the intestinal phosphate binder Lantharenol® in cats. BMC veterinary research 8, 1-8.

Schmitt, R., Smith, R., Lasch, J., Mosen, A., Olehy, D., Vasilevskis, J., 1963. Abundances of the fourteen rare-earth elements, scandium, and yttrium in meteoritic and terrestrial matter. Geochimica et Cosmochimica Acta 27, 577-622.

Semple, K.T., Doick, K.J., Jones, K.C., Burauel, P., Craven, A., Harms, H., 2004. Peer reviewed: defining bioavailability and bioaccessibility of contaminated soil and sediment is complicated. ACS Publications.

Sies, H., 1997. Oxidative stress: oxidants and antioxidants. Experimental Physiology: Translation and Integration 82, 291-295.

Somero, G.N., 1995. Proteins and temperature. Annual review of physiology 57, 43-68.

Sørensen, J.G., Kristensen, T.N., Loeschcke, V., 2003. The evolutionary and ecological role of heat shock proteins. Ecology letters 6, 1025-1037.

Tai, P., Zhao, Q., Su, D., Li, P., Stagnitti, F., 2010. Biological toxicity of lanthanide elements on algae. Chemosphere 80, 1031-1035.

Takaya, Y., Yasukawa, K., Kawasaki, T., Fujinaga, K., Ohta, J., Usui, Y., Nakamura, K., Kimura, J.-I., Chang, Q., Hamada, M., 2018. The tremendous potential of deep-sea mud as a source of rare-earth elements. Scientific reports 8, 1-8.

Uchida, N., Matsukami, H., Someya, M., Tue, N.M., Viet, P.H., Takahashi, S., Tanabe, S., Suzuki, G., 2018. Hazardous metals emissions from e-waste-processing sites in a village in northern Vietnam. Emerging Contaminants 4, 11-21.

Voncken, J.H.L., 2016. The rare earth elements: an introduction. Springer.

Wang, L., Groves, M.J., Hepburn, M.D., Bowen, D.T., 2000. Glutathione S-transferase enzyme expression in hematopoietic cell lines implies a differential protective role for T1 and A1 isoenzymes in erythroid and for M1 in lymphoid lineages. Haematologica 85, 573-579.

Wang, Y.-Y., Lu, H.-H., Liu, Y.-X., Yang, S.-M., 2016. Ammonium citrate-modified biochar: An adsorbent for La (III) ions from aqueous solution. Colloids and Surfaces A: Physicochemical and Engineering Aspects 509, 550-563.

Weltje, L., Heidenreich, H., Zhu, W., Wolterbeek, H.T., Korhammer, S., de Goeij, J.J., Markert, B., 2002. Lanthanide concentrations in freshwater plants and molluscs, related to those in surface water, pore water and sediment. A case study in The Netherlands. Science of the total environment 286, 191-214.

Wood, S.A., Gammons, C.H., Parker, S.R., 2006. The behavior of rare earth elements in naturally and anthropogenically acidified waters. Journal of alloys and compounds 418, 161-165.

Zeebe, R.E., Ridgwell, A., 2011. Past changes of ocean carbonate chemistry. Ocean acidification, 1-28.

Zhang, Z., Bai, W., Zhang, L., He, X., Ma, Y., Liu, Y., Chai, Z., 2012. Effects of rare earth elements La and Yb on the morphological and functional development of zebrafish embryos. Journal of Environmental Sciences 24, 209-213.

Zhi, Y., Zhang, C., Hjorth, R., Baun, A., Duckworth, O.W., Call, D.F., Knappe, D.R., Jones, J.L., Grieger, K., 2020. Emerging lanthanum (III)-containing materials for phosphate removal from water: A review towards future developments. Environment International 145, 106115.

PART TWO

BASELINE AND MONITORING REE LEVELS IN THE PORTUGUESE COAST AND NORTH ATLANTIC

Chapter 2

Rare earth elements biomonitoring using the mussel *Mytilus galloprovincialis* in the Portuguese coast: seasonal variations

Cátia Figueiredo [a,b,c,*] , Rui Oliveira [b] , Clara Lopes [b,d], Pedro Brito [b,d] , Miguel Caetano [b,d], Joana Raimundo [b,d]

[a] MARE, Marine and Environmental Sciences Centre, Laboratório Marítimo da Guia, Faculdade de Ciências da Universidade de Lisboa, Av. Nossa Senhora do Cabo 939, 2750-374, Cascais, Portugal

[b] IPMA, Portuguese Institute of Sea and Atmosphere, Rua Alfredo Magalhães Ramalho, 6, 1495-006 Lisbon, Portugal

[c] UCIBIO, REQUIMTE, Departamento de Química, Faculdade de Ciências e Tecnologia, Universidade NOVA de Lisboa, 2829-516 Caparica, Portugal

[d] CIIMAR, Marine and Environmental Research Center, Rua dos Bragas, 289, 4050-123 Porto, Portugal

* Corresponding author

Figueiredo, C., Oliveira, R., Lopes, C., Brito, P., Caetano, M., Raimundo, J. 2022. Rare earth elements biomonitoring using the mussel *Mytilus galloprovincialis* in the Portuguese coast: seasonal variations. Marine Pollution Bulletin 175, 113335. (DOI 10.1016/j.marpolbul.2022.113335)

ABSTRACT

Increased Rare earth elements (REE) usage culminates in discharges into the environment. Mussels have been chosen as models in biomonitoring, hence, REE concentrations in *Mytilus galloprovincialis* from six locations on the Portuguese coast were accessed to determine natural concentrations and possible linkage to local ecosystem characteristics and temporal variations, by determining them in distinct seasons (autumn and spring). Samples from Porto Brandão (located on the south bank of the Tagus estuary) exhibited the highest REE concentrations, while mussels from Aljezur (the southernmost point on the Portuguese coast) exhibited the lowest, in both seasons. Overall, ∑REE concentration was greater in the spring. LREE enrichment relative to HREE occurs and a negative Ce and Eu anomaly was observed. This study constitutes the first assessment of REE composition on this model species in the Portuguese coast, in two distinct seasons and contributes to a better understanding of REE uptake for future biomonitoring studies.

Keywords: European shale normalized REE; Ce and Eu anomaly; Northeast Atlantic; Bioindicator; *Mytilus galloprovincialis*.

2.1 INTRODUCTION

The lanthanides, from lanthanum (La) to lutetium (Lu), together with scandium (Sc) and yttrium (Y), constitute the group of rare earth elements (REE). These seventeen chemical elements present physicochemical properties alike, due to the lanthanide contraction, as the REE radii decrease uninterruptedly, with increasing atomic number (Hu et al., 2017). Their characteristics branded them of key importance in modern life and technologies. Nowadays, REE are widely applicated in, for example, the making of computer memories, batteries, mobile phones, wind turbine generators, solar panels, and as magnetic resonance imaging contrast-agents in complementary medicine diagnosis (Balaram, 2019). Furthermore, promoted use of REE occurs in many other areas such as agriculture, forestry, animal husbandry and aquaculture, in which they are used as components of bactericides or fertilizers (Gwenzi et al., 2018). Therefore, handover to aquatic systems is bound to continue and to increase in coming years. Industrial, agricultural, and domestic increased usage of REE culminates in great quantities of contaminated wastewater discharges into the environment by urban treatment systems and domestic and industrial effluents. The different anthropogenic sources of REE can alter their fractionation patterns in the aquatic environment. With increasing REE discharges, coastal and estuarine environments are subject to additional pressure. Such risks include the emergence of new contaminants, as REE (Lerat-Hardy et al., 2019), which are known to impose toxic responses in aquatic organisms (e.g., Bergsten-Torralba et al., 2020; Figueiredo et al., 2018; Figueiredo et al., 2020; Pinto et al., 2019).

Several intertidal and epibenthic species have been chosen as model species in biomonitoring studies (Phillips and Rainbow, 2013), including saltwater and freshwater mussels (e.g., Cai and Wang, 2019; Capolupo et al., 2017; Liu and Kueh, 2005). These filter-feeding species are known to accumulate REE (Akagi and Edanami, 2017; Freitas et al., 2020; Mestre et al., 2019). Mussels filter large quantities of water and are thus able to accumulate pollutants from water or particulate matter at elevated levels. Therefore, mussels are subject to this anthropogenic pressure and can be impacted by the increasing levels of REE in coastal and estuarine areas (e.g., Squadrone et al., 2016; Squadrone et al., 2019; Benaltabet et al., 2021). Additionally, mussels are widely distributed, sessile by nature, are easily sampled and thrive even in highly polluted areas

(Beyer et al., 2017). Accordingly, here we assessed REE concentrations in *Mytilus galloprovincialis* from six locations in the Portuguese coast with three main objectives: i) to determine the natural REE concentrations in feral organisms; ii) to investigate possible geographic differences, with linkage to local ecosystem characteristics, and iii) temporal variations by determining REE concentrations in two distinct seasons (Autumn and Spring).

2.2 MATERIAL AND METHODS

2.2.1 Sampling

Six points along the Portuguese coast covering areas with different anthropogenic inputs were surveyed in a single week in autumn (October 2020) and spring (April 2021) (Figure 2.1).

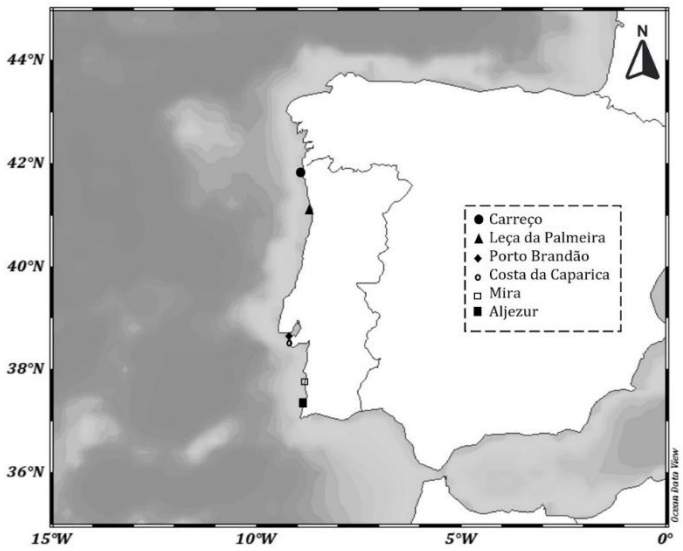

Figure 2.1 - Sample locations along the Portuguese (NE Atlantic Ocean) coastline

A total of six hundred and forty-nine *Mytilus galloprovincialis* specimens were handpicked during the low tide and kept cool in an icebox. Upon arrival at the laboratory and frozen at -20°C prior to further analyses.

2.2.2 Tissue sample preparation

After being thawed at room temperature, the shells were cleaned to remove limestone and debris. Specimens were measured for shell length and width, at the largest point, using a digital pachymeter and weighted. Mussels were then dissected, and their wet weight was determined. The whole soft body was used for sample preparation.

2.2.3 Rare earth elements analyses

Before the start of the analyses, all labware had been decontaminated with HNO_3 (20%) for 48h and rinsed with ultra-pure water (18.2 MΩ, Sartorius).

Each mussel was freeze-dried, grounded, and homogenized. After this, samples were digested with nitric acid (HNO_3, distilled, 65% v/v) and hydrogen peroxide (H_2O_2, Suprapur®, 30% v/v) in accordance with Raimundo et al. (2013). The concentrations of REE were determined in a Perkin-Elmer ICP-MS (NexION 2000C), equipped with a cyclonic spray chamber, a concentric Meinhard nebulizer and a dual detector. The isotopes used for quantification, free or subject to minimum isobaric and polyatomic interferences, were: ^{89}Y, ^{139}La, ^{140}Ce, ^{141}Pr, ^{146}Nd, ^{147}Sm, ^{151}Eu, ^{153}Eu, ^{157}Gd, ^{159}Tb, ^{163}Dy, ^{165}Ho, ^{166}Er, ^{169}Tm, ^{172}Yb, and ^{175}Lu. ^{115}In was the chosen internal standard (Merck, CertiPUR®). Polyatomic and isobaric interferences were minimized by setting the ratios $^{137}Ba{+}{+}/^{137}Ba$ and $^{140}Ce^{16}O/^{140}Ce$ ratios to 0.010 under routine operation conditions. ^{115}In was the chosen internal standard (Merck, CertiPUR®). Quality Control (QC) solutions were run every 20 samples batch and a 6-point calibration curve was used for quantification. Three procedural blanks were included within each batch to control the analytical quality of the method that always accounted for less than 1% variability of the REE concentration in the samples. The "Ce-anomaly" was calculated as $Ce/Ce^* = 3(Ce/Ce_{Eus})/(2(La/La_{Eus}) + (Nd/Nd_{Eus}))$ and the "Eu-anomaly" as $Eu/Eu^* = (Eu/Eu_{Eus})/((Sm/Sm_{Eus}) \times (Gd/ Gd_{Eus}))1/2$, where $_{Eus}$ represents the European Shale normalized value (Elderfield and Graves, 1982).

Lastly, the certified reference material BCR 668 (muscle of *Mytilus edulis*) was encompassed within the same batch of 20 samples to assess the accuracy of the analytical procedures, and the attained values were consistent with the certified ones ($p<0.05$).

Analytical blanks were used to obtain detection limits for each element. Rare earth elements detection limits for ICP-MS were: 20 ng g^{-1} for La, 28 ng g^{-1} for Ce, 5.5 ng g^{-1} for Pr, 17 ng g^{-1} for Nd, 2.4 ng g^{-1} for Sm, 1.3 ng g^{-1} for Eu, 15 ng g^{-1} for Gd, 0.60 ng g^{-1} for Tb, 2.3 ng g^{-1} for Dy, 10 ng g^{-1} for Y, 4.1 ng g^{-1} for Ho, 1.6 ng g^{-1} for Er, 0.41 ng g^{-1} for Tm, 4.3 ng g^{-1} for Yb and 0.5 ng g^{-1} for Lu.

2.2.4 Reporting

Although REE grouping is not consensual in the literature, here REE were sectioned into light rare earth elements (LREE) and heavy rare earth elements (HREE). The first group comprises the elements lanthanum (La), cerium (Ce), praseodymium (Pr), neodymium (Nd), promethium (Pm), samarium (Sm) and europium (Eu), while the latter includes gadolinium (Gd), terbium (Tb), dysprosium (Dy), holmium (Ho), erbium (Er), thulium (Tm), ytterbium (Yb), and lutetium (Lu) (Zepf, 2013).

The REE concentrations are presented in nanogram per gram of dry weight (ng g^{-1}, dw) and to simplify data visualization, REE were also normalized to the European Shale (EUS) according to Bau et al. (2018).

2.2.5 Statistical analyses

As the assumptions of normality were met, Pearson's correlation coefficient was applied to identify the correlation between REE content and specimens' size and weight. Later, an analysis of variance (one-way ANOVA) was performed to investigate elemental content differences between seasons, within different locations, and between locations within each season. Statistical analyses were performed at a significance level of 0.05 using the open-source software InVivoStat, version 4.2.

2.3 RESULTS AND DISCUSSION

Biometric data of the six hundred and forty-nine mussels *Mytilus galloprovincialis* sampled at six different locations on the Portuguese coast, between autumn 2020 and spring 2021 is presented in Table 2.1.

Table 2.1 - Shell length and width and respective total weight and soft body weight for *Mytilus galloprovincialis* from distinct geographical locations and seasons.

			Shell		Weight	
Location	**Season**	***n***	**Length (mm)**	**Width (mm)**	**Total (g)**	**Soft Body (g)**
Carreço	Fall	75	46 (34 - 65)	23 (19 - 30)	7.0 (2.6 - 19)	2.1 (1.0 - 4.5)
	Spring	60	46 (40 - 56)	24 (18 - 27)	8.0 (4.1 - 15)	2.5 (1.2 - 5.6)
Leça	Fall	55	49 (40 - 61)	26 (22 - 37)	7.8 (4.5 - 15)	2.3 (1.4 - 4.8)
	Spring	59	53 (42 - 63)	26 (22 -56)	7.9 (4.6 - 18)	2.3 (1.2 - 4.3)
Porto Brandão	Fall	49	50 (40 - 59)	28 (22 - 35)	13 (6.1 - 27)	3.8 (1.2 - 8.2)
	Spring	53	51 (43 - 61)	29 (25 - 35)	11 (7.0 - 17)	2.5 (1.5 - 4.8)
Costa da Caparica	Fall	52	45 (35 - 84)	25 (20 - 42)	10 (6.0 - 17)	3.6 (1.8 - 11)
	Spring	52	50 (43 - 60)	26 (21 - 34)	8.6 (5.1 - 15)	2.9 (1.6 - 5.0)
Mira	Fall	43	44 (34 - 60)	28 (23 - 40)	11 (5.3 - 30)	2.1 (1.3 - 4.6)
	Spring	60	57 (29 - 77)	35 (27 - 45)	14 (7.1 - 26)	4.9 (2.5 - 9.2)
Aljezur	Fall	43	52 (39 - 68)	28 (21 - 38)	11 (5.0 - 35)	3.6 (1.4 - 9.4)
	Spring	48	58 (47 - 74)	33 (27 - 38)	17 (9.5 - 30)	5.6 (2.7 - 11)

The statistical test based on Pearson's correlation coefficient showed no correlation between ∑REE, ∑LREE and ∑HREE and shell length, width, and total and soft body weight, for all locations and seasons ($p>0.05$), highlighting an unbiased and heterogeneous pool of mussels.

Median (minimum and maximum) REE concentrations in the mussels' whole soft body from the two sampling seasons are summarized in Table 2.2.

Table 2.2 - Median (Min - Max) rare earth elements concentrations in the studied mussel specimens (ng g^{-1}, dry weight)

		REE concentration (ng g^{-1}, dw)																	
Location	**Season**	**La**	**Ce**	**Pr**	**Nd**	**Sm**	**Eu**	**Gd**	**Tb**	**Dy**	**Y**	**Ho**	**Er**	**Tm**	**Yb**	**Lu**	**∑REE**	**∑LREE**	**∑HREE**
Carreço	Fall	318 (110 -726)	468 (164-1051)	75 (26-181)	319 (111-729)	63 (22-136)	10 (3.5-21)	52 (17-104)	6.1 (2.0-13)	33 (10-67)	238 (64-530)	6.1 (4.1-12)	14 (4.7-31)	1.7 (0.53-3.7)	10 (4.4-24)	1.4 (0.72-3.2)	1615 (544-3631)	1253 (436-2844)	125 (44-258)
	Spring	389 (156-1527)	777 (310-2966)	95 (37-345)	406 (170-1582)	90 (40-350)	15 (6.5-54)	81 (34-311)	9.3 (3.9-31)	45 (21-173)	194 (80-837)	7.6 (4.2-24)	19 (8.3-72)	1.9 (0.84-7.9)	10 (4.8-32)	0.85 (0.54-3.2)	2139 (877-8316)	1771 (720-6825)	174 (78-654)
Leça	Fall	270 (76-1001)	408 (116-1606)	67 (21-250)	288 (102-1066)	55 (21-201)	8.9 (3.6-28)	47 (19-166)	5.7 (2.1-22)	31 (12-117)	231 (78-1098)	5.8 (4.1-21)	14 (5.2-56)	1.6 (0.55-6.8)	9.5 (5.1-43)	1.4 (0.56-6.0)	1446 (466-5685)	1098 (339-4150)	117 (49-436)
	Spring	235 (108-607)	460 (208-1303)	57 (26-160)	281 (119-720)	65 (26-164)	12 (5-29)	62 (33-139)	8.0 (3.1-19)	40 (16-95)	176 (76-411)	7.0 (4.2-17)	16 (7.1-41)	1.6 (0.69-4.1)	8.3 (4.8-21)	0.69 (0.52-1.5)	1431 (638-3732)	1110 (493-2983)	144 (69-338)
Porto Brandão	Fall	340 (70-1170)	524 (91-1936)	84 (16-315)	356 (68-1351)	72 (13-290)	13 (2.7-56)	65 (18-251)	8.5 (1.6-33)	48 (8.7-183)	413 (54-1885)	10 (4.2-35)	23 (4.3-89)	2.7 (0.52-11)	17 (4.9-61)	2.4 (0.74-9)	1978 (358-7674)	1389 (261-5118)	176 (43-672)
	Spring	483 (76-1625)	928 (83-3516)	114 (10-426)	502 (54-1850)	113 (11-398)	18 (5.0-65)	93 (28-325)	13 (1.8-44)	64 (8.2-224)	282 (60-883)	12 (4.3-39)	27 (3.2-98)	3.1 (0.49-11)	16 (5.1-59)	1.2 (0.53-4.1)	2672 (351-9568)	2160 (240-7880)	230 (52-805)
Costa da Caparica	Fall	179 (84-1066)	268 (101-1420)	45 (16-239)	193 (70-1074)	39 (14-210)	6.9 (2.7-40)	36 (15-176)	4.3 (1.5-23)	25 (8.8-131)	191 (70-901)	7.1 (4.1-24)	13 (4.1-65)	1.5 (0.48-8)	10 (4.4-50)	1.3 (0.55-7)	1019 (396-5437)	743 (288-9880)	102 (39-1254)
	Spring	199 (70-690)	362 (77-1433)	46 (9.0-182)	225 (48-859)	48 (9-194)	10 (2.2-39)	51 (21-177)	4.9 (1.1-23)	29 (5.9-127)	148 (34-618)	6.6 (4.1-23)	12 (2.4-55)	1.4 (0.58-5.5)	7.3 (4.4-27)	1.0 (0.52-1.8)	1150 (289-4454)	889 (215-3397)	113 (40-439)
Mira	Fall	191 (67-1845)	258 (37-2657)	45 (8-461)	202 (37-2098)	43 (3.3-4.57)	9.0 (1.9-99)	40 (18-378)	4.3 (0.7-42)	23 (5.0-235)	122 (31-1167)	5.1 (4.2-40)	11 (2.3-111)	1.3 (0.46-13)	8.2 (4.4-76)	1.1 (0.58-11)	965 (221-9689)	748 (154-7617)	94 (35-906)
	Spring	423 (148-1218)	808 (266-2455)	95 (33-288)	398 (144-1200)	88 (34-264)	18 (6.9-53)	72 (28-206)	8.7 (3.4-25)	42 (16-115)	169 (67-470)	7.5 (4.2-20)	19 (7.5-53)	2.1 (0.84-5.7)	11 (4.6-32)	0.88 (0.53-2.4)	2161 (763-6408)	1830 (632-5478)	163 (65-460)
Aljezur	Fall	74 (26-276)	93 (30-383)	18 (7.2-65)	82 (28-292)	18 (6.4-66)	4.1 (1.5-15)	22 (15-63)	2.1 (0.7-7)	12 (4.6-60)	101 (39-278)	4.3 (4.2-7.5)	6.0 (2.3-19)	0.76 (0.45-2.2)	5.9 (4.4-13)	0.76 (0.54-1.9)	444 (171-1529)	288 (99-1097)	54 (32-154)
	Spring	98 (28-325)	167 (47-620)	22 (5.5-79)	108 (32-367)	27 (7.2-92)	4.3 (1.4-18)	26 (15-81)	1.9 (0.7-8.3)	15 (4.1-47)	94 (27-216)	5.6 (4.2-7.0)	6.4 (2.4-21)	0.77 (0.77-0.77)	5.4 (4.4-12)	0.76 (0.76-0.76)	582 (180-1895)	426 (121-1501)	62 (32-178)

The REE bioaccumulation depends on mussel growth, food availability (i.e., primary production, detritus, and particulate matter) and the physicochemical conditions of the environment. Furthermore, as sessile organisms that live close to the seabed, mussels may accumulate REE from sediment particles (Bonnail et al. 2017). The ∑REE concentration varied between sampling locations and ranged from 444 ng g^{-1} in Aljezur during the autumn up to 2672 ng g^{-1} in Porto Brandão during the spring. Overall, samples from Porto Brandão exhibited the highest REE concentrations, while mussels from Aljezur exhibited the lowest, in both autumn and spring (Table 2.2). The REE concentrations presented are in line with the range of concentrations described for mussels, in the environment, in other studies (Figure 2.2) (160–5000 ng g^{-1}; Briant et al., 2021; Costas-Rodríguez et al., 2010; MacMillan et al., 2017; Squadrone et al., 2019).

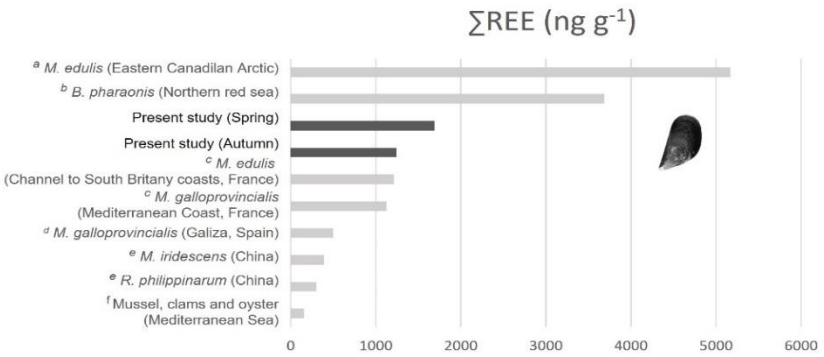

Figure 2.2 - ∑REE concentrations described for mussels, in the environment, in the present study in comparison to other studies. References: a – MacMillan et al. 2017; b – Benaltabet et al., 2021; c – Briant et al., 2021; d – Costas-Rodriguez et al., 2010; e – Wang et al., 2019; f – Squadrone et al., 2019.

Table 2.2 illustrates the occurrence of the greatest ∑REE in the area of the Tagus estuary mouth (Porto Brandão), which is subject of a great anthropogenic impact, being located on the south bank of the Tagus estuary, that runs across the dense urban Portuguese city, the capital Lisbon. Furthermore, Tagus transports high concentration of suspended material which is filtered by mussels and may in turn influence the accumulation of REE in their tissues. The physical and chemical features of estuarine sediments (pH, salinity, redox potential, organic matter content and grain size) can affect the REE mobility, availability, and absorption (Brito et al., 2018), and they seem to be greater in this location. Although the main anthropogenic REE emissions take place in surface waters (Slooff et al., 1993), REE concentration in the mussel tissues reflects the element availability in the water column because most sites are subjected to a vertical mixture due to waves, tides, and bottom topography. This availability is in turn

altered, also, by the elemental distribution in sediments. The distribution is controlled by scavenging processes, such as Fe-Mn oxides, redox conditions (Bau et al., 1997) and anthropogenic inputs (Borrego et al., 2012). Additionally, in the Tagus estuary, distinct sources of REE may occur: wastewater treatment plants effluents of about 2.8 million inhabitants, industries (chemical, cement, etc.), agriculture and the waste of an inactive chemical-industrial complex, that is responsible for an open-air phosphogypsum stack, originated from the production of phosphate fertilizer from phosphorite. This REE-rich residue contributes also to, for example, abnormal high contents of atmospheric dispersion of Y (Brito et al., 2018; Cánovas et al., 2018), as showcased in Table 2.2. Additionally, Y content appears to be greater in autumn, and this may be related to increased rain and surface runoff.

The concentration of ∑LREE varied between 288 ng g^{-1} in Aljezur during the autumn and 2160 ng g^{-1} in Porto Brandão during the spring. Far less concentrated (around 10-fold lower), ∑HREE ranged from 54 ng g^{-1} in Aljezur during the autumn up to 230 ng g^{-1} Porto Brandão during the spring. From spring to autumn, a significant difference in the ∑LREE concentration was found in the mussels from Carreço, Mira, Porto Brandão and Aljezur (Annex 2, Supplemental Table 2.1, $p<0.05$). Seasonal differences between the ∑HREE content were only found in mussels from Carreço, Leça da Palmeira and Mira, the two northernmost sample locations and an estuary impacted by mining activity and domestic effluents (Mil-Homens et al., 2014). Mussels sampled in Carreço and Mira also presented seasonal differences between their ∑REE content (Annex 2, Supplemental Table 2.1, $p<0.05$). Overall, ∑REE concentration appears to be greater in the spring. Within each season the different sampling locations presented significant differences among them regarding their ∑REE, ∑LREE and ∑HREE content (See Annex 2, Supplemental Table 2.2 A and B). This could be related to temperature variability between seasons and greater food availability in spring. Additionally, the reproductive cycle could also explain the observed seasonal variability, as gonad maturation occurs during spring. Leiniö and Lehtonen (2005) investigated the seasonal variation of enzyme activities in bivalves and described a stressed condition during the spring/early summer period and suggested that the reproductive cycle could explain it.

European shale normalized REE values are given in Table 2.3 and patterns are shown in Figure 2.3.

Table 2.3 - Rare earth elements (as the reason REE/European shale, dry weight) in the studied mussel specimens. Cerium and Eu anomalies are represented by Ce/Ce* and Eu/Eu*, respectively

		REE concentrations normalized to European shale																	
Location	**Season**	**La**	**Ce**	**Pr**	**Nd**	**Sm**	**Eu**	**Gd**	**Tb**	**Dy**	**Y**	**Ho**	**Er**	**Tm**	**Yb**	**Lu**	**Ce/Ce***	**Eu/Eu***	**La/Yb**
Carreço	Autumn	0.007 (0.002 – 0.016)	0.005 (0.002 - 0.012)	0.007 (0.002 – 0.017)	0.008 (0.003 – 0.018)	0.009 (0.003 – 0.019)	0.007 (0.002 – 0.014)	0.008 (0.003 – 0.016)	0.006 (0.002- 0.014)	0.006 (0.002- 0.011)	0.007 (0.002- 0.011)	0.005 (0.004- 0.010)	0.004 (0.001- 0.009)	0.003 (0.001- 0.007)	0.003 (0.001- 0.007)	0.003 (0.001- 0.007)	0.71	0.81	2.4
	Spring	0.009 (0.004- 0.034)	0.009 (0.003- 0.034)	0.009 (0.003- 0.033)	0.010 (0.004- 0.040)	0.012 (0.005- 0.048)	0.010 (0.004- 0.036)	0.013 (0.005- 0.049)	0.010 (0.004- 0.033)	0.008 (0.004- 0.030)	0.006 (0.002- 0.026)	0.006 (0.004- 0.020)	0.005 (0.002- 0.021)	0.004 (0.002- 0.016)	0.003 (0.001- 0.010)	0.002 (0.001- 0.006)	0.95	0.79	2.8
Leça	Autumn	0.006 (0.002 - 0.023)	0.005 (0.01- 0.018)	0.006 (0.002- 0.024)	0.007 (0.003- 0.027)	0.008 (0.003- 0.028)	0.006 (0.002- 0.019)	0.007 (0.003- 0.026)	0.006 (0.002- 0.023)	0.005 (0.002- 0.020)	0.007 (0.002- 0.034)	0.005 (0.003- 0.018)	0.004 (0.002- 0.016)	0.003 (0.001- 0.014)	0.003 (0.002 - 0.013)	0.003 (0.001 – 0.012)	0.71	0.80	2.1
	Spring	0.005 (0.002- 0.014)	0.005 (0.002- 0.015)	0.005 (0.002- 0.015)	0.007 (0.003- 0.018)	0.009 (0.004- 0.022)	0.008 (0.003- 0.020)	0.010 (0.005 - 0.022)	0.008 (0.003- 0.020)	0.007 (0.003 - 0.016)	0.006 (0.0052 -0.013)	0.006 (0.004- 0.014)	0.005 (0.002- 0.012)	0.003 (0.001 - 0.008)	0.003 (0.001 - 0.007)	0.001 (0.001 - 0.003)	0.88	0.88	2.1
Porto Brandão	Autumn	0.008 (0.002 - 0.026)	0.006 (0.001 - 0.022)	0.008 (0.001 - 0.030)	0.009 (0.002 – 0.034)	0.010 (0.002 - 0.040)	0.009 (0.002 - 0.038)	0.010 (0.003 - 0.040)	0.009 (0.002- 0.035)	0.008 (0.001 - 0.031)	0.013 (0.002- 0.059)	0.008 (0.004 - 0.030)	0.007 (0.001 - 0.026)	0.006 (0.001 - 0.021)	0.005 (0.002 - 0.019)	0.005 (0.002 – 0.019)	0.73	0.90	1.5
	Spring	0.011 (0.002 - 0.037)	0.010 (0.001- 0.040)	0.011 (0.001- 0.040)	0.013 (0.001- 0.047)	0.015 (0.002- 0.055)	0.012 (0.003- 0.044)	0.015 (0.004- 0.051)	0.014 (0.002- 0.047)	0.011 (0.001- 0.038)	0.009 (0.002- 0.028)	0.010 (0.004- 0.034)	0.008 (0.001- 0.029)	0.006 (0.001- 0.022)	0.005 (0.002- 0.018)	0.003 (0.001- 0.008)	0.91	0.82	2.2
Costa da Caparica	Autumn	0.004 (0.002 - 0.024)	0.003 (0.001- 0.016)	0.004 (0.002- 0.023)	0.005 (0.002 – 0.027)	0.006 (0.002- 0.029)	0.005 (0.002 - 0.027)	0.006 (0.002- 0.028)	0.005 (0.002- 0.025)	0.004 (0.002 - 0.022)	0.006 (0.002– 0.028)	0.006 (0.004– 0.021)	0.004 (0.001 - 0.019)	0.003 (0.001 – 0.016)	0.003 (0.001 - 0.015)	0.003 (0.001 - 0.015)	0.68	0.83	1.4
	Spring	0.004 (0.002- 0.016)	0.004 (0.001- 0.016)	0.004 (0.001- 0.017)	0.006 (0.001- 0.022)	0.007 (0.001- 0.027)	0.006 (0.001- 0.026)	0.008 (0.003- 0.028)	0.005 (0.001- 0.025)	0.005 (0.001- 0.022)	0.005 (0.001 - 0.019)	0.006 (0.003- 0.019)	0.004 (0.001- 0.016)	0.003 (0.001- 0.011)	0.002 (0.001- 0.008)	0.002 (0.001- 0.004)	0.84	0.89	2.0
Mira	Autumn	0.004 (0.002 - 0.042)	0.003 (0.0004 – 0.030)	0.004 (0.001 - 0.044)	0.005 (0.001 - 0.053)	0.006 (0.001- 0.063)	0.006 (0.001 - 0.067)	0.006 (0.003- 0.060)	0.005 (0.001 - 0.044)	0.004 (0.001- 0.040)	0.004 (0.001- 0.037)	0.004 (0.004– 0.034)	0.003 (0.001 - 0.032)	0.003 (0.001 – 0.026)	0.003 (0.001 – 0.023)	0.002 (0.001 - 0.022)	0.64	0.99	1.7
	Spring	0.010 (0.003- 0.027)	0.009 (0.003- 0.028)	0.009 (0.003- 0.027)	0.010 (0.004- 0.030)	0.012 (0.005- 0.036)	0.012 (0.005 - 0.036)	0.011 (0.004 - 0.032)	0.009 (0.004- 0.032)	0.007 (0.003- 0.020)	0.005 (0.002 - 0.015)	0.006 (0.004- 0.017)	0.005 (0.002- 0.016)	0.004 (0.002- 0.012)	0.003 (0.001- 0.010)	0.002 (0.001- 0.005)	0.94	1.04	2.8
Aljezur	Autumn	0.002 (0.001 – 0.006)	0.001 (0.0003 – 0.004)	0.002 (0.001 – 0.006)	0.002 (0.001 – 0.007)	0.002 (0.001- 0.009)	0.003 (0.001– 0.010)	0.003 (0.002- 0.010)	0.002 (0.001- 0.008)	0.002 (0.001– 0.007)	0.003 (0.001– 0.009)	0.004 (0.004- 0.006)	0.002 (0.001- 0.006)	0.002 (0.001- 0.004)	0.002 (0.001- 0.004)	0.002 (0.001- 0.004)	0.58	0.95	1.3
	Spring	0.002 (0.001 - 0.007)	0.002 (0.001 - 0.007)	0.002 (0.001- 0.007)	0.003 (0.001- 0.009)	0.004 (0.001- 0.013)	0.003 (0.001- 0.012)	0.004 (0.002- 0.013)	0.002 (0.001- 0.009)	0.002 (0.001- 0.008)	0.003 (0.001- 0.007)	0.005 (0.004- 0.006)	0.002 (0.001- 0.006)	0.002 (0.002- 0.002)	0.002 (0.001- 0.004)	0.002 (0.002- 0.002)	0.79	0.75	1.4

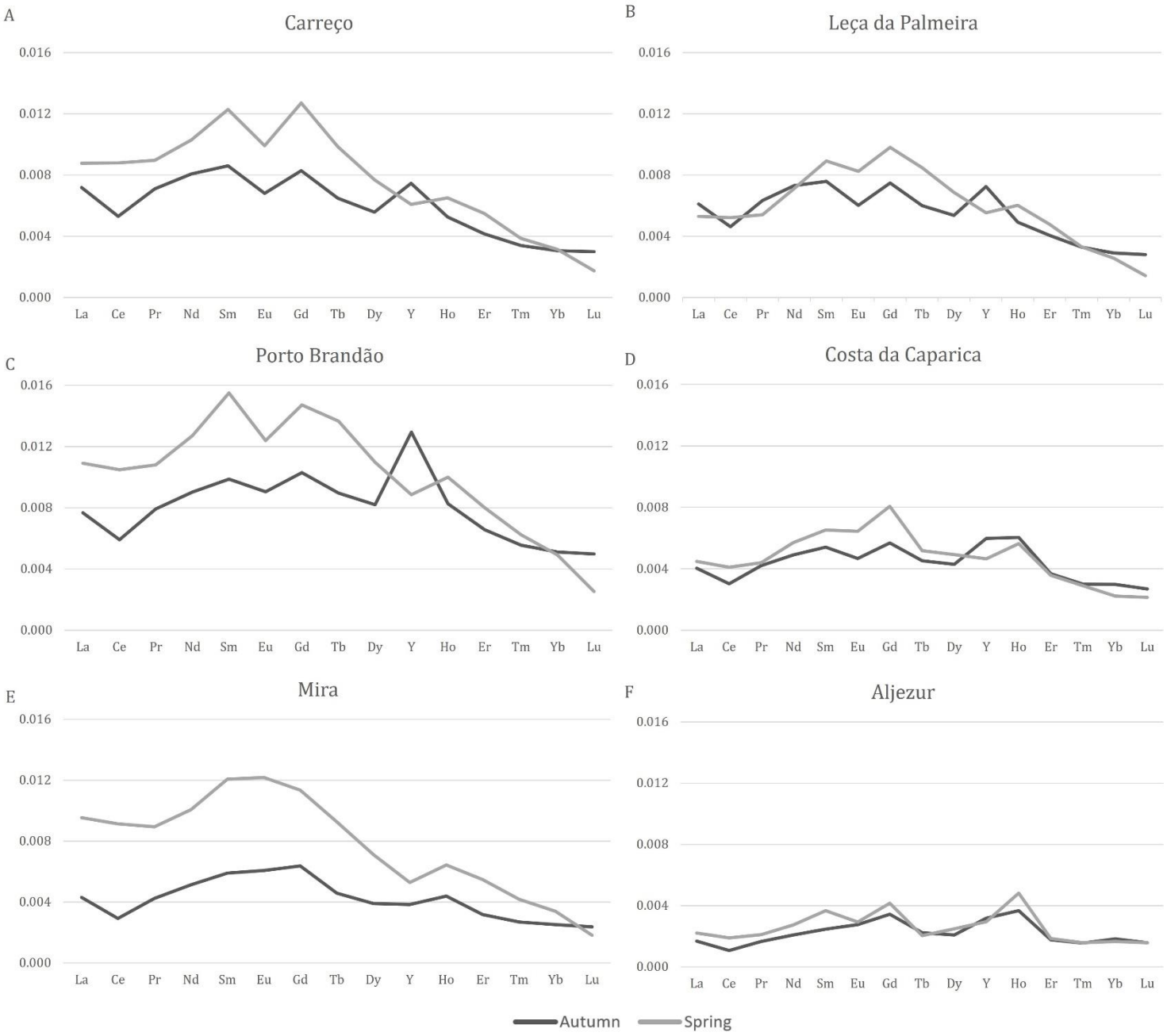

Figure 2.3 - European shale-normalized REE patterns for mussels sampled in a) Carreço; b) Leça da Palmeira; c) Porto Brandão; d) Costa da Caparica; e) Mira and f) Aljezur in both seasons (spring and autumn)

In this study, a LREE enrichment relative to HREE occurs. This pattern was also found in sediments from most of sites where mussels were collected (Brito et al., 2018; Araújo et al., 2002; Cesário et al., 2018). Furthermore, LREE are more soluble, which may indicate that they are more bioavailable than HREE (Pratas et al., 2017). Additionally, this pattern of fractionation between the light and heavy REE is in line with the REEs natural behavior in the environment and has already been described for mussels in other locations (Akagi and Edanami, 2017; Briant et al., 2021; Wang et al., 2019). Wang et al.

(2019) studied the REE concentrations in seven common species from the Maluan Bay (China) and found significant differences in total REEs concentration among species, even from the same phylum, suggesting a species- and element-dependent REE accumulation pattern. These results highlight the need to study a broader set of species over a larger spatial gradient, for the scientific community to pinpoint the prime organism for REE biomonitoring.

Overall, specimens showcase a negative Ce and Eu anomaly (Table 2.3). The negative Ce anomaly was more prominent in autumn and is consistent in all locations. These anomalies reveal a depletion of these elements in the water column or in their food. On one side, Ce is one of the naturally most abundant REE, while also being one of the highest applied in several industries, which suggests that the depletion was not expected, on another, no enrichment in relation to their pairs may exist presumably due to its insolubility in the most stable form (+4). Cerium and Eu are redox-sensitive elements (Brito et al., 2020). REE mainly occur as trivalent ions, however, among the LREE, Ce and Eu can occur in more than one redox state. Cerium can occur as a tri- or tetravalent ion (i.e., Ce^{3+}, Ce^{4+}), while Eu can occur as a di- or trivalent ion (i.e., Eu^{2+}, Eu^{3+}), depending on the oxidation-reduction conditions. For example, the tetravalent Ce ion is less soluble than the oxidized trivalent ion, and these characteristics may result in mobility alterations in the coastal system, which may then affect their uptake/bioavailability (Wang et al., 2019). Although Ce and Eu negative anomalies were found in most sediments, our results show that transfer has not occurred to the water column, neither were these elements incorporated by the mussels. Furthermore, this also indicates the lack of anthropogenic sources that may input these elements in the dissolved fraction.

Interestingly, all sites showed an increase of Gd respectively to their pair elements. This indicates an accumulation of this element from the dissolved fraction or associated with food. Increased concentration of this element has been found in wastewater treatment plants outfalls of the Tagus estuary (Brito et al., 2018) as a result of anthropogenic input from the contrast in the magnetic resonance imagery (Rogowska et al., 2018). This input was not specific from one site since this medical application has a wide use in Portugal. Pereto et al. (2020) studied the dissolved and total fraction of the water from a French river subject to strong urban pressure (Bordeaux area) and

exposed bivalves in situ for a three-month monitoring period and found the presence of Gd positive anomalies in the dissolved and total fractions as well as in the studied species *Corbicula fluminea*. The Gd anomaly observed in the water was also observed in *C. fluminea*, with a significant increase in the bioaccumulation of Gd. The input of the other elements, like Nd and Sm may result from other industrial activities and harbor pollution (Gwenzi et al., 2018). Although REE displays chemical characteristics alike, and may therefore behave homogenously by migrating as a whole, their bioavailability can be affected by a wide array of factors, which in turn is reflected in the element composition of the studied species. Even though the mechanisms driving REE anomalies in biota are yet not fully understood, this result indicated that both Ce and Eu were less available during autumn, probably due to the redox condition seasonal changes.

2.4 CONCLUSION

This study provides data on the REE content of mussels from 6 distinct locations on the Portuguese coast (NE Atlantic Ocean), in two distinct seasons. Here, samples from Porto Brandão (in the anthropogenic impacted Tagus River estuary) exhibited the highest REE concentrations, while mussels from Aljezur (the southernmost point) exhibited the lowest, in both autumn and spring. Overall, ∑REE concentration was greater in the spring. A LREE enrichment relative to HREE occurred and a negative Ce and Eu anomaly was observed. The negative Ce anomaly was more prominent in the autumn and is consistent in all locations probably due to the redox condition seasonal changes. Overall, this study constitutes the first assessment of the REE composition on this model species on the Portuguese coast, in two distinct seasons. The results presented demonstrated that this mollusk species can be considered as a bioindicator of REE contamination. Nevertheless, the REE content in the mussel specimens should be accompanied by environmental data from the sampling sites, for a critical understanding of the accumulation processes and the contamination levels. Furthermore, data on biomarkers should also fulfil the information on REE biomonitoring in upcoming studies.

ACKNOWLEDGEMENTS

This work was supported by Fundação para a Ciência e Tecnologia (FCT), through the strategic project UID/MAR/04292/2019 granted to MARE, and by the European Union's operation program Mar 2020 through the research project CEIC (MAR-01.04.02-FEAMP-0012) awarded to Joana Raimundo and SNMB-MONIT III (MAR-02.01.02-FEAMP-0213) awarded to Rui Oliveira. Cátia Figueiredo acknowledges the FCT-PhD grant SFRH/BD/130023/2017.

REFERENCES

Akagi, T., Edanami, K., 2017. Sources of rare earth elements in shells and soft-tissues of bivalves from Tokyo Bay. Marine Chemistry 194, 55-62.

Araújo, M., Jouanneau, J. M., Valério, P., Barbosa, T., Gouveia, A., Weber, O., Oliveira, A., Rodrigues, A., Dias, J. M. A., 2002. Geochemical tracers of northern Portuguese estuarine sediments on the shelf. Progress in Oceanography 52, 277-297.

Balaram, V., 2019. Rare earth elements: A review of applications, occurrence, exploration, analysis, recycling, and environmental impact. Geoscience Frontiers 10, 1285-1303.

Bau, M., Möller, P., Dulski, P., 1997. Yttrium and lanthanides in eastern Mediterranean seawater and their fractionation during redox-cycling. Marine Chemistry 56, 123-131.

Bau, M., Schmidt, K., Pack, A., Bendel, V., Kraemer, D., 2018. The European Shale: An improved data set for normalisation of rare earth element and yttrium concentrations in environmental and biological samples from Europe. Applied Geochemistry 90, 142-149.

Benaltabet, T., Gutner-Hoch, E., Torfstein, A., 2021. Heavy Metal, Rare Earth Element and Pb isotope dynamics in mussels during a depuration experiment in the Gulf of Aqaba, Northern Red Sea. Frontiers in Marine Science 8:669329.

Bergsten-Torralba, L., Magalhães, D., Giese, E., Nascimento, C., Pinho, J., Buss, D., 2020. Toxicity of three rare earth elements, and their combinations to algae, microcrustaceans, and fungi. Ecotoxicology and Environmental Safety 201, 110795.

Beyer, J., Green, N.W., Brooks, S., Allan, I.J., Ruus, A., Gomes, T., Bråte, I.L.N., Schøyen, M., 2017. Blue mussels (*Mytilus edulis* spp.) as sentinel organisms in coastal pollution monitoring: a review. Marine environmental research 130, 338-365.

Bonnail, E., Pérez-López, R., Sarmiento, A.M., Nieto, J.M., DelValls, T.Á., 2017. A novel approach for acid mine drainage pollution biomonitoring using rare earth elements bioaccumulated in the freshwater clam *Corbicula fluminea*. Journal of hazardous materials 338, 466-471.

Borrego, J., Carro, B., López-González, N., De La Rosa, J., Grande, J., Gómez, T., De La Torre, M., 2012. Effect of acid mine drainage on dissolved rare earth elements

geochemistry along a fluvial–estuarine system: the Tinto-Odiel Estuary (SW Spain). Hydrology Research 43, 262-274.

Briant, N., Le Monier, P., Bruzac, S., Sireau, T., Araújo, D.F., Grouhel, A., 2021. Rare Earth Element in Bivalves' Soft Tissues of French Metropolitan Coasts: Spatial and Temporal Distribution. Archives of Environmental Contamination and Toxicology, 1-12.

Brito, P., Mil-Homens, M., Caçador, I., Caetano, M., 2020. Changes in REE fractionation induced by the halophyte plant *Halimione portulacoides*, from SW European salt marshes. Marine Chemistry 223, 103805.

Brito, P., Prego, R., Mil-Homens, M., Caçador, I., Caetano, M., 2018. Sources and distribution of yttrium and rare earth elements in surface sediments from Tagus estuary, Portugal. Science of The Total Environment 621, 317-325.

Cai, C., Wang, W.-X., 2019. Inter-species difference of copper accumulation in three species of marine mussels: Implication for biomonitoring. Science of the Total Environment 692, 1029-1036.

Cánovas, C.R., Macías, F., López, R.P., Nieto, J.M., 2018. Mobility of rare earth elements, yttrium and scandium from a phosphogypsum stack: Environmental and economic implications. Science of the Total Environment 618, 847-857.

Capolupo, M., Franzellitti, S., Kiwan, A., Valbonesi, P., Dinelli, E., Pignotti, E., Birke, M., Fabbri, E., 2017. A comprehensive evaluation of the environmental quality of a coastal lagoon (Ravenna, Italy): Integrating chemical and physiological analyses in mussels as a biomonitoring strategy. Science of the Total Environment 598, 146-159.

Cesário, R., Brito, P., Caetano, M., Prego, R., 2018. Rare earth elements in the mira river estuary sediments. Paper presented at Seminário Ibérico de Química Marina (SIQUIMAR).

Costas-Rodríguez, M., Lavilla, I., Bendicho, C., 2010. Classification of cultivated mussels from Galicia (Northwest Spain) with European Protected Designation of Origin using trace element fingerprint and chemometric analysis. Analytica chimica acta 664, 121-128.

Elderfield, H., Graves, M., 1982. The rare earth elements in seawater. Nature 269, 214–219.

Figueiredo, C., Grilo, T.F., Lopes, C., Brito, P., Diniz, M., Caetano, M., Rosa, R., Raimundo, J., 2018. Accumulation, elimination and neuro-oxidative damage under lanthanum exposure in glass eels (*Anguilla anguilla*). Chemosphere 206, 414-423.

Figueiredo, C., Raimundo, J., Lopes, A.R., Lopes, C., Rosa, N., Brito, P., Diniz, M., Caetano, M., Grilo, T.F., 2020. Warming enhances lanthanum accumulation and toxicity promoting cellular damage in glass eels (*Anguilla anguilla*). Environmental research 191, 110051.

Freitas, R., Costa, S., Cardoso, C.E., Morais, T., Moleiro, P., Matias, A.C., Pereira, A.F., Machado, J., Correia, B., Pinheiro, D., 2020. Toxicological effects of the rare earth element neodymium in *Mytilus galloprovincialis*. Chemosphere 244, 125457.

Gwenzi, W., Mangori, L., Danha, C., Chaukura, N., Dunjana, N., Sanganyado, E., 2018. Sources, behaviour, and environmental and human health risks of high-technology rare earth elements as emerging contaminants. Science of the Total Environment 636, 299-313.

Hu, B., He, M., Jakubowski, N., Meinhardt, J., Meyer, F.M., Niederstraßer, J., Schramm, R., Sindern, S., Stosch, H.-G., Bertau, M., 2017. Handbook of Rare Earth Elements: Analytics. Walter de Gruyter GmbH & Co KG.

Leiniö, S., Lehtonen, K.K., 2005. Seasonal variability in biomarkers in the bivalves *Mytilus edulis* and *Macoma balthica* from the northern Baltic Sea. Comparative Biochemistry and Physiology Part C: Toxicology & Pharmacology 140, 408-421.

Lerat-Hardy, A., Coynel, A., Dutruch, L., Pereto, C., Bossy, C., Gil-Diaz, T., Capdeville, M.-J., Blanc, G., Schäfer, J., 2019. Rare Earth Element fluxes over 15 years into a major European Estuary (Garonne-Gironde, SW France): Hospital effluents as a source of increasing gadolinium anomalies. Science of The Total Environment 656, 409-420.

Liu, J., Kueh, C., 2005. Biomonitoring of heavy metals and trace organics using the intertidal mussel *Perna viridis* in Hong Kong coastal waters. Marine Pollution Bulletin 51, 857-875.

MacMillan, G.A., Chételat, J., Heath, J.P., Mickpegak, R., Amyot, M., 2017. Rare earth elements in freshwater, marine, and terrestrial ecosystems in the eastern Canadian Arctic. Environmental Science: Processes & Impacts 19, 1336-1345.

Mestre, N.C., Sousa, V.S., Rocha, T.L., Bebianno, M.J., 2019. Ecotoxicity of rare earths in the marine mussel *Mytilus galloprovincialis* and a preliminary approach to assess environmental risk. Ecotoxicology 28, 294-301.

Mil-Homens, M., Vale, C., Raimundo, J., Pereira, P., Brito, P., & Caetano, M., 2014. Major factors influencing the elemental composition of surface estuarine sediments: the case of 15 estuaries in Portugal. Marine pollution bulletin 84, 135-146.

Pereto, C., Coynel, A., Lerat-Hardy, A., Gourves, P.-Y., Schäfer, J., Baudrimont, M., 2020. *Corbicula fluminea*: A sentinel species for urban Rare Earth Element origin. Science of The Total Environment 732, 138552.

Phillips, D.J., Rainbow, P.S., 2013. Biomonitoring of trace aquatic contaminants. Springer Science & Business Media.

Pinto, J., Costa, M., Leite, C., Borges, C., Coppola, F., Henriques, B., Monteiro, R., Russo, T., Di Cosmo, A., Soares, A.M., 2019. Ecotoxicological effects of lanthanum in *Mytilus galloprovincialis*: Biochemical and histopathological impacts. Aquatic Toxicology 211, 181-192.

Pratas, J., Favas, P.J., Varun, M., D'Souza, R., Paul, M.S., 2017. Distribution of rare earth elements, thorium and uranium in streams and aquatic mosses of Central Portugal. Environmental Earth Sciences 76, 156.

Raimundo, J., Vale, C., Caetano, M., Giacomello, E., Anes, B., Menezes, G.M., 2013. Natural trace element enrichment in fishes from a volcanic and tectonically active region (Azores archipelago). Deep Sea Research Part II: Topical Studies in Oceanography 98, 137-147.

Rogowska, J., Olkowska, E., Ratajczyk, W., & Wolska, L. (2018). Gadolinium as a new emerging contaminant of aquatic environments. Environmental toxicology and chemistry 37, 1523-1534.

Slooff, W., Bont, P., Janus, J., Annema, J., 1993. Exploratory report rare earth metals and their compounds. RIVM Rapport 710401025.

Squadrone, S., Brizio, P., Stella, C., Prearo, M., Pastorino, P., Serracca, L., Ercolini, C., Abete, M.C., 2016. Presence of trace metals in aquaculture marine ecosystems of the northwestern Mediterranean Sea (Italy). Environmental Pollution 215, 77-93.

Squadrone, S., Brizio, P., Stella, C., Mantia, M., Battuello, M., Nurra, N., Sartor, R.M., Orusa, R., Robetto, S., Brusa, F., 2019. Rare earth elements in marine and

terrestrial matrices of Northwestern Italy: Implications for food safety and human health. Science of the Total Environment 660, 1383-1391.

Wang, Z., Yin, L., Xiang, H., Qin, X., Wang, S., 2019. Accumulation patterns and species-specific characteristics of yttrium and rare earth elements (YREEs) in biological matrices from Maluan Bay, China: Implications for biomonitoring. Environmental research 179, 108804.

Zepf, V., 2013. Rare earth elements: a new approach to the nexus of supply, demand and use: exemplified along the use of neodymium in permanent magnets. Springer Science & Business Media.

Chapter 3

Rare earth and trace elements in deep-sea sponges of the North Atlantic

Cátia Figueiredo [a,b,*], Miguel Caetano [b,c], Mário Mil-Homens [b], Inês Tojeira [d], Joana R. Xavier [d,e], Rui Rosa [a], Joana Raimundo [b,c]

[a] Laboratório Marítimo da Guia, MARE – Marine and Environmental Sciences Centre, Faculdade de Ciências da Universidade de Lisboa, Av. Nossa Senhora do Cabo, 939, 2750-374 Cascais, Portugal

[b] Division of Oceanography and Marine Environment, IPMA - Instituto Português do Mar e da Atmosfera, Av. Alfredo Magalhães Ramalho, 6, 1495-165 Algés, Portugal

[c] CIIMAR – Interdisciplinary Centre of Marine and Environmental Research of the University of Porto, 4450-208 Matosinhos, Portugal

[d] Task Group for the Extension of the Continental Shelf (EMEPC), R. Costa Pinto 165, 2770-047 Paço de Arcos, Portugal

[e] University of Bergen, Department of Biological Sciences and KG Jebsen Centre for Deep-Sea Research, 5006 Bergen, Norway

* Corresponding author

Figueiredo, C., Caetano, M., Mil-Homens, M., Tojeira I., Xavier, J. R., Rosa, R., Raimundo, J. 2021. Rare earth and trace elements in deep-sea sponges of the North Atlantic. Marine Pollution Bulletin 166, 112217. (DOI 10.1016/j.marpolbul.2021.112217)

ABSTRACT

The available data on trace elements (TE) of deep-sea organisms is scarce and nonexistent for rare earth elements (REE). Hence, this study characterizes REE and TE in five porifera genera (Jaspis, Geodia, Hamacantha, Leiodermatium, Poliopogon) collected in deep-sea areas (between 481 and 2656 m) of the North Atlantic. Aluminium was the most common TE while lead was the less abundant. These sponges showed an increased accumulation of TE compared with other probably influenced by volcanic activity. *Poliopogon amadou* sampled at the deepest location presented the highest concentration of all REE. All studied species exhibited a Light REE enrichment in comparison to Heavy REE and showed a negative Ce anomaly with a less conspicuous Eu depletion. Besides the establishment of a baseline for future comparisons, this study provides the first record of REE in a sessile deep-sea marine invertebrate group.

Keywords: Deep-sea; sponges; rare earth elements; trace elements.

3.1 INTRODUCTION

The deep-sea is the vastest environment of our planet and acts as an ultimate global repository for trace elements (TE) where rare earth elements (REE) are included. REE are crucial for numerous state-of-the-art environmental technologies namely: nuclear, solar, wind, bioenergy, carbon capture and storage. With limited supply but growing demand, their economic interest is steeply increasing (Malhotra et al., 2020). The significantly growing anthropogenic input into the environment may affect living organisms and demands for the study of these substances in the marine environment. Historically was often non-viable to determine low REE concentrations as the available analytical methods were not adequately sensitive (Markert and De Li, 1991). Hence, to this date, little is known about both the REE concentration in deep-sea organisms and their role in biogeochemical cycles. On other hand, trace elements have been detected in a wide range of environments and organisms (e.g., Bai et al., 2015; Benito et al., 1999; Kojadinovic et al., 2007; Purves, 2012; Subotić et al., 2013). The vast majority of REE-related studies have been conducted on sediments (e.g., Douville et al., 1999; Elderfield et al., 1981; Freslon et al., 2014; Yang et al., 2002) and volcanic plumes (e.g., Klinkhammer et al., 1994; Moune et al., 2010).

Sponges are sessile benthic animals that feed largely on microscopic size organic particles such as phytoplankton, bacteria and detritus (Kahn et al., 2015; Yahel et al., 2007) or dissolved organic carbon (de Goeij et al., 2013) while filtering large quantities of water that besides food also supplies oxygen and removes metabolic waste products (de Goeij et al., 2008; Van Soest et al., 2012). This feeding strategy brands sponges particularly vulnerable to seawater quality and element availability (Perez et al., 2003), which make them good biomonitors (Phillips and Rainbow, 2013). Hence, this study aims to characterize the elemental composition (namely 26 different elements, including REE) of seven sponges, belonging to five different genera (Jaspis, Geodia, Hamacantha, Leiodermatium, Poliopogon), from different North Atlantic deep-sea locations. Besides the establishment of a baseline for future comparisons, here we also provide, according to our knowledge, the first characterization of REE's in a sessile deep-sea marine invertebrate group.

3.2 MATERIAL AND METHODS

3.2.1 Sampling

The deep-sea environments within and beyond the Portuguese Exclusive Economic Zone were surveyed during three campaigns (EMEPC/LUSO/2009, EMEPC/M@rBis/SELVAGENS2010 and EMEPC/PEPC/LUSO/2013) undertaken in the scope of the Extension of the Portuguese Continental Shelf Programme (EMEPC). Deep-sea sponges were collected between 481 and 2656 m depth with the working class Remotely Operated Vehicle (ROV) Luso (model Bathyssaurus XL; rated 6000m depth) equipped with a 7-function arm and a suction sampler with 5 independent sampling chambers. Seven different specimens belonging to five porifera genera: Jaspis (n=1), Geodia (n=2), Hamacantha (n=1), Leiodermatium (n=2) and Poliopogon (n=1) were sampled in Irving and Meteor seamounts, Kings Trough area, East of Terceira, Selvagem Pequena and Selvagem Grande in the NE Atlantic (Figure 3.1). Following collection, sponge samples were stored in an on-board -80°C freezer. A detailed overview of samples used in the present study is provided in Table 3.1.

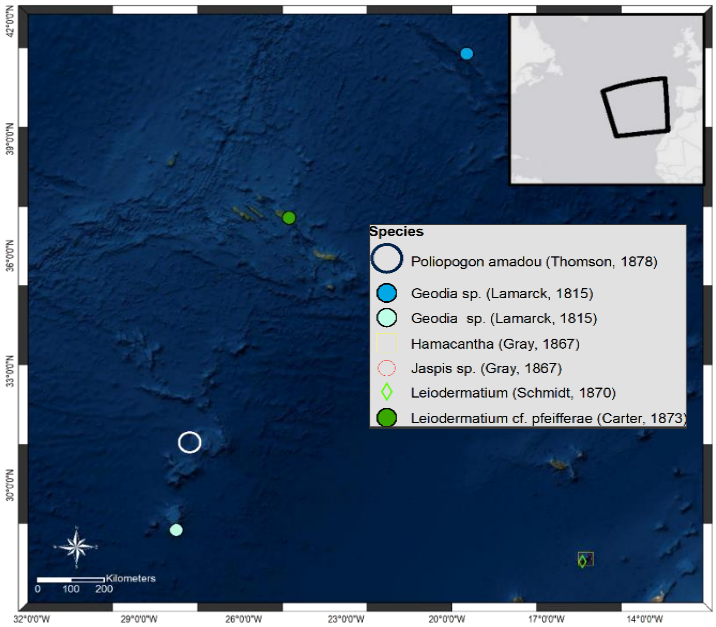

Figure 3.1 - Study area in the North Atlantic, with the locations where the different species were sampled.

Table 3.1 - Detailed overview of sponge samples used in the present study.

Class	Order	Family	Genus	Species	Collection site	Latitude (N)	Longitude (W)	Depth (m)
Demospongiae	Tetractinellida	Geodiidae	*Geodia*	*Geodia* sp. 1	Kings Trough	44° 6,6465'	-21° 57,838'	1874
				Geodia sp. 2	Meteor Seamount	29° 34.391'	-28° 20.271'	714
	-	Ancorinidae	*Jaspis*	*Jaspis* sp.	Selvagem Grande (Madeira Archipelago)	30° 06.284'	-15° 54.982'	699
	-	Azoricidae	*Leiodermatium*	*Leiodermatium* sp.	Selvagem Pequena (Madeira Archipelago)	30° 00.680’	-16° 00.164’	848
	-			*Leiodermatium* cf. *pfeifferae* Carter, 1873	East of Terceira island (Azores Archipelago)	38° 40.110'	-26° 51.465'	481
	Merliida	Hamacanthidae	*Hamacantha*	*Hamacantha* sp.	Selvagem Grande (Madeira Archipelago)	30° 06.284'	-15° 54.982'	699
Hexactinellida	Amphidiscosida	Pheronematidae	*Poliopogon*	*Poliopogon amadou* Thomson, 1878	Irving Seamount	32° 00.972'	-28° 27.762'	2656

3.2.2 Rare earth and trace elements analyses

Specimens were freeze-dried, ground, and homogenized prior to digestions. All labware was decontaminated with HNO_3 (20%) for two days and rinsed with Milli-Q water. Approximately 200 mg of the freeze-dried samples were digested in a microwave CEM MArsXpress in two steps using an in-house methodology. The first step used a mixture of 5 mL HNO_3 (suprapure, 65% v/v) and 2 mL HF (37% v/v) at 200°C during a hold of 15 minutes. In a second step, we added 4 mL of an oversaturated solution of H_3BO_3 at 170°C, for complexing the residual dissolved fluoride or re-dissolving insoluble fluorides formed during the digestion (Brito et al., 2020).

The concentrations of 14 REE: Lanthanum (La), Cerium (Ce), Praseodymium (Pr), Neodymium (Nd), Promethium (Pm), Samarium (Sm), Europium (Eu), Gadolinium (Gd), Terbium (Tb), Dysprosium (dy), Holmium (Ho), Erbium (Er), Thulium (Tm), Ytterbium (Yb) and Lutetium (Lu) and 13 TE: Aluminium (Al), Vanadium (V), Chromium (Cr), Manganese (Mn), Nickel (Ni), Copper (Cu), Zinc (Zn), Arsenic (As), Selenium (Se), Strontium (Sr), Molybdenum (Mo), Cadmium (Cd) and Lead (Pb) were determined in the same samples but in separate runs using a quadrupole ICP-MS (Thermo Elemental, X-Series) equipped with a Peltier Impact bead spray chamber and a concentric Meinhard nebulizer (Raimundo et al., 2013a). The selected analytical isotopes of the TE (^{27}Al, ^{51}V, ^{52}Cr, ^{55}Mn, ^{60}Ni, ^{65}Cu, ^{66}Zn, ^{75}As, ^{82}Se, ^{88}Sr, ^{95}Mo, ^{111}Cd and ^{208}Pb) and REE (^{139}La, ^{140}Ce, ^{141}Pr, ^{146}Nd, ^{147}Sm, ^{153}Eu, ^{157}Gd, ^{159}Tb, ^{163}Dy, ^{165}Ho, ^{166}Er, ^{169}Tm, ^{172}Yb and ^{175}Lu) were free or subject to minimum isobaric and polyatomic interferences. A 9-point calibration curve within a range of 0.1 to 400 mg L^{-1} was used to quantify trace elements, and a 9-point calibration curve within the range 0.05–20 mg L^{-1} was used to quantify REE concentrations.

3.2.3 Reporting

The REE were subdivided into Light Rare Earth Elements (LREE) and Heavy Rare Earth Elements (HREE) based on the 4-f electron configuration proposed by Zepf (2013). Thus, LREE include La, Ce, Pr, Nd, Pm, Sm, Eu and Gd and the following elements are included in the HREE group: Tb, Dy, Ho, Er, Tm, Yb and Lu.

Both TE and REE concentrations are presented in microgram per gram of dry weight (µg g^{-1}, dw). REE were also normalized to Chondrite (Cho) (McDonough and Sun, 1995). The positive or negative deviations of Ce and Eu from their neighbouring pairs of elements are considered as anomalies (Holser, 1997). For the “Ce-anomaly” we followed

the formulae $Ce/Ce^{*}=3(Ce/Ce_{Cho})/(2(La/La_{Cho})+(Nd/Nd_{Cho}))$ and for "Eu-anomaly" we followed $Eu/Eu^{*}=(Eu/Eu_{Cho})/((Sm/Sm_{Cho})\times(Gd/Gd_{Cho}))^{1/2}$, where $_{Cho}$ is the chondrite normalized value (Elderfield and Graves, 1982 and references therein).

3.2.4 Method reliability

The accuracy of the analytic methods was assessed through analysis of three international certificate reference materials (CRM) for trace elements [IAEA - 452, scallop (*Pecten maximus*), DORM-2, dogfish muscle and HISS-1, marine sediment] and for REE [BCR 668 – mussel tissue]. The results obtained for CRM did not differ significantly ($p<0.05$) from the certified values. Additionally, three procedural blanks were prepared using an equal analytical method and reagents and were included within each batch of samples. The blanks always delivered values of less than 1% of the total of the elements studied.

3.3 RESULTS

3.3.1 Rare earth elements

Table 3.2 shows the concentrations of REE for each species. Concentrations of ∑REE varied from 1.2 μg g^{-1} in *Leiodermatium* sp. up to 12 μg g^{-1} in *Poliopogon amadou* from Selvagem Pequena and Irving Seamount, respectively. The lowest ∑HREE of 0.046 μg g^{-1} was registered in *Geodia* sp. 2 from Meteor Seamount while the highest was recorded in *P. amadou* from Irving Seamount (1.4 μg g^{-1}). Concentrations of ∑LREE ranged from 1.1 μg g^{-1} in *Leiodermatium* sp. from Selvagem Pequena to 10 μg g^{-1} *in P. amadou* from the Irving Seamount. Lanthanum was the most abundant element, ranging from 1.1 μg g^{-1} in *Leidermatium* sp. from Selvagem Pequena to 2.1 μg g^{-1} in *P. amadou* from Irving seamount. *Poliopogon amadou* from Irving seamount presented the highest concentration of all REE.

Table 3.2 - Concentrations of rare earth elements in the studied sponge species (µg g^{-1}, dry weight). Rare earth elements detection limits for ICP-MS were: 0.015 µg g^{-1} for La, 0.055 µg g^{-1} for Ce, 0.0038 µg g^{-1} for Pr, 0.028 µg g^{-1} for Nd, 0.0075 µg g^{-1} for Sm, 0.0029 µg g^{-1} for Eu, 0.0056 µg g^{-1} for Gd, 0.0019 µg g^{-1} for Tb, 0.0026 µg g^{-1} for Dy, 0.0018 µg g^{-1} for Ho, 0.0076 µg g^{-1} for Er, 0.0010 µg g^{-1} for Tm, 0.0026 µg g^{-1} for Yb and 0.0010 µg g^{-1} for Lu.

			REE concentration (µg g^{-1}, dw)																
Collection site	**Depth (m)**	**Species**	**La**	**Ce**	**Pr**	**Nd**	**Sm**	**Eu**	**Gd**	**Tb**	**Dy**	**Ho**	**Er**	**Tm**	**Yb**	**Lu**	**∑LREE**	**∑HREE**	**∑REE**
Kings Trough	1874	*Geodia* sp. 1	2.0	1.1	0.13	0.63	0.10	0.024	0.099	0.014	0.090	0.018	0.056	0.007	0.052	0.007	4.1	0.25	4.3
Meteor Seamount	714	*Geodia* sp. 2	2.0	0.23	0.035	0.12	0.023	0.003	0.018	0.002	0.018	0.003	0.013	0.001	0.009	0.001	2.4	0.046	2.4
Selvagem Grande	699	*Hamacantha* sp.	1.8	2.9	0.47	1.8	0.32	0.084	0.33	0.047	0.29	0.052	0.16	0.021	0.14	0.019	7.8	0.73	8.5
Selvagem Grande	699	*Jaspis* sp.	1.1	0.17	0.050	0.19	0.033	0.008	0.038	0.004	0.032	0.006	0.021	0.002	0.016	0.001	1.6	0.083	1.7
Selvagem Pequena	848	*Leiodermatium* sp.	0.32	0.52	0.041	0.18	0.038	0.007	0.030	0.005	0.028	0.007	0.018	0.001	0.017	0.002	1.1	0.078	1.2
East of Terceira Island	481	*Leiodermatium* cf. *pfeifferae*	0.77	0.61	0.048	0.21	0.065	0.010	0.033	0.006	0.030	0.007	0.018	0.002	0.017	0.002	1.7	0.082	1.8
Irving Seamount	2656	*Poliopogon amadou*	2.1	3.0	0.74	3.1	0.62	0.15	0.65	0.094	0.56	0.11	0.31	0.042	0.26	0.036	10	1.4	12

Values of the chondrite REE normalized values are given in Table 3.3 and plotted in Figure 3.2. Overall, the studied species showed a negative Ce-anomaly (Ce/Ce* < 1, Table 3.3). The lowest anomalies were found in *Geodia* sp. 2 from Meteor seamount (0.03) and in *Jaspis* sp. from Selvagem Grande (0.09). The species that presented the Ce/Ce* values closer to the unit were *Leiodermatium* sp. (0.88) and *Hamacantha* sp. (0.74). The Eu anomaly varied in a narrower range from 0.52 in *Geodia* sp. 2 to 0.80 in *Hamacantha* sp. from Meteor seamount and Selvagem Grande, respectively.

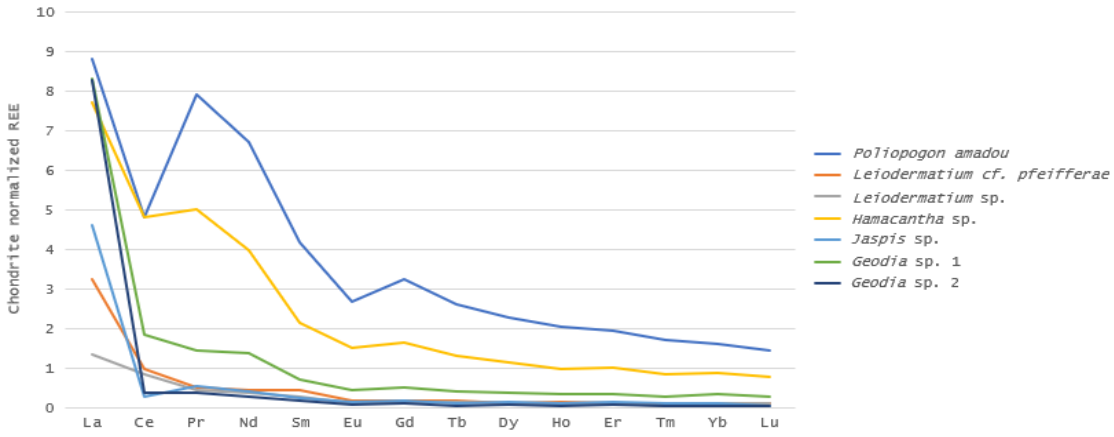

Figure 3.2 - Chondrite normalized REE patterns for the studied sponge species.

Table 3.3 - Rare earth elements (as the reason REE/Chondrite, dry weight) in the studied sponge species. Cerium and Eu anomalies are represented by Ce/Ce* and Eu/Eu*, respectively.

			REEs concentrations normalized to Chondrite															
Collection site	**Depth (m)**	**Species**	**La**	**Ce**	**Pr**	**Nd**	**Sm**	**Eu**	**Gd**	**Tb**	**Dy**	**Ho**	**Er**	**Tm**	**Yb**	**Lu**	**Ce/Ce***	**Eu/Eu***
Kings Trough	1874	*Geodia* sp. 1	8.3	1.8	1.4	1.4	0.69	0.43	0.50	0.40	0.37	0.33	0.35	0.29	0.33	0.27	0.31	0.66
Meteor seamount	714	*Geodia* sp. 2	8.3	0.38	0.37	0.27	0.16	0.06	0.09	0.05	0.07	0.05	0.08	0.04	0.06	0.03	0.06	0.52
Selvagem Grande	699	*Hamacantha* sp.	7.7	4.8	5.0	4.0	2.1	1.5	1.7	1.3	1.2	0.96	1.0	0.85	0.86	0.77	0.74	0.80
Selvagem Grande	699	*Jaspis* sp.	4.6	0.27	0.54	0.41	0.22	0.15	0.19	0.11	0.13	0.11	0.13	0.10	0.10	0.05	0.09	0.72
Selvagem Pequena	848	*Leiodermatium* sp.	1.4	0.85	0.44	0.39	0.26	0.12	0.15	0.14	0.11	0.12	0.11	0.05	0.10	0.10	0.88	0.61
East of Terceira Island	481	*Leiodermatium* cf. *pfeifferae*	3.2	0.99	0.51	0.45	0.44	0.17	0.17	0.17	0.12	0.14	0.11	0.08	0.10	0.10	0.43	0.63
Irving seamount	2656	*Poliopogon amadou*	8.8	4.8	7.9	6.7	4.2	2.7	3.2	2.6	2.3	2.0	2.0	1.7	1.6	1.4	0.59	0.72

3.3.2 Trace metals

Concentrations of the elements Al, V, Cr, Mn, Ni, Cu, Zn, As, Se, Sr, Mo, Cd and Pb are provided in Table 3.4. Aluminium was, by far, the most common element, followed by Sr. Concentrations of Al ranged from 19 µg g^{-1} in *Geodia* sp. 2 from Meteor seamount up to 3854 µg g^{-1} in *Hamacantha* sp. from Selvagem Grande. Levels of Sr varied in a narrow interval from 17 µg g^{-1} in *Leiodermatium* sp. from Selvagem Pequena to 921 µg g^{-1} in *P. amadou* from Irving Seamount. Succeeding, the element concentration decreased from Mn to Zn, Ni, As, Cu, Se, V, Mo, Cr, Cd and Pb was the least abundant element. Interestingly the non-essential element Cd hasn´t showed so low concentrations varying from 0.12 µg g^{-1} in *P. amadou* from the Irving Seamount and 2.2 µg g^{-1} in *Leiodermatium cf. pfeifferae* from the East of Terceira. Similarly, Pb concentrations ranged from 0.026 µg g^{-1} in *Geodia* sp. 2 from Meteor seamount to 4.7 µg g^{-1} in *Hamacantha* sp. from Selvagem Grande.

Table 3.4 - Concentrations of the trace elements Al, V, Cr, Mn, Ni, Cu, Zn, As, Se, Sr, Mo, Cd and Pb (μg g^{-1}, dw) for each studied specimen. N.D. – Not Determined. Trace elements detection limits for ICP-MS were: 1.5 μg g^{-1} for Al, 0.010 μg g^{-1} for V, 0.058 μg g^{-1} for Cr, 0.014 μg g^{-1} for Mn, 0.029 μg g^{-1} for Ni, 0.29 μg g^{-1} for Cu, 0.034 μg g^{-1} for Zn, 0.011 μg g^{-1} for As, 0.074 μg g^{-1} for Se, 0.026 μg g^{-1} for Sr, 0.048 μg g^{-1} for Mo, 0.033 μg g^{-1} for Cd and 0.019 μg g^{-1} for Pb.

			Trace elements concentration (μg g^{-1}, dw)												
Collection Site	**Depth (m)**	**Species**	**Al**	**V**	**Cr**	**Mn**	**Ni**	**Cu**	**Zn**	**As**	**Se**	**Sr**	**Mo**	**Cd**	**Pb**
Kings Trough	1874	*Geodia* sp. 1	910	4.5	1.2	62	46	7.6	99	19	19	132	2.7	1.4	1.4
Meteor seamount	714	*Geodia* sp. 2	19	0.39	0.07	7.6	58	12	33	40	14	39	2.9	0.40	0.026
Selvagem Grande	699	*Hamacantha* sp.	3854	8.3	2.3	175	22	9.1	18	7.9	8.0	490	1.0	1.0	4.7
Selvagem Grande	699	*Jaspis* sp.	297	2.7	2.6	11	44	9.1	19	23	9.4	38	2.5	0.78	0.89
Selvagem Pequena	848	*Leiodermatium* sp.	138	2.8	0.40	5.0	4.4	7.7	53	2.3	3.4	58	1.2	1.3	1.1
East of Terceira Island	481	*Leiodermatium* cf. *pfeifferae*	166	1.4	0.90	6.4	16	5.5	36	11	8.2	17	N.D.	2.2	0.92
Irving seamount	2656	*Poliopogon amadou*	2212	6.0	2.6	229	4.7	85	20	4.9	2.8	921	1.0	0.12	2.5

3.4 DISCUSSION

As sessile marine invertebrates, sponges live attached to the substrate in the same location for variable periods. Deep-sea sponges are assumed to be slow-growing and long-lived (Fallon et al., 2010; Kahn et al., 2016; Leys and Lauzon, 1998) and therefore likely to bioaccumulate over a long time (several decades). Fluids from hydrothermal activity at mid-ocean ridges display LREE enrichment over HREE (Douville et al., 1999; Mitra et al., 1994; Schmidt et al., 2010). Our samples exhibit an enrichment of LREE, concurring with previous findings. A negative anomaly of Ce was registered in the studied species, reflecting the low availability of this element in the water as similar findings were observed in Mitra et al. (1994), who described a negative Ce anomaly in the deep-sea water of the North Atlantic. The ability of sponges to bioaccumulate environmentally available trace elements, both dissolved in the seawater or adsorbed on particles, is well known (e.g., Batista et al. 2014; De Mestre et al., 2012; Illuminati et al., 2016; Pan et al., 2011). Nevertheless, their ability to bioaccumulate REE was unknown and is here, for the first time, described. Elderfield and Greaves (1982) observed that the concentrations of REE, except Ce, increase with depth in the North Atlantic Ocean and concomitantly *P. amadou* was sampled at the uppermost depth (2656m) and presents the highest REE concentrations. The vertical distribution of REE has been studied in sediment cores in the Azores area (e.g., Caetano et al., 2013; Dias et al., 2008), but these elements, according to our knowledge, have not been studied in sponges making comparison with the literature challenging. This highlights the importance of this study, which establishes a baseline for future comparisons. Caetano et al. (2013) showed that sediments showed a comparable normalized REE pattern with volcanic material, with LREE enrichment in comparison to HREE and no Eu anomalies. Concordantly, Dias et al. (2008) performed a geochemical investigation of a near-vent hydrothermal sediment core from the Lucky Strike site on the Mid-Atlantic Ridge and found a LREE enrichment, however, on another hand, found a pronounced positive Eu anomaly, suggesting that the sediment was composed of minerals directly precipitated from the vent fluids, negligibly mixed with seawater. This pronounced Eu anomaly was not found in the studied sponge species suggesting that they were not closer to hydrothermal vents neither influenced by their fluids.

Overall, our results show greater quantities (up to two orders of magnitude) of the studied trace elements when compared, for example, with different sponge species from India (Rao et al., 2009) and from Saudi Arabia (Pan et al., 2011, except Zn) but, in general, lower quantities when compared to freshwater sponges of lakes in Australia (De Mestre et al., 2012) and contaminated sites in the Mediterranean (Perez, 2004). The greater quantity of the studied elements in these sponge species, when compared to other marine species and non-contaminated sites, could be due to the geological nature of the study area. Volcanic activity has been recognized as a natural source of trace elements (Charlou et al., 2002; Douville et al., 2002; Raimundo et al., 2013b) and are characteristic of the deep seafloor in the Mid Atlantic area, possibly influencing the samples from East of Terceira Island, Irving and Meteor seamounts and Kings Through. Nevertheless, samples from the other locations showed similar quantities of trace elements and similar profiles of REE (Figure 3.2), which suggests that these sponges could have been in contact with other sources of major, trace and REE. There is also reported hydrothermal activity southern of the Madeira islands that may influence trace element accumulation. In fact, Frogner et al. (2001) showed that volcanic ash in contact with seawater can release great amounts of phosphate, iron, silica, and manganese. Deheyn et al. (2005) demonstrated that an active submarine volcano in the Antarctic Peninsula enhanced the bioavailability of trace elements. A study by Gentric et al. (2016) confirmed that marine sponges can concentrate most of metallic and organic contaminants, in some cases at higher rates than bivalves and for some of them in a species-specific manner. Other authors have also described that trace element accumulation varies between sponge species (Pan et al., 2011; Patel et al., 1985; Perez, 2004; Rao et al., 2009). Among sponge species evaluated, *Hamacantha* sp. presented some interesting characteristics, as it did not follow the trend of the other studied species of the same Class (that comprises over 85% of all sponge diversity), exhibiting very different quantities of Mn and Sr (Table 3.3). Genta-Jouve et al. (2012) described that sponge morphology is a key factor in metal bioaccumulation efficiency. This may be applied for *Hamacantha* sp. since it was sampled encrusting *Jaspis* sp., and explain the greater ability to accumulate several TEs and REE, when compared to its counterpart (*Jaspis* sp.) from the same location. Previous studies have also described sponge-associated bacteria that are capable of mineralizing elements (Padovan et al., 2012;

Keren et al., 2017). This diverse array of microbial symbionts appeared to be sponge-specific in some cases (Taylor et al., 2004), and this *Hamacantha* sp. specimen could comprise bacteria capable of mineralizing these elements, contributing to the higher values found in this study. Bauvais et al. (2015) also showed that the sponge *Spongia officinalis* collected in a contaminated site in the western Mediterranean Sea contained high levels of Zn, Pb and Cu, while also finding a sponge specific bacterial association that is highly tolerant to heavy metals. Marine sponges harbor dense and diverse microbial communities (Pita et al., 2016; Thomas et al., 2016), that are of considerable ecological importance, and these communities should be studied to better understand the sponge elemental load and their ability to bioaccumulate them.

We suggest for upcoming studies to compare species elemental concentration with that from the water and sediments from the location where the sponges were collected for evaluating their sensitivity to changes in the local environmental conditions and its potential as a tool for biomonitoring studies. Deep-sea sponge aggregations are considered particularly vulnerable to ongoing anthropogenic activities such as gas, oil and mining exploitation acting upon the deep seafloor. Uncertainties and gaps in scientific knowledge render baseline and impact assessments particularly difficult for the deep-sea. Additional insights into the speciation of these elements into the water column, the organisms and their symbionts will be of high interest to fully understand the processes behind TE and REE bioaccumulation. To assess whether the sponge elemental concentration is a consequence of a contaminated environment and/or a bioaccumulation process resulting from the animal metabolism is important to evaluate the behavior of a given species in a non-polluted environment and further studies should be able to make this comparison. Although sampling the deep-sea floor is challenging and hugely costly, we also suggest further studies to analyze a greater number of individuals. Nonetheless, this study is the first characterization of REE in a sessile deep-sea marine invertebrate group and sets a baseline for future studies.

ACKNOWLEDGEMENTS

This work was supported by Fundação para a Ciência e Tecnologia (FCT), through the project REEUSE (PTDC/QEQ-EPR/1249/2014) and the strategic project UID/MAR/04292/2019 granted to MARE. JR acknowledges the postdoctoral grant by FCT SFRH/BPD/91498/2012, RR the FCT-IF Development grant (IF/01373/3013) and CF the FCT-PhD grant SFRH/BD/130023/2017. JRX research is funded by the European Union's Horizon 2020 research and innovation program through the SponGES project (grant agreement No 679849) and further supported by national funds through FCT within the scope of UIDB/04423/2020 and UIDP/04423/2020, and CEECIND/00577/2018. The authors would also like to thank the scientists aboard the 2009, 2010 and 2013 expeditions of the Task Group for the Extension of the Continental Shelf Project and to the technical ROV team that made the sampling possible. Finally, the authors thank the anonymous reviewers for the useful comments for the improvement of this work.

REFERENCES

Bai, J., Zhao, Q., Lu, Q., Wang, J., Reddy, K.R., 2015. Effects of freshwater input on trace element pollution in salt marsh soils of a typical coastal estuary, China. Journal of Hydrology 520, 186-192.

Batista, D., Muricy, G., Rocha, R.C., Miekeley, N.F., 2014. Marine sponges with contrasting life histories can be complementary biomonitors of heavy metal pollution in coastal ecosystems. Environmental Science and Pollution Research 21, 5784-5794.

Bauvais, C., Zirah, S., Piette, L., Chaspoul, F., Domart-Coulon, I., Chapon, V., Gallice, P., Rebuffat, S., Pérez, T., Bourguet-Kondracki, M.-L., 2015. Sponging up metals: Bacteria associated with the marine sponge *Spongia officinalis*. Marine Environmental Research 104, 20-30.

Benito, V., Devesa, V., Munoz, O., Suner, M., Montoro, R., Baos, R., Hiraldo, F., Ferrer, M., Fernandez, M., Gonzalez, M., 1999. Trace elements in blood collected from birds feeding in the area around Doñana National Park affected by the toxic spill from the Aznalcóllar mine. Science of the total environment 242, 309-323.

Brito, P., Mil-Homens, M., Caçador, I., Caetano, M., 2020. Changes in YREE fractionation induced by the halophyte plant *Halimione portulacoides*, from SW European salt marshes. Marine Chemistry 223, 103805.

Caetano, M., Vale, C., Anes, B., Raimundo, J., Drago, T., Schimdt, S., Nogueira, M., Oliveira, A., Prego, R., 2013. The Condor seamount at Mid-Atlantic Ridge as a supplementary source of trace and rare earth elements to the sediments. Deep Sea Research Part II: Topical Studies in Oceanography 98, 24-37.

Cebrian, E., Uriz, M.J., Turon, X., 2007. Sponges as biomonitors of heavy metals in spatial and temporal surveys in northwestern Mediterranean: multispecies comparison. Environmental Toxicology and Chemistry 26, 2430-2439.

Charlou, J., Donval, J., Fouquet, Y., Jean-Baptiste, P., Holm, N., 2002. Geochemistry of high H_2 and CH_4 vent fluids issuing from ultramafic rocks at the Rainbow hydrothermal field (36 14’ N, MAR). Chemical Geology 191, 345-359.

de Goeij, J.M., van den Berg, H., van Oostveen, M.M., Epping, E.H., Van Duyl, F.C., 2008. Major bulk dissolved organic carbon (DOC) removal by encrusting coral reef cavity sponges. Marine Ecology Progress Series 357, 139-151.

De Mestre, C., Maher, W., Roberts, D., Broad, A., Krikowa, F., Davis, A.R., 2012. Sponges as sentinels: patterns of spatial and intra-individual variation in trace metal concentration. Marine Pollution Bulletin 64, 80-89.

Deheyn, D.D., Gendreau, P., Baldwin, R.J., Latz, M.I., 2005. Evidence for enhanced bioavailability of trace elements in the marine ecosystem of Deception Island, a volcano in Antartica. Marine Environmental Research 60, 1-33.

Dias, A., Mills, R., Taylor, R., Ferreira, P., Barriga, F., 2008. Geochemistry of a sediment push-core from the Lucky Strike hydrothermal field, Mid-Atlantic Ridge. Chemical Geology 247, 339-351.

Douville, E., Bienvenu, P., Charlou, J.L., Donval, J.P., Fouquet, Y., Appriou, P., Gamo, T., 1999. Yttrium and rare earth elements in fluids from various deep-sea hydrothermal systems. Geochimica Et Cosmochimica Acta 63, 627-643.

Douville, E., Charlou, J., Oelkers, E., Bienvenu, P., Colon, C.J., Donval, J., Fouquet, Y., Prieur, D., Appriou, P., 2002. The rainbow vent fluids (36 14’ N, MAR): the influence of ultramafic rocks and phase separation on trace metal content in Mid-Atlantic Ridge hydrothermal fluids. Chemical Geology 184, 37-48.

Elderfield, H., Hawkesworth, C., Greaves, M., Calvert, S., 1981. Rare earth element geochemistry of oceanic ferromanganese nodules and associated sediments. Geochimica Et Cosmochimica Acta 45, 513-528.

Elderfield, H., Graves, M., 1982. The rare earth elements in seawater. Nature 269, 214-219.

Fallon, S. J., James, K., Norman, R., Kelly, M. and Ellwood, M. J., 2010. A simple radiocarbon dating method for determining the age and growth rate of deep-sea sponges. Nuclear Instruments and Methods in Physics Research, Section B: Beam Interactions with Materials and Atoms, 268, 1241–1243.

Freslon, N., Bayon, G., Toucanne, S., Bermell, S., Bollinger, C., Chéron, S., Etoubleau, J., Germain, Y., Khripounoff, A., Ponzevera, E., 2014. Rare earth elements and neodymium isotopes in sedimentary organic matter. Geochimica Et Cosmochimica Acta 140, 177-198.

Gage, J.D., Tyler, P.A., 1991. Deep-sea biology: a natural history of organisms at the deep-sea floor. Cambridge University Press.

Genta-Jouve, G., Cachet, N., Oberhänsli, F., Noyer, C., Teyssié, J.-L., Thomas, O.P., Lacoue-Labarthe, T., 2012. Comparative bioaccumulation kinetics of trace elements in Mediterranean marine sponges. Chemosphere 89, 340-349.

Gentric, C., Rehel, K., Dufour, A., Sauleau, P., 2016. Bioaccumulation of metallic trace elements and organic pollutants in marine sponges from the South Brittany Coast, France. Journal of Environmental Science and Health, Part A 51, 213-219.

Holser, W.T., 1997. Evaluation of the application of rare-earth elements to paleoceanography. Palaeogeography Palaeoclimatology Palaeoecology 132, 309–323.

Illuminati, S., Annibaldi, A., Truzzi, C., Scarponi, G., 2016. Heavy metal distribution in organic and siliceous marine sponge tissues measured by square wave anodic stripping voltammetry. Marine Pollution Bulletin 111, 476-482.

Kahn, A.S., Yahel, G., Chu, J.W., Tunnicliffe, V., Leys, S.P., 2015. Benthic grazing and carbon sequestration by deep-water glass sponge reefs. Limnology and Oceanography, 60, 78-88.

Kahn, A.S., Vehring, L.J., Brown, R.R., Leys, S.P., 2016. Dynamic change, recruitment and resilience in reef-forming glass sponges. Journal of the Marine Biological Association of the United Kingdom, 96, 429–436.

Keren, R., Mayzel, B., Lavy, A., Polishchuk, I., Levy, D., Fakra, SC., Pokroy, B., Ilan, M., 2017. Sponge-associated bacteria mineralize arsenic and barium on intracellular vesicles. Nature Communications 8, 14393.

Klinkhammer, G., German, C.R., Elderfield, H., Greaves, M.J., Mitra, A., 1994. Rare earth elements in hydrothermal fluids and plume particulates by inductively coupled plasma mass spectrometry. Marine Chemistry 45, 179-186.

Kojadinovic, J., Potier, M., Le Corre, M., Cosson, R.P., Bustamante, P., 2007. Bioaccumulation of trace elements in pelagic fish from the Western Indian Ocean. Environmental Pollution 146, 548-566.

Leys, S. P. and Lauzon, N. R. J., 1998. Hexactinellid sponge ecology: growth rates and seasonality in deep water sponges. Journal of Experimental Marine Biology and Ecology 230, 111–129.

Malhotra, N., Hsu, H. S., Liang, S. T., Roldan, M. J. M., Lee, J. S., Ger, T. R., Hsiao, C. D., 2020. An Updated Review of Toxicity Effect of the Rare Earth Elements (REEs) on Aquatic Organisms. Animals 10, 1663.

Markert, B., De Li, Z., 1991. Natural background concentrations of rare-earth elements in a forest ecosystem. Science of the Total Environment 103, 27-35.

McDonough, W.F., Sun, S.S., 1995. The composition of the Earth. Chemical geology 120, 223-253.

Moune, S., Gauthier, P.J., Delmelle, P., 2010. Trace elements in the particulate phase of the plume of Masaya Volcano, Nicaragua. Journal of Volcanology and Geothermal Research, 193, 232-244.

Mitra, A., Elderfield, H., Greaves, M., 1994. Rare earth elements in submarine hydrothermal fluids and plumes from the Mid-Atlantic Ridge. Marine Chemistry 46, 217-235.

Padovan, A., Munksgaard, N., Alvarez, B., McGuinness, K., Parry, D., Gibb, K., 2012 Trace metal concentrations in the tropical sponge *Spheciospongia vagabunda* at a sewage outfall: synchrotron X-ray imaging reveals the micron-scale distribution of accumulated metals. Hydrobiologia 687, 275-288.

Pan, K., Lee, O.O., Qian, P.-Y., Wang, W.-X., 2011. Sponges and sediments as monitoring tools of metal contamination in the eastern coast of the Red Sea, Saudi Arabia. Marine Pollution Bulletin 62, 1140-1146.

Patel, B., Balani, M., Patel, S., 1985. Sponge 'sentinel' of heavy metals. Science of the Total Environment 41, 143-152.

Perez, T., Wafo, E., Fourt, M., Vacelet, J., 2003. Marine sponges as biomonitor of polychlorobiphenyl contamination: concentration and fate of 24 congeners. Environmental Science & Technology 37, 2152-2158.

Perez, T., 2004. In situ comparative study of several Mediterranean sponges as potential biomonitors of heavy metals. BMIB-Bollettino dei Musei e degli Istituti Biologici 68, 517-525.

Phillips, D.J., Rainbow, P.S., 2013. Biomonitoring of trace aquatic contaminants. Springer Science & Business Media.

Pita, L., Fraune, S., Hentschel, U., 2016. Emerging sponge models of animal-microbe symbioses. Frontiers in Microbiology 7, 2102.

Purves, D., 2012. Trace-element Contamination of the Environment. Elsevier.

Raimundo, J., Vale, C., Caetano, M., Anes, B., Porteiro, F., Silva, M., 2013a. Element concentrations in deep-sea gorgonians and black coral from Azores Arquipelago Deep Sea Research II 98, 129-136.

Raimundo, J., Vale, C., Caetano, M., Giacomello, E., Anes, B., Menezes, G.M., 2013b. Natural trace element enrichment in fishes from a volcanic and tectonically active region (Azores archipelago). Deep Sea Research Part II: Topical Studies in Oceanography 98, 137-147.

Rao, J.V., Srikanth, K., Pallela, R., Rao, T.G., 2009. The use of marine sponge, *Haliclona tenuiramosa* as bioindicator to monitor heavy metal pollution in the coasts of Gulf of Mannar, India. Environmental monitoring and assessment 156, 451-459.

Schmidt, K., Garbe-Schönberg, D., Bau, M., Koschinsky, A., 2010. Rare earth element distribution in > 400° C hot hydrothermal fluids from 5° S, MAR: The role of anhydrite in controlling highly variable distribution patterns. Geochimica et Cosmochimica Acta 74, 4058-4077.

Subotić, S., Spasić, S., Višnjić-Jeftić, Ž., Hegediš, A., Krpo-Ćetković, J., Mićković, B., Skorić, S., Lenhardt, M., 2013. Heavy metal and trace element bioaccumulation in target tissues of four edible fish species from the Danube River (Serbia). Ecotoxicology and environmental safety 98, 196-202.

Surugiu, V., Dauvin, J.-C., Gillet, P., Ruellet, T., 2008. Can seamounts provide a good habitat for polychaete annelids? Example of the northeastern Atlantic seamounts. Deep-Sea Research I 55, 1515-1531.

Taylor, M.W., Schupp, P.J., Dahllöf, I., Kjelleberg, S., Steinberg, P.D., 2004. Host specificity in marine sponge-associated bacteria, and potential implications for marine microbial diversity. Environmental Microbiology 6, 121-130.

Thomas, T., Moitinho-Silva, L., Lurgi, M., Björk, J.R., Easson, C., Astudillo-García, C., Olson, J.B., Erwin, P.M., López-Legentil, S., Luter, H., 2016. Diversity, structure and convergent evolution of the global sponge microbiome. Nature Communications 7, 11870.

Van Soest, R.W., Boury-Esnault, N., Vacelet, J., Dohrmann, M., Erpenbeck, D., De Voogd, N.J., Santodomingo, N., Vanhoorne, B., Kelly, M., Hooper, J.N., 2012. Global diversity of sponges (Porifera). PLoS one 7, e35105.

Yahel, G., Whitney, F., Reiswig, H.M., Eerkes-Medrano, D.I., Leys, S.P., 2007. In situ feeding and metabolism of glass sponges (Hexactinellida, Porifera) studied in a deep temperate fjord with remotely operated submersible. Limnology and oceanography 52, 428-440.

Yang, S.Y., Jung, H.S., Choi, M.S., Li, C.X., 2002. The rare earth element compositions of the Changjiang (Yangtze) and Huanghe (Yellow) river sediments. Earth and Planetary Science Letters 201, 407-419.

Zepf, V., 2013. Rare Earth Elements: What and where they are Rare Earth Elements: a new approach to the nexus of supply, demand and use. Springer Berlin Heidelberg pp. 11-39.

PART THREE

MULTIPLE STRESSORS IN A NEAR-FUTURE ENVIRONMENT

Chapter 4

Lanthanum and Gadolinium availability in aquatic mediums: new insights to ecotoxicology and environmental studies

Cátia Figueiredo [a,b,c*], Tiago F. Grilo [a], Clara Lopes [b], Pedro Brito [b], Miguel Caetano [b,d], Joana Raimundo [b,d]

[a] MARE – Marine and Environmental Sciences Centre, Faculdade de Ciências da Universidade de Lisboa, Campo Grande, 1749-016 Lisboa, Portugal

[b] Division of Oceanography and Marine Environment, IPMA – Portuguese Institute for Sea and Atmosphere, Av. Alfredo Magalhães Ramalho, 6, 1495-165 Algés, Portugal

[c] UCIBIO, REQUIMTE, Departamento de Química, Faculdade de Ciências e Tecnologia, Universidade NOVA de Lisboa, 2829-516 Caparica, Portugal

[d] CIIMAR – Interdisciplinary Centre of Marine and Environmental Research, Avenida General Norton de Matos S/N, 4450-208 Matosinhos, Portugal

* Corresponding author

Figueiredo, C., Grilo, T.F., Lopes, C., Brito, P., Caetano, M., Raimundo, J., 2022. Lanthanum and gadolinium availability in aquatic mediums: new insights to ecotoxicology and environmental studies. Submitted to Journal of Trace elements in Medicine and Biology.

ABSTRACT

Studies dealing with Rare Earth Elements (REE) ecotoxicological behavior are scattered and with potential conflicting results. Climate change impacts on aquatic biota and is known to modify contaminants toxicokinetic. Nevertheless, the current knowledge on the potential interactions between climate change and REE is virtually non-existent. Therefore, we focus our research on La and Gd as representatives of Light and Heavy REE that also are of great environmental concern. Experiments on different mediums (fresh-, brackish- and seawater) were designed to run at present-day and near-future conditions (T°=+4°C, pH=△-0.4). Sampling was taken at different time scales from minutes to hours for one day. The main challenge was to evaluate the availability of La and Gd under environmental conditions closely related to climate changes scenarios. Furthermore, this study will contribute to the baseline knowledge by which future research towards understanding REE patterns and toxicity will build upon. Lanthanum and Gd behave differently with salinity. Temperature also affects the availability of dissolved La in freshwater. On the other hand, pH reduction causes the decrease of Gd in freshwater. In this medium, concentrations reduce sharply, presumably due to sorption processes or precipitates. In the brackish water experiment only the dissolved La levels in the Warming (T°=+4°C) and Warming & Acidification (T°=+4°C, pH=△0.4) diminished significantly through time. Dissolved La and Gd levels in seawater were relatively constant with time. The speciation of both elements is also of great relevance for ecotoxicological experiments. The trivalent free ions (La^{3+} and Gd^{3+}) were the most common species in the trials. However, as ionic strength increases, the availability of other complexes rose, which should be subject of great attention for upcoming ecotoxicological studies.

Keywords: Rare earth elements; Salinity; Temperature; pH; Speciation.

4.1 INTRODUCTION

Rare earth elements (REE) are a group of fifteen lanthanides plus scandium and yttrium, found in the Earth's crust, that are irreplaceable in the making of high-end modern technology. Increased usage of these chemical elements has raised concern about their role as environmental emerging contaminants (Malhotra et al., 2020). The ever-growing demand for modern electronic equipment, which production relies on REE, engenders excessive amounts of e-waste and the REE recycling industry is expanding, however, it is still at the development stage (Haque et al., 2014). Among the REE, La and Gd are used in numerous industrial processes and medical treatments. With increasing production and demand, it is expected that both elements' availabilities in the environment will augment. This highlights the urgent need for a better understanding of their biogeochemical behavior. Although the number of studies dealing with their ecotoxicological behavior has been increasing, no hot spot species have been used, and the endpoints are scattered and with potential conflicting results (Malhotra et al., 2020). Therefore, it is key to run more studies on different environmental levels and organisms. Additionally, the increased human footprint since the industrial revolution has resulted in another great environmental concern: climate change. Since then, human activities have continuously increased the emission of greenhouse gases that in turn trap solar energy contributing to the well-known Greenhouse Effect (Al-Ghussain, 2019). According to the Intergovernmental Panel on Climate Change (IPCC), greenhouse gas emissions are causing the warming of the planet and the oceanic uptake of CO_2, which leads to pH dropping on a global scale (Field, 2014). These two phenomena are known as Ocean Warming and Acidification and, depending on the World's region, can occur isolated or combined. Climate change impacts aquatic biota, by altering their fitness, reproduction, recruitment, and distribution (Barange et al., 2018). In the last decade, a growing body of evidence became available on the broad potential negative impacts of climate change on the toxicity of environmental contaminants (e.g., Buckman et al., 2007). It is also known that climate change can modify contaminants' toxicokinetic, enhancing their biological effects. Hence, the scientific community increasingly became aware of the need to investigate the interaction between climate change and contaminants (Noyes et al., 2009; Schiedek et al., 2007). Nevertheless, the current knowledge on the potential

interactions between climate change and REE is virtually non-existent. The main challenge was to evaluate the availability of La and Gd under environmental conditions closely related to climate changes scenarios. This study will also contribute to the baseline knowledge by which future research towards understanding REE patterns and toxicity will build upon. Given this context, we designed an experiment with Lanthanum (La) and Gadolinium (Gd) levels (1.5 µg L^{-1} and 1 µg L^{-1}, respectively) in fresh-, brackish- and saltwater. Concentrations were monitored during eight sampling occasions over 24 hours in present-day and climate change conditions (T°=+4°C, pH=△0.4). The designed experiments also contribute to the discussion of methodology impairments in laboratory experiments used to study the ecotoxicological effects of REE.

4.2 MATERIAL AND METHODS

4.2.1 Experimental Setup

Although REE are known to behave coherently, their grouping is inconsistent among authors. Here, La and Gd were chosen as representatives of Light and Heavy rare earth elements (Anastopoulos, 2016), respectively. The dissolved concentration of both REEs vary in a broad range in the aquatic environment from ng L^{-1} to hundreds of µg L^{-1} (e.g., Trapasso et al., 2021). Therefore, it was optioned to select metal exposure concentrations in an average value avoiding the extremes where negligible or excessive changes may exist. The exposure experiment with La was performed with 1.5 µg L^{-1} while the Gd exposure was 1 µg L^{-1} of Gd. Furthermore, the selected environmentally relevant exposure concentrations fall within the exposure range of other experiments (e.g., Malhotra et al., 2020). Standard solutions of $LaCl_3$ and $GdCl_3$ were used as a source of both metals. The exposure experiments were conducted with freshwater (Sal=0), brackish water (Sal=15) and seawater (Sal=35) to reflect different aquatic environments, from rivers and lakes to estuaries and the open sea. Springwater collected at 41°28'05.8"N and 8°12'08.9"W (NE Portugal) was used for the freshwater experiment. For the seawater experiment, coastal water was collected in 38°40'45.5"N and 9°20'12.1"W (West Europe). Both freshwater and seawater were filtered through 0.45 µm membranes before use. By mixing the seawater with spring water, brackish water was obtained with salinity 15. The experiments were performed in individual 1L glass beakers. The different environmental conditions studied (temperature and acidification)

were set to mimic climate change scenarios taking the IPCC end-century predictions (Field, 2014): temperature increase of up to 4°C and a pH decrease of up to 0.4 units. All the used material was previously decontaminated with HNO_3 (20% v/v) and washed with ultra-pure water (18.2 MΩ.cm). Each beaker was filled with water (spring, brackish or seawater) and continuously aerated water and randomly distributed in two temperature-controlled water baths. The environmental conditions were altered to: i) Initial condition (Control T°C and pH); ii) Acidification (pH=△0.4); iii) Warming (T°=+4°C) and iv) Warming & Acidification (T°=+4°C, pH=△0.4). The experiment comprised twelve treatments as follow: i) Initial Cond; ii) Initial Cond + La; iii) Initial Cond + Gd; iv) Acidification; v) Acidification + La; vi) Acidification + Gd; vii) Warming; viii) Warming + La; ix) Warming + Gd; x) Warming & Acidification; xi) Warming & Acidification + La and xii) Warming & Acidification + Gd.

The temperature was kept stable in the two water baths (18 °C ± 0.3 °C for the control temperature treatments and 22±0.3 °C for the warming treatments) through submerged heaters (V2Therm 200W, TMC Iberia) and chillers (Hailea, HC-250 A). Water pH was automatically regulated by the controlling system Profilux 3.1T (GHL) connected to pH probes (GHL) which monitored pH in each glass beaker every 2 seconds. Upregulation was done with filtered air and downregulated via solenoid valves (Etopi) with CO_2 injection. Hysteresis was kept at ± 0.05 units of pH. Master parameters were measured with a portable pH and temperature probe (VWR pHenomenal) and salinity with a refractometer (V2, TMC Iberia). Carbonate system speciation was calculated from pH measurements and total alkalinity (Alkalinity checkers, Hanna® Instruments) using CO2SYS software (Pierrot et al., 2006). Due to the natural pH fluctuations inherent in the types of water studied, the freshwater pH was adjusted at 7.90±0.10 for the Control pH treatments and 7.52±0.11 for the Acidification treatments. The brackish water pH was kept at 8.07±0.05 for the Control pH treatments, and 7.70±0.11 for the Acidification treatments and the seawater pH was maintained at 8.29±0.06 and 7.83±0.11 for the Control pH and Acidification treatments, respectively.

Water aliquots were sampled after 15 minutes (15'), 30 minutes (30'), one hour (1h), two hours (2h), four hours (4h), six hours (6h), twelve hours (12h) and twenty-four hours (24h) of the exposure.

4.2.2 Lanthanum and Gadolinium quantification

Water aliquots (as triplicates) taken at each time were filtrated (0.45 µm, MF-Millipore TM, Merk) and acidified (2% Ultrapur® HNO_3). Dissolved La and Gd levels were determined using a quadrupole ICP-MS (Perkin-Elmer NexION 2000C), equipped with a cyclonic spray chamber, a concentric Meinhard nebulizer and a dual detector. The ^{139}La and ^{158}Gd were the quantified isotopes since they present minimum isobaric and polyatomic interferences by setting the ratios $^{137}Ba^{++}/^{137}Ba$ and $^{140}Ce^{16O}/^{140}Ce$ to 0.010 under routine operating conditions. Metals in spring waters samples were measured by direct aspiration into the ICP-MS, while brackish and seawater were diluted to salinity ~3 with Milli-Q water to minimize matrix interference.

Quality Control (QC) solutions were run every 20 samples, and a 6-point calibration curve within a range of 1 to 1000 µg L^{-1} was used for quantification, using ^{115}In as internal standard. Three reagent blanks and random sample duplicates were included within each batch of 20 samples to control the analytical quality of the method and accounted for less than 1% of the total La and Gd concentration in the samples. The detection limits were 0.022, 0.024 and 0.034 µg L^{-1} for La and 0.006, 0.016 and 0.010 µg L^{-1} for Gd in spring, brackish and seawater, respectively.

4.2.3 Statistical analyses

A one-way ANOVA approach was applied, for La and Gd levels, with Salinity as the treatment factor to investigate differences between salinities. This was followed by all pairwise comparisons between the predicted means of the salinity factor using Tukey's procedure (Braun, 1995). The analysis of variance two-way ANOVA was later used with temperature and pH as the treatment factors to identify differences in La and Gd levels, between treatments, for each salinity, and all pairwise comparisons using Tukey post hoc tests were assessed. Lastly, to evaluate the effect of time on La and Gd levels, a one-way ANOVA was applied for each spiked treatment, followed by all Tukey's pairwise comparisons. Whenever necessary, data were Log transformed to conform with the assumptions of normality (independence and homogeneity of variances). Statistical analyses were performed at a significance level of 0.05 using the open-source software InVivoStat, version 4.1.

4.3 RESULTS

A summary of seawater physicochemical parameters and specifics of the carbonate system for all treatments and salinities (mean ± standard deviation) is presented in Table 4.1.

Table 4.1 – Summary of physicochemical parameters and specifics of carbonate system for all treatments and salinities (mean ± standard deviation). Measured temperature (°C), pH (full scale) and total alkalinity (TA, µmol kg^{-1} SW) were used to calculate carbonate system parameters: pCO_2 (carbon dioxide partial pressure, µatm) and TC (total inorganic carbon, µmol kg^{-1} SW).

	Treatment		Temperature (°C)	pH (total scale)	TA (µmol kg^{-1} SW)	TC (µmol kg^{-1} SW)	pCO_2 (µatm)
Sal 0	Control	Present-day	18±0.2	7.89±0.10	520	323	230
		Acidification	18±0.2	7.54±0.09	360	401	1016
		Warming	22±0.4	7.87±0.11	580	477	276
		Warming & Acidification	22±0.2	7.52±0.10	700	745	1346
	La	Present-day	18±0.2	7.9±0.08	700	305	303
		Acidification	18±0.2	7.53±0.12	620	498	644
		Warming	22±0.3	7.91±0.09	780	475	337
		Warming & Acidification	22±0.4	7.52±0.12	600	650	656
	Gd	Present-day	18±0.3	7.89±0.13	380	384	243
		Acidification	18±0.4	7.49±0.09	520	547	729
		Warming	22±0.4	7.91±0.09	540	533	216
		Warming & Acidification	22±0.2	7.49±0.12	680	846	992
Sal 15	Control	Present-day	18±0.3	8.12±0.06	1760	1695	320
		Acidification	18±0.2	7.68±0.12	1760	1936	1003
		Warming	22±0.3	7.98±0.10	1760	1670	458
		Warming & Acidification	22±0.4	7.72±0.13	1980	2038	1161
	La	Present-day	18±0.3	8.11±0.04	1700	1632	317
		Acidification	18±0.3	7.67±0.15	1840	1918	1024
		Warming	22±0.2	8.13±0.05	1740	1655	310
		Warming & Acidification	22±0.4	7.73±0.10	1920	2068	946
	Gd	Present-day	18±0.4	8.01±0.04	1680	1635	405
		Acidification	18±0.3	7.69±0.09	1860	1914	1091
		Warming	22±0.3	7.99±0.03	1800	1718	461
		Warming & Acidification	22±0.3	7.70±0.06	1980	1993	1046
Sal 35	Control	Present-day	18±0.4	8.22±0.04	2700	2325	283
		Acidification	18±0.3	7.89±0.10	2980	2711	773
		Warming	22±0.3	8.18±0.05	2740	2314	318
		Warming & Acidification	22±0.3	7.88±0.11	2960	2605	788
	La	Present-day	18±0.4	8.20±0.07	2520	2248	278
		Acidification	18±0.3	7.86±0.13	2620	2579	818
		Warming	22±0.2	8.19±0.08	2600	2289	292
		Warming & Acidification	22±0.3	7.79±0.09	2680	2648	904
	Gd	Present-day	18±0.3	8.17±0.06	2580	2324	311
		Acidification	18±0.3	7.78±0.10	2640	2740	907
		Warming	22±0.4	8.21±0.08	2780	2454	296
		Warming & Acidification	22±0.3	7.77±0.15	2700	2752	960

Mean and standard deviation of dissolved La and Gd levels (µg L^{-1}) in freshwater (salinity 0), brackish water (salinity 15), and seawater (salinity 35) sampled at 15', 30', 1h, 2h, 4h, 6h, 12h and 24h are presented in Annex 3, Supplemental Table 4.1. The ANOVA results are shown in Annex 3, Supplemental Tables 4.2, 4.3 and 4.4 (A and B).

4.3.1 Salinity

Different salinities affected dissolved La and Gd levels ($p < 0.0001$, Annex 3, Supplemental Table 4.2). During the first 24h, La concentrations found in freshwater are significantly lower than in brackish- and seawater (Tukey test, $p<0.0001$). However, the levels did not vary significantly between brackish- and seawater (Tukey test, $p=0.53$). On the other hand, Gd concentrations presented significant differences between the three water types (Tukey test, $p<0.0001$), with higher values in sea-, followed by brackish- and freshwater.

4.3.2 Temperature and pH

Temperature is a significant factor ($p<0.0001$, Annex 3, Supplemental Table 4.3) for the availability of dissolved La in freshwater, unlike pH alone ($p=0.12$). All treatments showed differences amongst them, except Control T°C and pH vs Acidification ($p=0.74$). For dissolved Gd in freshwater, levels were significantly affected only by the interaction Temperature * pH ($p=0.021$). In fact, it was only when the Gd concentrations from the Control T°C and pH were compared with the Acidification treatment that significant differences were found ($p=0.011$).

Temperature, pH, and their interaction did not significantly influence dissolved La or Gd levels in brackish- and seawater ($p > 0.05$).

4.3.3 Time course evolution of La and Gd

For salinity 0 treatments without La or Gd added, both elements' concentrations were below detection limit (0.022 µg L^{-1} for La and 0.006 µg L^{-1} for Gd). Conversely, the La and Gd levels in different treatments varied significantly through time ($p<0.0001$, Annex 3, Supplemental Table 4.4A). The uppermost concentration of La was registered in the Warming (1.3±0.054 µg L^{-1}), after 15 minutes of exposure, followed by Warming & Acidification (1.1±0.039 µg L^{-1}) treatment (Figure 4.1A, Annex 3, Supplemental Table 4.1).

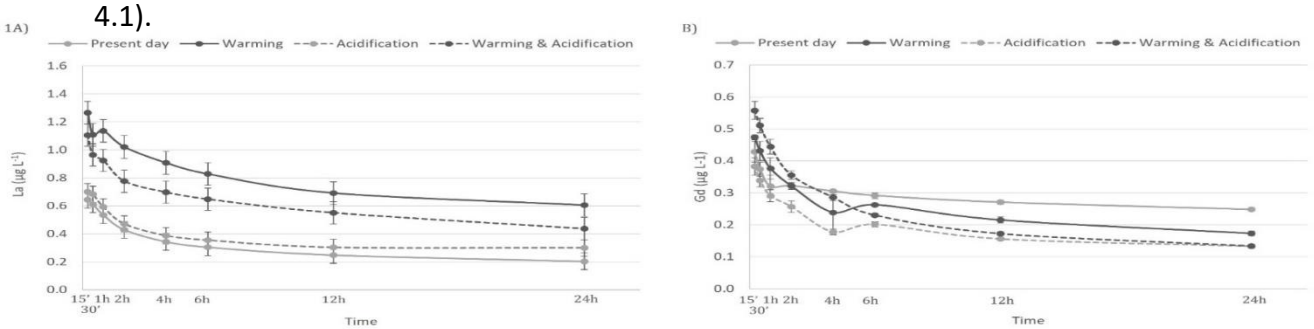

Figure 4.1 – Time course evolution of a) Lanthanum and b) Gadolinium levels (µg L^{-1}) in spiked treatments with 1.5 µg L^{-1} and 1 µg L^{-1}, respectively, for different sampling times (15', 30', 1h, 2h, 4h, 6h, 12h and 24h) at salinity 0. Values represent means ± SD.

The present-day treatment registered 0.64±0.031 µg L^{-1}, and the Acidification treatment 0.70±0.011 µg L^{-1}, after the same exposure time. In the course of 24 hours, the levels of dissolved La at present-day conditions dropped 67% to 0.20±0.010 µg L^{-1}, being the treatment that registered the largest decrease. The La concentrations in the Acidification treatment fell overtime 57% to 0.30±0.007 µg L^{-1}, and in the Warming & Acidification treatment dropped 56% to 0.44±0.011 µg L^{-1}. After 24h, the La values in the Warming treatment listed 0.61±0.011 µg L^{-1}, having dropped 53% then the values registered at 15'. Similarly, Gd levels also registered a great percentage decrease overtime (Figure 4.1B). The Warming & Acidification treatment registered the most significant Gd decrease (77%) from 0.56±0.028 µg L^{-1} at 15' to 0.13±0.004 µg L^{-1} at 24h, followed by the Acidification treatment (66%) from 0.38±0.027 µg L^{-1} to 0.13±0.006 µg L^{-1}, over the same period. The highest Gd level in the Warming treatment registered 0.47±0.007 µg L^{-1} at 15', and the lowest at 24 h (0.17±0.007 µg L^{-1}, 64% decrease). The Control T°C and pH treatment, at salinity 0, presented the minor Gd decline over time (42%) ranging from 0.43±0.033 µg L^{-1} at 15' to 0.25±0.005 µg L^{-1} at 24h (Annex 3, Supplemental Table 4.1).

For salinity 15, the baseline La levels in the control treatments varied between 0.03±0.001 µg L^{-1} and 0.09±0.007 µg L^{-1} (Annex 3, Supplemental Table 4.1). After 15 minutes of exposure, the La concentrations were higher than those observed in the salinity 0 trial (Figure 4.2A) and similar to the four treatments.

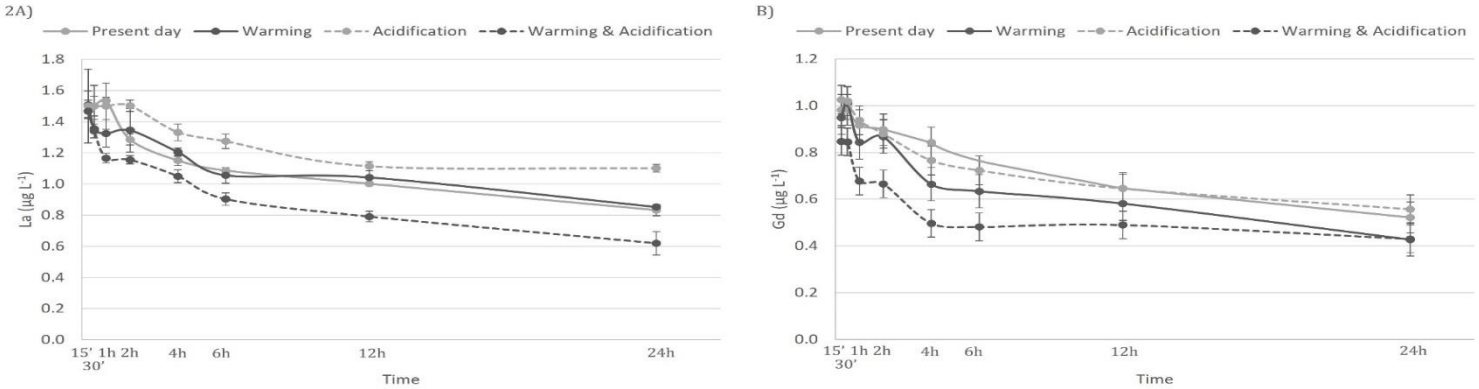

Figure 4.2 – Time course evolution of a) Lanthanum and b) Gadolinium levels (µg L^{-1}) in spiked treatments with 1.5 µg L^{-1} and 1 µg L^{-1}, respectively, for different sampling times (15', 30', 1h, 2h, 4h, 6h, 12h and 24h) at salinity 15. Values represent means ± SD.

Despite presenting globally higher La levels, the percentage of La decreased over time is comparable to that shown in salinity 0. The percentage is 45% in the Control T°C and pH treatment (0.83±0.036 µg L^{-1} at 24h), 43% in the Warming treatment (0.85±0.01 µg L^{-1} at 24h), 27% in the Acidification treatment (1.1±0.025 µg L^{-1} at 24h) and 59% in

the Warming & Acidification treatment (0.62±0.075 µg L^{-1} at 24h). The time course evolution of La in Warming and Warming & Acidification conditions varied significantly throughout the 24h (p=0.002 and p=0.001, respectively).

The baseline Gd levels in the salinity 15 experiments ranged between 0.02±0.001 µg L^{-1} and 0.09±0.007 µg L^{-1} (Annex 3, Supplemental Table 4.1). At 15 minutes Gd levels registered 1.0±0.043 µg L^{-1} in the Acidification treatment, 0.98±0.052 µg L^{-1} in the present-day treatment, 0.95±0.029 µg L^{-1} in the Warming treatment and 0.85±0.017 µg L^{-1} in the Warming & Acidification treatment (Figure 4.2B). During the 24 hours experiment the Gd in these treatments decreased 44, 47, 55 and 49%, to 0.56±0.014 µg L^{-1}, 0.52±0.022 µg L^{-1}, 0.43±0.007 µg L^{-1} and 0.43±0.021 µg L^{-1}, respectively. However, these time variations have no significance at the statistical level (p>0.05).

The baseline La levels in salinity 35 fluctuated between 0.04±0.001 µg L^{-1} and 0.09±0.006 µg L^{-1} (Annex 3, Supplemental Table 4.1).

The percentage of La also decrease over time as found in the other salinities, but not progressively (Figure 4.3A).

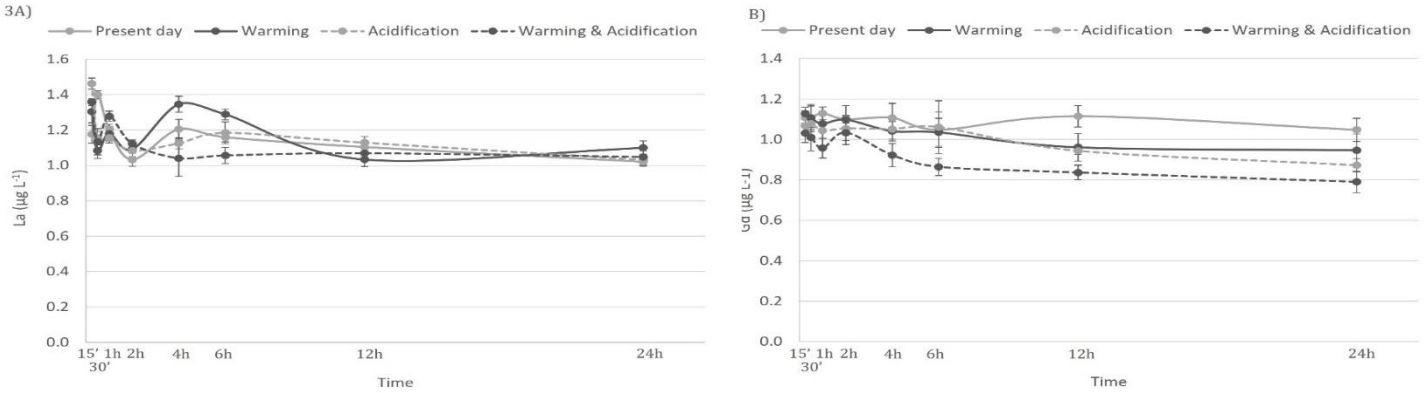

Figure 4.3 – a) Time course evolution of a) Lanthanum and b) gadolinium (µg L^{-1}) levels in spiked with 1.5 µg L^{-1} and 1 µg L^{-1}, treatments, respectively, in different sampling times (15', 30', 1h, 2h, 4h, 6h, 12h and 24h) at salinity 35. Values represent means ± SD.

The Acidification treatment presented 1.5±0.030 µg L^{-1} of dissolved La at 15' and 1.0±0.030 at 24h, representing a 29% decrease. The Warming & Acidification treatment showed a 23% La reduction from 1.4±0.020 µg L^{-1} at 15' to 1.1±0.034 µg L^{-1} at 24h. Lanthanum exposed to the Warming conditions peaked at 15' (1.3±0.064 µg L^{-1}) and decreased 15% on the course of 24h (1.1±0.040 µg L^{-1}). The lowest La percentage drop (14%) was exhibited by the Control T°C and pH treatment (1.2±0.050 µg L^{-1} at 15' to 1.0±0.025 µg L^{-1} at 24h). This up and down variability of La concentration in all treatments had no significance (p>0.05).

The Gd levels in the control treatments swung from 0.02±0.001 µg L^{-1} to 0.09±0.010 µg L^{-1} (Annex 3, Supplemental Table 4.1). The Gd level at the Control T°C and pH was the most stable of the experiment, having ranged from 1.1±0.034 µg L^{-1} to 1.1±0.057 µg L^{-1} (Figure 4.3B). The second lowest Gd decrease occurred in the Warming treatment (14%), with 1.1±0.031 µg L^{-1} after 15 minutes and 0.95±0.080 µg L^{-1} after 24hours. The Acidification and Warming & Acidification treatments registered a Gd decrease of 21%. The first sampled aliquots registered 1.1±0.041 µg L^{-1} and 1.0±0.048 µg L^{-1}, and 24h upon the spike both treatments registered 0.87±0.033 µg L^{-1} and 0.79±0.053 µg L^{-1}, respectively. The 24h experiment did not showcase significant differences in Gd levels in the studied treatments ($p>0.05$).

4.3.4 Lanthanum and Gd speciation

Lanthanum and Gd speciation analysis were carried out in Visual MINTEQ program (version 3.1), using the measured average pH, temperature, and La and Gd values for each treatment. The concentrations of major elements (i.e., Ca^{2+}, Na^{+}, Cl^{-}, CO_3^{2-}, Mg^{2+}, SO_4^{2-}) from the spring water and seawater (Pontié et al., 2014) was used as components for the speciation calculus (Gustafsson, 2011). The modelled percentage distribution among La and Gd species for all salinities is presented in Table 4.2.

Table 4.2 – Percentage distribution among La and Gd species for La (1.5 µg L^{-1}) and Gd (1 µg L^{-1}) treatments for salinity 0, 15 and 35.

		Treatment	La^{3+}	$LaCl^{2+}$	$LaOH^{2+}$						
Sal 0	La	Present day conditions	93.5	0.13	6.4						
		Acidification	97.2	0.13	2.7						
		Warming	91.9	0.13	8.0						
		Warming & Acidification	96.5	0.13	3.4						
			Gd^{3+}	$GdCl^{2+}$	$GdOH^{2+}$						
	Gd	Present day conditions	62.6	0.052	37.4						
		Acidification	80.7	0.067	19.2						
		Warming	55.5	0.046	44.5						
		Warming & Acidification	75.8	0.063	24.2						
			La^{3+}	$LaOH^{2+}$	LaF^{2+}	$LaCl^{2+}$	$La(SO_4)^{2-}$	$LaSO_4^{+}$	$LaHCO_3^{2+}$	$La(CO_3)^{2-}$	$LaCO_3^{+}$
Sal 15	La	Present day conditions	48.0	1.4	0.63	0.69	3.8	41.5	0.063	0.021	3.8
		Acidification	49.6	0.59	0.65	0.71	4.0	42.9	0.066	-	1.6
		Warming	45.9	1.7	0.62	0.67	4.3	42.8	0.065	0.024	3.9
		Warming & Acidification	47.5	0.72	0.64	0.69	4.5	44.3	0.069	-	1.7
			Gd^{3+}	$GdHCO_3^{2+}$	$GdOH^{2+}$	GdF^{2+}	GdF^{2+}	$GdCl^{2+}$	$Gd(SO_4)^{2-}$	$GdSO_4^{+}$	$Gd(CO_3)^{2-}$	$GdCO_3^{+}$
	Gd	Present day conditions	37.5	0.052	9.8	0.014	2.6	0.33	2.5	33.3	0.25	13.7
		Acidification	43.7	0.061	4.6	0.017	3.0	0.39	2.9	38.8	0.048	6.4
		Warming	34.8	0.052	12.1	0.012	2.4	0.31	2.6	33.7	0.28	13.7
		Warming & Acidification	41.3	0.063	5.7	0.015	2.9	0.36	3.1	39.9	0.054	6.6
			La^{3+}	$LaOH^{2+}$	LaF^{2+}	$LaCl^{2+}$	$La(SO_4)^{2-}$	$LaSO_4^{+}$	$LaHCO_3^{2+}$	$La(CO_3)^{2-}$	$LaCO_3^{+}$
Sal 35	La	Present day conditions	43.0	1.2	0.73	8.6	6.4	34.3	0.077	0.072	5.64
		Acidification	44.8	0.50	0.76	9.0	6.7	35.8	0.083	0.013	2.43
		Warming	43.9	1.4	0.71	8.3	7.1	32.6	0.079	0.081	5.76
		Warming & Acidification	45.9	0.60	0.75	8.7	7.4	34.0	0.086	0.014	2.50
			Gd^{3+}	$GdHCO_3^{2+}$	$GdOH^{2+}$	GdF^{2+}	GdF^{2+}	$GdCl^{2+}$	$Gd(SO_4)^{2-}$	$GdSO_4^{+}$	$Gd(CO_3)^{2-}$	$GdCO_3^{+}$
	Gd	Present day conditions	33.8	0.062	8.0	0.028	3.0	4.1	4.1	26.3	0.84	19.8
		Acidification	40.8	0.077	3.8	0.033	3.6	4.9	4.9	31.8	0.17	9.9
		Warming	34.2	0.062	9.9	0.024	2.8	3.7	4.3	24.4	0.91	19.7
		Warming & Acidification	41.8	0.079	4.8	0.029	3.4	4.6	5.3	29.8	0.19	10.0

Despite La^{3+} and Gd^{3+} being dominant in the three studied salinities, their percentage varied greatly between them. At salinity 0, La^{3+} was most present in the Acidification (97.2%) and Warming & Acidification treatment (96.5%), while presenting the lowest percentage in the Warming treatment (91.9%) followed by 93.5% in the Control TºC and pH treatment. The ion Gd^{3+} followed this trend, constituting 80.7% of species in the Acidification treatment and 75.8% in the Warming & Acidification treatment. In general, the fraction of the Gd free ion in solution was lower than the trivalent La. The lowest percentage of Gd^{3+} was 55.5% in the Warming treatment. At present-day conditions (Control T°C and pH), 62.6% of species were Gd^{3+}. The second most present form for both elements was the complexed $LaOH^{2+}$ and $GdOH^{2+}$, but with great percentage differences between them.

At salinity 15, both La^{3+} and Gd^{3+} were present at lower percentages than at salinity 0. The ions La^{3+} and Gd^{3+} were present at the lowest percentage in the Warming treatment (45.9% and 34.8%, correspondingly) and the highest percentage in the Acidification treatment (49.6% and 43.7%, respectively). The second most common species in salinity 15 were La and Gd sulfate complexes: $LaSO_4^+$ and $GdSO_4^+$, respectively

The percentage of the free ions La^{3+} and Gd^{3+} species decreased further at salinity 35. The highest percentage of La^{3+} occurred in the acidification treatment (43.7%) and lowest in the Warming treatment (34.8%). The trivalent Gd^{3+} peaked in the Warming & Acidification treatment (41.8%) and was lowest in the Control T°C and pH treatment (33.8%).

4.4 DISCUSSION

The REE show very similar geochemical behavior, although the lanthanide contraction (ionic radius decrease from La to Lu) leads to gradual changes in their physicochemical properties. The trivalent REE ions present different affinity towards surface adsorption and complexation with ligands (e.g., carbonates, phosphates and hydroxides) in solution due to this lanthanide contraction, which ultimately leads to HREE greater stability in solution and preferential adsorption of LREE on colloids and suspended particulate material (Erel and Stolper, 1993). Furthermore, REE bioavailability varies with ionic and ligand loads and decreases with free ions and organic or inorganic complexes (Borrego et al., 2012). This organic complexation are different

across La to Lu series (Byrne and Li, 1995; Ebrahimi and Barbieri, 2019). Therefore, it is challenging to fully understand REE behaviour in natural waters due to the formation of complexes, colloids, ion exchange and adsorption, which in turn can lead to fractionation (Biddau et al., 2002).

We showed that La and Gd behave differently from salinity 0 to 35. Our results showed that a temperature increase of 4°C in freshwater rises the availability of dissolved La. However, the decrease of 0.4 pH units has not changed the availability of both elements. On the other hand, Gd levels at present-day settings were higher than the ones at the Acidification treatment, both at the same T°C (18°C). Zhang et al. (2019) studied the REE dissolved distributions in small streams in China and found that anthropogenic Gd presented seasonal variations, being, for example, diluted by fresh rainwater. Additionally, the studied water masses exhibited HREE enrichment due to adsorption reactions that decreased the LREE in solution. At present-day conditions, for salinity 0, La decreased 67% over the 24h, while the Gd decreased 42%. This discrepancy may be related to increased La adsorption to all systems in the aquaria (glass, plastic air tubes, pH probe, etc.). Other hypothesis is the removal of both elements through the precipitation as hydroxides during the 24h experiment. On other hand, the IPCC projection of 4°C increase may be less extreme as the temperature variation exhibited in different seasons, or extreme events, which suggest an increased removal of La and Gd from the dissolved fraction. Sholkovitz (1995) determined how pH, salinity and colloids affect REE fractionation in the river and estuarine waters and described that both fractionation and concentration of dissolved REE in freshwaters are pH-dependent. Moermond et al. (2001) and Åström and Corin (2003) stated that REE concentration has an inverse correlation to river water pH and Goldstein and Jacobsen (1988) measured REE in several rivers in North America and found that low pH rivers present high REE concentrations while rivers with a pH of 8 exhibited low light REE concentrations and were HREE enriched. These findings are based on broad changes of pH, which was not mimicked in our study since we searched for REE differences associated with only increased acidification of 0.4 units. Therefore, it was expected no significant differences of La ($p>0.05$) at salinity 0 in the Control T°C and pH and Acidification treatments. Otherwise, this was not followed by Gd as their levels in the Acidification treatment were significantly lower ($p=0.011$) than the ones at the Control T°C and pH. Goldstein

and Jacobsen (1988) showed that in freshwater medium the temperature is a major driver affecting dissolved La availability presumably because minor pH variation was found in their work. The Warming and Warming & Acidification treatments presented significantly higher La levels than their Control T°C counterparts. The toxicity of several metals is pH-modulated (Luís et al., 2014) however very few studies reported this for REE, and are majorly focused on extreme events such as acid rains (Liang and Wang, 2013). Rivers are the major source of elements to the oceans and the behaviour of REE in freshwater should be further investigated. The concentration of La and Gd decreased greatly over 24h, at salinity 0, in all studied treatments (Annex 3, Supplemental Table 4.4 A and B), which bring additional challenges in ecotoxicology studies. Furthermore, this decrease has not reached a plateau pointing to continuous removal of both elements from the dissolved fraction. Therefore, in 24h studies, or longer, freshwater biota will be subject to different contamination levels and biological effects may change. The desired REE exposure concentration should be monitored in a shorter time scale or additional actions of changing the medium and re-spiking should be done to maintain conditions.

Regarding our results for salinity 15 (brackish water), the percentages of La and Gd removal was lower than those found in freshwater pointing to higher stability of both elements in the dissolved fraction. Most studies showed a higher removal of REE in the mixing area of fresh to seawater (Elderfield et al., 1990; Lawrence and Kamber, 2006; Pokrovsky et al., 2014). This removal is mainly related to the increase of particulate material, generation of colloids and precipitation of Al, Fe and Mn compounds (Kulaksiz and Bau, 2007; Tepe and Bau, 2016). These new particles promote sorption and precipitation reactions that scavenge REE into the solids. In our systems this perturbation of REE equilibria do not exit and therefore, dissolved species tend to be more stable in solution presumably due to increased complexation with chloride and sulphate ions. In the present study, temperature significantly affect the La levels in freshwater (Annex 3, Supplemental Table 4.3). Furthermore, seasonality and tides, which in turn may impose broader variability of temperature, may further impacting REE availability. Additionally, at salinity 15 the La levels in the Warming and Warming & Acidification treatment varied significantly through time, which highlights the effect of temperature in their availability. Dissolved La and Gd levels in seawater showed lower

variability than at salinity 0 and 15 since the percentage loss was the lowest and concentrations did not vary between treatments. In these seawater experiment, the speciation of both elements is much different from the observed in the other trials. Lower percentages of trivalent La and Gd free ions in solution and increased proportion of sulphate and chloride complexes were found in saltwater. The quantification of the total concentrations of REE in water is not directly linked to their potential interactions with the environment, bioaccumulation, and toxicological effects. Oral et al. (2010) described the toxicity of REE on sea urchin embryos and sperm and reported that levels ranged between 0.02 and 2 μg g^{-1} dry weight (dw), which were between 4 and 7 orders of magnitude above the concentration on the water. Studies evaluating the REE bioaccumulation and toxicity should investigate and report their availability in the water to provide a more comprehensive overview of these processes.

Yang et al. (1999) established a static aquatic microcosm to evaluate the distribution of five REEs, including La and Gd. They found that the sediment was the major reservoir for REE with 80-90% of both elements sediment, and a significant proportion in water reached 8% for La and 17% for Gd. This partitioning of REE in aquatic environments is key to understanding the intricacies of REE availability, accumulation, and toxicity. Trifuoggi et al. (2017) studied REE (Y, La, Ce, Nd, Sm, Eu and Gd) toxicology in the early life stages of two sea urchin species. They observed different toxicity patterns for individual REEs, and these patterns vary for each studied sea urchin species and treatment protocol. This highpoint the distinct toxicity patterns among REE and the urgent need to further study their behaviour. For example, Gd-based contrast agents are chelated and used as contrast media for magnetic resonance imaging (MRIs) that are globally considered safe to humans at recommended dosing levels (Rogosnitzky and Branch, 2016). This stability in the aquatic environment (sediment, water, suspended matter) is nevertheless understudied. Still, it is known that the decomposition of these compounds may lead to the release of free Gd ions to the solution, which is a more toxic form. Perrat et al. (2017) studied the Gd bioaccumulation in the digestive gland and gills of two edible bivalve species (i.e., *Dreissena rostriformis bugensis* and *Corbicula fluminea*) and showed that it could be accumulated in these tissues even as only present as the stable Gd-contrast agents, raising concerns regarding their toxicity. Our results

showed that at salinity 35, several Gd complexes are theoretically stable, which raises the relevance of studying each element speciation for ecotoxicological studies.

REE speciation depends on salinity, pH and the presence of anions (Aqeel Ashraf et al., 2012; Liang et al., 2005). The speciation, in turn, regulates solubility and bioavailability (Khan et al., 2017). Solubility is also dependent on pH and temperature. Speciation analysis conducted by Johannesson et al. (2004) in the organic-rich waters evidenced that dissolved REE bound with organic matter. Therefore, a clear understanding of metal speciation during the exposure phase in ecotoxicology trials is key to broadening our knowledge of toxicity to aquatic organisms. Carbonates, phosphates and hydroxides may decrease dissolved REE concentration in water (Delgado et al., 2012; Foucault-Collet et al., 2013). However, the dissolved complexes $LaSO_4^+$ and $GdSO_4^+$ were the second most common species at salinity 15 and 35. The availability of chloride and carbonate anions in brackish and seawater leads to a change of speciation of La and Gd with a significant decrease of free ions, which are considered the most toxic species (Das et al., 1988; Hirano et al., 1996). The trivalent REE ions, such as La^{3+}, chemically resemble Ca^{2+}, with comparable ionic radii, and are potential competitors for Ca uptake (Herrmann et al., 2016). This could inhibit Ca-channels, with deleterious effects on biota. Furthermore, free Gd^{3+} is extremely toxic (Rogosnitzky et al., 2016). However, even with greater REE removal at lower salinities over 24-hours, the high proportion of trivalent ions at salinity 0 may influence the toxicity responses and should be the subject of great attention for upcoming ecotoxicology studies.

4.5 CONCLUSIONS

The findings of this work showed that temperature affects the availability of La in freshwater systems and the pH decrease caused a reduction in Gd concentrations. La and Gd levels decreased over 24h, at salinity 0, which should lead to short-time scale monitoring of REE exposure concentrations. At salinity 15, La dissolved levels in the Warming (T°=+4°C) and Warming & Acidification (T°=+4°C, pH=△0.4) treatments decreased significantly through time, highlighting the interaction between climate change and the availability of this element in this medium. Dissolved La and Gd levels in seawater were kept at high levels and more stable with time. Nonetheless, with

demonstrated REE speciation changes from salinity 0 to 35, coming studies on the effects on biota should consider the baseline information presented in this study.

With virtually non-existent knowledge on the potential interactions between climate change and REE, we introduced new insights regarding REE availability and speciation in three salinities at present-day and near-future conditions. Nevertheless, the range of REE levels varies greatly depending on the aquatic system, and hence a broader assortment of concentrations should be tested in upcoming studies.

Climate change is forecasted to rise the occurrence and harshness of a wide array of pathogens, such as virus, parasites, toxins and to exacerbate the effects of pollutants. As verified, REE interactions with climate change variables are likely to occur. The lack of data and studies on both problematics highlights the urgent need to further assess this challenging topic.

ACKNOWLEDGEMENTS

This work was supported by Fundação para a Ciência e Tecnologia (FCT), through the project Climatoxeel (PTDC/AAG-GLO/3795/2014) awarded to Tiago F. Grilo and the strategic project UID/MAR/04292/2019 granted to MARE. Cátia Figueiredo acknowledges the FCT-PhD grant SFRH/BD/130023/2017 and the Early Career Research Grant awarded by National Geographic Society.

REFERENCES

Aharchaou, I., Beaubien, C., Campbell, P.G., Fortin, C., 2020. Lanthanum and cerium toxicity to the freshwater green alga *Chlorella fusca*: applicability of the Biotic Ligand Model. Environmental toxicology and chemistry 39, 996-1005.

Al-Ghussain, L., 2019. Global warming: review on driving forces and mitigation. Environmental Progress & Sustainable Energy 38, 13-21.

Anastopoulos, I., Bhatnagar, A., Lima, E.C., 2016. Adsorption of rare earth metals: A review of recent literature. Journal of Molecular Liquids 221, 954-962.

Aqeel Ashraf, M., Jamil Maah, M., Yusoff, I., Ghararibreza, M., 2012. Speciation of heavy metals in the surface waters of a former tin mining catchment. Chemical Speciation & Bioavailability 24, 1-12.

Åström, M., Corin, N., 2003. Distribution of rare earth elements in anionic, cationic and particulate fractions in boreal humus-rich streams affected by acid sulphate soils. Water research 37, 273-280.

Barange, M., Bahri, T., Beveridge, M.C., Cochrane, K.L., Funge-Smith, S., Poulain, F., 2018. Impacts of climate change on fisheries and aquaculture: synthesis of currrent knowledge, adaptation and mitigation options. FAO.

Biddau, R., Cidu, R., Frau, F., 2002. Rare earth elements in waters from the albitite-bearing granodiorites of Central Sardinia, Italy. Chemical Geology 182, 1-14.

Borrego, J., Carro, B., López-González, N., De La Rosa, J., Grande, J., Gómez, T., De La Torre, M., 2012. Effect of acid mine drainage on dissolved rare earth elements geochemistry along a fluvial–estuarine system: the Tinto-Odiel Estuary (SW Spain). Hydrology Research 43, 262-274.

Braun, H., 1995. The Collected Works of John W. Tukey: Vol. VIII, Multiple Comparisons 1948-1983. Journal of the Royal Statistical Society-Series A Statistics in Society 158, 629.

Buckman, A.H., Brown, S.B., Small, J., Muir, D.C., Parrott, J., Solomon, K.R., Fisk, A.T., 2007. Role of temperature and enzyme induction in the biotransformation of polychlorinated biphenyls and bioformation of hydroxylated polychlorinated biphenyls by rainbow trout (*Oncorhynchus mykiss*). Environmental science & technology 41, 3856-3863.

Byrne, R.H., Li, B., 1995. Comparative complexation behavior of the rare earths. Geochimica et Cosmochimica Acta 59, 4575-4589.

Das, T., Sharma, A., Talukder, G., 1988. Effects of lanthanum in cellular systems. Biological Trace Element Research 18, 201-228.

Delgado, J., Pérez-López, R., Galván, L., Nieto, J.M., Boski, T., 2012. Enrichment of rare earth elements as environmental tracers of contamination by acid mine drainage in salt marshes: a new perspective. Marine Pollution Bulletin 64, 1799-1808.

Ebrahimi, P., Barbieri, M., 2019. Gadolinium as an emerging microcontaminant in water resources: threats and opportunities. Geosciences 9, 93.

Elderfield, H., Upstill-Goddard, R., Sholkovitz, E., 1990. The rare earth elements in rivers, estuaries, and coastal seas and their significance to the composition of ocean waters. Geochimica et Cosmochimica Acta 54, 971-991.

Erel, Y., Stolper, E.M., 1993. Modeling of rare-earth element partitioning between particles and solution in aquatic environments. Geochimica et Cosmochimica Acta 57, 513-518.

Field, C.B., 2014. Climate change 2014–Impacts, adaptation and vulnerability: Regional aspects. Cambridge University Press.

Figueiredo, C., Raimundo, J., Lopes, A.R., Lopes, C., Rosa, N., Brito, P., Diniz, M., Caetano, M., Grilo, T.F., 2020. Warming enhances lanthanum accumulation and toxicity promoting cellular damage in glass eels (*Anguilla anguilla*). Environmental research 191, 110051.

Foucault-Collet, A., Gogick, K.A., White, K.A., Villette, S., Pallier, A., Collet, G., Kieda, C., Li, T., Geib, S.J., Rosi, N.L., 2013. Lanthanide near infrared imaging in living cells with Yb3+ nano metal organic frameworks. Proceedings of the National Academy of Sciences 110, 17199-17204.

Goldstein, S.J., Jacobsen, S.B., 1988. Rare earth elements in river waters. Earth and Planetary Science Letters 89, 35-47.

Gustafsson, J. P., 2011. Visual MINTEQ 3.0 user guide. KTH, Department of Land and Water Recources, Stockholm, Sweden.

Haque, N., Hughes, A., Lim, S., Vernon, C., 2014. Rare earth elements: Overview of mining, mineralogy, uses, sustainability and environmental impact. Resources 3, 614-635.

Herrmann, H., Nolde, J., Berger, S., Heise, S., 2016. Aquatic ecotoxicity of lanthanum–A review and an attempt to derive water and sediment quality criteria. Ecotoxicology and environmental safety 124, 213-238.

Hirano, S., Suzuki, K. T., 1996. Exposure, metabolism, and toxicity of rare earths and related compounds. Environmental health perspectives 104, 85-95.

Johannesson, K.H., Tang, J., Daniels, J.M., Bounds, W.J., Burdige, D.J., 2004. Rare earth element concentrations and speciation in organic-rich blackwaters of the Great Dismal Swamp, Virginia, USA. Chemical Geology 209, 271-294.

Khan, A.M., Bakar, N.K.A., Bakar, A.F.A., Ashraf, M.A., 2017. Chemical speciation and bioavailability of rare earth elements (REEs) in the ecosystem: a review. Environmental Science and Pollution Research 24, 22764-22789.

Kulaksız, S., Bau, M., 2007. Contrasting behaviour of anthropogenic gadolinium and natural rare earth elements in estuaries and the gadolinium input into the North Sea. Earth and Planetary Science Letters 260, 361-371.

Lawrence, M.G., Kamber, B.S., 2006. The behaviour of the rare earth elements during estuarine mixing—revisited. Marine Chemistry 100, 147-161.

Liang, C., Wang, W., 2013. Antioxidant response of soybean seedlings to joint stress of lanthanum and acid rain. Environmental Science and Pollution Research 20, 8182-8191.

Liang, T., Zhang, S., Wang, L., Kung, H.-T., Wang, Y., Hu, A., Ding, S., 2005. Environmental biogeochemical behaviors of rare earth elements in soil–plant systems. Environmental Geochemistry and Health 27, 301-311.

Luís, A.T., Bonet, B., Corcoll, N., Almeida, S.F., Da Silva, E.F., Figueira, E., Guasch, H., 2014. Experimental evaluation of the contribution of acidic pH and Fe concentration to the structure, function and tolerance to metals (Cu and Zn) exposure in fluvial biofilms. Ecotoxicology 23, 1270-1282.

Malhotra, N., Hsu, H.-S., Liang, S.-T., Roldan, M.J.M., Lee, J.-S., Ger, T.-R., Hsiao, C.-D., 2020. An Updated Review of Toxicity Effect of the Rare Earth Elements (REEs) on Aquatic Organisms. Animals 10, 1663.

Moermond, C.T., Tijink, J., van Wezel, A.P., Koelmans, A.A., 2001. Distribution, speciation, and bioavailability of lanthanides in the Rhine-Meuse estuary, The

Netherlands. Environmental Toxicology and Chemistry: An International Journal 20, 1916-1926.

Noyes, P.D., McElwee, M.K., Miller, H.D., Clark, B.W., Van Tiem, L.A., Walcott, K.C., Erwin, K.N., Levin, E.D., 2009. The toxicology of climate change: environmental contaminants in a warming world. Environment international 35, 971-986.

Oral, R., Bustamante, P., Warnau, M., d'Ambra, A., Guida, M., Pagano, G., 2010. Cytogenetic and developmental toxicity of cerium and lanthanum to sea urchin embryos. Chemosphere 81, 194-198.

Perrat, E., Parant, M., Py, J.-S., Rosin, C., Cossu-Leguille, C., 2017. Bioaccumulation of gadolinium in freshwater bivalves. Environmental Science and Pollution Research 24, 12405-12415.

Pierrot, D., Lewis, E., Wallace, D., 2006. MS Excel program developed for CO_2 system calculations. ORNL/CDIAC-105a. Carbon Dioxide Information Analysis Center, Oak Ridge National Laboratory, US Department of Energy, Oak Ridge, Tennessee 10.

Pokrovsky, O.S., Shirokova, L.S., Viers, J., Gordeev, V., Shevchenko, V.P., Chupakov, A., Vorobieva, T., Candaudap, F., Causserand, C., Lanzanova, A., 2014. Fate of colloids during estuarine mixing in the Arctic. Ocean Science 10, 107-125.

Pontié, M., Derauw, J.S., Plantier, S., Edouard, L., Bailly, L., 2013. Seawater desalination: nanofiltration—a substitute for reverse osmosis?, Desalination and Water Treatment 51, 485-494.

Rogosnitzky, M., Branch, S., 2016. Gadolinium-based contrast agent toxicity: a review of known and proposed mechanisms. Biometals 29, 365-376.

Schiedek, D., Sundelin, B., Readman, J.W., Macdonald, R.W., 2007. Interactions between climate change and contaminants. Marine pollution bulletin 54, 1845-1856.

Sholkovitz, E.R., 1995. The aquatic chemistry of rare earth elements in rivers and estuaries. Aquatic geochemistry 1, 1-34.

Strzeminska, I., Factor, C., Robert, P., Grindel, A.-L., Comby, P.-O., Szpunar, J., Corot, C., Lobinski, R., 2020. Long-term evaluation of gadolinium retention in rat brain after single injection of a clinically relevant dose of gadolinium-based contrast agents. Investigative radiology 55, 138.

Tepe, N., Bau, M., 2016. Behavior of rare earth elements and yttrium during simulation of arctic estuarine mixing between glacial-fed river waters and seawater and the impact of inorganic (nano-) particles. Chemical Geology 438, 134-145.

Trapasso, G., Chiesa, S., Freitas, R., & Pereira, E., 2021. What do we know about the ecotoxicological implications of the rare earth element gadolinium in aquatic ecosystems?. Science of the Total Environment, 146273.

Trifuoggi, M., Pagano, G., Guida, M., Palumbo, A., Siciliano, A., Gravina, M., Lyons, D.M., Burić, P., Levak, M., Thomas, P.J., 2017. Comparative toxicity of seven rare earth elements in sea urchin early life stages. Environmental Science and Pollution Research 24, 20803-20810.

Wang, L., Wang, W., Zhou, Q., Huang, X., 2014. Combined effects of lanthanum (III) chloride and acid rain on photosynthetic parameters in rice. Chemosphere 112, 355-361.

Yang, X., Yin, D., Sun, H., Wang, X., Dai, L., Chen, Y., Cao, M., 1999. Distribution and bioavailability of rare earth elements in aquatic microcosm. Chemosphere 39, 2443-2450.

Zhang, J., Wang, Z., Wu, Q., An, Y., Jia, H., Shen, Y., 2019. Anthropogenic rare earth elements: gadolinium in a small catchment in Guizhou Province, Southwest China. International journal of environmental research and public health 16, 4052.

Chapter 5

Accumulation, elimination, and neuro-oxidative damage under lanthanum exposure in glass eels (*Anguilla anguilla*)

Cátia Figueiredo [a,b,c*#], Tiago F. Grilo [a*], Clara Lopes [b], Pedro Brito [b,d], Mário Diniz [c], Miguel Caetano [b,d], Rui Rosa [a], Joana Raimundo [b,d]

[a] MARE, Marine and Environmental Sciences Centre, Laboratório Marítimo da Guia, Faculdade de Ciências da Universidade de Lisboa, Av. Nossa Senhora do Cabo 939, 2750-374, Cascais, Portugal

[b] IPMA, Portuguese Institute of Sea and Atmosphere, Rua Alfredo Magalhães Ramalho, 6, 1495-006 Lisbon, Portugal

[c] UCIBIO, REQUIMTE, Departamento de Química, Faculdade de Ciências e Tecnologia, Universidade NOVA de Lisboa, 2829-516 Caparica, Portugal

[d] CIIMAR, Marine and Environmental Research Center, Rua dos Bragas, 289, 4050-123 Porto, Portugal

Corresponding author:

* Authors equally contributed to the work.

Figueiredo, C.[#], Grilo, T. F.[#], Lopes, C., Brito, P., Diniz, M., Caetano, M., Rosa, R., Raimundo, J. 2018. Accumulation, elimination, and neuro-oxidative damage under lanthanum exposure in glass eels (*Anguilla anguilla*). Chemosphere 206, 414-423. (DOI 10.1016/j.chemosphere.2018.05.029)

ABSTRACT

Rare earth elements (REE) comprise elements from lanthanum to lutetium that together with yttrium and scandium are emergent contaminants of critical importance for numerous groundbreaking environmental technologies. Transfer to aquatic ecosystems is expected to increase, however, little information is known about their potential impacts in marine biota. Considering the endangered conservation status of the European eel (*Anguilla anguilla*) and the vulnerability of early fish life stages to contaminants, we exposed glass eels, through water, to an environmentally relevant concentration (120 ng L^{-1}) of lanthanum (La) for 7 days (plus 7 days of depuration). The aim was to study the accumulation and elimination of La in eel's body and subsequent quantification of acetylcholinesterase (AChE), lipid peroxidation and antioxidant enzymatic machinery. Accumulation peaked after 72h-exposure to La, decreasing afterwards, even in continuous exposure. Accumulation was higher in the viscera, followed by the skinless body and ultimately in the head, possibly as a protective mechanism to cope La neurotoxicity. A significant increase in AChE activity was observed in La-exposed glass eels, suggesting that La^{3+} may inhibit the binding of acetylcholine. A depression in lipid peroxidation was registered under La exposure, possibly indicating that La^{3+} may play physiological activities and functions as a free radical scavenger. Catalase activity was significantly inhibited in La-exposed glass eels after 72h, indicating that the availability of La may induce a physiological impairment. The quantification of Glutathione S-Transferase activity revealed no differences between control and La-exposed organisms. Further investigation is needed towards understanding the biological effects of REE.

Keywords: Rare Earth Elements; glass eels; lanthanum; bioaccumulation; lipid peroxidation; oxidative stress.

5.1 INTRODUCTION

Rare earth elements (REE) are subject of great economic interest as they are of critical importance for numerous groundbreaking environmental technologies and processes (EU Commission, 2010). The current utilization of REE has been disseminated rather rapidly with application in several areas, including modern electronic technology, medical and industry products, and also in agriculture, forestry, animal husbandry and aquaculture, in which they are components of bactericides or fertilizers (Wall, 2014). Transfer to aquatic ecosystems is, therefore, expected to increase in the form of wastewater and industrial emissions, surface run-off and atmospheric deposition (e.g. Kulaksız and Bau, 2011; Hatje et al., 2016). Thus, REE are considered of potential worldwide concern, since impacts in aquatic fauna and flora are still poorly documented. As a result, REE are currently being regarded as emergent contaminants, which in turn highlight the urgent need of a better understanding of their biogeochemical behavior and ecotoxicology. Among REE, Lanthanum (La) has been receiving further attention due to its unique physical and chemical properties and also because it is one of the most abundant REE in the environment (Herrmann et al., 2016). Lanthanum predominantly exists as the stable oxidation state +3 and by having a similar ionic radius (9.6-11.5 nm) as the calcium ion (9.9 nm). However, the higher valency (+3) of La may affect physiological functions by competing/substituting Ca^{2+} in the organism (Qinhai, 1996).

Eels are catadromous species that present a life cycle comprising two distinctive life phases (oceanic and continental). Mature Atlantic adult eels *Anguilla* spp. migrate to the Sargasso Sea to reproduce and die. The translucent leafshaped leptocephali larvae grow throughout their transatlantic voyage reaching the European coast with approximately 1-2 years old, where they metamorphose into glass eels (Lecomte-Finiger, 1994). Glass eels have elevated economic interest (SEG-Report, 2018) and increasing demand on a global scale, constituting a delicacy highly appreciated in southeast Asian and European countries (Houvenagel, 1989; Heinsbroek, 1991; Crook and Nakamura, 2013; ICES, 2016). As representatives of different aquatic ecosystems, from the open ocean to inland rivers and lakes, eels are considered good bioindicators and have been used as sentinels to assess environmental contamination, due its remarkable ability to incorporate pollutants from the surrounding environment (e.g., Arleny et al., 2007; Maes et al., 2008; Grilo et al., 2015). Therefore, the migratory trait

of this species institutes a particular risk towards exposure to La and other REE. It is well-known that contaminants may have detrimental effects on several levels of biological organization on eels, from subcellular, organ, individual up to population level (reviewed in Geeraerts and Belpaire, 2010). Moreover, toxic effects have been reported at different phases in eel's life cycle: during growing, silvering, migration, development of reproductive cells and larval stage (Geeraerts and Belpaire, 2010). The disturbance in acid-base balance caused by exposure to toxic-related stressors can often disrupt metabolic homeostasis of fishand lead to a reallocation of energy, usually required for growth, reproduction, and maintenance of basal metabolism, in order to cope with physiological stress. An increase in reactive oxygen species (ROS) may occur in response to these stressors and potentially affect cellular integrity and functioning, causing among the most common cellular injury processes, in which ROS react with membrane associated lipids, named peroxidation (e.g., Gravato et al., 2010).

Aerobic organisms have a constitutive antioxidant defense system of enzymatic and non-enzymatic molecules able to buffer toxic effects of ROS. Among antioxidant enzymes, superoxide dismutase (SOD), catalase (CAT) and glutathione-S-transferase (GST)] have been commonly used as efficient biomarkers of environmental contamination in fish and have been described as effective protective barriers against the formation of ROS, preventing oxidative cellular damage, as already reported specifically for glass eels (Gravato et al., 2010). To the best of our knowledge, only a single study has investigated the La-induced oxidative stress in fish, specifically in goldfish exposed to La-EDTA, resulting in a significant decrease in CAT activity (Chen et al., 2000).

In addition to biomarkers of oxidative stress, cholinesterases (e.g., ChEs) are responsible for the degradation of the neurotransmitter acetylcholine in cholinergic synapses and are considered biomarkers of neurotoxicity (Halliwell and Gutteridge, 2015). Experimental studies focusing on the La-induced neurotoxicity suggest that La could impair the learning ability due to a disruption of the homeostasis between trace elements, membrane-bound enzymes and neurotransmitter systems (Feng et al., 2006).

Considering the endangered conservation status (IUCN Red List) of the European eel and the vulnerability of early fish life stages to a wide range of contaminants, coupled with knowledge gaps and uncertainty about the REE' behavior, bioavailability and

impacts on aquatic systems, the main objective of the present study was to investigate the accumulation and elimination potential of La and subsequent quantification of acetylcholinesterase, lipid peroxidation and antioxidant enzymatic machinery, in the edible European glass eel. These endpoints will provide a holistic perspective about physiological processes occurring in glass eels under La exposure, including neurotransmission, cellular damage, protection against oxidative stress and detoxification, respectively, which are determinant for glass eels' survival and performance (Gravato et al., 2010). This work constitutes the first study addressing the potential impacts of an environmentally realistic exposure (120 ng L^{-1}, Herrmann et al., 2016) of La in early-life stages of the European eel, thus serving as a baseline for future research towards understanding of accumulation patterns of REE and associated oxidative stress responses.

5.2 MATERIAL AND METHODS

5.2.1 Sampling site

All glass eels were captured in a single night using fishing nets, during early autumn 2016, in the oligohaline section of the Mondego River (40º 08' 37'' N, 8º 42' 39'' W), on the central Atlantic coast of Portugal (Figure 5.1).

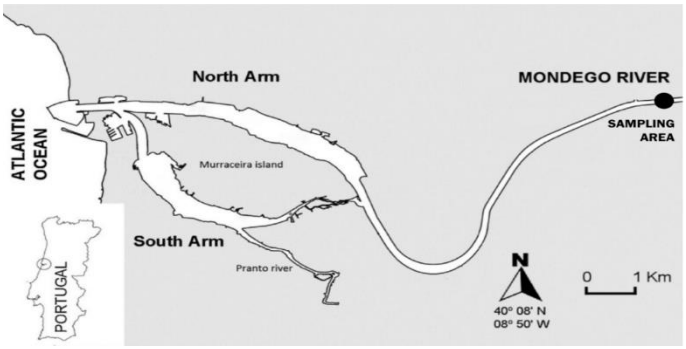

Figure 5.1 - Location of glass eels (*Anguilla anguilla*) sampling in the Mondego River, Portugal.

After being captured, the glass eels were immediately transported to the aquaculture facilities of the Laboratório Maritimo da Guia (LMG) and maintained in tanks with continuously aerated water from the same location of fishing, with no traces of metal contamination, following the procedure described in Grilo et al. (2015).

5.2.2 Experimental design

Prior to the start of the experiment glass eels were acclimated during two weeks under a 12h:12h light/dark photoperiod and physicochemical parameters mimicking those of the natural habitat: salinity = 0 (V2 refractometer, TMC Iberia, Portugal), water temperature = 18±1°C (TFX 430 Precision Thermometer, WTW GmbH, Germany) and pH=7.8±0.2 (SG8 – SevenGo pro™ pH/Ion meter, Mettler-Toledo International Inc., Switzerland). Glass eels were measured for total length (6.5±0.5 cm) and weighted (0.16±0.01 g, mean wet weight). Based on skin pigmentation, all organisms were classified between VI_{A1}-VI_{A2} stages, evidencing development of pigmentation along the whole dorsum and no clear preanal ventrolateral pigment but signs of postanal development (Elie et al., 1982).

The experiment lasted for 14 days in a controlled room temperature (18±1°C), comprising two distinct periods (i.e. exposure and post-exposure) and consisting of two treatments tested: control condition (no La addition) and exposure to 120 ng L^{-1} of lanthanum (III) chloride hidrate ($LaCl_3$), which was prepared using a La standard solution ($LaCl_3$; Merck) diluted in filtered freshwater. The La concentration chosen is within the range of levels used in exposure experiments with freshwater fishes (reviewed in Herrmann et al., 2016).

One hundred and eighty glass eels were randomly distributed within 5 independent glass tanks containing 7 L of dechlorinated tap water, filtered through a 0.45-µm pore size Millipore filters for particles removal. The tap water used throughout the experiment was previously dechlorinated by contact with air during some days, a common and efficient method to remove chlorine from the water, which is known to be toxic for glass eels. The water registered a pH value of 7.8±0.2 and a total water hardness of 105±5 mg L^{-1} $CaCO_3$ (moderately hard). The water of the tanks was renewed daily and contaminated with 120 ng L^{-1} of $LaCl_3$. Tanks were maintained in a controlled room temperature (18±1°C) with a 12 h light/dark cycle and were kept continuously aerated. Animals were fed with cod roe *ad libitum* 1 h before water change, every other day. Water aliquots were sampled every hour for the first 12 hours and after 24 h, of the first exposure, and acidified (2–20% ultrapure HNO_3) to measure La concentration.

During exposure phase, glass eels were sampled at two times: after 3 (T3) and 7 days (T7) of exposure to La. After 7 days of exposure, the remaining glass eels were

transferred to clean glass tanks filled with renewed freshwater, without residues of La, in order to begin the elimination phase which lasted 7 days (T14). At T3, T7 and at the end of decontamination period (T14), individuals were sacrificed and separated into three body parts: the head (separated from the body after the operculum), the viscera (containing all the internal organs) and the skinless body (obtained by removing the entire thin skin layer). Samples were stored at -80°C until further analyses.

5.2.3 Lanthanum quantification

Twelve pooled samples of each body part (2 specimens' body part per pool) were analyzed. Glass eels' body parts were freeze-dried, grounded, and homogenized. Lanthanum was determined in samples after digestion with the mixture of HNO_3 (sp, 65% v/v) and H_2O_2 (sp, 30% v/v) at different temperatures according to the method described in Ferreira et al. (1990). Prior to digestions all labware was decontaminated with HNO_3 (20%) for two days and rinsed with Milli-Q water. Procedural blanks were prepared using the analytical procedure. Concentrations of La were determined in a quadrupole ICP-MS (Thermo Elemental, X-Series). Procedural blanks always account for less than 1% of the total La concentration in the samples. The accuracy of the analytic method was assessed through analysis of international certified materials, BCR 668 (muscle of *Mytilus edulis*), DORM-4 (fish protein) and DOLT-2 (dogfish liver). The results obtained did not differ significantly ($p<0.05$) from the certified values (data not shown). Accumulation results are given in nanogram per gram of tissue dry weight (ng g^{-1}, dw).

5.2.4 Acetylcholinesterase, lipid peroxidation and antioxidant enzyme activities

5.2.4.1 Preparation of tissue extracts

Twelve samples of viscera and skinless body, from each experimental condition and sampling time, were analyzed for enzymatic activity and lipid peroxidation, in a total of 60 individuals. Samples were homogenized (Ultra-Turrax, Ika, Staufen, Germany) in accordance to body mass of each sample in homogenization buffer [phosphate buffered saline solution (PBS, pH 7.3): 0.14 M NaCl, 2.7 mM KCl, 8.1 mM Na_2HPO_4, 1.47 mM KH_2PO_4)] by using a glass/PTFE Potter–Elvehjem tissue grinder (Kartell, Italy). All homogenates were centrifuged (20 min at 14,000 x g at 4°C) and the enzyme activities quantified in the supernatant fraction. Each sample run in triplicate. Results were

normalized to total protein content by building a calibration curve using BSA standards (0–2.0 mg mL^{-1}), following the Bradford method (Bradford, 1976).

5.2.4.2 Acetylcholinesterase (AChE) activity

The AChE activity was determined exclusively in glass eels heads by homogenization on ice in 1.0 mL of PBS solution (0.14 M NaCl, 0.003 M KCl, 0.01 M Na_2HPO_4, 0.002 M KH_2PO_4, pH 7.4), using a Teflon tissue grinder for microtubes. The crude homogenates were then centrifuged (10 min at 14,000 x g at 4°C). The supernatant was collected, transferred to new microtubes and stored (−80°C) until further analysis. The enzymatic assay of acetylcholinesterase (EC 3.1.1.7; AChE) was performed based on an optimized Ellman method adapted to a 96-well microplate (Ellman et al., 1961; Magnotti et al., 1987). The thiocholine produced by the action of acetylcholinesterase forms a yellow (nitrobenzoate) color with 5,5'-dithiobis(2-nitrobenzoic acid), which is proportional to the AChE activity. All chemicals used in the assay were Sigma-Aldrich (Steinheim, Germany). Briefly, 50 µL of sample supernatant was diluted to 1:2 in assay buffer (50 mM KH_2PO_4, pH 7.5) and added to a 96-well microplate. Additionally, 50 µL of assay buffer was added to two microplate wells for blanks. Then, an acetylthiocholine reaction mixture was freshly prepared in ultra-pure water [50 mM phosphate buffer; 75 mM Acetylthiocholine iodide; 1.0 mM of 5,5'-dithiobis(2-nitrobenzoic acid)], and 250 µL added to each microplate well. Afterwards, the microplate was gently shaken for 30 seconds at room temperature and absorbance determined at 412 nm using a microplate reader (Bio-Rad, Benchmark model, USA) every minute during 10 minutes. For normalization purposes, total protein concentration in supernatant was determined by Bradford method (Bradford, 1976). The AChE activity (nmol min^{-1} mg^{-1} of total protein following normalization) was calculated considering that one unit of enzyme catalyzes the production of 1.0 µmol of thiocholine per minute under the assay conditions.

5.2.4.3 Lipid peroxidation assay [malondialdehyde (MDA) concentration]

Lipid peroxidation was determined in skinless body and viscera of glass eels by the quantification of malondialdehyde (MDA), a specific end-product of the oxidative degradation process of lipids. The thiobarbituric acid reactive substances (TBARS) assay was used to quantify MDA as described by Rosa et al. (2012). Homogenates were treated

with 8.1% sodium dodecyl sulfate, 20% trichloroacetic acid (pH 3.5), thiobarbituric acid and a 15:1 (v/v) mixture of n-butanol and pyridine. In the TBARS assay, the thiobarbituric acid reacts with the MDA to yield a fluorescent product, detected spectrophotometrically at 532 nm. MDA concentrations were calculated with a microplate reader (Asys UVM 340, Biochrom, USABIO-RAD, Benchmark, USA) based on an eight-point calibration curve (from 0 to 0.3 µM TBARS) using MDA bis (dimethyl acetal; Merck, Switzerland). The results were expressed in relation to the protein content of the samples (nmol min^{-1} mg^{-1} protein).

5.2.4.4 Catalase (CAT) activity

Catalase activity was determined in skinless body and viscera of glass eels according to the method described by Johansson and Borg (1988). Briefly, 20 µl of each sample, 100 µl of 100 mM potassium phosphate and 30 µl of methanol were added to a 96-well microplate, immediately shaken and incubated for 20 minutes. Subsequently, 30 µl of potassium hydroxide (10 M KOH) and 30 µl of purpald (34.2 mM in 0.5 M HCl) were added to each well, shaken and incubated for 10 minutes. Subsequently, 10 µl of potassium periodate (65.2 mM in 0.5 M KOH) was added to each well and a final incubation was performed for 5 minutes. Using a microplate reader (Asys UVM 340, Biochrom, USABIO-RAD, Benchmark, USA), enzymatic activity was determined spectrophotometrically at 540 nm. Formaldehyde concentration of the samples was calculated based on a calibration curve (from 0 to 75 µM formaldehyde). For the CAT activity was defined as the amount that will cause the formation of 1.0 nmol of formaldehyde per minute at 25°C. The results are expressed in relation to total protein content (nmol min^{-1} mg^{-1} protein).

5.2.4.5 Glutathione S-transferase (GST) activity

Glutathione S-transferase activity was determined in skinless body and viscera of glass eels according to the methodology described by Lopes et al. (2013), optimized for a 96-well microplate. This assay uses 1-chloro-2,4-dinitrobenzene (CDNB) as substrate, which conjugates with the thiol group of the glutathione (GSH), resulting in an increase in absorbance. The substrate solution (200 mM L-glutathione reduced, Dulbecco's PBS plus 100 mM CDNB solution) was added to each well of a 96-well Nunclon microplate (Thermo Scientific Nunc, USA), alongside with 20 µL of GST standard or sample. Equine liver GST was used as a positive control to validate the assay. The

enzyme activity was determined spectrophotometrically at 340 nm by quantifying the formation of the conjugate of GSH and CDNB. The absorbance was recorded every minute for 6 minutes, using a plate reader (BioRad, California, USA). The increase in absorbance per minute was estimated and the reaction rate was determined at 340nm using the CDNB extinction coefficient of 0.0053 εμM (μM^{-1} cm^{-1}). The results were expressed in relation to the protein content of the samples (nmol min^{-1} mg^{-1} protein).

5.2.5 La enrichment factor and elimination coefficient

Lanthanum enrichment factor was calculated to evaluate body part specific affinity for La and the rate of La elimination was estimated in order to clarify the recovery of each body part, through the calculus of an elimination coefficient, according to Pereira et al. (2015).

5.2.6 Statistical analyses

Data were tested for normality (Kolmogorov–Smirnov test) and for equality of variances (Levene's test) before using analysis of variance techniques to evaluate for potential differences in accumulation and biomarkers activities. Body part differences in bioaccumulation, AChE activity, lipid peroxidation (MDA levels) and antioxidant enzyme activities (CAT and GST) were tested via ANOVA followed by Tukey HSD *post hoc* tests. All statistical analyses were performed for a significance level of $p<0.05$, using STATISTICA™ 12 software (Statsoft, Inc., Tulsa, OK 74104, USA).

5.3 RESULTS

Ranges of La concentrations and of activity levels of Acetylcholinesterase (AChE), Malondialdehyde (MDA), Catalase (CAT) and Glutathione S-Transferase (GST) in the different body parts are presented in Table 5.1.

Table 5.1 - Ranges of La concentrations (ng g^{-1}, dry weight), acetylcholinesterase activity (AChE, nmol min^{-1} mg^{-1} total protein), lipid peroxidation values (MDA concentrations, nmol mg^{-1} total protein), catalase activity (CAT, nmol mg^{-1} total protein) and glutathione S-transferase activity (GST, nmol min^{-1} mg^{-1} total protein) of the control, exposed and post-exposed glass eels' head, skinless body, and viscera at T3, T7 and T14.

	Head		Skinless body				Viscera			
	Accumulation	AChE	Accumulation	LIPO	CAT	GST	Accumulation	LIPO	CAT	GST
T3 control	0.75-3.7	6.7-9.6	0.81-2.7	0.044-0.17	6.4-17	52-69	1.1-7.1	0.017-0.070	11-30	81-110
T3 exposed	1.6-4.7	12-77	1.1-6.7	0.047-0.093	0.77-8.1	54-62	4.8-13	0.011-0.053	0.63-1.9	73-119
T7 control	1.0-2.1	4.6-9.6	0.59-1.4	0.023-0.19	2.6-8.9	37-55	1.4-3.9	0.057-0.076	23-26	43-67
T7 exposed	0.39-4.3	10-68	0.64-2.1	0.021-0.065	4.3-7.5	38-69	1.1-4.6	0.014-0.051	23-42	59-100
T14 post-exposed	1.2-2.4	13-31	0.78-1.5	0.0017-0.0070	7.8-12	43-75	1.1-4.3	0.004-0.009	12-19	61-119

Baseline concentrations of La (T0) and concentrations in the water aliquots sampled every hour for the first 12 hours (T1-T12) and after 24h (T24) of exposure are presented in Annex 4, Supplemental Table 5.1.

5.3.1 Head

5.3.1.1 Bioaccumulation

Concentrations of La (ng g^{-1}, dry weight) in the glass eel heads are presented in figure 5.2a. After 3 and 7 days of exposure there were no significant differences between the eels exposed to La and those from the control (Tukey test, $p>0.05$).

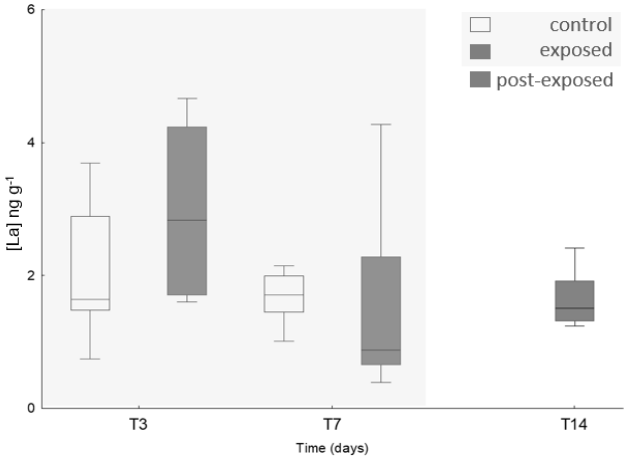

Figure 5.2 a - Median, percentile 25th and 75th, minimum and maximum values of concentration of La (ng g^{-1}) of the control, exposed and post-exposed glass eels' head for the different sampling times (T3, T7 and T14).

5.3.1.2 AChE activity

Median values of AChE activity (nmol min^{-1} mg^{-1} total protein) in the head are presented in figure 5.2b. At T3 and T7, such activity was significantly higher under La exposure than those found in control samples ($p=0.04$ and $p=0.02$, respectively), with a median value more than three times higher. In the post-exposure period, the AChE activity decreased almost by half ($p=0.25$).

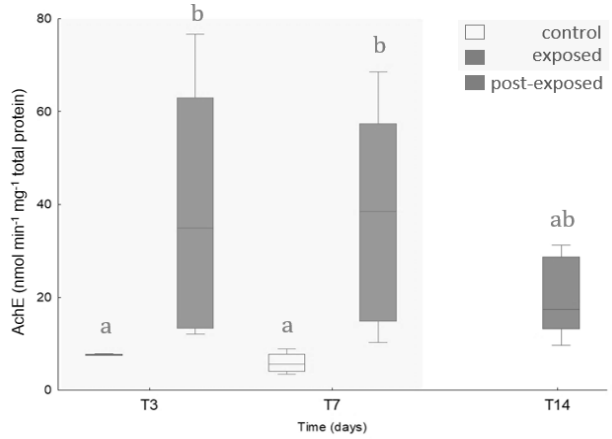

Figure 5.2b - Median, percentile 25th and 75th, minimum and maximum values of acetylcholinesterase activity (AChE, nmol min^{-1} mg^{-1} total protein) of the control, exposed and post-exposed glass eels' head for the different sampling times (T3, T7 and T14).

5.3.2 Skinless Body

5.3.2.1 Bioaccumulation

Median concentrations of La (ng g^{-1}, dry weight) in the skinless body are presented in Figure 5.3a.

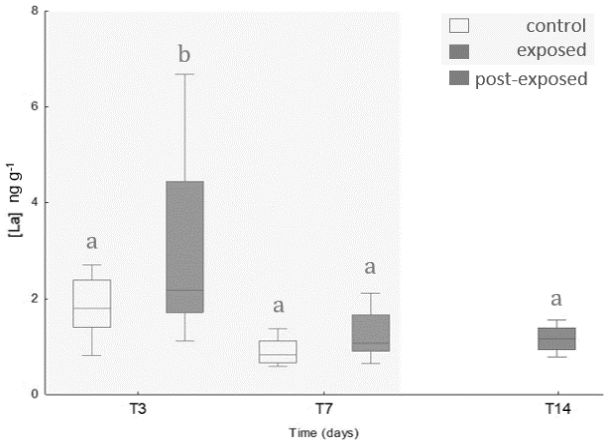

Figure 5.3a - Median, percentile 25th and 75th, minimum and maximum of concentration of La (ng g^{-1}) of the control, exposed and post-exposed glass eels' skinless body for the different sampling times (T3, T7 and T14). Different letters represent significant statistical differences ($p < 0.05$).

Exposed glass eels showed a significant tendency to accumulate La in the skinless body, most evident in the first 3 days, reaching 6.7 ng g^{-1} (p=0.004). After 7 days of exposure, La accumulation declined significantly, up to 2.1 ng g^{-1} La, more than 3-fold lower the values observed in the first 72h (T3, p=0.97). After seven days of decontamination (T14), the glass eels skinless body displayed La values similar to controls (p=0.88), reached on the T3 but not from exposed T7-glass eels.

5.3.2.2 MDA concentration

Median values of MDA concentration (nmol mg^{-1} total protein), in the skinless body, are presented in Figure 5.3b.

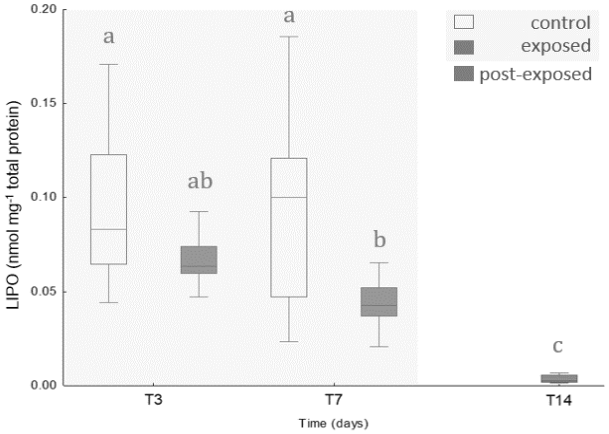

Figure 5.3b - Median, percentile 25th and 75th, minimum and maximum of lipid peroxidation values (MDA concentrations, nmol mg^{-1} total protein) of the control, exposed and post-exposed glass eels' skinless body for the different sampling times (T3, T7 and T14). Different letters represent significant statistical differences ($p < 0.05$).

Malondialdehyde values were considerably lower in contaminated samples, particularly in the T7, which was significantly lower than the control (p=0.04). After 7 days of elimination period, MDA concentration values dropped to values up to 0.0017-0.0070 nmol mg^{-1} total protein (p=0.15). MDA concentrations never exceeded 0.2 nmol mg^{-1} total protein.

5.3.2.3 *CAT activity*

Median values of catalase activity (CAT, nmol min^{-1} mg^{-1} total protein) in the skinless body are presented in figure 5.3c. Catalase uttermost activity was observed in the T3 control samples and the lowermost in the T3 contaminated samples (p=0.0001). On the T7 this deviation was diminished with analogous control and contaminated activity values (p=0.99). After the elimination, the CAT activity increased almost by 2-fold, displaying an opposite pattern of variation from the one observed during accumulation period (p=0.017).

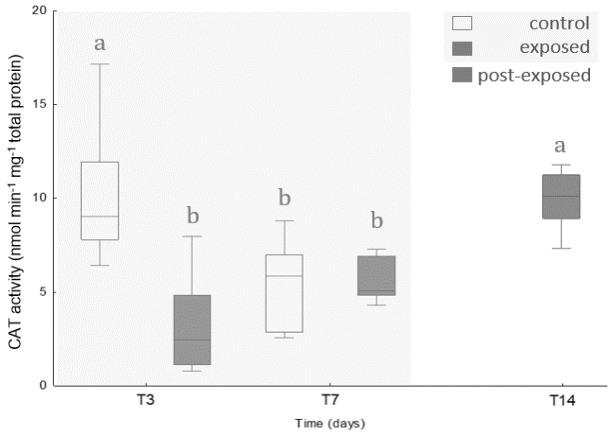

Figure 5.3c - Median, percentile 25th and 75th, minimum and maximum of catalase activity (CAT, nmol mg^{-1} total protein) of the control, exposed and post-exposed glass eels' skinless body for the different sampling times (T3, T7 and T14). Different letters represent significant statistical differences ($p < 0.05$).

5.2.2.4 GST activity

Median values of Glutathione S-transferase (GST) activity (nmol min^{-1} mg^{-1} total protein), in the skinless body, are presented in figure 5.3d. GST activity remained almost constant throughout the exposure (T3 and T7, p=0.99 and p=0.36, respectively) and elimination (T14) periods (p=0.79), with a slight lower activity in the T7 control (p=0.004).

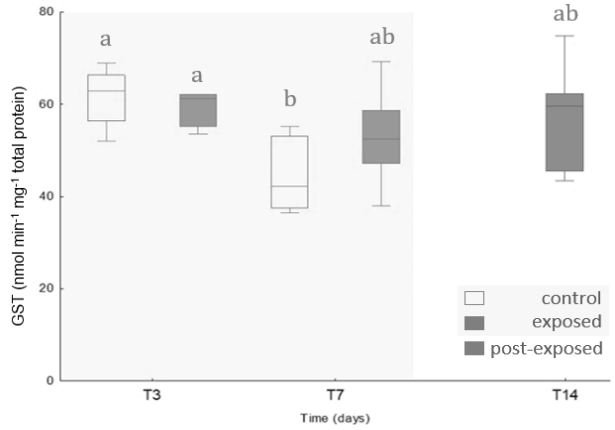

Figure 5.3d - Median, percentile 25th and 75th, minimum and maximum of glutathione S-transferase activity (GST, nmol min^{-1} mg^{-1} total protein) of the control, exposed and post-exposed glass eels' skinless body for the different sampling times (T3, T7 and T14). Different letters represent significant statistical differences ($p < 0.05$).

5.3.3 Viscera

5.2.3.1 *Bioaccumulation*

Median levels of La (ng g^{-1}, dry weight) in the viscera are shown in Figure 5.4a.

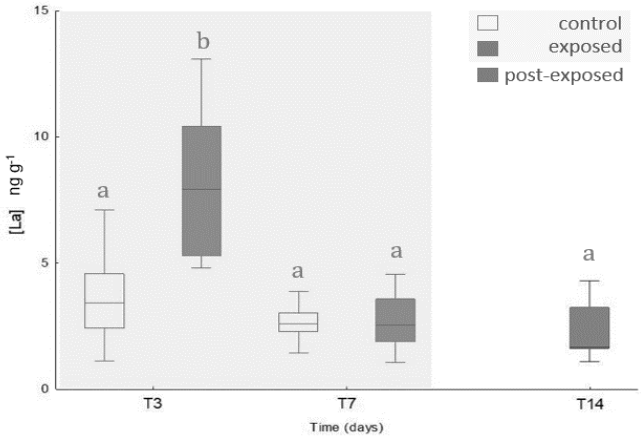

Figure 5.4a - Median, percentile 25th and 75th, minimum and maximum of concentration of La (ng g^{-1}) of the control, exposed and post-exposed glass eels' viscera for the different sampling times (T3, T7 and T14). Different letters represent significant statistical differences ($p < 0.05$).

Compared to the head and the skinless body, the viscera showed the highest levels of La. In the viscera, exposed T3 specimens presented significantly higher concentrations than their control counterparts (p=0.0003). After 7 days of exposure, the bioaccumulation dropped to values alike the controls (p=0.99). A similar range of values was sustained for the T14 (p=0.99).

5.3.3.2 *MDA concentration*

Median values of MDA concentration (nmol mg^{-1} total protein), in the viscera, are presented in figure 5.4b. As a common pattern observed for the skinless body, exposed glass eels presented low MDA levels, although on the T7 a statistically significant difference from the control equivalents was observed (p=0.034). The

concentration of MDA was significantly reduced on the T14, ranging from 0.004 to 0.009 nmol mg^{-1} total protein (p=0.031).

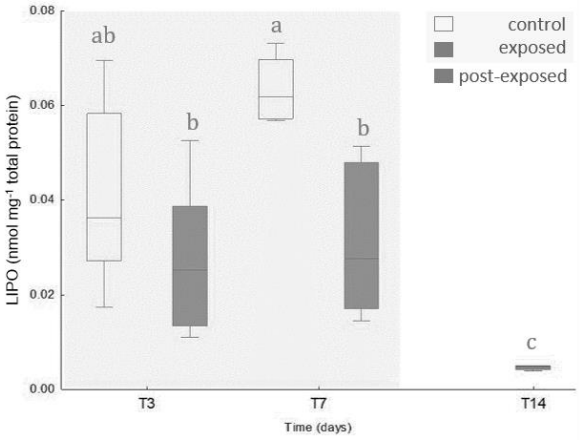

Figure 5.4b - Median, percentile 25th and 75th, minimum and maximum of lipid peroxidation values (MDA concentrations, nmol mg^{-1} total protein) of the control, exposed and post-exposed glass eels' viscera for the different sampling times (T3, T7 and T14). Different letters represent significant statistical differences ($p < 0.05$).

5.3.3.3 CAT activity

Median values of CAT activity (nmol min^{-1} mg^{-1} total protein), in the viscera, are presented in Figure 5.4c.

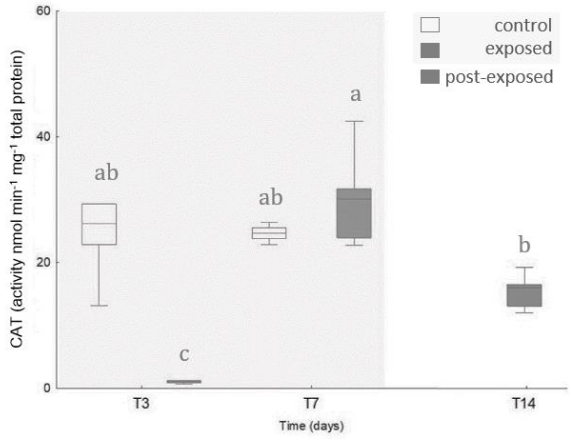

Figure 5.4c - Median, percentile 25th and 75th, minimum and maximum of catalase activity (CAT, nmol mg^{-1} total protein) of the control, exposed and post-exposed glass eels' viscera for the different sampling times (T3, T7 and T14). Different letters represent significant statistical differences ($p < 0.05$).

The time scale variation pattern of CAT activity in La-exposed glass eels was erratic. Catalase activity in the exposed specimens diminished significantly on the T3, attaining the lowest activity levels 0.63-1.9 nmol min^{-1} mg^{-1} total protein (p=0.0001). By the T7, CAT activity levels on exposed glass eels increased significantly to values equivalent to the control activity (p=0.57). The CAT activity dropped on the T14 to values ranging from 11.96 to 19.25 nmol min^{-1} mg^{-1} total protein (p=0.001).

5.3.3.4 GST activity

Median values of GST activity (nmol min^{-1} mg^{-1} total protein) in the viscera are presented in figure 5.4d. Overall, GST activity was relatively stable, varying within a narrow range of values throughout the experiment, independent of sampling time. A slight increase of GST was observed at exposed glass eels on T3 and T7 (p= 0.99 and p= 0.08, respectively).

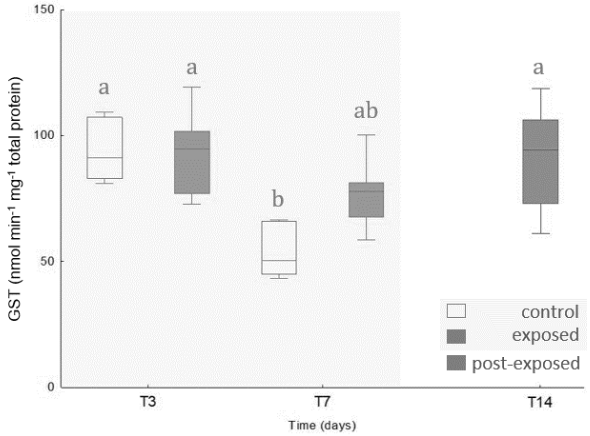

Figure 5.4d - Median, percentile 25th and 75th, minimum and maximum of glutathione S-transferase activity (GST, nmol min-1 mg-1 total protein) of the control, exposed and post-exposed glass eels' viscera for the different sampling times (T3, T7 and T14). Different letters represent significant statistical differences ($p < 0.05$).

5.3.4 La enrichment factor and elimination coefficient

After 3 days of exposure (T3) the highest enrichment factor was observed for the viscera, followed by the skinless body and finally the head (Figure 5.5). After 7 days of exposure (T7), the accumulation pattern changed with higher enrichment factors in skinless body followed by viscera and the head.

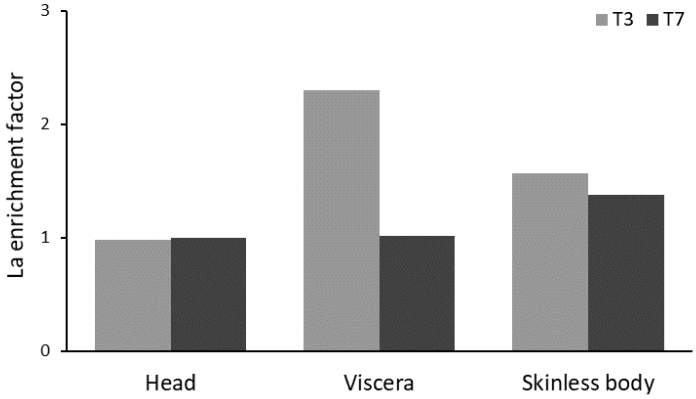

Figure 5.5 - Enrichment factor for the head, viscera, and skinless body of glass eels for the two exposed sampling times, T3 and T7.

The highest elimination (lowest coefficient) was registered for the viscera, followed by the head and ultimately the skinless body (Figure 5.6).

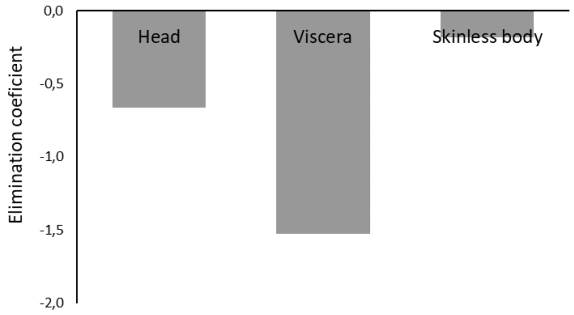

Figure 5.6 - Elimination coefficient for the head, viscera, and skinless body of glass eels.

5.4 DISCUSSION

It is known that La can be absorbed to particulate matter and be accumulated by organisms, interfering with cellular functions (e.g., Cui et al., 2012). However, information on its toxicity is very scarce and puzzling. The availability of La is strongly influenced by a wide range of confounding biotic (i.e. age dependent differences of exposed organisms) and abiotic factors, such as alkalinity (HCO^{3-}, CO_3^{2-}) and pH (reviewed in Herrmann et al., 2016). The La concentration measured in water aliquots (initially at each hour during 12 hours and then after 24 hour) remained relatively stable. In fact, median real total dissolved concentration did not vary more than 8.7% from the desired concentration (120 ng L^{-1}; Annex 4, Supplemental Table 5.1), during the contamination assay. At pH=7.8±0.2 up to 90% of the La is present as a cation with +3 valency (Bouyer et al., 2006). The La exposure concentration used in this experiment (120 ng L^{-1}) is environmentally realistic since it is within the levels already quantified in a European wastewater outlet (Brito et al., 2018). Glass eels used in the present study were in the same pigmentation stages (VI_{A1}-VI_{A2} stages) guarantying the ontogeny homogeneity, thus eliminating age influence in La variability. Water hardness can also influence the La availability and therefore their toxicity. In fact, La^{3+} behaves much like Ca^{2+} in biological systems, and an excess of Ca^{2+} ions in the water may directly compete with La^{3+} ions for biological binding sites, influencing La toxicity (Evans, 1983; Barry and Meehan, 2000). However, as emphasized by Herrmann et al. (2016), data published about this issue are insufficient to formulate a hardness dependency Environmental Quality Standard. Nonetheless, in the present study the water hardness (105±5 mg L^{-1} $CaCO_3$) was kept as moderately hard throughout the experiment to avoid ambiguous results.

In the present study, the highest La accumulation values were registered in the first 3 days of exposure, while after 7 days the accumulation dropped markedly, keeping relatively stable through the post-exposure period (T14) and reaching median values similar to the controls. This variability is not supported by published literature for other metals. Our data evidences, for the first time, that the bioaccumulation of La varied with body part and sampling time and that the first 72h are crucial for such bioaccumulation. After three days of exposure (T3) a higher accumulation (presented as an enrichment factor) was observed for the viscera, followed by the skinless body and finally the head (Figure 5.5). Such results are in agreement with previous studies confirming, for the majority of the elements, the viscera as the primary accumulation organ in fish (Mieiro et al., 2011; Raimundo et al., 2013; Pereira et al., 2015). The lowest enrichment factor was showcased by the head. This result was expected since this body part is associated with neuro-transmission and coordination in fish and low elemental concentrations are usually found in order to preserve these vital functions (Mieiro et al., 2011; Pereira et al., 2015). After 7 days of exposure (T7, when elimination period started) the accumulation pattern changed: higher enrichment factors were registered in skinless body followed by viscera and the head. The augment of La concentrations observed in the skinless body in T7 in comparison to the other sampled tissues may be related to the transfer of La from the viscera and head, osmosis, or by the association of La to the spine, which is Ca enriched, or by the presence of an unknown mechanism of the glass eels to cope with La contamination. Viscera presented the highest elimination as expected, since elimination tissues/organs (such as liver and bile) are included in this body part (Figure 5.6).

Noteworthy, among the studied body parts, the head presented the lowest enrichment factor but higher elimination coefficient than the skinless body. These results do not entirely support the findings of a study performed with seabreams exposed to Hg (Pereira et al., 2015) that showed a low elimination ability of the brain. This pattern was related with the presence of the Blood Brain Barrier, which can limit the release of elements into the bloodstream and, thus, their elimination. The possibility of brain effects can be further discussed since, in spite of the large variability in La bioaccumulation in the head, a very clear effect on AChE activity was found, with a median activity at least three times higher in exposed glass eels in both T3 and T7.

Acetylcholinesterase is involved in the termination of impulse transmission at synaptic junctions by rapid hydrolysis of the neurotransmitter acetylcholine (Ach; Colovic et al., 2013). Higher levels of AChE can be expected to change ACh balance, inducing secondary responses in the nervous system (Soreq and Seidman, 2001), and an accumulation of ACh can cause an alteration in mobility behavior of fish (Rao et al., 2005). The La exposure gave rise to an acetylcholine buildup, querying an over activity of AChE, which is linked to neurotransmission disruption and stress. Although several works evidence an opposite pattern of response of the AChE activity to contaminants (e.g. Nemcsók et al., 1984; Gravato et al., 2010; Tilton et al., 2011). Liapi et al. (2008) reported a significant increase (i.e., +23% compared to the control) in AChE activity in adult rat brains after a short-term exposure to La. This is known to inhibit the Ca-dependent neurotransmitter release (Przywara et al., 1992) and modulate the ion homeostasis within the central nervous system. As mentioned previously, this finding is of particular relevance since most studies have reported a general decline in AChE activity. These results raise pertinent questions about the potential ability of La to cross the blood–brain barrier of exposed organisms (Damment et al., 2007).

Romani et al. (2003) described an increase in the activity of AChE in the brain of the Mediterranean bony fish *Sparus auratus,* after a 20 days exposed to sub lethal concentrations of Cu, although the absence of significant accumulation. Cheng et al. (2014) also showed that Ce (second most abundant REE) accumulation increase the activity of cholinesterase in mice liver. Here we present the first evidence of a peaked AChE activity as a result of a REE accumulation in the fish head. Acetylcholine receptors are ion channels embedded in cell membranes, permeable to sodium, potassium and calcium (Vernino et al., 1992) and for this reason we suggest that this La^{3+} may bind to the acetylcholine receptors, substituting Ca, inhibiting the binding of acetylcholine. Thus, impairing the channel function, an increase in the content of acetylcholine could be expected, since it is not hydrolyzed, requiring and over activity of AChE. Miledi et al. (1980) showed an increase of acetylcholine in neuromuscular junctions treated with La which may affect physiological functions. The AChE activity disturbance evidence in the present study, sturdily demonstrates that La has an effect on glass eels physiology but the consequences associated with this effect are still unknown and require further investigation.

Malondialdehyde levels are a trustworthy indicator of lipid peroxidation (LPO). Lipid peroxidation promulgates damaging process, increasing the rigidity of cellular membranes (Nagarani et al., 2011). Peculiarly, the exposed glass eels have significantly lower values of MDA than the controls in the T7, for viscera and skinless body, and also in the elimination time T14. Reduced MDA contents may also reflect the absence of lipid membrane damage in glass eels exposed to protective effects of glass eel antioxidant system to La. Zheng et al. (2000) also reported a decrease of lipid peroxidation of plasma membranes under low La concentrations (i.e. < 60 μM $LaCl_3$), which is in accordance with our findings, but the opposite was observed under high concentrations (60-80 μM $LaCl_3$). According to these authors, within a specific range, La^{3+} may play some physiological activities and functions as a free radical scavenger, such as superoxide dismutase and peroxidase. This hypothesis was also suggested by Zeng et al. (1999). It is relevant, however, to highlight that Zheng et al. (2000) performed the research with rice (*Oryza sativa*) seedling roots, and Zeng et al. (1999) with wheat (*Triticum aestivum* L.) seedling leaves, and the complexity inherent to plants and animals is different as well as the mechanisms of action and toxicity of La. Arvela and Kärki (1971) also showed that the REE cerium reduced the activity of hepatic microsomal enzymes and induced changes in plasma concentrations of free fatty acids and liver phospholipids content. Because the REE are known to react especially with phospholipids, it was postulated that Cerium impairs the oxidation of lipids through interaction with these functionally important components. Another study described that low concentrations of REE can have positive effects on fish, and only a relatively high dosage of REE become toxic (Xu and Jiang, 2004). In addition, it is known that antioxidant enzymes are intrinsically linked and dependent upon the activity of one another (Lopes et al., 2013) and the tendency of LPO to decrease in the exposed organisms also show a relation with other enzymatic antioxidants since they were also impacted. Most of published literature presented concentrations of MDA in much higher orders of magnitude than the expressed in this study. The presented MDA concentration ranges from 0.021 to 0.093 (nmol mg^{-1} total protein) in the skinless body and 0.011 to 0.076 (nmol mg^{-1} total protein) in the viscera, while, for example, Fonseca et al. (2009) showed median values of MDA concentrations around 2 (nmol mg^{-1} total protein), in the liver of *Solea senegalensis* exposed to Cu, up to forty times greater than the ones here described for glass eels. Thus, with such an

undersized scale, it is proposed that the variance of MDA concentrations from control to exposed samples is unlikely to be an indicator of any damaging effects.

Catalase (CAT) converts H_2O_2 to H_2O and O_2 and thereby inhibits its accumulation in cells and tissues (Aebi, 1984). This biomarker exhibited an inverse pattern of variation in comparison to the accumulation, indicating a CAT inhibition in exposed samples. The inhibition is more evident in the T3, when accumulation of La reached the highest values. Exposure to La is known to cause a variety of biological effects in a time- and dose-dependent way (Zheng et al., 2000). Likewise, antioxidant defense strategies are tissue-specific and in this study the CAT inhibition was most evident in the viscera, which was the tissue with the highest La accumulation. Catalase inhibition constitutes a physiological impairment caused by the availability of La in the medium. The inhibition of CAT activity indicates that the time-dependent accumulation of La, with a peak in the first 72h, can cause oxidative damage to glass eels. Das et al. (1988) described the cytotoxic effects of the lanthanum-ion and Xiaorong (2000) also the CAT activity inhibition in fish liver upon exposure to La. Our results support the use of CAT activity as an indicator of La accumulation in glass eels and may deliver valuable information for future studies.

The antioxidant defense system includes other enzymes, such as a group of multifunctional enzymes GST, involved in the removal of highly reactive electrophilic components, which would otherwise be toxic; thereby protecting cells against ROS induced damage (Di Giulio et al., 1995; Lopes et al., 2013).

The absence of significant differences in GST activity between control, exposed and elimination samples, suggests that GST may not be the most suitable biomarker to evaluate oxidative stress in glass eels exposed to 120 ng L^{-1} of La. On the other hand, this concentration could be insufficient to cause significant alterations in GST activity. For a better understanding of the biological effects of La, future studies should encompass master water parameters (e.g., water hardness, temperature, pH, major ions) and higher levels of this L-REE. Complemented with determinations of non-enzymatic protective molecules, indicative of protein and DNA damage, for example. The timescale of the experiment should be better detailed in the first 72h of accumulation, which proved to be critical, to provide a more conclusive elucidation of the extended effects of this L-REE.

ACKNOWLEDGMENTS

This work was supported by Fundação para a Ciência e Tecnologia (FCT), through the project CLIMATOXEEL (PTDC/AAG-GLO/3795/2014) awarded to Tiago F. Grilo and the project REEUSE (PTDC/QEQ-EPR/1249/2014).

Joana Raimundo and Tiago F. Grilo acknowledge the post-doctoral grants by FCT SFRH/BPD/91498/2012 and SFRH/BPD/ 98590/2013, respectively. Cátia Figueiredo also acknowledges the PhD grant SFRH/BD/130023/2017 by FCT. The authors would also like to acknowledge the strategic project UID/MAR/04292/2013 granted to MARE.

Finally, the authors thank the two anonymous reviewers for the many useful comments and valuable advice for the improvement of this work.

REFERENCES

Aebi, H., 1984. Catalase *in vitro*. Methods In Enzymology 105, 121-126.

Arleny, I., Tabouret, H., Rodriguez Gonzalez, P.R., Bareille, G., Donard, O., Amouroux, D., 2007. Methylmercury bioconcentration in muscle tissue of the European eel (*Anguilla anguilla*) from the Adour estuary (Bay of Biscay, France). Marine Pollution Bulletin 54, 1031-1036.

Arvela, P., Kärki, N., 1971. Effect of cerium on drug metabolizing activity in rat liver. Cellular and Molecular Life Sciences 27, 1189-1190.

Barry, M.J., Meehan, B.J., 2000. The acute and chronic toxicity of lanthanum to *Daphnia carinata*. Chemosphere 41, 1669-1674.

Bouyer, F., Sanson, N., Destarac, M. and Gerardin, C., 2006. Hydrophilic block copolymer-directed growth of lanthanum hydroxide nanoparticles. New Journal of Chemistry 30, 399-408.

Bradford, M.M., 1976. A rapid and sensitive method for the quantitation of microgram quantities of protein utilizing the principle of protein-dye binding. Analytical Biochemistry 72, 248-254.

Brito, P., Prego, R., Mil-Homens, M., Caçador, I., & Caetano, M., 2018. Sources and distribution of yttrium and rare earth elements in surface sediments from Tagus estuary, Portugal. Science of The Total Environment 621, 317-325.

Chen, Y., Cao, X. D., Lu, Y., & Wang, X. R., 2000. Effects of rare earth metal ions and their EDTA complexes on antioxidant enzymes of fish liver. Bulletin Of Environmental Contamination And Toxicology 65, 357-365.

Cheng, J., Fei, M., Sang, X., Cheng, Z., Gui, S., Zhao, X., Sheng, L., Sun, Q., Hu, R., Wang, L., 2014. Gene expression profile in chronic mouse liver injury caused by long-term exposure to $CeCl_3$. Environmental Toxicology 29, 837-846.

Colovic, M.B., Krstic, D.Z., Lazarevic-Pasti, T.D., Bondzic, A.M., Vasic, V.M., 2013. Acetylcholinesterase inhibitors: pharmacology and toxicology. Current Neuropharmacology 11, 315-335.

Commission, E., 2010. Critical raw materials for the EU. Report of the Ad-hoc Working Group on defining critical raw materials. Ad-hoc Working Group: July 2010, 84.

Crook, V., Nakamura, M., 2013. Assessing supply chain and market impacts of a CITES listing on Anguilla species. Index Vol. 24: i–iv 9, 24.

Cui, J.a., Zhang, Z., Bai, W., Zhang, L., He, X., Ma, Y., Liu, Y., Chai, Z., 2012. Effects of rare earth elements La and Yb on the morphological and functional development of zebrafish embryos. Journal Of Environmental Sciences 24, 209-213.

Damment, S.J., De Broe, M.E., D'Haese, P.C., Bramall, N., Cox, A.G., McLeod, C.W., 2007. Incredulous effects of lanthanum? Toxicology Letters 168, 186-189.

Das, T., Sharma, A., Talukder, G., 1988. Effects of lanthanum in cellular systems. Biological Trace Element Research 18, 201-228.

Di Giulio, R., Benson, W., Sanders, B., Van Veld, P., 1995. Biochemical mechanisms: metabolism, adaptation, and toxicity. Fundamentals of Aquatic Toxicology 2, 523-560.

Dröge, W., 2002. Free radicals in the physiological control of cell function. Physiological Reviews 82, 47-95.

Elie, P., Lecomte-Finiger, R., Cantrelle, I., Charlon, N., 1982. Définition des limites des différents stades pigmentaires durant la phase civelle d'*Anguilla anguilla* L.(poisson téléostéen anguilliforme). Vie et Milieu 32, 149-157.

Ellman, G.L., Courtney, K.D., Andres, V., Featherstone, R.M., 1961. A new and rapid colorimetric determination of acetylcholinesterase activity. Biochemical Pharmacology 7, 88IN191-9095.

Evans, C.H., 1983. Interesting and useful biochemical properties of lanthanides. Trends in Biochemical Sciences 8, 445-449.

Feng, L., Xiao, H., He, X., Li, Z., Li, F., Liu, N., Zhao, Y., Huang, Y., Zhang, Z., Chai, Z., 2006. Neurotoxicological consequence of long-term exposure to lanthanum. Toxicology Letters 165, 112-120.

Ferreira, A., Cortesão, C., Castro, O., Vale, C., 1990. Accumulation of metals and organochlorines in tissues of the oyster *Crassostrea angulata* from the Sado Estuary, Portugal. Science of The Total Environment 97, 627-639.

Fonseca, V., Serafim, Â., Bebianno, M.J., Cabral, H., 2009. Effect of copper exposure on growth, condition indices and biomarker response in juvenile sole *Solea senegalensis*. Scientia Marina 73, 51-58.

Geeraerts, C., Belpaire, C., 2010. The effects of contaminants in European eel: a review. Ecotoxicology 19, 239-266.

Gravato, C., Guimarães, L., Santos, J., Faria, M., Alves, A., Guilhermino, L., 2010. Comparative study about the effects of pollution on glass and yellow eels (*Anguilla anguilla*) from the estuaries of Minho, Lima and Douro Rivers (NW Portugal). Ecotoxicology And Environmental Safety 73, 524-533.

Grilo, T., Mendes, T., Coelho, J., Pereira, E., Pardal, M., Cardoso, P., 2015. Kinetics of mercury accumulation and elimination in edible glass eel (*Anguilla anguilla*) and potential health public risks. Water, Air, & Soil Pollution 226, 166.

Halliwell, B., Gutteridge, J.M., 2015. Free radicals in biology and medicine. Oxford University Press, USA.

Hatje, V., Bruland, K.W., Flegal, A.R., 2016. Increases in anthropogenic gadolinium anomalies and rare earth element concentrations in San Francisco Bay over a 20 year record. Environmental Science & Technology 50, 4159-4168.

Heinsbroek, L., 1991. A review of eel culture in Japan and Europe. Aquaculture Research 22, 57-72.

Herrmann, H., Nolde, J., Berger, S., Heise, S., 2016. Aquatic ecotoxicity of lanthanum–A review and an attempt to derive water and sediment quality criteria. Ecotoxicology And Environmental safety 124, 213-238.

Houvenaghel, G. T., 1989. Assessment of the needs to culture the eel *Anguilla anguilla* in Europe. In N. De Pauw, E. Jaspers, H. Ackefors, & N. Wilkins (Eds.). Aquaculture – a biotechnology in progress, 169–178. Breden: European Aquaculture Society.

ICES, 2016. Report of the Working Group on Eels (WGEEL), 15–22 September 2016, Cordoba, Spain. ICES CM 2016/ACOM:19. 107 pp.

Johansson, L.H., Borg, L.H., 1988. A spectrophotometric method for determination of catalase activity in small tissue samples. Analytical Biochemistry 174, 331-336.

Kulaksız, S., Bau, M., 2011. Rare earth elements in the Rhine River, Germany: first case of anthropogenic lanthanum as a dissolved microcontaminant in the hydrosphere. Environment International 37, 973-979.

Lecomte-Finiger, R., 1994. The early life of the European eel. Nature 370, 424-424.

Liapi, C., Zarros, A., Galanopoulou, P., Theocharis, S., Skandali, N., Al-Humadi, H., Anifantaki, F., Gkrouzman, E., Mellios, Z., Tsakiris, S., 2008. Effects of Short-Term Exposure to Manganese on the Adult Rat Brain Antioxidant Status and the Activities of Acetylcholinesterase, (Na^+, K^+)-ATPase and Mg^{2+}-ATPase: Modulation by l-Cysteine. Basic & Clinical Pharmacology & Toxicology 103, 171-175.

Lopes, A.R., Trübenbach, K., Teixeira, T., Lopes, V.M., Pires, V., Baptista, M., Repolho, T., Calado, R., Diniz, M., Rosa, R., 2013. Oxidative stress in deep scattering layers: heat shock response and antioxidant enzymes activities of myctophid fishes thriving in oxygen minimum zones. Deep Sea Research Part I: Oceanographic Research Papers 82, 10-16.

Maes, J., Belpaire, C., Goemans, G., 2008. Spatial variations and temporal trends between 1994 and 2005 in polychlorinated biphenyls, organochlorine pesticides and heavy metals in European eel (*Anguilla anguilla* L.) in Flanders, Belgium. Environmental Pollution 153, 223-237.

Magnotti, R.A., Eberly, J.P., Quarm, D., Mcconnell, R.S., 1987. Measurement of acetylcholinesterase in erythrocytes in the field. Clinical chemistry 33, 1731-1735.

Mieiro, C.L., Pacheco, M., Pereira, M.E., Duarte, A.C., 2011. Mercury organotropism in feral European sea bass (*Dicentrarchus labrax*). Archives Of Environmental Contamination And Toxicology 61, 135-143.

Miledi, R., Molenaar, P., Polak, R., 1980. The effect of lanthanum ions on acetylcholine in frog muscle. The Journal Of Physiology 309, 199-214.

Nagarani, N., Devi, V.J., Kumaraguru, A., 2011. Mercuric chloride induced proteotoxicity and structural destabilization in marine fish (*Therapon jarbua*). Toxicological & Environmental Chemistry 93, 296-306.

Nemcsók, J., Nemeth, A., Buzás, Z., Boross, L., 1984. Effects of copper, zinc and paraquat on acetylcholinesterase activity in carp (*Cyprinus carpio* L.). Aquatic Toxicology 5, 23-31.

Pereira, P., Raimundo, J., Barata, M., Araújo, O., Pousão-Ferreira, P., Canário, J., Almeida, A., Pacheco, M., 2015. A new page on the road book of inorganic mercury in fish body–tissue distribution and elimination following waterborne exposure and post-exposure periods. Metallomics 7, 525-535.

Przywara, D.A., Bhave, S.V., Bhave, A., Chowdhury, P.S., Wakade, T.D., Wakade, A.R., 1992. Activation of K^+ channels by lanthanum contributes to the block of transmitter release in chick and rat sympathetic neurons. Journal Of Membrane Biology 125, 155-162.

Qiang, T., Xiao-Rong, W., Li-Qing, T., Le-Mei, D., 1994. Bioaccumulation of the rare earth elements lanthanum, gadolinium and yttrium in carp (*Cyprinus carpio*). Environmental Pollution 85, 345-350.

Qinhai, H., 1996. Distribution and accumulation of Lanthanum in *Ctenopharyngodon Idellus*. Agro-environmental Protection.

Raimundo, J., Anes, B., Caetano, M., Giacomello, E., Menezes, G., Vale, C., 2013. Trace-element concentrations in muscle and liver of 11 commercial fish species from Condor Seamount, Azores Archipelago (Portugal). Deep-Sea Research 98, 137-147.

Rao, J.V., Begum, G., Pallela, R., Usman, P., Rao, R.N., 2005. Changes in behavior and brain acetylcholinesterase activity in mosquito fish, *Gambusia affinis* in response to the sub-lethal exposure to chlorpyrifos. International Journal of Environmental Research And Public Health 2, 478-483.

Romani, R., Antognelli, C., Baldracchini, F., De Santis, A., Isani, G., Giovannini, E., Rosi, G., 2003. Increased acetylcholinesterase activities in specimens of *Sparus auratus* exposed to sublethal copper concentrations. Chemico-Biological Interactions 145, 321-329.

Rosa, R., Pimentel, M.S., Boavida-Portugal, J., Teixeira, T., Trübenbach, K., Diniz, M., 2012. Ocean warming enhances malformations, premature hatching, metabolic suppression and oxidative stress in the early life stages of a keystone squid. PLoS One 7, e38282.

SEG-Report:2018-1-V1 Quantifying the illegal trade in European glass eels (*Anguilla anguilla*): Evidences and Indicators" http://www.sustainableeelgroup.org/wp-content/uploads/2018/02/SEG-Report-2018-1-V1-1.pdf

Soreq, H., Seidman, S., 2001. Acetylcholinesterase—new roles for an old actor. Nature Reviews Neuroscience 2, 294-302.

Tilton, F.A., Bammler, T.K., Gallagher, E.P., 2011. Swimming impairment and acetylcholinesterase inhibition in zebrafish exposed to copper or chlorpyrifos

separately, or as mixtures. Comparative Biochemistry and Physiology Part C: Toxicology & Pharmacology 153, 9-16.

Vernino, S., Amador, M., Luetje, C.W., Patrick, J., Dani, J.A., 1992. Calcium modulation and high calcium permeability of neuronal nicotinic acetylcholine receptors. Neuron 8, 127-134.

Wall, F., 2014. Rare earth elements. Critical Metals Handbook, 312-339.

Xiaorong, C.Y.C.X.W., 2000. The effects of lanthanum and its complex compound (la-edta) on enzymes activities in fish liver. Environmental Chemistry 1, 006.

Xu, Z., Jiang, J., 2004. Effects of cerium on embryonic development of large yellow croaker, *Pseudosciaena crocea* (Richardson). Fisheries Science 23, 24-25.

Zeng, F., An, Y., Zhang, H., Zhang, M., 1999. The effects of La (III) on the peroxidation of membrane lipids in wheat seedling leaves under osmotic stress. Biological Trace Element Research, 69, 141-150.

Zheng, H.L., Zhao, Z.Q., Zhang, C.G., Feng, J.Z., Ke, Z.L., Su, M.J., 2000. Changes in lipid peroxidation, the redox system and ATPase activities in plasma membranes of rice seedling roots caused by lanthanum chloride. Biometals 13, 157-163.

Chapter 6

Warming enhances lanthanum accumulation and toxicity promoting cellular damage in glass eels (*Anguilla anguilla*)

Cátia Figueiredo [a,b,c,*,#], Joana Raimundo [a,d,#], Ana Rita Lopes [a,e], Clara Lopes [b,d], Nuno Rosa [b], Pedro Brito [b], Mário Diniz [c], Miguel Caetano [b,d], Tiago F. Grilo [a]

[a] MARE – Marine and Environmental Sciences Centre, Faculdade de Ciências da Universidade de Lisboa, Campo Grande, 1749-016 Lisboa, Portugal;

[b] Division of Oceanography and Marine Environment, IPMA – Portuguese Institute for Sea and Atmosphere, Av. Alfredo Magalhães Ramalho, 6, 1495-165 Algés, Portugal;

[c] UCIBIO, REQUIMTE, Departamento de Química, Faculdade de Ciências e Tecnologia, Universidade NOVA de Lisboa, 2829-516 Caparica, Portugal;

[d] CIIMAR – Interdisciplinary Centre of Marine and Environmental Research, Avenida General Norton de Matos S/N, 4450-208 Matosinhos, Portugal;

[e] MARE – Marine and Environmental Science Centre, ISPA – Instituto Universitário, R. Jardim do Tabaco 34, 1100-304 Lisboa, Portugal.

* Corresponding author:

[#] Authors equally contributed to the work.

Figueiredo, C.[#], Raimundo, J.[#], Lopes, A.R., Lopes, C., Rosa, N., Brito, P., Diniz, M., Caetano, M., Grilo, T.F. 2020. Warming enhances lanthanum accumulation and toxicity promoting cellular damage in glass eels (*Anguilla anguilla*). Environmental Research 191, 110051. (DOI 10.1016/j.envres.2020.110051)

ABSTRACT

Cumulative and continuing human emissions of greenhouse gases to the atmosphere are causing ocean warming. Rising temperature is a major threat to aquatic organisms and may affect physiological responses, such as acid-base balance, often compromising species fitness and survival. It is also expected that warming may influence the availability and toxicological effects of pollutants, including Rare Earth Elements. These are contaminants of environmental emerging concern with great economic interest. This group comprises yttrium, scandium, and lanthanides, being Lanthanum (La) one of the most common. The European eel (*Anguilla anguilla*) is critically endangered and constitutes a delicacy in Southeast Asia and Europe, being subject to an increasing demand on a global scale. Considering the vulnerability of early life stages to contaminants, we exposed glass eels to 1.5 µg L^{-1} of La for five days, plus five days of depuration, under a present-day temperature and warming scenarios (△T =+4°C). The aim of this study was to assess the bioaccumulation, elimination, and specific biochemical enzymatic endpoints in glass eels (*Anguilla anguilla*) tissues, under warming and La. Overall, our results showed that the accumulation and toxicity of La were enhanced with increasing temperature. The accumulation was higher in the viscera, followed by the head, and ultimately the body. Elimination was less effective under warming. Exposure to La did not impact acetylcholinesterase activity. Moreover, lipid peroxidation peaked after five days under the combined exposure of La and warming. The expression of heat shock proteins was majorly suppressed in glass eels exposed to La, at both tested temperatures. This result suggests that, when exposed to La, glass eels were unable to efficiently prevent cellular damage, with a particularly dramatic setup in a near-future scenario. Further studies are needed towards a better understanding of the effects of lanthanum in a changing world.

Keywords: Warming; Lanthanum; Glass eels; Cellular Damage; Heat Shock Proteins.

GRAPHICAL ABSTRACT

<table>
<tr><th colspan="2">Experimental design</th></tr>
<tr><td> 

T1; T3; T5; T10</td><td> 

T1; T3; T5; T10</td></tr>
<tr><th>Lanthanum bioaccumulation</th><th>Cellular damage markers</th></tr>
<tr><td> 
• Accumulation was higher in the viscera, followed by the head, and ultimately the body;
• Elimination was less effective in warming.</td><td> 
• La did not impact AChE activity;
• LPO peaked after five days under La and warming;
• La suppressed the expression of HSP, at both tested temperatures.</td></tr>
</table>

6.1 INTRODUCTION

The latest reports of the Intergovernmental Panel on Climate Change (IPCC) have been focusing on rising greenhouse gas emissions derived from human activities that are causing global warming (Aljerf, 2016). According to the IPCC's high greenhouse gas emission scenario (RCP8.5) the global mean surface air temperature may rise up to 4.9°C for the period 2081-2100, relative to the recent past (1986-2005) reference period (IPCC, 2019). In parallel, key ocean variables are experiencing profound changes associated with absorption of greenhouse gases by the ocean, manifested through alterations in temperature, pH, dissolved oxygen, among others (Doney et al., 2011; IPCC, 2019). In fact, warming is one of the biggest stressors to aquatic organisms, having the potential to disturb physiological responses, such as acid-base balance, which in turn can compromise species fitness and survival (Pankhurst and Munday, 2011; Pörtner and Peck, 2010). Under hostile environments (e.g., thermal stress), to cope with physiological stress and avoid cellular damage (Lushchak, 2011), aquatic organisms hold protective mechanisms and antioxidant defenses to counteract the overproduction of reactive oxygen species (ROS). Among the most frequent physiological strategies are protein repair and removal mechanisms, including the synthesis of heat shock proteins (HSPs) (Sørensen et al., 2003), which activity is temperature dependent (Alexandrov, 1969). Another mechanism is lipid peroxidation (LPO) which occurs when ROS react with lipids (Sachdeva et al., 2014). Warming can also interfere with acetylcholinesterase (AChE) activity, being able to modify the levels of the neurotransmitter acetylcholine (Halliwell and Gutteridge, 2015), that mediates nervous communication and ensures the optimal neuronal function. In addition, organisms proteome is responsible for genome repair, replication and expression, however it is expected that environmental stressors impact, to a certain degree, the DNA structure, causing DNA damage (Gueranger et al., 2014; Krisko et al., 2013). Reactive oxygen species can attack either DNA bases or the deoxyribose backbone, resulting, for example, in the oxidation of guanine in the C8 position that culminates in the easy formation of amongst studied DNA lesions suspected of mutagenicity – 8-hydroxy-2'-deoxyguanosine (8-OHdG). When 8-OHdG residues are present in DNA, GC to TA transversion occurs unless repaired prior to DNA replication (Cheng et al., 1992). 8-OHdG is an easier repairable genetic alteration than

irreversible chromosomal damage and has been used as a biomarker of environmental contamination, particularly in fish from polluted sites (Oliveira et al., 2010).

Besides temperature, an additional pressure that aquatic organisms are also dealing is contamination, manifested by the release of anthropogenic pollutants into the ocean as a consequence of increasing industrialization, technological progress and urbanization (Bukola et al., 2015). The great concern about contamination of aquatic ecosystems is reliant on potential interactions that may occur with other stressors, including temperature, since the availability and toxicological effects of pollutants may be altered by warming (Marques et al., 2010). Specifically, contaminants of environmental emerging concern have gathered the attention of the scientific community and regulatory authorities since the risks they may pose to human health and biota are still poorly understood (Herrmann et al., 2016; Pagano et al., 2015). As examples of these contaminants are the Rare Earth Elements (REE), in which are included the lanthanides, yttrium and scandium. Their use is key for numerous areas such as electronic technology, medical and industrial products, agriculture, and aquaculture, as bactericides or fertilizers (Wall, 2014). The increasing application of REE in these technologies and industries culminates in their transfer to aquatic ecosystems by means of both wastewater and industrial emission (Kulaksız and Bau, 2011). Furthermore, an ever-growing modern world demands state-of-the-art modern electronic devices of daily use, such as smartphones, screens, and tablets. The constant demand for newer and updated modern versions of these equipment has led to shorter lifespans which in turn is fasting the production of alarming quantities of electronic waste (e-waste) (Needhidasan et al., 2014). The dismantling, storage and burning of this e-waste may also represent REE contamination for the aquatic environment (Sepúlveda et al., 2010; Uchida et al., 2018). The urgent need for a better understanding of their impacts is evident when looking to the reviews available on the toxicity of REE (e.g. Herrmann et al. 2016 and references herein).

Lanthanum (La) is the second most common REE (Herrmann et al., 2016) and is mostly present in the stable oxidation state +3, and due to their comparable ionic radius, it is known to compete with the ion Ca^{2+} in organisms. (Qinhai, 1996; Zepf, 2013). This element is commonly used in many industrial applications (e.g., Rattanaphra et al. 2019), however very few studies exist on the toxicological effects of La in aquatic

systems (e.g., Cui et al., 2012; Moreira et al., 2020; Pinto et al., 2019), including a previous one dealing with juvenile stages of the European eel (*Anguilla anguilla*) (Figueiredo et al., 2018).

The natural populations of the European eel are critically endangered, according to the International Union for the Conservation of Nature, facing severe risk of extinction. A wide range of anthropogenic pressures are causative of the downfall of juvenile eel recruitment, such as overexploitation of this food resource, increasing contamination of its habitat and indirectly habitat loss, cumulative alien parasitoid species and climate change (Drouineau et al., 2018). The European eel has remarkable ecological features, typical of a catadromous species, comprising both oceanic and continental life phases, thus establishing the link between the open sea and inland rivers and lakes. Adult eels migrate from inland rivers to the Sargasso Sea to reproduce and die. The newborn leptocephali larvae migrate for up two years to reach the European coast. The larvae metamorphose then into glass eels and continue their journey through estuaries and upriver (Lecomte-Finiger, 1994). Glass eels are a delicacy in South East Asia and Europe (Crook and Nakamura, 2013), and their market price may reach thousands of euros, being therefore a lucrative resource subject to an increasing demand and illegal trafficking.

Fish early life stages have been recognized as more susceptible to climate change and pollutants than adult forms, which makes this juvenile eel stage even a more interesting model for experimentation, as demonstrated previously with lanthanum and mercury (e.g. Figueiredo et al., 2018; Grilo et al., 2015). Accordingly, the chief purpose of the present study was to assess the bioaccumulation and elimination of lanthanum-exposed glass eels tissues under present-day temperatures and warming (△T=+4°C) scenarios. In order to complement and understand better the physiological responses derived from La accumulation in eel tissues, specific biomarkers, indicative of cellular damage, will also be determined.

6.2 MATERIAL AND METHODS

6.2.1 Sampling site

Specimens were captured using hand-held dip nets and stow nets of 0.5-1.0 mm mesh size, in October 2018, in the oligohaline section of the Mondego River, on the

central Atlantic coast of Portugal (SW Europe), in a sole sampling occasion. Glass eels were immediately transferred to MARE-FCUL aquaculture facilities and maintained in tanks with continuously aerated water from the sample location, as in accordance with Grilo et al. (2015).

6.2.2 Experimental design

Three hundred and twenty glass eels were randomly distributed in tanks with continuously aerated dechlorinated tap water filtered through a 0.45-µm pore size membrane filter. Acclimation under a 12h light/12h dark photoperiod and salinity = 0 (V2 refractometer, TMC Iberia, Portugal), water temperature = 18±0.5°C (TFX 430 Precision Thermometer, WTW GmbH, Germany) and pH = 7.9±0.1 (SG8 e SevenGo pro™ pH/Ion meter, Mettler-Toledo International Inc., Switzerland), representing the natural habitat, lasted two weeks. Glass eels were measured (6.6±0.7 cm) and weighted (0.17±0.02 g, wet weight). In tanks mimicking the warming treatments, the water temperature was raised 1°C a day, to gradually allow acclimation before the start of the experiment. After the acclimation, the trial began with the following treatments: i) Control temperature (18°C, added La=0 µg L^{-1}); ii) exposed at the control temperature (18°C, added La=1.5 µg L^{-1}); iii) warming (22°C, added La=0 µg L^{-1}) and iv) exposed at the warming temperature (22°C, added La=1.5 µg L^{-1}). Throughout the experiment, a pH value of 7.9±0.1 and a total water hardness of 105±5 mg L^{-1} $CaCO_3$ (moderately hard) were registered. Water temperature was controlled through submerged heaters (V2Therm 200W aquarium heater, TMC Iberia, Portugal), and through seawater chillers (Hailea, HC-250A, Guangdong, China) in a water bath containing the experimental tanks. A La solution ($LaCl_3$, Merck), prepared in filtered freshwater, was added daily in the exposed treatments to warrant the La exposure. The water of the experimental tanks was completely renewed daily, at the same time, for the four treatments and the La concentration re-established with 1.5 µg L^{-1}, in the exposed treatments. The selected concentration is representative of levels present in polluted aquatic environments (e.g., Åström, 2001) and is comparable to other ecotoxicology trials (e.g., Moreira et al., 2020; Pinto et al., 2019). Water aliquots were sampled after 1h, 3h, 6h, 12h and 24h of the first exposure to measure dissolved La levels. One hour before the water renewal, individuals were fed ad libitum cod roe, every other day. Glass eels were sampled after 1 (T1), 3 (T3) and 5 (T5) days of exposure to La. Following this exposure phase, the

freshwater was renewed, and the elimination phase began, which lasted for 5 more days (T10). During this the water was also completely renewed daily at the same time, for all treatments, and animals kept being fed *ad libitum* every other day.

For the La quantification individuals were separated into three body parts: head, viscera (comprising the internal organs) and skinless body (the skin layer was removed). For the biomarkers' quantification individuals were separated into two body parts: head and remaining body (containing the internal organs and without the skin layer). Samples were stored at -80°C until further analyses.

6.2.3 Lanthanum quantification

Dissolved La concentrations (µg L^{-1}) were analyzed in filtrated and acidified (2% ultrapur HNO_3) water samples. In glass eels' tissues, La was determined in freeze-dried, grounded and homogenized samples (n=10 per treatment), after digestion with HNO_3 (destilled, 65% v/v) and H_2O_2 (suprapur, 30% v/v). Before digestions, labware was decontaminated with HNO_3 (20%) for two days and rinsed with ultra-pure water (Milli-Q water - 18.2 MΩ). A quadrupole ICP-MS (Thermo Elemental, X-Series) with a Peltier impact bead spray chamber and a concentric Meinhard nebulizer was used to determine La concentrations, following the experimental condition described in Raimundo et al. (2013).

La concentrations in glass eels body parts are presented in nanogram per gram of tissue dry weight (ng g^{-1}, dw).

6.2.3.1 Quality assurance and control

A nine-point calibration curve was used to quantify La, using a commercial solution of indium (In) as an internal standard (Merck, CertiPUR®). Three procedural blanks, prepared using the analytical procedure, and a quality control solution, used to evaluate the accuracy of the determinations, were included within each batch of 20 samples. Blanks accounted for less than 1% of the total La concentration in the samples.

The international certified reference material BCR 668 (muscle of *Mytilus edulis*), was also included within each batch of 20 samples to assess the accuracy of the analytic method.

6.2.4 Biomarkers

The heads and the remaining bodies (n=10 per treatment) of randomly collected individuals were homogenized (Ultra-Turrax, Staufen, Germany) in 0.5 mL of phosphate

buffered saline solution (PBS: 2.7 mM KCl, 0.14 M NaCl, 1.47 mM KH_2PO_4, 8.1 mM Na_2HPO_4 and, pH 7.4). Homogenates were centrifuged at 10.000 × g for 15 min at 4°C and then supernatants were frozen (-80°C) until further analyses. Each sample was run in technical replicates (triplicates), and the enzyme results were normalized to total protein content, as in Bradford (1976).

6.2.4.1 Neurotoxicity marker - Acetylcholinesterase

Acetylcholinesterase (AChE) activity was determined in the head of the glass eels according to an adaptation of the Ellman et al. (1961) method to 96-well microplates, as described by Figueiredo et al. (2018). For each sample, 25 µL of sample and 250 µL of a mix solution (50 mM of sodium phosphate, 75 mM acetylthiocholine iodide and 1 mM of 5,5'-dithio-bis-2-nitrobenzoic acid) were added to a 96-well microplate (Greiner Bio-one, Austria). The absorbance was read in a microplate reader at 415 nm (Biotek Synergy HTX multimode reader) every minute for 10 min. Acetylcholinesterase measurements were standardized to total protein concentration (nmol min^{-1} mg^{-1} total protein).

6.2.4.2 Oxidative damage markers – DNA damage and lipid peroxidation

DNA damage was measured in the head and remaining body of the glass eels, with an ELISA method and through quantification of 8-hydroxy-2'-deoxyguanosine (8-OHdG), as described in Lopes et al. (2019). This compound has been widely chosen as a biomarker of environmental contamination linked with DNA damage and its presence in cells may lead to mutagenesis and thus play a significant role in disease processes (Cooke et al., 2003; Oliveira et al., 2010). For our analysis, a total of 100 µL of each sample was added to 96-well microplates (Greiner Bio-one, Austria) and allowed to incubate overnight at 4°C. The plates were then washed three times with PBS-TWEEN 20, and incubated for 90 min at room temperature with 200 µL of 1% bovine serum albumin (BSA, NZYTech, 985, Portugal). After another washing procedure, microplates were incubated overnight with the primary antibody (anti-OHdG, clone 15 A3, Sigma-Aldrich, Germany). Microplates were again washed and incubated for 90 min at 37°C with the secondary antibody (alkaline phosphatase-conjugated anti-mouse IgG, Fab specific, Sigma-Aldrich, USA). After a final washing procedure, plates were incubated for 30 min at room temperature with the substrate (SIGMA FASTTM p-Nitrophenyl Phosphate Tablets, Sigma-Aldrich, USA). The reaction was stopped, after 30 min, through the

addition of 100 µL of 3 M NaOH. The absorbance was read at 405 nm using a microplate reader (Biotek Synergy HTX multi-mode reader).

Lipid peroxidation (LPO) was determined in glass eels' remaining body according to the thiobarbituric acid reactive substances (TBARS) assay (Uchiyama and Mihara, 1978), over the quantification of malondialdehyde (MDA), an end product of lipid damage.

Five µL of each sample, 45 µL of monobasic sodium phosphate buffer (50 mM), 12.5 µL of sodium dodecyl sulfate (8.1%), 93.5 µL of trichloroacetic acid (20%, pH 3.5), 93.5 µL of thiobarbituric acid (1%), and 50.5 µL of Milli-Q ultrapure water were added to a microtube. Subsequently microtubes were placed in boiling water (100°C) for 10 min. Then, microtubes were placed on ice until cool and 62.5 µL of Milli-Q ultrapure water was added. Finally, 150 µL of each sample was added to 96-well microplates (Greiner Bio-one, Austria), and the absorbance read at 532 nm (Biotek Synergy HTX multi-mode reader). Malondialdehyde (MDA) concentrations were calculated based on a calibration curve (0 - 0.3 µM MDA).

6.2.4.3 Heat shock proteins

Heat Shock Protein 70 (HSP) were quantified in the supernatants of the homogenate and centrifuged glass eels' remaining body through ELISA, as described in Lopes et al. (2018). In sum, 10 µL of sample diluted in 980 µL PBS was added to 96-well microplate (Microlon 600, Greiner, Austria) and allowed to incubate overnight at 4°C. On the next day, microplates were washed three times with PBS TWEEN-20 (0.05%). Later, 100 µL of BSA (1% bovine serum albumin, NZYtech, 98%, Portugal) was added to each well, and microplates incubated for 90 min at 37°C. Then, 50 µL of primary antibody 5 µg mL^{-1} of anti-HSP70/HSC70 in 1% BSA (Acris, USA) was added to each well. Microplates were once more incubated overnight at 4°C. After being washed three times, microplates were allowed to incubate for 90 min at 37°C with the second antibody [50 µL of 1 µg mL^{-1}; alkaline phosphatase-conjugated anti-mouse IgG (Fab specific, Sigma-Aldrich, USA)]. After the last washing procedure, 100 µL of the substrate (SIGMA FASTTM p-Nitrophenyl Phosphate Tablets, Sigma-Aldrich, USA) was added to each well and incubated for 30 min at room temperature. Finally, 50 µL of stop solution (3 M NaOH) was added to each well and the absorbances read at 405 nm (Biotek Synergy HTX multi-mode reader). HSP content was calculated from the calibration curve, based on

serial dilutions of purified HSP70 active protein (0 - 2.000 µg mL^{-1}, OriGene Technology, USA) and data normalized to sample protein (µg mg^{-1} total protein).

6.2.5 Statistical analyses

Normality and equality of variances were tested with Kolmogorov-Smirnov and Levene's tests, respectively. Differences between the four treatments within each sampling time, for lanthanum accumulation and elimination, AChE activity, DNA damage, LPO (MDA levels) and HSP were tested via ANOVA followed by Tukey HSD post hoc tests. These analyses were performed in STATISTICA™ 12 software (Statsoft, Inc., Tulsa, OK 74104, USA). A significance level of $p<0.05$ was applied.

6.3 RESULTS

Median La levels (µg L^{-1}) in the water aliquots sampled after 1, 3, 6, 12 and 24 hours of exposure are presented in Annex 5, Supplemental Table 6.1. Median concentrations in the first 24h were 0.034 µg L^{-1} in the 18°C and 0.057 µg L^{-1} in the 22°C non-spiked tanks. In the spiked tanks, dissolved median La concentrations were 1.3 and 1.6 µg L^{-1} in the 18°C and 22°C tanks, respectively. Concentrations in spiked tanks varied 6 to 13% from the nominal concentrations (1.5 µg L^{-1}).

6.3.1 Bioaccumulation and elimination

Median and ranges of La concentrations (ng g^{-1}, dry weight) in the head, skinless body and viscera are presented in Table 6.1.

Table 6.1 - Median and ranges of La concentration (ng g^{-1}, dry weight) of the control, exposed and post-exposed glass eels' head, skinless body, and viscera at T1, T3, T5 and T10, at 18°C and 22°C. Asterisk indicate the presence of concentrations below detection limit value (1.4 ng g^{-1}, dw).

Time	Treatment	Head	Skinless body (ng g^{-1}, dry weight)	Viscera
T1	18ºC control	3.4 (0.32 – 7.9)	0.96 (0.80 – 1.4)	29 (8.4 – 39)
	18ºC exposed	5.8 (2.1 – 18)	2.5 (0.74 – 3.0)	45 (14 – 91)
	22ºC control	12 (6.7 – 15)	0.61 (0.22 - 1.3)	8.18 (0.42 – 29)
	22ºC exposed	5.4 (4.1 – 23)	2.6 (2.0 – 7.0)	102 (70 - 144)
T3	18ºC control	8.1 (3.6 – 9.4)	0.74 (0.22 – 1.7)	26 (11 – 51)
	18ºC exposed	17 (8.4 – 22)	4.7 (3.5 – 6.8)	28 (14 – 30)
	22ºC control	6.7 (5.4 – 11)	2.2 (0.63 – 4.0)	20 (18 – 50)
	22ºC exposed	19 (18 – 23)	4.3 (0.91 – 8.2)	290 (132 – 582)
T5	18ºC control	22 (16 – 35)	1.4 (0.32 – 2.7)	39 (18 – 49)
	18ºC exposed	75 (27– 123)	2.8 (0.82 – 6.2)	67 (59 – 151)
	22ºC control	36 (24 – 47)	3.9 (1.7 – 5.6)	28 (25 – 37)
	22ºC exposed	141 (136 – 163)	7.1 (1.6 – 9.1)	119 (109 – 276)
T10	18ºC control	3.7*	0.84 (0.31 -1.1)	37 (19 – 55)
	18ºC post-exposed	8.9 (5.3 – 16)	1.2 (1.1 – 2.1)	25 (17 – 55)
	22ºC control	4.2 (1.2 – 4.4)	0.72 (0.38 – 1.0)	34 (20 – 34)
	22ºC post-exposed	62 (45 – 62)	2.2 (2.1 – 4.8)	15 (9.1 – 48)

6.3.1.1 Head

Concentrations of La (ng g^{-1}, dry weight) in the glass eels' heads are presented in Figure 6.1.

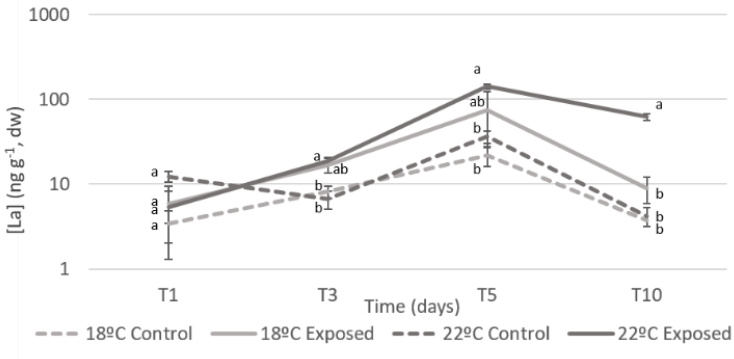

Figure 6.1 - Concentrations of lanthanum (ng g^{-1}, dry weight) of the control, La exposed and post-exposed glass eels' head at 18°C and 22°C in the different sampling times (T1, T3, T5 and T10). Values represent medians ± SE. Different letters represent significant differences between treatments within each sampling time ($p<0.05$).

After one day of exposure (T1) no significant differences were observed between the four treatments, yet after three days of exposure (T3) a significant accumulation occurred in the warming treatment ($p=0.026$). This significant difference from their corresponding control was higher after 5 days of exposure (T5, $p=0.004$). Interestingly, the exposed treatment at 18°C, although higher was never statistically different from their control counterpart, even though there was a trend for La to be accumulated at this temperature. A decrease in La concentration during the elimination phase was observed, nevertheless the post-exposed eels in warming treatment did not reach lanthanum concentrations similar to the control values ($p=0.022$).

6.3.1.2 Skinless Body

At 22°C there was a constant increase in the concentration of La in the exposed glass eels' body (Figure 6.2), for the 5 exposure days, although a statistically significant difference between the exposed and the control was only observed in T1 ($p=0.007$). This concentration decreased during elimination (T10), however not reaching control values ($p=0.003$). At 18°C, accumulation peaked at T3 ($p=0.02$). Interestingly, La concentration decreased from T3 onwards, in glass eels exposed at 18°C, even in a continuously contaminated environment.

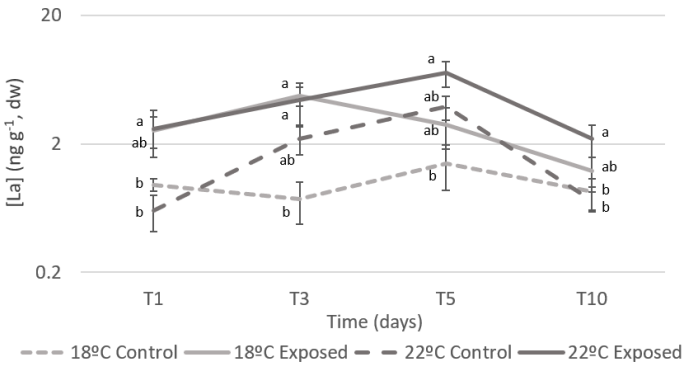

Figure 6.2 - Concentrations of lanthanum (ng g^{-1}, dry weight) of the control, La exposed and post-exposed glass eels' skinless body at 18°C and 22°C in the different sampling times (T1, T3, T5 and T10). Values represent medians ± SE. Different letters represent significant differences between treatments within each sampling time ($p<0.05$).

6.3.1.3 Viscera

Concentrations of La (ng g^{-1}, dry weight) in the glass eels' viscera are presented in Figure 6.3.

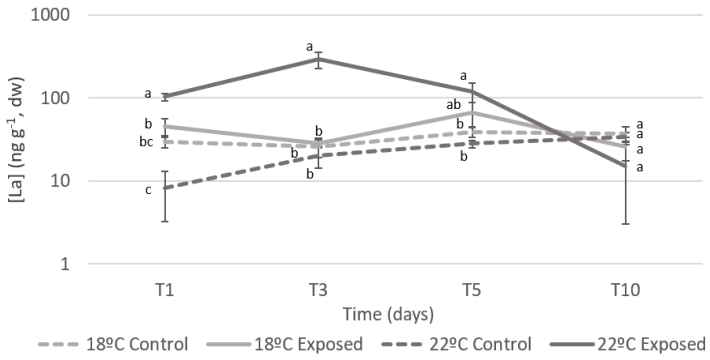

Figure 6.3 - Concentrations of lanthanum (ng g^{-1}, dry weight) of the control, La exposed and post-exposed glass eels' viscera at 18°C and 22°C in the different sampling times (T1, T3, T5 and T10). Values represent medians ± SE. Different letters represent significant differences between treatments within each sampling time ($p<0.05$).

Accumulation in the exposed eels at the warming treatment was greater than in the exposed eels at 18°C, except in T5. During the exposure phase, at the warming scenario, accumulation in the viscera occurred in the three sampling periods ($p=0.0001$, $p=0.0005$, $p=0.004$, respectively). There was no statistical difference between the exposed eels at 18°C and their control counterpart ($p>0.05$) over time. Lanthanum concentrations in exposed eels' viscera decreased, at both temperatures, during the post-exposure period to values comparable to the controls ($p>0.05$).

6.2.2 Biomarkers

Median and ranges of acetylcholinesterase activity (AChE, nmol min^{-1} mg^{-1} total protein), DNA damage (determined via the quantification of 8-OHdG, abs mg^{-1} protein), lipid peroxidation values (MDA concentrations, nmol mg^{-1} total protein) and heat shock protein 70 (µg mg^{-1} protein) in the head and body are presented in Table 6.2.

Table 6.2 - Median and ranges of acetylcholinesterase activity (AChE, nmol min^{-1} mg^{-1} total protein), lipid peroxidation values (MDA concentrations, nmol mg^{-1} total protein), heat shock proteins (µg mg^{-1} protein) and DNA damage (8-OHdG, abs mg^{-1} protein) of the control, La exposed and post-exposed glass eels' head and body at T1, T3, T5 and T10, at 18°C and 22°C.

Time	Treatment	Head		Body		
		AChE (nmol min^{-1} mg^{-1} total protein)	DNA Damage 8-OHdG (abs/mg protein)	LPO (nmol mg^{-1} total protein)	DNA Damage 8-OHdG (abs/mg protein)	HSP (µg mg $protein^{-1}$)
T1	18ºC control	292 (197 – 568)	0.054 (0.047 - 0.069)	0.028 (0.06 – 0.039)	0.058 (0.051 – 0.068)	1054 (526 – 1086)
	18ºC exposed	237 (178 – 284)	0.072 (0.061 – 0.088)	0.019 (0.010 – 0.025)	0.046 (0.042 – 0.059)	1045 (317 – 1385)
	22ºC control	287 (212 – 357)	0.053 (0.041 – 0.065)	0.017 (0.012 – 0.024)	0.052 (0.045 – 0.059)	1121 (681 – 1311)
	22ºC exposed	168 (144 – 243)	0.064 (0.051 – 0.092)	0.008 (0.003 – 0.015)	0.053 (0.050 – 0.066)	298 (235 – 888)
T3	18ºC control	252 (150 – 286)	0.067 (0.060 – 0.072)	0.022 (0.011 – 0.069)	0.054 (0.049 – 0.059)	821 (747 – 881)
	18ºC exposed	225 (150 - 352)	0.076 (0.058 – 0.094)	0.013 (0.007 – 0.025)	0.056 (0.046 – 0.068)	446 (316 – 760)
	22ºC control	218 (194 – 292)	0.069 (0.065 – 0.078)	0.018 (0.011 – 0.038)	0.052 (0.044 – 0.064)	1146 (856 – 1327)
	22ºC exposed	263 (214 – 296)	0.077 (0.072 – 0.084)	0.018 (0.011 – 0.019)	0.058 (0.053 – 0.069)	357 (253 – 695)
T5	18ºC control	231 (168 – 269)	0.063 (0.054 – 0.068)	0.028 (0.023 – 0.041)	0.047 (0.043 – 0.052)	820 (670 – 876)
	18ºC exposed	265 (164 – 369)	0.068 (0.066 – 0.099)	0.017 (0.016 -0.028)	0.067 (0.060 – 0.079)	414 (204 – 508)
	22ºC control	280 (236 – 327)	0.063 (0.063 – 0.064)	0.020 (0.012 – 0.025)	0.048 (0.045 – 0.054)	1239 (1089 – 1334)
	22ºC exposed	269 (202 – 321)	0.081 (0.073 – 0.098)	0.049 (0.021 – 0.097)	0.058 (0.055 – 0.063)	313 (201 – 695)
T10	18ºC control	234 (159 – 267)	0.075 (0.066 – 0.075)	0.035 (0.032 – 0.044)	0.065 (0.050 – 0.077)	943 (730 – 947)
	18ºC post-exposed	227 (200 – 297)	0.095 (0.094 – 0.095)	0.025 (0.022 – 0.055)	0.061 (0.052 – 0.066)	317 (264 – 368)
	22ºC control	223 (215 – 236)	0.078 (0.072 – 0.083)	0.018 (0.014 – 0.022)	0.064 (0.058 – 0.070)	1091 (927 – 1404)
	22ºC post-exposed	228 (207 – 337)	0.083 (0.070 – 0.093)	0.029 (0.014 – 0.043)	0.060 (0.054 – 0.075)	363 (299 – 631)

6.3.2.1 Head

6.3.2.1.1 AChE

Median values of AChE activity (nmol min^{-1} mg^{-1} total protein) in the head are presented in Figure 6.4a.

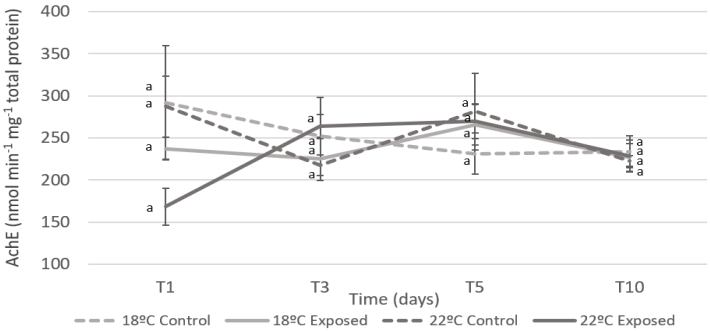

Figure 6.4 a - Acetylcholinesterase activity (AChE, nmol min^{-1} mg^{-1} total protein) of the control, La exposed and post-exposed glass eels' head at 18°C and 22°C in the different sampling times (T1, T3, T5 and T10). Values represent medians ± SE. Different letters represent significant differences between treatments within each sampling time ($p<0.05$).

There were no significant differences between the glass eels exposed to La and those non-exposed, at both temperatures ($p>0.05$), during both exposure (T1, T3, T5) and elimination phase (T10).

6.3.2.1.2 DNA damage

DNA damage (determined via the quantification of 8-OHdG, abs mg-1 total protein) occurred in the head of glass eels (Figure 6.4b) exposed at 22°C ($p=0.035$), after

just one day of exposure (T1), compared to the equivalent non-exposed La treatment at the same temperature.

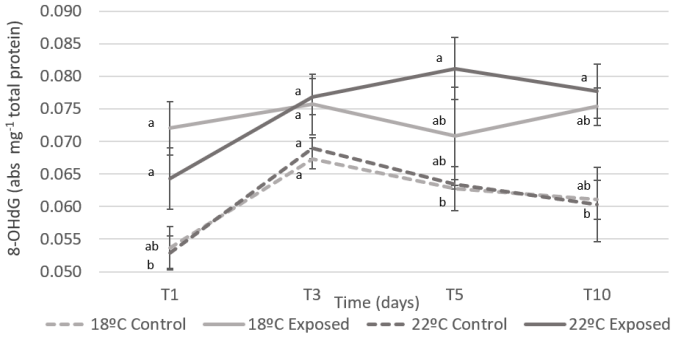

Figure 6.4 b - DNA damage, determined via the quantification of 8-OHdG (abs mg^{-1} protein) of the control, La exposed and post-exposed glass eels' head at 18°C and 22°C in the different sampling times (T1, T3, T5 and T10). Values represent medians ± SE. Different letters represent significant differences between treatments within each sampling time ($p<0.05$).

At T5, DNA damage peaked in glass eels' heads exposed at the warming treatment, but not statistically significantly different from their control. After the elimination period (T10), DNA Damage, for both temperatures, did not decrease significantly, still there were differences between glass eels exposed at 22°C and their equivalent controls at the same temperature.

6.3.2.2 Body

6.3.2.2.1 LPO

Malondialdehyde (MDA concentrations, nmol mg^{-1} total protein) medians (Figure 6.5A) were lower in the exposed glass eels' body than their equivalent controls, for both temperatures (18°C, $p=0.005$ and 22°C, $p=0.025$), after just one day of exposure (T1).

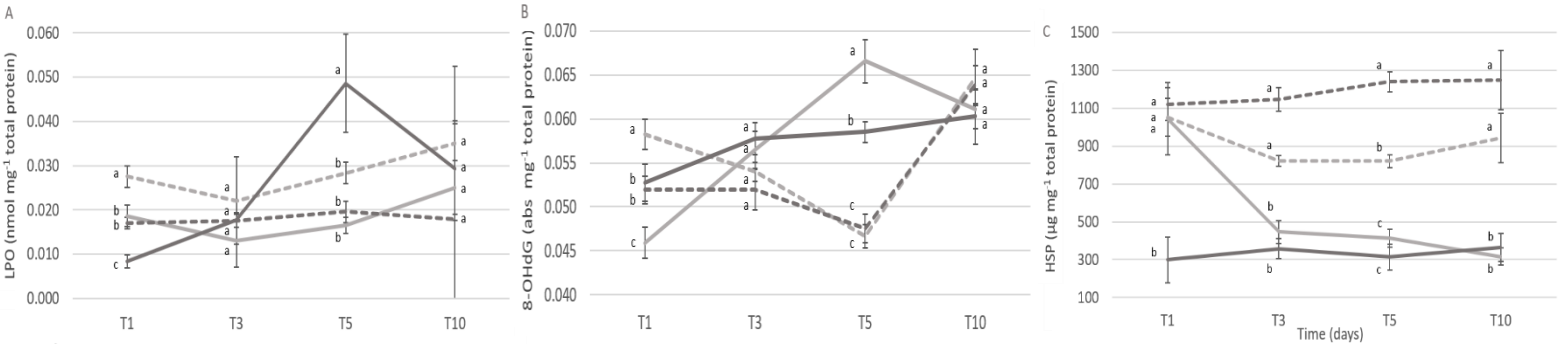

Figure 6.5 - A) Lipid peroxidation values (MDA concentrations, nmol mg^{-1} total protein), B) DNA damage, determined via the quantification of 8-OHdG (abs mg^{-1} protein) and C) Heat Shock Protein 70 (µg mg^{-1} protein) of the control, La exposed and post-exposed glass eels' body at 18°C and 22°C in the different sampling times (T1, T3, T5 and T10). Values represent medians±SE. Different letters represent significant differences between treatments within each sampling time ($p<0.05$).

Furthermore, the MDA values increased in the exposed glass eels' body in the warming scenario, reaching the highest values at T5. The exposed eels at 18°C did not follow this trend. After the elimination period (T10) the MDA values that had peaked at T5 for La exposed eels in a warming scenario, decreased to values similar to the controls.

6.3.2.2.2 DNA Damage

Median values of DNA damage (determined via the quantification of 8-OHdG, abs mg^{-1} total protein) in the body are presented in Figure 6.5b. Lanthanum exposed treatment at 18°C, at T1, exhibited lower values than their control counterpart (p=0.0005). However, these values increased significantly, reaching a peak at T5 and being different than their control (p=0.0002). Regarding glass eels exposed to a combined scenario of La and warming, it was only at T5, that values of DNA damage differed, when compared to their control counterparts (p=0.009). At T10 values of both exposed 18°C and 22°C matched with controls.

6.3.2.2.3 HSP

At T1 La exposed eels in a warming scenario showed a much lower expression of HSP (Figure 6.5C), than their control counterparts (p=0.004) and persisted fairly stable over time. Values of HSP decreased substantially in La exposed glass eels at 18°C at T3 and were different from their respective control (p=0.04). By the fifth day of exposure, the control at the warming scenario presented higher expression of HSP, than the control at 18°C (p=0.002). The five-day elimination phase was insufficient to restore the expression of HSP, with post-exposed glass eels at both temperatures, presenting lower expressions of HSP than their controls (18°C - p=0.004 and 22°C - p=0.0007).

6.4 DISCUSSION

The input of contaminants to the environment often results in deleterious effects on wildlife, and ultimately on human health. Warmer temperatures impose additional pressure on wildlife, by changing ecosystems structure (Cheung et al., 2009). Recent research confirmed that warming significantly decreased glass eels' survival (Borges et al., 2019). This reinforces the assumption that the combination of increasing loads of contaminants into the environment and warming would play a major role on *A. anguilla* fitness and, ultimately, survival. Overall, our results showed that in a warming scenario accumulation and toxic effects of lanthanum are enhanced. To ensure that age-

dependent differences of the organisms wouldn't influence the La accumulation, glass eels used in this study were in the same pigmentation stage to secure ontogeny similarity. Water pH and temperature are pointed has abiotic factors that influence La availability (Herrmann et al., 2016). Hence, pH was kept stable (7.9±0.1) at a level known to have 90% of La as a trivalent ion (Bouyer et al., 2006) that can compete with Ca^{2+} for biological binding sites, and affect La toxicity (Barry and Meehan, 2000; Evans, 1983). Although water hardness can also influence this element availability (reviewed in Herrmann et al., 2016), it is not clear to comprehend how, and for that reason, the water hardness was kept as moderately hard (105±5 mg L^{-1} $CaCO_3$) throughout the experiment, for all four treatments, in order to avoid bias. Here we began to unveil the influence of temperature in the availability of La. At 18°C there was a 24.4% loss of La, after 24h of exposure, either due to bioaccumulation, adsorption to particulate matter or glass tank walls. Interestingly, at 22°C the loss was shortened to 18.3%, after 24h of exposure. Alterations in the partitioning between the sediments, water, atmosphere, and biota of toxicants can be caused by climate change (Noyes et al., 2009). The increased temperature may interfere in air-surface exchange, deposition, and reaction rates (e.g., photolysis, biodegradation, oxidation in the air). The obtained results showed that in a warming scenario the bioavailability of La in water is slightly enhanced. The raised water temperature may as well alter contaminants to more bioactive metabolites, impairing homeostasis (reviewed in Noyes et al., 2009 and Manciocco et al., 2014).

In glass eels' heads, bioaccumulation increased consistently during the exposure period (5 days). At 18°C post-exposed eels were able to eliminate La to values as the controls, however at a warming temperature (22°C) this elimination was not so effective. To the best of our knowledge, this is the first study addressing the combined effects of a climate change variable, specifically thermal stress, and La, therefore comparison with other data is arduous. Warmer temperatures often enhance fish metabolism (Anacleto et al., 2018) which can lead to higher contaminants' uptake, either due to increased ventilation or enhanced feeding rates (Maulvault et al., 2016). On another hand, warmer temperatures may also promote contaminants' metabolization and elimination (Serra-Compte et al., 2018). This is in line with our results, where in a warming condition, a higher accumulation was not accompanied by an enhanced elimination. The blood-brain barrier can limit the release of elements into

the bloodstream, and thus affect elimination. Kiyatkin and Sharma (2009) described the permeability of this barrier as highly dependent on temperature by exposing rats to different temperatures. To preserve optimal neurotransmission and other vital functions, low elemental concentrations are usually found in the head (Mieiro et al., 2011). Interestingly, the skinless body of exposed glass eels presented globally lower accumulation values of La, than the head. Although this result is not in line with Figueiredo et al. (2018) presumably resulted from the higher (one order of magnitude) exposure concentration in the present experiment. At 18°C, La concentrations in exposed glass eels' skinless body reached a peak at T3 and afterward the concentrations decreased steadily, even in a continuously exposed medium. This interesting and baffling pattern of elimination in a continuously exposed medium suggest the existence of an unknown mechanism in glass eels to cope with La contamination. As expected, bioaccumulation was greater at higher temperatures in the viscera and this body part presented, globally, the higher accumulation values. This body part was also able to eliminate La, at both 18°C and 22°C, to non-exposed background values. This elimination ability was expected as, in fact, the viscera has been described as a primary accumulation and elimination organ in fish (e.g., Figueiredo et al., 2018; Pereira et al., 2015; Raimundo et al., 2013).

Aquatic communities can be resilient to environmental changes, such as thermal stress and increasing loads of pollutants (Snoeijs-Leijonmalm et al., 2017). However, these buffering capacities are limited and species can reach endpoints with permanent repercussions. The increased bio-activation or detoxification caused by warmer temperature will affect, accordingly, the toxicity of La. Acetylcholinesterase hydrolysis the neurotransmitter acetylcholine (Colovic et al., 2013) and when this process is impacted neurotransmission disturbance and stress occurs. In our previous study, we described a stimulatory AChE activity in exposed glass eels' heads, to 120 ng L^{-1} at 18°C. Interestingly, in the present study, glass eels' heads exposed to 1.5 µg L^{-1} La (12,5-fold higher), did not show similar AChE activity. Agathokleous et al. (2018) and Zhang et al. (2017), amongst other authors, have described the hormesis effect of La, in plants. Hormesis is a chemical phenomenon where stimulation can occur at low doses and inhibition can occur at high doses. Further dose-dependent effects of La have been demonstrated on the immune system of mammals. Foreman and Mongar (1973) also

stated dose-dependent effects of La in mammals, high concentrations of La suppressed histamine secretion in the peritoneal cavity of rats, while low-dose promoted histamine release. As far as we are aware, the hormesis effect has not been described for fish, however, La could have triggered a hormesis response, not interfering with the AChE activity. On the other hand, DNA damage occurred in exposed glass eels' heads after one day at 18°C, being therefore caused by La exposure alone, and was exacerbated by warming. At 22°C, La non-exposed eel's heads did not show DNA damage, dismissing the effect of temperature. The DNA damage values of the glass eels' head previously exposed to La, did not recover during the elimination phase (5 days), at both temperatures. This highlights the effects of La on the DNA, and the inability of eels to recover after being exposed to a La-contaminated environment. Overall, DNA damage values were greater in the head, than in the remaining body, which denotes the neurotoxic effects of La. The synergetic effect caused by warming and La accumulation on DNA, can be a result of ROS interaction with the DNA chain, which in turn can cause base oxidation, base-pair disparities, and breaks, and ultimately trigger mutations with unknown consequences. This DNA damage can also be caused by protein damage, as damage in the proteasome is intrinsically related to genome repair mechanisms (Gueranger et al., 2014; Krisko and Radman, 2013).

Lipid peroxidation is caused by the reaction of ROS with lipids (Sachdeva et al., 2014). When lipid molecules are broken into LPO by-products such as malondialdehyde, lipid damage occurs. In exposed glass eels' body, LPO values reached a peak after 5 days of exposure to warming and La contamination. Since they occur in a chain of reaction manner, this peak suggests that the antioxidant enzymatic activity was insufficient to cope with both stressors and was unable to avoid lipid damage. In fact, previous studies have described an increasing antioxidant enzymatic activity in fish that is still insufficient in avoiding lipid peroxidation (e.g., Pimentel et al., 2015), in a climate change scenario. This damage did not occur in the non-exposed glass eels' body under warming, nor at La exposed glass eels' body at 18°C, suggesting that the effects of warming and La exposure on LPO are synergetic.

The heat shock response is a set of physiological mechanisms that aquatic organisms possess to evade deleterious effects caused by environmental stressors (Lesser, 2006). This response includes the synthesis of heat shock proteins that are vital

in the stabilization and refolding of denatured protein (Tomanek, 2010). Increasing temperatures can lead to protein unfolding and thus interfere with their function (Dong et al., 2008). In this scenario HSP's are triggered. Our results revealed, as expected, the highest expressions of HSP in the non-exposed glass eel's body under warming. Remarkably, the expression of HSP was majorly suppressed in glass eels exposed to La. One day of exposure to La was insufficient to cause this inhibition at 18°C, nonetheless after T3 this suppression was evident. At 22°C, where normally HSP's are triggered, one day of exposure to La was sufficient to repress these vital proteins. Wang et al. (2011) exposed hydroponically cultivated *Vicia faba* seedlings to different concentrations of La, and described a hormetic dose-response, with HSP production enhanced at low doses and suppressed at higher doses. However, the lower dose in this paper (0.25 mg L^{-1}) is up to 150 times higher than the concentration used in this study (1.5 µg L^{-1}), which could point to a species-specific reaction to La. Our results suggest that, when exposed to La, glass eels' will be unable to stabilize and refold denatured proteins, and prevent cellular damage, with a particular dramatic setup in a near-future scenario.

Dose responses are vital in toxicology and the assessment of the effects of La will depend on them. Furthermore, the influence of other water parameters, such as water hardness and major ions content, in the La availability and toxicity should also be considered. This is the first study to unveil the combined effects of warming and La and will set the baseline on which future studies dealing with this emergent problematic will build upon. Nevertheless, to better understand the effects of La in a changing world, the effects of global climate change (i.e., the combined effect of ocean acidification and warming) on REEs toxicity need to be scrutinized.

Concomitantly, the empirical data deriving from these studies will be pivotal for the decision-making process of policy makers (e.g., governments and environmental agencies) when legislating for these new emergent pollutants and timely environmental policies.

ACKNOWLEDGMENTS

Tiago F. Grilo acknowledges the Junior Researcher contract attributed by FCT (CEECIND/03517/2017). The authors would also like to acknowledge the strategic project UID/MAR/04292/2019 granted to MARE. Cátia Figueiredo also acknowledges the PhD grant SFRH/BD/130023/2017 by FCT. The authors acknowledge all colleagues

who provided technical and scientific insights. Finally, the authors thank the two anonymous reviewers for the useful comments and valuable advice for the improvement of this work.

REFERENCES

Agathokleous, E., Kitao, M., Calabrese, E.J., 2018. The rare earth element (REE) lanthanum (La) induces hormesis in plants. Environmental Pollution 238, 1044-1047.

Alexandrov, V.Y., 1969. Conformatonal flexibility of proteins, their resistance to proteinases and temperature conditions of life. Biosystems 3, 9-19.

Aljerf, L., 2016. Reduction of gas emission resulting from thermal ceramic manufacturing processes through development of industrial conditions. Scientific Journal of King Faisal University 17, 1-10.

Anacleto, P., Figueiredo, C., Baptista, M., Maulvault, A.L., Camacho, C., Pousão-Ferreira, P., Valente, L.M., Marques, A., Rosa, R., 2018. Fish energy budget under ocean warming and flame retardant exposure. Environmental Research 164, 186-196.

Åström, M., 2001. Abundance and fractionation patterns of rare earth elements in streams affected by acid sulphate soils. Chemical Geology 175, 249-258.

Barry, M.J., Meehan, B.J., 2000. The acute and chronic toxicity of lanthanum to *Daphnia carinata*. Chemosphere 41, 1669-1674.

Bouyer, F., Sanson, N., Destarac, M., Gerardin, C., 2006. Hydrophilic block copolymer-directed growth of lanthanum hydroxide nanoparticles. New Journal of Chemistry 30, 399-408.

Borges, F.O., Santos, C.P., Sampaio, E., Figueiredo, C., Paula, J.R., Antunes, C., Rosa, R., Grilo, T.F., 2019. Ocean warming and acidification may challenge the riverward migration of glass eels. Biology Letters 15, 20180627.

Bradford, M.M., 1976. A rapid and sensitive method for the quantitation of microgram quantities of protein utilizing the principle of protein-dye binding. Analytical biochemistry 72, 248-254.

Bukola, D., Zaid, A., Olalakan, E.I., Falilu, A., 2015. Consequences of anthropogenic activities on fish and the aquatic environment. Poultry, Fisheries & Wildlife Sciences 3, 138.

Cheng, K.C., Cahill, D.S., Kasai, H., Nishimura, S., Loeb, L.A., 1992. 8-Hydroxyguanine, an abundant form of oxidative DNA damage, causes G-T and A-C substitutions. Journal of Biological Chemistry 267, 166–172.

Cheung, W.W., Lam, V.W., Sarmiento, J.L., Kearney, K., Watson, R., Pauly, D., 2009. Projecting global marine biodiversity impacts under climate change scenarios. Fish and Fisheries 10, 235-251.

Colovic, M.B., Krstic, D.Z., Lazarevic-Pasti, T.D., Bondzic, A.M., Vasic, V.M., 2013. Acetylcholinesterase inhibitors: pharmacology and toxicology. Current Neuropharmacology 11, 315-335.

Cooke, M.S., Evans, M.D., Dizdaroglu, M., Lunec, J., 2003. Oxidative DNA damage: mechanisms, mutation, and disease. The FASEB Journal 17, 1195–1214.

Crook, V., Nakamura, M., 2013. Assessing supply chain and market impacts of a CITES listing on Anguilla species. Traffic Bulletin 25, 24-30.

Cui, J.A., Zhang, Z., Bai, W., Zhang, L., He, X., Ma, Y., Liu, Y., Chai, Z., 2012. Effects of rare earth elements La and Yb on the morphological and functional development of zebrafish embryos. Journal of Environmental Sciences 24, 209-213.

Doney, S.C., Ruckelshaus, M., Duffy, J.E., Barry, J.P., Chan, F., English, C.A., Galindo, H.M., Grebmeier, J.M., Hollowed, A.B., Knowlton, N., Polovina, J., Rabalais, N.N., Sydeman, W.J., Talleu, L.D., 2011. Climate change impacts on marine ecosystems. Annual Review of Marine Science 4, 11-37.

Dong, Y., Miller, L.P., Sanders, J.G., Somero, G.N., 2008. Heat-shock protein 70 (Hsp70) expression in four limpets of the genus Lottia: interspecific variation in constitutive and inducible synthesis correlates with in situ exposure to heat stress. Biology Bulletin 215, 173-181.

Drouineau, H., Durif, C., Castonguay, M., Mateo, M., Rochard, E., Verreault, G., Yokouchi, K., Lambert, P., 2018. Freshwater eels: A symbol of the effects of global change. Fish and Fisheries 19, 903-930.

Ellman, G.L., Courtney, K.D., Andres, V., Featherstone, R.M., 1961. A new and rapid colorimetric determination of acetylcholinesterase activity. Biochemical Pharmacology 7, 88-95.

Evans, C.H., 1983. Interesting and useful biochemical properties of lanthanides. Trends in Biochemical Sciences 8, 445-449.

Figueiredo, C., Grilo, T.F., Lopes, C., Brito, P., Diniz, M., Caetano, M., Rosa, R., Raimundo, J., 2018. Accumulation, elimination, and neuro-oxidative damage under lanthanum exposure in glass eels (*Anguilla anguilla*). Chemosphere 206, 414-423.

Foreman, J.C. and Mongar J.L., 1973. The action of lanthanum and manganese on anaphylatic istamine secretion. British Journal of Pharmacology 48, 527-537.

Grilo, T., Mendes, T., Coelho, J., Pereira, E., Pardal, M., Cardoso, P., 2015. Kinetics of mercury accumulation and elimination in edible glass eel (*Anguilla anguilla*) and potential health public risks. Water Air Soil Pollution 226: 166.

Gueranger, Q., Li, F., Peacock, M., Larnicol-Fery, A., Brem, R., Macpherson, P., Egly, J.-M., Karran, P., 2014. Protein oxidation and DNA repair inhibition by 6-thioguanine and UVA radiation. Journal of Investigative Dermatology 134, 1408-1417.

Halliwell, B., Gutteridge, J.M., 2015. Free radicals in biology and medicine. Oxford University Press, USA.

Herrmann, H., Nolde, J., Berger, S., Heise, S., 2016. Aquatic ecotoxicity of lanthanum–A review and an attempt to derive water and sediment quality criteria. Ecotoxicology and Environmental Safety 124, 213-238.

IPCC, 2019: IPCC Special Report on the Ocean and Cryosphere in a Changing Climate [H.-O. Pörtner, D.C. Roberts, V. Masson-Delmotte, P. Zhai, M. Tignor, E. Poloczanska, K. Mintenbeck, A. Alegría, M. Nicolai, A. Okem, J. Petzold, B. Rama, N.M. Weyer (eds.)]. In press.

Kiyatkin, E.A., Sharma, H.S., 2009. Permeability of the blood–brain barrier depends on brain temperature. Neuroscience 161, 926-939.

Krisko, A., Radman, M., 2013. Phenotypic and genetic consequences of protein damage. PLoS genetics 9, e1003801.

Kulaksız, S., Bau, M., 2011. Rare earth elements in the Rhine River, Germany: first case of anthropogenic lanthanum as a dissolved microcontaminant in the hydrosphere. Environmental International 37, 973-979.

Lecomte-Finiger, R., 1994. The early life of the European eel. Nature 370, 424-424.

Lesser, M.P., 2006. Oxidative stress in marine environments: biochemistry and physiological ecology. Annual Review of Physiology 68, 253-278.

Lopes, A.R., Sampaio, E., Santos, C., Couto, A., Pegado, M.R., Diniz, M., Munday, P.L., Rummer, J.L., Rosa, R., 2018. Absence of cellular damage in tropical newly hatched sharks (*Chiloscyllium plagiosum*) under ocean acidification conditions. Cell Stress Chaperones 23, 837-846.

Lopes, A.R., Borges, F.O., Figueiredo, C., Sampaio, E., Diniz, M., Rosa, R., Grilo, T.F., 2019. Transgerational exposure to ocean acidification induces biochemical distress in a keystone amphipod species (*Gammarus locusta*). Environmental Research 170, 168-177.

Lushchak, V.I., 2011. Environmentally induced oxidative stress in aquatic animals. Aquatic Toxicology 101, 13-30.

Manciocco, A., Calamandrei, G., Alleva, E., 2014. Global warming and environmental contaminants in aquatic organisms: the need of the etho-toxicology approach. Chemosphere 100, 1-7.

Marques, A., Nunes, M.L., Moore, S.K., Strom, M.S., 2010. Climate change and seafood safety: Human health implications. Food Research International 43, 1766-1779.

Maulvault, A.L., Barbosa, V., Alves, R., Custódio, A., Anacleto, P., Repolho, T., Ferreira, P.P., Rosa, R., Marques, A., Diniz, M., 2017. Ecophysiological responses of juvenile seabass (*Dicentrarchus labrax*) exposed to increased temperature and dietary methylmercury. Science of the Total Environment 586, 551-558.

Maulvault, A.L., Custódio, A., Anacleto, P., Repolho, T., Pousão, P., Nunes, M.L., Diniz, M., Rosa, R., Marques, A., 2016. Bioaccumulation and elimination of mercury in juvenile seabass (*Dicentrarchus labrax*) in a warmer environment. Environmental Research 149, 77-85.

Mieiro, C.L., Pacheco, M., Pereira, M.E., Duarte, A.C., 2011. Mercury organotropism in feral European sea bass (*Dicentrarchus labrax*). Archives of Environmental Contamination and Toxicology 61, 135-143.

Moreira, A., Henriques, B., Leite, C., Libralato, G., Pereira, E., Freitas, R., 2020. Potential impacts of lanthanum and yttrium through embryotoxicity assays with *Crassostrea gigas*. Ecology Indicators 108, 105687.

Needhidasan, S., Melvin, S., Ramalingam, C., 2014. Electronic waste - an emerging threat to the environment of urban India. Journal of Environmental Health Science and Engineering 12, 1-36.

Noyes, P.D., McElwee, M.K., Miller, H.D., Clark, B.W., Van Tiem, L.A., Walcott, K.C., Erwin, K.N., Levin, E.D., 2009. The toxicology of climate change: environmental contaminants in a warming world. Environment International 35, 971-986.

Oliveira, M., Ahmad, I., Maria, V.L., Ferreira, C.S., Serafim, A., Bebianno, M.J., Pacheco, M., Santos, M.A., 2010. Evaluation of oxidative DNA lesions in plasma and nuclear abnormalities in erythrocytes of wild fish (*Liza aurata*) as an integrated approach for genotoxicity assessment. Mutation Research - Genetic Toxicology and Environmental Mutagenesis 703, 83-89.

Pagano, G., Guida, M., Tommasi, F., Oral, R., 2015. Health effects and toxicity mechanisms of rare earth elements - Knowledge gaps and research prospects. Ecotoxicology and Environmental Safety 115, 40-48.

Pankhurst, N.W., Munday, P.L., 2011. Effects of climate change on fish reproduction and early life history stages. Marine and Freshwater Research 62, 1015-1026.

Pereira, P., Raimundo, J., Barata, M., Araújo, O., Pousão-Ferreira, P., Canário, J., Almeida, A., Pacheco, M., 2015. A new page on the road book of inorganic mercury in fish body–tissue distribution and elimination following waterborne exposure and post-exposure periods. Metallomics 7, 525-535.

Pimentel, M.S., Faleiro, F., Diniz, M., Machado, J., Pousão-Ferreira, P., Peck, M.A., Pörtner, H.O., Rosa, R., 2015. Oxidative stress and digestive enzyme activity of flatfish larvae in a changing ocean. PloS one 10, e0134082.

Pinto, J., Costa, M., Leite, C., Borges, C., Coppola, F., Henriques, B., Monteiro, R., Russo, T., Di Cosmo, A., Soares, A.M., 2019. Ecotoxicological effects of lanthanum in *Mytilus galloprovincialis*: biochemical and histopathological impacts. Aquatic Toxicology 211, 181-192.

Pörtner, H.O., Peck, M., 2010. Climate change effects on fishes and fisheries: towards a cause-and-effect understanding. Journal of Fish Biology 77, 1745-1779.

Qinhai, H., 1996. Distribution and accumulation of Lanthanum in *Ctenopharyngodon ldellus*. Agro-environmental Protection 15, 218-220.

Raimundo, J., Vale, C., Caetano, M., Giacomello, E., Anes, B., Menezes, G.M., 2013. Natural trace element enrichment in fishes from a volcanic and tectonically active region (Azores archipelago). Deep Sea Res. Pt II 98, 137-147.

Rattanaphra, D., Soodjit, P., Thanapimmetha, A., Saisriyoot, Srinophakun, P., 2019. Synthesis, characterization and catalytic activity studies of lanthanum oxide from Thai monazite ore for biodiesel production. Renewable Energy 13, 1128-1137.

Sachdeva, M., Karan, M., Singh, T., Dhingra, S., 2014. Oxidants and antioxidants in complementary and alternative medicine: A review. Spatula DD 4, 1-16.

Sepúlveda, A., Schluep, M., Renaud, F.G., Streicher, M., Kuehr, R., Hagelüken, C., Gerecke, A.C., 2010. A review of the environmental fate and effects of hazardous substances released from electrical and electronic equipments during recycling: Examples from China and India. Environmental Impact Assessment Rev. 30, 28-41.

Serra-Compte, A., Maulvault, A.L., Camacho, C., Álvarez-Muñoz, D., Barceló, D., Rodríguez-Mozaz, S., Marques, A., 2018. Effects of water warming and acidification on bioconcentration, metabolization and depuration of pharmaceuticals and endocrine disrupting compounds in marine mussels (*Mytilus galloprovincialis*). Environmental Pollution 236, 824-834.

Snoeijs-Leijonmalm, P., Schubert, H., Radziejewska, T., 2017. (Eds.) Biological oceanography of the Baltic Sea. Springer Science & Business Media.

Sørensen, J.G., Kristensen, T.N., Loeschcke, V., 2003. The evolutionary and ecological role of heat shock proteins. Ecology Letters 6, 1025-1037.

Tomanek, L., 2010. Variation in the heat shock response and its implication for predicting the effect of global climate change on species' biogeographical distribution ranges and metabolic costs. Journal of Experimental Biology 213, 971-979.

Uchida, N., Matsukami, H., Someya, M., Tue, N.M., Viet, P.H., Takahashi, S., Tanabe, S., Suzuki, G., 2018. Hazardous metals emissions from e-waste-processing sites in a village in northern Vietnam. Emerging Contaminants 4, 11-21.

Uchiyama, M., Mihara, M., 1978. Determination of malonaldehyde precursor in tissues by thiobarbituric acid test. Analytical Biochemistry 86, 271-278.

Wall, F., 2014. Rare earth elements. Gunn, A.G. (Ed.), Critical metals handbook. John Wiley & Sons, pp. 312-339.

Wang, C., He, M., Shi, W., Wong, J., Cheng, T., Wang, X., Hu, L., Chen, F., 2011. Toxicological effects involved in risk assessment of rare earth lanthanum on roots of *Vicia faba* L. seedlings. International Journal of Environmental Science and Technology 23, 1721-1728.

Zepf, V., 2013. Rare Earth Elements: What and where they are, Rare Earth Elements. Springer, pp. 11-39.

Zhang, F., Cheng, M., Sun, Z., Wang, L., Zhou, Q., Huang, X., 2017. Combined acid rain and lanthanum pollution and its potential ecological risk for nitrogen assimilation in soybean seedling roots. Environmental Pollution 231, 524-532.

Chapter 7

Differential tissue accumulation in the invasive manila clam, *Ruditapes philippinarum* under two environmentally relevant lanthanum concentrations

Cátia Figueiredo [a,b,c,#], Tiago F. Grilo [a], Ana Rita Lopes [a,d], Clara Lopes [b], Pedro Brito [b], Miguel Caetano [b,e], Joana Raimundo [b,e]

[a] MARE – Marine and Environmental Sciences Centre, Faculdade de Ciências da Universidade de Lisboa, Campo Grande, 1749-016 Lisboa, Portugal;

[b] Division of Oceanography and Marine Environment, IPMA – Portuguese Institute for Sea and Atmosphere, Av. Alfredo Magalhães Ramalho, 6, 1495-165 Algés, Portugal;

[c] UCIBIO, REQUIMTE, Departamento de Química, Faculdade de Ciências e Tecnologia, Universidade NOVA de Lisboa, 2829-516 Caparica, Portugal;

[d] MARE – Marine and Environmental Science Centre, ISPA – Instituto Universitário, R. Jardim do Tabaco 34, 1149-041 Lisboa, Portugal.

[e] CIIMAR – Interdisciplinary Centre of Marine and Environmental Research, Avenida General Norton de Matos S/N, 4450-208 Matosinhos, Portugal;

Corresponding author

Figueiredo, C., Grilo, T.F., Lopes, A.R., Lopes, C., Brito, P., Caetano, M., Raimundo, J., 2022. Differential tissue accumulation in the invasive manila clam, *Ruditapes philippinarum* under two environmentally relevant lanthanum concentrations. Environmental Monitoring and Assessment 194:11. DOI 10.1007/s10661-021-09666-y

ABSTRACT

Amongst the environmental emerging concern rare earth elements, lanthanum (La) is one of the most common and reactive. Lanthanum is widely used in numerous modern technologies and applications, and its intense usage results in increasing discharges into the environment, with potentially deleterious consequences to earthlings. Therefore, we exposed the important food resource and powerful monitoring tool manila clam to two environmentally relevant concentrations of La (0.3 μg L^{-1} and 0.9 μg L^{-1}) for six days, through water, to assess the bioaccumulation pattern in the gills, digestive gland, and remaining body. The La bioaccumulation was measured after one (T1), two (T2), and six (T6) days of exposure. Lanthanum was bioaccumulated after two days, and the levels increased in all tissues in a dose-dependent manner. When exposed to 0.3 μg L^{-1} the enrichment factor pattern was gills>body>digestive gland. However, when exposed to 0.9 μg L^{-1} the pattern appears to change to gills>digestive gland>body. Tissue portioning appears to be linked with exposed concentration: in higher exposure levels digestive gland seems to gain importance, probably associated with detoxification mechanisms. Here we describe for the first time La bioaccumulation in these different tissues in a bivalve species. Future studies dealing with the bioaccumulation and availability of La should connect them with additional water parameters (such as temperature, pH, and major cations).

Keywords: *Ruditapes philippinarum*; dose-dependent bioaccumulation; enrichment factor; emergent contaminant; lanthanum.

7.1 INTRODUCTION

Most high technology equipment relies on Rare Earth Elements (REE) to be manufactured, such as electric and hybrid vehicles, smartphones, digital cameras, etc. (Wall, 2014). REE are also applied in low carbon energy technologies like nuclear, solar, eolic, bioenergy, carbon capture and storage, and electricity grids (Wall, 2014). The rising demand for up-to-date electronic equipment engenders enormous quantities of e-waste. Insufficient public knowledge on its recycling accoupled with inefficient recycling methodologies culminates in REE build-up in the environment (Tansel, 2017), highlighting the urgent need to study their speciation, availability, and ecotoxicological behavior and impacts. This has also led to REE being considered contaminants of environmental emerging concern.

REE are naturally present in small concentrations (from thousands of μg to tens of ng per gram), however, near mining and industrial locations, these can increase up to hundreds of times (Liang et al., 2014). Rare earth elements enter aquatic ecosystems through domestic and industrial wastewater discharges and leaching of REE enriched soils. Although REE exists in very low concentrations in non-contaminated seawater (in the pg L^{-1} range, Wang and Yamada, 2007), they are known to be bioaccumulated by marine organisms (i.e., squids, krill, Nautilus, etc.; Palmer et al., 2006; Pernice et al., 2009).

Lanthanum (La) is the first REE, with the major atomic radius is of the most reactive amidst them (Herrmann et al., 2016). Lanthanum is an essential catalyst for oil refineries and is fundamental for alloy making, alkali-resistant glass, hydrogen storage, battery-electrodes, and camera lenses (Sanghera and Aggarwal, 1998). The complex Lanthanum carbonate is applied in Medicine, to treat end-stage kidney disease, as it is capable to captivate excess phosphate in the blood (Albaaj and Hutchison, 2005). With increasing production and demand, it is expected that La availability in the environment will augment. The aquatic La speciation is powerfully affected by pH and other cations (Herrmann et al., 2016; Moermond et al., 2001). In seawater, La-carbonates complexes and free ions are the dominant species, while sulfates, humic complexes, and phosphates are a slight amount (Moermond et al., 2001).

Bivalves are well known as indicators of pollution, which brands them useful for monitoring studies due to their known ability to accumulate contaminants in their

tissues. The manila clam, *Ruditapes philippinarum*, is broadly distributed. Although presenting a long-life cycle, reaches maturity at ~30 mm in shell length, before 1-year-old (Moura et al., 2018). Given that this species is a worldwide commercially important food resource, can reach great economic worth. The manila clam is the most cultured clam species, representing approximately 25% of global mollusk production in 2018 (Sofia, 2018). It also demonstrates a high propensity to bioaccumulate pollutants (e.g., carbon nanoparticles, drugs, trace metals), under both natural and laboratory conditions (De Marchi et al., 2017; Won et al., 2016).

Within this framework, the purpose of this study was to assess the bioaccumulation ability of the manila clam to two different La concentrations. The chosen environmentally realistic La exposure concentrations fall within the levels quantified in a European wastewater outlet (Brito et al., 2018): low La: 0.3 µg L^{-1} and high La: 0.9 µg L^{-1}. The bioaccumulation was assessed by analysing the La content present in the gills, digestive gland, and remaining body (containing the siphon, adductor muscle, mantle, and foot, and hereafter called body).

7.2 MATERIAL AND METHODS

7.2.1 Sampling

Manila clam (*Ruditapes philippinarum*) specimens were collected in a single sampling event in July 2018, during the low tide, in a subtidal zone at Ria de Aveiro, Portugal (SW Europe). After sampling, specimens were transported to the MARE-FCUL aquaculture facilities and depurated for seven days under a 12h light/12h dark photoperiod. Individuals were kept in filtered (0.35 µm, Harmsco, Florida, USA) and UV-irradiated (Vecton 600, TMC Iberia) natural seawater with parameters as those measured in the sampling event: salinity = 35±0.1 (V2 refractometer, TMC Iberia), temperature = 16.2±0.1°C (TFX 430 Precision Thermometer, WTW GmbH) and pH = 8.19±0.03 (SevenGo pro™, Mettler Toledo).

7.2.2 Experimental design

One hundred and fifty manila clam individuals were randomly assigned to fifteen 5L glass tanks, with continuously aerated, filtered and UV-irradiated natural seawater directly pumped from the ocean (38°70'99.7"N and 9°48'69.2"W), into three treatments: control (La=0 µg L^{-1}), low La concentration (La=0.3 µg L^{-1}) and high La

concentration (La=0.9 µg L^{-1}). In each sampling event, 10 clams were randomly collected from the 5 replicates of each treatment. The temperature was kept constant by immersing the experimental tanks in a bath with submerged heaters (V_2Therm 200W aquarium heater, TMC Iberia) and chillers (HC-250A, Hailea). Dissolved La levels were warranted through the addition of a La solution in the seawater. This solution was prepared with a $LaCl_3$ standard solution (Merck) diluted in filtered ultra-pure water (18.2 MΩ, Milli-Q, Merck). The water was renewed daily, at the same time, for the three treatments to keep dissolved inorganic carbon speciation, due to bacterial activity minor, and afterwards, the respective La solution was added, in the exposed treatments. Water aliquots were sampled every hour, for the first 12 hours of the first exposure, to evaluate the variation of dissolved La levels. Individuals were fed with a commercially concentrated mixture of green and brown marine phytoplankton – Reef Phytoplankton™, Seachem – every day, one hour before water change to minimize the potential removal of La.

Clams were sampled before the beginning of the trial (T0) and after 1 (T1), 2 (T2), and 6 (T6) days of exposure to La.

7.2.3 Lanthanum quantification

To quantify the total dissolved La levels (µg L^{-1}), water triplicates were filtrated (0.45 µm, MF-Milipore ^{TM}, Merk) and acidified (2% Ultrapur® HNO_3).

Clams were dissected into gills, digestive gland, and remaining body and kept at -80°C until further analyses. Lanthanum concentrations were determined in freeze-dried, grounded, and homogenized gills, digestive gland, and remaining body, after digestion with nitric acid (HNO_3, distilled, 65% v/v) and hydrogen peroxide (H_2O_2, Suprapur®, 30% v/v) in accordance to Raimundo et al. (2013). All labware was previously decontaminated with HNO_3 (20%) for 48h and rinsed with ultra-pure water (18.2 MΩ, Milli-Q, Merck).

The concentration of La was determined in a quadrupole ICP-MS (Thermo Elemental, X-Series) and the experimental ICP-MS parameters for La determinations are detailed in Caetano et al. (2009). ^{115}In was the internal standard (Merck, CertiPUR®) chosen. The ^{139}La was the isotope selected for the quantification that has minimum isobaric and polyatomic interferences. Quality Control (QC) solutions were run every 20 samples. The coefficients of variation for counts (n=5) were lower than 2%, and a 5-point

calibration from 0.005 to 5 ppm was used for quantification. Accumulation results are given in milligram per kilogram of dry weight tissue (mg Kg^{-1}, dw).

To control the analytical quality of the method, three procedural blanks were prepared, using the same analytical procedure described above, and included within each batch of 20 samples. Blanks accounted for less than 1% of the total La concentration in all the samples. Additionally, a certified reference material BCR 668 (muscle of *Mytilus edulis*) was included within each batch of 20 samples to evaluate the accuracy of all analytical procedures, and the obtained values were consistent with the certified ones.

7.2.4 Lanthanum enrichment factor

To estimate the La specific affinity for the body, the digestive gland, and the gill, the enrichment factor was determined as the quotient of the median La levels in exposed and control samples, for T1, T2, and T6, according to Pereira et al. (2015).

7.2.5 Seawater carbonate system

Temperature (°C), salinity, and pH were measured four times for each treatment, in each sampling day (T0, T1, T2, and T6). The total alkalinity (TA) and pH total scale (pH_T) were used to calculate the specifics of the seawater carbonate system (e.g., pCO_2, HCO_3^-, ΩCa, ΩAr), using the CO2SYS software.

7.2.6 Statistical analyses

Kolmogorov-Smirnov and Levene's tests were used to test data for normality and equality of variances and non-compliance of these parametric assumptions led to the practice of the Mann-Whitney non-parametric test. All pairwise differences in La concentrations between treatments within and between sampling times were assessed. Differences between La concentrations in different body parts for each treatment were also tested.

Given that the water was renewed entirely daily, the seawater carbonate system was measured every sampling day in experimental water representative of only that day. For that reason, the differences between each seawater physicochemical parameter were tested only between treatments and not between sampling days.

Statistical analyses were performed in STATISTICA™ 12 software (Statsoft, Inc., Tulsa, OK 74104, USA), using a significance level of $p < 0.05$.

7.3 RESULTS

7.3.1 Dissolved lanthanum levels

The total dissolved La levels (µg L^{-1}) in the water samples collected every hour, for 12h, after La spike are presented in Annex 6, Supplemental Table 7.1. Average concentrations in the first 12h were 0.25±0.10 µg L^{-1} in the low exposure concentration treatment and 0.84±0.09 µg L^{-1} in the higher exposure concentration treatment.

In the present study, the La levels quantified in the spiked water stabilized after 6h, for the lower La concentration, and remained stable for the following period (Annex 6, Supplemental Table 7.1). This period of non-equilibrium was lower for the higher spiked concentration. The average dissolved concentration was very similar to the desired exposure concentration for both exposed treatments, and its presence was assured by adding the same concentration to a renewed medium every day. The constancy of the total dissolved La concentration points that minor precipitation may have occurred.

7.3.2 Lanthanum accumulation

Median and ranges of La concentrations (mg Kg^{-1}, dry weight) in the three studied parts, namely body, digestive gland, and gills are presented in Table 7.1.

Table 7.1 - Median and ranges of La concentration (mg Kg^{-1}, dry weight) in manila clams' body, digestive gland and gills after 0 (T0), 1 (T1), 2 (T2) and 6 (T6) days of exposure to control (0 µg L^{-1}), low (0.3 µg L^{-1}) and high (0.9 µg L^{-1}) La concentration, through water.

Time	N	Treatment	Body	Digestive Gland (mg Kg^{-1}, dry weight)	Gills
T0	10	Control	0.18 (0.14 - 0.29)	0.22 (0.17 - 0.26)	0.29 (0.25 - 0.34)
T1	10	Control	0.28 (0.27 - 0.38)	0.51 (0.44 - 0.59)	0.49 (0.42 - 0.56)
	10	Low La	0.30 (0.20 - 0.37)	0.54 (0.29 - 0.68)	0.63 (0.36 - 0.80)
	10	High La	0.36 (0.29 - 0.43)	0.69 (0.42 - 0.86)	0.66 (0.52 - 0.93)
T2	10	Control	0.21 (0.20 - 0.29)	0.34 (0.32 - 0.36)	0.37 (0.37 - 0.42)
	10	Low La	0.42 (0.28 - 0.59)	0.61 (0.53 - 0.88)	0.78 (0.70 - 0.94)
	10	High La	0.46 (0.44 - 0.64)	0.71 (0.49 - 1.2)	0.82 (0.48 - 1.1)
T6	10	Control	0.28 (0.28 - 0.30)	0.48 (0.46 - 0.50)	0.34 (0.31 - 0.36)
	10	Low La	0.70 (0.34 - 0.82)	1.0 (0.72 - 1.7)	1.5 (0.70 - 1.7)
	10	High La	1.1 (0.52 - 1.7)	1.9 (1.5 - 2.6)	1.8 (1.1 - 2.9)

Concentrations of La (mg Kg^{-1}, dw) in the manila clams' body are presented in Figure 7.1.

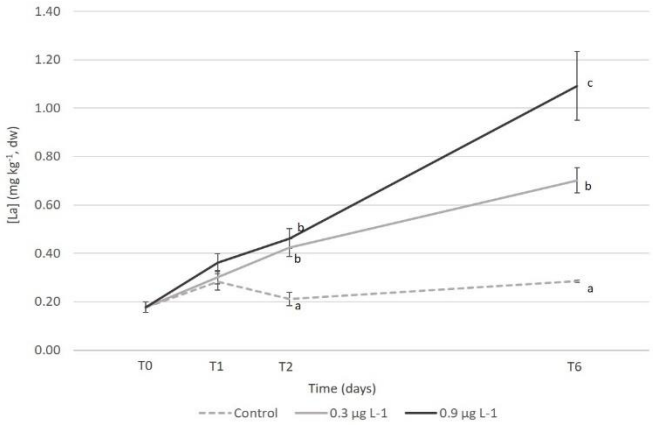

Figure 7.1 - Concentrations of lanthanum (mg Kg^{-1}, dry weight) in manila clams' body under control (0 µg L^{-1}), low La (0.3 µg L^{-1}) and high La (0.9 µg L^{-1}) at different sampling times (T0, T1, T2, and T6). Values represent medians ± SE. Different letters represent significant differences between treatments within each sampling time ($p<0.05$). For additional significant differences see Annex 6, Supplemental Table 7.2.

Levels on the control treatment varied in a narrow range between 0.18 and 0.28 mg Kg^{-1}, without significant differences between sampling times ($p>0.05$, statistical differences shown in Annex 6, Supplemental Table 7.2a, b, and c, Online Resources 1, 2 and 3). The concentration of La found in the body of both exposed treatments increased with time. For the low La treatment (0.3 µg L^{-1}) median levels of La in the body reached their lowest at T1 (0.30 mg Kg^{-1}) and its highest at T6 (0.70 mg Kg^{-1}). The same trend occurred in the bodies of the manila clams exposed to high La (0.9 µg L^{-1}), with concentrations ranging from 0.36 mg Kg^{-1} at T1 to 1.1 mg Kg^{-1} at T6.

One day of exposure to La (T1) was insufficient to display significant differences between the three treatments ($p > 0.05$), however significant differences between the control and both exposure concentrations were found on the second day (T2, $p=0.032$ and $p=0.037$, respectively). The accumulation of La in the body did not show significant differences between the two different exposure concentrations after two days of exposure ($p=0.213$). Nevertheless, at T6, the three treatments were significantly different among them ($p<0.05$).

The same trend was observed for the digestive gland (Figure 7.2).

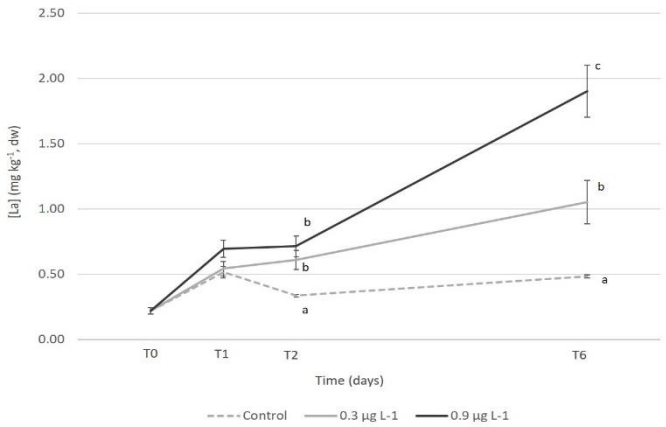

Figure 7.2 - Concentrations of lanthanum (mg Kg^{-1}, dry weight) in Manila clams' digestive gland under control (0 µg L^{-1}), low La (0.3 µg L^{-1}) and high La (0.9 µg L^{-1}) at different sampling times (T0, T1, T2, and T6). Values represent medians ± SE. Different letters represent significant differences between treatments within each sampling time ($p < 0.05$). For additional significant differences see Annex 6, Supplemental Table 7.2.

At T1, no significant differences were shown between treatments (p>0.05), with La values varying from 0.51 mg Kg^{-1} in the control, 0.54 mg Kg^{-1} in low La, and to 0.69 mg Kg^{-1} in high La concentrations. After two days of exposure (T2), accumulation was evident, with the control digestive glands exhibiting significantly lower concentrations than the ones registered in digestive glands exposed to 0.3 µg L^{-1} (p=0.020) and 0.9 µg L^{-1} of La (p=0.008). As expected, the highest accumulation value occurred after 6 days of exposure (T6) and in the treatment with higher La concentration (1.9 mg Kg^{-1}, dw). This level was significantly different from their control counterpart (p=0.037) and also from the digestive glands exposed to low La (p=0.023).

Lanthanum concentrations in the manila clams' gills are shown in Figure 7.3.

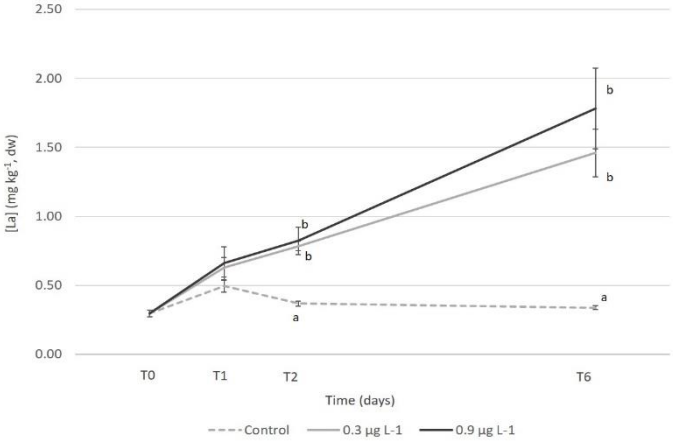

Figure 7.3 - Concentrations of lanthanum (mg Kg^{-1}, dry weight) in manila clams' gills under control (0 µg L^{-1}), low La (0.3 µg L^{-1}) and high La (0.9 µg L^{-1}) at different sampling times (T0, T1, T2, and T6). Values represent medians ± SE. Different letters represent significant differences between treatments within each sampling time ($p < 0.05$). For additional significant differences see Annex 6, Supplemental Table 7.2

The accumulation of La in the gills increased steadily over time till day 6 (T6). As found in the other tissues, one day of exposure was not sufficient to induce measurable La bioaccumulation. Nevertheless, after two days of exposure, the low and high La treatments differed from the control (p=0.028, for both La treatments). At T6, this significant difference between the control and the exposed treatments was upheld, but the exposed treatments did not show a significant difference between them (p=0.298).

7.3.3 La enrichment factor

The highest enrichment factor occurred after 6 days of exposure in the gills, for both La concentrations (Figure 7.4), and it was greater, for all body parts, at the high La concentration. When exposed to 0.3 µg L^{-1} La the highest enrichment factor was observed in the gills, followed by the body and ultimately the digestive gland. However, even though not significantly (p>0.05), when exposed to 0.9 µg L^{-1} La, the accumulation pattern appears to change, and the highest enrichment factor was observed in the gills, followed by the digestive gland and ultimately the body.

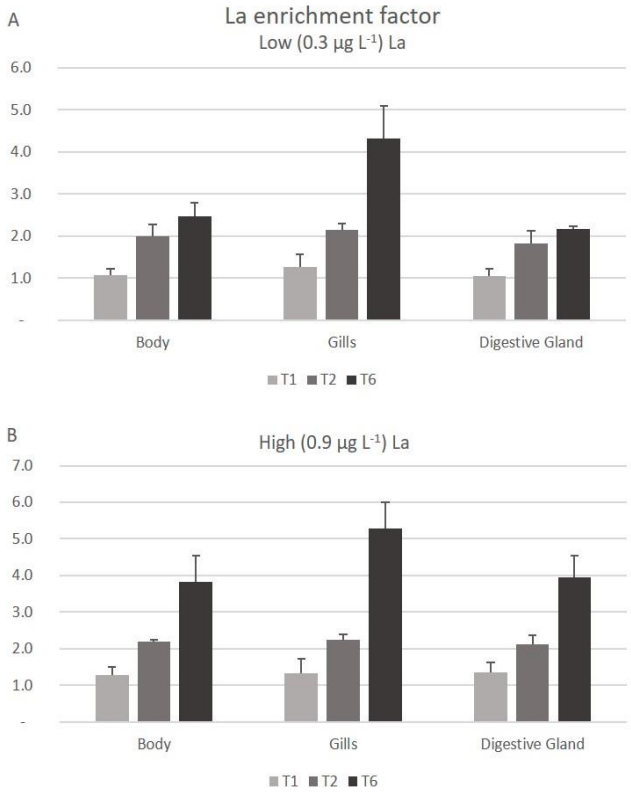

Figure 7.4 - Enrichment factor for the body, gills and digestive gland of the Manila clam for the three exposed sampling times, T1, T2 and T6. Values represent medians ± SE

7.3.4 Seawater carbonate system

Seawater physicochemical parameters and specifics of the seawater carbonate system are presented in Table 7.2.

Table 7.2 - Seawater physicochemical parameters and specifics of the seawater carbonate system for the three treatments (median ± SD).

Treatment	Temperature (°C)	Salinity	pH	Total Alkalinity (µmol kg^{-1} SW)	pCO_2 (µatm)	HCO_3^- (µmol kg^{-1} SW)	OH^- (µmol kg^{-1} SW)	ΩCa	ΩAr
Control	16.1±0.1	35±0.1	8.2±0.03	2570±382	318±53	1981±325	4.1±0.44	5.8±0.75	3.7±0.48
Low La (0.3 µg L^{-1})	16.3±0.1	35±0.1	8.2±0.03	2213±361	259±59	1690±308	4.2±0.27	5.0±0.71	3.2±0.46
High La (0.9 µg L^{-1})	16.2±0.1	35±0.1	8.2±0.03	2460±355	308±62	1956±312	4.1±0.52	4.9±0.67	3.2±0.43

The temperature, salinity, and pH were kept stable for the three treatments (control, 0.3 µg L^{-1} La and 0.9 µg L^{-1} La) and the total alkalinity was 2570±382 (µmol kg^{-1} SW) in the control treatment and slightly lower for the added lanthanum treatments: 2213±361 (µmol kg^{-1} SW) for the low La treatment and 2460±355 for the high La treatment. Nevertheless, the studied water parameters (TA, pCO_2, HCO_3^-, OH^-, ΩCa and ΩAr) remained comparable between treatments (p>0.05).

7.4 DISCUSSION

The availability of REE in the environment is increasing and they are becoming worldwide-ranging contaminants. Their behavior has been described in the water, particulate matter, sediments, and organisms living in rivers, estuaries, and oceans (e.g. Akagi and Edanami, 2017). Nevertheless, studies evaluating the availability and bioaccumulation of La under-laboratory conditions are still scarce. To the best of our knowledge, this is the first study on the differential tissue accumulation of La in a bivalve species. Therefore, any comparison with the literature is hampered and can only be achieved with other chemical elements, that may have distinct toxicokinetic or other species.

One day of exposure to La, at both concentrations, was insufficient to trigger accumulation in the three studied body parts. The ability of bivalves to reduce filtration rates when exposed to pollutants is well known (e.g., Almeida et al., 2015). This is achieved by valve closing and diminishing the respiration and filtration rates, to avoid pollutant accumulation. Our results showed that this could have happened upon La

exposure. Pinto et al. (2019) exposed the mussel *M. galloprovincialis* to different levels of La (0, 0.1, 1, 10 mg L^{-1}), and after measuring accumulation in the whole soft body, they found that as La exposure concentration increased, the bioconcentration factor (the ratio between the concentration in the organisms and the water) decreased. In fact, just after one day of exposure to La, the exposed body parts showed very similar values to the control ones, which may corroborate the hypothesis that this species presents an ability to deal with La in a short-time frame. This ability seems to be very limited as after 2 days of exposure accumulation occurred in all body parts. However, at this point, we did not find significant differences between the body parts exposed to low and high La concentrations, which could still be due to this ability to reduce respiration and filtration, and therefore pollutants accumulation. In the face of this adaptation to La-induced environmental stress, bivalves may not get adequate energy from feeding, which may impair other physiological processes, such as growth and reproduction. Future studies should further investigate this ability by means of, for example, quantification of stress biomarkers in the first days of exposure to the same range of environmental realistic La concentrations.

The La bioaccumulation partly depends on the element bioavailability that is influenced by a complex array of factors, such as water hardness, alkalinity, dissolved organic carbon, and pH. Furthermore, the bioaccumulation is influenced by the physicochemical characteristics of the exposed organisms (Herrmann et al., 2016). On another side, bioaccumulation will depend on the uptake and elimination kinetics, and such processes may be species-specific, and on the biologically active fractions of the element (Khan et al., 2017). Cánovas et al. (2020) studied REE exposure in aquatic organisms using diffusive gradient in thin-films (DGT), and observed that element retention in DGTs was related to total concentration in water (dissolved + particulate), suggesting that a relation between the DGT-labile concentration and the accumulated levels in organisms exists. These findings corroborate our results since a dose-dependent accumulation was found, which relates to the total and labile concentration in water. In fact, our research showcases the great ability of the environmentally realistic La concentrations to be accumulated in a swift timeframe. Additionally, Bonnail et al. (2017) showed a *Corbicula fluminea*' REE uptake proportional to the pollution degree, and the REE geochemical signature of the environment was preserved in their soft

tissue. Furthermore, Cánovas et al. (2020) showed that in brackish-seawater REE-CO_3 complexes prevail over free ions, Cl^-, F^-, Sc^- and O/OH^-complexes. Nevertheless, the CO_3 complexes showed the lowest contribution for La (~60% of all species), in comparison to the remaining REE (up to 96% of all species).

In our study, the body presented the lowest accumulation values, which is consistent with previous ecotoxicological studies with other metals on the same species. Jang et al. (2009) exposed the manila clam to different concentrations of cadmium (Cd) and described the gills as the tissue with the higher accumulation, followed by the digestive gland and ultimately the residual tissues. Furthermore, Liu et al. (2017) investigated the tissue-specific bioaccumulation of heavy metals (Cr, Cu, Hg, Zn, As, Cd, and Pb) in the manila clam demonstrating that the visceral masses tended to accumulate more efficiently than the muscle. The gills have been indicated as a temporary target organ for pollutants in bivalves, that are later transferred to the digestive organs, such as the digestive gland (Guo-Qing and Dong-Feng, 2016). In our study the gills and the digestive gland accumulated similar quantities of La. However, in the gills, no significant difference was discerned between the two exposed treatments at T6. The La accumulation similarity in both the gills and the digestive gland may be related to the short exposure period used in this trial (6 days). Perhaps in a long exposure experiment a clear difference between the gills, a key interface for the uptake of contaminants from the water, and the digestive gland, a vital detoxification tissue, may occur. Won et al. (2016) characterized the target organs (gill, mantle, digestive gland, siphons, adductor muscle, and foot) of the manila clam by exposing them to copper (Cu) and lead (Pb) and described a linear uptake and that the order of accumulation rate in laboratory exposure was not concomitant with that of the field study, suggesting that different routes of metal uptake and exposure duration may induce distinct partitioning of metals in *R. philippinarum*. Hence, in order to better understand the La uptake, we suggest that more than three data sets (T1, T2 and T6) should be applied, with particular emphasis on the first days due to this bivalve species ability to cope with La exposure. More studies on La toxicity should be carried out, and this study provides key information on which future studies will build upon.

Focusing attention on the enrichment factors calculated in the present study, they were higher in the gills, followed by the body and ultimately the digestive gland for

the manila clams exposed to 0.3 µg L^{-1} La. However, when the exposure concentration tripled, the enrichment factor was higher in the gills followed by the digestive gland and ultimately the body. It could be interesting to see if this changed accumulation pattern would become more noticeable with a higher concentration exposure. Considering this, we suggest that future studies perform these trials with an increased gap between the environmentally realistic exposure concentrations studied. Additionally, the manila clam presented an increase in La concentration level when exposed to a higher concentration, and this might have increased even more if a higher concentration was applied.

If the contamination route used in our study would be through the diet (i.e., by adding La to the concentrated marine phytoplankton used to feed the manila clams), the results might likely be different. The gills would probably reach lower La enrichment factors than the digestive gland attending the contamination vehicle would not pass directly by them. This highlights the importance of differential tissue accumulation studies, and the organ specificity of La accumulation should be further investigated.

Here the accumulation increased in all body parts till T6, and therefore, an extension of the exposure duration should also happen in upcoming studies as Figueiredo et al. (2018) found that the accumulation of La peaked and decreased afterwards even in a continuously exposed medium, in freshwater glass eels (*Anguilla anguilla*). Unfortunately, we lost the six-day elimination phase samples and were unable to process them, and therefore advise researchers to evaluate the elimination rate of this element in future studies.

The increased usage of modern electronic technologies, and other activities, is rising the availability of La in the aquatic environment, which is in turn being accumulated by commercially important food resources. The information on the toxicity of La is unfortunately scarce and still quite puzzling. Therefore, we also suggest that future studies should investigate its effects, equally on a cellular, tissue, and individual level as we must adopt a holistic approach to better understand REE toxicology and its effects on species sustainability and human health.

7.5 CONCLUSION

The findings described in this article revealed that environmentally realistic concentrations of La (0.3 µg L^{-1} and 0.9 µg L^{-1}) were not bioaccumulated by *R. phillipinarum* in the first 24 hours of exposure. Nevertheless, on the second day of exposure, accumulation occurred in the three studied body parts (digestive gland, gills, and remaining body). The accumulation was upheld until the sixth day of exposure and occurred in a dose-dependent manner. Having into consideration that the studied concentrations represent environmentally realistic concentrations, like the ones present at a European wastewater outlet, the results highlight the bivalve propensity to accumulate La in its' tissues. Owing to the limited information about these emerging contaminants, the evidence added by this study is of key importance from an ecological and food safety point of view.

ACKNOWLEDGMENTS

This work was supported by Fundação para a Ciência e Tecnologia (FCT), through the project Climatoxeel (PTDC/AAG-GLO/3795/2014) and the Junior Researcher contract (CEECIND/03517/2017), both awarded to Tiago F Grilo and the strategic project UID/MAR/04292/2019 granted to MARE. Cátia Figueiredo acknowledges the FCT-PhD grant SFRH/BD/130023/2017. Finally, the authors thank the anonymous reviewers for the useful comments and valuable advice for the improvement of this work.

REFERENCES

Akagi, T., Edanami, K., 2017. Sources of rare earth elements in shells and soft tissues of bivalves from Tokyo Bay. Marine Chemistry 194, 55-62.

Albaaj, F., Hutchison, A., 2005. Lanthanum carbonate (Fosrenol®): a novel agent for the treatment of hyperphosphataemia in renal failure and dialysis patients. International journal of clinical practice 59, 1091-1096.

Almeida Â., Freitas R., Calisto V., Esteves V., Schneider R., Soares A.M.V.M., Figueira E., 2015. Chronic toxicity of the antiepileptic carbamazepine on the clam *Ruditapes philippinarum*. *Comparative Biochemistry and Physiology – Part C: Toxicology & Pharmacology*. 172-173: 26-35.

Bonnail, E., Pérez-López, R., Sarmiento, A. M., Nieto, J. M., DelValls, T. Á., 2017. A novel approach for acid mine drainage pollution biomonitoring using rare earth elements bioaccumulated in the freshwater clam *Corbicula fluminea*. Journal of hazardous materials, 338, 466-471.

Brito, P., Prego, R., Mil-Homens, M., Caçador, I., Caetano, M., 2018. Sources and distribution of yttrium and rare earth elements in surface sediments from Tagus estuary, Portugal. Science of The Total Environment 621, 317-325.

Caetano, M., Prego, R., Vale, C., de Pablo, H., Marmolejo-Rodríguez, J., 2009. Record of diagenesis of rare earth elements and other metals in a transitional sedimentary environment. Marine Chemistry 116, 36-46.

Cánovas, C. R., Basallote, M. D., & Macías, F., 2020. Distribution and availability of rare earth elements and trace elements in the estuarine waters of the Ria of Huelva (SW Spain). Environmental Pollution, 267, 115506.

De Marchi, L., Neto, V., Pretti, C., Figueira, E., Chiellini, F., Soares, A.M., Freitas, R., 2017. The impacts of emergent pollutants on *Ruditapes philippinarum*: biochemical responses to carbon nanoparticles exposure. Aquatic Toxicology 187, 38-47.

Figueiredo, C., Grilo, T.F., Lopes, C., Brito, P., Diniz, M., Caetano, M., Rosa, R., Raimundo, J., 2018. Accumulation, elimination and neuro-oxidative damage under lanthanum exposure in glass eels (*Anguilla anguilla*). Chemosphere 206, 414-423.

Guo-Qing, H., & Dong-Feng, W., 2016. Effects of lanthanum on the cadmium uptake of pacific oyster *Crassostrea gigas*. Indian Journal of Geo-Marine Science 45, 653-657.

Herrmann, H., Nolde, J., Berger, S., Heise, S., 2016. Aquatic ecotoxicity of lanthanum–A review and an attempt to derive water and sediment quality criteria. Ecotoxicology and environmental safety 124, 213-238.

Jang, S.-W., Kim, S.-G., Choi, O.-I., Kim, S.-S., Kang, J.-C., 2009. Cadmium accumulation and elimination in the tissues of the manila Clam, *Ruditapes philippinarum*, after Sub-chronic Cadmium Exposure. The Korean society of fisheries and aquatic science 12: 324-330.

Khan, A. M., Bakar, N. K. A., Bakar, A. F. A., & Ashraf, M. A., 2017. Chemical speciation and bioavailability of rare earth elements (REEs) in the ecosystem: a review. Environmental Science and Pollution Research 24, 22764-22789

Liang, T., Li, K., Wang, L., 2014. State of rare earth elements in different environmental components in mining areas of China. Environmental monitoring and assessment 186, 1499-1513.

Liu, J., Cao, L., Dou, S., 2017. Bioaccumulation of heavy metals and health risk assessment in three benthic bivalves along the coast of Laizhou Bay, China. Marine pollution bulletin 117, 98-110.

Moermond, C.T., Tijink, J., van Wezel, A.P., Koelmans, A.A., 2001. Distribution, speciation, and bioavailability of lanthanides in the Rhine-Meuse estuary, The Netherlands. Environmental Toxicology and Chemistry: An International Journal 20, 1916-1926.

Moura, P., Vasconcelos, P., Pereira, F., Chainho, P., Costa, J.L., Gaspar, M.B., 2018. Reproductive cycle of the manila clam (*Ruditapes philippinarum*): an intensively harvested invasive species in the Tagus Estuary (Portugal). Marine Biological Association of the United Kingdom. Journal of the Marine Biological Association of the United Kingdom 98, 1645-1657.

Palmer, A.S., Snape, I., Stark, J.S., Johnstone, G.J., Townsend, A.T., 2006. Baseline metal concentrations in Paramoera walkeri from East Antarctica. Marine pollution bulletin 52, 1441-1449.

Pereira, P., Raimundo, J., Barata, M., Araújo, O., Pousão-Ferreira, P., Canário, J., Almeida, A., Pacheco, M., 2015. A new page on the road book of inorganic mercury in fish body–tissue distribution and elimination following waterborne exposure and post-exposure periods. Metallomics 7, 525-535.

Pernice, M., Boucher, J., Boucher-Rodoni, R., Joannot, P., Bustamante, P., 2009. Comparative bioaccumulation of trace elements between *Nautilus pompilius* and *Nautilus macromphalus* (Cephalopoda: Nautiloidea) from Vanuatu and New Caledonia. Ecotoxicology and environmental safety 72, 365-371.

Pinto, J., Costa, M., Leite, C., Borges, C., Coppola, F., Henriques, B., Monteiro, R., Russo, T., Di Cosmo, A., Soares, A.M., 2019. Ecotoxicological effects of lanthanum in *Mytilus galloprovincialis*: biochemical and histopathological impacts. Aquatic toxicology 211, 181-192.

Raimundo, J., Vale, C., Caetano, M., Giacomello, E., Anes, B., Menezes, G.M., 2013. Natural trace element enrichment in fishes from a volcanic and tectonically active region (Azores archipelago). Deep Sea Research Part II: Topical Studies in Oceanography 98, 137-147.

Sanghera, J., Aggarwal, I.D., 1998. Infrared fiber optics. CRC Press.

SOFIA, F., 2018. The State of World Fisheries and Aquaculture 2018-Meeting the sustainable development goals. Fisheries and Aquaculture Department, Food and Agriculture Organization of the United Nations, Rome.

Tansel, B., 2017. From electronic consumer products to e-wastes: Global outlook, waste quantities, recycling challenges. Environment international 98, 35-45.

Wall, F., 2014. Rare earth elements. Critical metals handbook, 312-339.

Wang, Z.L., Yamada, M., 2007. Geochemistry of dissolved rare earth elements in the Equatorial Pacific Ocean. Environmental geology 52, 779-787.

Won, E.J., Kim, K.T., Choi, J.Y., Kim, E.S., Ra, K., 2016. Target organs of the manila clam Ruditapes philippinarum for studying metal accumulation and biomarkers in pollution monitoring: laboratory and in-situ transplantation experiments. Environmental monitoring and assessment 188, 478.

Chapter 8

Single and combined ecotoxicological effects of ocean warming, acidification and lanthanum exposure on the surf clam (*Spisula solida*)

Cátia Figueiredo [a,b,c*], Tiago F. Grilo [a], Rui Oliveira [b], Inês João Ferreira [d], Clara Lopes [b,e], Pedro Brito [b,e], Pedro Ré [a], Miguel Caetano [b,e], Mário Diniz [c,f], Joana Raimundo [b,e]

[a] MARE – Marine and Environmental Sciences Centre, Faculdade de Ciências da Universidade de Lisboa, Campo Grande, 1749-016 Lisboa, Portugal;

[b] Division of Oceanography and Marine Environment, IPMA – Portuguese Institute for Sea and Atmosphere, Av. Alfredo Magalhães Ramalho, 6, 1495-165 Algés, Portugal;

[c] UCIBIO – Applied Molecular Biosciences Unit, Department of Chemistry / Department of Life Sciences, School of Science and Technology, NOVA University Lisbon, 2819-516 Caparica, Portugal

[d] LAQV-REQUIMTE, Chemistry Department, NOVA School of Science and Technology, 2829-516 Caparica, Portugal

[e] CIIMAR – Interdisciplinary Centre of Marine and Environmental Research, Avenida General Norton de Matos S/N, 4450-208 Matosinhos, Portugal;

[f] Associate Laboratory i4HB - Institute for Health and Bioeconomy, School of Science and Technology, NOVA University Lisbon, 2819-516 Caparica, Portugal

* Corresponding author

Figueiredo, C., Grilo, T.F., Oliveira, R., Ferreira, I.J., Gil, F., Lopes, C., Brito, P., Ré, P., Caetano, M., Diniz, M., Raimundo, J., 2022. Single and combined ecotoxicological effects of ocean warming, acidification and lanthanum exposure on the surf clam (*Spisula solida*). Submitted to Environmental Pollution.

ABSTRACT

Lanthanum (La) is one of the most abundant emergent rare earth elements. Its release into the environment is enhanced by its use in various industrial applications. In the aquatic environment, emerging contaminants are one of the stressors with the ability to compromise the fitness of its inhabitants. Climate changes can also affect their resilience and are another consequence of the growing human footprint on the planet. However, as far as we know, a study on the effects of ocean warming, acidification, and their interaction with La were never carried out. Hence, we exposed the surf clam (*Spisula solida*) to 15 µg L^{-1} of La and warming (+4°C) and acidification (-0.4) for 7 days, plus a 7-day depuration period, with the objective of exploring the effects, combined and as single stressors, of ocean warming, acidification, and La accumulation and elimination. Furthermore, we quantified a robust set of membrane-associated, protein, and antioxidant enzymes and non-enzymatic biomarkers (LPO, HSP, Ub, SOD, CAT, GPx, GST, TAC). Lanthanum was bioaccumulated after just one day of exposure, in both present-day and climate change scenarios. A 7-day depuration phase was insufficient to achieve control values and in a warming scenario La elimination was more efficient. A biochemical response was triggered, as highlighted by enhanced SOD, CAT, GST, and TAC levels, however as lipoperoxidation was observed, it was insufficient to detoxify La and avoid damage. The HSP were mostly inhibited in La treatments combined with warming and acidification. Concomitantly, Lipoperoxidation was highest in clams exposed to La, warming and acidification combined. The results emphasize the toxic effects of La on bivalve species, and its enhanced potential in a changing world.

KEYWORDS: Bioaccumulation; Rare earth elements; Elimination; Climate change; Oxidative stress; Cellular damage

8.1 INTRODUCTION

Lanthanum (La) is the chemical element with atomic number 57, being the first of the lanthanide (Ln) series, and the second most reactive of them (Emsley, 2011). The lanthanides, scandium, and yttrium compose the Rare Earth Elements (REE). Although less concentrated than other metals, hence their name, the REE holds an essential part in the development of innovative technologies. As one of the most abundant Ln in the environment, La has been receiving additional attention (Herrmann et al., 2016). Currently regarded as an emergent contaminant, La is used in several industrial applications such as alloying agent, for hydrogen storage, hybrid car batteries, optical glasses, superconductor, amongst others (Voncken, 2016). This intense and wide use potentiates La release into the hydrosphere through industrial emissions, and La mining and ore processing (Khan et al., 2017; Kulaksız and Bau, 2011). Furthermore, as La strongly binds to carbonate and phosphate, La salts have been used in medicine to impound excess phosphate in humans with kidney disease (Schmidt et al., 2012). Though, La has been described as carcinogenic to human beings and genotoxic with particularly damaging consequences to human lymphocytes (Wang et al., 2016). The trivalent La^{3+} is bioavailable and capable of affecting biological responses. This ion competes with Ca^{2+} ions, as both present similar ionic radii, and can inhibit Ca-channels, affecting cell membrane enzymes, with consequences to the normal functioning of cells (Das et al., 1988). Nonetheless, the assessment of the consequences of rather recent increased La levels in the environment is still to be achieved and few studies exist on its toxicological outcomes.

In the aquatic environment, emerging contaminants are one of the stressors with the ability to compromise their inhabitant's fitness. Abiotic variations, such as climate change-related ones may also affect their resilience and are another result of the growing human footprint on the planet. Greenhouse gas emissions, such as carbon dioxide (CO_2), methane (CH_4), and ozone (O_3) are increasing into the atmosphere because of fossil fuel burn. The atmospheric layer created by the abnormal quantities of these gases absorbs and traps solar energy, in the form of heat, which increases global average temperatures (Black and Weisel 2010). Most of this energy is stored in the ocean, and according to the predictions of the Intergovernmental Panel on Climate Change (IPCC) in the Northern Hemisphere, temperate coastal areas of the Atlantic

Ocean can experience a temperature increase of 4ºC by 2100 (IPCC, 2021). The continuing emission of CO_2 has led to an increased CO_2 partial pressure (pCO_2) oceanic uptake, with direct consequences in seawater chemistry. Dissolved CO_2 reacts with the water molecule (H_2O) and produces carbonic acid (H_2CO_3). The H_2CO_3 is later separated into bicarbonate (HCO_3^-) and hydrogen (H^+), which ultimately decreases the water pH (Zeebe and Ridgwell 2011). With unreduced anthropogenic CO_2 emissions, by the end of the century, a drop of up to 0.4 pH units in temperate coastal areas of the Atlantic Ocean is likely to occur (IPCC, 2021; McNeil and Sasse, 2016). Both climate-change-related variations can occur isolated or combined with other stressors, such as the anthropogenic exacerbated levels of La. To the best of our knowledge, a study dealing with the effects of ocean warming, acidification, and their interaction with La was never conducted. Intending to downsize this knowledge gap, we selected the surf clam (*Spisula solida*) as the biological model. Due to the species ability to accumulate pollutants (Mesquita et al., 2011; Pousse et al., 2020) and its wide geographical distribution (Eastern Atlantic and the Mediterranean), *S. solida* is prone to be impacted by climate change and pollution, and their single and joint effects need to be investigated. This species holds a considerable environmental and economic significance, as an important human food source. In this framework, the main aim of the present study was to investigate the combined effects of ocean warming, acidification, and La accumulation and elimination in the surf clam *S. solida.* Furthermore, we intended to assess their ecotoxicological effects by measuring the oxidative stress-related responses. Here we quantified a robust set of biomarkers, namely lipid peroxidation (LPO), heat shock response (HSP), ubiquitin (Ub), superoxide dismutase (SOD), catalase (CAT), glutathione peroxidase (GPx), glutathione S-transferase (GST) and total antioxidant capacity (TAC) levels.

Therefore, to achieve this objective, we exposed adult surf clams for 7 days to increased temperature (Δ = +4°C), CO_2 (Δ = −0.4 pH units), and La levels (~ 15 µg L^{-1}), through water, followed by a 7-day depuration period.

8.2 MATERIAL AND METHODS

8.2.1 Sampling

Specimens were dredged in Setúbal, Portugal (North Atlantic, SW Europe) in a single sampling event in April 2021. After sampling, individuals were transferred to the aquaculture facilities of *Aquarium Vasco da Gama*, in Lisbon, and maintained in 12.5 L tanks with continuously aerated water mirroring the natural habitat conditions. Clams were depurated for seven days in filtered seawater in a 12h light/12h dark photoperiod. During this phase, physicochemical parameters were kept as salinity = 35±0.1 (V2 refractometer, TMC Iberia, Portugal); water temperature = 15.2±0.1°C (TFX 430 Precision Thermometer, WTW GmbH, Germany) and pH 8.0±0.03 (SG8 e SevenGo pro™ pH/Ion meter, Mettler-Toledo International Inc., Switzerland).

8.2.2 Experimental design

Two hundred and eighty-eight clams were randomly distributed in 8 glass tanks representative of the following treatments: i) control (15°C, pH= 8.0, no La added); ii) high CO_2 (15°C, pH=7.6, no La added); iii) La exposed at control temperature and pH (15°C, pH= 8.0, added La=15 µg L^{-1}); iv) La exposed at control temperature and high CO_2 (15°C, pH= 7.6, added La=15 µg L^{-1}); v) warming (19ºC, pH=8.0, no La added); vi) warming and high CO_2 (19°C, pH=7.6, no La added); vii) La exposed at warming (19°C, pH=8.0, added La=15 µg L^{-1}); viii) La exposed at warming and high CO_2 (19°C, pH=7.6, added La=15 µg L^{-1}). In tanks representative of warming and acidification treatments, the temperature was raised 1°C, and the pH was diminished 0.1, respectively, a day, to gradually acclimate the clams before the beginning of the trial.

The water temperature was kept stable by submerging the experimental tanks in a water bath controlled by heaters (V_2Therm 200 W aquarium heater, TMC Iberia) and chillers (Hailea, HC-250 A). The water pH was mechanically controlled by a Profilux 3.1T (GHL) system linked to pH probes (GHL) which monitored pH every 2 seconds. Upregulation was done with filtered air and downregulated via solenoid valves (Etopi) with CO_2 injection. Hysteresis was kept at ± 0.05 units of pH.

The experimental water was renewed every other day, at the same time, and a La solution ($LaCl_3$, Merck), prepared in filtered ultra-pure water (18.2 MΩ, Milli-Q, Merck), was afterward added to the exposed treatments. Specimens were fed *ad libitum*

with a mixture of green and brown marine phytoplankton (Reef Phytoplankton™, Seachem), every other day, before water change.

Clams were sampled before the beginning of the trial (T0) and after 1 (T1), 3 (T3), and 7 (T7) days of exposure to La. Subsequently to this exposure, the elimination phase began, which lasted an additional 7 days (T14).

Total alkalinity was hand-measured for every sampling event (Alkalinity checkers, Hanna® Instruments) and then the carbonate system speciation was calculated using CO2SYS software (Pierrot et al., 2006).

8.2.3 Lanthanum quantification

Lanthanum concentrations in clams were determined in freeze-dried, grounded, and homogenized samples (n=5 per treatment), after digestion with HNO_3 (distilled, 65% v/v) and H_2O_2 (suprapur, 30% v/v). Labware was previously decontaminated with HNO_3 (20%) and cleaned with ultra-pure water (Milli-Q water - 18.2 MΩ). A quadrupole ICP-MS (NexION 2000) with a cyclonic spray chamber, a concentric Meinhard nebulizer and a dual detector was used to determine La concentrations (Figueiredo et al., 2020). A nine-point calibration curve was used to quantify La, using a commercial solution of indium (In) as an internal standard (Merck, CertiPUR®).

Quality Control (QC) solutions were run every 20 samples. Three procedural blanks were also included within each batch of 20 samples. Blanks accounted for less than 1% of the total La concentration. Furthermore, a certified reference material BCR 668 (muscle of *Mytilus edulis*) was included within each batch of 20 samples, and the measured concentrations were consistent with the certified ones.

La concentrations in clam's whole soft are presented in microgram per gram of tissue dry weight (μg g^{-1}, dw).

8.2.4 Biomarkers

Samples (n=3 per treatment) were homogenized using an Ultra-Turrax (Staufen, Germany), in 3 mL of phosphate-buffered saline solution (PBS: 0.14 M NaCl, 2.7 mM KCl, 8.1 mM Na_2HPO_4, and 1.47 mM KH_2PO_4, pH 7.4). Homogenates were centrifuged at 10.000 x g for 10 min at 4°C and frozen (-80°C) until further analyses. Each sample was run in duplicates (technical replicates), and all the results were normalized to total protein content, as described by Bradford (1976).

8.2.4.1 Oxidative damage markers

Lipid peroxidation

Lipid peroxidation (LPO) was determined according to the thiobarbituric acid reactive substances (TBARS) assay (Uchiyama and Mihara, 1978), over the quantification of malondialdehyde (MDA), an end product of lipid damage. Briefly, 5 µL of each sample, 45 µL of monobasic sodium phosphate buffer (50 mM), 12.5 µL of sodium dodecyl sulfate (8.1%), 93.5 µL of trichloroacetic acid (20%, pH 3.5), 93.5 µL of thiobarbituric acid (1%), and 50.5 µL of Milli-Q ultrapure water were added to a microtube. Later, microtubes were positioned in dry bath (Labnet, 100°C) for 10 min. After cooling on ice, 62.5 µL of Milli-Q ultrapure water was added. Finally, 150 µL of the mixture was added to 96-well microplates (Greiner Bio-one, Germany), and the absorbance was read at 532 nm (Biotek Synergy HTX multi-mode reader). Malondialdehyde (MDA) concentrations were calculated using a calibration curve (0 - 0.1 µM MDA).

8.2.4.2 Protein repair and removal mechanisms

Heat shock proteins

Heat Shock Protein 70 (HSP) was quantified in the supernatants of the samples homogenates through ELISA, as described in Lopes et al. (2019). Ten µL of sample diluted in 980 µL PBS was added to a 96-well microplate (Microlon 600, Greiner, Bio-One, Germany) and allowed to incubate overnight at 4°C. Microplates were then washed three times with PBS TWEEN-20 (0.05%). Following, the microplates were incubated for 90 min at 37 °C, after 100 µL of BSA (1% bovine serum albumin, NZYtech, 98%, Portugal) was added to each well. Formerly, 50 µL of primary antibody 5 µg mL^{-1} of anti-HSP70/HSC70 in 1% BSA (Acris, USA) was added to each well. Microplates incubated overnight at 4°C. Microplates were incubated for 90 min at 37 °C with the secondary antibody [50 µL of 1 µg mL^{-1}; alkaline phosphatase-conjugated anti-mouse IgG (Fc specific, Sigma-Aldrich, USA), after being washed three times with PBS TWEEN-20 (0.05%). After the last washing procedure, 100 µL of the substrate (SIGMA FASTTM p-Nitrophenyl Phosphate Tablets, Sigma-Aldrich, USA) was added to each well and incubated for 30 min at room temperature. Then, 50 µL of stop solution (3 M NaOH) was added to each well and the absorbances read at 405 nm (Biotek Synergy HTX multi-mode reader, USA). HSP content was calculated from the calibration curve, based on serial dilutions of purified HSP70 active protein (0 - 2.000 µg mL^{-1}, OriGene Technology, USA).

Total Ubiquitin

Total Ubiquitin (Ub) content was assessed through a direct ELISA, according to Lopes et al. (2019). Briefly, 100 µL of the supernatant of each sample was added to 96-well microplates (Microlon 600, Greiner, Bio-One, Germany) and incubated overnight at 4°C. After this incubation, microplates were washed with PBS-TWEEN (0.05%) three times. Afterward, 100 µL of blocking solution [1% bovine serum albumin (BSA)] was added and microplates were incubated for 90 min at 37°C. Later, 50 µL of primary antibody (200 µg mL^{-1}; P4D1, sc-8017, HRP conjugate, Santa Cruz, USA) was added, and after overnight incubation (4°C), microplates were washed three times with PBS TWEEN-20 (0.05%). Subsequently, 100 µL of TMB/E substrate (Temecula California, Merck Millipore) was added to each well and incubated for 30 min at RT. Lastly, 100 µL of stop solution (1M HCL) was added to each well and the absorbances were read at 415 nm, using a microplate reader (Biotek Synergy HTX multi-mode reader, USA).

The Ub content was calculated using a dilution of purified ubiquitin (0 - 1 µg $mL^{-1,}$ UbpBio, E-1100, USA).

8.2.4.3 Antioxidant responses

Superoxide dismutase

Superoxide dismutase (SOD), percentage of inhibition, was determined through an adaptation of the method described by McCord and Fridovich (1969) to 96-well microplates. Each sample (10 µL of the supernatant), as well as 180 µL of a reaction mix (deionized ultrapure water, 50 mM potassium phosphate, 0.1 mM ethylenediaminetetraacetic acid, 0.01 mM cytochrome c, and 0.05 mM xanthine), were added to a 96-well microplate. Afterward, 10 µL of xanthine oxidase (0.005 units) initiated the reaction. The absorbance was read at 550 nm using a microplate reader (Biotek Synergy HTX multi-mode reader, USA).

Catalase

Catalase (CAT) activity was determined by the method described by Johansson and Borg (1988). In short, 20 µl of each sample, 100 µl of 100 mM potassium phosphate, and 30 µl of methanol were added to each well of a microplate (Greiner, Bio-One, Germany), shaken, and incubated for 20 minutes. Then, 30 µl of potassium hydroxide (10 M KOH) and 30 µl of purpald (34.2 mM in 0.5 M HCl) were added to each well, shaken, and incubated for 10 minutes. Subsequently, 10 µl of potassium periodate (65.2

mM in 0.5 M KOH) was added to each well and a final incubation was performed for 5 minutes. Using a microplate reader (Biotek Synergy HTX multi-mode reader, USA), enzymatic activity was determined spectrophotometrically at 540 nm. Formaldehyde concentration was calculated based on a calibration curve (from 0 to 75 µM formaldehyde).

Glutathione peroxidase

Glutathione peroxidase (GPx) activity was determined according to Lawrence and Burk (1976). Twenty µL of each sample, 120 µL of 50 mM phosphate buffer (pH 7.6), fifty µL co-substrate mixture (0.8 mM β-NADPH, 4 mM Glutathione, 4 U/mL glutathione reductase, and 4 mM sodium azide), and twenty µL 15 mM cumene hydroperoxide (C9H12O2) were added to each of the 96 well of a microplate, and the absorbance was read at 340 nm (Biotek Synergy HTX multi-mode reader, USA), every minute for 6 min. The GPx activity was determined using the β-NADPH coefficient extinction (3,73 mM^{-1} cm^{-1}).

Glutathione S-transferase

Glutathione S-transferase (GST) activity was determined according to Lopes et al. (2019). A substrate solution (200 mM L-glutathione reduced, Dulbecco's PBS plus 100 mM CDNB solution) was added to a 96-well microplate (Greiner, Bio-One, Germany), together with 20 µL of GST standard or sample. The GST activity was read spectrophotometrically at 340 nm, every minute for 6 minutes, using a plate reader (Biotek Synergy HTX multi-mode reader, USA). The reaction rate was calculated using the CDNB extinction coefficient of 0.0053 εµM (μM^{-1} cm^{-1}).

Total antioxidant capacity

The total antioxidant capacity (TAC) was determined according to Kambayashi et al. (2009). Ten µL of each sample together with 90 µM myoglobin (10 µL), 600 µM 2,2'-azino-bis (3-ethylbenzothiazoline-6-sulphonic acid) (150 µL) and 500 µM hydrogen peroxide (40 µL) were added to the wells of a microplate (Greiner, Bio-One, Germany). Microplates were incubated at room temperature for 5 min and the absorbance was read at 410 nm (Biotek Synergy HTX multi-mode reader, USA). The TAC was calculated based on a series of Trolox (0 – 0.33 mM).

8.2.5 Statistical analyses

To investigate differences between the experimental treatments, for T1, T3 T7 and T14, a three-way ANOVA was applied with Temperature, pH and Contamination as treatment factors, followed by all pairwise comparisons between the predicted means of the treatment factors using Tukey's procedure (Braun, 1995). In the case of T0, a two-way ANOVA was applied with Temperature and pH as treatment factors. Lastly, a one-way ANOVA was carried out to identify differences in La concentrations in clam's exposed to climate change variables and La, between sampling times. These analyses were repeated for each of the studied biomarkers.

To compel the assumptions of normality and stabilize the variance, data were $\log_{10}$ transformed.

The analyses were performed at a significance level of 0.05 using the open-source software InVivoStat, version 4.3.

8.3 RESULTS

The physicochemical and carbonate system-specific parameters of water in every experimental treatment are shown in Table 8.1.

Table 8.1 - Seawater physicochemical parameters and specifics of carbonate system for all treatments (mean ± standard deviation). Measured temperature, pH and total alkalinity were utilized to calculate the carbonate system parameter: carbon dioxide partial pressure (pCO_2).

Treatments	Temperature (°C)	Salinity	pH	Total Alkalinity (µmol kg^{-1} SW)	$pCO2$ (µatm)
Control	15.1±0.2	35±0.1	8.01±0.10	1928±109	367±67
High CO_2	15.1±0.3	35±0.1	7.59±0.10	1643±64	893±73
La exposed	15.0±0.1	35±0.1	8.02±0.07	2250±112	408±29
High CO_2 and La exposed	15.2±0.1	35±0.1	7.58±0.11	1522±88	847±20
Warming	19.1±0.2	35±0.1	8.03±0.06	2307±102	442±65
High CO_2	19.2±0.3	35±0.1	7.61±0.14	1707±83	897±22
Warming and La exposed	19.2±0.1	35±0.1	8.00±0.05	2169±140	382±56
Warming, High CO_2 and La exposed	19.1±0.1	35±0.1	7.62±0.12	1696±97	868±44

8.3.1 Lanthanum bioaccumulation and elimination

Median and ranges of La concentration (µg g^{-1}, dry weight) are shown in Table 8.2. Concentrations of La (µg g^{-1}, dry weight) in surf clams exposed to La and climate change scenarios are presented in Figure 8.1.

Table 8.2 - Median, minimum and maximum La concentrations (µg g^{-1}, dry weight) in *Spisula solida*' soft body at T0, T1, T3, T7 and T14, exposed to control; acidification; La; acidification + La; warming; warming + acidification; warming + La and warming + acidification + La. The ICP-MS detection limit for La stood at 0.078 µg g^{-1}, dw.

	[La] (µg g^{-1} dry weight)				
	T0	**T1**	**T3**	**T7**	**T14**
Control	0.18 (0.11 -0.23)	0.16 (0.14 -0.18)	0.12 (0.11 - 0.19)	0.21 (0.19 - 0.29)	0.22 (0.15 - 0.35)
High CO_2	0.14 (0.11 - 0.23)	0.18 (0.14 - 0.22)	0.18 (0.13 - 0.20)	0.23 (0.20 - 0.30)	0.12 (0.092 - 0.17)
La exposed		1.6 (1.4 -1.8)	2.0 (2.0 - 3.8)	5.3 (4.5 - 6.1)	3.1 (2.9 - 3.7)
High CO_2 and La exposed		1.3 (1.2 -1.7)	2.5 (1.7 - 3.7)	3.9 (3.1 - 6.1)	3.2 (2.8 - 3.7)
Warming	0.17 (0.13 - 0.23)	0.10 (0.075 -0.16)	0.18 (0.15 - 0.20)	0.13 (0.10 - 0.16)	0.16 (0.14 - 0.20)
Warming and High CO_2	0.14 (0.11 - 0.18)	0.13 (0.13 -0.14)	0.12 (0.087 - 0.19)	0.21 (0.13 - 1.1)	0.18 (0.17 - 0.20)
Warming and La exposed		2.1 (1.7 - 2.4)	3.0 (2.1 - 3.4)	3.2 (2.9 - 3.2)	1.3 (1.0 - 1.5)
Warming, High CO_2 and La exposed		1.9 (1.0 - 2.9)	2.7 (2.4 - 3.7)	4.7 (2.7 - 4.9)	1.8 (1.6 - 1.9)

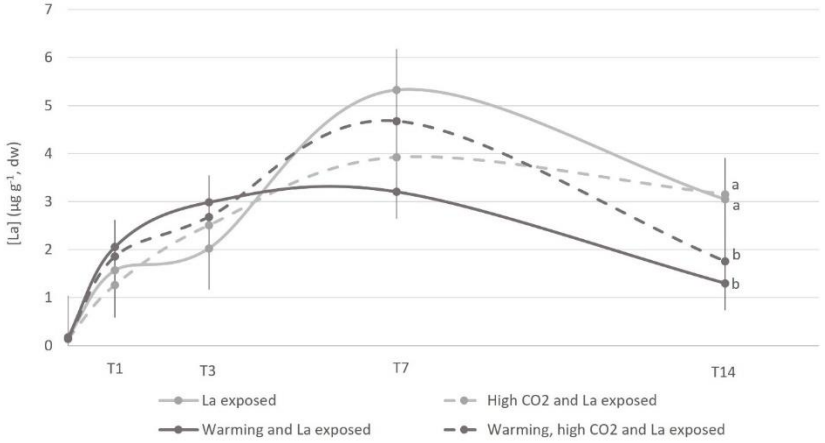

Figure 8.1 – Lanthanum concentration (µg g^{-1}, dry weight) in in *Spisula solida*' soft body at T1, T3, T7 and T14, exposed La; acidification + La; warming + La and warming + acidification + La. Values represent medians ± SE. Different letters represent significant differences between exposure treatment, within sampling time (p<0.05).

The Tukey's pairwise comparisons of La concentrations between all treatments, within each sampling time, are presented in Annex 7, Supplemental Table 8.1 A and the comparisons of the La concentrations in spiked treatments between sampling times are presented in Annex 7, Supplemental Table 8.1 B.

The baseline La values remained comparable for the T0 and the non-La exposed treatments throughout the experiment (T1-T14; Annex 7, Supplemental Table 8.1 A) as they varied between 0.12 µg g^{-1} (Warming and high CO_2 and control treatments at T3) and 0.23 µg g^{-1} (high CO_2 treatment at T7; Table 8.2).

After just one day of exposure, La accumulation occurred in all four exposure treatments as they exhibited significant differences from their control counterparts (p<0.0001, Annex 7, Supplemental Table 8.1 A). At this time the clams exposed to warming and La accumulated a median±SE of 2.1±0.20 µg g^{-1}, while the ones exposed to warming, high CO_2, and La accumulated 1.9±0.54 µg g^{-1}. The clams exposed to La accumulated 1.6±0.16 µg g^{-1}, while the clams exposed to high CO_2 and La accumulated

1.3±0.16 μg g^{-1}. The La concentrations increased in T3, being higher in the surf clams exposed to La at a warming temperature. The clams exposed to warming and La presented a La concentration of 3.0±0.31 μg g^{-1}, and the ones exposed to warming + CO_2 + La exhibited 2.7±0.28 μg g^{-1}. The peak of accumulation occurred at T7 for all treatments, being highest in the clams exposed to La, at the control temperature (5.3±1.1 μg g^{-1}), followed by the ones exposed to warming, high CO_2, and La (4.7±0.52 μg g^{-1}). The La concentration of clams exposed to high CO_2 and La was 3.9±0.51 μg g^{-1}, and of the clams exposed to warming and La was 3.2±0.11 μg g^{-1}. At T14, after 7 days of La elimination, the values decreased but were still different than their control counterparts (p<0.05, Annex 7, Supplemental Table 8.1 A). Lanthanum exposed clams presented a concentration of 3.1±0.73 μg g^{-1}, whilst clams of the acidification treatment showed 3.2±0.24 μg g^{-1}. The clams exposed to warming and La showed 1.3±0.09 μg g^{-1}, and the clams previously exposed to La in a warming and high CO_2 setting revealed 1.8±0.14 μg g^{-1}, after the exposure period. The La elimination was highest in clams under this latter treatment, declining roughly 60% from T7 (4.7±0.52 μg g^{-1}) to T14 (1.8±0.14 μg g^{-1}). At T14 we observed significant differences between the La exposure treatments (p<0.0001, Annex 7, Supplemental Table 8.1 A), showcasing different elimination patterns. At a control temperature, the La elimination was greater. At T14, the La concentrations in the exposure treatments varied accordingly to temperature as significant differences were found between treatments at control and warming temperatures (p<0.001, Annex 7, Supplemental Table 8.1 A) and not between treatments at the same temperature (i.e., La exposed vs High CO_2 and La exposed and Warming and La exposed vs Warming, High CO_2 and La exposed).

Throughout time the concentrations of La from clams exposed to La, at a control temperature and pH (T=15°C, pH=8.0), varied significantly from T1 to T7 (p=0.0035, Annex 7, Supplemental Table 8.1b), and from T3 to T7 (p=0.032). Regarding the concentration in clams exposed to acidification and La, they only varied significantly between T1 and T7 (p=0.0018) and T1 and T14 (p=0.02). In the warming + La exposed treatment, the La concentration showed significant differences between T1 and T14 (p=0.017), T3 and T14 (p=0.0002), and T7 and T14 (p=0.0002). Lastly, in the treatment that combined both climate change variables and La exposure, the concentrations were only significantly different between T1 and T7 (p=0.033).

8.3.2 Biomarkers

Mean±standard deviation levels of lipid peroxidation (LPO); ubiquitin (Ub); superoxide dismutase (SOD); catalase (CAT); glutathione peroxidase (GPx); glutathione S-transferase (GST) and total antioxidant capacity (TAC) are presented in Table 8.3 and in Figure 8.2. The three-way ANOVA with the Temperature, pH and Contamination as factors followed by significant Tukey's pairwise comparisons for TAC, SOD, GST, GPx, HSP, CAT, LPO and Ub, for each sampling time are presented in Annex 7, Supplemental Table 8.2a. Tukey's pairwise comparisons between times for TAC, SOD, GST, GPx, HSP, CAT, LPO and Ub values in the four La exposed treatments are presented in Annex 7, Supplemental Table 8.2 B.

Table 8.3 - Mean ± standard deviation levels of Lipid peroxidation (LPO, nmol mg protein $^{-1}$); Heat Shock Protein 70 (HSP, µg mg^{-1} protein); Total Ubiquitin (Ub, µg mg^{-1} protein); Superoxide dismutase (SOD, % inhibition min^{-1} mg^{-1} protein); Catalase (CAT, nmol min^{-1} mg^{-1} protein); Glutathione peroxidase (GPx, nmol min^{-1} mg^{-1} protein); Glutathione S-transferase (GST, nmol min^{-1} mg^{-1} total protein) and total antioxidant capacity (TAC, mM Trolox mg^{-1} total protein) in *S. solida*' soft body at T0, T1, T3, T7 and T14.

		LIPO (nmol mg protein $^{-1}$)	**HSP** (µg mg^{-1} protein)	**Ub** Ub (µg mg^{-1} protein)	**SOD** (% inhibition min^{-1} mg^{-1} protein)	**CAT** (nmol min^{-1} mg^{-1} protein)	**GPx** (nmol min^{-1} mg^{-1} protein	**GST** (nmol min^{-1} mg^{-1} total protein)	**TAC** (mM Trolox mg^{-1} total protein)
T0	Control	4.5±0.47	54±4.8	1.8±0.24	5.5±0.71	1.1±0.34	5.2±0.65	30±4.3	0.73±0.050
	High CO_2	6.2±2.9	58±5.3	1.9±0.87	4.5±1.6	1.2±0.39	5.8±0.89	35±3.3	0.83±0.11
	Warming	5.7±0.74	60±5.4	1.8±0.030	5.1±1.3	0.90±0.16	6.0±1.7	34±4.3	0.84±0.010
	Warming and high CO_2	5.1±0.83	54±2.7	2.4±0.27	5.6±0.69	1.1±0.35	5.6±1.1	38±2.2	0.74±0.15
T1	Control	5.6±1.2	48±5.6	1.6±1.1	5.7±0.66	1.2±0.29	5.1±1.2	30±3.3	0.78±0.070
	La exposed	3.2±0.19	62±12	1.3±0.070	4.0±0.66	0.70±0.020	5.4±0.31	35±2.4	0.77±0.010
	High CO_2	4.9±2.5	56±11	2.1±0.90	4.6±0.34	1.4±0.020	5.9±0.21	33±2.9	0.80±0.010
	High CO_2 and La exposed	3.6±0.67	54±11	1.5±0.85	3.6±0.65	1.0±0.070	5.5±0.65	36±1.5	0.70±0.17
	Warming	6.1±1.7	56±7.1	1.9±0.78	5.6±0.58	0.80±0.030	5.7±0.34	32±1.4	0.71±0.070
	Warming and La exposed	5.4±1.3	73±9.0	2.5±0.73	4.3±0.36	0.80±0.11	5.2±0.35	41±2.7	0.91±0.070
	Warming and high CO_2	4.9±1.1	46±8.7	2.4±0.49	6.4±1.2	1.0±0.31	5.7±1.9	38±4.0	0.77±0.35
	Warming, high CO_2 and La exposed	3.8±1.1	61±19	2.6±0.43	3.8±0.64	1.0±0.020	5.5±0.41	39±4.3	1.2±0.56
T3	Control	2.9±0.90	45±9.3	2.0±1.4	5.5±0.15	1.1±0.040	4.6±0.24	27±1.9	1.1±0.0002
	La exposed	1.5±0.59	56±5.8	2.9±0.68	4.4±0.64	0.80±0.14	3.0±0.52	34±1.5	1.1±0.11
	High CO_2	2.8±0.89	46±6.2	2.6±0.65	4.9±1.0	1.4±0.020	3.6±0.56	30±4.1	1.2±0.30
	High CO_2 and La exposed	2.5±0.40	36±4	2.6±0.14	4.8±0.97	0.80±0.080	2.6±0.72	38±0.70	1.2±0.42
	Warming	3.4±0.47	46±8.9	2.2±0.67	6.9±0.68	0.90±0.10	4.7±0.22	29±3.4	1.7±0.15
	Warming and La exposed	3.1±1.0	25±12	1.2±0.50	5.8±1.4	1.0±0.13	4.2±0.53	41±1.7	1.7±0.08
	Warming and high CO_2	3.3±0.53	37±8.9	2.2±0.10	6.3±2.0	1.0±0.10	4.1±0.46	33±5.5	1.4±0.33
	Warming, high CO_2 and La exposed	3.7±0.69	31±2.7	2.2±0.93	4.4±0.62	1.0±0.01	3.6±0.38	38±2.7	2.4±0.41
T7	Control	3.8±0.33	41±7.4	1.4±0.65	4.6±1.0	1.4±0.030	4.1±0.40	31±2.6	1.4±0.060
	La exposed	7.3±1.3	50±9.0	2.6±0.45	4.2±0.30	2.3±0.13	3.2±0.33	34±4.5	2.2±0.65
	High CO_2	4.2±0.71	44±8.3	2.3±1.2	4.0±0.84	2.1±0.070	3.0±0.63	31±3.3	1.6±0.020
	High CO_2 and La exposed	9.4±1.3	16±0.40	2.6±0.26	6.8±0.23	2.3±0.24	2.8±0.41	36±2.0	2.4±0.24
	Warming	12±2.3	54±12	2.8±0.16	8.2±0.89	2.1±0.20	3.8±0.61	31±2.6	3.3±0.47
	Warming and La exposed	14±0.08	25±3.6	0.80±0.29	7.9±0.83	2.1±0.090	2.8±0.78	34±2.4	2.7±0.13
	Warming and high CO_2	14±3.4	32±3.9	4.2±0.19	7.1±0.43	2.0±0.17	2.5±0.31	30±5.5	2.7±0.18
	Warming, high CO_2 and La exposed	20±2.5	34±1.2	4.2±0.27	8.9±0.62	2.3±0.19	2.4±0.90	38±1.8	3.1±0.16
T14	Control	3.5±0.20	33±4.9	1.7±0.18	6.0±0.47	1.4±0.18	3.5±0.36	30±4.8	1.3±0.30
	La exposed	4.6±2.8	33±3.3	1.6±0.36	7.5±0.33	1.9±0.050	4.2±0.47	33±0.92	1.7±0.37
	High CO_2	2.6±0.38	41±1.3	1.7±0.28	6.6±0.97	1.8±0.13	3.4±0.31	30±4.1	1.7±0.23

Table 8.3 Cont.

		LIPO (nmol mg protein $^{-1}$)	HSP (µg mg^{-1} protein)	Ub (µg mg^{-1} protein)	SOD (% inhibition min^{-1} mg^{-1} protein)	CAT (nmol min^{-1} mg^{-1} protein)	GPx (nmol min^{-1} mg^{-1} protein	GST (nmol min^{-1} mg^{-1} total protein)	TAC (mM Trolox mg^{-1} total protein)
T14	High CO_2 and La exposed	3.1±1.1	32±9.6	2.0±0.01	7.1±0.92	1.6±0.080	3.1±0.63	34±3.7	1.9±0.060
	Warming	7.6±0.38	47±9.7	1.0±0.12	7.7±0.49	1.9±0.11	3.7±0.40	29±3.4	3.2±0.40
	Warming and La exposed	3.0±0.31	40±13	3.0±0.060	7.2±0.49	1.4±0.28	2.8±0.78	34±3.8	2.1±0.44
	Warming and high CO_2	7.0±1.1	43±9.2	3.7±0.46	8.0±0.02	2.2±0.18	3.0±1.1	32±0.25	2.2±0.11
	Warming, high CO_2 and La exposed	2.9±0.080	32±14	2.3±0.090	7.6±0.41	1.7±0.20	2.7±0.56	35±2.2	2.3±0.11

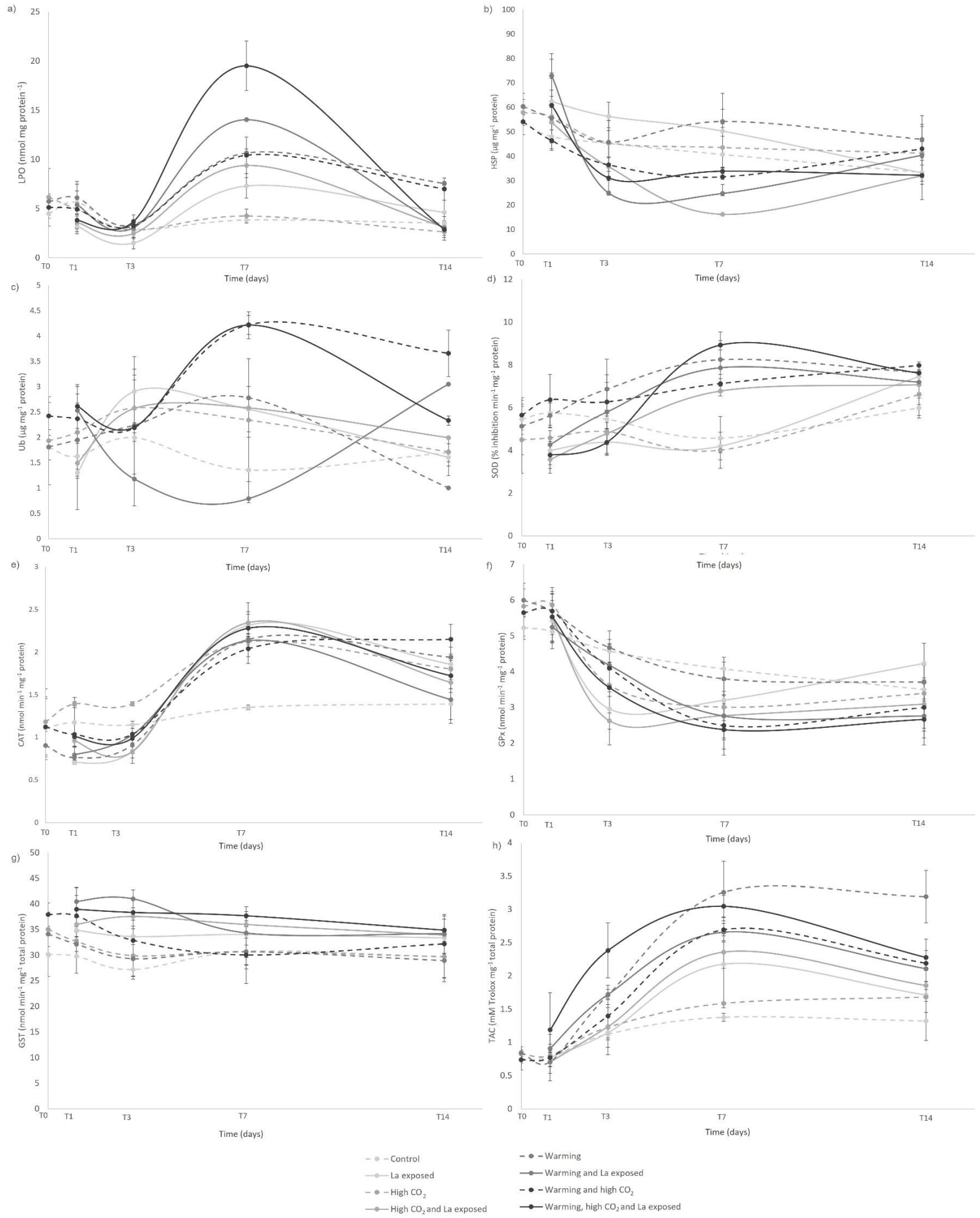

Figure 8.2 – a) Lipid peroxidation (LPO, nmol mg protein $^{-1}$); b) Heat Shock Protein 70 (HSP, µg mg^{-1} protein); c) Ubiquitin (Ub, µg mg^{-1} protein); d) Superoxide dismutase (SOD, (% inhibition min^{-1} mg^{-1} protein); e) Catalase (CAT, nmol min^{-1} mg^{-1} protein); f) Glutathione peroxidase (GPx, nmol min^{-1} mg^{-1} protein); g) Glutathione S-transferase (GST, nmol min^{-1} mg^{-1} total protein) and h) total antioxidant capacity (TAC, mM Trolox mg^{-1} total protein) in *Spisula solida*' soft body at T0, T1, T3, T7 and T14 exposed to: control; high CO_2; La; high CO_2 and La; Warming; Warming and La; Warming and high CO_2; Warming, high CO_2 and La. Values correspond to mean ± SD.

8.3.2.1 Lipid peroxidation

On the third day of the experiment (T3), significant differences in LPO were observed between the La exposed treatments and the controls (p<0.05, Annex 7, Supplemental Table 8.2a; Figure 8.2a), as this showed lower values than the latter.

The impact of climate change alone on lipid peroxidation was observed on T7 when the clams from the warming treatment and the warming and high CO_2 exhibited significantly higher values than their control temperature counterparts (p=0.0009 and p=0.0004, respectively). Additionally, clams from these two treatments also exhibited significantly higher values than clams kept in just a high CO_2 scenario (p=0.0037 and p=0.0016, respectively).

At this time, La exposed clams exhibited significantly higher (p=0.0486) values than the control equivalents. Concomitantly, a significant difference was also observed between clams exposed to high CO_2 and La and the ones kept in high CO_2 (p=0.0127). Furthermore, clams exposed to the three stressors: warming, high CO_2 and La showed higher lipid peroxidation than clams exposed to high CO_2 and La (p=0.0002).

At T14, lipid peroxidation values of the La exposed treatments decreased to control-like values. Clams of the warming and warming and high CO_2 treatments exhibited the greatest lipid peroxidation values.

Lipid peroxidation results were significantly different between day 3 (T3) and day 7 (T7) in the four La exposed treatments (p<0.05, Annex 7, Supplemental Table 8.2b). Furthermore, the LPO levels were significantly different between T1 and T7 and between T7 and T14 in La exposed treatments, at higher CO_2, temperature, and both combined.

8.3.2.2 Heat shock proteins

It was only at T7 that the effect of La in the HSP expression was noted (Annex 7, Supplemental table 8.2a; Figure 8.2b). Clams exposed for 7 days to La showed a significantly lower HSP expression than the clams kept at high CO_2 and La (p=0.0072). The latter showed significantly lower HSP expression than the clams kept in a high CO_2 treatment (p=0.0154). Finally, clams inhabiting a warmer condition showed higher HSP values than the clams exposed to La in a warmer scenario (p=0.0246).

The clams from the warming and La treatment showed significantly lower HSP values from T1 to T3 and T7 (p=0.0191 and p=0.0278, respectively). Heat shock proteins also decreased from T1 to T7 in the clams exposed to high CO_2 and La (p=0.02, Annex 7, Supplemental Table 8.2b).

8.3.2.3 Total Ubiquitin

Again, here, it was only at T7 that significant differences in Ub values between treatments were observed. Ubiquitin values on La exposed clams were significantly higher than on La exposed clams in a warming temperature (p=0.0336). The total Ub levels were the highest in the warming, high CO_2, and La exposed treatment and this proved to be statistically higher than the clams in the warming and La treatment (p=0.0025). On another hand, the Ub values on the warming and La treatment were significantly lower than the warming treatment (p=0.0129).

By the end of the elimination phase, only the total Ub levels in clams from the warming treatment were significantly lower than the ones from the warming and high CO_2 trial (p=0.0465).

The Ub levels were different in La exposed treatment between T1 and T3 (p=0.0444, Annex 7, Supplemental Table 8.2 B) and differed from T1 to T7 in the warming and La exposed treatment (p=0.019).

8.3.2.4 Superoxide dismutase

At T1, the four La exposed treatments presented overall lower SOD (% inhibition) values than their control counterparts (Figure 8.2d). Although at T1, several significant pairwise comparisons were observed between all experimental treatments, the most striking is the one between SOD levels of clams exposed to warming, high CO_2, and La and the clams exposed to warming and La (p<0.0001), being the former significantly lower. Curiously, at T3, as overall SOD values in La exposed treatments rose, no significant differences were observed between treatments. On another hand, at T7 several significant differences come from the exposure to La and climate change, together and as single stressors. The effect of temperature was clear through the significant difference found between SOD values in the clams at the control treatment and the ones exposed to a warmer temperature (p<0.0001). Likewise, clams that were kept in the high CO_2 treatment showed significantly lower SOD than the ones in the warming and high CO_2 (p<0.0001). The effect of pH decrease was also obvious as the

SOD values of clams exposed for 7 days to La were significantly lower than the ones exposed to La in a high CO_2 environment. Noteworthily, clams exposed to La and high CO_2 exhibited significantly higher SOD values than the ones in the high CO_2 treatment (p<0.0001).

At T14, differences between the control treatment and the warming and warming and high CO_2 treatments were showcased (p=0.01 and p=0.0151, respectively), as the latter two exhibited higher SOD levels.

In the La exposed treatment, the SOD activity varied between T1 and T14 (p=<0.0001), and between T3 and T14 (p=0.0003), with enhanced levels in T14. In the remaining three La exposed treatments, the T1 and T3 were different from all the other sampling times, apart from T1 vs T3 in the Warming, high CO_2, and La exposed treatment (p=0.2779, Annex 7, Supplemental Table 8.2b).

8.3.2.5 Catalase

There were no significant differences in CAT values in T0 and T1 (p>0.05). At T3, clams exposed to La and high CO_2 showed significantly diminished CAT values than the ones exposed to only high CO_2. This difference was not observed in T7, as the CAT values increased, overall, in all exposure treatments. In fact, on the 7th day of the experiment, the control treatment showed significantly lower CAT values than all the other treatments (p<0.05, Annex 7, Supplemental Table 8.2a).

At 14, CAT values on the control treatment were kept significantly different than the Warming and Warming and high CO_2 treatments (p=0.0137 and p=0.0022, respectively), highlighting the effects of increased temperature on CAT activity. The CAT activity values of the previously La exposed four treatments decreased from T7 to T14, in a way that none were different than their respective control.

Catalase activity varied greatly between sampling times, for all four La exposure treatments, except between T1 and T3 (Annex 7, Supplemental Table 8.2b). Furthermore, between T7 and T14 the clams in the La exposed treatment and in the warming and La exposed treatment did not show significantly different CAT activity.

8.3.2.6 Glutathione peroxidase

After 3 days of exposure to La, clams showed significantly inhibited GPx levels, when compared to the control (p<0.0001; Figure 8.2f). Here both temperature and pH

seemed to affect the GPx values. Clams exposed to La and high CO_2 showed significantly lower GPx values than the ones exposed to just high CO_2 (p=0.0139) and, curiously, lower than the ones exposed to warming, high CO_2, and La (p=0.0213). Additionally, La exposed clams displayed significantly lower levels of GPx than the ones exposed to La in a warmer temperature (p=0.0024). At T7, only the clams exposed to three stressors: warming, high CO_2, and La exhibited significantly lower GPx values than the control (p=0.0049).

Between T1 and T7 and T1 and T14, the GPx values decreased significantly for all La exposed treatments (Annex 7, Supplemental Table 8.2b). As the decrease of GPx values was greater in clams exposed to La and exposed to high CO_2 and La, these two treatments showed significant differences between T1 and T3. The GPx levels of the two La exposed treatments at a warmer temperature were different between T3 and T7.

8.3.2.7 Glutathione S-transferase

At the beginning of the experiment (T0), a significantly lower GST activity in control clams was found in comparison to the clams acclimated to Warming and high CO_2 (p=0.0219; Figure 8.2g). At T1, when the 8 experimental treatments were analyzed together, the control proved to only be different than the warming and La exposed treatment (p=0.0354). After 3 days, the four La exposed treatments showed significantly enhanced GST values, in comparison to the temperature and pH control treatment (Annex 7, Supplemental Table 8.2a). Additionally, clams exposed to warming and La exhibited significantly higher GST values than the ones exposed to only La and significantly higher GST values than the ones exposed to warming (p=0.0008). Finally, at this time, the warming and La treatment originated higher GST values than the warming and high CO_2 treatment (p=0.0203). With increasing exposure time (T7), the clams exposed to warming, high CO_2 and La, presented higher values than the warming and high CO_2 treatment (p=0.0225). At T14, no significant differences were observed between treatments.

Only in the warming and La exposed treatment that GST differences over time occurred (p<0.05, Annex 7, Supplemental Table 2b). The levels varied between T1 and T7; T1 and T14; T3 and T7 and T3 and T14.

8.3.2.8 Total antioxidant capacity

At T3, the total antioxidant capacity of the clams exposed to warming, high CO_2, and La were significantly higher than the control clams (p=0.0108), the bivalves exposed to La alone (p=0.0055), and those exposed to high CO_2 and La (p=0.0205; Figure 8.2h). At T7, the warming treatment showed enhanced TAC levels, in comparison to the control temperature (p=0.0288). The control treatment was also statistically different than the warming, high CO_2, and La one (p=0.0437). After the elimination period, no statistical differences were observed between TAC levels in the different treatments (p=0.1653).

Between T1 and T3 significantly higher TAC values were detected in all La exposed treatments (Annex 7, Supplemental Table 8.2b). The same was observed between T1 and T7, apart from the TAC levels displayed by clams exposed to warming, high CO_2, and La.

8.4 DISCUSSION

Bivalves acquire their food sources through filter-feeding processes, which predispose them to be particularly vulnerable to water elemental load and overall quality. In fact, bivalves are known to accumulate both environmentally available and laboratory spiked REEs (e.g., Akagi and Edanami, 2017; Bonnail et al., 2017; Wang et al. 2019). In the present study, an exposure to 15 µg L^{-1} of $LaCl_3$ rendered La bioaccumulation just after one day, in a temperature and pH control setting but also, in an acidified medium, warmer one, and both combined. As far as we are aware, this is the first study to investigate REE accumulation in an ocean warming and acidification scenario which hardens comparison with previously published data. Nevertheless, Figueiredo et al. (2020) exposed glass eels (*Anguilla anguilla*) to 1.5 µg L^{-1} of La for five days in a warming scenario (△T = +4 °C) and described enhanced accumulation with increasing temperature in this fish species. It must be highlighted, however, that this experiment waws carried out in freshwater, which, in addition to being performed with a vertebrate, may explain the different results obtained in the present study as we did not observe effects of warming and acidification on La bioaccumulation. On another hand, Serra-Compte et al. (2018) exposed mussels (*Mytilus galloprovincialis*) to pharmaceuticals and endocrine-disrupting compounds in a warming and acidification

scenario and described antagonistic effects. Warming increased the bioconcentration factor (BCF) of sulfamethoxazole and sotalol, while acidification increased the BCF of sulfamethoxazole, sotalol, and methylparaben. Distinctively, acidification decreased triclosan, while both stressors decreased venlafaxine and citalopram BCFs. Furthermore, Romero-Freire et al. (2020) exposed the same mussel species to dissolved trace metals (Cu, Co, Pb, Cd, Cr, As and Ni) in a warming and CO_2 increase setting and described that the increasing CO_2 alone did not impact bioaccumulation, however, the combined stressors may have led to an increase in the bioaccumulation for some elements. The conflicting results of bivalves exposed to different pollutants in a climate change scenario point to a species and/or element-specific bioaccumulation and/or elimination/detoxifying pattern. This highlights the huge knowledge gap on the effects of climate change on REE accumulation and toxicity and illustrates the novelty of the present study. Pinto et al. (2019) exposed *M. galloprovincialis* to different La concentrations (0, 0.1, 1, 10 mg L^{-1}), for 28 days, under controlled temperature (18±1.0°C) and showed that La concentrations increased in higher exposure concentrations, while BCF's strongly decreased with increasing exposure concentrations, indicating that organisms could limit La accumulation. Hanana et al. (2017) described a similar trend for 28 days La exposed freshwater *Dreissena polymorpha* mussels. Here we exposed clams to a much lower environmentally realistic La concentration, and for fewer days, which could have been insufficient to trigger the bivalve capacity to reduce filtration rates and hence decrease BCF's with increasing pollutant concentration. Nevertheless, in the present study, the concentrations increased in all La exposure treatments and seemed to not be affected by the increased temperature or CO_2. This is an unexpected result, as previously discussed, and the lack of significant differences between the four La exposure treatments at different abiotic climate change conditions may likely be due to interindividual variability and/or short exposure duration. Hence, we suggest that further studies should take this into consideration and, if possible, increase the number of individuals studied and the duration of the exposure itself. In our study, a 7-day elimination phase was insufficient to counterbalance a 7-day exposure. At 14, La concentrations in the clams' whole soft body did not reach control like values and we observed an effect of temperature in La elimination. The ratio of La concentration on T14/T7 indicates greater elimination at a

warming temperature, in the acidified treatment followed by the control pH than at the two La exposure treatments at a control temperature. This is supported by the results of Maulvault et al. (2018), which assessed the bioaccumulation and elimination of other emerging chemical contaminants in marine bivalves (*Mytilus galloprovincialis* and *Ruditapes philippinarum*) and showed that warming facilitated the elimination of some contaminants. Information on REE elimination on bivalves is extremely scarce, particularly in a climate change scenario. Here we provide information on which future studies may build upon.

Normal metabolic processes, that need molecular O_2 to produce energy, lead to the creation of reactive oxygen species (ROS), due to electrons escaping the electron transport chain (Lushchak, 2011). The cellular reduction of molecular O_2 to H_2O, generates reactive intermediates, like the superoxide ion (O_2^-), hydrogen peroxide (H_2O_2), and the hydroxyl radical (HO), that may cause deleterious outcomes for biological systems. Regoli and Giuliani (2014) described how pollutants can cause ROS overproduction, which can alter biological membranes, causing oxidative degradation of lipids, if not eliminated by the antioxidant enzymes. In regular conditions, these deleterious outcomes can be prevented by a set of antioxidant defense mechanisms, that include antioxidant enzymes. Superoxide dismutase is responsible for removing O_2^- while forming H_2O_2. Catalase (CAT) and GPx reduce the H_2O_2 into H_2O (Regoli and Giuliani, 2014). If the excess O_2^- is not removed, protein, lipid, and DNA damage may occur (González et al., 2015). Additionally, H_2O_2 can cross biological membranes, damaging cellular components, prompting cell death pathways (Lesser 2006). Glutathione S-transferases (GST) play a key role in the second phase of the detoxification process by detoxifying both ROS and some xenobiotics. When in stressful environments, such as increased temperature, CO_2, and enhanced emerging contaminants the antioxidant system proficiency may be compromised. Overall, our results showed that just after one day of exposure, concurring with bioaccumulation significant values, SOD was inhibited in La exposure treatments, in the present-day scenario, and climate change ones. A decrease in antioxidant enzyme activity may occur directly caused by oxidative damage or ultimately due to altered enzyme gene expression (Freitas et al., 2020b). Nevertheless, this rapid inhibition was overcome as SOD values increased over

time. Furthermore, at T7, SOD values were higher in climate change treatments, when compared to their control counterpart. Enhanced SOD values in bivalves exposed to warming had been previously described (e.g., Hornstein et al., 2018; Matozzo et al., 2013). Here we showed that at T7, when exposed to both high CO_2 and La, SOD levels were enhanced, in comparison to clams exposed to just La, showcasing a synergistic effect of acidification and La.

Catalase activity increased over time in climate change- and La-exposed treatments while GPx activity was hindered in the four La exposed treatments, after 3 days. These results are not following the ones described by Pinto et al. (2019) that showed increase activity of antioxidant enzymes in *M. galloprovincialis* exposed to La. This could be related to differences in La exposure concentrations, as in that study, the activation of the antioxidant defenses SOD and GPx occurred in mussels exposed to 100 μg L^{-1} and 1000 μg L^{-1} La, roughly 10 and 100-fold higher than the environmentally realistic one applied in the present study. On another hand, in the present study, GST values were globally higher in La exposed clams, which suggests that La triggered a biochemical response in this clam species, especially in a climate change environment. Furthermore, GST values varied significantly with La exposure time and were upheld even after the elimination phase, suggesting a lasting effect on the oxidative stress response, with probable consequences on individuals' fitness.

Marine organisms display a robust protein repair and removal method. Proteins are temperature-dependent, and their stability is affected by temperature and stress (Hazel and Prosser, 1974). Hence, when exposed to environmental stress a heat shock response is activated, through the synthesis of chaperones as the heat shock proteins (Sørensen et al., 2003). In the present study, after 7 days of the experiment, heat shock proteins (HSP) were repressed in the warming and La exposed treatments, in comparison to the warming treatment. Additionally, La exposure in an acidification setting constrained HSP expression, in comparison to La exposure alone. This highlights that La exposure will trigger a particularly deleterious outcome in a climate change scenario. This HSP pattern also suggests that although the superfamily GST was activated, it was insufficient to detoxify La.

Ubiquitin (Ub) sustains cellular homeostasis as it targets damaged proteins for degradation. When HSP fail to maintain optimal protein conformation, ubiquitin targets

damaged protein and removes them (Sørensen et al., 2003). In this study, a very peculiar Ub pattern was observed, as clams exposed to warming, high CO_2, and La exhibited much higher Ub levels than the ones exposed to warming and La. On another hand, clams exposed to warming and La showed significantly lower Ub levels than the ones kept in the warming treatment. Pousse et al. (2020) studied the energetic response of the surfclam *Spisula solidissima* to ocean acidification resulting in increased metabolic loss and suggesting a rise in energy expenditure under an acidified medium. The results emphasize the sensitivity of surf clams to ocean acidification, with some temporary resilience. Furthermore, it is known that protein synthesis is an energetically demanding process and thus ubiquitination can be impaired if organisms enter physiological failure (Araújo et al., 2018). Hence, natural Ub levels could have been altered due to the exposure to warming, La, and high CO_2, together and as single stressors.

When the previously discussed biomarkers fail to balance antioxidant-prooxidant levels, excess ROS cause oxidative damage in the form of, for example, lipid peroxidation. Lipid peroxidation (LPO) is caused by the reaction of ROS with lipids (Sachdeva et al., 2014) and is commonly measured by the content of malondialdehyde. Here, we showed that lipid damage occurred on the 7^{th} day of exposure to climate change alone and was greater in clams exposed to warming and acidification together with La, which highlights the enhanced toxic effects of this REE in near future conditions. Exposure of the mussel *M. galloprovincialis* to two other REE, dysprosium (Dy) (Freitas et al., 2020a) and neodymium (Nd) (Freitas et al., 2020b), for 28 days, resulted in cellular damage and loss of redox balance as a consequence of REE exposure, at a control temperature.

Finally, we observed increased antioxidant capacity in clams exposed to warming, high CO_2, and La. TAC values increased in all La exposed treatments from day one to day 7. This molecule is known as a non-enzymatic complement to the antioxidant system, helping in the prevention of oxidative damage. Nevertheless, here, increased levels of TAC were inadequate to evade lipid damage. Joyner-Matos et al. (2009) performed single- and dual-stressor laboratory experiments (hypoxia, warming, hyposalinity, and combined warming and hyposalinity) on the clam *Mercenaria mercenaria* and showed that there was no relationship between the studied biomarkers

and the effects observed at the whole-organisms level (e.g., survival and burial ability) and therefore we suggest future studies should measure additional outcomes (e.g., behavior, feeding rates, respirometry). This emphasizes the intricacies of climate change consequences on biota and how overwhelming the task of understanding the physiological and biochemical impairments in aquatic organisms of poorly known emergent contaminants in a changing world can be.

8.5 CONCLUSION

To which extend multiple climate change stressors interact with rare earth elements and their impacts on marine organisms was never explored before this experiment. Hence, this study constitutes a valuable source of information on the interactions of ocean warming, ocean acidification, and La in a clam species with a great ecological and economic stance. The findings here described showed *S. solida* capacity to swiftly accumulate La, at present-day conditions and at similar rates in near future conditions. Elimination of La was more effective in a warmer temperature. Lanthanum triggered a biochemical response, however as lipid damage occurred, the oxidative stress response activation was insufficient do detoxify La. Total antioxidant capacity increased in all La exposed treatments from day one to day 7, still inadequately to evade lipid damage. The present results emphasize the toxic effects of La to bivalve species, and their enhanced potential in a changing world with prospective consequences on bivalve species fitness and ultimately survival.

ACKNOWLEDGMENTS

This work was supported by Fundação para a Ciência e Tecnologia (FCT), through the project Climatoxeel (PTDC/AAG-GLO/3795/2014) and the Junior Researcher contract (CEECIND/03517/2017), both awarded to Tiago F. Grilo and the strategic project UID/MAR/04292/2019 granted to MARE and by the Applied Molecular Biosciences Unit UCIBIO financed by national funds from FCT (UIDP/04378/2020 and UIDB/04378/2020). Cátia Figueiredo acknowledges the FCT-PhD grant SFRH/BD/130023/2017 and the Early Career Research Grant awarded by National Geographic Society.

REFERENCES

Akagi, T. and Edanami, K., 2017. Sources of rare earth elements in shells and soft-tissues of bivalves from Tokyo Bay. Marine Chemistry 194, 55-62.

Araújo, J.E., Madeira, D., Vitorino, R., Repolho, T., Rosa, R. Diniz, M., 2018. Negative synergistic impacts of ocean warming and acidification on the survival and proteome of the commercial sea bream, *Sparus aurata*. Journal of sea research 139, 50-61.

Black, B.C., Weisel, G.J., 2010. Global Warming. Santa Barbara, CA: Greenwood.

Bonnail, E., Pérez-López, R., Sarmiento, A.M., Nieto, J.M. and DelValls, T.Á. ,2017. A novel approach for acid mine drainage pollution biomonitoring using rare earth elements bioaccumulated in the freshwater clam *Corbicula fluminea*. Journal of hazardous materials 338, 466-471.

Bradford, M.M., 1976. A rapid and sensitive method for the quantitation of microgram quantities of protein utilizing the principle of protein-dye binding. Analytical biochemistry 72, 248-254.

Braun, H., 1995. The Collected Works of John W. Tukey: Vol. VIII, Multiple Comparisons 1948-1983. Journal of the Royal Statistical Society-Series A Statistics in Society 158, 629.

Das, T., Sharma, A., Talukder, G., 1988. Effects of lanthanum in cellular systems. Biological Trace Element Research 18, 201-228.

Emsley, J. (2011) Nature's building blocks: an AZ guide to the elements, Oxford University Press.

Figueiredo, C., Raimundo, J., Lopes, A.R., Lopes, C., Rosa, N., Brito, P., Diniz, M., Caetano, M., Grilo, T.F., 2020. Warming enhances lanthanum accumulation and toxicity promoting cellular damage in glass eels (*Anguilla anguilla*). Environmental research 191, 110051.

Freitas, R., Cardoso, C.E., Costa, S., Morais, T., Moleiro, P., Lima, A.F., Soares, M., Figueiredo, S., Águeda, T.L., Rocha, P., 2020a. New insights on the impacts of e-waste towards marine bivalves: The case of the rare earth element Dysprosium. Environmental Pollution 260, 113859.

Freitas, R., Costa, S., Cardoso, C.E., Morais, T., Moleiro, P., Matias, A.C., Pereira, A.F., Machado, J., Correia, B., Pinheiro, D., 2020b. Toxicological effects of the rare earth element neodymium in *Mytilus galloprovincialis.* Chemosphere 244, 125457.

González, P.M., Malanga, G., Puntarulo, S., 2015. Cellular oxidant/antioxidant network: update on the environmental effects over marine organisms. The Open Marine Biology Journal 9, 1-13.

Hanana, H., Turcotte, P., Pilote, M., Auclair, J., Gagnon, C., Gagné, F., 2017. Biomarker assessment of lanthanum on a freshwater invertebrate, *Dreissena polymorpha*. SOJ Biochemistry 3, 1-9.

Hazel, J.R., Prosser, C.L., 1974. Molecular mechanisms of temperature compensation in poikilotherms. Physiological reviews 54, 620-677.

Herrmann, H., Nolde, J., Berger, S., Heise, S., 2016. Aquatic ecotoxicity of lanthanum–A review and an attempt to derive water and sediment quality criteria. Ecotoxicology and Environmental Safety 124, 213-238.

Hornstein, J., Espinosa, E.P., Cerrato, R.M., Lwiza, K.M., Allam, B., 2018. The influence of temperature stress on the physiology of the Atlantic surfclam, *Spisula solidissima*. Comparative Biochemistry and Physiology Part A: Molecular & Integrative Physiology 222, 66-73.

IPCC, 2021: Summary for Policymakers. In: Climate Change 2021: The Physical Science Basis. Contribution of Working Group I to the Sixth Assessment Report of the Intergovernmental Panel on Climate Change [Masson-Delmotte, V., P. Zhai, A. Pirani, S.L. Connors, C. Péan, S. Berger, N. Caud, Y. Chen, L. Goldfarb, M.I. Gomis, M. Huang, K. Leitzell, E. Lonnoy, J.B.R. Matthews, T.K. Maycock, T. Waterfield, O. Yelekçi, R. Yu, and B. Zhou (eds.)]. In Press.

Johansson, L.H., Borg, L.H., 1988. A spectrophotometric method for determination of catalase activity in small tissue samples. Analytical biochemistry 174, 331-336.

Joyner-Matos, J., Andrzejewski, J., Briggs, L., Baker, S.M., Downs, C.A., Julian, D., 2009. Assessment of cellular and functional biomarkers in bivalves exposed to ecologically relevant abiotic stressors. Journal of aquatic animal health 21, 104-116.

Khan, A.M., Bakar, N.K.A., Bakar, A.F.A., Ashraf, M.A., 2017. Chemical speciation and bioavailability of rare earth elements (REEs) in the ecosystem: a review. Environmental Science and Pollution Research 24, 22764-22789.

Kulaksız, S., Bau, M., 2011. Rare earth elements in the Rhine River, Germany: first case of anthropogenic lanthanum as a dissolved microcontaminant in the hydrosphere. Environment International 37, 973-979.

Lesser, M.P., 2006. Oxidative stress in marine environments: biochemistry and physiological ecology. Annual Review of Physiology 68, 253-278.

Lopes, A.R., Borges, F.O., Figueiredo, C., Sampaio, E., Diniz, M., Rosa, R., Grilo, T.F., 2019. Transgenerational exposure to ocean acidification induces biochemical distress in a keystone amphipod species (*Gammarus locusta*). Environmental research 170, 168-177.

Lushchak, V.I., 2011. Environmentally induced oxidative stress in aquatic animals. Aquatic toxicology 101, 13-30.

Matozzo, V., Chinellato, A., Munari, M., Bressan, M., Marin, M.G., 2013. Can the combination of decreased pH and increased temperature values induce oxidative stress in the clam *Chamelea gallina* and the mussel *Mytilus galloprovincialis*?. Marine Pollution Bulletin 72, 34-40.

Maulvault, A.L., Camacho, C., Barbosa, V., Alves, R., Anacleto, P., Fogaça, F., Kwadijk, C., Kotterman, M., Cunha, S.C., Fernandes, J.O., 2018. Assessing the effects of seawater temperature and pH on the bioaccumulation of emerging chemical contaminants in marine bivalves. Environmental research 161, 236-247.

McNeil, B.I., Sasse, T.P., 2016. Future ocean hypercapnia driven by anthropogenic amplification of the natural CO_2 cycle. Nature 529, 383-386.

Mesquita, J.R., Vaz, L., Cerqueira, S., Castilho, F., Santos, R., Monteiro, S., Manso, C.F., Romalde, J.L., Nascimento, M.S.J., 2011. Norovirus, hepatitis A virus and enterovirus presence in shellfish from high quality harvesting areas in Portugal. Food Microbiology 28, 936-941.

Pierrot, D., Lewis, E., Wallace, D., 2006. MS Excel program developed for CO2 system calculations. ORNL/CDIAC-105a. Carbon Dioxide Information Analysis Center, Oak Ridge National Laboratory, US Department of Energy, Oak Ridge, Tennessee 10.

Pinto, J., Costa, M., Leite, C., Borges, C., Coppola, F., Henriques, B., Monteiro, R., Russo, T., Di Cosmo, A., Soares, A.M., 2019. Ecotoxicological effects of lanthanum in *Mytilus galloprovincialis*: Biochemical and histopathological impacts. Aquatic toxicology 211, 181-192.

Pousse, E., Poach, M.E., Redman, D.H., Sennefelder, G., White, L.E., Lindsay, J.M., Munroe, D., Hart, D., Hennen, D., Dixon, M.S., 2020. Energetic response of Atlantic surfclam *Spisula solidissima* to ocean acidification. Marine Pollution Bulletin 161, 111740.

Regoli, F., Giuliani, M.E., 2014. Oxidative pathways of chemical toxicity and oxidative stress biomarkers in marine organisms. Marine environmental research 93, 106-117.

Romero-Freire, A., Lassoued, J., Silva, E., Calvo, S., Pérez, F.F., Bejaoui, N., Babarro, J.M. and Cobelo-García, A., 2020. Trace metal accumulation in the commercial mussel *M. galloprovincialis* under future climate change scenarios. Marine Chemistry 224, 103840.

Schmidt, B.H., Dribusch, U., Delport, P.C., Gropp, J.M., van der Staay, F.J., 2012. Tolerability and efficacy of the intestinal phosphate binder Lantharenol® in cats. BMC veterinary research 8, 1-8.

Serra-Compte, A., Maulvault, A.L., Camacho, C., Alvarez-Munoz, D., Barceló, D., Rodriguez-Mozaz, S., Marques, A., 2018. Effects of water warming and acidification on bioconcentration, metabolization and depuration of pharmaceuticals and endocrine disrupting compounds in marine mussels (*Mytilus galloprovincialis*). Environmental pollution 236, 824-834.

Sørensen, J.G., Kristensen, T.N., Loeschcke, V., 2003. The evolutionary and ecological role of heat shock proteins. Ecology letters 6, 1025-1037.

Uchiyama, M., Mihara, M., 1978. Determination of malonaldehyde precursor in tissues by thiobarbituric acid test. Analytical biochemistry 86, 271-278.

Voncken, J.H.L., 2016. The rare earth elements: an introduction, Springer.

Wang, Y.Y., Lu, H.H., Liu, Y.X. and Yang, S.M., 2016. Ammonium citrate-modified biochar: An adsorbent for La (III) ions from aqueous solution. Colloids and Surfaces A: Physicochemical and Engineering Aspects 509, 550-563.

Wang, Z., Yin, L., Xiang, H., Qin, X., Wang, S., 2019. Accumulation patterns and species-specific characteristics of yttrium and rare earth elements (YREEs) in biological matrices from Maluan Bay, China: Implications for biomonitoring. Environmental research 179, 108804.

Zeebe, R.E., Ridgwell, A., 2011. Past changes of ocean carbonate chemistry. Ocean acidification, 1-28.

Chapter 9

Enhanced ecotoxicity of Gadolinium in a warmer and acidified changing ocean using a multibiomarker approach: the case of the surf clam *Spisula solida*

Cátia Figueiredo [a,b,c*], Tiago F. Grilo [a], Rui Oliveira [b], Inês João Ferreira [d], Clara Lopes [b,e], Pedro Brito [b,e], Pedro Ré [a], Miguel Caetano [b,e], Mário Diniz [c,f], Joana Raimundo [b,e]

[a] MARE – Marine and Environmental Sciences Centre, Faculdade de Ciências da Universidade de Lisboa, Campo Grande, 1749-016 Lisboa, Portugal;

[b] Division of Oceanography and Marine Environment, IPMA – Portuguese Institute for Sea and Atmosphere, Av. Alfredo Magalhães Ramalho, 6, 1495-165 Algés, Portugal;

[c] UCIBIO – Applied Molecular Biosciences Unit, Department of Chemistry / Department of Life Sciences, School of Science and Technology, NOVA University Lisbon, 2819-516 Caparica, Portugal

[d] LAQV-REQUIMTE, Chemistry Department, NOVA School of Science and Technology, 2829-516 Caparica, Portugal

[e] CIIMAR – Interdisciplinary Centre of Marine and Environmental Research, Avenida General Norton de Matos S/N, 4450-208 Matosinhos, Portugal;

[f] Associate Laboratory i4HB - Institute for Health and Bioeconomy, School of Science and Technology, NOVA University Lisbon, 2819-516 Caparica, Portugal

* Corresponding author

Figueiredo, C., Grilo, T.F., Oliveira, R., Ferreira, I.J., Gil, F., Lopes, C., Brito, P., Ré, P., Caetano, M., Diniz, M, Raimundo, J., 2022. Enhanced ecotoxicity of Gadolinium in a warmer and acidified changing ocean using a multibiomarker approach: the case of the surf clam *Spisula solida*. Submitted to Science of the Total Environment.

ABSTRACT

Humans have exhaustively exploited natural resources, combusted fossil fuels, and release pollutants into the environment, at continuously faster rates resulting in global average temperatures increase and seawater pH decrease. Furthermore, climate change is forecasted to exacerbate the effects of pollutants such as the emergent rare earth elements. Therefore, the objective of this study was to assess for the first time the combined effects of rising temperature (Δ = +4°C) and decreasing pH (Δ = −0.4 pH units) on the bioaccumulation and elimination of gadolinium (Gd) in the bioindicator bivalve species *Spisula solida.* We exposed surf clams to 10 µg L^{-1} of $GdCl_3$ for seven days, followed by a depuration phase lasting for another seven days and then investigated oxidative stress-related responses after 1, 3 and 7 days of exposure and the elimination phase. Gadolinium accumulated after just one day of exposure with values increasing with exposure time and reaching the highest value at T7. Gadolinium was not proficiently eliminated after 7 days of depuration. Even though no significant differences in Gd concentration were observed between animals exposed to Gd under current conditions, warming, acidification, and warming & acidification conditions, their interaction impacted the clams' biochemical response. Our results showed that Gd was the main driver of the oxidative stress response, however, its impact was exacerbated by warming and acidification. To limit the extent of oxidative stress, the first response was greater in clams exposed to acidification & Gd and warming, acidification & Gd. Ultimately, lipid damage was greater in clams exposed to warming & Gd, which emphasizes the enhanced toxic effects of Gd in a changing ocean.

Keywords: Rare earth elements; Emergent pollutants; Climate change; Oxidative stress; Cellular damage

9.1 INTRODUCTION

Since the late 18th century, humans have exhaustively exploited natural resources, combusted fossil fuels, and release pollutants into the environment, at continuously faster rates. The burning of fossil fuels has led to the emission of greenhouse gases (GHG), which in turn created the known Greenhouse Effect (Field and Barros, 2014). This layer absorbs and traps solar energy, in the form of heat, increasing global average temperatures (Black and Weisel, 2010). An increase of up to 4 to 5°C is expected in coastal areas of the Atlantic Ocean by 2100 (IPCC, 2014; IPCC, 2019). Additionally, the continuous emission of GHG has led to increased CO_2 partial pressure (*p*CO2) oceanic uptake, which in turn leads to average seawater pH decrease at a global scale, in the known Ocean Acidification phenomenon (IPCC, 2014). In a worst-case scenario, at today's rate, by the end of the century, a drop of 0.4 pH units in temperate coastal areas of the Atlantic Ocean is projected to occur (IPCC, 2014; McNeil and Sasse, 2016). Furthermore, climate change is forecasted to exacerbate the effects of pollutants (Maulvault et al. 2018), such as emergent Critical Metals (Figueiredo et al., 2020). The rare earth elements (REE) are a prime example of those and are composed by the 15 chemical elements of the lanthanide group, plus scandium (Sc) and yttrium (Y), as defined by the International Union of Applied and Pure Chemistry (Damhus et al., 2005). These elements show comparable electron configurations, and are present mostly in a +3 valence, while some elements may also be present in different oxidation states, such as +2 and +4. They exhibit physical and chemical characteristics that allow their usage in a wide array of modern technologies, such as the manufacture of batteries, lasers, optics, magnets, superconductors, and several other applications in the chemical and medical industries. This highlights their role in the functioning of the world's economy (Gonzalez et al. 2014). Among the elements used in medical applications lies gadolinium (Gd). Gadolinium is widely used as a contrast agent in magnetic resonance imaging (MRI). Here, this element must be applied complexed with organic ligands that shield the known toxic effects of the Gd^{3+} ion (Pagano et al., 2015). As a free ion, Gd^{3+} hinders biological processes by interfering with Ca^{2+} channels (Caravan et al., 1999). The Gd-contrast shows a brief human body residence and is swiftly released through sewage. Gadolinium is not efficiently removed in wastewater treatment plant processes (Rabiet

et al., 2009) and is therefore discharged into the environment. This input of anthropogenic Gd occurs mainly in fresh and coastal bodies of water and although Gd is applied as a complexed contrast agent, both the contrast and the free ion are known to be accumulated by bivalves and other aquatic organisms (Lingott et al., 2016; Perrat et al., 2017).

The benthic filter-feeding bivalves are key organisms in coastal ecosystems, while also being important food sources to several species and humans. Bivalves inhabit coastal regions that are particularly vulnerable to both acidification and thermal stress, and both are known to impose negative impacts on these commercially important species such as slowed growth, increased metabolism, and mortality (Stevens and Gobler, 2018). The sand-burrowing surf clam (*Spisula solida*) is found in the continental shelf of the Eastern North Atlantic coastal waters, from Iceland to Portugal, and was chosen as the biological model due to its known ability to bioaccumulate a wide array of pollutants and susceptibility to climate change (e.g. Mesquita et al., 2011; Pousse et al., 2020).

The study of the environmental hazard linked to Gd has received little attention from the scientific community, so far, and the study of multiple stressors, such as warming, acidification, and their interaction with this emerging pollutant follows the same trend. Therefore, the objective of this study was to assess for the first time the combined effects of rising temperature (Δ = +4°C) and decreasing pH (Δ = −0.4 pH units) on the bioaccumulation and elimination of Gd in the bioindicator bivalve species *S. solida.* Here, we exposed surf clams to 10 µg L^{-1} of $GdCl_3$ for seven days, followed by an elimination phase that lasted another seven days. Furthermore, we investigated oxidative stress-related responses. Specifically, we measured some biomarkers, such as lipid peroxidation (LIPO), total antioxidant capacity (TAC), oxidative stress enzymes (SOD, CAT, GPx, GST), and chaperoning (HSP) and ubiquitin-proteasome system mechanisms (Ub).

9.2 MATERIAL AND METHODS

9.2.1 Organisms collection

Clams were collected by dredging in Comporta (Setubal, Portugal, North Atlantic, SW Europe) in April 2021 and transported to the aquaculture facilities of *Aquarium*

Vasco da Gama, in Lisbon. Specimens were kept in constantly aerated water and in stable conditions, mimicking their natural environment. Organisms were depurated under the following physicochemical parameters: 12h light/12h dark photoperiod, salinity= 35±0.1 PSU (V2 refractometer, TMC Iberia), water temperature = 15.2±0.1 °C (TFX 430 Precision Thermometer, WTW GmbH) and pH 8.02 ± 0.05 (SG8 e SevenGo pro™ pH/Ion meter, Mettler-Toledo International Inc), for seven days.

9.2.2 Warming, Gd and CO_2 exposure

Individuals (n=8 per treatment and sampling time) were randomly distributed in tanks illustrative of eight treatments: i) Control (15.1°C, pH=8.01); ii) Acidification (15.1°C, pH=7.59); iii) Gd (15.1°C, pH=8.09, added Gd=10 µg L^{-1}); iv) Acidification & Gd (15.2°C, pH=7.62, added Gd=10 µg L^{-1}); v) Warming (19.1°C, pH=8.03); vi) Warming & Gd (19.3°C, pH=8.08, added Gd=10 µg L^{-1}); vii) Warming & acidification (19.2°C, pH=7.61); viii) Warming, acidification & Gd (19.2°C, pH=7.63, added Gd=10 µg L^{-1}). In the warming and acidification treatments, the temperature was raised 1°C, and the pH was reduced by 0.1, respectively, per day, before the beginning of the trial, to gradually acclimate the clams to the experimental conditions. The Gd exposure concentration was selected to like other Gd exposure trials with bioindicator bivalve species (e.g., Hanana et al., 2017; Henriques et al., 2019; Perrat et al., 2017).

The water temperature was maintained with access to a water bath controlled by heaters (V_2Therm 200 W aquarium heater, TMC) and chillers (Hailea, HC-250 A). The pH was routinely controlled by a Profilux 3.1T (GHL) system and pH probes (GHL), which measured pH every 2 seconds. Upregulation was done with filtered air, via an air compressor (Hailea, ACO 328) and downregulation with CO_2 injection, via electric solenoid valves (Etopi). To obtain the most stable pH values, hysteresis was kept at the lowest possible (0.05 units of pH).

Water was renewed every other day, at the same time, and a Gd solution ($GdCl_3$, Merck), prepared in filtered ultra-pure water (18.2 MΩ, Sartorius), was afterwards spiked in the exposed treatments. Specimens were fed green and brown marine phytoplankton (Reef Phytoplankton™, Seachem), *ad libitum,* every other day.

Clams were sampled before the beginning of the test (T0) and after 1 (T1), 3 (T3), and 7 (T7) days. Subsequently to this exposure period, clams were kept in renewed water and the elimination phase began, which lasted 7 days (T14).

Total alkalinity was measured (Alkalinity checkers, Hanna® Instruments) and the carbonate system speciation was calculated (CO2SYS software, Pierrot et al. 2006).

9.2.3 Gadolinium quantification

Clam samples (n=5) were freeze-dried, grounded, and homogenized before being digested with HNO_3 (distilled, 65% v/v) and H_2O_2 (suprapur, 30% v/v) in labware that had been previously decontaminated with HNO_3 (20%) and cleaned with ultra-pure water (Milli-Q water - 18.2 MΩ).

Gadolinium concentrations were determined in a quadrupole ICP-MS (NexION 2000) equipped with a concentric Meinhard nebulizer, a cyclonic spray chamber and a dual detector (Figueiredo et al., 2020).

Three procedural blanks, a quality control solution, and the certified reference material BCR 668 (muscle of *Mytilus edulis*) were run within every 20 samples. Gadolinium concentrations are shown in microgram per gram of tissue dry weight ($\mu g\ g^{-1}$, dw).

9.2.4 Biomarkers

Three clams per treatment were homogenized (Ultra-Turrax, Staufen), in 3 mL of PBS (phosphate-buffered saline solution: 0.14 M NaCl, 2.7 mM KCl, 8.1 mM Na_2HPO_4 and 1.47 mM KH_2PO_4, pH 7.4), centrifuged (10.000 x g for 15 min at 4 °C) and frozen (-80 °C) until further analyses. The 3 samples were run in duplicates. Results were normalized to total protein concentration (Bradford, 1976).

9.2.4.1 Lipid peroxidation

As an indicator of cellular damage, LIPO was ascertained by the quantification of malondialdehyde (MDA) according to Uchiyama and Mihara (1978). Briefly, 5 µL of the homogenized and centrifuged sample, 45 µL of monobasic sodium phosphate buffer (50 mM), 12.5 µL of sodium dodecyl sulfate (8.1%), 93.5 µL of trichloroacetic acid (20%, pH 3.5), 93.5 µL of thiobarbituric acid (1%), and 50.5 µL of Milli-Q ultrapure water were placed in a microtube that was positioned in 100 °C water bath for 10 min. After chilling in ice until room temperature, 62.5 µL of Milli-Q ultrapure water was added. Finally, 150 µL of the microtube content was added to 96-well microplates (Greiner Bio-one,

Germany). The absorbance was read at 532 nm (Biotek Synergy HTX multi-mode reader, USA). Malondialdehyde (MDA) was determined using a calibration curve (0 - 0.3 µM MDA).

9.2.4.2 Total antioxidant capacity

Total antioxidant capacity was ascertained agreeing to Kambayashi et al. (2009). Each homogenized and centrifuged sample (10 µL) and 10 µL of myoglobin (90 µM), 150 µL of 2,2'-azino-bis (3-ethylbenzothiazoline-6-sulphonic acid, 600 µM) and 40 µL of hydrogen peroxide (500 µM) were comprised in a microplate that was incubated at room temperature for 5 min. The absorbance was read at 410 nm (Biotek Synergy HTX multi-mode reader, USA). The TAC was computed from a calibration curve, based on a series of Trolox (0 – 0.3 Mm).

9.2.4.3 Oxidative stress enzymes

Superoxide dismutase

Superoxide dismutase inhibition was established through an adjustment of the method described by McCord and Fridovich (1969). Samples (10 µL) and 180 µL of a reaction mix (deionized ultrapure water, 50 mM potassium phosphate, 0.1 mM ethylenediaminetetraacetic acid, 0.01 mM cytochrome c and 0.05 mM xanthine) were included in a 96-well microplate. Then, 10 µL of xanthine oxidase (0.005 units) were added to initiate the reaction. The absorbance was read at 550 nm (Biotek Synergy HTX multi-mode reader, USA).

Catalase

Catalase activity was determined based on Johansson and Borg (1988). Briefly, 20 µl of the sample, 100 µl of potassium phosphate, and 30 µl of methanol were added to a microplate. The microplate was then shaken and incubated at room temperature for 20 minutes. Later, 30 µl of potassium hydroxide (10 M KOH) and 30 µl of purpald reagent (34.2 mM in 0.5 M HCl) were included in each well, agitated, and incubated for another 10 minutes. Successively, 10 µl of potassium periodate (65.2 mM in 0.5 M KOH) was added to the wells and incubated for 5 minutes. The absorbance was read at 540 nm (Biotek Synergy HTX multi-mode reader, USA). As one unit of catalase is defined as the amount that will cause the formation of 1.0 nmol of formaldehyde per minute at 25

°C, formaldehyde concentration was calculated based on a calibration curve (from 0 to 75 µM formaldehyde) to assess CAT activity.

Glutathione peroxidase

Glutathione peroxidase was measured corresponding to Lawrence and Burk (1976). Sample (20 µL), 50 mM phosphate buffer (pH 7.6), co-substrate mixture (0.8 Mm β-NADPH, 4 mM Glutathione, 4 U/mL glutathione reductase, and 4 mM sodium azide) and 15 mM cumene hydroperoxide ($C_9H_{12}O_2$) were added to a microplate, and the absorbance was read at 340 nm (Biotek Synergy HTX multi-mode reader, USA), every minute for 6 min. The GPx activity was determined using the β-NADPH coefficient extinction.

Glutathione S-transferase

Glutathione S-transferase was determined according to Lopes et al. (2019). A substrate solution (200 mM L-glutathione reduced, Dulbecco's PBS plus 100 mM CDNB solution) was added to a Nunclon microplate (Thermo Scientific Nunc, USA), with either 20 µL of GST standard or sample. The GST activity was read spectrophotometrically at 340 nm, every minute for 6 minutes, using a plate reader (Biotek Synergy HTX multi-mode reader, USA). The reaction rate was calculated using the CDNB extinction coefficient (εµM) of 0.0053 ($\mu M^{-1}\ cm^{-1}$).

9.2.4.4 Chaperoning and ubiquitin-proteasome system mechanisms

Heat shock proteins

Heat Shock Protein 70 was quantified through ELISA, as described in (Lopes et al., 2019). Ten µL of homogenate sample diluted in 980 µL PBS was added to each well of a microplate (Microlon 600, Greiner, Bio-One, Germany) and incubated overnight at 4 °C. Microplates were washed with PBS TWEEN-20 (0.05%) three times and incubated for 90 min at 37 °C after 100 µL of BSA (1% bovine serum albumin, NZYtech, 98%, Portugal) was added. Fifty µL of primary antibody 5 µg mL^{-1} of anti-HSP70/HSC70 in 1% BSA (OriGene, USA) was added, and microplates were incubated overnight at 4 °C. Microplates were incubated for 90 min at 37 °C with the second antibody [50 µL of 1 µg mL^{-1}; alkaline phosphatase-conjugated anti-mouse IgG (Fc specific, Sigma-Aldrich, USA)], after being washed three times. After, 100 µL of the substrate (SIGMA FASTTM p-Nitrophenyl Phosphate Tablets, Sigma-Aldrich, USA) was added and incubated for 30

min at room temperature. Finally, 50 µL of stop solution (3 M NaOH) was added. The absorbances were read at 405 nm (Biotek Synergy HTX multi-mode reader, USA). HSP content was calculated from a calibration curve, of purified HSP70 active protein (0 - 2.000 µg mL^{-1}, OriGene Technology, USA) dilutions.

Total ubiquitin

Ubiquitin content was measured through ELISA, according to Lopes et al. (2019). Briefly, 100 µL of the sample was added to 96-well microplates (Microloan 600, Greiner, Bio-One, Germany) and incubated overnight at 4 °C. Microplates were then washed with PBS-TWEEN three times. Afterwards, 100 µL of blocking solution [1% bovine serum albumin (BSA)] was added and microplates were incubated for 90 min at 37 °C. Later, 50 µL of primary antibody (200 µg mL^{-1}; P4D1, sc-8017, HRP conjugate, Santa Cruz, USA) was included, and after overnight incubation (4 °C), microplates were washed three times. Subsequently, 100 µL of TMB/E substrate (Temecula California, Merck Millipore) was added and the microplates were incubated for 30 min at room temperature. Lastly, 100 µL of stop solution (1 M HCL) was added. Absorbances were read at 415 nm, using a microplate reader (Biotek Synergy HTX multi-mode reader, USA).

The Ub content was calculated using a dilution of purified ubiquitin (0 - 1 µg $mL^{-1,}$ UbpBio, E-1100, USA).

9.2.5 Statistical analyses

A one-way ANOVA was utilized to explore significant variations in Gd concentration and biomarkers activity between the eight experimental treatments at each sampling time. To investigate differences of Gd accumulation and biomarkers values between sampling times, for each exposure treatment, a one-way ANOVA was applied. Whenever an ANOVA table proved to be significant, all pairwise comparisons using Tukey's procedure (Braun, 1995) were carried out. When needed data were Log_{10} transformed to conform with the assumptions of normality. Statistical analyses were performed in InVivoStat, version 4.1 at a significance level of 0.05.

9.3 RESULTS

A summary of the water physicochemical and carbonate system-specific parameters are presented in Table 9.1.

Table 9.1 – Summary of physicochemical water parameters and carbonate system specifics. Temperature, pH and total alkalinity measured values were used to calculate pCO_2 (carbon dioxide partial pressure). Values represent mean ± standard deviation.

Treatment	Temperature (°C)	Salinity	pH	Total Alkalinity (µmol kg^{-1} SW)	pCO_2 (µatm)
Control	15.1 ± 0.2	35 ± 0.1	8.01 ± 0.10	1928 ± 109	367 ± 67
Acidification	15.1 ± 0.3	35 ± 0.1	7.59 ± 0.10	1643 ± 64	893 ± 73
Gd exposed	15.1 ± 0.2	35 ± 0.1	8.09 ± 0.04	2536 ± 43	372 ± 28
Acidification & Gd	15.2 ± 0.1	35 ± 0.1	7.62 ± 0.09	1769 ± 108	894 ± 35
Warming	19.1 ± 0.2	35 ± 0.1	8.03 ± 0.06	2307 ± 102	442 ± 65
Warming & acidification	19.2 ± 0.3	35 ± 0.1	7.61 ± 0.14	1550 ± 83	812 ± 22
Warming & Gd	19.3 ± 0.1	35 ± 0.1	8.08 ± 0.04	2206 ± 69	338 ± 38
Warming, acidification & Gd	19.2 ± 0.2	35 ± 0.1	7.63 ± 0.10	1671 ± 95	834 ± 28

9.3.1 Gadolinium accumulation and clearance

Concentrations of Gd (µg g^{-1}, dry weight) in spiked treatments are represented in Figure 9.1. Median, minimum, and maximum Gd concentrations (µg g^{-1}, dry weight), in the whole clam's soft body, are featured in Table 9.2 and described below.

Table 9.2 - Median and ranges of Gd concentration (µg g^{-1}, dry weight) in the clams' whole soft body exposed to control; acidification; Gd; acidification & Gd; warming; warming & acidification; warming & Gd and warming, acidification & Gd at T0, T1, T3, T7 and T14. The detection limit was 0.025 µg g^{-1}, dw.

	[Gd] (µg g^{-1} dry weight)				
Treatments	**T0**	**T1**	**T3**	**T7**	**T14**
Control	0.066 (0.046 - 0.10)	0.098 (0.091 - 0.11)	0.090 (0.031 - 0.095)	0.099 (0.095 - 0.10)	0.085 (0.070 - 0.098)
Acidification	0.070 (0.036 - 0.089)	0.095 (0.079 - 0.13)	0.086 (0.073 - 0.095)	0.11 (0.10 + 0.12)	0.088 (0.063 - 0.161)
Gd		1.1 (0.84 - 1.2)	2.6 (1.2 - 3.8)	2.7 (2.6 - 2.7)	2.1 (1.4 - 2.9)
Acidification & Gd		1.5 (1.2 - 2.7)	2.5 (1.6 - 4.9)	4.1 (3.2 - 4.9)	2.8 (1.1 - 3.3)
Warming	0.076 (0.063 - 0.084)	0.069 (0.029 - 0.11)	0.13 (0.11 - 0.16)	0.13 (0.048 - 0.19)	0.17 (0.14 - 0.18)
Warming & acidification	0.078 (0.076 - 0.088)	0.076 (0.046 - 0.11)	0.066 (0.026 - 0.12)	0.21 (0.18 – 0.21)	0.16 (0.092 - 0.19)
Warming & Gd		1.7 (1.2 - 2.3)	2.6 (1.4 + 3.8)	3.8 (2.7 - 6.5)	1.9 (1.4 - 3.0)
Warming, acidification & Gd		1.7 (1.4 - 3.1)	2.8 (2.4 - 2.9)	3.0 (2.5 - 3.4)	2.0 (1.1 - 2.4)

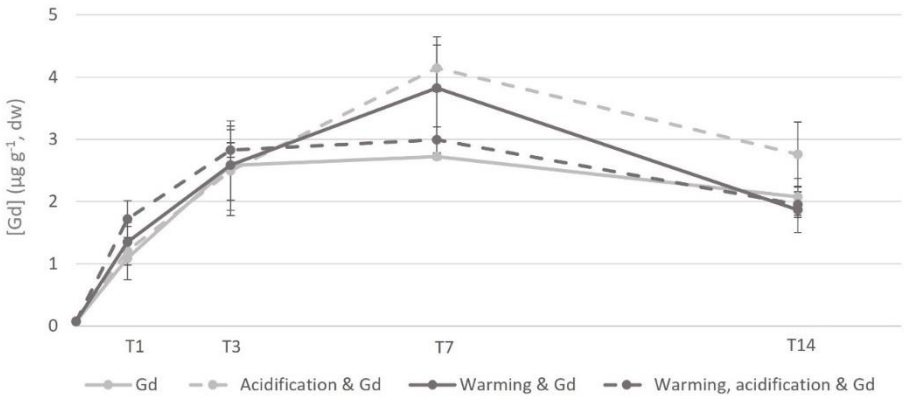

Figure 9.1 – Concentrations of Gadolinium (µg g^{-1}, dry weight) in the clams' whole soft body exposed to Gd; acidification & Gd; warming & Gd and warming, acidification & Gd in the different sampling times (T1, T3, T7 and T14). Values correspond to medians ± SE.

Just before the beginning of the trial, Gd concentrations varied between 0.066 μg g^{-1} in the Control temperature and pH treatment and 0.078 μg g^{-1} in the Warming and acidification treatment. These represent baseline concentrations of Gd in non-exposed clams and, in fact, throughout the experiment, the Gd concentrations in clams from non-exposed treatments remained stable and did not show significant differences among them ($p>0.05$, Table 9.1, Annex 8, Supplemental Table 9.1 A). At one day of exposure (T1), Gd accumulation occurred in all four Gd exposure treatments (Annex 8, Supplemental Table 9.1 A). Clams from the Gd exposed treatment presented a median±SE concentration of 1.1±0.11 μg g^{-1}, while those exposed at a lower pH (acidification & Gd) presented 1.5±0.46 μg g-1 of Gd. At a simulated warming scenario, Gd exposed clams accumulated 1.7±0.25 μg g^{-1}, independently of pH. After 3 days of exposure (T3) the highest accumulation value occurred in the clams exposed to Warming, acidification & Gd (2.8±0.12 μg g^{-1}) followed by the clams exposed to Warming & Gd and just Gd, both showcasing 2.6±0.72 and 2.6±0.56 μg g^{-1}, respectively. The clams exposed to Acidification & Gd, at a present-day temperature, presented Gd concentrations of 2.5±0.72 μg g^{-1}. The highest accumulation values were observed after 7 days. At T7, the highest accumulation value occurred in clams from the Acidification & Gd treatment (4.1±0.37 μg g^{-1}). The second highest Gd accumulation was detected in the Warming & Gd treatment (3.8±0.82 μg g^{-1}). Intriguingly, surf clams exposed to Gd, at a present-day temperature and pH, and exposed to Warming, acidification & Gd presented similar Gd concentrations (2.7±0.051 and 3.0±0.21 μg g^{-1}, respectively). After a 7-day elimination period (T14), the previously accumulated Gd values did not diminish to control-like values. All the Gd exposure treatments remained statistically different from their control counterparts ($p<0.0001$) and presented values similar to the ones sampled at T3. At T14, the highest Gd concentration was exhibited by clams previously exposed to Acidification & Gd (2.8±0.51 μg g^{-1}), followed by the ones exposed to Gd alone (2.1±0.30 μg g^{-1}). In the Warming, acidification & Gd treatment a concentration of 2.0±0.21 μg g^{-1} was observed.

Overall, we did not observe significant differences between the Gd exposed treatments, at each sampling time ($p>0.05$, Annex 8, Supplemental Table 9.1 A). For the Gd exposed clams, at control temperature and pH, the Gd concentrations were

significantly different between T1 and T7 (p=0.047, Annex 8, Supplemental Table 9.1 B). In the Warming & Gd exposed treatment, the Gd concentrations were significantly different between T1 and T7 (p=0.041), but also T7 and T14 (p=0.042). The Gd concentrations in the clams exposed to Warming, acidification & Gd were only different between T7 and T14 (p=0.041). In the Acidification & Gd treatment the Gd concentration did not vary significantly through time (p>0.05, Annex 8, Supplemental Table 9.1 B).

9.3.2 Biochemical responses

Mean ± standard deviation values of biochemical outputs in *Spisula solida'* soft body are presented in Table 9.3.

9.3.2.1 Lipid peroxidation

Before the 7th day of exposure, no significant differences between the LIPO levels of clams exposed to the different experimental treatments were found (Figure 9.2a). At T7 the effects of temperature on lipid peroxidation levels were highlighted as the control and the acidification treatments proved to be significantly different than the Warming and Warming & Gd and Warming & acidification (Annex 8, Supplemental Table 9.2 B). At T14, these differences were not upheld as no significant differences occurred between treatments.

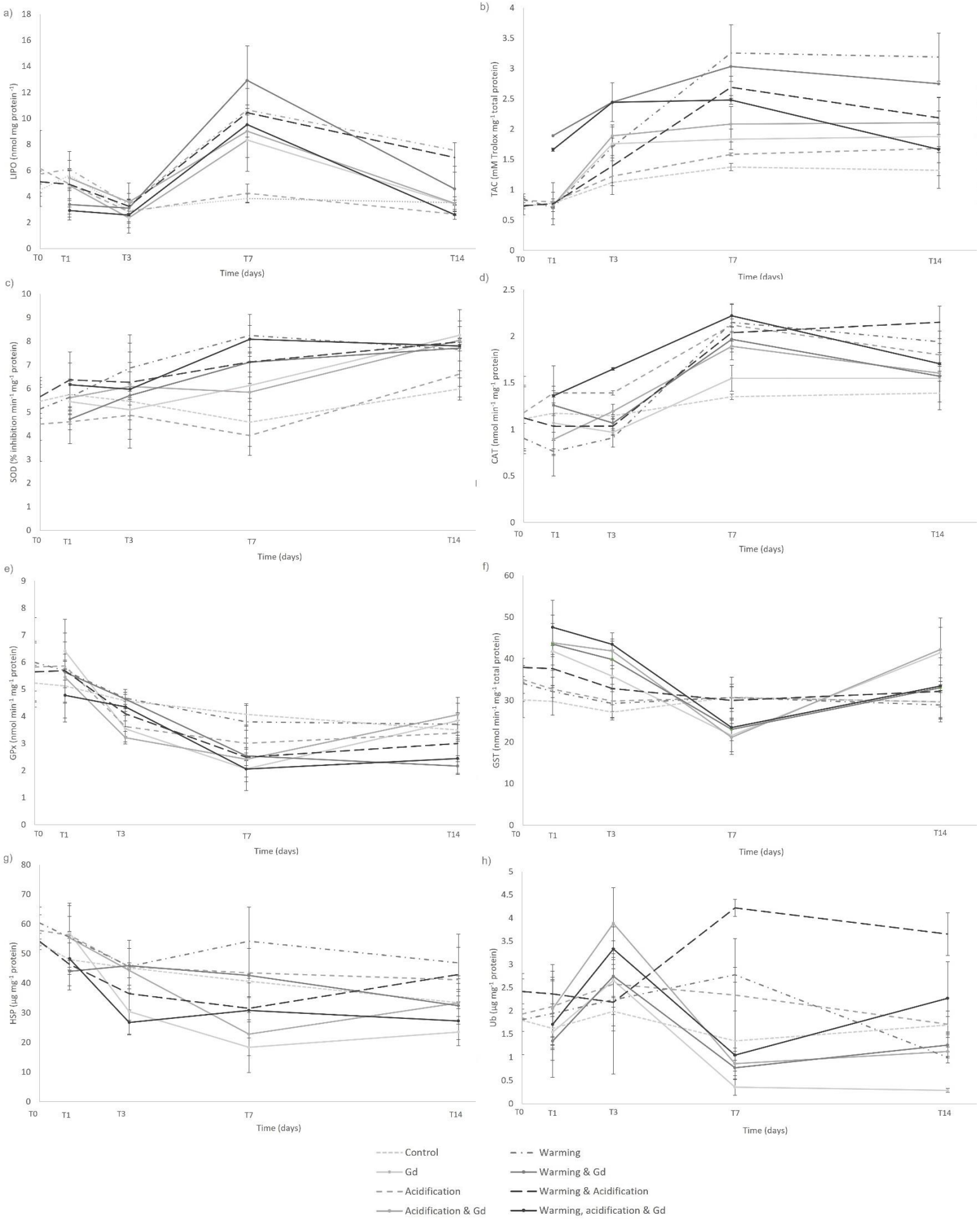

Figure 9.2 – Mean ± SD values of a) Lipid peroxidation (LIPO, nmol mg protein $^{-1}$); b) total antioxidant capacity (TAC, mM Trolox mg^{-1} total protein); c) Superoxide dismutase (SOD, % inhibition min^{-1} mg^{-1} protein); d) Catalase (CAT, nmol min^{-1} mg^{-1} protein); e) Glutathione peroxidase (GPx, nmol min^{-1} mg^{-1} protein); f) Glutathione S-transferase (GST, nmol min^{-1} mg^{-1} total protein); g) Heat Shock Protein 70 (HSP, µg mg^{-1} protein) and h) Ubiquitin (Ub, µg mg^{-1} protein) in *Spisula solida*' soft body.

Table 9.3 - Mean ± standard deviation values in *Spisula solida*' soft body at T0, T1, T3, T7 and T14 of Lipid peroxidation (LIPO, nmol mg protein $^{-1}$); total antioxidant capacity (TAC, mM Trolox mg^{-1} total protein); Superoxide dismutase (SOD, % inhibition min^{-1} mg^{-1} protein); Catalase (CAT, nmol min^{-1} mg^{-1} protein); Glutathione peroxidase (GPx, nmol min^{-1} mg^{-1} protein); Glutathione S-transferase (GST, nmol min^{-1} mg^{-1} total protein) Heat Shock Protein 70 (HSP, µg mg^{-1} protein) and Ubiquitin (Ub, µg mg^{-1} protein).

		LIPO (nmol mg protein $^{-1}$)	TAC (mM Trolox mg^{-1} total protein)	SOD (% inhibition min^{-1} mg^{-1} protein)	CAT (nmol min^{-1} mg^{-1} protein)	GPx (nmol min^{-1} mg^{-1} protein	GST (nmol min^{-1} mg^{-1} total protein)	HSP (µg mg^{-1} protein)	Ub (µg mg^{-1} protein)
T0	Control	4.5±0.47	0.73±0.050	5.5±0.71	1.1±0.34	5.2±0.65	30±4.3	54±4.8	1.8±0.24
	Acidification	6.2±2.9	0.83±0.11	4.5±1.6	1.2±0.39	5.8±0.89	35±3.3	58±5.3	1.9±0.87
	Warming	5.7±0.74	0.84±0.010	5.1±1.3	0.90±0.16	6.0±1.65	34±4.3	60±5.4	1.8±0.030
	Warming & acidification	5.1±0.83	0.74±0.15	5.6±0.69	1.1±0.35	5.6±1.12	38±2.2	54±2.7	2.4±0.27
T1	Control	5.6±1.2	0.78±0.070	5.7±0.66	1.2±0.29	5.1±1.2	30±3.3	48±5.6	1.6±1.1
	Gd	4.8±1.1	0.74±0.22	5.4±0.95	1.1±0.10	6.4±0.68	42±1.3	57±9.3	1.5±0.61
	Acidification	4.9±2.5	0.80±0.010	4.6±0.34	1.4±0.020	5.9±0.21	33±2.9	56±11	2.1±0.90
	Acidification & Gd	5.4±0.73	0.74±0.04	5.6±0.71	0.90±0.39	5.4±0.32	44±6.7	55±1.7	2.0±0.60
	Warming	6.1±1.7	0.71±0.070	5.6±0.58	0.80±0.03	5.7±0.34	32±1.4	56±7.1	1.9±0.78
	Warming & Gd	3.4±1.2	1.9±0.27	4.7±1.0	1.3±0.11	5.6±1.1	43±5.0	44±0.40	1.3±0.080
	Warming & acidification	4.9±1.1	0.77±0.35	6.4±1.2	1.0±0.31	5.7±1.9	38±4.0	46±8.7	2.4±0.49
	Warming, acidification & Gd	2.9±0.27	1.7±0.030	6.2±0.92	1.4±0.32	4.8±0.28	48±6.5	48±9.2	1.7±0.45
T3	Control	2.9±0.88	1.1±0.0001	5.5±0.15	1.1±0.040	4.6±0.24	27±1.9	45±9.3	2.0±1.4
	Gd exposed	2.4±0.77	1.8±0.28	5.1±0.43	1.0±0.020	3.5±0.29	36±3.7	30±7.7	2.7±0.35
	Acidification	2.8±0.89	1.2±0.30	4.9±1.0	1.4±0.020	3.6±0.56	30±4.1	46±6.2	2.6±0.65
	Acidification & Gd	3.6±0.68	1.9±0.18	6.1±0.61	1.2±0.080	3.2±0.23	42±4.3	44±2.5	3.9±0.77
	Warming	3.4±0.47	1.7±0.15	6.9±0.68	0.90±0.10	4.7±0.22	29±3.4	46±8.9	2.2±0.67
	Warming & Gd	3.1±1.9	2.4±0.18	5.7±2.2	1.1±0.090	4.6±0.36	40±4.4	46±0.90	2.7±1.1
	Warming & acidification	3.3±0.53	1.4±0.33	6.3±2.0	1.0±0.10	4.1±0.46	33±5.5	37±8.9	2.2±0.10
	Warming, acidification & Gd	2.6±0.080	2.4±0.32	6±1.1	1.6±0.020	4.4±0.32	43±1.3	27±4.2	3.3±0.18
T7	Control	3.8±0.33	1.4±0.060	4.6±1.0	1.4±0.030	4.1±0.40	31±2.6	41±7.4	1.4±0.65
	Gd exposed	8.3±2.4	1.8±0.17	6.1±1.0	1.5±0.14	2.1±0.30	22±3.9	18±8.5	0.40±0.17
	Acidification	4.2±0.71	1.6±0.020	4.0±0.84	2.1±0.070	3.0±0.63	31±3.3	44±8.3	2.3±1.2
	Acidification & Gd	9.0±2.0	2.1±0.29	5.8±0.39	1.9±0.14	2.4±0.23	21±4.1	23±7.3	0.90±0.34
	Warming	12±2.3	3.3±0.47	8.2±0.89	2.1±0.20	3.8±0.61	31±2.6	54±12	2.8±0.16
	Warming & Gd	13±2.7	3.0±0.74	7.1±0.63	2.0±0.14	2.5±0.95	23±2.7	43±0.50	0.80±0.17
	Warming & acidification	14±3.4	2.7±0.18	7.1±0.43	2.0±0.17	2.5±0.31	30±5.5	32±3.9	4.2±0.19
	Warming, acidification & Gd	9.5±0.97	2.5±0.080	8.1±0.58	2.2±0.12	2.1±0.80	24±2.3	31±9.3	1.0±0.010
T14	Control	3.5±0.20	1.3±0.30	6.0±0.47	1.4±0.18	3.5±0.36	30±4.8	33±4.9	1.7±0.18
	Gd	3.4±0.56	1.9±0.64	8.3±0.37	1.5±0.26	3.8±0.64	41±6.0	24±2.6	0.3±0.040
	Acidification	2.6±0.38	1.7±0.23	6.6±0.97	1.8±0.12	3.4±0.31	30±4.1	41±1.3	1.7±0.28
	Acidification & Gd	3.5±0.10	2.1±0.42	8.0±0.060	1.6±0.020	4.1±0.64	42±7.6	33±4.5	1.1±0.10
	Warming	7.6±0.38	3.2±0.40	7.7±0.49	1.9±0.11	3.7±0.40	29±3.4	47±9.7	1.0±0.12
	Warming & Gd	4.6±1.8	2.8±0.68	7.7±1.6	1.6±0.050	2.2±0.27	33±7.2	32±9.0	1.3±0.28
	Warming & acidification	7.0±1.1	2.2±0.11	8.0±0.020	2.2±0.17	3.0±1.1	32±0.30	43±9.2	3.7±0.46
	Warming, acidification & Gd	2.6±0.070	1.7±0.050	7.8±1.1	1.7±0.010	2.4±0.11	33±5.1	27±8.4	2.3±0.79

Lipid peroxidation values on the Gd exposed treatment decreased from T1 to T3 (p=0.0401), increased from T3 to T7 (p=0.0041), and decreased again from T7 to T14 (p=0.0284, Annex 8, Supplemental Table 9.2 B). From T3 to T7, LIPO values were raised in all four Gd exposure treatments. From T1 to T7 the LIPO values varied significantly in the Warming & Gd and Warming, acidification & Gd treatment (p=0.0452 and p=<0.0001, respectively). Finally, from the end of the exposure phase (T7) until the end of the elimination phase (T14), LIPO varied in all Gd exposure treatments, except for the Warming & Gd (p=0.113).

9.3.2.2 Total antioxidant capacity

One day of exposure (T1) was enough to trigger significant differences between TAC levels of clams from the Warming treatment and the Warming & Gd (p=0.0455, Annex 8, Supplemental table 9.2 A, Figure 9.2b). Total antioxidant capacity levels were also higher in the Warming & Gd treatment in comparison to the Warming & acidification (p=0.0302). Overall, the treatments exposed to Gd exhibited higher TAC levels. On T3, although a global effect was shown (p=0.358, Annex 8, Supplemental Table 9.2 A), non-significant post-hoc effects occurred. At T7, only clams exposed to the warming treatment showed significantly higher TAC levels than the control (p=0.0375). After the elimination phase (T14), no significant differences were found between treatments.

Total antioxidant capacity changed through time in the Acidification & Gd and Warming, acidification & Gd treatments (Annex 8, Supplemental Table 9.2 B). The first varied from T1 to T3 (p=0.0077), T1 to T7 (p=0.0054) and from T1 to T14 (p=0.0052). The second treatment varied from T1 to T3 (p=0.0082) and from T1 to T7 (p=0.0099).

9.3.2.3 Oxidative stress enzymes

Superoxide dismutase

It took 7 days of exposure to induce significant differences in SOD levels between treatments (Figure 9.2c). The control clams exhibited significantly lower SOD values than the four treatments at a warming temperature, and the Gd exposure treatment (Annex 8, Supplemental Table 9.2 A). Furthermore, clams kept at the acidification treatment showed lower SOD than those kept at the Acidification & Gd (p=0.0004). On another hand, the Acidification & Gd treatment clams exhibited lower SOD than the

ones exposed to Warming, acidification & Gd (p=0.0026). No SOD level differences were present at T14.

Superoxide dismutase levels varied in clams exposed to Gd and climate change from T1 to T14 (Annex 8, Supplemental Table 9.2 B). Additionally, the SOD values in T1 were significantly lower than the ones in T7, for the Warming & Gd (p=0.0389) and Warming, acidification & Gd treatments (p=0.0121). In the Warming, acidification & Gd the SOD levels were also different between T3 and T7 (p=0.0109) and between T3 and T14 (p=0.0295). Superoxide dismutase values also varied between T3 and T14, and T7 and T14 in clams exposed to Gd and Acidification & Gd.

Catalase

Catalase activity was similar in all experimental treatments at T0 and T1 (Figure 9.2d). At T3, several post-hoc differences of CAT activity between treatments were shown. Noteworthily, the CAT activity was highest in the Warming, acidification & Gd treatment, being significantly different than the activity shown in clams of the Warming & Gd treatment (p=0.0007, Annex 8, Supplemental Table 9.2 A) and the Acidification & Gd (p=0.0089). The effects of Gd on CAT activity were illustrated as clams from this treatment also showcased significantly higher activity levels than the ones maintained in the Warming & acidification treatment (p=0.0004). Finally, the effect of temperature was also shown as clams kept in an acidified environment showed higher CAT activity than those from the Warming & acidification treatment (p=0.0163). At T7, the impacts of climate change on CAT activity were also shown. The controls were significantly different from the acidification (p=0.0008) and warming (p=0.0003) treatments. Both showed higher CAT activity values than their control counterparts. Clams exposed to both warming & Gd showed significantly enhanced CAT activity values than the ones just exposed to Gd (p=0.0463). At T14, the control shows significantly lower levels than the warming (p=0.0182) and the warming & acidification treatment (p=0.0023).

From T1 to T7 and from T3 to T7 CAT activity was significantly enhanced in clams exposed to Gd, Acidification & Gd and Warming & Gd. From T1 to T14, this activity was significantly different in the clams exposed to Gd and Acidification & Gd. Finally, CAT concentrations exhibited at T3 were different than that of T14 in clams from the Gd and Warming & Gd exposure treatments (Annex 8, Supplemental Table 9.2 B).

Glutathione peroxidase

Overall, glutathione peroxidase decreased with time (Figure 9.2e). At T3 clams exposed to Gd presented significantly lower GPx levels than the ones kept in control conditions (p=0.0038, Annex 8, Supplemental Table 9.2 A). At this time, clams exposed to Acidification & Gd exhibited the overall lowest GPx values and these were significantly lower than the levels of clams exposed to Warming, acidification & Gd (p=0.0024). At T7, the control clams showed significantly higher GPx levels than the clams from the four treatments exposed to Gd (i.e., Gd; Acidification & Gd; Warming & Gd; Warming, acidification & Gd). Furthermore, clams kept in a warming environment showed significantly higher GPx values than the ones exposed to Warming, acidification & Gd (p=0.0265). After the elimination phase, GPx values of clams in the treatment previously exposed to Gd showed higher values than the ones exposed to Warming & Gd (T14, p=0.0154).

Glutathione peroxidase levels of T1 and T3 were significantly higher than the ones of T7 and T14 for all four Gd exposure treatments, apart from T3 vs T14 in the Gd exposed one (Annex 8, Supplemental table 9.2 B). Furthermore, GPx levels of the Gd treatment and the Acidification & Gd displayed significant differences between T1 and T3, and T7 and T14.

Glutathione S-transferase

At T0, clams previously acclimated to warming and acidification showed lower GST levels than the control (*p*=0.0219, Figure 9.2f). After just one day of exposure (T1), the four treatments exposed to Gd showed higher GST levels than the control (Annex 8, Supplemental Table 9.2a). Additionally, clams exposed to Warming & acidification presented significantly lower GST levels than those exposed to Warming, acidification & Gd (p=0.0491). At T3, the significant difference between the four Gd exposed treatments and the control was upheld. Clams exposed to acidification showed significantly lower GST levels than those exposed to Acidification & Gd (p=0.0001). Furthermore, clams exposed to Warming & Gd and Warming, acidification & Gd presented enhanced GST levels, in comparison to the ones kept in the Warming treatment (p=0.0098 and p=0.0002, respectively).

An overall decrease of GST levels in the Gd exposed treatments occurred from T3 to T7. In fact, unlike T1 and T3, at T7 the Gd exposed, Acidification & Gd, and Warming & Gd treatments were significantly lower than the control (p=0.0028, p=0.0012, and p=0.0173, respectively). Furthermore, clams exposed to Acidification & Gd showed lower GST values than the ones in the acidification treatment (p=0.0025). Similarly, clams exposed to Warming & Gd presented significantly lower GST values than the clams exposed to Warming (p=0.0192).

Glutathione S transferase levels were significantly different from T1 to T7, from T3 to T7 and from T7 to T14 in all Gd exposure treatments (Annex 8, Supplemental Table 9.2b). Furthermore, GST levels registered at T3 were different than the ones at T7, in the Warming & Gd and Warming, acidification & Gd treatments. Finally, exposure to Warming, acidification & Gd triggered significantly lower GST levels from T3 to T14.

9.3.2.4 Chaperoning and ubiquitin-proteasome system mechanism

Heat Shock Protein

Heat shock proteins expression during the experiment was not linear (Figure 9.2g). A significant lower HSP concentration in clams exposed to Gd than clams exposed to warming was observed at T7 (p=0.0117, Annex 8, Supplemental Table 9.2 A). At T14 the effects of climate change on HSP expression were evident. The Warming and Warming & acidification treatments showed enhanced HSP expression when compared to the control (p=0.0241 and p=0.0444, respectively). Likewise, clams that had been exposed to Warming & acidification had higher HSP levels than those in the acidification treatment (p=0.0021).

Regarding the Acidification & Gd treatment, it was only between T1 and T7 that different HSP expression occurred (p=0.0155, Annex 8, Supplemental Table 9.2 B).

Total Ubiquitin

At T7, the Gd exposed clams showed lower Ub levels than the four non-exposed treatments (i.e., Control; Acidification; Warming; Warming & acidification; Figure 9.2h). Interestingly, the Ub levels of the previously exposed clams to Gd did not recover during the clearance phase and the Ub levels were kept as the lowest in T14, and as significantly different from all the other experimental treatments (Annex 8, Supplemental Table 9.2 A). However, at this time, Ub levels in the Warming & acidification treatment were

significantly greater than in the Warming treatment (p=0.0175, Annex 8, Supplemental Table 9.2 A).

Clams exposed to Gd showed Ub levels significantly different from T1 to T7 (p=0.0075), from T1 to T14 (p=0.0031), from T3 to T7 (p=0.0007), and from T7 to T14 (p=0.0013), with the lowest levels being registered at T14. The values of Ub were also significantly different between T3 and T7 in the Acidification & Gd and Warming, acidification & Gd treatments (p=0.0234 and p=0.0219, Annex 8, Supplemental Table 9.2 B).

9.4 DISCUSSION

The effects of climate change-related variables on surf clams have previously been studied (e.g., Hornstein et al. 2018, Stevens and Gobler 2018). Although, for example, there is evidence of enhanced energy metabolism and filtration rate reduction in clams exposed to warmer temperatures, warming and acidification interacted both antagonistically and synergistically, with unpredicted outcomes from the responses to individual stressors. Above this puzzling information, the assessment of warming and acidification impacts on Gd bioaccumulation, elimination, and ecotoxicity was, before this study, never achieved, which obstructs comparison with the literature.

Bivalves are known to accumulate a wide array of contaminants, including Gd, as their food sources are suctioned across their siphons, in a non-selective filter-feeding process, in both their soft tissues and shells (Akagi and Edanami, 2017). Furthermore, marine and freshwater mussels are known to accumulate Gd under laboratory exposure experiments (Hanana et al., 2017; Henriques et al., 2019; Perrat et al. 2017). Hanana et al. (2017) exposed the freshwater mussel (*Dreissena polymorpha*), for 28 days, to 10 µg L^{-1} Gd, while Henriques et al. (2019) exposed the mussel *Mytilus galloprovincialis* for the same period to increasing concentrations of Gd (0, 15, 30, 60, 120 µg L^{-1}), however, both only evaluated the accumulation at the end of the exposure period. Perrat et al. (2017) exposed the freshwater bivalves *Dreissena rostriformis bugensis* and *Corbicula fluminea* for 7 and 21 days to 1 and 10 µg L^{-1} of Gd, respectively. However, information on the first days of exposure to Gd in bivalve species was not available. Our data showed that Gd accumulation occurred just after one day of exposure (T1), in all Gd exposed

treatments. Overall, the accumulation increased with exposure time and was highest in T7. Our accumulation results are not in agreement with the ones described by Henriques et al. (2019), as the mussels *M. galloprovincialis* exposed to 15 and 30 µg L^{-1} of Gd showed levels below the ICP-MS detection limit (0.38 µg g^{-1} Gd), on the 28th day of exposure. This could be related to an unknown Gd detoxifying mechanism. Accordingly, Figueiredo et al. (2018) described that *Anguilla anguilla* exposed to 120 ng L^{-1} Lanthanum (La) for 7 days, peaked accumulation of this REE on the third day of exposure, and the concentration decreased afterwards, even in a continuously exposed medium. This highlights the importance of understanding the REE accumulation pattern by employing more frequent sampling events within the exposure period. On another hand, the discrepancy in these results could be related to intrinsic species-specific responses to REE. Despite we did not observe any effects of warming and acidification on Gd accumulation and elimination in clams, increased temperature enhanced bioaccumulation of another rare earth element (La) in *Anguilla anguilla* glass eels (Figueiredo et al., 2020). Even though no significant differences in Gd concentration were observed between Gd exposed in present-day, Warming, Acidification, and Warming & acidification conditions, their interaction could nonetheless impact the organism response to the bioaccumulation. Data also showed that during the 7-day elimination period the Gd concentrations did not diminish to control like values (T14). This may be related to the fact that Gd^{3+} is insoluble at physiologic pH, which prompts delayed systemic excretion (reviewed in Ramalho et al., 2016). In the previously discussed articles that studied Gd bioaccumulation on bivalve species, the Gd elimination was not assessed which highpoints the knowledge gap on organisms' capacity to withhold pollution events. Hence, comparison with the literature is hindered and we suggest that further studies on REE bioaccumulation and ecotoxicity, both in present-day and near-future conditions, take this into notice.

The current knowledge on the ecotoxicological outcomes of REE in aquatic biota is very limited and far from being considered conclusive. Bivalves are known to overproduce reactive oxygen species (ROS) in the presence of contaminants (e.g., Renault, 2015). Under control circumstances, the ROS buildup consequences are avoided through a set of antioxidant defense mechanisms, that include SOD, CAT, and GPx. Superoxide dismutase removes O_2 while forming H_2O_2 that is later reduced to H_20

by CAT and GPx (Regoli and Giuliani, 2014). Our data showed that on T7 SOD was greater in Gd exposed clams, than in the control animals. Climate change variables enhanced the Gd impacts on SOD as clams exposed to both Acidification & Gd showed greater values than the ones exposed to acidification, furthermore, clams exposed to Warming, acidification & Gd showed increased levels in comparison to the ones exposed to Acidification & Gd. Moreover, at T3 the highest CAT levels were observed in clams exposed to Warming, acidification & Gd. On T7, synergistic effects of warming and Gd were observed as clams exposed to these stressors showed higher CAT values than clams exposed to Gd. Concerning GPx, values were hindered in Gd exposed treatments at T7, regardless of temperature and pH. Our results showed that Gd is the main driver of this oxidative stress response, however, their impacts may be exacerbated by warming and/or acidification. A significant decrease in GPx values in mussels *M. galloprovincialis* in the presence of Neodynium has been reported (Freitas et al. 2020b). However, this was not observed when the same species was exposed for the same period (28 days) to similar concentrations of Dysprosium (Freitas et al., 2020a), which suggests that bivalve species may display an REE specific oxidative stress response. Accordingly, Andrade et al. (2022) intended to foresee how climate change events would affect Gd accumulation and for that assessed the biochemical modifications in mussels, *M. galloprovincialis*, exposed to 10 µg L^{-1} Gd at different salinities (20, 30 and 40) for 28 days and the authors observed that Gd caused cellular damage at all salinities, but specimens showed distinct approaches under each salinity to limit the extent of oxidative stress.

Glutathione S-transferases (GST) are key in a phase II response by detoxifying ROS and toxic xenobiotics. This enzyme is typically activated under stress conditions to prevent subsequent deleterious effects caused by the toxic substances' buildup. In the first days of exposure (T1 and T3), clams exposed to Gd in present-day and near-future conditions showcased enhanced GST values. On another hand, at T7, the values had been significantly hindered, in comparison to control values. These results are not in agreement with Henriques et al. (2019) that described enhanced SOD, CAT, and GST values in mussels *M. galloprovinciallis* exposed to Gd for 28 days. On one hand, this may be due to the previously discussed lack of sampling points during the exposure phase,

to understand the enzymatic behavior, on another hand may be related to a species-specific strategy to cope with Gd accumulation or to the different exposure durations. Martino et al. (2017) studied Gd effects on the embryonic development of European sea urchin species *Paracentrotus lividus* and *Arbacia lixula* and Australian ones, *Heliocidaris tuberculata* and *Centrostephanus rodgersii* from Australia and described different sensitivities to Gd, while arguing that Gd may display distinct toxicity levels on marine organisms, even within the same taxonomic group.

If the antioxidant defense system of a particular organisms is unable of eliminating excess ROS the free radical may react with membrane lipids, altering membrane permeability with deleterious consequences on a cellular level. Lipid peroxidation (oxidation of polyunsaturated fatty acids, LIPO) indicates oxidative degradation of cell membrane lipids. At T7 the climate change impacts on LIPO were evident through the visible synergistic effects of Warming & Gd, as clams exposed to this scenario showed higher LIPO values than the controls. Similarly, Hanana et al. (2017) found a SOD increase after exposure of freshwater zebra mussels to $GdCl_3$ for 28 days, while CAT and GST were downregulated and no effects on LIPO were observed, at a control temperature.

A heat shock reaction mediated by HSPs' is the first cell response to thermal stress. The damaged structure of thermally unfolded proteins is reestablished through this response (Somero 2020). In our study, we observed reduced HSP levels in Gd exposed clams, in comparison to the control, at T7, and the effects of increasing temperature were only observed on T14. Martino et al. (2021) investigated the combined effects of thermal stress and Gd in the embryos and larvae of the sea urchin *Paracentrotus lividus* and described that those elevated temperatures reduced the Gd effects by means of lower abnormality percentage and improved skeleton growth while Gd was the main driver for the induction of HSP expression. The author reasoned that near future warmer conditions will mitigate the negative Gd effects, which was not underlined by data derived in the present study. If HSP fails to reestablish the unfolded proteins, Ub target these proteins for degradation. Again, in this study, at T7, the level of this biomarker was lower for all the four Gd exposed treatments, in comparison to their control counterparts. Furthermore, at T14, previously Gd exposed clams exhibited lower Ub levels, in comparison to the remaining treatments. Hence, we propose that

the heat shock response was incapable of guaranteeing ideal protein function and ubiquitin, in the presence of Gd, could not target those proteins to be eliminated. Although we did not observe mortality during the experimental period this may cause serious deleterious outcomes on organisms' physiological function with consequences on feeding, growth, reproduction, and ultimately resilience and survival. About the non-enzymatic antioxidant reaction, we observed increased TAC values on clams exposed to Warming, and Warming & Gd, in comparison to the control. The observed resilience of the surf clam to climate change variables was expected as this species inhabits shallow coastal habitats that are subject to everyday abiotic variations. However, clams were not able to proficiently regulate the oxidative stress response in the presence of multiple stressors and the combination of Warming & Gd triggered lipid damage, which emphasizes the enhanced toxic effects of Gd in a changing ocean.

9.5 CONCLUSION

Through various sampling periods during the first 7 days of exposure to the studied multi-stressors we provided a new insight into the reaction time and were able to monitor the first biochemical responses. The results derived from this study showcased the rapid ability of the surf clam *Spisula solida* to accumulate Gd. This accumulation increased steadily in the first 7 days of exposure and was independent of temperature and pH. Furthermore, we showed a slight ability to eliminate Gd, derived from a 7-day elimination period. Nevertheless, Gd accumulation in a Warming, Acidification, and Warming & acidification scenario further impacted the clams' biochemical response. The results herein illustrate the enhanced toxic effects of Gd in a changing ocean which suggest that deleterious impacts to the population of surf clams are likely to be exacerbated in the near future.

ACKNOWLEDGMENTS

This work was supported by Fundação para a Ciência e Tecnologia (FCT), through the project Climatoxeel (PTDC/AAG-GLO/3795/2014) and the Junior Researcher contract (CEECIND/03517/2017), both awarded to Tiago F. Grilo, by the European Union's operation program Mar 2020 through the research project CEIC (MAR-01.04.02-

FEAMP-0012) awarded to Joana Raimundo and the strategic project UID/MAR/04292/2019 granted to MARE and by the Applied Molecular Biosciences Unit UCIBIO financed by national funds from FCT (UIDP/04378/2020 and UIDB/04378/2020). Cátia Figueiredo acknowledges the FCT-PhD grant SFRH/BD/130023/2017 and the Early Career Research Grant awarded by National Geographic Society.

REFERENCES

Akagi, T., Edanami, K., 2017. Sources of rare earth elements in shells and soft-tissues of bivalves from Tokyo Bay. Marine Chemistry 194, 55-62.

Andrade, M., Soares, A.M., Solé, M., Pereira, E., Freitas, R., 2022. Will climate changes enhance the impacts of e-waste in aquatic systems?. Chemosphere 288, 132264.

Black, B.C., Weisel, G.J., 2010. Global Warming. Santa Barbara, CA: Greenwood.

Bradford, M.M., 1976. A rapid and sensitive method for the quantitation of microgram quantities of protein utilizing the principle of protein-dye binding. Analytical biochemistry 72, 248-254.

Braun, H., 1995. The Collected Works of John W. Tukey: Vol. VIII, Multiple Comparisons 1948-1983. Journal of the Royal Statistical Society-Series A Statistics in Society 158, 629.

Caravan, P., Ellison, J.J., McMurry, T.J., Lauffer, R.B., 1999. Gadolinium (III) chelates as MRI contrast agents: structure, dynamics, and applications. Chemical reviews 99, 2293-2352.

Damhus, T., Hartshorn, R., Hutton, A., 2005. Nomenclature of inorganic chemistry: IUPAC recommendations 2005. CHEMISTRY International.

Field, C.B., Barros, V.R., 2014. Climate change 2014–Impacts, adaptation and vulnerability: Regional aspects, Cambridge University Press.

Figueiredo, C., Grilo, T.F., Lopes, C., Brito, P., Diniz, M., Caetano, M., Rosa, R., Raimundo, J., 2018. Accumulation, elimination and neuro-oxidative damage under lanthanum exposure in glass eels (*Anguilla anguilla*). Chemosphere 206, 414-423.

Figueiredo, C., Raimundo, J., Lopes, A.R., Lopes, C., Rosa, N., Brito, P., Diniz, M., Caetano, M., Grilo, T.F., 2020. Warming enhances lanthanum accumulation and toxicity promoting cellular damage in glass eels (*Anguilla anguilla*). Environmental research 191, 110051.

Freitas, R., Cardoso, C.E., Costa, S., Morais, T., Moleiro, P., Lima, A.F., Soares, M., Figueiredo, S., Águeda, T.L., Rocha, P., 2020a. New insights on the impacts of e-waste towards marine bivalves: The case of the rare earth element Dysprosium. Environmental Pollution 260, 113859.

Freitas, R., Costa, S., Cardoso, C.E., Morais, T., Moleiro, P., Matias, A.C., Pereira, A.F., Machado, J., Correia, B., Pinheiro, D., 2020b. Toxicological effects of the rare earth element neodymium in *Mytilus galloprovincialis*. Chemosphere 244, 125457.

Gonzalez, V., Vignati, D.A., Leyval, C. and Giamberini, L., 2014. Environmental fate and ecotoxicity of lanthanides: are they a uniform group beyond chemistry?. Environment international 71, 148-157.

Hanana, H., Turcotte, P., André, C., Gagnon, C., Gagné, F., 2017. Comparative study of the effects of gadolinium chloride and gadolinium–based magnetic resonance imaging contrast agent on freshwater mussel, *Dreissena polymorpha*. Chemosphere 181, 197-207.

Henriques, B., Coppola, F., Monteiro, R., Pinto, J., Viana, T., Pretti, C., Soares, A., Freitas, R., Pereira, E., 2019. Toxicological assessment of anthropogenic Gadolinium in seawater: Biochemical effects in mussels *Mytilus galloprovincialis*. Science of the Total Environment 664, 626-634.

Hornstein, J., Espinosa, E.P., Cerrato, R.M., Lwiza, K.M., Allam, B., 2018. The influence of temperature stress on the physiology of the Atlantic surfclam, *Spisula solidissima*. Comparative Biochemistry and Physiology Part A: Molecular & Integrative Physiology 222, 66-73.

IPCC, 2019: IPCC Special Report on the Ocean and Cryosphere in a Changing Climate [H.-O. Pörtner, D.C. Roberts, V. Masson-Delmotte, P. Zhai, M. Tignor, E. Poloczanska, K. Mintenbeck, A. Alegría, M. Nicolai, A. Okem, J. Petzold, B. Rama, N.M. Weyer (eds.)].

IPCC, 2021: Summary for Policymakers. In: Climate Change 2021: The Physical Science Basis. Contribution of Working Group I to the Sixth Assessment Report of the Intergovernmental Panel on Climate Change [Masson-Delmotte, V., P. Zhai, A. Pirani, S.L. Connors, C. Péan, S. Berger, N. Caud, Y. Chen, L. Goldfarb, M.I. Gomis, M. Huang, K. Leitzell, E. Lonnoy, J.B.R. Matthews, T.K. Maycock, T. Waterfield, O. Yelekçi, R. Yu, and B. Zhou (eds.)]. In Press.

Johansson, L.H., Borg, L.H., 1988. A spectrophotometric method for determination of catalase activity in small tissue samples. Analytical biochemistry 174, 331-336.

Lingott, J., Lindner, U., Telgmann, L., Esteban-Fernández, D., Jakubowski, N., Panne, U., 2016. Gadolinium-uptake by aquatic and terrestrial organisms-distribution determined by laser ablation inductively coupled plasma mass spectrometry. Environmental Science: Processes & Impacts 18, 200-207.

Lopes, A.R., Borges, F.O., Figueiredo, C., Sampaio, E., Diniz, M., Rosa, R., Grilo, T.F., 2019. Transgenerational exposure to ocean acidification induces biochemical distress in a keystone amphipod species (*Gammarus locusta*). Environmental research 170, 168-177.

Martino, C., Bonaventura, R., Byrne, M., Roccheri, M., Matranga, V., 2017. Effects of exposure to gadolinium on the development of geographically and phylogenetically distant sea urchins species. Marine environmental research 128, 98-106.

Martino, C., Byrne, M., Roccheri, M.C., Chiarelli, R., 2021. Interactive effects of increased temperature and gadolinium pollution in *Paracentrotus lividus* sea urchin embryos: a climate change perspective. Aquatic Toxicology 232, 105750.

Maulvault, A.L., Camacho, C., Barbosa, V., Alves, R., Anacleto, P., Fogaça, F., Kwadijk, C., Kotterman, M., Cunha, S.C., Fernandes, J.O., 2018. Assessing the effects of seawater temperature and pH on the bioaccumulation of emerging chemical contaminants in marine bivalves. Environmental research 161, 236-247.

McNeil, B.I., Sasse, T.P., 2016. Future ocean hypercapnia driven by anthropogenic amplification of the natural CO_2 cycle. Nature 529, 383-386.

Mesquita, J.R., Vaz, L., Cerqueira, S., Castilho, F., Santos, R., Monteiro, S., Manso, C.F., Romalde, J.L., Nascimento, M.S.J., 2011. Norovirus, hepatitis A virus and enterovirus presence in shellfish from high quality harvesting areas in Portugal. Food Microbiology 28, 936-941.

Pagano, G., Guida, M., Tommasi, F., Oral, R., 2015. Health effects and toxicity mechanisms of rare earth elements—Knowledge gaps and research prospects. Ecotoxicology and environmental safety 115, 40-48.

Perrat, E., Parant, M., Py, J.S., Rosin, C., Cossu-Leguille, C., 2017. Bioaccumulation of gadolinium in freshwater bivalves. Environmental Science and Pollution Research 24, 12405-12415.

Pierrot, D., Lewis, E., Wallace, D., 2006. MS Excel program developed for CO_2 system calculations. ORNL/CDIAC-105a. Carbon Dioxide Information Analysis Center, Oak Ridge National Laboratory, US Department of Energy, Oak Ridge, Tennessee 10.

Pousse, E., Poach, M.E., Redman, D.H., Sennefelder, G., White, L.E., Lindsay, J.M., Munroe, D., Hart, D., Hennen, D., Dixon, M.S., 2020. Energetic response of Atlantic surfclam *Spisula solidissima* to ocean acidification. Marine Pollution Bulletin 161, 111740.

Rabiet, M., Brissaud, F., Seidel, J., Pistre, S., Elbaz-Poulichet, F., 2009. Positive gadolinium anomalies in wastewater treatment plant effluents and aquatic environment in the Hérault watershed (South France). Chemosphere 75, 1057-1064.

Ramalho, J., Semelka, R., Ramalho, M., Nunes, R., AlObaidy, M., Castillo, M., 2016. Gadolinium-based contrast agent accumulation and toxicity: an update. American Journal of Neuroradiology 37, 1192-1198.

Regoli, F., Giuliani, M.E., 2014. Oxidative pathways of chemical toxicity and oxidative stress biomarkers in marine organisms. Marine environmental research 93, 106-117.

Renault, T., 2015. Immunotoxicological effects of environmental contaminants on marine bivalves. Fish & shellfish immunology 46, 88-93.

Somero, G.N., 2020. The cellular stress response and temperature: Function, regulation, and evolution. Journal of Experimental Zoology Part A: Ecological and Integrative Physiology 333, 379-397.

Stevens, A.M., Gobler, C.J., 2018. Interactive effects of acidification, hypoxia, and thermal stress on growth, respiration, and survival of four North Atlantic bivalves. Marine Ecology Progress Series 604, 143-161.

Uchiyama, M., Mihara, M., 1978. Determination of malonaldehyde precursor in tissues by thiobarbituric acid test. Analytical biochemistry 86, 271-278.

Chapter 10

A triple threat: ocean warming, acidification and REE exposure triggers a superior antioxidant response and pigment production in the adaptable *Ulva rigida*

Cátia Figueiredo [a,b,c*], Tiago F. Grilo [a], Rui Oliveira [b], Inês João Ferreira [d], Fátima Gil [e], Clara Lopes [b,f], Pedro Brito [b,f], Pedro Ré [a], Miguel Caetano [b,f], Mário Diniz [c,g], Joana Raimundo [b,f]

[a] MARE – Marine and Environmental Sciences Centre, Faculdade de Ciências da Universidade de Lisboa, Campo Grande, 1749-016 Lisboa, Portugal;

[b] Division of Oceanography and Marine Environment, IPMA – Portuguese Institute for Sea and Atmosphere, Av. Alfredo Magalhães Ramalho, 6, 1495-165 Algés, Portugal;

[c] Associate Laboratory i4HB - Institute for Health and Bioeconomy, School of Science and Technology, NOVA University Lisbon, 2819-516 Caparica, Portugal

[d] LAQV-REQUIMTE, Chemistry Department, NOVA School of Science and Technology, 2829-516 Caparica, Portugal

[e] Aquário Vasco da Gama, Rua Direita do Dafundo, 1495-718 Cruz Quebrada, Portugal

[f] CIIMAR – Interdisciplinary Centre of Marine and Environmental Research, Avenida General Norton de Matos S/N, 4450-208 Matosinhos, Portugal;

[g] UCIBIO – Applied Molecular Biosciences Unit, Department of Chemistry / Department of Life Sciences, School of Science and Technology, NOVA University Lisbon, 2819-516 Caparica, Portugal

* Corresponding author

Figueiredo, C., Grilo, T.F., Oliveira, R., Ferreira, I.J., Gil, F., Lopes, C., Brito, P., Caetano, M., Ré, P., Caetano, M, Diniz, M., Raimundo, J., 2022. A triple threat: ocean warming, acidification and REE exposure triggers a superior antioxidant response and pigment production in the adaptable *Ulva rigida*. Submitted to Aquatic toxicology.

ABSTRACT

Anthropogenic increased atmospheric CO_2 concentrations will lead to a drop of 0.4 units of seawater pH and ocean warming up to 4.8 °C by 2100. Contaminant's toxicity is known to increase under a climate change scenario. Rare earth elements (REE) are emerging contaminants, as they became vital to new technologies. Studies of REE bioaccumulation, elimination, and toxicity in a multi-stressor environment (e.g., warming and acidification) are lacking. Hence, we investigated the algae phytoremediation capacity, the ecotoxicological responses and total chlorophyll and carotenoid contents in *Ulva rigida* during 7 days of co-exposure to La or Gd (15 µg L^{-1} or 10 µg L^{-1}, respectively), and warming (+4 °C) and acidification (-0.4 pH units). Additionally, we assessed these metals elimination, after a 7-day phase. After one day of experiment La and Gd clearly showed accumulation/adsorption in different patterns, at future conditions. Unlikely for Gd, Warming and Acidification contributed to the lowest La accumulation, and increased elimination. Lanthanum and Gd triggered an adequate activation of the antioxidant defence system, by avoiding lipid damage. Nevertheless, REE exposure in a near-future scenario triggered an overproduction of ROS that requested an enhanced antioxidant response. Additionally, an increase in total chlorophyll and carotenoids could also indicate an unforeseen energy expense, as a response to a multi-stressor environment. The obtained results suggest that the outcomes of REE exposure on this species in a changing world may be more severe than foreseen.

KEYWORDS: Green macroalgae; Lanthanum; Gadolinium; Oxidative stress; Total chlorophyll; Carotenoid content.

10.1 INTRODUCTION

Since the industrial revolution that exacerbated anthropogenic CO_2 emissions are striking physicochemical changes in seawater. The Intergovernmental Panel on Climate Change (IPCC) projects that these abnormal atmospheric CO_2 concentrations will lead to a drop of around 0.4 units of seawater pH, by the end of the 21st century (IPCC, 2021). Besides this known ocean acidification phenomenon, increasing atmospheric CO_2 levels will also allude, among others, to global average temperature increase, with direct implications in seawater temperature. The IPCC predicts warming of the global mean sea surface temperature up to 4°C for the same timeframe (IPCC, 2021). Climate change is expected to impact coastal ecosystems, with profound implications to animal welfare and human health. The enhancement of contaminants toxicity is also known to be caused by climate change (Figueiredo et al. 2020). The increase in seawater temperature can affect the bioavailability of pollutants, through transport and change in speciation, while altering the metabolism of the biota, its physiology and aptitude, affecting the patterns of bioaccumulation and elimination of contaminants (Maulvault et al. 2016). Added to these challenges posed by rising temperatures and CO_2 levels, emerging contaminants constitute another difficulty, particularly to coastal environments and their inhabitants. Rare earth elements (REE) belong to this category of contaminants (i.e., emergent), as they have become in recent years of chief importance to the manufacture of new technologies. The REE are a family of 17 elements, composed of the 15 lanthanides, plus yttrium, and scandium. In the present study, Lanthanum (La) and Gadolinium (Gd) were chosen as representatives of Light (LREE) and Heavy REE (HREE), respectively. These chemical elements exhibit unique magnetic and catalytic properties, which branded them essential for modern electronic and clean energy technologies. They are also applied in medicine as magnetic resonance imaging contrast, agriculture, animal husbandry, and aquaculture, in which they are used as components of bactericides or fertilizers (Gwenzi et al. 2018). Additionally, the growing demand for modern electronic products has led to an alarming build-up of electronic waste (e-waste). E-waste dismantling, storage, and burning can release its components into the environment (Uchida et al. 2018). Furthermore, the recycling of REE is until recently rarely applied due to inefficient techniques (Binnemans

et al., 2021). Increased REE usage, in the recent past, has resulted in increased discharge into the environment and the transfer to aquatic ecosystems is expected to be upheld. Gadolinium and La availability are affected by temperature and pH (Byrne and Sholkovitz 1996), which suggests that interactions with climate change variables are likely to occur. The risks associated with excess REE availability in the aquatic environment have gathered the scientific community's attention in recent years, however still little and quite puzzling information is available on its uptake and toxicity to aquatic organisms. Furthermore, integrated studies dealing with REE bioaccumulation and toxicity in a multi-stressor environment (e.g., warming and acidification) are lacking. Another human created problematic is the increased urbanization and coastal zone use that leads to coastal eutrophication (Smith et al. 1999). The changing climatic conditions together with the enhanced nutrient input promotes green tide events, which are blooms of great macroalgae biomass. These are of global concern due to their impacts both on an ecological and economic level. *Ulva* sp. (Chlorophyta) are generally the dominant genus of green tides (reviewed in Fletcher 1996). This genus is common worldwide and is dominant along marine coasts (Uchimura et al., 2004). Species of *Ulva* sp. present high growth rates, with strong CO_2 capture capacities (Fan et al. 2014). Macroalgae can accumulate a wide array of metals, and this has led to their appliance as biomonitors of water contamination. Additionally, *Ulva* spp. are known to accumulate REE (e.g., Pinto et al. 2020). Nevertheless, to the best of our knowledge, a study of the interactive effects of ocean warming, acidification, and REE with an algae species has never been conducted. In this context, we investigated the potential for phytoremediation, the ecotoxicological responses (antioxidant enzymes and cellular oxidative damage) and total chlorophyll and carotenoid contents in *U. rigida* after 7 days of co-exposure to La or Gd (15 µg L^{-1} or 10 µg L^{-1}, respectively), and warming (ΔT°C = +4 °C) and acidification (ΔpH = -0.4 units). Furthermore, we assessed the bioaccumulation and elimination of La or Gd, after a seven-day exposure and seven-day elimination period.

10.2 MATERIAL AND METHODS

10.2.1 Specimens acquisition

Fresh *U. rigida* thalli were collected manually in a single sampling event in April 2021 at a land-based aquaculture system (ALGAplus Ltda). This company produces

macroalgae at Ria de Aveiro lagoon (40º 36' 44.7'' N, 8º 40' 27.0'' W) in coastal Portugal under the EU organic aquaculture standards (EC710/ 2009). *Ulva rigida* was immediately transported in aerated and controlled temperature seawater from its source of origin, under refrigerated conditions (+4°C), until reaching the aquaculture facilities of Aquário Vasco da Gama, in Lisbon. Before acclimation, the seaweed blades were rinsed with filtered seawater to remove epiphytes and debris. Roughly eight thousand and two hundred thalli disks of 15 mm in diameter were cut to warrant homogeneity in weight and exposure area and placed in gently aerated filtered seawater in a 12h:12h light-dark cycle (irradiance of 45 µmol photons m^{-2} s^{-1}, fluorescent tubes, Philips) and at the same physicochemical parameters as the sample location (T = 18 °C, pH = 8.1, salinity = 35 PSU). The disks were acclimated for 5 days.

10.2.2 Experimental design

Seaweed disks were distributed in glass tanks representative of 12 experimental treatments: i) Control temperature and pH (18°C, pH = 8.1, ~400 µatm pCO_2); ii) Acidification (18°C, pH = 7.7, ~900 µatm pCO_2); iii) La exposure (18°C, pH = 8.1, ~400 µatm pCO_2, added La = 15 µg L^{-1}); iv) Acidification & La (18°C, pH = 7.7, ~900 µatm pCO_2, added La = 15 µg L^{-1}); v) Gd exposure (18°C, pH = 8.1, ~400 µatm pCO_2, added Gd = 10 µg L^{-1}); vi) Acidification & Gd (18°C, pH = 7.7, ~900 µatm pCO_2, added Gd = 10 µg L^{-1}); vii) Warming (22°C, pH = 8.1, ~400 µatm pCO_2); viii) Warming & acidification (22°C, pH = 7.7, ~900 µatm pCO_2); ix) Warming & La (22°C, pH = 8.1, ~400 µatm pCO_2, added La = 15 µg L^{-1}); x) Warming, acidification & La (22°C, pH = 7.7, ~900 µatm pCO_2, added La = 15 µg L^{-1}); xi) Warming & Gd (22°C, pH = 8.1, ~400 µatm pCO_2, added Gd = 10 µg L^{-1}); xii) Warming, acidification & Gd (22°C, pH = 7.7, ~900 µatm pCO_2, added Gd = 10 µg L^{-1}).

Natural seawater was pumped directly from the ocean, and subsequently filtered (0.35 µm filters) and UV-sterilized (Vecton600, TMC Iberia). Seawater temperature was adjusted by heaters (V2Therm, TMC Iberia) and chillers (HC-250A, Hailea) submerged in a water bath, together with the twelve experimental glass tanks. Seawater pH was automatically regulated through a Profilux system (3.1, GHL), coupled to pH probes (GHL). Solenoid valves connected to this system downregulated automatically the seawater pH through injecting CO_2 enriched air. Upregulation was done by injecting filtered air. The seawater temperature (thermometer TFX 430, WTW GmbH), pH (pH/ion

meter SG8, Mettler-Toledo) and salinity (V2 Refractometer, TMC) were hand monitored daily. Seawater carbonate system speciation was calculated every sampling day from total alkalinity (Alkalinity checker, Hanna) and pH measurements, using the CO2SYS software.

A La or a Gd spike-solution ($LaCl_3$ and $GdCl_3$, Merck, respectively) was added to the water every other day in the corresponding exposure treatments to assure the dissolved levels. Water aliquots were sampled after 24h of exposure in every experimental tank, filtered for particles removal (0.45 μm Millipore), and acidified (20% ultrapure HNO_3) to determine La and Gd levels.

Ulva rigida was sampled immediately before the beginning of the trial (T0), and after 1 (T1), 3 (T3), and 7 days (T7). Following, a 7-day elimination phase began (T14), where no La nor Gd solutions were added. During the entire experiment, the media was completely renewed every two days.

After being sampled, *U. rigida* was stored at -80 °C until further analyses.

10.2.3 Lanthanum and Gd quantification

Five pools of 30 *U. rigida* disks were used for La and Gd quantification. The pools were freeze-dried, grounded, and homogenized before being digested in a microwave CEM MArsXpress with nitric acid (HNO_3, distilled, 65% v/v) as in Brito et al. (2020). The labware used in this procedure was previously decontaminated with HNO_3 (20%).

Concentrations of La and Gd were determined in a quadrupole ICP-MS (NexION 2000C). ^{115}In was used as an internal standard (Alfa Aesar, Plasma Standard Solution, Specpure®, In 1,000 μg mL^{-1}). The ^{139}La and ^{158}Gd were the quantified isotopes, as they present minimum isobaric and polyatomic interferences under routine conditions ($^{137}Ba^{++}/^{137}Ba$ and $^{140}Ce^{16}O/^{140}Ce \approx 0.010$). Three procedural blanks were included within each batch of 20 samples and accounted for less than 1% of the total concentrations determined in the samples. The accuracy of the analytic method was also evaluated through the evaluation of an international certified material (BCR 668). The results obtained did not differ significantly ($p>0.05$) from the certified values. The La and Gd ICP-MS detection limit for *U. rigida* samples were 0.12 and 0.032 μg L^{-1}, respectively.

Water samples were preconcentrated using an automated Elemental Scientific Inc. SeaFAST system (SeaFASTpico™) prior to analysis by ICP-MS (NexION 2000C) following the methodology described by Hatje et al. (2014). Succinctly, acidified

seawater sampled were spiked with a standard containing known isotopic ratios. Like the algae samples, water samples were run with blanks, seawater quality controls and certified reference materials (CASS-6 and NASS-7). A six-point calibration curve was used, and the detection limit was determined through the method blanks. The La and Gd ICP-MS detection limit for seawater samples were 0.008 and 0.003 µg L^{-1}, respectively.

Accumulated concentrations are presented in microgram per gram of tissue dry weight (µg g^{-1}, dw) and La and Gd levels in water are presented in microgram per litre (µg L^{-1}).

10.2.4 Biochemical analyses

A total of n=4 disks for each of the 12 treatments were sampled for biochemical analyses, each sampling time.

10.2.4.1 Sample preparation

Ulva rigida disks were individually homogenized in a chilled glass mortar and pestle in 500 µl of phosphate saline buffer (PBS: 0.14 M NaCl, 2.7 mM KCl, 8.1 mM Na_2HPO_4, and 1.47 mM KH_2PO_4, pH 7.4). Homogenates were centrifuged at 15000 x g for 5 min at 4 °C and stored at -80 °C.

Samples were run in triplicates (technical replicates) and all the results were normalized to total protein content by the method of Lowry et al. (1951).

10.2.4.2 Antioxidant enzymes

i) The percentage of inhibition of superoxide dismutase (SOD) was ascertained adapting Sun et al. (1988) method. Concisely, 200 µl of 50 mM phosphate buffer (pH 8.0) (Merck, Germany), 10 µl of 3 mM EDTA (Riedel-de Haën), 10 µl of 3 mM xanthine (Merck), 10 µl of 0.75 mM NBT (Merck) and 10 µl of SOD standard or sample were added to each well of a 96-well microplate (Greiner Bio-one, Germany). Following, 10 µl of 100 mU xanthine-oxidase (XOD, Sigma-Aldrich) was added to begin the reaction and the absorbance was read at 560 nm in a plate reader (Biotek Synergy HTX multi-mode reader, USA). The absorbance was recorded every 2 minutes for 26 minutes. SOD (Merck) was used as a standard and positive control, and a negative control included all components (except SOD or sample). SOD activity is expressed as % inhibition mg^{-1} of total protein.

ii) Catalase (CAT) activity was measured according to the method described in Johansson and Borg (1988). Twenty microliters of a sample, 100 µL of 100 mM potassium phosphate, and 30 µL of methanol were added to each well of a 96-well microplate (Greiner Bio-one, Germany) and incubated for 20 minutes. Subsequently, 30 µL of potassium hydroxide (10 M KOH) and 30 µL of Purpald Reagent (34.2 mM in 0.5 M HCl) were added, and the plate was incubated for 10 minutes. Then, 10 µL of potassium metaperiodate (65.2 mM in 0.5 M KOH) was added and incubated for 5 minutes. The activity was assessed spectrophotometrically at 540 nm, in a microplate reader (Biotek Synergy HTX multi-mode reader, USA). Formaldehyde concentration of the samples was calculated based on a calibration curve (from 0 to 75 µM formaldehyde). The results are presented in nmol min^{-1} mg^{-1} protein.

iii) Glutathione S-transferase (GST) was determined by adapting a method previously described by Habig et al. (1974), and adapted to 96-well microplates (Greiner Bio-one Germany). Accordingly, 180 µl of substrate solution (100 mM 1-chloro-2,4-dinitrobenzene (CDNB), 200 mM L-glutathione and Dulbecco's PBS), 20 µl sample were included in each well of the microplate and the absorbance was read at 340 nm (Biotek Synergy HTX multi-mode reader, USA) six times, once every minute. Equine liver GST (Merck, Germany) was used as a positive control to validate the assay and GST activity calculated using the molar extinction coefficient for CDNB of 5.3 εµM (μM^{-1} cm^{-1}). The results were expressed according to the total protein of the sample (nmol min^{-1} mg^{-1} total protein).

10.2.4.3 Cellular oxidative damage

Lipid peroxidation (LIPO) was established by malondialdehyde (MDA) quantification, a by-product of lipid damage, according to the thiobarbituric acid reactive substances (TBARS) assay (Uchiyama and Mihara 1978). Briefly, 10 µL of each sample, 45 µL of PBS, 12.5 µL of sodium dodecyl sulfate (8.1%), 93.5 µL of trichloroacetic acid (20%, pH 3.5), and 93.5 µL of thiobarbituric acid (1%), were added in a 1.5 mL microtube. A total of 50.5 µL of Milli-Q ultrapure water was added to the microtube, mixed, and incubated in a dry bath (Labnet, USA) at 100 °C for 10 min. Afterward, this mixture was cooled on ice. After colling, 62.5 µL of Milli-Q ultrapure water and one hundred and fifty µL of supernatant was added to 96-well microplates, and absorbance was read at 532 nm in a microplate reader (Biotek Synergy HTX multi-mode reader,

USA). Malondialdehyde concentrations were calculated based on a calibration curve (0 - 0.1 µM) using MDA bis (dimethyl acetal) standards.

10.2.5 Chlorophylls and carotenoids

Chlorophylls were determined through an adaptation of the method described by Arnon (1949). A pool of n=3 disks corresponding approximately to 0.15 g wet weight (ww) of *U. rigida* was extracted in 10 mL of 80% (v/v) acetone (Merck) in glass vials that were protected from light and kept at 4 °C for 24h. Samples were run in triplicates (technical replicates) and the absorbance of the supernatants was measured at 663 nm and 645 nm in a UV-spectrophotometer (Biotek Synergy HTX multi-mode reader, USA). To ascertain total chlorophyll (total Chl), the content of chlorophyll a (Chl a) and chlorophyll b (Chl b) were calculated as by Rodrigues et al. (2021):

Chl a (µg g^{-1} ww) = 12.25 A_{663} – 2.79 A_{645}

Chl b (µg g^{-1} ww) = 21.5 A_{645} – 5.10 A_{663}

Total Chl (µg g^{-1} ww) = Chl a + Chl b

The carotenoid content was measured in the same extract used for chlorophyll a and b estimation by the method of Kirk and Allen (1965). Briefly, the extract was measured at 480 nm and the content was calculated as:

Carotenoid (µg g^{-1} ww) = A_{480} + (0.114 A_{663}) – (0.638 A_{645})

A = absorbance at each respective wavelength

10.2.6 Data analyses

Two- and Three-way ANOVAs followed by significant Tukey's pairwise comparisons with Temperature, pH, and Contamination as factors for the outputs La or Gd accumulation, SOD, CAT, GST, LIPO, Total Chlorophyll and Carotenoids in each respective sampling time (two-way for T0, three-way for T1, T3, T7 and T14) were performed to explore significant differences between treatments. A one-way ANOVA was performed to explore differences in La and Gd concentrations in La and Gd exposure treatments, between sampling times.

Analyses were performed at a significance level of 0.05 in InVivoStat, version 4.3.

10.3 RESULTS

Table 10.1 comprises measured master water parameters and calculated pCO_2 values for every experimental treatment.

Table 10.1 - Means ± SD (standard deviation) of seawater and carbonate system parameters for all experimental treatments. Hand measured parameters (temperature, pH and total alkalinity) were used to calculate pCO_2 (carbon dioxide partial pressure).

Treatment	Temperature (°C)	Salinity	pH	Total Alkalinity (µmol kg^{-1} SW)	pCO_2 (µatm)
Control temperature and pH	17.9±0.2	35±0.1	8.11±0.08	2783±88	398±42
La	18.0±0.1	35±0.2	8.12±0.09	2922±83	407±38
Gd	18.0±0.1	35±0.1	8.14±0.04	2956±74	389±30
Acidification	18.1±0.1	35±0.1	7.71±0.10	2182±46	892±37
Acidification & La	17.8±0.3	35±0.1	7.69±0.09	2254±66	923±40
Acidification & Gd	18.1±0.2	35±0.1	7.70±0.08	2237±82	915±54
Warming	22.2±0.1	35±0.2	8.10±0.09	2771±82	404±32
Warming & La	21.8±0.2	35±0.2	8.09±0.11	2804±78	422±34
Warming & Gd	21.9±0.2	35±0.1	8.10±0.05	2896±91	424±44
Warming & Acidification	22.1±0.3	35±0.1	7.68±0.04	2002±99	891±65
Warming, acidification & La	22.0±0.2	35±0.1	7.72±0.09	2084±102	838±77
Warming, acidification & Gd	22.1±0.1	35±0.1	7.71±0.15	2147±88	863±39

10.3.1 Lanthanum and Gd bioaccumulation and elimination

Lanthanum concentrations (µg g^{-1}, dry weight) in La spiked *U. rigida* are shown in Figure 10.1a while Gd concentrations (µg g^{-1}, dry weight) in Gd exposed treatments are shown in Figure 10.1b.

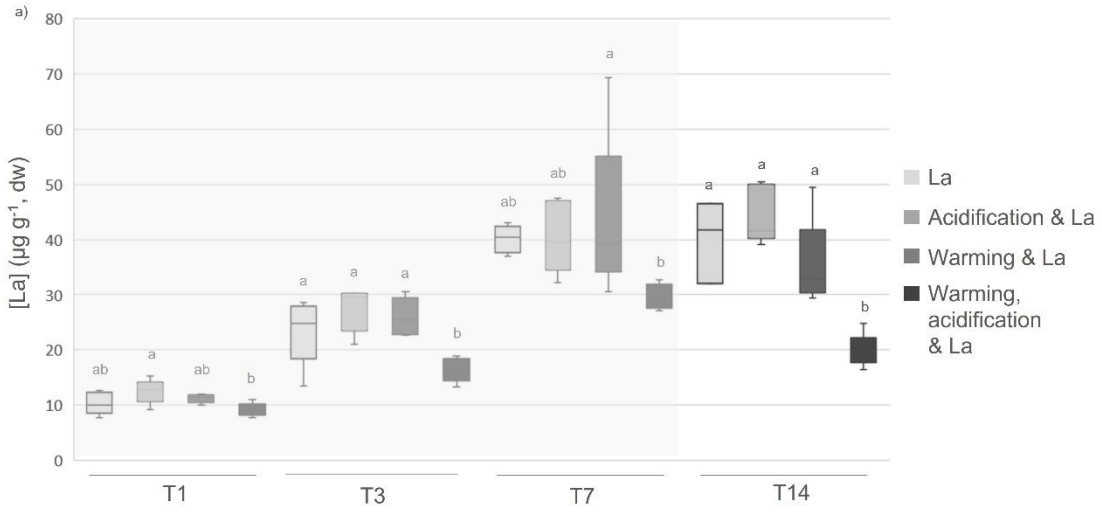

Figure 10.1 a – Median, percentile 25th and 75th, minimum and maximum values of Lanthanum (µg $^{-1}$) concentrations in *Ulva rigida* exposed to 15 µg L^{-1} in different sampling times (T1, T3, T7 and T14). Different letters represent significant differences between exposure treatments within sampling times.

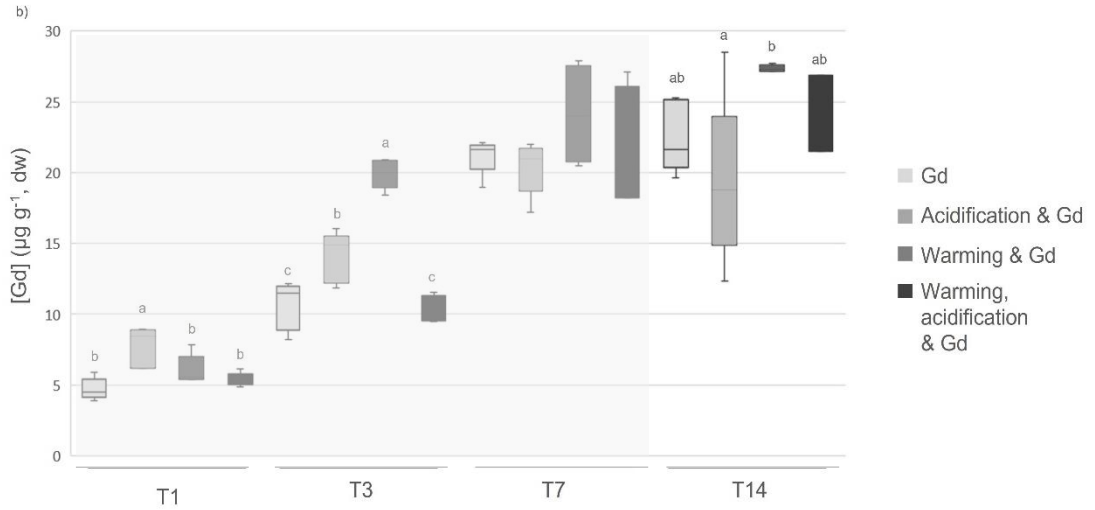

Figure 10.1 b – Median, percentile 25th and 75th, minimum and maximum values of gadolinium (µg $^{-1}$) concentrations in *Ulva rigida* exposed to 10 µg L^{-1} in different sampling times (T1, T3, T7 and T14). Different letters represent significant differences between exposure treatments within sampling times.

Table 10.2 shows median (minimum-maximum) La and Gd concentrations (µg g^{-1}, dry weight) in *U. rigida* samples for each experimental condition.

Table 10.2 - Median, minimum, and maximum La and Gd concentrations (µg g^{-1}, dry weight) in *Ulva rigida* exposed to: control/present-day temperature and pH; Acidification; La; Acidification & La; Gd; Acidification & Gd; Warming; Warming & acidification; Warming & La; Warming & Gd; Warming, acidification & La; Warming, acidification & Gd at T0, T1, T3, T7 and T14. BDL stands for below detection limit. Detection limits were 0.12 µg L^{-1} for La and 0.032 µg L^{-1} for Gd.

			[La] (µg g^{-1} dry weight)		
	T0	**T1**	**T3**	**T7**	**T14**
Control temperature & pH	BDL	0.12 (0.12-0.18)	0.23 (0.19-0.28)	0.34 (0.28-0.39)	0.20 (0.12-0.24)
Acidification	BDL	0.12 (0.12-0.14)	0.14 (0.12-0.16)	0.16 (0.12-0.20)	BDL
La		10 (7.7-13)	24 (14-27)	40 (37-43)	42 (32-46)
Acidification & La		13 (9.2-15)	30 (21-30)	40 (32-47)	41 (39-50)
Warming	BDL	0.12 (0.12-0.64)	BDL	0.12 (0.12-0.12)	BDL
Warming & Acidification	BDL	BDL	BDL	0.21 (0.20-0.76)	BDL
Warming & La		11 (0.12-12)	25 (23-30)	39 (31-69)	33 (29-49)
Warming, acidification & La		9.2 (7.7-11)	16 (13-19)	29 (27-33)	19 (16-25)
			[Gd] (µg g^{-1} dry weight)		
	T0	**T1**	**T3**	**T7**	**T14**
Control temperature & pH	BDL	0.038 (0.032-0.046)	0.048 (0.032-0.060)	BDL	BDL
Acidification	BDL	0.032 (0.032-0.054)	0.057 (0.043-0.060)	0.064 (0.043-0.11)	0.033 (0.032-0.14)
Gd		4.5 (3.9-5.9)	11 (8.2-12)	22 (19-22)	22 (20-25)
Acidification & Gd		8.4 (6.2-9.0)	15 (12-16)	21 (17-22)	19 (12-28)
Warming	BDL	BDL	0.042 (0.032-0.046)	BDL	BDL
Warming & Acidification	BDL	BDL	BDL	BDL	BDL
Warming & Gd		5.5 (5.4-7.8)	20 (18-21)	24 (20-28)	21 (18-27)
Warming, acidification & Gd		5.3 (4.9-6.2)	10 (9.5-12)	27 (27-28)	26 (22-27)

Table 10.3 presents the La and Gd levels in the water (µg L^{-1}) aliquots sampled after 24h (immediately before T1) in all experimental treatments.

Table 10.3 - Levels of La and Gd in the water (µg L^{-1}) aliquots sampled after 24h (immediately before T1) of exposure in all experimental treatments

	[La] (µg L^{-1}) 24 h	[Gd] (µg L^{-1}) 24 h
Control temperature & pH	0.010	0.004
La	**0.72**	-
Gd	-	**0.60**
Acidification	0.013	0.009
Acidification & La	**0.63**	-
Acidification & Gd	-	**0.76**
Warming	0.008	0.004
Warming & La	**1.8**	-
Warming & Gd	-	**0.74**
Warming & Acidification	0.009	0.004
Warming, acidification & La	**1.7**	-
Warming, acidification & Gd	-	**3.7**

All *U. rigida* pools from T0 registered La and Gd values below the detection limit. Throughout the experiment, regarding the non-spiked treatments, the highest La median value registered was 0.34±0.003 µg g^{-1}, observed in algae exposed to control temperature and pH, vulgo present-day conditions, at T7 and the highest median Gd concentration was 0.064±0.012 µg g^{-1}, in the Acidification treatment at T7.

We observed La accumulation just after 24h, as the La spiked treatments showcased significant differences from their control counterparts ($p<0.0001$, Annex 9, Supplemental Table 10.1a), and the La accumulation was greater in the Acidification & La treatment than in the Warming, acidification & La one ($p=0.0022$, Annex 9, Supplemental Table 10.1a). At T1, the median La concentration was highest in *U. rigida* exposed to Acidification & La (13±0.98 µg g^{-1}), followed by the samples in the Warming & La treatment (11±0.37 µg g^{-1}). The lowest concentrations were found in the Warming, acidification & La treatment (9.2±0.55 µg g^{-1}) followed by *U. rigida* disks exposed to La (10±0.89 µg L^{-1}). On the first day of exposure, the La water levels diminished in the Acidification & La treatment 96% (Table 3), followed by 95% in the La treatment. The La reduction was lowest in the Warming & La treatment (88%), closely followed by the La exposure treatment (89%). Regarding the La trial at T3, the La accumulation was upheld and increased, the highest accumulation occurred in the Acidification & La treatment (30±1.8 µg g^{-1}), followed by the Warming & La (25±1.5 µg g^{-1}), that was in turn closely followed by *U. rigida* exposed to La (24±3.0 µg g^{-1}). The lowest median La concentration

was measured in algae exposed to Warming, acidification & La (16±0.98 µg g^{-1}). At this time of exposure, La concentrations were significantly lower in the Warming, acidification & La than the other three La exposed treatments ($p<0.05$, Annex 9, Supplemental Table 10.1a). At T7, the lowest La accumulation value was also registered in the Warming, acidification & La treatment (29±1.0 µg g^{-1}). The alga exposed to La and Acidification & La presented overall the same accumulation values (40 µg g^{-1}). The algae disks exposed to Warming & La for 7 days showed 39±6.7 µg g^{-1} of La. Here we only observed significant lower La levels in the Warming, acidification & La than the Warming & La treatment ($p=0.0152$, Annex 9, Supplemental Table 10.1a). At T14, for the La trial, the highest La concentration was measured in algae previously exposed to La (42±4.2 µg g^{-1}), followed by the Acidification & La treatment (41±2.3 µg g^{-1}). The lowest La levels were observed in the Warming, acidification & La treatment (19±1.4 µg g^{-1}). The Warming & La treatment revealed 33±3.6 µg g^{-1} of La.

Considering the Gd exposure trial, after one day of exposure, Gd accumulation occurred in all Gd exposed treatments ($p<0.0001$, Annex 9, Supplemental Table 10.1a). The Gd accumulation trend was similar to the La trial: the highest median Gd accumulation occurred in the Acidification & Gd treatment (8.4±0.63 µg g^{-1}), followed by Warming & Gd (5.5±0.46 µg g^{-1}). The lowest median value was observed in *U. rigida* exposed to Gd (4.5±0.34 µg g^{-1}), followed by the Warming, acidification & Gd exposure treatment (5.3±0.21 µg g^{-1}). Here the accumulation was greater in the Acidification & Gd treatment than the Gd treatment ($p=<0.0001$), the Warming & Gd ($p=0.0004$), and the Warming, acidification & Gd ($p=<0.0001$, Annex 9, Supplemental Table 10.1a). The Gd reduction from water, in the first 24h, was greatest in the Gd exposure treatment 94% (Table 3) followed by the Warming & Gd (93%), the Acidification & Gd treatment (92%). The lowest reduction was exhibited in the Warming, acidification & Gd (63%). At T3, the highest Gd concentration was observed in the algae exposed to Warming & Gd (20±0.45 µg g^{-1}), followed by the Acidification & Gd treatment (15±0.79 µg g^{-1}). On the contrary, the lowest values were observed in the Warming, acidification & Gd (10±0.46 µg g^{-1}), and Gd (11±0.75 µg g^{-1}) treatments. In fact, the Gd exposure treatment showed significantly lower accumulation values than the algae exposed to both Warming & Gd ($p<0.0001$, Annex 9, Supplemental Table 10.2a) and Acidification & Gd ($p=0.0001$, Annex

9, Supplemental Table 10.2a). The Warming & Gd also showed significantly higher values than the Acidification & Gd treatment (p=<0.0001, Annex 9, Supplemental Table 10.2a). Lastly, the Warming, acidification & Gd treatment showed significantly lower values than the Acidification & Gd and Warming & Gd treatments (p<0.0001 and p<0.0001, respectively, Annex 9, Supplemental Table 10.1a). At T7, the Gd accumulation values ranged between 21±0.84 μg g^{-1} in the Acidification & Gd treatment and 27±0.13 μg g^{-1} in the Warming, acidification & Gd treatment. *Ulva rigida* exposed to Gd for 7 days accumulated 22±0.57 μg g^{-1}, while the one exposed to Warming & Gd accumulated 24±1.8 μg g^{-1}. No differences in Gd accumulation were found between the Gd exposed treatments (p>0.05, Annex 9, Supplemental Table 10.2a). At T14, for the Gd trial, the highest concentration was observed in the Warming, acidification & Gd treatment (26±1.6 μg g^{-1}), followed by 22±1.1 μg g^{-1} in the previously Gd exposed algae. The Acidification & Gd treatment showed median Gd levels of 19±2.6 μg g^{-1} while the Warming & Gd presented 21±2.1 μg $g^{-1}$of Gd.

Regarding the elimination phase, 7 days of elimination were insufficient. At T14, every La and Gd exposed treatment remained different than their control counterpart (Annex 9, Supplemental Table 10.2a). Additionally, the concentration values presented at T14 were very similar to the ones at T7. In fact, from time T7 to T14 we only observed a significant difference in the Warming, acidification & La treatment (p<0.0001, Annex 9, Supplemental Table 10.1b). The first sampling time for the La and Gd concentrations in the exposed treatments, respectively, was different from all the other (T1 vs T3, T7, and T14, p<0.05, Annex 9, Supplemental Table 10.1b). The La and Gd concentrations in T3 were significantly lower than T7 for all spiked treatments and the same occurred between T3 and T14 apart from the treatments Warming & La (p=0.3412), Warming, acidification & La (p=0.114), and Acidification & Gd (p=0.0935, Annex 9, Supplemental Table 10.1b).

10.3.2 Oxidative stress-related biomarkers

Oxidative stress-related biomarkers values for every experimental treatment and time are presented in Table 10.4.

Table 10.4 - Mean ± standard deviation values of Superoxide dismutase (SOD, % inhibition min^{-1} mg^{-1} protein); Catalase (CAT, nmol min^{-1} mg^{-1} protein); Glutathione S-transferase (GST, nmol min^{-1} mg^{-1} total protein); Lipid peroxidation (LPO, nmol mg protein $^{-1}$); Total Chlorophyll (mg g^{-1}, ww); Carotenoid (mg g^{-1}, ww) in *Ulva rigida* at T0, T1, T3, T7 and T14 in all experimental treatments.

		SOD (% inhibition min^{-1} mg^{-1} protein)	CAT (nmol min^{-1} mg^{-1} protein)	GST (nmol min^{-1} mg^{-1} total protein)	LIPO (nmol mg protein $^{-1}$)	Total Chlorophyll (mg g^{-1}, ww)	Carotenoids (mg g^{-1}, ww)
T0	Control	175±67	1.2±0.04	33±2.7	0.037±0.008	1.3±0.036	0.065±0.004
	Acidification	152±14	1.1±0.20	29±3.8	0.029±0.0002	1.3±0.005	0.077±0.001
	Warming	131±24	1.1±0.22	32±8.0	0.032±0.006	1.3±0.049	0.075±0.002
	Warming & Acidification	134±40	1.1±0.04	39±3.9	0.030±0.004	1.2±0.013	0.058±0.004
T1	Control	181±21	1.2±0.31	38±4.3	0.028±0.008	1.2±0.17	0.055±0.006
	La	293±27	1.4±0.44	49±10	0.034±0.018	1.7±0.025	0.042±0.009
	Gd	336±65	1.6±0.42	55±4.1	0.026±0.014	1.0±0.033	0.043±0.001
	Acidification	184±76	1.2±0.16	30±3.4	0.027±0.015	1.3±0.086	0.051±0.015
	Acidification & La	292±51	1.5±0.37	41±9.0	0.040±0.013	1.4±0.30	0.042±0.0001
	Acidification & Gd	314±84	1.6±0.39	52±4.2	0.039±0.008	0.90±0.010	0.042±0.007
	Warming	361±84	1.3±0.35	36±2.0	0.028±0.007	1.4±0.11	0.045±0.007
	Warming & La	348±90	1.3±0.31	50±6.3	0.059±0.019	1.9±0.73	0.038±0.012
	Warming & Gd	273±92	1.2±0.34	57±3.4	0.044±0.025	1.5±0.030	0.093±0.017
	Warming & acidification	267±58	1.3±0.17	45±3.9	0.031±0.009	1.2±0.65	0.062±0.020
	Warming, acidification & La	212±88	1.0±0.14	50±11	0.056±0.015	2.1±0.34	0.06±0.008
	Warming, acidification & Gd	212±66	1.4±0.05	48±5.4	0.051±0.019	1.6±0.47	0.052±0.005
T3	Control	234±59	1.2±0.30	41±5.2	0.038±0.009	0.90±0.030	0.035±0.0005
	La	341±35	0.66±0.15	45±16	0.067±0.025	1.2±0.060	0.04±0.001
	Gd	486±58	0.51±0.09	53±20	0.06±0.011	1.0±0.022	0.043±0.011
	Acidification	270±24	1.0±0.08	37±8.9	0.051±0.014	1.3±0.080	0.049±0.002
	Acidification & La	336±58	0.54±0.18	46±7.0	0.061±0.038	1.6±0.018	0.060±0.0
	Acidification & Gd	468±21	0.47±0.2	56±7.2	0.066±0.001	1.3±0.083	0.059±0.020
	Warming	404±30	1.0±0.14	52±13	0.067±0.05	1.4±0.042	0.065±0.004
	Warming & La	419±47	0.65±0.1	51±3.5	0.066±0.022	1.6±0.23	0.057±0.010
	Warming & Gd	545±66	0.62±0.21	58±12	0.071±0.012	1.4±0.041	0.054±0.001
	Warming & acidification	370±49	0.92±0.19	42±14	0.056±0.019	1.0±0.045	0.050±0.023
	Warming, acidification & La	439±72	0.71±0.09	55±15	0.068±0.02	2.0±0.036	0.079±0.0002
	Warming, acidification & Gd	491±63	0.6±0.22	45±18	0.074±0.006	1.8±0.025	0.067±0.004
T7	Control	250±15	1.2±0.13	40±5.9	0.036±0.013	1.6±0.026	0.063±0.001
	La	343±66	0.75±0.17	48±11	0.068±0.027	1.6±0.060	0.061±0.002
	Gd	478±49	0.67±0.11	49±5.3	0.08±0.026	1.7±0.077	0.059±0.012
	Acidification	430±54	0.91±0.18	40±5.4	0.056±0.02	1.6±0.32	0.078±0.010
	Acidification & La	305±60	0.66±0.04	37±14	0.073±0.042	1.7±0.098	0.084±0.005
	Acidification & Gd	482±49	0.5±0.12	53±8.0	0.07±0.009	1.6±0.073	0.066±0.007
	Warming	386±48	0.85±0.11	49±12	0.047±0.024	1.5±0.074	0.076±0.004
	Warming & La	453±39	0.73±0.21	47±7.8	0.069±0.028	1.7±0.006	0.067±0.009
	Warming & Gd	575±54	0.74±0.25	85±11	0.083±0.012	1.5±0.31	0.080±0.001
	Warming & acidification	438±90	0.84±0.02	39±2.2	0.05±0.02	1.3±0.018	0.053±0.001
	Warming, acidification & La	585±45	0.56±0.13	65±10	0.077±0.008	1.9±0.054	0.077±0.011
	Warming, acidification & Gd	639±87	0.53±0.18	72±8.8	0.084±0.025	2.0±0.43	0.087±0.011
T14	Control	286±38	1.1±0.15	38±5	0.031±0.004	1.5±0.10	0.059±0.002
	La	259±61	0.56±0.06	38±3.3	0.043±0.028	1.5±0.14	0.056±0.012
	Gd	419±81	0.62±0.11	36±17	0.063±0.002	1.6±0.17	0.063±0.001
	Acidification	342±63	0.94±0.05	38±8.4	0.048±0.033	1.5±0.027	0.057±0.010
	Acidification & La	259±40	0.61±0.15	35±13	0.055±0.013	1.6±0.008	0.077±0.012
	Acidification & Gd	379±16	0.87±0.35	39±4.5	0.056±0.038	1.6±0.24	0.066±0.003
	Warming	361±43	0.92±0.42	33±6.9	0.059±0.02	1.7±0.008	0.057±0.005

Table 10.4 Cont.

		SOD (% inhibition min^{-1} mg^{-1} protein)	CAT (nmol min^{-1} mg^{-1} protein)	GST (nmol min^{-1} mg^{-1} total protein)	LIPO (nmol mg $protein^{-1}$)	Total Chlorophyll (mg g^{-1}, ww)	Carotenoids (mg g^{-1}, ww)
T14	Warming & La	415±110	0.69±0.23	33±5.4	0.058±0.03	1.4±0.013	0.062±0.006
	Warming & Gd	440±116	0.82±0.13	82±4.6	0.062±0.023	1.7±0.098	0.067±0.004
	Warming & acidification	375±41	0.85±0.08	32±10	0.059±0.013	1.4±0.16	0.061±0.002
	Warming, acidification & La	401±124	0.61±0.13	54±9.0	0.048±0.023	1.7±0.52	0.081±0.007
	Warming, acidification & Gd	402±61	0.82±0.41	58±17	0.064±0.05	1.8±0.011	0.072±0.001

10.3.2.1 Superoxide dismutase

The superoxide dismutase (SOD, % inhibition min^{-1} mg^{-1} protein) levels for the La and Gd trials are shown in Figures 10.2a and b, respectively.

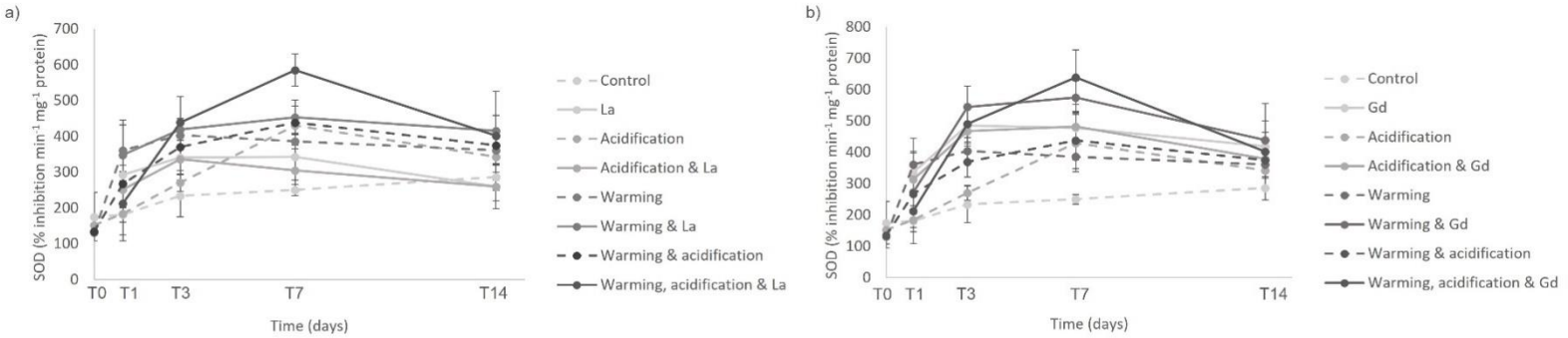

Figure 10.2 a) and b) - Mean ± SD values of Superoxide dismutase (SOD, % inhibition min^{-1} mg^{-1} protein). a) represents the La exposure trial and b) represents the Gd exposure trial.

For the La trial, warming induced SOD values, just after one day as *U. rigida* kept in a warmer condition showed increased values in comparison to the control (p=0.0308, Annex 9, Supplemental Table 10.2a) and the Acidification treatment (p=0.0058, Annex 9, Supplemental Table 10.2a). The impacts of climate change on increased SOD values were also visible at T3, and the four La exposure treatments showed enhanced SOD levels in comparison to the control samples (Annex 9, Supplemental Table 10.2a). At T7, the La exposure treatments remained significantly higher than the control, except for the Acidification & La treatment (p>0.05). Additionally, we observed that La in conjugation with climate change (i.e., Acidification & Warming) triggered an enhanced SOD activity, in comparison to La exposure (p=0.0193 and p=<0.0001, Annex 9, Supplemental Table 10.2a). On another hand, the Acidification & La treatment caused diminished SOD values, in comparison to the Acidification treatment (p=0.0027). The Warming & La treatment provoked significantly higher SOD than the Acidification & La

(p=0.0007, Annex 9, Supplemental Table 10.2a). At the end of the elimination period (T14), we observed that the treatments Warming & La and Warming, acidification & La displayed enhanced SOD, analogous to the La exposure treatment (p=0.0181 and p=0.018, respectively). Furthermore, *U. rigida* exposed to Warming & acidification for 14 days, showed higher SOD levels than *U. rigida* previously exposed to La (p=0.022, Annex 9, Supplemental Table 10.2a).

Regarding the Gd exposure, in the effect on SOD activity was clear in the first treatment day. *Ulva rigida* disks exposed for 24 h to Gd showcased enhanced SOD levels in comparison to the control (p=0.0176) and the Acidification treatments (p=0.0027). In addition, the Acidification & Gd showed higher values than the Acidification treatment (p=0.0123, Annex 9, Supplemental Table 10.2a). On the third exposure day, all four Gd exposure treatments showed higher SOD levels than the control (Annex 9, Supplemental Table 10.2a). Gadolinium exposure caused higher SOD levels than Acidification (p<0.0001), and Warming & acidification combined (p=0.0131, Annex 9, Supplemental Table 10.2a). The combination of Acidification & Gd also triggered enhanced SOD levels, in comparison to just Acidification (p=<0.0001, Annex 9, Supplemental Table 10.2a). Finally, at T3, SOD levels were greater in Warming, acidification & Gd than in the Warming & acidification treatment (p=0.0093). On the 7th day, all four Gd exposure treatments showed higher SOD than the control (p<0.05, Annex 9, Supplemental Table 10.2a). The combination of Warming, acidification & Gd resulted in the highest SOD levels, and these were significantly higher than the ones showcased by all the other treatments: Control (p=<0.0001), Acidification (p=<0.0001), Acidification & Gd (p<0.0001), Gd (p<0.0001), Warming (p=0.0008), Warming & Gd (p=0.0002) and Warming & acidification (p=<0.0001, Annex 9, Supplemental Table 10.2a). At T14, the previously enhanced SOD levels from the four Gd exposure treatments decreased to control-like values, and we did not observe significant differences between experimental treatments.

10.3.2.2 Catalase

Catalase (CAT, nmol min^{-1} mg^{-1} total protein) values are shown in Figures 10.2 c and d.

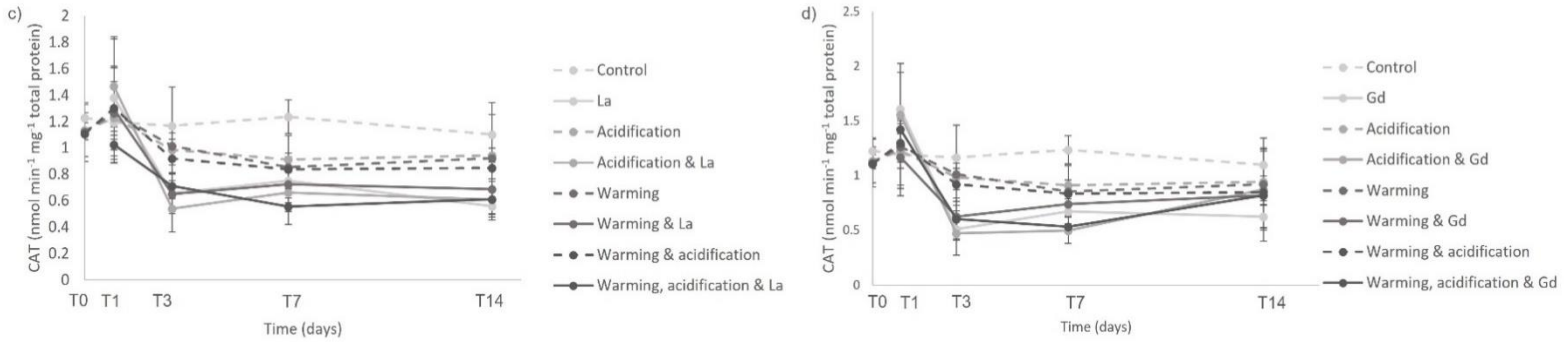

Figure 10.2 c) and d) - Mean ± SD values of Catalase (CAT, nmol min^{-1} mg^{-1} total protein). c) represents the La exposure trial and d) represents the Gd exposure trial.

On the La trial, significant differences between treatments were only visible at T3 and T14. On the Gd trial, we only observed differences at T3. On T3, *U. rigida* exposed to Acidification & La showed lower CAT levels than the control (p=0.0277, Annex 9, Supplemental Table 10.2a). At T14, the previously exposed algae to La, Acidification & La and Warming, acidification & La showed an inhibition of CAT in comparison to the control (p=0.008, p=0.0198, p=0.0226, respectively, Annex 9, Supplemental Table 10.2b).

At T3, Acidification & Gd exposure inhibited CAT expression in comparison to the control (p=0.0196) and the warming treatment (p=0.0331, Annex 9, Supplemental Table 10.2a).

For the La trial, the CAT levels were higher in T1 than the other experimental times (T3, T7, and T14) for the four La exposure treatments, apart from T1 *versus* T3 in the Warming, acidification & La (p=0.1109, Annex 9, Supplemental Table 10.2b). Regarding the Gd trial, T1 was different from the other experimental times for the Gd and Warming, acidification & Gd treatments. In the Acidification & Gd CAT levels decreased from T1 to T3 (p=0.0059) and T7 (p=0.0109, Annex 9, Supplemental Table 10.2b).

10.3.2.3 Glutathione S-transferase

Glutathione S-transferase (GST, nmol min^{-1} mg^{-1} total protein) levels for the La and Gd experiments, and their respective controls, are presented in Figures 10.2e and f, respectively.

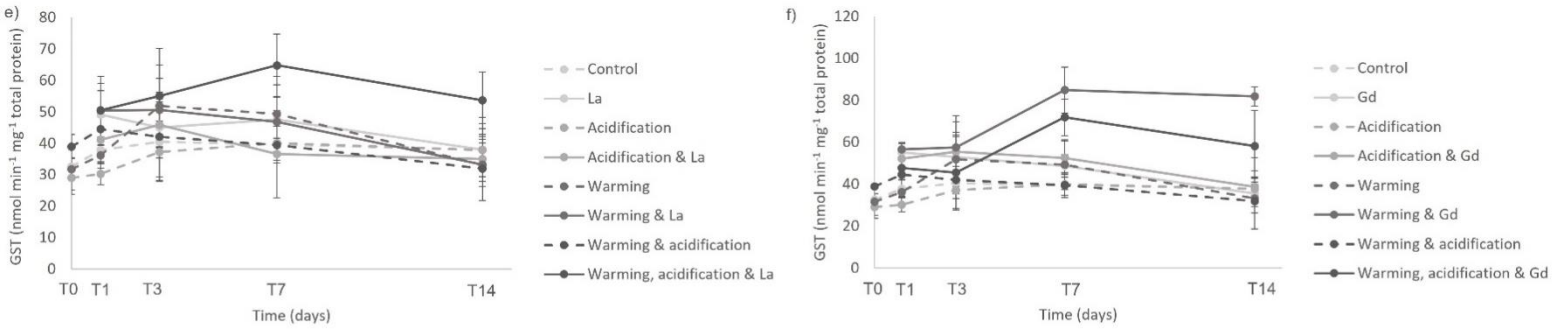

Figure 10.2 e) and f) - Mean ± SD values of Glutathione S-transferase (GST, nmol min^{-1} mg^{-1} total protein). e) represents the La exposure trial and f) represents the Gd exposure trial.

At T1, the combination of La and climate change variables synergistically enhanced GST expression (Figure 10.2e). Acidification & La exposure prompted higher GST levels than Acidification exposure (p=0.0443, Annex 9, Supplemental Table 10.2a) and Warming & La prompted higher levels than Warming as a single stressor (p=0.0244). Furthermore, Warming, Acidification & La showed increased levels than Warming (p=0.0166, Annex 9, Supplemental Table 10.2a). After 7 days of exposure to the combination of Warming, acidification & La, *U. rigida* specimens presented significantly higher GST values than specimens exposed to Acidification & La (p=0.0032) and Acidification (p=0.014, Annex 9, Supplemental Table 10.2a). After the elimination period (T14), the enhanced GST levels triggered by the exposure to Warming, Acidification & La decreased slightly and remained the highest, being significantly higher than the Warming (p=0.0317), Warming & La (p=0.0317), and Warming & Acidification (p=0.0106, Annex 9, Supplemental Table 10.2a).

After just one day of exposure (T1) all the Gd exposure treatments showcased significantly higher GST values than the control (p<0.05, Annex 9, Supplemental Table 10.2a). Furthermore, Gd exposure triggered higher GST expression than Acidification (p=<0.0001) and Warming (p<0.0001, Annex 9, Supplemental Table 10.2a). The Acidification & Gd also showed higher GST levels than Acidification alone (p<0.0001) while Warming & Gd showed higher GST levels than Warming alone (p<0.0001). Warming, acidification & Gd triggered enhanced GST expression in comparison to Warming (p=0.0017) and Acidification (p=<0.0001, Annex 9, Supplemental Table 10.2a).

At T7, Warming & Gd elicited enhanced GST values, in comparison to the control (p=0.0004), to the Gd exposure (p=0.0049), and the Warming treatment (p=0.0012, Annex 9, Supplemental Table 10.2a). Moreover, Warming, acidification & Gd prompted greater GST levels than the control (p=0.0112), and the Warming & acidification treatment (p=0.0076, Annex 9, Supplemental Table 10.2a). At the end of the elimination phase, the GST values presented by the *U. rigida* exposed to Warming & Gd remained significantly higher than those found in the control (p=0.0004) and the Gd exposure treatment (p=0.0001). At this time, T14, Warming, Acidification & Gd showed significantly greater GST values than Warming & Acidification (p=0.0027), Warming (p=0.0093), and Gd exposure treatment (p=0.0376, Annex 9, Supplemental Table 10.2a).

10.3.2.4 Lipid peroxidation

Lipid peroxidation (LIPO, nmol mg protein^{-1}) levels in *Ulva rigida* samples exposed to La and Gd, in present-day and predicted climate change conditions are shown in Figures 10.2g and h, respectively.

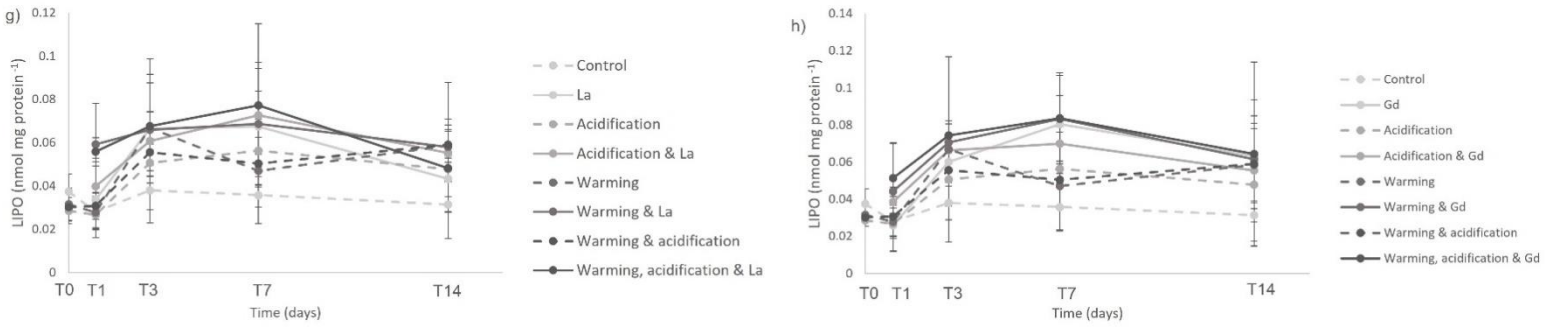

Figure 10.2 g) and h) - Mean ± SD values of Lipid peroxidation (LIPO, nmol mg protein^{-1}). g) represents the La exposure trial and h) represents the Gd exposure trial.

Although we did not observe significant differences in the LIPO levels between the exposure treatments, along the experimental times the levels increased from T1 to T3 (p=0.0493, Annex 9, Supplemental Table 2b) and T7 (p=0.0141) in the Gd exposure treatment and from T1 to T7 (p=0.0441, Annex 9, Supplemental Table 10.2b) in the Acidification & Gd treatment.

10.3.3 Total Chlorophyll and Carotenoid content

Contents of total chlorophyll and carotenoids are given in Table10.4 and illustrated in Figures 10.3a-d.

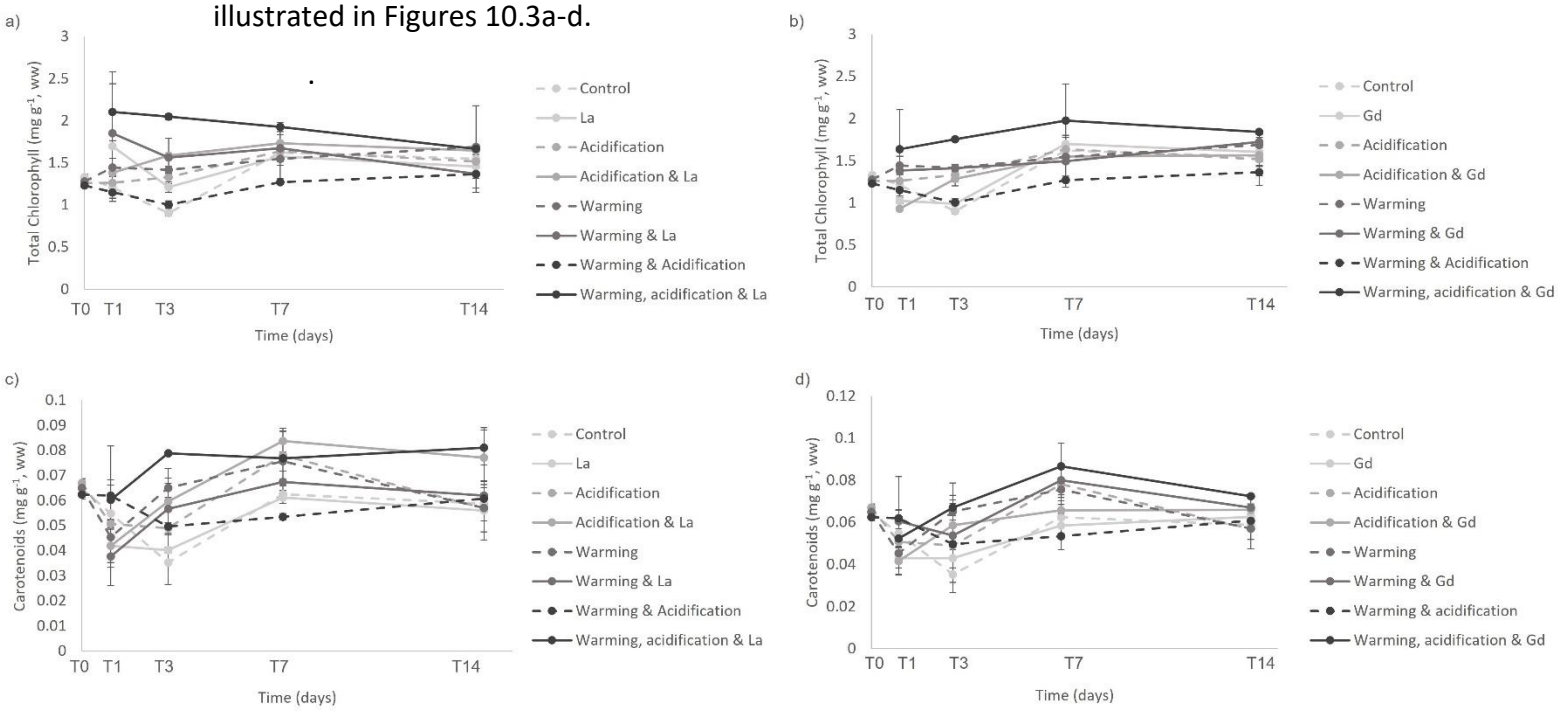

Figure 10.3 Mean ± SD values of Total Chlorophyll (mg g^{-1}, ww) and Carotenoid content (mg g^{-1}, ww) in *Ulva rigida* at T1, T3, T7 and T14 in the La (a and c) and Gd (b and d) trials for the four La and Gd exposed treatments, respectively.

At T0, the algae samples acclimated to Warming & acidification showed significantly lower chlorophyll values than the ones kept in control conditions (p=0.0305, Annex 9, Supplemental Table 10.2a; Figure 10.3a). The effects of climate change, acting alone or in combination were also noticeable at T1. Additionally, at this sampling time, the four La exposure treatments presented significantly higher total chlorophyll values than the control (p<0.05, Annex 9, Supplemental Table 10.2a). The highest chlorophyll content was registered in *U. rigida* disks exposed to Warming, acidification & La, and these were significantly greater than the values presented by all the other treatments (p<0.05, Annex 9, Supplemental Table 10.2a). T1 showed higher total chlorophyll values than at T3 (p=0.0006) and T14 (p=0.0479). On the contrary, T3 showed significantly lower values than T7 (p=0.0029) and T14 (p=0.0253, Annex 9, Supplemental Table 10.2b). At T7, Warming, acidification & La evoked greater chlorophyll content than Warming & acidification (p=0.0041, Annex 9, Supplemental Table 10.2a).

Regarding the Gd trial, at T1, Acidification & Gd showed lower total chlorophyll content than Warming & acidification ($p=0.0278$, Annex 9, Supplemental Table 10.2a; Figure 3b). At T3, Gd exposure in conjugation with climate change variables acting alone and together elicited increased chlorophyll content in comparison to the control ($p<0.05$, Annex 9, Supplemental Table 10.2a), but not Gd exposure alone. While Gd exposure alone revealed greater chlorophyll content than Acidification & Gd ($p=0.0001$), Warming & Gd exposure triggered greater values than Gd exposure alone ($p<0.0001$). Alike the La trial, exposure to the three stressors, Warming, acidification & Gd caused enhanced chlorophyll content in comparison to the remaining treatments ($p<0.05$, Annex 9, Supplemental Table 10.2a). No differences were observed at T7 and T14 regarding total chlorophyll content.

We did not observe significant differences concerning carotenoid content between treatments at T0 and T1 (Figure 10.3c). At T3, Acidification & La showed a greater carotenoid content than the control ($p=0.0178$, Annex 9, Supplemental Table 10.2a), while the Warming, acidification & La elicited enhanced carotenoid content than the control ($p=0.0015$) and the La exposure alone ($p=0.0065$, Annex 9, Supplemental Table 10.2a). At T7, these three stressors in combination (Warming, Acidification & La), caused increased carotenoid content than Warming & acidification ($p=0.0273$). For the Acidification & La treatment, carotenoid content increased from T1 to T3 ($p=0.0138$), to T7 ($p=0.001$), and ultimately T14 ($p=0.0019$), while also being significantly greater at T7 than at T3 ($p=0.0161$). For the La exposure treatment values increased significantly from T1 to T3 ($p=0.0426$) and from T3 to T7 ($p=0.0234$, Annex 9, Supplemental Table 10.2b). At T14, even though total carotenoid content was greater in the Warming, acidification & La followed by Acidification & La treatment, no significant differences among treatments occurred.

Significant differences in carotenoid content of the Gd exposure trial were only found at T7 (Figure 10.3d). Here, Warming, acidification & Gd elicited greater carotenoid values than the Gd exposure alone ($p=0.0375$) and Warming & acidification ($p=0.0116$, Annex 9, Supplemental Table 10.2a). At T14 we did not observe differences between treatments.

10.4 DISCUSSION

Here we showed *U. rigida*'s outstanding ability to uptake La and Gd, in mono-element exposure trials, at great levels. Macroalgae are known to significantly bioaccumulate pollutants (e.g., Bonanno et al. 2020), and recent attention has been given to their role in REE removal (Cao et al. 2021), although scarce data on macroalgae interaction with REE is still available. Furthermore, a study encompassing exposure to various stressors related to climate change, such as ocean warming and acidification, and REE with this bioindicator species, has never been carried out.

The literature describes two distinct processes for elemental uptake by algae: i) adsorption onto the cell wall and ii) intracellular absorption (Davis et al. 2003). Although the used methodology is not able to differentiate the two processes, it was clear that one day of exposure proved to be sufficient for La and Gd to be accumulated/adsorbed. Although REE are known to be a chemically coherent group, we observed distinct La and Gd accumulation patterns, under future climate-change conditions. *Ulva rigida* exposed to Warming, acidification & La showed the overall lowest accumulation values, while this trend was not observed for Gd. Figueiredo et al. (2020) described enhanced La accumulation in warming scenario for a fish species (*Anguilla anguilla*) and Andrade et al. (2022) described significantly different Gd accumulation values at different salinities (20, 30, and 40) in the mussel *Mytilus galloprovincialis*. Future climate change conditions are thus likely to interfere with REE accumulation, elimination, and toxicity, yet different results must derive from phylogenetically related differences and the absence of information on these pertinent issues highlights the urgent need for further studies to be conducted on a wider array of model species in forecasted climate change scenarios.

The green *U. rigida* presents a lobed laminar foliaceous thallus, that encompasses two cell layers (Olivares et al. 2016), which brands the algae to present a large surface area in contact with seawater, contributing to great REE accumulation ability. Previous studies found distinct accumulation patterns to be related to different algae physical characteristics (e.g., Pinto et al. 2021). This was surpassed by the use of algae disks with the same weight, size and area. Ferreira et al. (2020) studied the Gd accumulation (10, 157 and 500 µg L^{-1}) using three different marine macroalgae (e.g., *Ulva lactuca*, *Fucus spiralis* and *Gracilaria* sp.), for 72 h, and all accumulated Gd, with a

removal efficiency of around 85%. Moreover, when exposed to a mixture of REE (Y, La, Ce, Pr, Nd, Eu, Tb, Dy) and other elements (Cr, Ni, Cu, Cd, Hg, Pb), at salinity 10 and 30, the removal efficiency was kept (~84%). In the present study, for the same exposure concentration (10 μg L^{-1}), we observed lower uptake percentages, which may be related with the shorter exposure time that we used. Furthermore, this comparison is relative, since has not taken into consideration the algae surface area in contact with the solution. In fact, Pinto et al. (2020) studied REE (Y, La, Ce, Pr, Nd, Eu, Gd, Tb, Dy) removal from laboratory-prepared seawater for 72 h and described that has occurred mainly in the first 24 h, and an equilibrium was not reached until the end of the trial. On another hand, we observed amounts of removal in the Acidification and Gd treatment as those reported in the cited studies.

The pH is key for REE adsorption onto algae as this is highly dependent on the speciation and the projected pH decrease by the end of the century appears to increase both La and Gd accumulation. As discussed by Cao et al. (2021), REE mostly exist as positively charged ions and thus exhibit electrostatic attraction towards the negatively charged constituents of the algae surface. When the pH is lower in solution than inside the algae, the REE sorption is obstructed, when the solution pH is higher electrostatic attraction occurs and algae may absorb REE. This may be related to REE speciation shifts, which in turn are regulated by pH, water hardness, alkalinity, ionic strength, and complexing agents (reviewed in Herrmann et al. 2016). In the present study, we also did not observe an equilibrium as the concentrations kept increasing until T7, and this could be related to a short exposure time. Sakamoto et al. (2008) determined REE in several seaweeds species and observed concentrations of about 100 times higher than those in seawater. These results suggest that REE uptake is greater in the first hours of exposure, however the uptake can be upheld for a long period, and future studies should increase exposure duration without disregarding frequent sampling of biological material and quantification of REE levels in the water.

The literature reveals a great information gap on REE elimination in macroalgae. Most research focus on REE recycling using micro and macroalgae (e.g. Jacinto et al. 2018), nevertheless, the study of REE elimination by these organisms has been majorly overlooked. Here we showed that neither La nor Gd were eliminated in a 7-day elimination period. In fact, the La and Gd concentrations measured only diminished

between T7 and T14 for the Warming, acidification & La treatment. Both climate change stressors combined, Warming and Acidification, contributed to the lowest La accumulation values, in all exposure times and appear to increase La elimination, but not Gd. Here we showed that in a future climate change scenario a different accumulation and elimination pattern between the LREE La and the HREE Gd occurs.

Climate change impacts alone on the green tide forming *Ulva* sp. have been described and this genus presents remarkable adaptability to them. Wang et al. (2021) described that elevated CO_2 promoted *Ulva* species propagation through enhanced photosynthetic and respiration efficiency while reducing energy demand to maintain external pH. Gao et al. (2017) also described that higher temperature increased reproduction in *U. rigida*, and this would be increased in combination with acidification. On the other hand, Gao et al. (2018) described that the positive effect of increasing temperature on *U. rigida* growth rate turned negative on the second, fourth, and sixth week of exposure to increasing temperatures. This was discussed to be related to induced reproductive events. In our study, we conducted a shorter 14-day experiment, and thus this induction is unlikely to have occurred. Nevertheless, algae are affected by a wide array of factors such as light, nutrients, temperature, and pH, among others. Temperature is known to affect photosynthesis directly, and growth and reproduction indirectly, by regulating enzyme activity. Furthermore, increased CO_2 (that in turn is responsible for pH decrease), can promote algae growth (Cao et al. 2021). Even though *U. rigida* is carbon-saturated at present-day CO_2 conditions, the species harbors a carbon-concentrating mechanism (Mercado et al. 1998), and as a result increased CO_2 concentrations may affect the species fitness in the near future. Although the assessment of the impacts of climate change on this macroalgae was not the objective of the present study, all these factors may interact with our results.

A full factorial experimental design was employed to better identify the impacts of single and the combination of two and three stressors. Exposure to single and multiple stressors, as climate change and emergent pollutants, is expected to increase the production of reactive oxygen species (ROS). The presence of ROS induces a set of defence mechanisms towards preventing the establishment or neutralizing oxidizing species. When this defence mechanisms fail, the structure and functionality of cells is

compromised. For example, if a cell membrane is oxidized by ROS, its rigidity and permeability may be altered with profound consequences to its functionality. Superoxide dismutase (SOD) and catalase (CAT) are the first enzymatic antioxidant's reaction towards ROS. Glutathione-S-transferases (GST) constitute a second line non-enzymatic antioxidant response. In these processes, malondialdehyde is produced and this is used as a biomarker of oxidative stress as an indicator of lipid peroxidation (LIPO). Higher antioxidant activity levels have been described in *U. rigida* exposed to heavy metals. Olivares et al. (2016) described enhanced antioxidant activity in this algae species in areas with great mining activities. Positive effects of REE in algae have also been described (Goecke et al. 2015). REE are applied in agriculture and have shown to, for example, increase crop productivity (reviewed by Tyler (2004). However, these results are still not completely clear as several toxic outcomes from REE exposure have similarly been described. Joonas et al. (2017) described the toxic effects of REE on the green microalgae *Raphidocelis subcapitata* and observed growth inhibition within 72 h. Suitable concentrations of REE have been described to increase SOD, and CAT levels, together with higher content of carotenoids, increasing plants' resistance to abiotic stressors, to a threshold as excessive concentration have caused damage to chloroplasts (reviewed in Kovaříková et al. 2019). In fact, Ippolito et al. (2010) described enhanced antioxidant enzymatic responses and glutathione activity in the common duckweed, *Lemna minor* exposed to REE before signs of stress symptoms were observed. A biphasic effect was noted, from antioxidant defence mechanism activation to growth inhibition. In the present study, exposure to La and Gd triggered the activation of the antioxidant defence system. The response of this system seems to be quicker in the case of Gd exposure, however, on the third day of exposure the four La exposed treatments and the four Gd exposed treatments showed enhanced SOD levels. Furthermore, we observed that this response was higher when the studied REE were combined with climate change variables. The CAT response appeared to be reduced when La and Gd were spiked in an acidification scenario. This is not in line with the response of *Ulva* sp. to other metals as Pereira et al. (2009) showed enhanced CAT activity in specimens environmentally exposed to greater Cu and Ni concentrations. This may be related to a REE specific response. Furthermore, a second line response was activated, highlighted by increased GST levels in REE exposed treatments. Overall, the levels were greater in

algae exposed to Warming, Acidification & La, in the La trial while being greater in algae exposed to Warming & Gd, followed by Warming, Acidification & Gd (Gd trial). This response shows that REE exposure in a near future scenario triggers an overproduction of ROS that requests a superior antioxidant response, which in turn may compromise energy requirements and overall species fitness. This response appears to be adequate in avoiding lipid damage as LIPO activity revealed no significant differences. Nevertheless, we observed a trend for greater LIPO values in exposed algae to La and Gd and for that we advise future studies to increase the number of samples studied as we encounter great variability. Furthermore, a broader set of environmentally realistic exposure concentrations may be applied as a previously discussed biphasic effect may occur with increasing concentrations. This intertidal species shows an extraordinary adaptation ability. In the present study we observed increased total chlorophyll in REE exposure treatments, particularly when combined with climate change, after 3 days of exposure. This was not so obvious on T7 and T14 probably due to this species' previously discussed outstanding adaptation capacity. Nevertheless, an increase in chlorophyll a, chlorophyll b and carotenoids could indicate an unforeseen energy expense to the biosynthesis of pigments, at the cost of growth and reproduction, as a response to a multi-stressor environment. This indicates that although the antioxidant defence system was activated and appeared to prevent lipid damage, the outcomes of REE exposure in a changing world may be more severe than foreseen. In fact, Ashraf et al. (2021) studied the effects of nanomolar La concentrations on the freshwater green microalga *Desmodesmus quadricauda* and observed that La had no direct effects on growth, but increasing concentrations led to decrease in cell number, and La also inhibited photosynthesis with posterior consequences on growth. Furthermore, La^{3+} is known to precipitate as a phosphate in water, which may lead to phosphorus reduction, that is vital for algae growth, reproduction an ultimately survival (González et al. 2015). Ngwenya et al. (2009) described that heavy REE, such as Gd, are more prone to carboxylate, in this sense exacerbated La concentrations may stand a harsher toxicological threat than Gd to algae species. In the environment, REE often occur together, and some studies have tried to understand the interaction between mixtures of REE and macroalgae. Jacinto et al. (2018) studied the REE removal ability of red

seaweed *Gracilaria gracilis* by exposing them to mono- and multi-elements REE solutions (Y, Ce, Nd, Eu and La) and observed up to 70% removal in 48h. Removal was greater in multi elemental exposure trials; however, selectivity was not observed. Costa et al. (2020) studied if the presence of Cd, Cr, Cu, Pb, Hg and Ni, interferes with the ability of macroalgae (*Ulva intestinalis*, *Ulva lactuca*, *Fucus spiralis*, *Fucus vesiculosus*, *Gracilaria* sp. and *Osmundea pinnatifida*) to remove REE (La, Ce, Pr, Nd, Eu, Gd, Tb, Dy and Y) and found that competition of REE to macroalgae sorption sites was minor. Hence, the REE accumulation in mono and multi elemental exposure trials does not seem to be significantly different. Furthermore, the understanding of mono-elemental exposure is still limited, and this study constitutes a great contribution to lessen the knowledge gap regarding the REE individual behavior while starting to unveil their combined effects to a near future setting.

10.5 CONCLUSIONS

The present study is the first assessment of the impacts of ocean warming and acidification on La and Gd accumulation and elimination, through mono-elemental exposure in a factorial design on the green tidal forming *U. rigida* through quantification of an array of non- and enzymatic antioxidant responses and total chlorophyll and carotenoid contents. Overall, we observed distinct La and Gd accumulation patterns in future climate-change conditions and showed that La and Gd are not proficiently eliminated. The exposure to La and Gd triggered the activation of the antioxidant defence system, and this response seems to be quicker in the case of Gd exposure. The response also appears to be adequate in avoiding lipid damage. In a near-future scenario, REE exposure overproduces ROS, which engenders the need for a superior antioxidant response, which may enhance energy requirements with downstream impacts to species fitness.

ACKNOWLEDGMENTS

This work was supported by Fundação para a Ciência e Tecnologia (FCT), through the project Climatoxeel (PTDC/AAG-GLO/3795/2014) and the Junior Researcher contract (CEECIND/03517/2017), both awarded to Tiago F. Grilo, by the European Union's operation program Mar 2020 through the research project CEIC (MAR-01.04.02-

FEAMP-0012) awarded to Joana Raimundo and the strategic project UID/MAR/04292/2019 granted to MARE and by the Applied Molecular Biosciences Unit UCIBIO financed by national funds from FCT (UIDP/04378/2020 and UIDB/04378/2020). Cátia Figueiredo acknowledges the FCT-PhD grant SFRH/BD/130023/2017 and the Early Career Research Grant awarded by National Geographic Society.

REFERENCES

Andrade, M., Soares, A.M., Solé, M., Pereira, E., Freitas, R., 2022. Will climate changes enhance the impacts of e-waste in aquatic systems? Chemosphere 288, 132264.

Arnon, D.I., 1949. Copper enzymes in isolated chloroplasts. Polyphenoloxidase in Beta vulgaris. Plant physiology 24, 1.

Ashraf, N., Vítová, M., Cloetens, P., Mijovilovich, A., Bokhari, S.N.H., Küpper, H., 2021. Effect of nanomolar concentrations of lanthanum on Desmodesmus quadricauda cultivated under environmentally relevant conditions. Aquatic Toxicology 235, 105818.

Binnemans, .K., McGuiness, P., Jones, P. T., 2021. Rare-earth recycling needs market intervention. Nature Reviews Materials 6, 459-461.

Bonanno, G., Veneziano, V., Raccuia, S.A., Orlando-Bonaca, M., 2020. Seagrass Cymodocea nodosa and seaweed Ulva lactuca as tools for trace element biomonitoring. A comparative study. Marine Pollution Bulletin 161, 111743.

Brito, P., Mil-Homens, M., Caçador, I., Caetano, M., 2020. Changes in REE fractionation induced by the halophyte plant *Halimione portucaloides,* from SW European salt marshes. Marine Chemistry 223, 103805.

Byrne, R., Sholkovitz, E., 1996. Marine chemistry and geochemistry of the lanthanides. Handbook on the physics and chemistry of rare earths 23, 497-593.

Cao, Y., Shao, P., Chen, Y., Zhou, X., Yang, L., Shi, H., Yu, K., Luo, X., Luo, X., 2021. A critical review of the recovery of rare earth elements from wastewater by algae for resources recycling technologies. Resources, Conservation and Recycling 169, 105519.

Costa, M., Henriques, B., Pinto, J., Fabre, E., Dias, M., Soares, J., Carvalho, L., Vale, C., Pinheiro-Torres, J., Pereira, E., 2020. Influence of toxic elements on the simultaneous uptake of rare earth elements from contaminated waters by estuarine macroalgae. Chemosphere 252, 126562.

Davis, T.A., Volesky, B., Mucci, A., 2003. A review of the biochemistry of heavy metal biosorption by brown algae. Water research 37, 4311-4330.

Fan, X., Xu, D., Wang, Y., Zhang, X., Cao, S., Mou, S., Ye, N., 2014. The effect of nutrient concentrations, nutrient ratios and temperature on photosynthesis and nutrient uptake by Ulva prolifera: implications for the explosion in green tides. Journal of Applied Phycology 26, 537-544.

Ferreira, N., Ferreira, A., Viana, T., Lopes, C.B., Costa, M., Pinto, J., Soares, J., Pinheiro-Torres, J., Henriques, B., Pereira, E., 2020. Assessment of marine macroalgae potential for gadolinium removal from contaminated aquatic systems. Science of the Total Environment 749, 141488.

Figueiredo, C., Raimundo, J., Lopes, A.R., Lopes, C., Rosa, N., Brito, P., Diniz, M., Caetano, M., Grilo, T.F., 2020. Warming enhances lanthanum accumulation and toxicity promoting cellular damage in glass eels (*Anguilla anguilla*). Environmental research 191, 110051.

Fletcher, R., 1996. The occurrence of "green tides"—a review. Marine benthic vegetation, 7-43.

Gao, G., Clare, A.S., Rose, C., Caldwell, G.S., 2017. Eutrophication and warming-driven green tides (Ulva rigida) are predicted to increase under future climate change scenarios. Marine Pollution Bulletin 114, 439-447.

Gao, G., Clare, A.S., Rose, C., Caldwell, G.S., 2018. *Ulva rigida* in the future ocean: potential for carbon capture, bioremediation and biomethane production. Gcb Bioenergy 10, 39-51.

Goecke, F., Jerez, C.G., Zachleder, V., Figueroa, F.L., Bišová, K., Řezanka, T., Vítová, M., 2015. Use of lanthanides to alleviate the effects of metal ion-deficiency in *Desmodesmus quadricauda* (Sphaeropleales, Chlorophyta). Frontiers in microbiology 6, 2.

González, V., Vignati, D.A., Pons, M.-N., Montarges-Pelletier, E., Bojic, C., Giamberini, L., 2015. Lanthanide ecotoxicity: First attempt to measure environmental risk for aquatic organisms. Environmental Pollution 199, 139-147.

Gwenzi, W., Mangori, L., Danha, C., Chaukura, N., Dunjana, N., Sanganyado, E., 2018. Sources, behaviour, and environmental and human health risks of high-technology rare earth elements as emerging contaminants. Science of the Total Environment 636, 299-313.

Habig, W.H., Pabst, M.J., Jakoby, W.B., 1974. Glutathione S-transferases: the first enzymatic step in mercapturic acid formation. Journal of biological chemistry 249, 7130-7139.

Hatje, V., K.W. Bruland, A.R. Flegal, 2014. Determination of rare earth elements after pre-concentration using NOBIAS-chelate PA-1®resin: Method development and application in the San Francisco Bay plume. Marine Chemistry 160, 34–41

Herrmann, H., Nolde, J., Berger, S., Heise, S., 2016. Aquatic ecotoxicity of lanthanum–A review and an attempt to derive water and sediment quality criteria. Ecotoxicology and Environmental Safety 124, 213-238.

IPCC, 2021: Summary for Policymakers. In: Climate Change 2021: The Physical Science Basis. Contribution of Working Group I to the Sixth Assessment Report of the Intergovernmental Panel on Climate Change [Masson-Delmotte, V., P. Zhai, A. Pirani, S.L. Connors, C. Péan, S. Berger, N. Caud, Y. Chen, L. Goldfarb, M.I. Gomis, M. Huang, K. Leitzell, E. Lonnoy, J.B.R. Matthews, T.K. Maycock, T. Waterfield, O. Yelekçi, R. Yu, and B. Zhou (eds.)]. In Press.

Ippolito, M., Fasciano, C., d'Aquino, L., Morgana, M., Tommasi, F., 2010. Responses of antioxidant systems after exposition to rare earths and their role in chilling stress in common duckweed (*Lemna minor* L.): a defensive weapon or a boomerang? Archives of environmental contamination and toxicology 58, 42-52.

Jacinto, J., Henriques, B., Duarte, A., Vale, C. and Pereira, E., 2018. Removal and recovery of Critical Rare Elements from contaminated waters by living *Gracilaria gracilis*. Journal of hazardous materials 344, 531-538.

Johansson, L.H., Borg, L.H., 1988. A spectrophotometric method for determination of catalase activity in small tissue samples. Analytical biochemistry 174, 331-336.

Joonas, E., Aruoja, V., Olli, K., Syvertsen-Wiig, G., Vija, H., Kahru, A., 2017. Potency of (doped) rare earth oxide particles and their constituent metals to inhibit algal growth and induce direct toxic effects. Science of the Total Environment 593, 478-486.

Kirk, J., Allen, R., 1965. Dependence of chloroplast pigment synthesis on protein synthesis: effect of actidione. Biochemical and Biophysical Research Communications 21, 523-530.

Kovaříková, M., Tomášková, I., Soudek, P., 2019. Rare earth elements in plants. Biologia plantarum 63, 20-32.

Lowry, O.H., Rosebrough, N.J., Farr, A.L., Randall, R.J., 1951. Protein measurement with the Folin phenol reagent. Journal of biological chemistry 193, 265-275.

Maulvault, A.L., Custódio, A., Anacleto, P., Repolho, T., Pousão, P., Nunes, M.L., Diniz, M., Rosa, R., Marques, A., 2016. Bioaccumulation and elimination of mercury in juvenile seabass (*Dicentrarchus labrax*) in a warmer environment. Environmental research 149, 77-85.

Mercado, J.M., Gordillo, F.J.L., Figueroa, F.L., Niell, F.X., 1998. External carbonic anhydrase and affinity for inorganic carbon in intertidal macroalgae. Journal of Experimental Marine Biology and Ecology 221, 209-220.

Ngwenya, B.T., Mosselmans, J.F.W., Magennis, M., Atkinson, K.D., Tourney, J., Olive, V., Ellam, R.M., 2009. Macroscopic and spectroscopic analysis of lanthanide adsorption to bacterial cells. Geochimica et Cosmochimica Acta 73, 3134-3147.

Olivares, H.G., Lagos, N.M., Gutierrez, C.J., Kittelsen, R.C., Valenzuela, G.L., Lillo, M.E.H., 2016. Assessment oxidative stress biomarkers and metal bioaccumulation in macroalgae from coastal areas with mining activities in Chile. Environmental monitoring and assessment 188, 1-11.

Pereira, P., de Pablo, H., Rosa-Santos, F., Pacheco, M., Vale, C., 2009. Metal accumulation and oxidative stress in *Ulva* sp. substantiated by response integration into a general stress index. Aquatic Toxicology 91, 336-345.

Pinto, J., Costa, M., Henriques, B., Soares, J., Dias, M., Viana, T., Ferreira, N., Vale, C., Pinheiro-Torres, J., Pereira, E., 2021. Competition among rare earth elements on sorption onto six seaweeds. Journal of Rare Earths 39, 734-741.

Pinto, J., Henriques, B., Soares, J., Costa, M., Dias, M., Fabre, E., Lopes, C.B., Vale, C., Pinheiro-Torres, J., Pereira, E., 2020. A green method based on living macroalgae for the removal of rare-earth elements from contaminated waters. Journal of environmental management 263, 110376.

Rodrigues, L.A., Cardeira, M., Leonardo, I.C., Gaspar, F.B., Redovniković, I.R., Duarte, A.R.C., Paiva, A., Matias, A.A., 2021. Deep eutectic systems from betaine and polyols–Physicochemical and toxicological properties. Journal of Molecular Liquids 335, 116201.

Sakamoto, N., Kano, N., Imaizumi, H., 2008. Determination of rare earth elements, thorium and uranium in seaweed samples on the coast in Niigata Prefecture by inductively coupled plasma mass spectrometry. Applied Geochemistry 23, 2955-2960.

Smith, V.H., Tilman, G.D., Nekola, J.C., 1999. Eutrophication: impacts of excess nutrient inputs on freshwater, marine, and terrestrial ecosystems. Environmental pollution 100, 179-196.

Sun, Y., Oberley, L.W., Li, Y., 1988. A simple method for clinical assay of superoxide dismutase. Clinical chemistry 34, 497-500.

Tyler, G., 2004. Rare earth elements in soil and plant systems-A review. Plant and soil 267, 191-206.

Uchida, N., Matsukami, H., Someya, M., Tue, N.M., Viet, P.H., Takahashi, S., Tanabe, S., Suzuki, G., 2018. Hazardous metals emissions from e-waste-processing sites in a village in northern Vietnam. Emerging Contaminants 4, 11-21.

Uchimura, M., Yoshida, G., Hiraoka, M., Komatsu, T., Arai, S., Terawaki, T., 2004. Ecological studies of green tide, *Ulva* spp.(chlorophyta) in hiroshima bay, the seto inland sea. Japanese Journal of Phycology 52, 17–22.

Uchiyama, M., Mihara, M., 1978. Determination of malonaldehyde precursor in tissues by thiobarbituric acid test. Analytical biochemistry 86, 271-278.

Wang, Y., Xu, D., Ma, J., Zhang, X., Fan, X., Zhang, Y., Wang, W., Sun, K., Ye, N., 2021. Elevated CO_2 accelerated the bloom of three *Ulva* species after one life cycle culture. Journal of Applied Phycology, 1-11.

PART FOUR

GENERAL CONSIDERATIONS AND FUTURE RESEARCH PERSPECTIVES

Chapter 11

The present PhD thesis constitutes a valuable contribution towards the understanding of REE bioaccumulation, elimination, the effects of the possible interactions of warming and/or acidification with it, and their induced ecotoxicological responses in aquatic significant species. The main goal of this thesis was to deliver key knowledge on these emergent problematics. Data provided by this PhD dissertation, interpreted in an integrated way, replied to the previously asked research questions while leading to the rise of several research perspectives that future studies should address to complement the information delivered by this dissertation.

1. Will depth, location and season affect REE bioaccumulation in good biomonitoring species?

Rare earth elements concentrations in *Mytilus galloprovincialis* from six locations along the Portuguese coast during autumn and spring, described in chapter 2, revealed that samples from Porto Brandão showed the highest REE concentrations. In the Tagus estuary, where Porto Brandão is located, wastewater treatment plants effluents of about 2.8 million inhabitants, industries, agriculture, and an inactive chemical-industrial complex constitute important sources of REE that contribute to the greatest concentration of REE in this samples. Furthermore, increased rain and surface runoff in autumn appear to contribute to increased Y concentrations in this samples as they are subject of an open-air phosphogypsum stack (Brito et al., 2018; Cánovas et al., 2018). On another hand, ∑REE concentration was greater in the spring. LREE enrichment relative to HREE occurred which is in line with the REEs natural behavior in the environment (Akagi and Edanami, 2017; Briant et al., 2021; Wang et al., 2019). Furthermore, LREE are more soluble, which may indicate that they are more bioavailable than HREE (Pratas et al., 2017). Finally, a negative Ce and Eu anomaly was observed which indicates that both were less available during autumn, probably due to the redox condition seasonal changes.

Rare earth element levels in five porifera genera (*Jaspis, Geodia, Hamacantha, Leiodermatium, Poliopogon*) collected in deep-sea areas (between 481 and 2656 m) of the North Atlantic, described in chapter 3, showed an increased REE concentration compared with other sponge specimens from different locations, probably influenced by volcanic activity as this has been recognized as a natural source of trace elements (Charlou et al., 2002; Douville et al., 2002; Raimundo et al., 2013b) and are characteristic of the deep-seafloor in the Mid Atlantic area. Alike the previously described study, the specimens presented LREE enrichment in comparison to HREE and a negative Ce anomaly with a less pronounced Eu depletion, reflecting the low availability of these elements in the water (Mitra et al., 1994).

Overall, depth, location, and season impact REE bioaccumulation. The results suggest that the studied mollusk species may be deemed as a good bioindicator of REE contamination, however future research should accompany these records with environmental data, for an integrated and critical understanding of the REE accumulation processes. Furthermore, biomarkers information should also integrate upcoming studies on REE biomonitoring. Likewise, future research should compare sponge species elemental load with that of the water and sediments from the same sample locations to better evaluate its potential as tools for biomonitoring studies. Further insights into the speciation of REE into the water column, the organisms and their symbionts will be key to unveil the processes behind REE bioaccumulation. Finally, sampling the deep-sea floor is challenging and enormously expensive, and obtained samples are of extreme importance/value, however further studies should attempt to analyze a greater number of individuals.

2. Will warming and acidification affect REE availability in water?

The knowledge on the interactions between climate change (i.e., warming and acidification) and REE was, before this dissertation, non-existent. Although described as chemically analogous, La and Gd behaved differently at different salinities, as illustrated in chapter 4. A temperature rise of 4°C in freshwater increases La availability while a pH decrease of 0.4 points decreases Gd availability. At present day conditions, for salinity 0, La decreased 67% over 24h, while the Gd decreased 42%. This divergence may be related to greater La adsorption to the glass beaker, air tubes or the pH probe, and due

to other confounding factors, such as the concentration of free ions (Aharchaou et al., 2020). The La and Gd removal were lower at salinity 15, due to adsorption and/or precipitation reactions. At salinity 15 the La levels in the Warming and Warming & Acidification treatment differed across time, which emphasizes the effect of temperature in their availability. Although dissolved La and Gd levels in seawater were the most stable, the free ions La^{3+} and Gd^{3+} presented globally lower availability which may influence the toxicity responses. Hence, in studies longer than 24h, biota will be exposed to different elemental species and levels and the derived biological effects may shift. Therefore, the desired REE exposure concentration should be monitored in a shorter time scale or additional actions of changing the medium and re-spiking should be done to maintain conditions in future studies. Therefore, future research on REE bioaccumulation and toxicity, in present day and near future conditions, should explore and show REE availability in the exposure medium (e.g., water) to deliver a more complete outline of the accumulation, elimination and toxicological processes. Furthermore, as the range of REE concentrations varies greatly depending on the aquatic system, a broader assortment of concentrations should be tested in upcoming studies. Nevertheless, the objective of setting the baseline knowledge by which future research towards understanding REE patterns and toxicity in climate change conditions will build upon was attained.

3. Will warming and/or acidification interact with REE bioaccumulation and affect species' ecotoxicological responses?

The empirical findings gathered in this dissertation and described in chapter 5 show that 120 ng L^{-1} La in freshwater aliquots remained relatively stable in the first 24h, which is not in accordance with the previous La availability results in freshwater, probably due to the different exposure concentrations used. When glass eels (*Anguilla anguila*) were exposed to 120 ng L^{-1} of La, the highest La accumulation values were registered in the first 3 days of exposure, and afterwards the La levels dropped. Exposed eels showed lower MDA, which could reflect the absence of lipid membrane damage. On another hand, catalase inhibition in exposed samples occurred, showcasing the physiological impairment caused by La and that this element caused oxidative damage

to glass eels. Hence, for a better understanding of the biological effects of La, future studies should encompass master water parameters (e.g., water hardness, temperature, pH, major ions) and different levels of La, complemented with determinations of non-enzymatic protective molecules, indicative of protein and DNA damage, for example. The timescale of the experiment should be better detailed in the first 72h of accumulation, which proved to be critical, to provide a more decisive elucidation of the extended effects of environmental relevant concentrations of La in fish species.

Considering the scientific knowledge derived from the previous experiment, a slightly higher La exposure concentration in European glass eels (*A. anguilla*) was applied La (1.5 µg L^{-1}). As expressed in chapter 6, in a warming scenario the bioavailability of La in freshwater is slightly enhanced. The increased temperature may interfere in air-surface exchange, deposition, and reaction rates (e.g., photolysis, biodegradation, oxidation in the air). Overall, the accumulation and toxicity of La were enhanced with increasing temperature. Although with a distinct accumulation patter, an unknown mechanism to cope with La contamination was also evident, such as in Figueiredo et al. (2018). Nevertheless, elimination was less efficient under warming. When exposed to La, glass eels' will be unable to stabilize and refold denatured proteins, and prevent cellular damage, with a particular dramatic setup in a near-future scenario. The results highlight the effects of La on the DNA, and the inability of eels to recover after being exposed to a La-contaminated environment. This was the first study addressing the combined effects of a climate change variable, specifically thermal stress, and La. Dose responses are vital in toxicology and the assessment of the effects of La will depend on them. Furthermore, the influence of other water parameters, such as water hardness and major ions content, in the La availability and toxicity should also be considered in future studies.

On the first study on the differential tissue accumulation of La in a bivalve species, the manila clam (*Ruditapes phillipinarum*) one day of exposure to La, was insufficient to trigger accumulation, probably due to the ability of bivalves to reduce filtration rates when exposed to pollutants (e.g., Almeida et al., 2015), as discussed in Chapter 7. This ability seems to be limited as after 2 days of exposure accumulation occurred in all body parts. The body presented the lowest accumulation values, which is consistent with previous ecotoxicological studies with other metals on the same species.

The gills and the digestive gland accumulated similar quantities of La, which may be related to the short exposure period used in this trial (6 days). In a longer exposure experiment a clear difference between the gills, a key interface for the uptake of contaminants from the water, and the digestive gland, a vital detoxification tissue, could occur and this should be taken into consideration in upcoming research. Furthermore, future studies should replicate these trials with an increased gap between the environmentally realistic exposure concentrations studied while evaluating the elimination rate of this element. Furthermore, future studies should investigate La effects, equally on a cellular, tissue, and individual level, by means of, for example, quantification of stress biomarkers in the first days of exposure to the same range of environmental realistic La concentrations, as we must adopt a holistic approach to better understand REE toxicology and its effects on species sustainability and human health.

On the study described in chapter 8, La was bioaccumulated by the surf clam (*Spisula solida*) after just one day, in all exposure experimental treatments. Concentrations increased overtime and seemed to not be affected by the increased temperature or CO_2. The results indicate a lasting effect on the oxidative stress response, with probable consequences on individuals' fitness. Additionally, La exposure in an acidification setting constrained HSP expression, in comparison to La exposure alone. This highlights that La exposure will trigger a particularly deleterious outcome in a climate change scenario. This result also highpoints that although the superfamily GST was activated, it was insufficient to detoxify La. Lipid damage occurred on the 7^{th} day of exposure to climate change alone and was greater in clams exposed to warming and acidification together with La, which highpoints the enhanced toxic effects of this REE in near future conditions. As a no relationship between biomarker levels and the effects of climate change on bivalve species whole-organisms level (e.g., survival and burial ability) have been described (Joyner-Matos et al. 2009), future studies on the interactions of REE and climate change should complement biomarker information with additional outcomes (e.g., behavior, feeding rates and respirometry).

Regarding the trial with the similar experimental design exposing the same model to 10 µg L^{-1} Gd, presented in Chapter 9, synergetic effects of warming and Gd

were observed. Overall, results show that Gd is the main driver of the oxidative stress response, however, their impact may be exacerbated by warming and/or acidification. The heat shock response was incapable of guaranteeing ideal protein function and ubiquitin, in the presence of Gd, could not target those proteins to be eliminated. Clams were not able to proficiently regulate the oxidative stress response in the presence of multiple stressors and the combination of Warming & Gd triggered lipid damage, which emphasizes the enhanced toxic effects of Gd in a changing ocean and suggest that deleterious impacts to the population of surf clams are likely to be exacerbated soon. Overall, results emphasize the significance of better understanding the REE accumulation pattern by employing more frequent sampling events within the exposure period and having in consideration the knowledge gap information on both La and Gd elimination, future studies should complement the information derived in this dissertation on organisms' capacity to withhold pollution events.

Upon assessing the ecotoxicological responses and total chlorophyll and carotenoid content of *Ulva rigida* after 7 days of exposure to La or Gd (15 µg L^{-1} or 10 µg L^{-1}, respectively), and warming (+4°C) and acidification (-0.4 pH units), as stated in Chapter 10, results show that one day was sufficient for La and Gd to be accumulated and/or adsorbed. Interestingly, a distinct La and Gd accumulation pattern, in future conditions, occurred as Warming and Acidification contributed to the lowest La levels, and increased La elimination, but not Gd. Neither La nor Gd were eliminated in a 7-day elimination period, as occurred in the bivalve species *S. solida* exposed to the same concentration of these elements. The *Ulva rigida*' accumulation results suggest that REE uptake is greater in the first hours of exposure, however the uptake can be upheld for a long period, and future research should increase exposure duration without disregarding frequent sampling of biological material and quantification of REE levels in water. The exposure to both elements adequately activated the antioxidant defense system, by avoiding lipid damage and this response seemed to be quicker in the case of Gd exposure. REE exposure in a near future scenario triggered an overproduction of ROS. Furthermore, an increased total chlorophyll and carotenoids in REE exposure treatments, particularly when combined with climate change, could indicate an unforeseen energy expense to the biosynthesis of pigments, at the cost of growth and reproduction, as a response to a multi-stressor environment. This indicates that

although the antioxidant defense system was activated and appeared to prevent lipid damage, the outcomes of REE exposure in a changing environment may be more severe.

The severe lack of scientific knowledge on the pertinent issues that relate the combined effects of climate change variables on REE accumulation, elimination, and toxicological outcomes, highlights the urgent necessity for further studies to be conducted on a wider array of model species and REE elements in forecasted climate change scenarios. Whenever possible, future studies should also increase the number of samples studied as great variability in stress biomarkers were encountered. Furthermore, a broader set of environmentally realistic exposure concentrations may be applied as a previously discussed biphasic effect may occur with increasing concentrations. Finally, future research should also consider a broader set of climate change-related stressors such as dissolved oxygen, UV-radiation, salinity, and other altered variables in a regional point of view. This is of extreme importance towards understanding the impacts of climate change and emergent pollutants on aquatic ecosystems across the globe as it is being affected differently.

REFERENCES

Aharchaou, I., Beaubien, C., Campbell, P.G., Fortin, C., 2020. Lanthanum and cerium toxicity to the freshwater green alga Chlorella fusca: applicability of the Biotic Ligand Model. Environmental toxicology and chemistry 39, 996-1005.

Akagi, T., Edanami, K., 2017. Sources of rare earth elements in shells and soft-tissues of bivalves from Tokyo Bay. Marine Chemistry 194, 55-62.

Almeida A., Freitas R., Calisto V., Esteves V., Schneider R., Soares A. M. V. M., Figueira, E., 2015. Chronic toxicity of the antiepileptic carbamazepine on the clam *Ruditapes philippinarum*. Comparative Biochemistry and Physiology – Part C: Toxicology & Pharmacology, 172– 173, 26–35.

Briant, N., Le Monier, P., Bruzac, S., Sireau, T., Araújo, D.F., Grouhel, A., 2021. Rare Earth Element in Bivalves' Soft Tissues of French Metropolitan Coasts: Spatial and Temporal Distribution. Archives of Environmental Contamination and Toxicology, 1-12.

Brito, P., Prego, R., Mil-Homens, M., Caçador, I., Caetano, M., 2018. Sources and distribution of yttrium and rare earth elements in surface sediments from Tagus estuary, Portugal. Science of The Total Environment 621, 317-325.

Cánovas, C.R., Macías, F., López, R.P., Nieto, J.M., 2018. Mobility of rare earth elements, yttrium and scandium from a phosphogypsum stack: Environmental and economic implications. Science of the Total Environment 618, 847-857.

Figueiredo, C., Grilo, T.F., Lopes, C., Brito, P., Diniz, M., Caetano, M., Rosa, R., Raimundo, J., 2018. Accumulation, elimination and neuro-oxidative damage under lanthanum exposure in glass eels (*Anguilla anguilla*). Chemosphere 206, 414-423.

Figueiredo, C., Raimundo, J., Lopes, A. R., Lopes, C., Rosa, N., Brito, P., Diniz, M., Caetano, M., Grilo, T. F., 2020. Warming enhances lanthanum accumulation and toxicity promoting cellular damage in glass eels (*Anguilla anguilla*). Environmental research, 191, 110051.

Freitas, R., Costa, S., Cardoso, C.E., Morais, T., Moleiro, P., Matias, A.C., Pereira, A.F., Machado, J., Correia, B., Pinheiro, D., 2020. Toxicological effects of the rare earth element neodymium in *Mytilus galloprovincialis*. Chemosphere 244, 125457.

Joyner-Matos, J., Andrzejewski, J., Briggs, L., Baker, S.M., Downs, C.A., Julian, D., 2009. Assessment of cellular and functional biomarkers in bivalves exposed to ecologically relevant abiotic stressors. Journal of aquatic animal health 21, 104-116.

Pratas, J., Favas, P.J., Varun, M., D'Souza, R., Paul, M.S., 2017. Distribution of rare earth elements, thorium and uranium in streams and aquatic mosses of Central Portugal. Environmental Earth Sciences 76, 156.

Ramalho, J., Semelka, R., Ramalho, M., Nunes, R., AlObaidy, M., Castillo, M., 2016. Gadolinium-based contrast agent accumulation and toxicity: an update. American Journal of Neuroradiology 37, 1192-1198.

Wang, Z., Yin, L., Xiang, H., Qin, X., Wang, S., 2019. Accumulation patterns and species-specific characteristics of yttrium and rare earth elements (YREEs) in biological matrices from Maluan Bay, China: Implications for biomonitoring. Environmental research 179, 108804.

ANNEXES

ANNEX 1

THESIS SCIENTIFIC OUTPUTS, GRANTS AND AWARDS

PUBLICATIONS

Figueiredo, C., Oliveira, R., Lopes, C., Brito, P., Caetano, M., Raimundo, J., 2022. Rare earth elements biomonitoring using the mussel *Mytilus galloprovincialis* in the Portuguese coast: seasonal variations. Marine Pollution Bulletin 175, 113335**. DOI 10.1016/j.marpolbul.2022.113335**

Figueiredo, C., Caetano, M., Mil-Homens, M., Tojeira, I., Xavier, J.R., Rosa, R., Raimundo, R., 2021. Rare earth and trace elements in deep-sea sponges of the North Atlantic. Marine Pollution Bulletin **DOI 10.1016/j.marpolbul.2021.112217**

Figueiredo, C., Grilo T.F., Lopes, C., Brito, P., Caetano, M., Raimundo, J., 2022. Lanthanum and gadolinium availability in aquatic mediums: new insights to ecotoxicology and environmental studies. Journal of Trace elements in Medicine and Biology 71, 136957. **DOI 10.1016/j.jtemb.2022.126957**

Figueiredo, C.[#], Grilo, T.F.[#], Lopes, C., Brito, P., Diniz, M., Caetano, M., Rosa, R., Raimundo, J., 2018. Accumulation, elimination and neuro-oxidative damage under lanthanum exposure in glass eels (*Anguilla anguilla*). Chemosphere 70, 35-42. **DOI 10.1016/j.chemosphere.2018.05.029**

Figueiredo, C.*, Raimundo, J.*, Lopes, A.R., Lopes, C., Rosa, N., Brito, P., Diniz, M., Caetano, M., Grilo, T.F., 2020. Warming enhances lanthanum accumulation and toxicity promoting celular damage in glass eels (*Anguilla anguilla*). Environmental Research 191, 110051. **DOI 10.1016/j.envres.2020.110051**

Figueiredo, C., Grilo, T.F., Lopes, A.R., Lopes, C., Brito, P., Caetano, M., Raimundo, J., 2022. Differential tissue accumulation in the invasive manila clam, *Ruditapes philippinarum* under two environmentally relevant lanthanum concentrations. Environmental Monitoring and Assessment 194:11. **DOI 10.1007/s10661-021-09666-y**

Figueiredo, C., Grilo, T.F., Oliveira, R., Ferreira, I.J., Gil, F., Lopes, C., Brito, P., Ré, P., Caetano, M., Diniz, M., Raimundo, J., 2022. Single and combined ecotoxicological effects of ocean warming, acidification and lanthanum exposure on the surf clam (*Spisula solida*). Chemosphere 302, 134850. **DOI 10.1016/j.chemosphere.2022.134850**

Figueiredo, C., Grilo, T.F., Oliveira, R., Ferreira, I.J., Gil, F., Lopes, C., Brito, P., Ré, P., Caetano, M., Diniz, M, Raimundo, J., 2022. Enhanced ecotoxicity of Gadolinium in a warmer and acidified changing ocean using a multibiomarker approach: the case of the surf clam *Spisula solida*. Accepted for publication in Aquatic Toxicology.

Figueiredo, C., Grilo, T.F., Oliveira, R., Ferreira, I.J., Gil, F., Lopes, C., Brito, P., Caetano, M., Ré, P., Caetano, M, Diniz, M., Raimundo, J., 2022. A triple threat: ocean warming, acidification and REE exposure triggers a superior antioxidant response and pigment production in the adaptable *Ulva rigida*. Environmental Advances 8, 100235. **DOI 10.1016/j.envadv.2022.100235**

ORAL PRESENTATIONS

Figueiredo, C., Lopes, A. R., Carvalho, F., Pinto, E., Lopes, C., Diniz, M., Caetano, M., Grilo, T. F., Raimundo, J. (2019) Lanthanum accumulation, elimination and Lipid and DNA damage in glass eels (*Anguilla anguilla*) under a warming scenario. CHEERS – Global changes in estuarine and coastal systems: innovative approaches and assessment tools, November 4-8, Bordeaux, France.

Figueiredo, C., Lopes, A. R., Carvalho, F., Pinto, E., Lopes, C., Diniz, M., Rosa, R., Caetano, M., Grilo, T.F., Raimundo, J. (2019) Lanthanum accumulation, elimination and lipid and DNA damage in glass eels (*Anguilla anguilla*) under a warming scenario. Final meeting of COST Action TD1407 (Technology-critical elements – Sources chemistry and toxicology), 2-3 April, Zagreb, Croatia.

Figueiredo, C., Grilo, T.F., Sampaio, E., Borges, F., Brito, P., Lopes, C., Caetano, M., Rosa, R., Raimundo, J. (2017) Accumulation and elimination potential of lanthanum-exposed glass eels and linked oxidative stress responses. PRIMO – 19th International Symposium on Pollutant Responses of Marine Organisms. Matsuyama, Japan

POSTER PRESENTATIONS

Figueiredo, C., Lopes, C., Diniz, M., Grilo, T. F., Raimundo, J. (2019) Accumulation, elimination, and oxidative stress in glass eels (*Anguilla Anguilla*) exposed to Lanthanum under a warming scenario. 42nd CIESM Congress – The Mediterranean Science Commission. 7-11 November, Estoril, Portugal.

Figueiredo, C., Grilo, T.F., Lopes, C., Brito, P., Diniz, M., Caetano, M., Rosa, R., Raimundo, R. (2018) Accumulation, elimination, and neuro-oxidative damage under lanthanum exposure in glass eles (*Anguilla anguilla*). SETAC North America 39th Annual Meeting – Bridging Divides Between Environmental Stewardship and Economic Development. 4-8 November, Sacramento, CA, USA.

Figueiredo, C., Grilo, T.F., Lopes, C., Brito, P., Diniz, M., Caetano, M., Rosa, R., Raimundo, R. (2018) Accumulation, elimination, and cellular responses under lanthanum exposure in glass eles (*Anguilla Anguilla*) and potential shifts in a changing ocean. 4th International Climate Change Symposium, The Effects of Climate Change in the World's Oceans (PICES). 2-8 June, Washington, USA.

BEST PRESENTATION AWARD

Birgit Daus AWARD – best 'out-of-the box' communication in the final meeting of COST Action TD1407 (Technology-critical elements – Sources, chemistry, and toxicology), Zagreb 2-3 April 2019.

PhD GRANT

Thesis topic: "Effects of Rare Earth Elements on marine organisms under a changing ocean", 2017-2021. Fully funded PhD grant by Fundação para a Ciência e Tecnologia.

FINANCIAL SUPPORT GRANTS

Final meeting "Technology-critical elements – Sources chemistry and toxicology" in Zagreb, Croatia (2019). Fully paid expenses (708€) by COST Action TD1407.

Support for Woman and Dependent Care (2018). (2197 USD) sponsored by National Geographic.

CONFERENCE GRANT

"Host-Parasite interactions (TiBE 2018)". Registration and travel expenses (400 €) sponsored by tebu-bio, Innovative Lab Services & Reagents.

TRAVEL GRANTS

"SETAC North America 39th Annual Meeting – Bridging Divides Between Environmental Stewardship and Economic Development. 4-8 November 2018, Sacramento, CA, USA". Travel expenses (400 USD) sponsored by SETAC North America.

"PRIMO - 19th International Symposium on Pollutant Responses of Marine Organisms,

2017 Matsuyama, Japan". Travel expenses (JPYen 50,000) sponsored by PRIMO.

SCIENTIFIC PROJECT GRANT

4,400 USD for the project: "Effects of Rare Earth Elements on marine organisms under a changing ocean" (2019). Sponsored by National Geographic Society's Committee for Research and Exploration as an Early Career Research Grant.

VOLUNTEERING

Volunteer in the organization of the "42nd CIESM Congress" by CIESM – The Mediterranean Science Committee in Estoril, Portugal 6-12 October 2019.

ANNEX 2

SUPPLEMENTARY INFORMATION FOR CHAPTER 2

Supplemental Table 2.1 - Statistical comparisons (1-way ANOVA) of REE, LREE and HREE content between different seasons (Autumn and Spring). Bold indicate significant differences ($p < 0.05$).

		1-way ANOVA effect	df	Sum of Squares	Mean sum of squares	F-test	p-value
Carreço	REE+Y	Autumn vs Spring	1	0.031	0.031	12.20	**0.0007**
		Residual	131	0.337	0.003		
	LREE	Autumn vs Spring	1	0.013	0.013	17.77	**<0.0001**
		Residual	131	0.092	0.001		
	HREE	Autumn vs Spring	1	0.005	0.005	11.90	**0.0008**
		Residual	131	0.060	0.000		
Leça da Palmeira	REE+Y	Autumn vs Spring	1	0.003	0.003	1.69	0.1961
		Residual	112	0.166	0.001		
	LREE	Autumn vs Spring	1	0.000	0.000	1.10	0.2958
		Residual	112	0.034	0.000		
	HREE	Autumn vs Spring	1	0.002	0.002	4.81	**0.0304**
		Residual	112	0.037	0.000		
Porto Brandão	REE+Y	Autumn vs Spring	1	0.032	0.032	2.83	0.0959
		Residual	100	1.148	0.011		
	LREE	Autumn vs Spring	1	0.019	0.019	7.69	**0.0066**
		Residual	100	0.242	0.002		
	HREE	Autumn vs Spring	1	0.006	0.006	2.23	0.1385
		Residual	100	0.250	0.003		
Costa da Caparica	REE+Y	Autumn vs Spring	1	0.021	0.021	1.79	0.1839
		Residual	102	1.221	0.012		
	LREE	Autumn vs Spring	1	0.001	0.001	0.70	0.4034
		Residual	102	0.206	0.002		
	HREE	Autumn vs Spring	1	0.006	0.006	2.23	0.1387
		Residual	102	0.290	0.003		
Mira	REE+Y	Autumn vs Spring	1	0.082	0.082	13.79	**0.0003**
		Residual	101	0.597	0.006		
	LREE	Autumn vs Spring	1	0.030	0.030	19.16	**<0.0001**
		Residual	101	0.160	0.002		
	HREE	Autumn vs Spring	1	0.011	0.011	9.69	**0.0024**
		Residual	101	0.115	0.001		
Aljezur	REE+Y	Autumn vs Spring	1	0.000	0.000	1.10	0.2973
		Residual	89	0.028	0.000		
	LREE	Autumn vs Spring	1	0.000	0.000	7.39	**0.0079**
		Residual	89	0.006	0.000		
	HREE	Autumn vs Spring	1	0.000	0.000	0.13	0.7199
		Residual	89	0.006	0.000		

| ANNEX 2

Supplemental Table 2.2 a) - 1-way ANOVA with locations as factor for REE, LREE and HREE content, for Spring and for Fall. Bold indicate significant differences ($p < 0.05$).

		1-way ANOVA effect	df	Sum of Squares	Mean sum of squares	F-test	p-value
Spring	REE	All locations	5	0.657	0.131	30.48	**<0.0001**
		Residual	326	1.405	0.004		
	LREE	All locations	5	0.165	0.033	29.71	**<0.0001**
		Residual	326	0.362	0.001		
	HREE	All locations	5	0.144	0.029	33.45	**<0.0001**
		Residual	326	0.280	0.001		
Fall	REE	All locations	5	0.347	0.069	10.23	**<0.0001**
		Residual	309	2.093	0.007		
	LREE	All locations	5	0.056	0.011	9.18	**<0.0001**
		Residual	309	0.378	0.001		
	HREE	All locations	5	0.084	0.017	10.88	**<0.0001**
		Residual	309	0.478	0.002		

Supplemental Table 2.2 b) - Tukey's pairwise comparisons for each location, in each season. Bold indicate significant differences ($p < 0.05$).

Tukey's pairwise comparison p value								
			Carreço	Leça da Palmeira	Porto Brandão	Costa da Caparica	Mira	Aljezur
Fall	REE	Carreço		0.9924	**0.0119**	0.9697	0.6432	**0.0005**
		Leça da Palmeira	0.9924		**0.0039**	0.8003	0.9357	**0.0084**
		Porto Brandão	**0.0119**	**0.0039**		0.165	**0.0002**	**< 0.0001**
		Costa da Caparica	0.9697	0.8003	0.165		0.2786	**< 0.0001**
		Mira	0.6432	0.9357	**0.0002**	0.2786		0.1718
		Aljezur	**0.0005**	**0.0084**	**< 0.0001**	**< 0.0001**	0.1718	
			Carreço	Leça da Palmeira	Porto Brandão	Costa da Caparica	Mira	Aljezur
	LREE	Carreço		0.9479	0.3014	0.9996	0.5027	**< 0.0001**
		Leça da Palmeira	0.9479		0.0658	0.9948	0.9545	**0.0014**
		Porto Brandão	0.3014	0.0658		0.2356	**0.0085**	**< 0.0001**
		Costa da Caparica	0.9996	0.9948	0.2356		0.7541	**0.0002**
		Mira	0.5027	0.9545	**0.0085**	0.7541		**0.0449**
		Aljezur	**< 0.0001**	**0.0014**	**< 0.0001**	**0.0002**	**0.0449**	
			Carreço	Leça da Palmeira	Porto Brandão	Costa da Caparica	Mira	Aljezur
	HREE	Carreço		0.999	**0.0013**	0.6851	0.8376	**0.0032**
		Leça da Palmeira	0.999		**0.0008**	0.5162	0.9672	**0.0199**
		Porto Brandão	**0.0013**	**0.0008**		0.1806	**< 0.0001**	**< 0.0001**
		Costa da Caparica	0.6851	0.5162	0.1806		0.1561	**< 0.0001**
		Mira	0.8376	0.9672	**< 0.0001**	0.1561		0.2193
		Aljezur	**0.0032**	**0.0199**	**< 0.0001**	**< 0.0001**	0.2193	
			Carreço	Leça da Palmeira	Porto Brandão	Costa da Caparica	Mira	Aljezur
Spring	REE	Carreço		0.1295	**0.0001**	**0.002**	1	**< 0.0001**
		Leça da Palmeira	0.1295		**< 0.0001**	0.7088	0.0881	**< 0.0001**
		Porto Brandão	**0.0001**	**< 0.0001**		**< 0.0001**	**0.0003**	**< 0.0001**
		Costa da Caparica	**0.002**	0.7088	**< 0.0001**		0.0011	**0.0081**
		Mira	1	0.0881	**0.0003**	**0.0011**		**< 0.0001**
		Aljezur	**< 0.0001**	**< 0.0001**	**< 0.0001**	**0.0081**	**< 0.0001**	

Supplemental Table 2.2 b Cont.

Tukey's pairwise comparison p value							
		Carreço	Leça da Palmeira	Porto Brandão	Costa da Caparica	Mira	Aljezur
LREE	Carreço		**0.006**	**0.012**	**0.0001**	0.9917	**< 0.0001**
	Leça da Palmeira	**0.006**		**< 0.0001**	0.8654	**0.0006**	**0.0006**
	Porto Brandão	**0.012**	**< 0.0001**		**< 0.0001**	0.0654	**< 0.0001**
	Costa da Caparica	**0.0001**	0.8654	**< 0.0001**		**< 0.0001**	**0.0402**
	Mira	0.9917	**0.0006**	0.0654	**< 0.0001**		**< 0.0001**
	Aljezur	**< 0.0001**	**0.0006**	**< 0.0001**	**0.0402**	**< 0.0001**	
		Carreço	Leça da Palmeira	Porto Brandão	Costa da Caparica	Mira	Aljezur
HREE	Carreço		0.6594	**< 0.0001**	**0.0162**	1	**< 0.0001**
	Leça da Palmeira	0.6594		**< 0.0001**	0.4804	0.7723	**< 0.0001**
	Porto Brandão	**< 0.0001**	**< 0.0001**		**< 0.0001**	**< 0.0001**	**< 0.0001**
	Costa da Caparica	**0.0162**	0.4804	**< 0.0001**		**0.0281**	**0.001**
	Mira	1	0.7723	**< 0.0001**	**0.0281**		**< 0.0001**
	Aljezur	**< 0.0001**	**< 0.0001**	**< 0.0001**	**0.001**	**< 0.0001**	

ANNEX 3

SUPPLEMENTARY INFORMATION FOR CHAPTER 4

Supplemental Table 4.1 – Mean and SD (standard deviation) of La and Gd levels (µg L^{-1}) in non-spiked and spiked fresh-(Sal 0), brackish- (Sal 15), and saltwater seawater (Sal 35) sampled at 15', 30', 1h, 2h, 4h, 6h, 12h and 24h for all treatments. * Due to technical issues this sampling point could not be evaluated.

Lanthanum

		Control				La (µg L^{-1}) treatments			
	Time	Present-day conditions	Warming	Acidification	Warming + Acidification	Present-day conditions	Warming	Acidification	Warming + Acidification
Sal 0	15'	< 0.022				0.64±0.031	1.3±0.054	0.70±0.011	1.1±0.039
	30'					0.61±0.025	1.1±0.018	0.68±0.016	0.96±0.023
	1h					0.53±0.021	1.1±0.018	0.59±0.018	0.92±0.038
	2h					0.43±0.016	1.0±0.01	0.47±0.004	0.78±0.036
	4h					0.34±0.011	0.91±0.006	0.39±0.018	0.70±0.017
	6h					0.30±0.008	0.83±0.02	0.35±0.007	0.65±0.018
	12h					0.25±0.010	0.69±0.003	0.30±0.010	0.55±0.017
	24h					0.20±0.010	0.61±0.011	0.30±0.007	0.44±0.011
Sal 15	15'	< 0.024	0.05±0.008	0.08±0.004	0.04±0.001	1.5±0.237	1.5±0.088	1.5±0.039	1.5±0.041
	30'	0.07±0.002	< 0.024	0.07±0.004	0.03±0.001	1.5±0.063	1.4±0.059	1.5±0.134	1.3±0.046
	1h	0.06±0.002	< 0.024	0.05±0.002	< 0.024)	1.5±0.022	1.3±0.088	1.5±0.148	1.2±0.031
	2h	< 0.024	0.08±0.002	0.03±0.002	0.08±0.003	1.3±0.035	1.4±0.139	1.5±0.036	1.2±0.026
	4h	0.07±0.006	< 0.024	< 0.024	0.1±0.002	1.2±0.032	1.2±0.026	1.3±0.054	1.1±0.04
	6h	0.07±0.004	0.07±0.013	< 0.024	< 0.024	1.1±0.005	1.1±0.05	1.3±0.047	0.90±0.041
	12h	< 0.024	0.06±0.017	< 0.024	< 0.024	1.0±0.012	1.0±0.042	1.1±0.029	0.79±0.033
	24h	< 0.024	< 0.024	0.09±0.007	< 0.024	0.83±0.036	0.85±0.01	1.1±0.025	0.62±0.075
Sal 35	15'	< 0.034	< 0.034	< 0.034	< 0.034	1.2±0.050	1.3±0.064	1.5±0.030	1.4±0.020
	30'	0.09±0.003	< 0.034	< 0.034	< 0.034	1.4±0.023	1.1±0.044	1.2±0.038	1.1±0.075
	1h	0.09±0.003	< 0.034	0.04±0.001	< 0.034	1.2±0.027	1.2±0.041	1.2±0.030	1.3±0.028
	2h	0.04±0.001	0.07±0.005	< 0.034	0.08±0.004	1.0±0.037	1.1±0.052	1.1±0.035	1.1±0.021
	4h	0.07±0.010	0.06±0.009	< 0.034	< 0.034	1.2±0.055	1.4±0.046	1.1±0.031	1.0±0.102
	6h	0.09±0.006	< 0.034	< 0.034	0.05±0.001	1.2±0.026	1.3±0.032	1.2±0.061	1.1±0.045
	12h	< 0.034	0.05±0.001	< 0.034	0.04±0.003	1.1±0.036	1.0±0.040	1.1±0.034	1.1±0.032
	24h	0.04±0.007	0.04±0.002	< 0.034	< 0.034	1.0±0.025	1.1±0.040	1.0±0.030	1.1±0.034

Gadolinium

		Control				Gd (µg L^{-1}) treatment			
	Time	Present-day conditions	Warming	Acidification	Warming + Acidification	Present-day conditions	Warming	Acidification	Warming + Acidification
Sal 0	15'	< 0.006				0.43±0.033	0.47±0.007	0.38±0.027	0.56±0.028
	30'					0.37±0.022	0.43±0.030	0.34±0.020	0.51±0.022
	1h					0.32±0.035	0.38±0.033	0.29±0.019	0.44±0.023
	2h					0.32±0.010	0.32±0.011	0.26±0.018	0.36±0.013
	4h					0.31±0.004	0.24±0.057	0.18±0.082	0.29±0.010
	6h					0.29±0.009	0.26±0.003	0.20±0.008	0.23±0.005
	12h					0.27±0.006	0.22±0.009	0.16±0.005	0.17±0.005
	24h					0.25±0.005	0.17±0.007	0.13±0.006	0.13±0.004
Sal 15	15'	0.10±0.003	0.06±0.002	< 0.016	0.04±0.003	0.98±0.052	0.95±0.029	1.0±0.043	0.85±0.017
	30'	0.09±0.007	0.06±0.002	0.06±0.003	0.07±0.005	0.98±0.037	1.0±0.029	1.0±0.054	0.84±0.043
	1h	0.05±0.003	0.03±0.003	< 0.016	0.03±0.008	0.92±0.034	0.84±0.02	0.94±0.024	0.68±0.035
	2h	0.02±0.003	0.08±0.239	< 0.016	0.04±0.004	0.90±0.028	0.87±0.051	0.88±0.062	0.67±0.003
	4h	0.02±0.002	< 0.016	< 0.016	0.03±0.003	0.84±0.023	0.66±0.016	0.77±0.011	0.50±0.018
	6h	0.02±0.002	< 0.016	0.04±0.001	0.03±0.001	*	0.63±0.02	0.72±0.022	0.48±0.014
	12h	0.04±0.006	0.07±0.002	0.03±0.005	0.03±0.001	0.65±0.026	0.58±0.014	0.65±0.032	0.49±0.017
	24h	0.02±0.001	0.03±0.007	< 0.016	0.02±0.004	0.52±0.022	0.43±0.007	0.56±0.014	0.43±0.021
Sal 35	15'	0.08±0.005	0.09±0.002	0.07±0.008	0.09±0.006	1.1±0.034	1.1±0.031	1.1±0.041	1.0±0.048
	30'	< 0.010	0.04±0.006	< 0.010	0.09±0.010	1.1±0.059	1.1±0.068	1.1±0.020	1.0±0.066
	1h	0.06±0.006	0.08±0.005	0.06±0.007	0.05±0.002	1.1±0.031	1.1±0.040	1.0±0.077	0.96±0.049
	2h	0.05±0.002	0.02±0.004	0.08±0.003	0.02±0.003	1.1±0.019	1.1±0.070	1.1±0.060	1.0±0.059
	4h	0.02±0.002	0.02±0.003	0.02±0.001	< 0.010	1.1±0.071	1.0±0.048	1.1±0.051	0.92±0.058
	6h	0.03±0.007	0.05±0.020	< 0.010	0.05±0.002	1.1±0.088	1.0±0.070	1.1±0.130	0.86±0.043
	12h	0.02±0.004	0.02±0.001	0.05±0.002	0.06±0.004	1.1±0.053	0.96±0.068	0.94±0.018	0.84±0.036
	24h	< 0.010	0.04±0.001	0.04±0.001	< 0.010	1.1±0.057	0.95±0.080	0.87±0.033	0.79±0.053

Supplemental Table 4.2 - Statistical comparisons (1-way ANOVA followed by pairwise comparisons) between different salinities (0, 15 and 35). Bold indicate significant differences ($p < 0.05$).

1-way ANOVA effect	La df	La Sum of Squares	La Mean sum of squares	La F-test	La p-value	Gd df	Gd Sum of Squares	Gd Mean sum of squares	Gd F-test	Gd p-value
Salinity	2.0	8.8	4.4	39	**< 0.0001**	2.0	11	5.6	79	**< 0.0001**
Residual	285	33	0.11			285	20	0.071		
Tukey's pairwise comparisons	**Difference**	**Lower 95% CI**	**Upper 95% CI**	**Std error**	**p-value**	**Difference**	**Lower 95% CI**	**Upper 95% CI**	**Std error**	**p-value**
0 x 15	-0.40	-0.49	-0.30	0.049	**< 0.0001**	-0.30	-0.38	-0.23	0.039	**< 0.0001**
0 x 35	-0.34	-0.44	-0.25	0.049	**< 0.0001**	-0.48	-0.56	-0.40	0.039	**< 0.0001**
15 x 35	0.052	-0.044	0.15	0.049	0.53	-0.18	-0.25	-0.10	0.039	**< 0.0001**

Supplemental Table 4.3 – Statistical comparisons (2-way ANOVA with Temperature and pH as factors followed by Tukey's pairwise comparisons) between different treatments (Present day conditions, Warming, Acidification and Warming & Acidification) for each salinity. Bold indicate significant differences ($p < 0.05$).

		La					Gd				
	2-way ANOVA effects	**df**	**Sum of Squares**	**Mean sum of squares**	**F-test**	**p-value**	**df**	**Sum of Squares**	**Mean sum of squares**	**F-test**	**p-value**
Sal 0	Temperature	1	3.9	3.9	101	**< 0.0001**	1.0	0.046	0.046	1.6	0.21
	pH	1	0.094	0.094	2.4	0.12	1.0	0.129	0.129	4.5	0.036
	Temperature * pH	1	0.34	0.34	8.9	**0.0036**	1.0	0.157	0.157	5.5	**0.021**
	Residual	92	3.5	0.038			92	2.618	0.028		
	Tukey's pairwise comparisons	**Difference**	**Lower 95% CI**	**Upper 95% CI**	**Std error**	**p-value**	**Difference**	**Lower 95% CI**	**Upper 95% CI**	**Std error**	**p-value**
	Present day conditions vs Warming	-0.52	-0.63	-0.41	0.057	**< 0.0001**	0.037	-0.059	0.13	0.049	0.87
	Present day conditions vs Acidification	0.057	-0.055	0.17	0.057	0.74	-0.15	-0.25	-0.057	0.049	**0.011**
	Present day conditions vs Warming & Acidification	0.34	0.23	0.45	0.057	**< 0.0001**	-0.030	-0.13	0.067	0.049	0.93
	Acidification vs Warming	-0.46	-0.58	-0.35	0.057	**< 0.0001**	-0.11	-0.21	-0.020	0.049	0.084
	Acidification vs Warming & Acidification	-0.28	-0.39	-0.17	0.057	**< 0.0001**	-0.12	-0.22	-0.028	0.049	0.059
	Warming vs Warming & Acidification	-0.18	-0.30	-0.07	0.057	**0.0094**	0.007	-0.089	0.10	0.049	0.99
	2-way ANOVA effects	**df**	**Sum of Squares**	**Mean sum of squares**	**F-test**	**p-value**	**df**	**Sum of Squares**	**Mean sum of squares**	**F-test**	**p-value**
Sal 15	Temperature	1.0	0.004	0.004	0.03	0.87	1.0	0.18	0.18	2.5	0.12
	pH	1.0	0.012	0.012	0.07	0.79	1.0	0.088	0.088	1.2	0.28
	Temperature * pH	1.0	0.46	0.46	2.8	0.098	1.0	0.003	0.003	0.040	0.84
	Residual	92	15	0.17			92	6.9	0.075		
	Tukey's pairwise comparisons	**Difference**	**Lower 95% CI**	**Upper 95% CI**	**Std error**	**p-value**	**Difference**	**Lower 95% CI**	**Upper 95% CI**	**Std error**	**p-value**
	Present day conditions vs Warming	-0.13	-0.36	0.11	0.12	0.71	0.076	-0.08	0.23	0.079	0.77
	Present day conditions vs Acidification	0.12	-0.12	0.35	0.12	0.75	-0.049	-0.21	0.11	0.079	0.92
	Present day conditions vs Warming & Acidification	-0.035	-0.27	0.20	0.12	0.99	-0.15	-0.3	0.009	0.079	0.25
	Acidification vs Warming	-0.008	-0.24	0.23	0.12	0.99	0.027	-0.13	0.18	0.079	0.99
	Acidification vs Warming & Acidification	0.15	-0.081	0.39	0.12	0.57	0.098	-0.058	0.26	0.079	0.60
	Warming vs Warming & Acidification	-0.16	-0.39	0.073	0.12	0.52	-0.071	-0.23	0.085	0.079	0.80
	2-way ANOVA effects	**df**	**Sum of Squares**	**Mean sum of squares**	**F-test**	**p-value**	**df**	**Sum of Squares**	**Mean sum of squares**	**F-test**	**p-value**
Sal 35	Temperature	1.0	0.42	0.42	4.6	0.56	1.0	0.0	0.0	0.0	0.95
	pH	1.0	0.026	0.026	0.29	0.59	1.0	0.067	0.067	0.83	0.36
	Temperature * pH	1.0	0.054	0.054	0.59	0.44	1.0	0.010	0.010	0.12	0.73
	Residual	92	8.5	0.092			92	7.5	0.081		
	Tukey's pairwise comparisons	**Difference**	**Lower 95% CI**	**Upper 95% CI**	**Std error**	**p-value**	**Difference**	**Lower 95% CI**	**Upper 95% CI**	**Std error**	**p-value**
	Present day conditions vs Warming	-0.081	-0.26	0.093	0.088	0.79	0.024	-0.14	0.19	0.082	0.99
	Present day conditions vs Acidification	-0.085	-0.26	0.089	0.088	0.77	-0.073	-0.24	0.090	0.082	0.81
	Present day conditions vs Warming & Acidification	-0.099	-0.27	0.075	0.088	0.67	-0.056	-0.22	0.11	0.082	0.90
	Acidification vs Warming	0.014	-0.16	0.19	0.088	0.99	-0.049	-0.21	0.11	0.082	0.93
	Acidification vs Warming & Acidification	-0.17	-0.34	0.009	0.088	0.24	-0.017	-0.18	0.15	0.082	0.99
	Warming vs Warming & Acidification	-0.18	-0.35	-0.006	0.088	0.18	-0.032	-0.20	0.13	0.082	0.98

Supplemental Table 4.4 a) - 1-way ANOVA with Time as factor for each La and Gd spiked treatment (Control TºC and pH, Warming, Acidification and Warming & Acidification), in each salinity. Bold indicate significant differences ($p < 0.05$).

			La spiked					Gd spiked				
		1-way ANOVA effect	df	Sum of Squares	Mean sum of squares	F-test	p-value	df	Sum of Squares	Mean sum of squares	F-test	p-value
Sal 0	Control TºC and pH	Time	0.58	7	0.08	250	**<0.0001**	0.070	7	0.01	26	**<0.0001**
		Residual	0.01	16	0.0			0.006	16	0.0		
	Warming	Time	1.2	7	0.17	76	**<0.0001**	0.25	7	0.036	38	**<0.0001**
		Residual	0.04	16	0.002			0.015	16	0.001		
	Acidification	Time	0.58	7	0.08	360	**<0.0001**	0.18	7	0.025	21	**<0.0001**
		Residual	0.004	16	0.0			0.019	16	0.001		
	Warming & Acidification	Time	1.1	7	0.16	72	**<0.0001**	0.54	7	0.078	129	**<0.0001**
		Residual	0.035	16	0.002			0.010	16	0.001		
Sal 15	Control TºC and pH	Time	1.4	7	0.21	0.79	0.61	0.35	7	0.049	0.51	0.82
		Residual	4.2	16	0.26			1.6	16	0.097		
	Warming	Time	1.1	7	0.16	5.5	**0.002**	0.65	7	0.093	1.4	0.26
		Residual	0.45	16	0.03			1.0	16	0.065		
	Acidification	Time	1.2	7	0.17	0.54	0.79	0.48	7	0.068	0.61	0.74
		Residual	4.9	16	0.31			1.8	16	0.11		
	Warming & Acidification	Time	1.5	7	0.22	6.8	**0.001**	0.48	7	0.069	2.1	0.11
		Residual	0.51	16	0.03			0.54	16	0.034		
Sal 35	Control TºC and pH	Time	0.32	7	0.05	0.24	0.97	0.019	7	0.003	0.03	1.0
		Residual	3.1	16	0.19			1.6	16	0.099		
	Warming	Time	0.34	7	0.05	1.5	0.23	0.1	7	0.015	0.14	0.99
		Residual	0.5	16	0.03			1.7	16	0.11		
	Acidification	Time	0.37	7	0.05	0.33	0.93	0.12	7	0.017	0.12	1.0
		Residual	2.6	16	0.16			2.3	16	0.14		
	Warming & Acidification	Time	0.46	7	0.07	1.2	0.36	0.23	7	0.033	0.37	0.91
		Residual	0.88	16	0.06			1.4	16	0.089		

Supplemental Table 4.4 b) - Tukey's pairwise comparisons for each La and Gd spiked treatment (Control T°C and pH, Warming, Acidification and Warming & Acidification), in each salinity. Bold indicate significant differences ($p < 0.05$).

Tukey's pairwise comparisons p-value		La spiked								Gd spiked							
		15'	30'	1h	2h	4h	6h	12h	24h		15'	30'	1h	2h	4h	6h	12h	24h
Control T°C and pH	15'		0.39	**<0.0001**	**<0.0001**	**<0.0001**	**<0.0001**	**<0.0001**	**<0.0001**	15'		0.055	**<0.0001**	**0.0001**	**<0.0001**	**<0.0001**	**<0.0001**	**<0.0001**
	30'	0.39		**0.002**	**<0.0001**	**<0.0001**	**<0.0001**	**<0.0001**	**<0.0001**	30'	0.055		0.057	0.071	**0.009**	**0.002**	**0.0002**	**<0.0001**
	1h	**<0.0001**	**0.002**		**<0.0001**	**<0.0001**	**<0.0001**	**<0.0001**	**<0.0001**	1h	**<0.0001**	0.057		1.0	0.98	0.62	0.093	**0.006**
	2h	**<0.0001**	**<0.0001**	**<0.0001**		**0.001**	**<0.0001**	**<0.0001**	**<0.0001**	2h	**0.0001**	0.071	1.0		0.95	0.55	0.075	**0.005**
	4h	**<0.0001**	**<0.0001**	**<0.0001**	**0.001**		**0.22**	**0.0002**	**<0.0001**	4h	**<0.0001**	**0.009**	0.98	0.95		0.99	0.41	**0.038**
	6h	**<0.0001**	**<0.0001**	**<0.0001**	**<0.0001**	**0.22**		**0.029**	**<0.0001**	6h	**<0.0001**	**0.002**	0.62	0.55	0.99		0.88	0.18
	12h	**<0.0001**	**<0.0001**	**<0.0001**	**<0.0001**	**0.0002**	**0.029**		0.11	12h	**<0.0001**	**0.0002**	0.093	0.075	0.41	0.88		0.83
	24h	**<0.0001**	**<0.0001**	**<0.0001**	**<0.0001**	**<0.0001**	**<0.0001**	0.11		24h	**<0.0001**	**<0.0001**	**0.006**	**0.005**	**0.038**	0.18	0.83	
		15'	30'	1h	2h	4h	6h	12h	24h		15'	30'	1h	2h	4h	6h	12h	24h
Warming	15'		**0.015**	0.061	**0.0002**	**<0.0001**	**<0.0001**	**<0.0001**	**<0.0001**	15'		0.70	**0.025**	**0.0004**	**<0.0001**	**<0.0001**	**<0.0001**	**<0.0001**
	30'	**0.015**		0.99	0.36	**0.0016**	**<0.0001**	**<0.0001**	**<0.0001**	30'	0.70		0.42	**0.010**	**<0.0001**	**<0.0001**	**<0.0001**	**<0.0001**
	1h	0.061	0.99		0.12	**0.0004**	**<0.0001**	**<0.0001**	**<0.0001**	1h	**0.025**	0.42		0.42	**0.0011**	**0.001**	**0.0002**	**<0.0001**
	2h	**0.0002**	0.36	0.12		0.12	**<0.0001**	**<0.0001**	**<0.0001**	2h	**0.0004**	**0.010**	0.42		0.071	0.052	**0.012**	**0.001**
	4h	**<0.0001**	**0.0016**	**0.0004**	0.12		**0.015**	**0.001**	**<0.0001**	4h	**<0.0001**	**<0.0001**	**0.0011**	0.071		1.0	0.98	0.23
	6h	**<0.0001**	**<0.0001**	**<0.0001**	**<0.0001**	**0.015**		0.78	**0.026**	6h	**<0.0001**	**<0.0001**	**0.001**	0.052	1.0		0.99	0.30
	12h	**<0.0001**	**<0.0001**	**<0.0001**	**<0.0001**	**0.001**	0.78		0.37	12h	**<0.0001**	**<0.0001**	**0.0002**	**0.012**	0.98	0.99		0.71
	24h	**<0.0001**	**<0.0001**	**<0.0001**	**<0.0001**	**<0.0001**	**0.026**	0.37		24h	**<0.0001**	**<0.0001**	**<0.0001**	**0.001**	0.23	0.30	0.71	
Sal 0		15'	30'	1h	2h	4h	6h	12h	24h		15'	30'	1h	2h	4h	6h	12h	24h
Acidification	15'		0.82	**<0.0001**	**<0.0001**	**<0.0001**	**<0.0001**	**<0.0001**	**<0.0001**	15'		0.78	0.079	**0.008**	**<0.0001**	**<0.0001**	**<0.0001**	**<0.0001**
	30'	0.82		**<0.0001**	**<0.0001**	**<0.0001**	**<0.0001**	**<0.0001**	**<0.0001**	30'	0.78		0.70	0.14	**0.001**	**0.001**	**0.0002**	**<0.0001**
	1h	**<0.0001**	**<0.0001**		**<0.0001**	**<0.0001**	**<0.0001**	**<0.0001**	**<0.0001**	1h	0.079	0.70		0.92	0.019	**0.019**	**0.004**	**0.001**
	2h	**<0.0001**	**<0.0001**	**<0.0001**		**<0.0001**	**<0.0001**	**<0.0001**	**<0.0001**	2h	**0.008**	0.14	0.92		0.17	0.17	**0.044**	**0.009**
	4h	**<0.0001**	**<0.0001**	**<0.0001**	**<0.0001**		**0.016**	**0.0001**	**<0.0001**	4h	**<0.0001**	**0.0007**	0.019	0.17		1.0	0.99	0.76
	6h	**<0.0001**	**<0.0001**	**<0.0001**	**<0.0001**	**0.016**		0.20	0.13	6h	**<0.0001**	**0.0007**	0.019	0.17	1.0		0.99	0.76
	12h	**<0.0001**	**<0.0001**	**<0.0001**	**<0.0001**	**0.0001**	0.20		1.0	12h	**<0.0001**	**0.0002**	**0.0043**	**0.044**	0.99	0.99		0.99
	24h	**<0.0001**	**<0.0001**	**<0.0001**	**<0.0001**	**<0.0001**	0.13	1.0		24h	**<0.0001**	**<0.0001**	**0.0009**	**0.009**	0.76	0.76	0.99	
		15'	30'	1h	2h	4h	6h	12h	24h		15'	30'	1h	2h	4h	6h	12h	24h
Warming & Acidification	15'		**0.034**	**0.005**	**<0.0001**	**<0.0001**	**<0.0001**	**<0.0001**	**<0.0001**	15'		0.33	**0.0008**	**<0.0001**	**<0.0001**	**<0.0001**	**<0.0001**	**<0.0001**
	30'	**0.034**		0.96	**0.003**	**<0.0001**	**<0.0001**	**<0.0001**	**<0.0001**	30'	0.33		0.069	**<0.0001**	**<0.0001**	**<0.0001**	**<0.0001**	**<0.0001**
	1h	**0.005**	0.96		**0.024**	**0.001**	**<0.0001**	**<0.0001**	**<0.0001**	1h	**0.0008**	0.069		**0.007**	**<0.0001**	**<0.0001**	**<0.0001**	**<0.0001**
	2h	**<0.0001**	**0.003**	**0.024**		0.48	**0.002**	**0.001**	**<0.0001**	2h	**<0.0001**	**<0.0001**	**0.007**		**0.050**	**<0.0001**	**<0.0001**	**<0.0001**
	4h	**<0.0001**	**<0.0001**	**0.001**	0.48		0.083	**0.025**	**<0.0001**	4h	**<0.0001**	**<0.0001**	**<0.0001**	**0.050**		**0.008**	**0.001**	**<0.0001**
	6h	**<0.0001**	**<0.0001**	**<0.0001**	**0.002**	0.083		0.99	**0.039**	6h	**<0.0001**	**<0.0001**	**<0.0001**	**<0.0001**	**0.008**		0.90	**0.081**
	12h	**<0.0001**	**<0.0001**	**<0.0001**	**0.001**	**0.025**	0.99		0.12	12h	**<0.0001**	**<0.0001**	**<0.0001**	**<0.0001**	**0.001**	0.90		0.54
	24h	**<0.0001**	**<0.0001**	**<0.0001**	**<0.0001**	**<0.0001**	**0.039**	0.12		24h	**<0.0001**	**<0.0001**	**<0.0001**	**<0.0001**	**<0.0001**	**0.081**	0.54	

Supplemental Table 4.4b Cont.

Tukey's pairwise comparisons p-value		La spiked							
		15'	30'	1h	2h	4h	6h	12h	24h
	15'		0.94	0.92	0.85	0.33	**0.024**	**0.035**	**0.004**
	30'	0.94		1.0	1.0	0.92	0.19	0.25	**0.035**
	1h	0.92	1.0		1.0	0.94	0.20	0.28	**0.040**
Warming	2h	0.85	1.0	1.0		0.98	0.28	0.37	0.057
	4h	0.33	0.92	0.94	0.98		0.79	0.88	0.29
	6h	**0.024**	0.19	0.21	0.28	0.79		1.0	0.98
	12h	**0.035**	0.25	0.28	0.37	0.88	1.0		0.94
	24h	**0.004**	**0.035**	**0.040**	0.057	0.29	0.98	0.94	
Sal 15		15'	30'	1h	2h	4h	6h	12h	24h
	15'		0.98	0.63	0.41	0.15	**0.012**	**0.009**	**0.001**
	30'	0.98		0.98	0.90	0.55	0.070	0.052	**0.007**
	1h	0.63	0.98		0.99	0.96	0.31	0.24	**0.039**
Warming & Acidification	2h	0.41	0.90	0.99		0.99	0.50	0.41	0.079
	4h	0.15	0.55	0.96	0.99		0.87	0.79	0.24
	6h	**0.012**	0.070	0.31	0.50	0.87		1.0	0.92
	12h	**0.009**	0.052	0.24	0.41	0.79	1.0		0.96
	24h	**0.001**	**0.007**	**0.039**	0.079	0.24	0.92	0.96	

ANNEX 4

SUPPLEMENTARY INFORMATION FOR CHAPTER 5

Supplemental Table 5.1 - Concentrations of La in the water (ng L^{-1}) aliquots sampled every hour for the first 12 hours (T1-T12) and after 24h (T24) of exposure. The naturally presented values in the water (T0) were deducted from the exposed water values.

	T0	T1	T2	T3	T4	T5	T6	T7	T8	T9	T10	T11	T12	T24
[La] ng L^{-1}	31,91	136,4	129,4	129,0	137,0	119,3	111,9	117,6	120,1	114,8	109,4	104,4	121,3	100,2

ANNEX 5

SUPPLEMENTARY INFORMATION FOR CHAPTER 6

Supplemental Table 6.1 - Concentrations of La in the water (µg L^{-1}) aliquots sampled after 1, 3, 6, 12 and 24 hours of exposure.

[La] µg L^{-1}	1h	3h	6h	12h	24h
18ºC control	0.049	0.031	0.033	0.028	0.029
18ºC La exposed	1.6	1.4	1.3	1.2	1.2
22ºC control	0.045	0.065	0.085	0.048	0.041
22ºC La exposed	1.9	1.6	1.5	1.4	1.5

ANNEX 6

SUPPLEMENTARY INFORMATION FOR CHAPTER 7

Supplemental Table 7.1 - Concentrations of La in the water (µg L^{-1}) aliquots sampled every hour of the first twelve hours after La spike, for both exposed treatments.

[La]	Low concentration (0.3 µg L^{-1})	High concentration (0.9 µg L^{-1})
1h	0.081	0.79
2h	0.15	0.73
3h	0.13	0.79
4h	0.16	0.68
5h	0.18	0.99
6h	0.33	1.0
7h	0.30	0.87
8h	0.34	0.84
9h	0.29	0.84
10h	0.34	0.85
11h	0.37	0.87
12h	0.35	0.84

Supplemental Table 7.2 a) – Statistical comparisons (Mann-Whitney non-parametric test) between treatments for each tissue. Asterisks indicate significant differences ($p < 0.05$).

Body	**T1**	**T2**	**T6**
Control x 0.3 µg L^{-1}	U=8 Z=0.456 p=0.649	U=1 Z=-2.14 p=0.032*	U=0 Z=-2.35 p=0.019*
Control x 0.9 µg L^{-1}	U=2 Z=-1.24 p=0.216	U=0 Z=-2.09 p=0.037*	U=0 Z=-2.40 p=0.016*
0.3 µg L^{-1} x 0.9 µg L^{-1}	U=7 Z=-1.23 p=0.219	U=11 Z=-1.24 p=0.213	U=13 Z=-2.17 p=0.030*
Digestive Gland	**T1**	**T2**	**T6**
Control x 0.3 µg L^{-1}	U=11 Z=-0.102 p=0.919	U=0 Z=-2.33 p=0.020*	U=0 Z=-2.28 p=0.023*
Control x 0.9 µg L^{-1}	U=4 Z=-1.16 p=0.245	U=0 Z=-2.63 p=0.008*	U=0 Z=-2.09 p=0.037*
0.3 µg L^{-1} x 0.9 µg L^{-1}	U=10 Z=-1.74 p=0.081	U=20 Z=0 p=1	U=3 Z=-2.27 p=0.023*
Gills	**T1**	**T2**	**T6**
Control x 0.3 µg L^{-1}	U=6 Z=-0.645 p=0.519	U=0 Z=-2.20 p=0.028*	U=0 Z=-2.19 p=0.028*
Control x 0.9 µg L^{-1}	U=1 Z=-1.31 p=0.190	U=0 Z=-2.20 p=0.028*	U=0 Z=-2.19 p=0.028*
0.3 µg L^{-1} x 0.9 µg L^{-1}	U=7 Z=-0.387 p=0.699	U=16 Z=-0.240 p=0.810	U=11 Z=1.04 p=0.298

Supplemental Table 7.2 b) – Statistical comparisons (Mann-Whitney non-parametric test) between sampling times for each tissue. Asterisks indicate significant differences ($p < 0.05$).

Body	**T0 vs T1**	**T0 vs T2**	**T0 vs T6**	**T1 vs T2**	**T1 vs T6**	**T2 vs T6**
Control	U=2 Z=-1.82 p=0.068	U=6 Z=-0.912 P=0.362	U=2 Z=-1.80 p=0.068	U=2 Z=0.873 p=0.383	U=3 Z=-0.44 p=0.663	U=2 Z=-0.873 p=0.383
0.3 µg L^{-1}				U=8 Z=-2.26 p=0.024*	U=2 Z=-2.95 p=0.003*	U=6 Z=-2.68 p=0.007*
0.9 µg L^{-1}				U=0 Z=-2.33 p=0.020*	U=0 Z=-2.70 p=0.007*	U=2 Z=-2.67 p=0.008*
Digestive Gland	**T0 vs T1**	**T0 vs T2**	**T0 vs T6**	**T1 vs T2**	**T1 vs T6**	**T2 vs T6**
Control	U=0 Z=-1.74 p=0.081	U=0 Z=-1.94 p=0.052	U=0 Z=-1.75 p=0.081	U=0 Z=1.94 p=0.052	U=3 Z=0.436 p=0.663	U=0 Z=-1.94 p=0.052
0.3 µg L^{-1}				U=10 Z=-1.39 p=0.164	U=0 Z=-3.183 p=0.001*	U=6 Z=-1.79 p=0.074
0.9 µg L^{-1}				U=21 Z=-0.323 p=0.747	U=0 Z=-2.65 p=0.008*	U=0 Z=-2.85 p=0.004*
Gills	**T0 vs T1**	**T0 vs T2**	**T0 vs T6**	**T1 vs T2**	**T1 vs T6**	**T2 vs T6**
Control	U=0 Z=-1.75 p=0.081	U=0 Z=-1.75 p=0.081	U=2 Z=-0.87 p=0.383	U=1 Z=1.31 p=0.190	U=0 Z=1.75 p=0.081	U=0 Z=1.75 p=0.081
0.3 µg L^{-1}				U=5 Z=-2.00 p=0.045*	U=3 Z=-2.32 p=0.020*	U=7 Z=-1.68 p=0.093
0.9 µg L^{-1}				U=7 Z=-0.387 p=0.699	U=0 Z=-2.19 p=0.028*	U=1 Z=-2.64 p=0.008*

Supplemental Table 7.2 c) - Statistical comparisons (Mann-Whitney non-parametric test) between body, digestive gland and gills (La concentration) for each sampling time (T0, T1, T2 and T6). Asterisks indicate significant differences ($p < 0.05$).

Control	**T0**	**T1**	**T2**	**T6**
Body x Digestive Gland	U=10 Z=0.00 p=1.00	U=0 Z=-1.75 p=0.081	U=0 Z=-1.944 p=0.052	U=0 Z=-1.75 p=0.081
Body x Gills	U=2 Z=-1.82 p=0.068	U=0 Z=-1.74 p=0.081	U=0 Z=-1.746 p=0.081	U=0 Z=-1.75 p=0.081
Digestive Gland x Gills	U=1 Z=-1.30 p=0.190	U=3 Z=0.436 p=0.663	U=0 Z=-1.94 p=0.052	U=6 Z=1.75 p=0.081
0.3 µg L^{-1}	**T0**	**T1**	**T2**	**T6**
Body x Digestive Gland		U=8 Z=-2.26 p=0.024*	U=2 Z=-2.56 p=0.010*	U=6 Z=-2.49 p=0.013*
Body x Gills		U=1 Z=-2.79 p=0.005*	U=0 Z=-3.034 p=0.002*	U=4 Z=-2.52 p=0.012*
Digestive Gland x Gills		U=15 Z=-1.10 p=0.272	U=10 Z=-0.822 p=0.411	U=17 Z=-0.5 p=0.617
0.9 µg L^{-1}	**T0**	**T1**	**T2**	**T6**
Body x Digestive Gland		U=1 Z=-2.24 P=0.025*	U=5 Z=-2.56 p=0.010*	U=1 Z=-2.8 p=0.005*
Body x Gills		U=0 Z=-1.94 p=0.052	U=4 Z=-2.36 p=0.018*	U=7 Z=-2.90 p=0.022*
Digestive Gland x Gills		U=9 Z=0 p=1	U=20 Z=-0.452 p=0.651	U=17 Z=0.50 p=0.617

ANNEX 7

SUPPLEMENTARY INFORMATION FOR CHAPTER 8

Supplemental Table 8.1 a) - Tukey's pairwise comparisons between experimental treatments, for La concentrations. Bold point significant differences ($p < 0.05$).

	T0	T1	T3	T7	T14
Control vs High CO_2	0.56	1.0	0.94	1.00	0.98
Control vs Warming	0.99	0.76	0.77	0.26	0.99
Control vs Warming and High CO_2	0.67	0.99	0.99	0.99	0.99
High CO_2 vs Warming	0.61	0.39	0.99	0.16	1.00
High CO_2 vs Warming and High CO_2	0.99	0.92	0.71	1.0	0.99
Warming vs Warming and High CO_2	0.72	0.94	0.45	0.99	1.0
Control vs La exposed		**< 0.0001**	**< 0.0001**	**< 0.0001**	**< 0.0001**
Control vs High CO_2 and La exposed		**< 0.0001**	**< 0.0001**	**< 0.0001**	**< 0.0001**
Control vs Warming and La exposed		**< 0.0001**	**< 0.0001**	**< 0.0001**	**< 0.0001**
Control vs Warming, High CO_2 and La exposed		**< 0.0001**	**< 0.0001**	**< 0.0001**	**< 0.0001**
High CO_2 vs La exposed		**< 0.0001**	**< 0.0001**	**< 0.0001**	**< 0.0001**
High CO_2 vs High CO_2 and La exposed		**< 0.0001**	**< 0.0001**	**< 0.0001**	**< 0.0001**
High CO_2 vs Warming and La exposed		**< 0.0001**	**< 0.0001**	**< 0.0001**	**< 0.0001**
High CO_2 vs Warming, High CO_2 and La exposed		**< 0.0001**	**< 0.0001**	**< 0.0001**	**< 0.0001**
Warming vs La exposed		**< 0.0001**	**< 0.0001**	**< 0.0001**	**< 0.0001**
Warming vs High CO_2 and La exposed		**< 0.0001**	**< 0.0001**	**< 0.0001**	**< 0.0001**
Warming vs Warming and La exposed		**< 0.0001**	**< 0.0001**	**< 0.0001**	**< 0.0001**
Warming vs Warming, High CO_2 and La exposed		**< 0.0001**	**< 0.0001**	**< 0.0001**	**< 0.0001**
Warming and High CO_2 vs La exposed		**< 0.0001**	**< 0.0001**	**< 0.0001**	**< 0.0001**
Warming and High CO_2 vs High CO_2 and La exposed		**< 0.0001**	**< 0.0001**	**< 0.0001**	**< 0.0001**
Warming and High CO_2 vs Warming and La exposed		**< 0.0001**	**< 0.0001**	**< 0.0001**	**< 0.0001**
Warming and High CO_2 vs Warming, High CO_2 and La exposed		**< 0.0001**	**< 0.0001**	**< 0.0001**	**< 0.0001**
La exposed vs High CO_2 and La exposed		0.77	1.0	0.98	1.0
La exposed vs Warming and La exposed		0.99	0.99	0.78	**< 0.0001**
La exposed vs Warming, High CO_2 and La exposed		1.0	0.99	0.97	**< 0.0001**
High CO_2 and La exposed vs Warming and La exposed		0.59	0.97	0.98	**< 0.0001**
High CO_2 and La exposed vs Warming, High CO_2 and La exposed		0.94	0.97	1.0	**< 0.0001**
Warming and La exposed vs Warming, High CO_2 and La exposed		0.99	1.0	0.99	0.13

Supplemental Table 8.1 b) - Tukey's pairwise comparisons between times for La concentration in the four La exposed treatments. Bold point significant differences ($p < 0.05$).

	La exposed	High CO_2 and La exposed	Warming and La exposed	Warming, high CO_2 and La exposed
T1 vs T3	0.45	0.13	0.11	0.28
T1 vs T7	**0.0035**	**0.0018**	0.051	**0.033**
T1 vs T14	0.054	**0.02**	**0.017**	1
T3 vs T7	**0.032**	0.081	0.88	0.51
T3 vs T14	0.59	0.55	**0.0002**	0.38
T7 vs T14	**0.13**	0.71	**0.0002**	0.065

Supplemental Table 8.2 a) - Three-way ANOVA with temperature, pH and contamination as factors followed by Tukey's pairwise comparisons for TAC, SOD, GST, GPx, HSP, CAT, LIPO and Ub, for each sampling time. Bold point significant differences ($p < 0.05$).

			Sum of squares	Degrees of freedom	Mean square	F-value	p-value
T0	**LIPO**	Temperature	0.001	1	0.001	0.08	0.7881
		pH	0.002	1	0.002	0.14	0.7272
		Temperature * pH	0.013	1	0.013	0.92	0.3918
		Residual	0.056	4	0.014		
	HSP	Temperature	0	1	0	0.01	0.9247
		pH	0	1	0	0	0.9876
		Temperature * pH	0.003	1	0.003	0.57	0.4766
		Residual	0.036	7	0.005		
	Ub	Temperature	0.007	1	0.007	0.23	0.6545
		pH	0.005	1	0.005	0.15	0.7149
		Temperature * pH	0.006	1	0.006	0.19	0.6794
		Residual	0.166	5	0.033		
	SOD	Temperature	0.006	1	0.006	0.26	0.6191
		pH	0.002	1	0.002	0.11	0.745
		Temperature * pH	0.022	1	0.022	0.98	0.3393
		Residual	0.317	14	0.023		
	CAT	Temperature	0.005	1	0.005	0.34	0.5926
		pH	0.006	1	0.006	0.38	0.5687
		Temperature * pH	0.002	1	0.002	0.12	0.7457
		Residual	0.065	4	0.016		
	GPx	Temperature	0.001	1	0.001	0.15	0.7056
		pH	0.001	1	0.001	0.09	0.7699
		Temperature * pH	0.005	1	0.005	0.62	0.4407
		Residual	0.139	17	0.008		
	GST	Temperature	0.01	1	0.01	3.72	0.0718
		pH	0.016	1	0.016	6.1	**0.0251**
		Temperature * pH	0	1	0	0.16	0.6903
		Residual	0.043	16	0.003		
		significant pair-wise comparison				control vs Warming and high CO_2	**0.0219**
	TAC	Temperature	0	1	0	0.01	0.9274
		pH	0	1	0	0.03	0.8702
		Temperature * pH	0.006	1	0.006	2.1	0.2213
		Residual	0.012	4	0.003		
T1	**LIPO**	Temperature	0.031	1	0.031	1.72	0.2091
		pH	0.031	1	0.031	1.74	0.2069
		Contamination	0.09	1	0.09	5.04	**0.0403**
		Temperature * pH	0.013	1	0.013	0.73	0.4065
		Temp * Contamination	0.01	1	0.01	0.56	0.465
		pH * Contamination	0.002	1	0.002	0.11	0.7496
		Temperature * pH * Contamination	0.015	1	0.015	0.85	0.3716
		Residual	0.269	15	0.018		
	HSP	Temperature	0.002	1	0.002	0.06	0.8091
		pH	0.016	1	0.016	0.55	0.47
		Contamination	0.02	1	0.02	0.68	0.4221
		Temperature * pH	0.022	1	0.022	0.76	0.3979
		Temp * Contamination	0.002	1	0.002	0.08	0.7867
		pH * Contamination	0.017	1	0.017	0.59	0.4551
		Temperature * pH * Contamination	0.002	1	0.002	0.06	0.8047
		Residual	0.4	14	0.029		
	Ub	Temperature	0.182	1	0.182	3.94	0.0687
		pH	0.011	1	0.011	0.25	0.6264
		Contamination	0	1	0	0	0.9544
		Temperature * pH	0	1	0	0	0.9481
		Temp * Contamination	0.023	1	0.023	0.5	0.4917
		pH * Contamination	0.01	1	0.01	0.22	0.6498
		Temperature * pH * Contamination	0.001	1	0.001	0.01	0.9082
		Residual	0.601	13	0.046		
	SOD	Temperature	0.018	1	0.018	4.35	**0.0454**

Supplemental Table 8.2a Cont.

			Sum of squares	Degrees of freedom	Mean square	F-value	p-value
T1	**SOD**	pH	0.013	1	0.013	3.09	0.0888
		Contamination	0.207	1	0.207	49.06	**< 0.0001**
		Temperature * pH	0.01	1	0.01	2.47	0.1259
		Temp * Contamination	0.003	1	0.003	0.62	0.4356
		pH * Contamination	0.002	1	0.002	0.41	0.5281
		Temperature * pH * Contamination	0.012	1	0.012	2.95	0.0957
		Residual	0.131	31	0.004		
		significant pair-wise comparisons				Control vs High CO_2 and La exposed	**0.0083**
						Control vs Warming, high CO_2 and La exposed	**0.0277**
						La exposed vs Warming	**0.0111**
						La exposed vs Warming and high CO_2	**0.0004**
						High CO_2 and La exposed vs Warming	**0.0004**
						High CO_2 and La exposed vs Warming and high CO_2	**< 0.0001**
						Warming vs Warming high CO_2 and La exposed	**0.0021**
						Warming and La exposed vs Warming and high CO_2	**0.0061**
						Warming, high CO_2 and La exposed vs Warming and high CO_2	**< 0.0001**
	CAT	Temperature	0	1	0	0.03	0.8685
		pH	0.002	1	0.002	0.46	0.5121
		Contamination	0	1	0	0	0.9617
		Temperature * pH	0.015	1	0.015	2.88	0.1203
		Temp * Contamination	0.008	1	0.008	1.52	0.2454
		pH * Contamination	0.041	1	0.041	8.07	**0.0175**
		Temperature * pH * Contamination	0.023	1	0.023	4.46	0.0609
		Residual	0.051	10	0.005		
	GPx	Temperature	0	1	0	0.02	0.8865
		pH	0.004	1	0.004	0.97	0.3318
		Contamination	0	1	0	0.12	0.7319
		Temperature * pH	0.003	1	0.003	0.68	0.4148
		Temp * Contamination	0.001	1	0.001	0.19	0.6637
		pH * Contamination	0	1	0	0.07	0.7886
		Temperature * pH * Contamination	0.006	1	0.006	1.6	0.215
		Residual	0.113	30	0.004		
	GST	Temperature	0.015	1	0.015	3.41	0.0737
		pH	0.003	1	0.003	0.6	0.4439
		Contamination	0.046	1	0.046	10.5	**0.0027**
		Temperature * pH	0.001	1	0.001	0.32	0.5733
		Temp * Contamination	0.001	1	0.001	0.25	0.6173
		pH * Contamination	0.003	1	0.003	0.76	0.3908
		Temperature * pH * Contamination	0	1	0	0.05	0.8286
		Residual	0.148	34	0.004		
		significant pair-wise comparison				Control vs warming and La exposed	**0.0354**
	TAC	Temperature	0.01	1	0.01	0.68	0.4289
		pH	0.001	1	0.001	0.08	0.7821
		Contamination	0.015	1	0.015	1.07	0.3263
		Temperature * pH	0.005	1	0.005	0.34	0.5737
		Temp * Contamination	0.037	1	0.037	2.59	0.1387
		pH * Contamination	0	1	0	0.01	0.917
		Temperature * pH * Contamination	0.006	1	0.006	0.4	0.542
		Residual	0.144	10	0.014		
T3	**LIPO**	Temperature	0.148	1	0.148	11.22	**0.0041**
		pH	0.032	1	0.032	2.45	0.1373
		Contamination	0.047	1	0.047	3.58	0.0767
		Temperature * pH	0.008	1	0.008	0.6	0.451
		Temp * Contamination	0.045	1	0.045	3.43	0.0827
		pH * Contamination	0.047	1	0.047	3.57	0.0772
		Temperature * pH * Contamination	0.007	1	0.007	0.53	0.4784

Supplemental Table 8.2 a Cont.

			Sum of squares	Degrees of freedom	Mean square	F-value	p-value
T3	**LIPO**	Residual	0.211	16	0.013		
		significant pair-wise comparisons				La exposed vs Warming	**0.0196**
						La exposed vs Warming, high CO_2 and La exposed	**0.0095**
						La exposed vs Warming and high CO_2	**0.0281**
	HSP	Temperature	0.101	1	0.101	4.44	0.0589
		pH	0.011	1	0.011	0.48	0.5049
		Contamination	0.031	1	0.031	1.37	0.2667
		Temperature * pH	0.01	1	0.01	0.45	0.5153
		Temp * Contamination	0.029	1	0.029	1.25	0.2865
		pH * Contamination	0.002	1	0.002	0.07	0.7958
		Temperature * pH * Contamination	0.067	1	0.067	2.92	0.1155
		Residual	0.251	11	0.023		
	Ub	Temperature	0.079	1	0.079	1.93	0.1954
		pH	0.028	1	0.028	0.68	0.4299
		Contamination	0	1	0	0.01	0.9296
		Temperature * pH	0.002	1	0.002	0.06	0.8159
		Temp * Contamination	0.062	1	0.062	1.5	0.2488
		pH * Contamination	0.003	1	0.003	0.07	0.7935
		Temperature * pH * Contamination	0.075	1	0.075	1.81	0.2079
		Residual	0.411	10	0.041		
	SOD	Temperature	0.039	1	0.039	3.4	0.074
		pH	0.023	1	0.023	2.05	0.1617
		Contamination	0.055	1	0.055	4.76	**0.0363**
		Temperature * pH	0.014	1	0.014	1.19	0.2838
		Temp * Contamination	0.006	1	0.006	0.52	0.4765
		pH * Contamination	0.001	1	0.001	0.1	0.7597
		Temperature * pH * Contamination	0.01	1	0.01	0.89	0.352
		Residual	0.378	33	0.011		
	CAT	Temperature	0.001	1	0.001	0.63	0.4445
		pH	0.005	1	0.005	2.27	0.1598
		Contamination	0.031	1	0.031	15.82	**0.0022**
		Temperature * pH	0	1	0	0.24	0.6323
		Temp * Contamination	0.045	1	0.045	22.95	**0.0006**
		pH * Contamination	0.007	1	0.007	3.51	0.0879
		Temperature * pH * Contamination	0	1	0	0.02	0.8895
		Residual	0.022	11	0.002		
		significant pair-wise comparisons				La exposed vs High CO_2	**0.0062**
						High CO_2 and La exposed vs High CO_2	**0.0061**
						High CO_2 vs Warming	**0.0121**
	GPx	Temperature	0.083	1	0.083	22.66	**< 0.0001**
		pH	0.055	1	0.055	14.94	**0.0005**
		Contamination	0.134	1	0.134	36.66	**< 0.0001**
		Temperature * pH	0.001	1	0.001	0.19	0.6657
		Temp * Contamination	0.034	1	0.034	9.25	**0.0044**
		pH * Contamination	0.001	1	0.001	0.27	0.6078
		Temperature * pH * Contamination	0.002	1	0.002	0.64	0.4294
		Residual	0.128	35	0.004		
		significant pair-wise comparisons				control vs La exposed	**< 0.0001**
						control vs high CO_2 and La exposed	**< 0.0001**
						La exposed vs Warming	**0.0002**
						La exposed vs Warming and La exposed	**0.0024**
						La exposed vs Warming and high CO_2	**0.0075**
						High CO_2 and La exposed vs High CO_2	**0.0139**
						High CO_2 and La exposed vs Warming	**< 0.0001**
						High CO_2 and La exposed vs Warming and La exposed	**0.0001**
						High CO_2 and La exposed vs Warming, high CO_2 and La exposed	**0.0213**
						High CO_2 and La exposed vs Warming and high CO_2	**0.0004**

Supplemental Table 8.2 a Cont.

			Sum of squares	Degrees of freedom	Mean square	F-value	p-value
T3	**GST**	Temperature	0.013	1	0.013	7.26	**0.012**
		pH	0.005	1	0.005	2.93	0.0986
		Contamination	0.081	1	0.081	45.32	**< 0.0001**
		Temperature * pH	0.002	1	0.002	1.28	0.2685
		Temp * Contamination	0	1	0	0.13	0.7221
		pH * Contamination	0.002	1	0.002	1.19	0.2845
		Temperature * pH * Contamination	0.004	1	0.004	1.98	0.1712
		Residual	0.048	27	0.002		
		significant pair-wise comparisons				control vs La exposed	**0.0218**
						control vs high CO_2 and La exposed	**0.007**
						control vs Warming and La exposed	**< 0.0001**
						control vs Warming, high CO_2 and La exposed	**0.0007**
						La vs Warming and La exposed	**0.042**
						High CO_2 vs Warming and La exposed	**0.0001**
						High CO_2 vs Warming, high CO_2 and La exposed	**0.0186**
						Warming vs Warming and La exposed	**0.0008**
						Warming vs Warming, high CO_2 and La exposed	**0.0366**
						Warming and La exposed vs Warming and high CO_2	**0.0203**
	TAC	Temperature	0.144	1	0.144	25.27	**0.0004**
		pH	0.003	1	0.003	0.47	0.5093
		Contamination	0.016	1	0.016	2.89	0.1174
		Temperature * pH	0	1	0	0.01	0.9436
		Temp * Contamination	0.015	1	0.015	2.7	0.1288
		pH * Contamination	0.014	1	0.014	2.46	0.145
		Temperature * pH * Contamination	0.016	1	0.016	**2.88**	0.1179
		Residual	0.063	11	0.006		
		significant pair-wise comparisons				control vs Warming, high CO_2 and La exposed	**0.0108**
						La exposed vs Warming, high CO_2 and La exposed	**0.0055**
						high CO_2 and La exposed vs Warming, high CO_2 and La exposed	**0.0205**
						High CO_2 vs Warming, high CO_2 and La exposed	**0.0217**
T7	**LIPO**	Temperature	0.691	1	0.691	106.75	**< 0.0001**
		pH	0.032	1	0.032	4.87	**0.0518**
		Contamination	0.197	1	0.197	30.36	**0.0003**
		Temperature * pH	0	1	0	0.06	0.8187
		Temp * Contamination	0.042	1	0.042	6.55	**0.0284**
		pH * Contamination	0.006	1	0.006	0.93	0.3571
		Temperature * pH * Contamination	0	1	0	0.01	0.9344
		Residual	0.065	10	0.006		
		significant pair-wise comparisons				control vs La exposed	**0.0486**
						control vs high CO_2 and La exposed	**0.0025**
						control vs Warming	**0.0009**
						control vs Warming and La exposed	**0.0003**
						control vs Warming, high CO_2 and La exposed	**< 0.0001**
						control vs Warming and high CO_2	**0.0004**
						La exposed vs Warming, high CO_2 and La exposed	**0.0059**
						high CO_2 and La exposed vs high CO_2	**0.0127**
						high CO_2 and La exposed vs Warming, high CO_2 and La exposed	**0.0242**
						high CO_2 vs Warming	**0.0037**
						high CO_2 vs Warming and La exposed	**0.0012**
						high CO_2 vs Warming, high CO_2 and La exposed	**0.0002**
						high CO_2 vs Warming and high CO_2	**0.0016**

Supplemental Table 8.2 a Cont.

			Sum of squares	Degrees of freedom	Mean square	F-value	p-value
T7	**HSP**	Temperature	0	1	0	0.01	0.9156
		pH	0.1	1	0.1	9.6	**0.0092**
		Contamination	0.114	1	0.114	10.97	**0.0062**
		Temperature * pH	0.046	1	0.046	4.42	0.0572
		Temp * Contamination	0	1	0	0	0.9716
		pH * Contamination	0.005	1	0.005	0.46	0.5121
		Temperature * pH * Contamination	0.224	1	0.224	21.59	**0.0006**
		Residual	0.124	12	0.01		
		significant pair-wise comparisons				control vs high CO_2 and La exposed	**0.0314**
						La exposed vs high CO_2 and La exposed	**0.0072**
						High CO_2 and La exposed vs high CO_2	**0.0154**
						high CO_2 and La exposed vs Warming	**0.0021**
						Warming vs Warming and La exposed	**0.0246**
	Ub	Temperature	0.026	1	0.026	1.19	0.2961
		pH	0.429	1	0.429	19.38	**0.0009**
		Contamination	0.008	1	0.008	0.37	0.5565
		Temperature * pH	0.149	1	0.149	6.75	**0.0233**
		Temp * Contamination	0.253	1	0.253	11.42	**0.0055**
		pH * Contamination	0.028	1	0.028	1.28	0.2798
		Temperature * pH * Contamination	0.178	1	0.178	8.06	**0.0149**
		Residual	0.266	12	0.022		
		significant pair-wise comparisons				control vs Warming, high CO_2 and La exposed	**0.0335**
						control vs Warming and high CO_2	**0.0331**
						La exposed vs Warming and La exposed	**0.0336**
						high CO_2 and La exposed vs Warming and La exposed	**0.0145**
						Warming vs Warming and La exposed	**0.0129**
						Warming and La exposed vs Warming, high CO_2 and La exposed	**0.0025**
						Warming and La exposed vs Warming and high CO_2	**0.0024**
	SOD	Temperature	0.434	1	0.434	141.82	**< 0.0001**
		pH	0.011	1	0.011	3.7	0.0646
		Contamination	0.042	1	0.042	13.73	**0.0009**
		Temperature * pH	0.013	1	0.013	4.33	**0.0468**
		Temp * Contamination	0.009	1	0.009	2.81	0.1051
		pH * Contamination	0.077	1	0.077	25.15	**< 0.0001**
		Temperature * pH * Contamination	0.011	1	0.011	3.65	0.0664
		Residual	0.086	28	0.003		
		significant pair-wise comparisons				control vs High CO_2 and La exposed	**0.0048**
						control vs Warming	**< 0.0001**
						control vs Warming and La exposed	**< 0.0001**
						control vs Warming, high CO_2 and La exposed	**< 0.0001**
						control vs Warming and high CO_2	**0.0005**
						La exposed vs high CO_2 and La exposed	**0.0018**
						La exposed vs Warming	**< 0.0001**
						La exposed vs Warming and La exposed	**< 0.0001**
						La exposed vs Warming, high CO_2 and La exposed	**< 0.0001**
						La exposed vs Warming and high CO_2	**0.0002**
						High CO_2 and La exposed vs high CO_2	**< 0.0001**
						High CO_2 vs Warming	**< 0.0001**
						High CO_2 vs Warming and La exposed	**< 0.0001**
						High CO_2 vs Warming, high CO_2 and La exposed	**< 0.0001**
						High CO_2 vs Warming and high CO_2	**< 0.0001**
	CAT	Temperature	0.005	1	0.005	4.7	0.0583
		pH	0.011	1	0.011	10.98	**0.009**
		Contamination	0.027	1	0.027	26.75	**0.0006**
		Temperature * pH	0.01	1	0.01	9.76	**0.0122**

Supplemental Table 8.2 a Cont.

			Sum of squares	Degrees of freedom	Mean square	F-value	p-value
T7	**CAT**	Temp * Contamination	0.014	1	0.014	13.53	**0.0051**
		pH * Contamination	0.005	1	0.005	5.02	0.0518
		Temperature * pH * Contamination	0.015	1	0.015	14.95	**0.0038**
		Residual	0.009	9	0.001		
		significant pair-wise comparisons				control vs La exposed	**0.0007**
						control vs high CO_2 and La exposed	**0.0006**
						control vs high CO_2	**0.0026**
						control vs Warming	**0.0011**
						control vs Warming and La exposed	**0.0024**
						control vs Warming, high CO_2 and La exposed	**0.0009**
						control vs Warming and high CO_2	**0.0051**
	GPx	Temperature	0.042	1	0.042	3.93	0.0566
		pH	0.119	1	0.119	11.16	**0.0023**
		Contamination	0.061	1	0.061	5.72	**0.0232**
		Temperature * pH	0.002	1	0.002	0.18	0.6772
		Temp * Contamination	0.002	1	0.002	0.2	0.6612
		pH * Contamination	0.017	1	0.017	1.58	0.2185
		Temperature * pH * Contamination	0	1	0	0.04	0.8525
		Residual	0.321	30	0.011		
		significant pair-wise comparison				control vs Warming, high CO_2 and La exposed	**0.0049**
	GST	Temperature	0	1	0	0.05	0.8307
		pH	0.002	1	0.002	0.87	0.3565
		Contamination	0.049	1	0.049	23.63	**< 0.0001**
		Temperature * pH	0	1	0	0	0.9523
		Temp * Contamination	0.001	1	0.001	0.52	0.4772
		pH * Contamination	0.005	1	0.005	2.35	0.1341
		Temperature * pH * Contamination	0	1	0	0.21	0.6465
		Residual	0.077	37	0.002		
		significant pair-wise comparison				Warming, high CO_2 and La exposed vs Warming and high CO_2	**0.0225**
	TAC	Temperature	0.162	1	0.162	21.14	**0.0013**
		pH	0.001	1	0.001	0.13	0.7307
		Contamination	0.032	1	0.032	4.16	0.0718
		Temperature * pH	0.006	1	0.006	0.75	0.4094
		Temp * Contamination	0.036	1	0.036	4.64	0.0597
		pH * Contamination	0.005	1	0.005	0.71	0.4197
		Temperature * pH * Contamination	0.009	1	0.009	1.11	0.3189
		Residual	0.069	9	0.008		
		significant pair-wise comparisons				control vs Warming	**0.0288**
						control vs Warming, high CO_2 and La exposed	**0.0437**
T14	**LIPO**	Temperature	0.092	1	0.092	7.3	**0.0222**
		pH	0.027	1	0.027	2.18	0.1708
		Contamination	0.115	1	0.115	9.08	**0.013**
		Temperature * pH	0.013	1	0.013	1	0.3414
		Temp * Contamination	0.23	1	0.23	18.19	**0.0017**
		pH * Contamination	0	1	0	0	0.9888
		Temperature * pH * Contamination	0	1	0	0.01	0.9204
		Residual	0.126	10	0.013		
		significant pair-wise comparisons				High CO_2 vs Warming	**0.0184**
						High CO_2 vs Warming and high CO_2	**0.0289**
						Warming vs Warming, high CO_2 and La exposed	**0.0314**
						Warming, high CO_2 and La exposed vs Warming and high CO_2	**0.0496**
	HSP	Temperature	0.015	1	0.015	0.71	0.4178
		pH	0.002	1	0.002	0.09	0.7718
		Contamination	0.026	1	0.026	1.26	0.2847
		Temperature * pH	0.013	1	0.013	0.65	0.4375
		Temp * Contamination	0.004	1	0.004	0.2	0.6625
		pH * Contamination	0.014	1	0.014	0.67	0.4293
		Temperature * pH * Contamination	0.002	1	0.002	0.09	0.7673

Supplemental Table 8.2 a Cont.

			Sum of squares	Degrees of freedom	Mean square	F-value	p-value
T14	**HSP**	Residual	0.227	11	0.021		
	Ub	Temperature	0.037	1	0.037	2.1	0.1853
		pH	0.058	1	0.058	3.28	0.1078
		Contamination	0.026	1	0.026	1.46	0.262
		Temperature * pH	0.019	1	0.019	1.09	0.3267
		Temp * Contamination	0.015	1	0.015	0.84	0.3875
		pH * Contamination	0.088	1	0.088	4.95	0.0568
		Temperature * pH * Contamination	0.154	1	0.154	8.69	**0.0185**
		Residual	0.142	8	0.018		
		significant pair-wise comparison				Warming vs Warming and high CO_2	**0.0465**
	SOD	Temperature	0.02	1	0.02	14.04	**0.0009**
		pH	0.002	1	0.002	1.12	0.2991
		Contamination	0.003	1	0.003	1.93	0.1768
		Temperature * pH	0	1	0	0.25	0.6198
		Temp * Contamination	0.014	1	0.014	9.55	**0.0047**
		pH * Contamination	0.002	1	0.002	1.14	0.2959
		Temperature * pH * Contamination	0.002	1	0.002	1.71	0.2022
		Residual	0.038	26	0.001		
		significant pair-wise comparisons				control vs La exposed	**0.0486**
						control vs Warming	**0.01**
						control vs Warming, high CO_2 and La exposed	**0.0048**
						control vs Warming and high CO_2	**0.0151**
	CAT	Temperature	0.005	1	0.005	2.81	0.1193
		pH	0.01	1	0.01	5.8	**0.033**
		Contamination	0.006	1	0.006	3.4	0.0899
		Temperature * pH	0.001	1	0.001	0.69	0.4221
		Temp * Contamination	0.03	1	0.03	17.15	**0.0014**
		pH * Contamination	0.005	1	0.005	2.95	0.1115
		Temperature * pH * Contamination	0.012	1	0.012	7	**0.0214**
		Residual	0.021	12	0.002		
	GPx	Temperature	0.062	1	0.062	7.89	**0.009**
		pH	0.045	1	0.045	5.72	**0.0238**
		Contamination	0.02	1	0.02	2.53	0.1231
		Temperature * pH	0.005	1	0.005	0.58	0.4515
		Temp * Contamination	0.015	1	0.015	1.89	0.1798
		pH * Contamination	0	1	0	0.05	0.8178
		Temperature * pH * Contamination	0.016	1	0.016	2.05	0.1633
		Residual	0.218	28	0.008		
		significant pair-wise comparisons				control vs Warming and La exposed	**0.034**
						control vs Warming, high CO_2 and La exposed	**0.0359**
						La exposed vs Warming and La exposed	**0.0213**
						La exposed vs Warming, high CO_2 and La exposed	**0.0224**
	GST	Temperature	0.001	1	0.001	0.5	0.4852
		pH	0.002	1	0.002	0.83	0.3716
		Contamination	0.022	1	0.022	9.34	**0.0053**
		Temperature * pH	0.001	1	0.001	0.54	0.4699
		Temp * Contamination	0	1	0	0.01	0.919
		pH * Contamination	0.001	1	0.001	0.23	0.6349
		Temperature * pH * Contamination	0.001	1	0.001	0.32	0.5753
		Residual	0.059	25	0.002		
	TAC	Temperature	0.131	1	0.131	16.1	**0.0025**
		pH	0	1	0	0.04	0.8527
		Contamination	0	1	0	0	0.9997
		Temperature * pH	0.022	1	0.022	2.66	0.1342
		Temp * Contamination	0.03	1	0.03	3.71	**0.0831**
		pH * Contamination	0.004	1	0.004	0.51	0.4917
		Temperature * pH * Contamination	0.021	1	0.021	2.59	0.1385
		Residual	0.081	10	0.008		
		significant pair-wise comparison				control vs Warming	**0.0107**

Supplemental Table 8.2 b - Tukey's pairwise comparisons between times for TAC, SOD, GST, GPx, HSP, CAT, LIPO and Ub in the four La exposed treatments. Bold point significant differences ($p < 0.05$).

		La exposed	High CO_2 and La exposed	Warming and La exposed	Warming, high CO_2 and La exposed
LIPO	T1 vs T3	0.1089	0.1801	0.0934	0.9999
	T1 vs T7	0.1527	**0.0024**	**0.018**	**0.0008**
	T1 vs T14	0.8496	0.8156	0.1476	0.6227
	T3 vs T7	**0.0095**	**0.0003**	**0.0017**	**0.0007**
	T3 vs T14	0.0594	0.6434	0.9999	0.6578
	T7 vs T14	0.4591	**0.0019**	**0.0029**	**0.0003**
HSP	T1 vs T3	0.9965	0.5031	**0.0191**	0.6417
	T1 vs T7	0.932	**0.02**	**0.0278**	0.8093
	T1 vs T14	0.2839	0.2924	0.3069	0.698
	T3 vs T7	0.9841	0.1127	0.9894	0.9972
	T3 vs T14	0.4512	0.9594	0.372	1
	T7 vs T14	0.647	0.1906	0.5005	0.997
Ub	T1 vs T3	**0.0444**	0.2212	0.1424	0.9812
	T1 vs T7	0.0758	0.1731	**0.019**	0.6108
	T1 vs T14	0.7309	0.5674	0.8848	0.9953
	T3 vs T7	0.9064	1	0.5945	0.4437
	T3 vs T14	0.1069	0.7975	0.0844	0.9996
	T7 vs T14	0.1976	0.7504	**0.0144**	0.5583
SOD	T1 vs T3	0.6121	**0.0374**	**0.0151**	0.2779
	T1 vs T7	0.9235	**0.0002**	**< 0.0001**	**< 0.0001**
	T1 vs T14	**< 0.0001**	**< 0.0001**	**< 0.0001**	**< 0.0001**
	T3 vs T7	0.9787	**0.0284**	**0.0038**	**< 0.0001**
	T3 vs T14	**0.0003**	**0.003**	**0.0386**	**< 0.0001**
	T7 vs T14	**0.0006**	0.9892	0.7077	0.1452
CAT	T1 vs T3	0.2489	0.3264	0.2619	0.9805
	T1 vs T7	**< 0.0001**	**0.0003**	**0.0026**	**0.0004**
	T1 vs T14	**0.0002**	**0.002**	**0.0244**	**0.0416**
	T3 vs T7	**0.0002**	**0.0001**	**0.0067**	**0.0004**
	T3 vs T14	**0.0008**	**0.0007**	0.133	**0.0317**
	T7 vs T14	0.1526	**0.013**	0.0999	**0.0016**
GPx	T1 vs T3	**< 0.0001**	**< 0.0001**	0.1117	0.0719
	T1 vs T7	**< 0.0001**	**< 0.0001**	**< 0.0001**	**0.0002**
	T1 vs T14	**0.0419**	**0.0003**	**< 0.0001**	**0.0017**
	T3 vs T7	0.6309	0.9404	**0.0025**	**0.0297**
	T3 vs T14	**0.0017**	0.4855	**0.0005**	0.2305
	T7 vs T14	**0.0167**	0.7931	0.996	0.6943
GST	T1 vs T3	0.8946	0.9128	0.9896	0.9965
	T1 vs T7	0.9266	1	**0.0063**	0.9484
	T1 vs T14	0.8591	0.5829	**0.0043**	0.3196
	T3 vs T7	0.9994	0.8937	**0.0031**	0.9936
	T3 vs T14	0.9993	0.3535	**0.0021**	0.5358
	T7 vs T14	0.995	0.5042	0.9982	0.6305
TAC	T1 vs T3	0.1956	0.135	**0.0011**	0.0762
	T1 vs T7	**0.0088**	**0.0044**	**0.0001**	**0.0363**
	T1 vs T14	**0.0256**	**0.0165**	**0.0005**	0.1196
	T3 vs T7	**0.0438**	0.0515	0.0136	0.6887
	T3 vs T14	0.1901	0.2518	0.2634	0.9985
	T7 vs T14	0.6093	0.6053	0.1833	0.6665

ANNEX 8

SUPPLEMENTARY INFORMATION FOR CHAPTER 9

Supplemental Table 9.1 a)- Tukey's pairwise comparisons between experimental treatments, for Gd concentrations. Bold point significant differences ($p < 0.05$).

	T0	T1	T3	T7	T14
Control vs Acidification	0.9996	1	0.9724	1	0.9724
Control vs Warming	0.9593	0.7922	0.1923	1	0.0616
Control vs Warming & Acidification	0.7118	0.9653	1	0.9976	0.2803
Acidification vs Warming	0.92	0.6675	0.7364	1	0.1389
Acidification vs Warming & Acidification	0.6098	0.9255	0.9307	0.9955	0.5112
Warming vs Warming & Acidification	0.9267	0.9967	0.1327	0.9963	0.9979
Control vs Gd		**< 0.0001**	**< 0.0001**	**0.0012**	**< 0.0001**
Control vs Acidification & Gd		**< 0.0001**	**< 0.0001**	**< 0.0001**	**< 0.0001**
Control vs Warming & Gd		**< 0.0001**	**< 0.0001**	**< 0.0001**	**< 0.0001**
Control vs Warming, acidification & Gd		**< 0.0001**	**< 0.0001**	**0.0001**	**< 0.0001**
Acidification vs Gd		**< 0.0001**	**< 0.0001**	**0.0003**	**< 0.0001**
Acidification vs Acidification & Gd		**< 0.0001**	**< 0.0001**	**< 0.0001**	**< 0.0001**
Acidification vs Warming & Gd		**< 0.0001**	**< 0.0001**	**< 0.0001**	**< 0.0001**
Acidification vs Warming, acidification & Gd		**< 0.0001**	**< 0.0001**	**< 0.0001**	**< 0.0001**
Warming vs Gd		**< 0.0001**	**< 0.0001**	**0.0003**	**< 0.0001**
Warming vs Acidification & Gd		**< 0.0001**	**< 0.0001**	**0.0014**	**< 0.0001**
Warming vs Warming & Gd		**< 0.0001**	**< 0.0001**	**< 0.0001**	**< 0.0001**
Warming vs Waming, acidification & Gd		**< 0.0001**	**< 0.0001**	**< 0.0001**	**< 0.0001**
Warming & Acidification vs Gd		**< 0.0001**	**< 0.0001**	**< 0.0001**	**< 0.0001**
Warming & Acidification vs Acidification & Gd		**< 0.0001**	**< 0.0001**	**< 0.0001**	**< 0.0001**
Warming & Acidification vs Warming & Gd		**< 0.0001**	**< 0.0001**	**< 0.0001**	**< 0.0001**
Warming & Acidification vs Warming, acidification & Gd		**< 0.0001**	**< 0.0001**	**< 0.0001**	**< 0.0001**
Gd vs Acidification & Gd		0.9926	0.9937	0.403	0.9996
Gd vs Warming & Gd		1	1	0.0688	0.9957
Gd vs Warming & Acidification & Gd		0.8872	0.9981	0.9986	0.999
Acidification & Gd vs Warming & Gd		0.9945	0.999	0.9885	0.9337
Acidification & Gd vs Warming, acidification & Gd		0.9998	1	0.6749	0.9659
Warming & Gd vs Warming, acidification & Gd		0.9269	0.9998	0.1503	1

Supplemental Table 9.1 b) - Tukey's pairwise comparisons between times for Gd concentration in the four Gd exposed treatments. Bold point significant differences ($p < 0.05$).

	Gd exposed	Acidification & Gd	Warming & Gd	Warming, acidification & Gd
T1 vs T3	0.094	0.44	0.75	0.15
T1 vs T7	**0.047**	0.097	**0.041**	0.062
T1 vs T14	0.12	0.81	0.99	0.99
T3 vs T7	0.92	0.61	0.22	0.96
T3 vs T14	0.99	0.9	0.81	0.1
T7 vs T14	0.79	0.31	**0.042**	**0.041**

Supplemental Table 9.2 a) – Two and three-way ANOVAs with Temperature and pH and Temperature, pH, and Contamination as factors, respectively, followed by significant Tukey's pairwise comparisons for LIPO, TAC, SOD, CAT, GPx, GST, HSP and Ub, for T0, T1, T3, T7 and T14. Bold represent statistical differences ($p < 0.05$).

		Effect	Sum of squares	Degrees of freedom	Mean square	F-value	p-value
T0	**LIPO**	Temperature	0.001	1	0.001	0.08	0.7881
		pH	0.002	1	0.002	0.14	0.7272
		Temperature * pH	0.013	1	0.013	0.92	0.3918
		Residual	0.056	4	0.014		
	TAC	Temperature	0	1	0	0.01	0.9274
		pH	0	1	0	0.03	0.8702
		Temperature * pH	0.006	1	0.006	2.1	0.2213
		Residual	0.012	4	0.003		
	SOD	Temperature	0.006	1	0.006	0.26	0.6191
		pH	0.002	1	0.002	0.11	0.745
		Temperature * pH	0.022	1	0.022	0.98	0.3393
		Residual	0.317	14	0.023		
	CAT	Temperature	0.005	1	0.005	0.34	0.5926
		pH	0.006	1	0.006	0.38	0.5687
		Temperature * pH	0.002	1	0.002	0.12	0.7457
		Residual	0.065	4	0.016		
	GPx	Temperature	0.001	1	0.001	0.15	0.7056
		pH	0.001	1	0.001	0.09	0.7699
		Temperature * pH	0.005	1	0.005	0.62	0.4407
		Residual	0.139	17	0.008		
	GST	Temperature	0.01	1	0.01	3.72	0.0718
		pH	0.016	1	0.016	6.1	0.0251
		Temperature * pH	0	1	0	0.16	0.6903
		Residual	0.043	16	0.003		
		significant pair-wise comparison				Control - Warming and acidification	**0.0219**
	HSP	Temperature	0	1	0	0.01	0.9247
		pH	0	1	0	0	0.9876
		Temperature * pH	0.003	1	0.003	0.57	0.4766
		Residual	0.036	7	0.005		
	Ub	Temperature	0.007	1	0.007	0.23	0.6545
		pH	0.005	1	0.005	0.15	0.7149
		Temperature * pH	0.006	1	0.006	0.19	0.6794
		Residual	0.166	5	0.033		
T1	**LIPO**	Temperature	0.044	1	0.044	2.46	0.1395
		pH	0.011	1	0.011	0.61	0.4484
		Treatment	0.072	1	0.072	4.04	0.0641
		Temperature * pH	0.003	1	0.003	0.18	0.6771
		Temperature * Treatment	0.08	1	0.08	4.48	0.0528
		pH * Treatment	0.012	1	0.012	0.68	0.4241
		Temperature * pH * Treatment	0.004	1	0.004	0.24	0.6314
		Residual	0.25	14	0.018		
	TAC	Temperature	0.12	1	0.12	10.03	0.0114
		pH	0	1	0	0.02	0.8937
		Treatment	0.138	1	0.138	11.53	**0.0079**
		Temperature * pH	0.001	1	0.001	0.09	0.7658
		Temperature * Treatment	0.192	1	0.192	16.07	**0.0031**
		pH * Treatment	0.001	1	0.001	0.11	0.7505
		Temperature * pH * Treatment	0.001	1	0.001	0.06	0.8055
		Residual	0.108	9	0.012		
		significant pair-wise comparisons				Warming - Warming & Gd	**0.0455**
						Warming & Gd - Warming & acidification	**0.0302**
	SOD	Temperature	0.005	1	0.005	1.05	0.3142
		pH	0.004	1	0.004	0.82	0.3724
		Treatment	0.001	1	0.001	0.16	0.6926
		Temperature * pH	0.034	1	0.034	6.7	0.0147
		Temperature * Treatment	0.013	1	0.013	2.5	0.1245
		pH * Treatment	0.019	1	0.019	3.68	0.0646

Supplemental Table 9.2 a Cont.

		Effect	Sum of squares	Degrees of freedom	Mean square	F-value	p-value
		Temperature * pH * Treatment	0.001	1	0.001	0.15	0.6972
		Residual	0.151	30	0.005		
	CAT	Temperature	0.009	1	0.009	0.94	0.3524
		pH	0.014	1	0.014	1.46	0.2519
		Treatment	0.057	1	0.057	6.15	**0.0306**
		Temperature * pH	0.043	1	0.043	4.63	0.0545
		Temperature * Treatment	0.038	1	0.038	4.14	0.0667
		pH * Treatment	0.002	1	0.002	0.18	0.6765
		Temperature * pH * Treatment	0.005	1	0.005	0.54	0.4778
		Residual	0.102	11	0.009		
	GPx	Temperature	0.005	1	0.005	1.23	0.2761
		pH	0.004	1	0.004	1	0.3244
		Treatment	0	1	0	0	0.9782
		Temperature * pH	0.004	1	0.004	0.91	0.3486
		Temperature * Treatment	0.012	1	0.012	2.76	0.1068
		pH * Treatment	0.021	1	0.021	4.81	**0.036**
		Temperature * pH * Treatment	0.005	1	0.005	1.06	0.3102
		Residual	0.133	31	0.004		
	GST	Temperature	0.007	1	0.007	1.43	0.2402
		pH	0.01	1	0.01	1.9	0.1769
		Treatment	0.196	1	0.196	37.87	**< 0.0001**
		Temperature * pH	0	1	0	0.01	0.9375
		Temperature * Treatment	0	1	0	0	0.9558
		pH * Treatment	0	1	0	0.02	0.8778
		Temperature * pH * Treatment	0.001	1	0.001	0.16	0.6873
		Residual	0.181	35	0.005		
		significant pair-wise comparisons				Control - Gd	**0.0418**
						Control - Acidification & Gd	**0.0111**
						Control - Warming & Gd	**0.0124**
						Control - Warming, acidification & Gd	**0.0011**
						Acidification - Warming, acidification and Gd	**0.0273**
						Warming - Warming, acidification & Gd	**0.0063**
						Warming, acidification & Gd - Warming & acidification	**0.0491**
	HSP	Temperature	0.01	1	0.01	1.04	0.3285
		pH	0	1	0	0.01	0.9063
		Treatment	0	1	0	0.01	0.9287
		Temperature * pH	0.004	1	0.004	0.36	0.5585
		Temperature * Treatment	0.009	1	0.009	0.94	0.3508
		pH * Treatment	0	1	0	0.01	0.9382
		Temperature * pH * Treatment	0.014	1	0.014	1.46	0.2499
		Residual	0.119	12	0.01		
	Ub	Temperature	0.009	1	0.009	0.21	0.6529
		pH	0.044	1	0.044	0.98	0.3392
		Treatment	0.02	1	0.02	0.46	0.5103
		Temperature * pH	0	1	0	0	0.9709
		Temperature * Treatment	0.032	1	0.032	0.71	0.4132
		pH * Treatment	0	1	0	0	0.9944
		Temperature * pH * Treatment	0	1	0	0	0.9881
		Residual	0.575	13	0.044		
T3	**LIPO**	Temperature	0.003	1	0.003	0.15	0.7037
		pH	0.006	1	0.006	0.33	0.577
		Treatment	0.01	1	0.01	0.55	0.4679
		Temperature * pH	0.017	1	0.017	0.97	0.3391
		Temperature * Treatment	0.013	1	0.013	0.75	0.4013
		pH * Treatment	0.013	1	0.013	0.71	0.4136
		Temperature * pH * Treatment	0.016	1	0.016	0.9	0.358
		Residual	0.267	15	0.018		
	TAC	Temperature	0.071	1	0.071	7.32	**0.0242**
		pH	0	1	0	0	0.9817

Supplemental Table 9.2 a Cont.

		Effect	Sum of squares	Degrees of freedom	Mean square	F-value	p-value
T3	**TAC**	Treatment	0.151	1	0.151	15.57	**0.0034**
		Temperature * pH	0.009	1	0.009	0.94	0.3568
		Temperature * Treatment	0	1	0	0.05	0.8269
		pH * Treatment	0.004	1	0.004	0.39	0.5468
		Temperature * pH * Treatment	0.001	1	0.001	0.11	0.7529
		Residual	0.087	9	0.01		
	SOD	Temperature	0.022	1	0.022	1.82	0.1871
		pH	0	1	0	0.01	0.9353
		Treatment	0	1	0	0.04	0.8519
		Temperature * pH	0.001	1	0.001	0.11	0.7403
		Temperature * Treatment	0.016	1	0.016	1.38	0.2488
		pH * Treatment	0.031	1	0.031	2.65	0.1131
		Temperature * pH * Treatment	0	1	0	0.04	0.8495
		Residual	0.379	32	0.012		
	CAT	Temperature	0.001	1	0.001	0.71	0.4164
		pH	0.053	1	0.053	48.72	**< 0.0001**
		Treatment	0.005	1	0.005	4.92	**0.0466**
		Temperature * pH	0.002	1	0.002	1.47	0.2482
		Temperature * Treatment	0.051	1	0.051	47.35	**< 0.0001**
		pH * Treatment	0.006	1	0.006	5.31	**0.0398**
		Temperature * pH * Treatment	0.005	1	0.005	4.37	0.0585
		Residual	0.013	12	0.001		
		significant pair-wise comparisons				Control - Warming, acidification & Gd	**0.0076**
						Gd - Acidification	**0.0077**
						Gd - Warming, acidification & Gd	**0.0003**
						Acidification & Gd - Warming	**0.0129**
						Acidification & Gd - Warming, acidification & Gd	**0.0089**
						Acidification - Warming	**0.0008**
						Acidification - Warming & Gd	**0.0344**
						Acidification - Warming & acidification	**0.0163**
						Warming - Warming, acidification & Gd	**< 0.0001**
						Warming & Gd - Warming, acidification & Gd	**0.0007**
						Warming, acidification & Gd - Warming & acidification	**0.0004**
	GPx	Temperature	0.056	1	0.056	34.27	**< 0.0001**
		pH	0.031	1	0.031	19.11	**0.0001**
		Treatment	0.011	1	0.011	6.52	**0.0158**
		Temperature * pH	0.002	1	0.002	1.29	0.2646
		Temperature * Treatment	0.02	1	0.02	11.86	**0.0017**
		pH * Treatment	0.005	1	0.005	3.15	0.0857
		Temperature * pH * Treatment	0.001	1	0.001	0.36	0.5553
		Residual	0.051	31	0.002		
		significant pair-wise comparisons				Control - Gd	**0.0038**
						Control - Acidification & Gd	**< 0.0001**
						Control - Acidification	**0.0021**
						Gd - Warming	**0.0044**
						Gd - Warming & Gd	**0.0022**
						Acidification & Gd - Warming	**< 0.0001**
						Acidification & Gd - Warming & Gd	**< 0.0001**
						Acidification & Gd - Warming, acidification & Gd	**0.0024**
						Acidification & Gd - Warming & acidification	**0.0069**
						Acidification - Warming	**0.0029**
						Acidification - Warming & Gd	**0.0011**
	GST	Temperature	0.011	1	0.011	5.12	**0.0301**
		pH	0.023	1	0.023	10.51	**0.0027**
		Treatment	0.171	1	0.171	77.2	**< 0.0001**
		Temperature * pH	0	1	0	0.11	0.7476
		Temperature * Treatment	0	1	0	0.02	0.8936
		pH * Treatment	0	1	0	0.13	0.7188
		Temperature * pH * Treatment	0.001	1	0.001	0.37	0.5472

Supplemental Table 9.2 a Cont.

		Effect	Sum of squares	Degrees of freedom	Mean square	F-value	p-value
T3	**GST**	Residual	0.075	34	0.002		
		significant pair-wise comparisons				Control - Gd	**0.0025**
						Control - Acidification & Gd	**< 0.0001**
						Control - Warming & Gd	**< 0.0001**
						Control - Warming, acidification & Gd	**< 0.0001**
						Acidification & Gd - Acidification	**0.0001**
						Acidification & Gd - Warming	**0.0011**
						Acidification & Gd - Warming & acidification	**0.0227**
						Acidification - Warming & Gd	**0.0022**
						Acidification - Warming, acidification & Gd	**< 0.0001**
						Warming - Warming & Gd	**0.0098**
						Warming - Warming, acidification & Gd	**0.0002**
						Warming, acidification & Gd - Warming & acidification	**0.0048**
	HSP	Temperature	0.013	1	0.013	0.49	0.5015
		pH	0.02	1	0.02	0.78	0.3971
		Treatment	0.031	1	0.031	1.19	0.3017
		Temperature * pH	0.096	1	0.096	3.71	0.083
		Temperature * Treatment	0.001	1	0.001	0.04	0.8392
		pH * Treatment	0	1	0	0	0.9933
		Temperature * pH * Treatment	0.025	1	0.025	0.95	0.3529
		Residual	0.259	10	0.026		
	Ub	Temperature	0.005	1	0.005	0.14	0.7163
		pH	0.049	1	0.049	1.26	0.2854
		Treatment	0.119	1	0.119	3.06	0.108
		Temperature * pH	0.016	1	0.016	0.4	0.539
		Temperature * Treatment	0.002	1	0.002	0.04	0.8441
		pH * Treatment	0.011	1	0.011	0.29	0.5999
		Temperature * pH * Treatment	0.011	1	0.011	0.28	0.6056
		Residual	0.428	11	0.039		
T7	**LIPO**	Temperature	0.44	1	0.44	31.13	**0.0002**
		pH	0	1	0	0.01	0.9254
		Treatment	0.073	1	0.073	5.17	**0.044**
		Temperature * pH	0.004	1	0.004	0.31	0.5868
		Temperature * Treatment	0.158	1	0.158	11.19	**0.0065**
		pH * Treatment	0.013	1	0.013	0.91	0.3599
		Temperature * pH * Treatment	0.006	1	0.006	0.44	0.5202
		Residual	0.156	11	0.014		
		significant pair-wise comparisons				Control - Warming	**0.0135**
						Control - Warming & Gd	**0.0038**
						Control - Warming & acidification	**0.0064**
						Acidification - Warming	**0.0432**
						Acidification - Warming & Gd	**0.0159**
						Acidification - Warming & acidification	**0.0214**
	TAC	Temperature	0.189	1	0.189	23.97	**0.0012**
		pH	0.001	1	0.001	0.15	0.7078
		Treatment	0.009	1	0.009	1.19	0.3073
		Temperature * pH	0.022	1	0.022	2.84	0.1306
		Temperature * Treatment	0.021	1	0.021	2.63	0.1436
		pH * Treatment	0	1	0	0.01	0.9344
		Temperature * pH * Treatment	0	1	0	0.03	0.8697
		Residual	0.063	8	0.008		
		significant pair-wise comparison				Control - Warming	**0.0375**
	SOD	Temperature	0.337	1	0.337	107.28	**< 0.0001**
		pH	0.004	1	0.004	1.26	0.2693
		Treatment	0.054	1	0.054	17.26	**0.0002**
		Temperature * pH	0.003	1	0.003	0.9	0.3496
		Temperature * Treatment	0.061	1	0.061	19.32	**0.0001**
		pH * Treatment	0.016	1	0.016	4.99	**0.0321**
		Temperature * pH * Treatment	0.004	1	0.004	1.28	0.2651

Supplemental Table 9.2 a Cont.

		Effect	Sum of squares	Degrees of freedom	Mean square	F-value	p-value
T7	**SOD**	Residual	0.107	34	0.003		
		significant pair-wise comparisons				Control - Gd	**0.0195**
						Control - Warming	**< 0.0001**
						Control - Warming & Gd	**0.0002**
						Control - Warming, acidification & Gd	**< 0.0001**
						Control - Warming & acidification	**0.0004**
						Gd - Acidification	**< 0.0001**
						Gd - Warming	**0.006**
						Gd - Warming, acidification & Gd	**0.0109**
						Acidification & Gd - Acidification	**0.0004**
						Acidification & Gd - Warming	**0.0014**
						Acidification & Gd - Warming, acidification & Gd,	**0.0026**
						Acidification - Warming	**< 0.0001**
						Acidification - Warming & Gd	**< 0.0001**
						Acidification - Warming, acidification & Gd	**< 0.0001**
						Acidification - Warming & acidification	**< 0.0001**
	CAT	Temperature	0.038	1	0.038	39.26	**< 0.0001**
		pH	0.029	1	0.029	30.32	**0.0001**
		Treatment	0	1	0	0.01	0.9055
		Temperature * pH	0.019	1	0.019	19.67	**0.0008**
		Temperature * Treatment	0	1	0	0.02	0.8898
		pH * Treatment	0	1	0	0.34	0.5732
		Temperature * pH * Treatment	0.01	1	0.01	10.4	**0.0073**
		Residual	0.012	12	0.001		
		significant pair-wise comparisons				Control - Acidification & Gd	**0.0045**
						Control - Acidification	**0.0008**
						Control - Warming	**0.0003**
						Control - Warming & Gd	**0.0018**
						Control - Warming, Acidification & Gd	**0.0001**
						Control - Warming & acidification	**0.0018**
						Gd - Acidification	**0.0135**
						Gd - Warming	**0.0053**
						Gd - Warming & Gd	**0.0463**
						Gd - Warming, acidification & Gd	**0.0023**
						Gd - Warming & acidification	**0.0345**
	GPx	Temperature	0.009	1	0.009	0.9	0.3495
		pH	0.059	1	0.059	6.15	**0.0192**
		Treatment	0.247	1	0.247	25.6	**< 0.0001**
		Temperature * pH	0.021	1	0.021	2.16	0.1528
		Temperature * Treatment	0.004	1	0.004	0.4	0.5309
		pH * Treatment	0.049	1	0.049	5.07	**0.0321**
		Temperature * pH * Treatment	0.007	1	0.007	0.71	0.4063
		Residual	0.28	29	0.01		
		significant pair-wise comparisons				Control - Gd	**0.0011**
						Control - Acidification & Gd	**0.0133**
						Control - Warming & Gd	**0.0117**
						Control - Warming, acidification & Gd	**0.0029**
						Gd - Warming	**0.0179**
						Warming - Warming, acidification & Gd	**0.0265**
	GST	Temperature	0.003	1	0.003	0.85	0.3626
		pH	0	1	0	0.06	0.8107
		Treatment	0.2	1	0.2	55.14	**< 0.0001**
		Temperature * pH	0	1	0	0.02	0.8935
		Temperature * Treatment	0.006	1	0.006	1.68	0.2038
		pH * Treatment	0	1	0	0.04	0.8411
		Temperature * pH * Treatment	0.001	1	0.001	0.19	0.6678
		Residual	0.127	35	0.004		
		significant pair-wise comparisons				Control - Gd	**0.0028**
						Control - Acidification & Gd	**0.0012**

Supplemental Table 9.2 a Cont.

		Effect	Sum of squares	Degrees of freedom	Mean square	F-value	p-value
T7	**GST**					Control - Warming & Gd	**0.0173**
						Gd - Acidification	**0.0057**
						Gd - Warming	**0.0031**
						Gd - Warming & acidification	**0.0088**
						Acidification & Gd - Acidification	**0.0025**
						Acidification & Gd - Warming	**0.0013**
						Acidification & Gd - Warming & acidification	**0.0038**
						Acidification - Warming & Gd	**0.0321**
						Warming - Warming & Gd	**0.0192**
	HSP	Temperature	0.088	1	0.088	4.72	**0.0489**
		pH	0.023	1	0.023	1.25	0.2834
		Treatment	0.18	1	0.18	9.71	**0.0082**
		Temperature * pH	0.08	1	0.08	4.3	0.0586
		Temperature * Treatment	0.083	1	0.083	4.48	0.054
		pH * Treatment	0.01	1	0.01	0.55	0.4726
		Temperature * pH * Treatment	0	1	0	0.01	0.9047
		Residual	0.241	13	0.019		
		significant pair-wise comparison				Gd - Warming	**0.0117**
	Ub	Temperature	0.325	1	0.325	11.41	**0.0062**
		pH	0.269	1	0.269	9.44	**0.0106**
		Treatment	1.3	1	1.3	45.62	**< 0.0001**
		Temperature * pH	0.023	1	0.023	0.82	0.3836
		Temperature * Treatment	0.006	1	0.006	0.22	0.6495
		pH * Treatment	0.002	1	0.002	0.07	0.7992
		Temperature * pH * Treatment	0.014	1	0.014	0.49	0.4978
		Residual	0.313	11	0.028		
		significant pair-wise comparisons				Control - Gd	**0.0473**
						Gd - Acidification	**0.0088**
						Gd - Warming	**0.0021**
						Gd - Warming & acidification	**0.0008**
						Acidification & Gd - Warming & acidification	**0.0121**
						Warming & Gd - Warming & acification	**0.0165**
T14	**LIPO**	Temperature	0.149	1	0.149	25.2	**0.0005**
		pH	0.039	1	0.039	6.61	**0.0279**
		Treatment	0.082	1	0.082	13.93	**0.0039**
		Temperature * pH	0.005	1	0.005	0.92	0.3594
		Temperature * Treatment	0.158	1	0.158	26.65	**0.0004**
		pH * Treatment	0.001	1	0.001	0.15	0.7029
		Temperature * pH * Treatment	0.03	1	0.03	5.16	**0.0465**
		Residual	0.059	10	0.006		
		significant pair-wise comparisons				Gd - Warming	**0.0096**
						Gd - Warming & acidification	**0.0184**
						Acidification & Gd - Warming	**0.0213**
						Acidification & Gd - Warming & acidification	**0.0391**
						Warming - Warming, acidification & Gd	**0.0023**
						Warming & acidification - Warming, acidification & Gd	**0.004**
						Control - Warming	**0.0241**
						Control - Warming & acidification	**0.0444**
						Warming - Acidification	**0.0012**
						Acidification - Warming & acidification	**0.0021**
	TAC	Temperature	0.098	1	0.098	10.22	**0.0085**
		pH	0.011	1	0.011	1.16	0.3041
		Treatment	0.001	1	0.001	0.12	0.7403
		Temperature * pH	0.086	1	0.086	8.98	**0.0122**
		Temperature * Treatment	0.055	1	0.055	5.71	**0.0359**
		pH * Treatment	0.003	1	0.003	0.34	0.5698
		Temperature * pH * Treatment	0	1	0	0	0.96
		Residual	0.106	11	0.01		
		significant pair-wise comparison					**0.0157**
	SOD	Temperature	0.007	1	0.007	2.03	0.1682

Supplemental Table 9.2 a Cont.

		Effect	Sum of squares	Degrees of freedom	Mean square	F-value	p-value
T14	**SOD**	pH	0.001	1	0.001	0.38	0.5444
		Treatment	0.018	1	0.018	4.84	**0.0386**
		Temperature * pH	0	1	0	0	0.9858
		Temperature * Treatment	0.024	1	0.024	6.6	**0.0175**
		pH * Treatment	0.001	1	0.001	0.39	0.5374
		Temperature * pH * Treatment	0.001	1	0.001	0.21	0.6551
		Residual	0.081	22	0.004		
	CAT	Temperature	0.02	1	0.02	11.32	**0.0056**
		pH	0.014	1	0.014	7.59	**0.0174**
		Treatment	0.012	1	0.012	6.42	**0.0262**
		Temperature * pH	0.001	1	0.001	0.47	0.5078
		Temperature * Treatment	0.01	1	0.01	5.8	**0.033**
		pH * Treatment	0.003	1	0.003	1.79	0.2053
		Temperature * pH * Treatment	0.002	1	0.002	1.25	0.2858
		Residual	0.022	12	0.002		
		significant pair-wise comparisons				Control - Warming	**0.0182**
						Control - Warming & acidification	**0.0023**
						Gd - Warming & acidification	**0.0188**
	GPx	Temperature	0.123	1	0.123	16.22	**0.0006**
		pH	0.003	1	0.003	0.44	0.5145
		Treatment	0.024	1	0.024	3.12	0.092
		Temperature * pH	0	1	0	0.01	0.9306
		Temperature * Treatment	0.055	1	0.055	7.2	**0.0139**
		pH * Treatment	0.025	1	0.025	3.24	0.0864
		Temperature * pH * Treatment	0.002	1	0.002	0.29	0.5956
		Residual	0.159	21	0.008		
		significant pair-wise comparisons				Control - Warimng & Gd	**0.0015**
						Gd - Warming & Gd	**0.0154**
						Acidification & Gd - Warming & Gd	**0.0028**
						Acidification - Warming & Gd	**0.0491**
	GST	Temperature	0.014	1	0.014	2.81	0.106
		pH	0.002	1	0.002	0.42	0.5241
		Treatment	0.061	1	0.061	12.29	**0.0017**
		Temperature * pH	0.001	1	0.001	0.24	0.6257
		Temperature * Treatment	0.025	1	0.025	5.04	**0.0339**
		pH * Treatment	0.001	1	0.001	0.11	0.7467
		Temperature * pH * Treatment	0.001	1	0.001	0.17	0.6806
		Residual	0.124	25	0.005		
		significant pair-wise comparison				Control-Gd	**0.0378**
	HSP	Temperature	0.013	1	0.013	1.08	0.3183
		pH	0.007	1	0.007	0.57	0.4662
		Treatment	0.108	1	0.108	9.18	**0.0105**
		Temperature * pH	0.042	1	0.042	3.54	0.0844
		Temperature * Treatment	0.006	1	0.006	0.51	0.4894
		pH * Treatment	0	1	0	0	0.9679
		Temperature * pH * Treatment	0.002	1	0.002	0.14	0.7153
		Residual	0.141	12	0.012		
	Ub	Temperature	0.278	1	0.278	22.49	**0.0015**
		pH	0.509	1	0.509	41.16	**0.0002**
		Treatment	0.299	1	0.299	24.22	**0.0012**
		Temperature * pH	0.005	1	0.005	0.37	0.5617
		Temperature * Treatment	0.208	1	0.208	16.82	**0.0034**
		pH * Treatment	0.031	1	0.031	2.5	0.1523
		Temperature * pH * Treatment	0.216	1	0.216	17.45	**0.0031**
		Residual	0.099	8	0.012		
		significant pair-wise comparisons				Control - Gd	**0.0011**
						Gd - Acidification & Gd	**0.0057**
						Gd - Acidification	**0.0011**
						Gd - Warming	**0.0096**
						Gd - Warming & Gd	**0.0036**

Supplemental Table 9.2a Cont.

	Effect	Sum of squares	Degrees of freedom	Mean square	F-value	p-value
T14	**Ub**				Gd - Warming, acidification & Gd	**0.0005**
					Gd - Warming & acidification	**0.0001**
					Acidification & Gd - Warming & acidification	**0.0308**
					Warming - Warming & acidfication	**0.0175**

Supplemental table 9.2 b) - Tukey's pairwise comparisons for LIPO, TAC, SOD, CAT, GPx, GST, HSP and Ub between times in the treatments exposed to Gd. Bold indicate significant differences ($p < 0.05$).

		Gd	Acidification & Gd	Warming & Gd	Warming, acidification & Gd
LIPO	T1 vs T3	**0.0401**	0.3576	0.9677	0.401
	T1 vs T7	0.18	0.3298	**0.0452**	**< 0.0001**
	T1 vs T14	0.4392	0.4145	0.8899	0.4667
	T3 vs T7	**0.0041**	**0.0336**	**0.0166**	**< 0.0001**
	T3 vs T14	0.3129	0.9999	0.6353	0.9989
	T7 vs T14	**0.0284**	**0.0509**	0.113	**< 0.0001**
TAC	T1 vs T3	0.2443	**0.0077**	0.5854	**0.0082**
	T1 vs T7	0.182	**0.0054**	0.2197	**0.0099**
	T1 vs T14	0.1844	**0.0052**	0.3604	1
	T3 vs T7	0.9885	0.8924	0.7342	0.9915
	T3 vs T14	0.99	0.874	0.9458	**0.0048**
	T7 vs T14	1	1	0.9516	**0.0065**
SOD	T1 vs T3	0.9038	0.495	0.7404	0.9746
	T1 vs T7	0.4826	0.8637	**0.0389**	**0.0121**
	T1 vs T14	**0.0027**	**0.002**	**0.0113**	**0.0364**
	T3 vs T7	0.1539	0.8969	0.3542	**0.0109**
	T3 vs T14	**0.0006**	**0.0132**	0.1694	**0.0295**
	T7 vs T14	**0.0257**	**0.005**	0.9709	0.951
CAT	T1 vs T3	0.8094	0.3151	0.1225	0.3543
	T1 vs T7	**0.0478**	**0.0161**	**0.0008**	0.016
	T1 vs T14	**0.0327**	**0.0629**	0.0594	0.2555
	T3 vs T7	**0.027**	**0.0981**	**0.0001**	0.1108
	T3 vs T14	**0.0193**	0.4155	**0.0038**	0.9889
	T7 vs T14	0.9999	0.7948	0.0589	0.1592
GPx	T1 vs T3	**< 0.0001**	**< 0.0001**	0.6397	0.8758
	T1 vs T7	**< 0.0001**	**< 0.0001**	**0.0002**	**0.0002**
	T1 vs T14	**0.0002**	**0.0021**	**< 0.0001**	**0.0015**
	T3 vs T7	**< 0.0001**	**0.0013**	**0.0008**	**0.001**
	T3 vs T14	0.8575	**0.0203**	**0.0003**	**0.0093**
	T7 vs T14	**< 0.0001**	**< 0.0001**	0.8802	0.4386
GST	T1 vs T3	0.1916	0.9695	0.7708	0.5928
	T1 vs T7	**< 0.0001**	**< 0.0001**	**< 0.0001**	**< 0.0001**
	T1 vs T14	0.9955	0.9783	**0.0246**	**0.0009**
	T3 vs T7	**< 0.0001**	**< 0.0001**	**< 0.0001**	**< 0.0001**
	T3 vs T14	0.2401	1	0.1857	**0.0093**
	T7 vs T14	**< 0.0001**	**< 0.0001**	**0.0062**	**0.0023**
HSP	T1 vs T3	0.2591	0.6033	0.9932	0.4244
	T1 vs T7	0.0201	**0.0155**	0.9976	0.6432
	T1 vs T14	0.102	0.1035	0.2636	0.5643
	T3 vs T7	0.3784	0.0892	0.9652	0.9245

Supplemental Table 9.2 b Cont.

		Gd	Acidification & Gd	Warming & Gd	Warming, acidification & Gd
	T3 vs T14	0.8901	0.6158	0.1389	0.9897
	T7 vs T14	0.7694	0.2876	0.3316	0.9911
Ub	T1 vs T3	0.1908	0.2783	0.5008	0.1157
	T1 vs T7	**0.0075**	0.1837	0.5744	0.2856
	T1 vs T14	**0.0031**	0.5961	0.9977	0.6475
	T3 vs T7	**0.0007**	**0.0234**	0.1038	**0.0219**
	T3 vs T14	0.8034	0.0831	0.4128	0.3683
	T7 vs T14	**0.0013**	0.8422	0.6677	0.0914

ANNEX 9

SUPPLEMENTARY INFORMATION FOR CHAPTER 10

Supplemental Table 10.1 a) - Tukey's pairwise comparison, for La and Gd concentrations for the La and Gd trial, respectively, between all experimental treatments. Bold point significant differences ($p < 0.05$).

	La trial						Gd trial			
	T0	**T1**	**T3**	**T7**	**T14**		**T0**	**T1**	**T3**	**T7**	**T14**
Control vs Acidification	1	1	1	1	1	Control vs Acidification	1	1	1	1	1
Control vs Warming	1	1	1	1	1	Control vs Warming	1	1	1	1	1
Control vs Warming & acidification	1	1	1	1	0.7009	Control vs Warming & acidification	1	1	1	1	0.9596
Acidification vs Warming	1	1	1	1	1	Acidification vs Warming	1	1	1	1	0.9999
Acidification vs Warming & acidification	1	1	1	1	0.6897	Acidification vs Warming & Acidification	1	1	1	1	0.9369
Warming vs Warming & acidification	1	1	1	1	0.8517	Warming vs Warming & acidification	1	1	1	1	0.9948
Control vs La		**< 0.0001**	**< 0.0001**	**< 0.0001**	**< 0.0001**	Control vs Gd		**< 0.0001**	**< 0.0001**	**< 0.0001**	**< 0.0001**
Control vs acidification & La		**< 0.0001**	**< 0.0001**	**< 0.0001**	**< 0.0001**	Control vs Acidification & Gd		**< 0.0001**	**< 0.0001**	**< 0.0001**	**< 0.0001**
Control vs Warming & La		**< 0.0001**	**< 0.0001**	**< 0.0001**	**< 0.0001**	Control vs Warming & Gd		**< 0.0001**	**< 0.0001**	**< 0.0001**	**< 0.0001**
Control vs Warming, acidification & La		**< 0.0001**	**< 0.0001**	**< 0.0001**	**< 0.0001**	Control vs Warming, acidification & Gd		**< 0.0001**	**< 0.0001**	**< 0.0001**	**< 0.0001**
Acidification vs La		**< 0.0001**	**< 0.0001**	**< 0.0001**	**< 0.0001**	Acidification vs Gd		**< 0.0001**	**< 0.0001**	**< 0.0001**	**< 0.0001**
Acidification vs Acidification & La		**< 0.0001**	**< 0.0001**	**< 0.0001**	**< 0.0001**	Acidification vs Acidification & Gd		**< 0.0001**	**< 0.0001**	**< 0.0001**	**< 0.0001**
Warming vs La		**< 0.0001**	**< 0.0001**	**< 0.0001**	**< 0.0001**	Warming vs Gd		**< 0.0001**	**< 0.0001**	**< 0.0001**	**< 0.0001**
Warming vs Acidification & La		**< 0.0001**	**< 0.0001**	**< 0.0001**	**< 0.0001**	Warming vs Acidification & Gd		**< 0.0001**	**< 0.0001**	**< 0.0001**	**< 0.0001**
Warming vs Warming & La		**< 0.0001**	**< 0.0001**	**< 0.0001**	**< 0.0001**	Warming vs Warming & Gd		**< 0.0001**	**< 0.0001**	**< 0.0001**	**< 0.0001**
Warming vs Warming, acidification & La		**< 0.0001**	**< 0.0001**	**< 0.0001**	**< 0.0001**	Warming vs Warming, acidification & Gd		**< 0.0001**	**< 0.0001**	**< 0.0001**	**< 0.0001**
Warming & acidification vs Warming & La		**< 0.0001**	**< 0.0001**	**< 0.0001**	**< 0.0001**	Warming & acidification vs Warming & Gd		**< 0.0001**	**< 0.0001**	**< 0.0001**	**< 0.0001**
Warming & acidification vs Warming, acidification & La		**< 0.0001**	**< 0.0001**	**< 0.0001**	**0.001**	Warming & acidification vs Warming, acidification & Gd		**< 0.0001**	**< 0.0001**	**< 0.0001**	**< 0.0001**
La vs Acidification & La		0.1001	0.4095	1	0.9142	Gd vs Acidification & Gd		**< 0.0001**	**0.0001**	0.9969	0.5356
La vs Warming & La		0.9086	0.8608	0.9813	0.8888	Gd vs Warming & Gd		0.3718	**< 0.0001**	0.3608	0.1496
La vs Warming, acidification & La		0.791	**0.01**	0.1298	**< 0.0001**	Gd vs Warming, Acidification & Gd		0.6457	0.9998	1	0.9346
Acidification & La vs Warming & La		0.7034	0.9937	0.9897	0.1001	Acidification & Gd vs Warming & Gd		**0.0004**	**< 0.0001**	0.1132	**0.0019**
Acidification & La vs Warming, acidification & La		**0.0022**	**< 0.0001**	0.1075	**< 0.0001**	Acidification & Gd vs Warming, acidification & Gd		**< 0.0001**	**< 0.0001**	0.9737	0.1215
Warming & La vs Warming, acidification & La		0.1374	**0.0002**	**0.0152**	**0.0004**	Warming & Gd vs Warming, acidification & Gd		0.9992	**< 0.0001**	0.6248	0.8939

Supplemental table 10.1 b) - Tukey's pairwise comparisons between times for La and Gd concentrations in the four La exposed treatments and four Gd exposed treatments, respectively. Bold point significant differences ($p < 0.05$).

	La	**Acidification & La**	**Warming & La**	**Warming, acidification & La**	**Gd**	**Acidification & Gd**	**Warming & Gd**	**Warming, acidification & Gd**
T1 vs T3	**0.0021**	**0.0007**	**0.0001**	**0.0007**	**0.0002**	**0.0333**	**< 0.0001**	**< 0.0001**
T1 vs T7	**< 0.0001**	**< 0.0001**	**< 0.0001**	**< 0.0001**	**< 0.0001**	**< 0.0001**	**< 0.0001**	**< 0.0001**
T1 vs T14	**< 0.0001**	**< 0.0001**	**0.0021**	**< 0.0001**	**< 0.0001**	**0.0002**	**< 0.0001**	**< 0.0001**
T3 vs T7	**0.0002**	**0.0024**	**0.0253**	**< 0.0001**	**< 0.0001**	**0.0354**	**0.0197**	**< 0.0001**
T3 vs T14	**0.001**	**0.0002**	0.3412	0.114	**< 0.0001**	0.0935	**0.0002**	**< 0.0001**
T7 vs T14	1	0.5656	0.4718	**< 0.0001**	0.6147	0.955	0.1057	0.4691

| ANNEX 9

Supplemental Table 10.2 a) – Two- and Three-way ANOVAs followed by significant Tukey's pairwise comparisons with Temperature, pH, and Contamination as factors for the outputs SOD, CAT, GST, LIPO, Total Chlorophyll and Carotenoids in each respective sampling time (two-way for T0, three-way for T1, T3, T7 and T14). Bold represent statistical differences ($p < 0.05$).

			Sum of squares	Degrees of freedom	Mean square	F-value	p-value
T0	**SOD**	Temperature	0.022	1	0.022	1.74	0.2231
		pH	0.001	1	0.001	0.1	0.7648
		Temperature * pH	0.001	1	0.001	0.11	0.7489
		Residual	0.099	8	0.012		
	CAT	Temperature	0.002	1	0.002	0.64	0.4409
		pH	0.001	1	0.001	0.33	0.5773
		Temperature * pH	0.001	1	0.001	0.38	0.5496
		Residual	0.036	10	0.004		
	GST	Temperature	0.013	1	0.013	1.57	0.2254
		pH	0.001	1	0.001	0.17	0.6888
		Temperature * pH	0.025	1	0.025	3.13	0.0928
		Residual	0.152	19	0.008		
	LPO	Temperature	0.002	1	0.002	0.33	0.5809
		pH	0.011	1	0.011	2.01	0.194
		Temperature * pH	0.006	1	0.006	1.13	0.3196
		Residual	0.045	8	0.006		
	Chloropyll	Temperature	0	1	0	4.05	0.0841
		pH	0.001	1	0.001	8.52	0.0224
		Temperature * pH	0	1	0	0.19	0.6722
		Residual	0.001	7	0		
		Pairwise comparison				Control vs Warming & acidification	0.0305
	Carotenoid	Temperature	0	1	0	2.41	0.1811
		pH	0	1	0	0.02	0.9043
		Temperature * pH	0.001	1	0.001	3.27	0.1302
		Residual	0.001	5	0		

Supplemental Table 10.2a Cont.

			La trial								Gd trial				
			Sum of squares	**Degrees of freedom**	**Mean square**	**F-value**	**p-value**				**Sum of squares**	**Degrees of freedom**	**Mean square**	**F-value**	**p-value**
T1	**SOD**	Temperature	0.159	1	0.159	7.07	**0.0111**	**T1**	**SOD**	Temperature	0.028	1	0.028	1.77	0.1907
		pH	0.164	1	0.164	7.28	**0.0101**			pH	0.061	1	0.061	3.88	0.0553
		Contamination	0.025	1	0.025	1.1	0.3015			Contamination	0.054	1	0.054	3.44	0.0704
		Temperature * pH	0.034	1	0.034	1.51	0.2262			Temperature * pH	0.022	1	0.022	1.43	0.2389
		Temperature * Contamination	0.168	1	0.168	7.45	**0.0093**			Temperature * Contamination	0.428	1	0.428	27.44	**< 0.0001**
		pH * Contamination	0.023	1	0.023	1.03	0.3163			pH * Contamination	0	1	0	0.01	0.9352
		Temperature * pH * Contamination	0	1	0	0	0.9832			Temperature * pH * Contamination	0.001	1	0.001	0.08	0.7828
		Residual	0.922	41	0.022					Residual	0.671	43	0.016		
		Pairwise comparisons				Control vs Warming	**0.0308**			Pairwise comparisons				Control vs Gd	**0.0176**
						Acidification vs Warming	**0.0058**							Control vs Warming	**0.0046**
						Acidification vs Warming & La	**0.0313**							Gd vs Acidification	**0.0027**
														Gd vs Warming, acidification & Gd	**0.045**
														Acidification & Gd vs Acidification	**0.0123**
														Acidification vs Warming	**0.0005**
														Warming vs Warming, acidification & Gd	**0.0105**
	CAT	Temperature	0.006	1	0.006	0.58	0.4557		**CAT**	Temperature	0.005	1	0.005	0.52	0.4787
		pH	0	1	0	0.02	0.9036			pH	0.006	1	0.006	0.56	0.4644
		Contamination	0.001	1	0.001	0.06	0.803			Contamination	0.021	1	0.021	2.11	0.1646
		Temperature * pH	0.007	1	0.007	0.66	0.4251			Temperature * pH	0.004	1	0.004	0.45	0.5132
		Temperature * Contamination	0.021	1	0.021	1.95	0.1777			Temperature * Contamination	0.017	1	0.017	1.75	0.2036
		pH * Contamination	0.005	1	0.005	0.46	0.5032			pH * Contamination	0	1	0	0.05	0.827
		Temperature * pH * Contamination	0.008	1	0.008	0.69	0.4144			Temperature * pH * Contamination	0.004	1	0.004	0.42	0.5245
		Residual	0.228	21	0.011					Residual	0.17	17	0.01		
	GST	Temperature	0.04	1	0.04	9.46	**0.0041**		**GST**	Temperature	0.01	1	0.01	4.56	**0.0396**
		pH	0.005	1	0.005	1.1	0.3017			pH	0.007	1	0.007	3.02	0.0907
		Contamination	0.117	1	0.117	27.47	**< 0.0001**			Contamination	0.245	1	0.245	111.03	**< 0.0001**

Supplemental Table 10.2 a Cont.

			La trial								Gd trial				
			Sum of squares	Degrees of freedom	Mean square	F-value	p-value				Sum of squares	Degrees of freedom	Mean square	F-value	p-value
T1	**GST**	Temperature * pH	0.046	1	0.046	10.76	**0.0024**	**T1**	**GST**	Temperature * pH	0.012	1	0.012	5.34	**0.0267**
		Temperature * Contamination	0.002	1	0.002	0.41	0.5286			Temperature * Contamination	0.02	1	0.02	9.02	**0.0048**
		pH * Contamination	0.003	1	0.003	0.76	0.3907			pH * Contamination	0.005	1	0.005	2.22	0.1449
		Temperature * pH * Contamination	0.007	1	0.007	1.7	0.2009			Temperature * pH * Contamination	0.036	1	0.036	16.26	**0.0003**
		Residual	0.149	35	0.004					Residual	0.079	36	0.002		
		Pairwise comparisons				Control vs Warming, acidification & La	**0.0353**			Pairwise comparisons				Control vs Gd	**< 0.0001**
						La vs Acidification	**0.0003**							Control vs Acidification & Gd	**0.0001**
						Acidification & La vs Acidification	**0.0443**							Control vs Acidification	**0.0299**
						Acidification vs Warming & La	**< 0.0001**							Control vs Warming & Gd	**< 0.0001**
						Acidification vs Warming, acidification & La	**< 0.0001**							Control vs Warming, acidification & Gd	**0.0062**
						Acidification vs Warming & acidification	**0.0214**							Gd vs Acidification	**< 0.0001**
						Warming vs Warming & La	**0.0244**							Gd vs Warming	**< 0.0001**
						Warming vs Warming, acidification & La	**0.0166**							Acidification & Gd vs Acidification	**< 0.0001**
														Acidification & Gd vs Warming	**< 0.0001**
														Acidification vs Warming & Gd	**< 0.0001**
														Acidification vs Warming, acidification & Gd	**< 0.0001**
														Acidification vs Warming & acidification	**0.0004**
														Warming vs Warming & Gd	**< 0.0001**
														Warming vs Warming, acidification & Gd	**0.0017**
	LPO	Temperature	0.144	1	0.144	3.75	0.0653		**LPO**	Temperature	0.051	1	0.051	0.87	0.3615
		pH	0	1	0	0.01	0.9299			pH	0.084	1	0.084	1.44	0.2424
		Contamination	0.358	1	0.358	9.35	**0.0056**			Contamination	0.07	1	0.07	1.2	0.2839

Supplemental Table 10.2 a Cont.

			La trial							Gd trial				
			Sum of squares	Degrees of freedom	Mean square	F-value	p-value			Sum of squares	Degrees of freedom	Mean square	F-value	p-value
T1	**LPO**	Temperature * pH	0	1	0	0	0.968	**T1**	**LPO**	Temperature * pH	0.01	1	0.01	0.17	0.6829
		Temperature * Contamination	0.043	1	0.043	1.13	0.2994			Temperature * Contamination	0.003	1	0.003	0.05	0.8256
		pH * Contamination	0.008	1	0.008	0.2	0.6602			pH * Contamination	0.129	1	0.129	2.22	0.1502
		Temperature * pH * Contamination	0.031	1	0.031	0.8	0.379			Temperature * pH * Contamination	0.007	1	0.007	0.12	0.7327
		Residual	0.882	23	0.038					Residual	1.344	23	0.058		
	Chlor opyll	Temperature	0.027	1	0.027	3.39	0.0854		**Chloro pyll**	Temperature	0.029	1	0.029	3.91	0.068
		pH	0.001	1	0.001	0.16	0.6953			pH	0.005	1	0.005	0.67	0.4261
		Contamination	0.083	1	0.083	10.56	**0.0054**			Contamination	0.023	1	0.023	3.07	0.1017
		Temperature * pH	0.003	1	0.003	0.39	0.5431			Temperature * pH	0.01	1	0.01	1.31	0.2718
		Temperature * Contamination	0.005	1	0.005	0.66	0.4301			Temperature * Contamination	0.007	1	0.007	0.9	0.3577
		pH * Contamination	0	1	0	0.02	0.8865			pH * Contamination	0.014	1	0.014	1.86	0.1947
		Temperature * pH * Contamination	0.023	1	0.023	2.97	0.1053			Temperature * pH * Contamination	0.038	1	0.038	5.02	**0.0417**
		Residual	0.118	15	0.008					Residual	0.105	14	0.008		
	Carot enoid	Temperature	0.003	1	0.003	0.18	0.6793		**Carot enoid**	Temperature	0.012	1	0.012	0.78	0.3938
		pH	0.002	1	0.002	0.13	0.7274			pH	0.001	1	0.001	0.08	0.7782
		Contamination	0.001	1	0.001	0.08	0.7784			Contamination	0.001	1	0.001	0.06	0.811
		Temperature * pH	0.064	1	0.064	3.51	0.0854			Temperature * pH	0.001	1	0.001	0.08	0.7845
		Temperature * Contamination	0	1	0	0	0.9598			Temperature * Contamination	0.03	1	0.03	2	0.1803
		pH * Contamination	0.001	1	0.001	0.04	0.8381			pH * Contamination	0.003	1	0.003	0.21	0.6573
		Temperature * pH * Contamination	0.018	1	0.018	1.01	0.3348			Temperature * pH * Contamination	0.007	1	0.007	0.49	0.4973
		Residual	0.217	12	0.018					Residual	0.196	13	0.015		
T3	**SOD**	Temperature	0.244	1	0.244	59.16	**< 0.0001**	**T3**	**SOD**	Temperature	0.128	1	0.128	37.28	< 0.0001
		pH	0.001	1	0.001	0.29	0.5959			pH	0.001	1	0.001	0.15	0.7056
		Contamination	0.086	1	0.086	21	**< 0.0001**			Contamination	0.424	1	0.424	123	< 0.0001
		Temperature * pH	0.005	1	0.005	1.26	0.2678			Temperature * pH	0.013	1	0.013	3.89	0.0566

Supplemental Table 10.2 a Cont.

			La trial								Gd trial				
			Sum of squares	Degrees of freedom	Mean square	F-value	p-value				Sum of squares	Degrees of freedom	Mean square	F-value	p-value
T3	**SOD**	Temperature * Contamination	0.022	1	0.022	5.28	**0.0271**	**T3**	**SOD**	Temperature * Contamination	0.062	1	0.062	18.08	0.0001
		pH * Contamination	0	1	0	0.09	0.7616			pH * Contamination	0.005	1	0.005	1.57	0.2188
		Temperature * pH * Contamination	0.014	1	0.014	3.37	0.0741			Temperature * pH * Contamination	0.004	1	0.004	1.2	0.2801
		Residual	0.161	39	0.004					Residual	0.121	35	0.003		
		Pairwise comparisons				Control vs La	**0.0011**			Pairwise comparisons				Control vs Gd	**< 0.0001**
						Control vs Acidification & La	**0.0057**							Control vs Acidification & Gd	**< 0.0001**
						Control vs W	**< 0.0001**							Control vs Warming	**< 0.0001**
						Control vs Warming & La	**< 0.0001**							Control vs Warming & Gd	**< 0.0001**
						Control vs Warming, acidification & La	**< 0.0001**							Control vs Warming, acidification & Gd	**< 0.0001**
						Control vs Warming & acidification	**< 0.0001**							Control vs Warming & acidification	**< 0.0001**
						Acidification vs W	**0.0032**							Gd vs Acidification	**< 0.0001**
						Acidification vs Warming & La	**0.0002**							Gd vs Warming & acidification	**0.0131**
						Acidification vs Warming, acidification & La	**< 0.0001**							Acidification & Gd vs Acidification	**< 0.0001**
						Acidification vs Warming & acidification	**0.0086**							Acidification vs Warming	**0.0012**
														Acidification vs Warming & Gd	**< 0.0001**
														Acidification vs Warming, acidification & Gd	**< 0.0001**
														Acidification vs Warming & acidification	**0.0035**
														Warming & Gd vs Warming & acidification	**0.0009**
														Warming, acidification & Gd vs Warming & acidification	**0.0093**
	CAT	Temperature	0.002	1	0.002	0.17	0.6869		**CAT**	Temperature	0.007	1	0.007	0.35	0.5602
		pH	0.007	1	0.007	0.58	0.4541			pH	0.012	1	0.012	0.59	0.4502
		Contamination	0.262	1	0.262	21.28	**0.0002**			Contamination	0.542	1	0.542	25.63	**< 0.0001**

Supplemental Table 10.2 a Cont.

			La trial								Gd trial				
			Sum of squares	Degrees of freedom	Mean square	F-value	p-value				Sum of squares	Degrees of freedom	Mean square	F-value	p-value
T3	**CAT**	Temperature * pH	0.006	1	0.006	0.49	0.4926	**T3**	**CAT**	Temperature * pH	0	1	0	0.02	0.895
		Temperature * Contamination	0.015	1	0.015	1.23	0.2808			Temperature * Contamination	0.028	1	0.028	1.31	0.2648
		pH * Contamination	0	1	0	0.03	0.8623			pH * Contamination	0	1	0	0	0.9791
		Temperature * pH * Contamination	0.009	1	0.009	0.69	0.4154			Temperature * pH * Contamination	0.001	1	0.001	0.06	0.8138
		Residual	0.246	20	0.012					Residual	0.465	22	0.021		
		Pairwise comparisons				Control vs Acidification & La	**0.0277**			Pairwise comparisons				Control vs Acidification & Gd	**0.0196**
														Warming vs Acidification & Gd	**0.0331**
	GST	Temperature	0.047	1	0.047	3.76	0.0611		**GST**	Temperature	0.003	1	0.003	0.21	0.6529
		pH	0.003	1	0.003	0.26	0.6108			pH	0.029	1	0.029	2.11	0.1547
		Contamination	0.042	1	0.042	3.39	0.0744			Contamination	0.093	1	0.093	6.8	**0.0132**
		Temperature * pH	0	1	0	0.04	0.8517			Temperature * pH	0.02	1	0.02	1.43	0.2402
		Temperature * Contamination	0	1	0	0	0.974			Temperature * Contamination	0.027	1	0.027	1.99	0.1664
		pH * Contamination	0.018	1	0.018	1.44	0.2385			pH * Contamination	0.001	1	0.001	0.05	0.8238
		Temperature * pH * Contamination	0	1	0	0.03	0.8591			Temperature * pH * Contamination	0.01	1	0.01	0.7	0.4095
		Residual	0.41	33	0.012					Residual	0.493	36	0.014		
	LPO	Temperature	0.052	1	0.052	0.97	0.337		**LPO**	Temperature	0.048	1	0.048	1.64	0.2146
		pH	0.002	1	0.002	0.04	0.8386			pH	0.023	1	0.023	0.78	0.3862
		Contamination	0.078	1	0.078	1.44	0.244			Contamination	0.173	1	0.173	5.91	**0.0246**
		Temperature * pH	0	1	0	0.01	0.9372			Temperature * pH	0.012	1	0.012	0.42	0.5226
		Temperature * Contamination	0.003	1	0.003	0.06	0.8065			Temperature * Contamination	0.004	1	0.004	0.13	0.7241
		pH * Contamination	0.026	1	0.026	0.48	0.4965			pH * Contamination	0.003	1	0.003	0.1	0.7591
		Temperature * pH * Contamination	0.032	1	0.032	0.58	0.4533			Temperature * pH * Contamination	0.007	1	0.007	0.22	0.6409
		Residual	1.135	21	0.054					Residual	0.587	20	0.029		
	Chlor opyll	Temperature	0.027	1	0.027	45.97	**< 0.0001**		**Chloro pyll**	Temperature	0.042	1	0.042	138.8	**< 0.0001**
		pH	0.02	1	0.02	35.22	**< 0.0001**			pH	0.016	1	0.016	51.72	**< 0.0001**
		Contamination	0.107	1	0.107	184.2	**< 0.0001**			Contamination	0.025	1	0.025	84.05	**< 0.0001**

Supplemental Table 10.2 a Cont.

			La trial								Gd trial				
			Sum of squares	Degrees of freedom	Mean square	F-value	p-value				Sum of squares	Degrees of freedom	Mean square	F-value	p-value
T3	**Chlorophyll**	Temperature * pH	0.035	1	0.035	61.13	**< 0.0001**	**T3**	**Chlorophyll**	Temperature * pH	0.04	1	0.04	132.83	**< 0.0001**
		Temperature * Contamination	0.008	1	0.008	13.67	**0.0024**			Temperature * Contamination	0.017	1	0.017	56.58	**< 0.0001**
		pH * Contamination	0.017	1	0.017	30.09	**< 0.0001**			pH * Contamination	0.013	1	0.013	43.17	**< 0.0001**
		Temperature * pH * Contamination	0.037	1	0.037	63.15	**< 0.0001**			Temperature * pH * Contamination	0.032	1	0.032	105.16	**< 0.0001**
		Residual	0.008	14	0.001					Residual	0.004	14	0		
		Pairwise comparison				Control vs La	**0.0003**			Pairwise comparisons				Control vs Acidification & Gd	**< 0.0001**
						Control vs Acidification & La	**< 0.0001**							Control vs Acidification	**< 0.0001**
						Control vs Acidification	**< 0.0001**							Control vs Warming	**< 0.0001**
						Control vs W	**< 0.0001**							Control vs Warming & Gd	**< 0.0001**
						Control vs Warming & La	**< 0.0001**							Control vs Warming, acidification & Gd	**< 0.0001**
						Control vs Warming, acidification & La	**< 0.0001**							Gd vs Acidification & Gd	**0.0001**
						La vs Acidification & La	**0.0007**							Gd vs Acidification	**< 0.0001**
						La vs Warming & La	**0.0042**							Gd vs Warming	**< 0.0001**
						La vs Warming, acidification & La	**< 0.0001**							Gd vs Warming & Gd	**< 0.0001**
						La vs Warming & acidification	**0.0065**							Gd vs Warming, acidification & Gd	**< 0.0001**
						Acidification & La vs Acidification	**0.0244**							Acidification & Gd vs Warming, acidification & Gd	**< 0.0001**
						Acidification & La vs Warming, acidification & La	**0.0012**							Acidification & Gd vs Warming & acidification	**< 0.0001**
						Acidification & La vs Warming & acidification	**< 0.0001**							Acidification vs Warming, acidification & Gd	**< 0.0001**
						Acidification vs Warming, acidification & La	**< 0.0001**							Acidification vs Warming & acidification	**< 0.0001**
						Acidification vs Warming & acidification	**0.0002**							Warming vs Warming, acidification & Gd	**0.0008**
						W vs Warming, acidification & La	**< 0.0001**							Warming vs Warming & acidification	**< 0.0001**

Supplemental Table 10.2 a Cont.

			Sum of squares	La trial Degrees of freedom	Mean square	F-value	p-value				Sum of squares	Gd trial Degrees of freedom	Mean square	F-value	p-value
						W vs Warming & acidification	**< 0.0001**							Warming & Gd vs Warming, acidification & Gd	**0.0002**
						Warming & La vs Warming, acidification & La	**0.0016**							Warming & Gd vs Warming & acidification	**< 0.0001**
						Warming & La vs Warming & acidification	**< 0.0001**							Warming, acidification & Gd vs Warming & acidification	**< 0.0001**
						Warming, acidification & La vs Warming & acidification	**< 0.0001**								
	Carotenoid	Temperature	0.079	1	0.079	18.28	**0.0011**		**Carotenoid**	Temperature	0.054	1	0.054	6.98	**0.0215**
		pH	0.031	1	0.031	7.05	**0.021**			pH	0.016	1	0.016	2	0.1827
		Contamination	0.028	1	0.028	6.42	**0.0262**			Contamination	0.014	1	0.014	1.74	0.2113
		Temperature * pH	0.029	1	0.029	6.6	**0.0246**			Temperature * pH	0.031	1	0.031	3.96	0.0699
		Temperature * Contamination	0	1	0	0.03	0.8753			Temperature * Contamination	0.001	1	0.001	0.18	0.6757
		pH * Contamination	0.03	1	0.03	6.95	**0.0217**			pH * Contamination	0.015	1	0.015	1.96	0.187
		Temperature * pH * Contamination	0.02	1	0.02	4.69	0.0513			Temperature * pH * Contamination	0.018	1	0.018	2.38	0.1492
		Residual	0.052	12	0.004					Residual	0.093	12	0.008		
		Pairwise comparisons				Control vs Acidification & La	**0.0178**								
						Control vs W	**0.0133**								
						Control vs Warming, acidification & La	**0.0015**								
						La vs Warming, acidification & La	**0.0065**								
T7	**SOD**	Temperature	0.262	1	0.262	66.6	**< 0.0001**	**T7**	**SOD**	Temperature	0.097	1	0.097	35.3	< 0.0001
		pH	0.084	1	0.084	21.3	**< 0.0001**			pH	0.07	1	0.07	25.39	< 0.0001
		Contamination	0.023	1	0.023	5.85	**0.0201**			Contamination	0.287	1	0.287	104.15	< 0.0001
		Temperature * pH	0	1	0	0.07	0.7882			Temperature * pH	0.013	1	0.013	4.62	0.0384
		Temperature * Contamination	0.037	1	0.037	9.3	**0.004**			Temperature * Contamination	0	1	0	0.03	0.8564
		pH * Contamination	0.036	1	0.036	9.1	**0.0044**			pH * Contamination	0.035	1	0.035	12.67	0.0011

Supplemental Table 10.2 a Cont.

			La trial							Gd trial				
			Sum of squares	Degrees of freedom	Mean square	F-value	p-value			Sum of squares	Degrees of freedom	Mean square	F-value	p-value
T7	**SOD**	Temperature * pH * Contamination	0.084	1	0.084	21.46	**< 0.0001**	**T7**	**SOD**	Temperature * pH * Contamination	0.031	1	0.031	11.39	0.0018
		Residual	0.161	41	0.004					Residual	0.099	36	0.003		
		Pairwise comparisons				Control vs La	**0.0298**			Pairwise comparisons				Control vs Gd	**< 0.0001**
						Control vs Acidification	**< 0.0001**							Control vs Acidification & Gd	**< 0.0001**
						Control vs W	**0.0004**							Control vs Acidification	**< 0.0001**
						Control vs Warming & La	**< 0.0001**							Control vs Warming	**< 0.0001**
						Control vs Warming, acidification & La	**< 0.0001**							Control vs Warming & Gd	**< 0.0001**
						Control vs Warming & acidification	**< 0.0001**							Control vs Warming, acidification & Gd	**< 0.0001**
						La vs Warming & La	**0.0193**							Control vs Warming & acidification	**< 0.0001**
						La vs Warming, acidification & La	**< 0.0001**							Gd vs Warming	**0.0207**
						Acidification & La vs Acidification	**0.0027**							Gd vs Warming, acidification & Gd	**0.0085**
						Acidification & La vs Warming & La	**0.0007**							Acidification & Gd vs Warming	**0.0279**
						Acidification & La vs Warming, acidification & La	**< 0.0001**							Acidification & Gd vs Warming, acidification & Gd	**0.0201**
						Acidification & La vs Warming & acidification	**0.0076**							Acidification vs Warming & Gd	**0.0123**
						Acidification vs Warming, acidification & La	**0.0057**							Acidification vs Warming, acidification & Gd	**0.0003**
						W vs Warming, acidification & La	**< 0.0001**							Warming vs Warming & Gd	**0.0001**
						Warming, acidification & La vs Warming & acidification	**0.0273**							Warming vs Warming, acidification & Gd	**< 0.0001**
														Warming & Gd vs Warming & acidification	**0.0374**
														Warming, acidification & Gd vs Warming & acidification	**0.0014**
	CAT	Temperature	0.021	1	0.021	1.07	0.312		**CAT**	Temperature	0.002	1	0.002	0.09	0.7625
		pH	0.023	1	0.023	1.14	0.2974			pH	0.056	1	0.056	2.53	0.1254

Supplemental Table 10.2 a Cont.

			La trial								Gd trial				
			Sum of squares	Degrees of freedom	Mean square	F-value	p-value				Sum of squares	Degrees of freedom	Mean square	F-value	p-value
T7	**CAT**	Contamination	0.132	1	0.132	6.68	**0.0173**	**T7**	**CAT**	Contamination	0.267	1	0.267	12.04	**0.0021**
		Temperature * pH	0	1	0	0	0.9642			Temperature * pH	0.001	1	0.001	0.05	0.8244
		Temperature * Contamination	0	1	0	0	0.9536			Temperature * Contamination	0.013	1	0.013	0.59	0.4512
		pH * Contamination	0.004	1	0.004	0.2	0.6571			pH * Contamination	0.022	1	0.022	0.97	0.3349
		Temperature * pH * Contamination	0.006	1	0.006	0.31	0.5827			Temperature * pH * Contamination	0.002	1	0.002	0.08	0.7838
		Residual	0.414	21	0.02					Residual	0.511	23	0.022		
	GST	Temperature	0.089	1	0.089	6.08	**0.018**		**GST**	Temperature	0.161	1	0.161	14.07	**0.0006**
		pH	0.007	1	0.007	0.48	0.4932			pH	0.017	1	0.017	1.47	0.2327
		Contamination	0.049	1	0.049	3.35	0.0745			Contamination	0.407	1	0.407	35.52	**< 0.0001**
		Temperature * pH	0.027	1	0.027	1.86	0.1799			Temperature * pH	0.02	1	0.02	1.74	0.1948
		Temperature * Contamination	0.02	1	0.02	1.34	0.254			Temperature * Contamination	0.058	1	0.058	5.04	**0.0303**
		pH * Contamination	0.011	1	0.011	0.78	0.3828			pH * Contamination	0.004	1	0.004	0.36	0.5533
		Temperature * pH * Contamination	0.074	1	0.074	5.07	**0.0299**			Temperature * pH * Contamination	0.001	1	0.001	0.09	0.7659
		Residual	0.588	40	0.015					Residual	0.458	40	0.011		
		Pairwise comparisons				Acidification & La vs Warming, acidification & La	**0.0032**			Pairwise comparisons				Control vs Warming & Gd	**0.0004**
						Acidification vs Warming, acidification & La	**0.014**							Control vs Warming, acidification & Gd	**0.0112**
														Gd vs Warming & Gd	**0.0049**
														Acidification & Gd vs Warming & Gd	**0.0216**
														Acidification vs Warming, acidification & Gd	**0.0005**
														W vs Warming & Gd	**0.0012**
														Warming & Gd vs Warming & acidification	**0.0002**
														Warming, acidification & Gd vs Warming & acidification	**0.0076**
	LPO	Temperature	0.049	1	0.049	0.58	0.4539		**LPO**	Temperature	0.077	1	0.077	1.23	0.2785

Supplemental Table 10.2 a Cont.

			La trial								Gd trial				
			Sum of squares	Degrees of freedom	Mean square	F-value	p-value				Sum of squares	Degrees of freedom	Mean square	F-value	p-value
T7	**LPO**	pH	0.211	1	0.211	2.5	0.1279	**T7**	**LPO**	pH	0.096	1	0.096	1.52	0.2299
		Contamination	0.386	1	0.386	4.58	**0.0437**			Contamination	0.7	1	0.7	11.16	**0.003**
		Temperature * pH	0.037	1	0.037	0.44	0.5134			Temperature * pH	0.066	1	0.066	1.06	0.315
		Temperature * Contamination	0.038	1	0.038	0.46	0.5065			Temperature * Contamination	0.019	1	0.019	0.31	0.5841
		pH * Contamination	0.051	1	0.051	0.6	0.4456			pH * Contamination	0.141	1	0.141	2.25	0.1479
		Temperature * pH * Contamination	0.132	1	0.132	1.56	0.2241			Temperature * pH * Contamination	0.089	1	0.089	1.42	0.2459
		Residual	1.855	22	0.084					Residual	1.38	22	0.063		
										Pairwise comparisons				Control vs Warming & Gd	**0.0475**
	Chlor opyll	Temperature	0.001	1	0.001	0.59	0.4573		**Chloro pyll**	Temperature	0.002	1	0.002	0.51	0.4886
		pH	0	1	0	0.05	0.8206			pH	0	1	0	0	0.9704
		Contamination	0.015	1	0.015	11.04	**0.0068**			Contamination	0.008	1	0.008	1.79	0.2081
		Temperature * pH	0.001	1	0.001	0.82	0.3835			Temperature * pH	0.002	1	0.002	0.39	0.5461
		Temperature * Contamination	0.011	1	0.011	8.14	**0.0157**			Temperature * Contamination	0.008	1	0.008	1.72	0.2166
		pH * Contamination	0.01	1	0.01	7.4	**0.0199**			pH * Contamination	0.008	1	0.008	1.83	0.2029
		Temperature * pH * Contamination	0.003	1	0.003	2.21	0.1648			Temperature * pH * Contamination	0.017	1	0.017	3.85	0.0754
		Residual	0.015	11	0.001					Residual	0.049	11	0.004		
	Carot enoid	Temperature	0.002	1	0.002	1.05	0.3278		**Carot enoid**	Temperature	0.009	1	0.009	3.8	0.0799
		pH	0.005	1	0.005	3.1	0.1061			pH	0	1	0	0.11	0.7507
		Contamination	0.004	1	0.004	2.66	0.1312			Contamination	0.004	1	0.004	1.89	0.1992
		Temperature * pH	0.03	1	0.03	17.98	**0.0014**			Temperature * pH	0.019	1	0.019	8.45	**0.0156**
		Temperature * Contamination	0.002	1	0.002	1.1	0.3167			Temperature * Contamination	0.031	1	0.031	13.63	**0.0042**
		pH * Contamination	0.018	1	0.018	10.4	**0.0081**			pH * Contamination	0.006	1	0.006	2.43	0.1503
		Temperature * pH * Contamination	0.008	1	0.008	4.54	0.0565			Temperature * pH * Contamination	0.014	1	0.014	5.99	**0.0345**
		Residual	0.019	11	0.002					Residual	0.023	10	0.002		
		Pairwise comparisons				Acidification & La vs Warming & acidification	**0.0098**			Pairwise comparisons				Gd vs Warming, acidification & Gd	**0.0375**

Supplemental Table 10.2 a Cont.

			Sum of squares	La trial Degrees of freedom	Mean square	F-value	p-value
T7	**Carotenoid**					Acidification vs Warming & acidification	**0.0182**
						Warming, acidification & La vs Warming & acidification.	**0.0252**
T14	**SOD**	Temperature	0.183	1	0.183	21.82	**< 0.0001**
		pH	0.004	1	0.004	0.44	0.5118
		Contamination	0.008	1	0.008	0.9	0.35
		Temperature * pH	0.005	1	0.005	0.63	0.4313
		Temperature * Contamination	0.036	1	0.036	4.26	**0.046**
		pH * Contamination	0.008	1	0.008	0.97	0.3306
		Temperature * pH * Contamination	0.001	1	0.001	0.07	0.7925
		Residual	0.311	37	0.008		
		Pairwise comparisons				La vs Warming & La	**0.0181**
						La vs Warming, acidification & La	**0.018**
						La vs Warming & acidification	**0.022**
	CAT	Temperature	0.002	1	0.002	0.25	0.6243
		pH	0.003	1	0.003	0.32	0.5784
		Contamination	0.252	1	0.252	25.96	**< 0.0001**
		Temperature * pH	0	1	0	0.01	0.9361
		Temperature * Contamination	0.024	1	0.024	2.45	0.1327
		pH * Contamination	0.001	1	0.001	0.14	0.7085
		Temperature * pH * Contamination	0.007	1	0.007	0.76	0.3923
		Residual	0.204	21	0.01		
		Pairwise comparisons				Control vs La	**0.008**
						Control vs Acidification & La	**0.0198**
						Control vs Warming, acidification & La	**0.0226**

			Sum of squares	Gd trial Degrees of freedom	Mean square	F-value	p-value
T7	**Carotenoid**					Warming, acidification & Gd vs Warming & acidification	**0.0116**
T14	**SOD**	Temperature	0.014	1	0.014	1.74	0.1957
		pH	0.002	1	0.002	0.3	0.5901
		Contamination	0.051	1	0.051	6.35	0.0163
		Temperature * pH	0	1	0	0.02	0.8881
		Temperature * Contamination	0.014	1	0.014	1.69	0.2024
		pH * Contamination	0.01	1	0.01	1.24	0.2737
		Temperature * pH * Contamination	0.007	1	0.007	0.85	0.3621
		Residual	0.29	36	0.008		
	CAT	Temperature	0.019	1	0.019	1.2	0.2853
		pH	0.002	1	0.002	0.12	0.7374
		Contamination	0.122	1	0.122	7.68	**0.0115**
		Temperature * pH	0.014	1	0.014	0.89	0.355
		Temperature * Contamination	0.004	1	0.004	0.26	0.6129
		pH * Contamination	0.003	1	0.003	0.16	0.6953
		Temperature * pH * Contamination	0.039	1	0.039	2.45	0.1326
		Residual	0.334	21	0.016		

Supplemental Table 10.2 a Cont.

			La trial								Gd trial				
			Sum of squares	Degrees of freedom	Mean square	F-value	p-value				Sum of squares	Degrees of freedom	Mean square	F-value	p-value
T14	**GST**	Temperature	0	1	0	0	0.9849	**T14**	**GST**	Temperature	0.113	1	0.113	11.13	**0.002**
		pH	0.013	1	0.013	1.22	0.2758			pH	0.011	1	0.011	1.08	0.3059
		Contamination	0.025	1	0.025	2.29	0.1382			Contamination	0.253	1	0.253	24.9	**< 0.0001**
		Temperature * pH	0.05	1	0.05	4.7	**0.0366**			Temperature * pH	0.034	1	0.034	3.32	**0.0771**
		Temperature * Contamination	0.047	1	0.047	4.43	**0.0419**			Temperature * Contamination	0.299	1	0.299	29.37	**< 0.0001**
		pH * Contamination	0.028	1	0.028	2.66	0.1114			pH * Contamination	0.003	1	0.003	0.28	0.6027
		Temperature * pH * Contamination	0.054	1	0.054	5	**0.0313**			Temperature * pH * Contamination	0.031	1	0.031	3.07	0.0883
		Residual	0.407	38	0.011					Residual	0.356	35	0.01		
		Pairwise comparisons				W vs Warming, acidification & La	**0.0317**			Pairwise comparisons				Control vs Warming & Gd	**0.0004**
						Warming & La vs Warming, acidification & La	**0.0317**							Gd vs Warming & Gd	**0.0001**
						Warming, acidification & La vs Warming & acidification	**0.0106**							Gd vs Warming, acidification & Gd	**0.0376**
														Acidification & Gd vs Warming & Gd	**0.0003**
														Acidification vs Warming & Gd	**0.0002**
														Warming vs Warming, acidification & Gd	**0.0093**
														Warming, acidification & Gd vs Warming & acidification	**0.0027**
	LPO	Temperature	0.094	1	0.094	1.6	0.2225		**LPO**	Temperature	0.074	1	0.074	1.88	0.1881
		pH	0.016	1	0.016	0.26	0.6132			pH	0.001	1	0.001	0.03	0.8708
		Contamination	0	1	0	0.01	0.9419			Contamination	0.057	1	0.057	1.46	0.2441
		Temperature * pH	0.056	1	0.056	0.96	0.3408			Temperature * pH	0	1	0	0.01	0.925
		Temperature * Contamination	0.044	1	0.044	0.76	0.3962			Temperature * Contamination	0.056	1	0.056	1.44	0.2473
		pH * Contamination	0	1	0	0.01	0.9338			pH * Contamination	0.031	1	0.031	0.79	0.3878
		Temperature * pH * Contamination	0.017	1	0.017	0.28	0.6028			Temperature * pH * Contamination	0.008	1	0.008	0.2	0.6618
		Residual	1.059	18	0.059					Residual	0.668	17	0.039		
	Chlor opyll	Temperature	0.001	1	0.001	0.1	0.7577		**Chloro pyll**	Temperature	0.002	1	0.002	2.01	0.1899

Supplemental Table 10.2 a Cont.

		La trial					Gd trial				
		Sum of squares	**Degrees of freedom**	**Mean square**	**F-value**	**p-value**	**Sum of squares**	**Degrees of freedom**	**Mean square**	**F-value**	**p-value**
	pH	0	1	0	0.02	0.8838	0.002	1	0.002	1.58	0.2398
	Contamination	0	1	0	0.01	0.933	0.007	1	0.007	5.85	**0.0387**
	Temperature * pH	0.001	1	0.001	0.27	0.6141	0.001	1	0.001	0.42	0.5351
	Temperature * Contamination	0	1	0	0.04	0.8494	0.003	1	0.003	2.78	0.1298
	pH * Contamination	0.014	1	0.014	2.63	0.1358	0.004	1	0.004	3.06	0.1141
	Temperature * pH * Contamination	0.003	1	0.003	0.5	0.4948	0.004	1	0.004	3.48	0.0949
	Residual	0.053	10	0.005			0.011	9	0.001		
							Pairwise comparison			Warming, acidification & Gd vs Warming & acidification	**0.0337**
Carotenoid	Temperature	0.002	1	0.002	0.66	0.437	0.002	1	0.002	2.09	0.1826
	pH	0.02	1	0.02	5.79	**0.037**	0.001	1	0.001	1.26	0.2913
	Contamination	0.019	1	0.019	5.44	**0.0418**	0.015	1	0.015	15.84	**0.0032**
	Temperature * pH	0	1	0	0.03	0.8679	0.001	1	0.001	0.89	0.3712
	Temperature * Contamination	0.001	1	0.001	0.25	0.6301	0.001	1	0.001	0.74	0.4123
	pH * Contamination	0.017	1	0.017	4.89	0.0515	0.001	1	0.001	0.57	0.4682
	Temperature * pH * Contamination	0.001	1	0.001	0.4	0.5418	0	1	0	0.31	0.5907
	Residual	0.035	10	0.003			0.009	9	0.001		

| ANNEX 9

Supplemental table 10.2 b) - Tukey's pairwise comparisons between times for SOD, CAT, GST, LIPO, Total Chlorophyll and Carotenoid in the four La and Gd exposed treatments, respectively. Bold point significant differences ($p < 0.05$).

		La	Acidification & La	Warming & La	Warming, acidification & La	Gd	Acidification & Gd	Warming & Gd	Warming, acidification & Gd
SOD	T1 vs T3	0.5309	0.2146	0.3851	**0.0002**	**0.0025**	**0.0015**	**0.0244**	**< 0.0001**
	T1 vs T7	0.5401	0.427	0.1921	**< 0.0001**	**0.0018**	**0.0002**	**0.0153**	**< 0.0001**
	T1 vs T14	0.5684	0.9136	0.5867	**0.0012**	0.1057	0.0614	0.2907	**0.0005**
	T3 vs T7	0.9999	0.9511	0.9478	0.2042	0.9984	0.9932	0.9948	0.2712
	T3 vs T14	**0.0192**	0.5923	0.9977	0.8486	0.3934	0.16	0.5234	0.4989
	T7 vs T14	**0.017**	0.8547	0.9088	**0.0374**	0.4211	**0.0492**	0.3929	**0.0339**
CAT	T1 vs T3	**0.0082**	**0.003**	**0.0142**	0.1109	**< 0.0001**	**0.0059**	0.2327	**0.033**
	T1 vs T7	**0.0188**	**0.0155**	**0.0478**	**0.0057**	**0.0006**	**0.0109**	0.4587	**0.0181**
	T1 vs T14	**0.0012**	**0.0048**	**0.0284**	**0.0175**	**0.0003**	0.1989	0.621	**0.0382**
	T3 vs T7	0.8681	0.6518	0.9618	0.2682	0.2428	0.9761	0.9094	0.9654
	T3 vs T14	0.8453	0.8915	0.9987	0.6359	0.4902	0.151	0.8194	0.9995
	T7 vs T14	0.3642	0.9425	0.9894	0.8824	0.9458	0.2754	0.9934	0.9373
GST	T1 vs T3	0.8265	0.9035	0.999	0.9286	0.985	0.7981	1	0.8459
	T1 vs T7	0.9889	0.7441	0.9646	0.0732	0.8007	1	**0.0012**	**0.0177**
	T1 vs T14	0.2177	0.6493	**0.0076**	0.9337	**0.0264**	**0.0006**	**0.0085**	0.5961
	T3 vs T7	0.932	0.3971	0.9318	0.388	0.9785	0.8166	**0.0007**	**0.005**
	T3 vs T14	0.7683	0.3438	**0.0056**	0.9999	0.1204	**< 0.0001**	**0.0063**	0.2515
	T7 vs T14	0.3129	0.9913	**0.0462**	0.3036	0.1188	**0.0009**	0.9835	0.3339
LIPO	T1 vs T3	0.3825	0.9342	0.9955	0.9094	**0.0493**	0.0639	0.3398	0.5709
	T1 vs T7	0.3845	0.5584	0.9997	0.6106	**0.0141**	**0.0441**	0.1456	0.3659
	T1 vs T14	0.9865	0.8819	0.9996	0.8304	0.0911	0.7289	0.4425	0.9893
	T3 vs T7	1	0.9083	0.9855	0.9345	0.8579	0.9952	0.9753	0.993
	T3 vs T14	0.5626	0.9967	0.9897	0.4615	0.998	0.5675	0.9873	0.78
	T7 vs T14	0.5651	0.9818	1	0.209	0.9639	0.4624	0.8539	0.5945
Total Chlorophyll	T1 vs T3	**0.0006**	0.5453	0.9704	0.9994	0.8269	**0.0222**	0.9502	0.9059
	T1 vs T7	0.459	0.31	0.9985	0.955	**0.0002**	**0.0031**	0.9005	0.5345
	T1 vs T14	**0.0479**	0.477	0.8055	0.3921	**0.0004**	**0.003**	0.6774	0.7513
	T3 vs T7	**0.0029**	0.9012	0.9936	0.978	**0.0001**	0.1948	0.9985	0.8832
	T3 vs T14	**0.0253**	0.9913	0.9709	0.4466	**0.0002**	0.1877	0.9042	0.986
	T7 vs T14	0.3869	0.9823	0.8997	0.6589	0.6846	1	0.9484	0.9781
Carotenoids	T1 vs T3	**0.0426**	**0.0138**	0.2793	0.1266	0.9984	0.3579	**0.0214**	0.0657
	T1 vs T7	0.9709	**0.001**	0.1192	0.1337	0.3013	0.1476	**0.0028**	**0.0009**
	T1 vs T14	0.9573	**0.0019**	0.1764	0.0585	0.1668	0.1427	0.2475	**0.0108**
	T3 vs T7	**0.0234**	**0.0161**	0.8068	0.9886	0.2549	0.8745	**0.0002**	0.0618
	T3 vs T14	0.0861	0.0518	0.96	0.9938	0.1402	0.8627	**0.0035**	0.7648
	T7 vs T14	0.7895	0.6723	0.9717	0.9189	0.9661	1	**0.0133**	0.1598